

ACTA POLONIAE PHARMACEUTICA

VOL. 72 No. 1 January/February 2015

ISSN 2353-5288

Drug Research



EDITOR

Aleksander P. Mazurek

National Medicines Institute, The Medical University of Warsaw

ASSISTANT EDITOR

Jacek Bojarski

Medical College, Jagiellonian University, Kraków

EXECUTIVE EDITORIAL BOARD

Mirosława Furmanowa	The Medical University of Warsaw
Bożenna Gutkowska	The Medical University of Warsaw
Roman Kaliszan	The Medical University of Gdańsk
Jan Pachecka	The Medical University of Warsaw
Jan Pawlaczyk	K. Marcinkowski University of Medical Sciences, Poznań
Janusz Pluta	The Medical University of Wrocław
Witold Wieniawski	Polish Pharmaceutical Society, Warsaw
Pavel Komarek	Czech Pharmaceutical Society
Henry Ostrowski-Meissner	Charles Sturt University, Sydney
Erhard Röder	Pharmazeutisches Institut der Universität, Bonn
Phil Skolnick	DOV Pharmaceutical, Inc.
Zoltán Vincze	Semmelweis University of Medicine, Budapest

This Journal is published bimonthly by the Polish Pharmaceutical Society (Issued since 1937)

The paper version of the Publisher magazine is a prime version.

The electronic version can be found in the Internet on page
www.actapoloniaepharmaceutica.pl

An access to the journal in its electronics version is free of charge

Impact factor (2013):	0.693
MNiSW score (2013):	15 points
Index Copernicus (2012):	13.18

Charges

Annual subscription rate for 2014 is US \$ 210 including postage and handling charges. Prices subject to change.
Back issues of previously published volumes are available directly from Polish Pharmaceutical Society, 16 Długa St., 00-238 Warsaw, Poland.

Payment should be made either by banker's draft (money order) issued to „PTFarm” or to our account Millennium S.A. No. 29 1160 2202 0000 0000 2770 0281, Polskie Towarzystwo Farmaceutyczne, ul. Długa 16, 00-238 Warszawa, Poland, with the memo Acta Poloniae Pharmaceutica - Drug Research.

Warunki prenumeraty

Czasopismo Acta Poloniae Pharmaceutica - Drug Research wydaje i kolportaż prowadzi Polskie Towarzystwo Farmaceutyczne, ul. Długa 16, 00-238 Warszawa.

Cena prenumeraty krajowej za rocznik 2014 wynosi 207,90 zł (w tym 5% VAT). Prenumeratę należy wpłacać w dowolnym banku lub Urzędzie Pocztowym na rachunek bankowy Wydawcy:

Millennium S.A.
29 1160 2202 0000 0000 2770 0281
Polskie Towarzystwo Farmaceutyczne
ul. Długa 16, 00-238 Warszawa

z dopiskiem: prenumerata Acta Poloniae Pharmaceutica - Drug Research.

Warunki prenumeraty zagranicznej - patrz tekst angielski.

CONTENTS

REVIEW

3. Muhammad Khurram Waqas, Naveed Akhtar, Rehan Mustafa, Muhammad Jamshaid, Haji Muhammad Shoaib Khan, Ghulam Murtaza
Dermatological and cosmeceutical benefits of *Glycine max* (soybean) and its active components.
13. Łukasz Dobrek, Piotr J. Thor
The role of prostanoids in the urinary bladder function and a potential use of prostanoid-targeting pharmacological agents in bladder overactivity treatment.

ANALYSIS

21. Kinga Lange, Teresa Gierlach-Hładoń
Solid state characterization of α -tocopherol in inclusion complexes with cyclodextrins.
31. Urszula Hubicka, Barbara Żuromska-Witek, Joanna Piotrowska, Jan Krzek
Determination of neomycin in the form of neomycin derivative with dabsyl chloride by thin layer chromatography and densitometry.
39. Anna Petruczynik, Karol Wróblewski, Monika Waksmundzka-Hajnos
Effect of chromatographic conditions on retention behavior and system efficiency for HPTLC of selected psychotropic drugs on chemically bonded stationary phases.

DRUG BIOCHEMISTRY

49. Anna Bilska-Wilkosz, Magdalena Dudek, Joanna Knutelska, Lidia Włodek
Effect of lipoic administration on the urinary excretion of thiocyanate in rats exposed to potassium cyanide.

DRUG SYNTHESIS

53. Jerzy Cieplik, Marcin Stolarczyk, Janusz Pluta, Olaf Gubrynowicz, Iwona Bryndał, Tadeusz Lis, Marcin Mikulewicz
Synthesis and antibacterial properties of pyrimidine derivatives.
65. Mostafa M. Ghorab, Mansour S. Alsaïd, Yassin M. Nissan
Novel pyrrolopyrimidines and triazolopyrrolopyrimidines carrying a biologically active sulfonamide moieties as anticancer agents
79. Mostafa M. Ghorab, Mansour S. Alsaïd, Abdullah-Al-Dhfyān, Reem K. Arafa
Cytotoxic activity of some novel sulfonamide derivatives.
89. Anna Maria Waszkielewicz, Agnieszka Gunia-Krzyżak, Marek Cegła, Henryk Marona
Synthesis and evaluation of anticonvulsant activity of N-(2,5-dimethylphenoxy) and N-[(2,3,5-trimethylphenoxy)alkyl]aminoalkanoles.
101. Anna Nowicka, Hanna Liszkiewicz, Wanda P. Nawrocka, Joanna Wietrzyk, Agnieszka Zubiak, Wojciech Kołodziejczyk
Synthesis and antiproliferative activity *in vitro* of new 2-thioxoimidazo[4,5-b]pyridine derivatives.

NATURAL DRUGS

113. Alamgeer, Uzma Mazhar, Muhammad Naveed Mushtaq, Hafeez Ullah Khan, Safirah Maheen, Muhammad Nasir Hayat Malik, Taseer Ahmad, Fouzia Latif, Nazia Tabassum, Abdul Qayyum Khan, Haseeb Ahsan, Wasim Khan, Inrahim Javed, Haider Ali
Evaluation of anti-inflammatory, analgesic and antipyretic activities of *Thymus serpyllum* Linn. in mice.
119. Talent Chipiti, Mohammed Auwal Ibrahim, Neil Anthony Koorbanally, Md. Shahidul Islam
In vitro antioxidant activity and GC-MS analysis of the ethanol and aqueous extracts of *Cissus cornifolia* (Baker) Splanck (Vitaceae) parts.
129. Muhammad Asif, Muhammad Atif, Amin Malik, Shah Abdul Majid, Sabbar Dahham, Sawsan Al Ravi, Zahari Che Dan
Diuretic activity of aqueous extract of *Nigella sativa* in Albino rats.

137. Marina T. Tomovic, Snezana M. Cupara, Marija T. Popovic-Milenkovic, Biljana T. Ljujic, Marina J. Kostic, Slobodan M. Jankovic Antioxidant and anti-inflammatory activity of *Potentilla reptans* L.
147. Emmanuel E. Nyong, Michael A. Odeniyi, Jones O. Moody *In vitro* and *in vivo* antimicrobial evaluation of alkaloidal extracts of *Enantia chlorantha* stem bars and their formulated ointments.
153. Rachel Dorothy Wilson, Md. Shahidul Islam Effects of white mulberry (*Morus alba*) leaf tea investigated in a type 2 diabetes model of rats.

PHARMACEUTICAL TECHNOLOGY

161. Witold Musiał, Jiří Michálek The influence of low process temperature on the hydrodynamic radius of polyNIPAM-co-PEG thermosensitive nanoparticles presumed as drug carriers for bioactive proteins.
171. Ehab I. Taha, Saleh A. Al-Suwayeh, Moustafa M. Tayel, Mohamed M. Badran Fast ultra-fine self-nanoemulsifying drug delivery system for improving *in vitro* gastric dissolution of poor water soluble drug
179. Sofiane Fatmi, Lamine Bournine, Mokrane Iguer-Ouada, Malika Lahiani-Skiba, Fatiha Bouchal, Mohamed Skiba Amorphous solid dispersion studies of camptothecin–cyclodextrin inclusion complexes in PEG 6000.
193. Venkata Srikanth Meka, Shreeni Pillai, Senthil Rajan Dharmalingham, Ravi Sheshala, Adinarayana Gorajana Preparation and *in vitro* characterization of non-effervescent floating drug delivery system for poorly soluble drug, glipizide.

PHARMACOLOGY

205. Monika Rykaczewska-Czerwińska, Piotr Oleś, Michał Oleś, Mariola Kuczer, Danuta Konopińska, Andrzej Plech Effect of alloferon 1 on central nervous system in rats.

SHORT COMMUNICATION

213. Olivera Z. Milovanovic, Jasmina R. Milovanovic, Aleksandar Djukic, Milovan Matovic, Aleksandra Tomic Lucic, Nenad Glumbic, Ana M. Radovanovic, Slobodan M. Jankovic Variation in vitamin D plasma levels according to study load of biomedical students.

REVIEW

DERMATOLOGICAL AND COSMECEUTICAL BENEFITS
OF *GLYCINE MAX* (SOYBEAN) AND ITS ACTIVE COMPONENTSMUHAMMAD KHURRAM WAQAS¹, NAVEED AKHTAR¹, REHAN MUSTAFA¹,
MUHAMMAD JAMSHAD², HAJI MUHAMMAD SHOAB KHAN¹ and GHULAM MURTAZA^{3*}¹Department of Pharmacy, Faculty of Pharmacy and Alternative Medicines,
The Islamia University of Bahawalpur, Bahawalpur, Pakistan²Department of Pharmacy, University of Central Punjab, Lahore, Pakistan³Department of Pharmaceutical Sciences, COMSATS Institute of Information Technology,
Abbottabad, 22060 Pakistan

Abstract: *Glycine max*, known as the soybean or soya bean, is a species of legume native to East Asia. Soya beans contain many functional components including phenolic acids, flavonoids, isoflavonoids (quercetin, genistein, and daidzein), small proteins (Bowman-Birk inhibitor, soybean trypsin inhibitor) tannins, and proanthocyanidins. Soybean seeds extract and fresh soymilk fractions have been reported to possess the cosmeceutical and dermatological benefits such as anti-inflammatory, collagen stimulating effect, potent anti-oxidant scavenging peroxy radicals, skin lightening effect and protection against UV radiation. Thus, present review attempts to give a short overview on dermatological and cosmeceutical studies of soybean and its bioactive compounds.

Keywords: *Glycine max*, soybean, isoflavonoids, genistein, cosmeceutical, dermatological

The soybean (*Glycine max*) is an annual legume of the Fabaceae family. It is indigenous to East Asia and China but now is extensively cultivated in many temperate regions of the world (1). Traditionally, soybean has been an excellent source of proteins (2). Despite of proteins it is rich in dietary fiber and a variety of micronutrients and phytochemicals. Soybeans are unique among the legumes because they are a concentrated source of isoflavones (3). Soybean seeds extract and fresh soy milk is used in cosmetic dermatology for the improvement of skin tone, pigmentation and other photo-aging attributes (4). In this review, several cosmeceutical and dermatological studies of *Glycine max* commonly known as soybean and its bioactive compounds are described.

Active constituents

Phenolic acids

The term phenolics comprises of approximately 8000 naturally occurring compounds, all of which possess one common structural feature, a phenol (an aromatic ring bearing at least one hydroxyl sub-

stituent). Phenolics are plant secondary metabolites and they are commonly found in herbs and fruits, vegetables, grains, tea, coffee beans, propolis, and red wine as a color and flavoring agents and are an integral part of human diet (5). Naturally occurring phenolic acids contain two distinguishing constitutive carbon frameworks: the hydroxycinnamic and hydroxybenzoic acid structures. The phenolics, particularly polyphenols exhibit a wide variety of beneficial biological activities in mammals, including antiviral, antibacterial, immune-stimulating, antiallergic, antihypertensive, antiischemic, antiarrhythmic, antithrombotic, hypocholesterolemic, antilipo-peroxidant, hepatoprotective, anti-inflammatory, and anti-carcinogenic actions. They are powerful antioxidants *in vitro* (6). In the past decade, the antioxidant activity of herbal phenolics, namely phenolic acids and flavonoids has been given much attention. Therefore, the phenolics may be beneficial in preventing UV-induced oxygen free radical generation and lipid peroxidation, i.e., events involved in pathological states such as photoaging and skin cancer (7). The concentration of phenolic com-

* Corresponding author: e-mail: gmdogar356@gmail.com; mobile: 0092-314-2082826; fax: 0092-922-383441

pounds in the mature seeds is in ranges from 1–3 mg/g (8). Defatted soy flakes contained 4 mg of total phenolics/g of sample, which was distributed as about 28% of phenolic acids. The major phenolic acids present in soy bean are syringic, ferulic, and sinapic acids (9) (Fig. 1).

Flavonoids

Flavonoids is a collective term of polyphenolic compounds and ubiquitously exist in all parts of plants (10). They are categorized into flavonols, flavones, flavanones, isoflavones, catechins, anthocyanidins and chalcones in the light of chemical structures (11, 12). Isoflavones are a subclass of a large group called flavonoids. Because of its estrogenic activity, are also known as phytoestrogens (13). In soybean there are basically three types of isoflavones that are normally present in four different isoforms: glucosides (daidzingenistin and glycytin); acetylglucosides (acetyl daidzin, acetylgenistin and acetylglycytin) malonylglucosides (malonyl daidzin, malonylgenistin and malonylglycytin) and structure unconjugated aglycone (daidzein, genistein and glycitein) (14). Isoflavones are found in highest amounts in soybeans and soy foods, although they are also present in other beans and legumes. Soy foods generally contain 1.2–3.3 mg

isoflavones/g dry weight, with the precise amount depending on numerous factors, including the type of soy food as well as soybean variety, harvest year and geographical location (15) (Fig. 2).

Soy proteins

Protein is the major constituent of the soybean (30 to 50 g/100 g) (16). It contributes to the supply of essential amino acids and nitrogen to human and animals (17). The major components of soy proteins are storage proteins known as β -conglycinin (7S) and glycinin (11S), which represent 65% to 80% of total seed proteins. Whole soybean contains about 7–9% of protease inhibitors that are in the grain cotyledon (18–20). The proteins STI, a Kunitz-type trypsin inhibitor or soybean trypsin inhibitor and BBI, the Bowman-Birk protease inhibitor (21, 22) were first isolated from soybeans in the early 1940's. STI (21) is a protein of 181 amino acid residues and a tertiary structure which is dependent on two disulfide bridges (23). BBI is an 8 kDa protein with 81 amino acid residues and seven disulfide bonds that is a weak trypsin inhibitor and a strong chymotrypsin inhibitor (24). STI is heat labile (23), while BBI has a stable conformation even after its disulfide bonds are broken by heating or treatment with acid and pepsin (21). STI and BBI are found

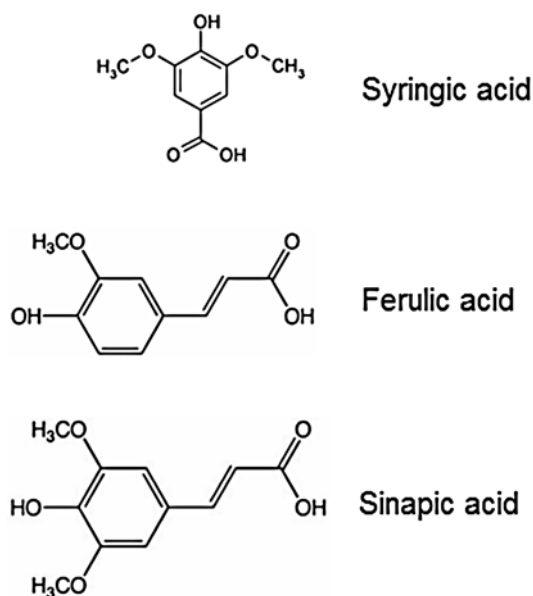


Figure 1. Chemical structure of major phenolic acids present in soy bean

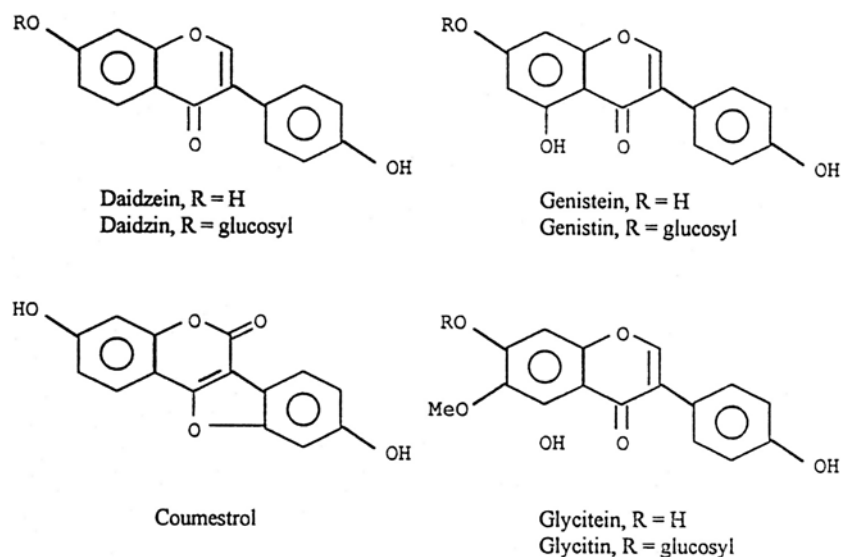


Figure 2. Chemical structures of soy isoflavones

only in the bean, and not in any other part of the soy plant (21).

Dermatological and cosmeceutical benefits

Anti-inflammatory effects

Isoflavones, a major class of flavonoids mainly present in soybean, has been shown to possess antioxidant activity, reduce risk of cardiovascular disease, and inhibit cancer cell growth (25–28). Several recent studies also demonstrated that isoflavones may exhibit anti-inflammatory activity (29–31). Inflammation, a primary component of innate immunity, can result in killing or degradation of outer microorganisms by neutrophils in blood and macrophage in tissues through combination with polysaccharides on the microorganism's surface (32). Pus can thus be formed after the death of neutrophils that have entered damaged tissues because of infection. Meanwhile, macrophages can secrete several soluble proteins called cytokines, including interleukin-1 (IL-1), interleukin-6 (IL-6), interleukin-8 (IL-8), interleukin-12 (IL-12), and tumor necrosis factor receptor (TNF-R). Among these cytokines, IL-1, IL-6, and TNF-R have attracted more attention as they can be localized to the infected tissue, manifested systemically throughout the body, and cause vasodilation as well as inflammation symptoms such as redness, swelling, heat and pain (32). Other cytokines, such as IL-8 and IL-12,

were seldom investigated. Both IL-1 and TNF-R have been reported to increase expression of intercellular adhesion molecule-1 (ICAM-1) and vascular cell adhesion molecule-1 (VCAM-1), resulting in adhesion of neutrophils, monocytes and macrophages to vessel wall and subsequent inflammation of infected tissues (32). In addition to cytokines, macrophages can secrete inflammation mediators such as prostaglandin E₂ (PGE₂) and nitric oxide (NO), causing sepsis, septic shock and systemic inflammatory response syndrome (33). Chronic inflammation has been linked to numerous skin diseases and conditions, including skin aging (34) and many skin care products, therefore, contain anti-inflammatory agents. Additionally, inflammation has been linked to epithelial skin-tumors, and anti-inflammatory drugs are being studied for the prevention and treatment of non-melanoma skin cancers (35). Cyclooxygenase-2 (COX-2), the main UV-responsive COX isoform in human skin, is involved in UV-induced skin inflammation and carcinogenesis (36). UV-induced COX-2 expression plays a major role in UV-induced inflammation, edema, keratinocytes proliferation and epidermal hyperplasia, as well as in the generation of oxidative DNA damage. Repeated exposure to UV leads to chronic up-regulation of COX-2 expression and chronic inflammation, contributing both to accelerated skin aging and to an increased risk of skin can-

cer. The induction of COX-2 expression by UV is higher in aged human skin as compared to young human skin, and aged human skin produces higher amounts of prostaglandin E₂ (PGE₂, the product of the COX-2 pathway) relative to young skin (9). Aging of the skin may increase the susceptibility for developing both photo-aging and carcinogenic processes. Oral and topical COX-2 inhibitors have chemopreventive activity against chemically- and UV-induced skin cancer in numerous animal models (36). The topical applications of soy isoflavones to mouse skin before UVB exposure reduced the expression of COX-2 (37). Several studies dealing with the inhibition of inflammation by isoflavones are available in the literature (38). Several papers also suggested that genistein could activate peroxisomal proliferator-activated receptor- γ (PPAR- γ) and in turn, retard adhesion of monocytes to human vascular endothelial cells which may be associated with the A ring in the isoflavone structure (39, 40). It is found that with an isoflavone-containing diet intra-peritoneal lipopolysaccharide (LPS) injection in mice led to a decrease in the liver antioxidant glutathione level and prevention of the inflammation-associated induction of metallothionein in the intestine (40). In a later study, it was demonstrated that dietary isoflavones have beneficial effects on C-reactive protein (CRP) concentrations, but not on other inflammatory biomarkers of cardiovascular disease risk in postmenopausal women, and may improve VCAM-1 response in an ER gene polymorphic subgroup. Similarly, the CRP level could be raised in the blood of patients with end-stage renal disease, but both IL-6 and TNF-R were unaffected (41). In a recent study, it is further pointed out that isoflavones extracted from *Puerariathum bergiana* could suppress LPS-induced release of NO and TNF-R in primary cultured microglia and cell lines (42). Kao et al. reported the use of soybean cake as raw material for processing into powder and to evaluate the anti-inflammatory activity. Eleven treatments, including powders of malonyl-glucoside, glucoside, acetylglucoside, aglycone, as well as genistein standard, γ -PGA, control, normal, and PDTC (ammonium pyrrolidine dithiocarbamate), were used for evaluation. A total of 77 mice were provided daily with tube feeding for 4 weeks at a dose of 0.3 mL of aqueous solution from each treatment, and inflammation was induced with intraperitoneal injection of 1 mg/kg of body weight lipopolysaccharides (LPS). Results showed that all of the isoflavone powders and genistein standard were effective in inhibiting LPS-induced inflammation, lowering leukocyte number in mice blood and

reducing production of IL-1, IL-6, NO, and PGE₂ in both peritoneal exudates, cell supernatant and peritoneal exudate fluid (43).

Skin lightening effects

Skin pigmentary abnormalities are seen as esthetically unfavorable and have led to the development of cosmetic and therapeutic treatment modalities of varying efficacy. Hence, several putative depigmenting agents aimed at modulating skin pigmentation are currently being researched or sold in commercially available products (44). Melanocytes, the pigment producing cells of the follicular and interfollicular epidermis, produce a specialized lysosomal related organelle termed the melanosome. Within the melanosome, biopolymers of the pigment melanin are synthesized to give hair and skin, as well as other tissue, its color. This melanin synthesis involves a bipartite process in which structural proteins are exported from the endoplasmic reticulum and fuse with melanosome-specific regulatory glycoproteins released in coated vesicles from the Golgi apparatus. Melanin synthesis ensues subsequent to the sorting and trafficking of these proteins to the melanosome (45). Each melanocyte resides in the basal epithelial layer and, by virtue of its dendrites, interacts with approximately 36 keratinocytes to transfer melanosomes and protect the skin from photo-induced carcinogenesis. Furthermore, the amount and type of melanin produced and transferred to the keratinocytes with subsequent incorporation, aggregation and degradation influences skin pigmentation (46). Hyperpigmentary disorders of the skin such as melasma, age spots or solar lentigo can result from the overproduction and accumulation of melanin (47). The protease-activated receptor 2 (PAR-2) (48–50) is a seven transmembrane G-protein-coupled receptor that is activated by a serine-protease cleavage, creating a tethered ligand. Trypsin and mast cell tryptase are the only known natural activators of PAR-2 (51, 52). PAR-2 is expressed in keratinocytes (53) but not in melanocytes (47) and is involved in the regulation of pigmentation (54–56). The pigmentary effect of PAR-2 modulation by serine protease inhibitors is possible only when keratinocyte-melanocyte contact is established (57).

Melanocytes alone do not respond to PAR-2 modulating agents with pigmentary changes (54). PAR-2 activation was shown to increase keratinocyte phagocytosis (57) resulting in increased melanosome ingestion and transfer (55) even in the absence of melanocytes. Serine protease inhibitors that interfere with PAR-2 activation were shown to

reduce melanosome transfer and ingestion by keratinocytes, resulting in depigmentation both *in vitro* and *in vivo* (54, 55).

For medical and cosmetic reasons, it is often desired to alter skin color. Currently available topical agents used to treat hyperpigmentation include tyrosinase inhibitors, retinoids, hydroquinones, and melanocyte-cytotoxic agents. Unfortunately, the results of these treatments are sometimes disappointing (58) and there is a need for more effective, safer, and less irritating depigmenting therapies. Moreover, a move towards natural therapies created a demand for a natural, safe, and efficacious depigmenting treatment.

Soybean seeds have been used in Asia for centuries as a dietary source of protein (57). Soymilk and the soymilk-derived proteins STI and BBI inhibit PAR-2 activation and thus induce skin depigmentation by reducing the phagocytosis of melanosomes by keratinocytes, thus reducing melanin transfer. Such agents may serve as an alternative, natural treatment for hyperpigmentation (57). The depigmenting activity of these agents, as well as their ability to prevent UV-induced pigmentation, was demonstrated both *in vitro* and *in vivo* (57). Importantly, the non-denatured soybean extracts were superior to either STI or BBI alone in their depigmenting effect, even though the concentrations of STI and BBI within these extracts were much lower than when tested individually (57).

Soybean trypsin and Bowman-Birk inhibitors inhibit activation of the protease-activated receptor-2 (PAR-2) and therefore, inhibit the melanosome transfer. PAR-2 is expressed in keratinocytes but not in melanocytes, and is involved in the regulation of pigmentation (58). PAR-2 is a phagocytic receptor and inhibition of PAR-2 results in impaired melanosomes transfer from the melanocytes to the keratinocytes. The inhibition of PAR-2 by serine protease inhibitors results in reduced pigment deposition and skin color lightening (59). Non-denatured soybean extracts contain two serine protease inhibitory proteins, i.e., soybean trypsin inhibitor and Bowman-Birk inhibitor. Soybean trypsin inhibitor, Bowman-Birk inhibitor, and non-denatured soybean extracts inhibit PAR-2 activation, resulting in skin depigmentation *in vitro*, *in vivo* and in human skins transplanted onto immune-compromised mice (60). The first documentation of a clinical skin lightening activity by the non-denatured soybeans extracts was published in 2000 (61), with a follow-up study in 2002 (62). A study of skin color suggests that these extracts are excellent choice for the treatment of post-inflammatory hyperpigmenta-

tion and melasma (63). In a recent review, these non-denatured soybean extracts were discussed as topical alternatives to hydroquinone (64, 65).

Elastin and collagen stimulating effects

Elastin fiber production is reduced with aging (66, 67). The age-induced decline in skin elasticity results from slower tissue regeneration, from lower elastin synthesis levels and from the increased production and secretion of elastases. UV exposure further decreases the functionality of the elastic fiber network, as excessive elastin production and abnormal cross-linking create elastotic material ("solar elastosis") with reduced elastic capacity (67, 68). Preventing or reversing skin ageing includes the use of sunscreens and sun avoidance behavior, the use of anti-oxidants, and the use of agents like retinoids, which inhibit collagenases and promote collagen production (69). Only a few agents are available to directly enhance the balanced synthesis and assembly of the elastic fiber network. The inhibition of fibroblast-derived elastases following chronic UVB irradiation was found to protect the dermal elastic network of the skin from fragmentation and to reduce wrinkle formation in rodents (70, 71).

Searching for botanical extracts for anti-aging skin care use, the non-denatured soybean extracts were found to have elastase-inhibitory activities (72). In addition, non-denatured soybean extracts were found to induce the synthesis of collagen and elastin, and to promote the correct assembly of new elastin fibers, providing a complete protection and restoration to the dermal extracellular matrix (73). *In vitro* studies using both purified elastases and cultured fibroblasts demonstrated that non-denatured soybean extracts could affect the extracellular matrix. The enzymatic activity of several elastases was inhibited by these extracts, and, to a lesser extent, by STI or BBI, while soy isoflavones did not show any elastase-inhibitory activity (72). The non-denatured soybean extracts also protected elastic fibers produced by cultured fibroblasts from degradation by exogenously-added elastases (72). Additionally, these extracts exhibited elastin-enhancement activities. A dose-dependent induction of expression of the elastin gene was documented using an elastin promoter-luciferase reporter gene, and was confirmed by mRNA analysis of treated fibroblasts. The synthesis of new tropoelastin monomers, as well as of elastin-accessory proteins, and the assembly of new elastin fibers, was documented by histological staining (72). The elastin-enhancing activity of the non-denatured soybean extracts was confirmed *in vivo*. Histological analysis

of mice and swine skins topically treated with non-denatured soybean extracts showed a significant increase in the elastic fibers network, with an accompanied increase in elastin mRNA and in desmosine content (72). When human skins, transplanted onto immuno-deficient mice, were topically treated with these extracts, an increase was documented in the expression of elastin, elastin-accessory proteins, and collagen (72). Human skin explants treated *ex-vivo* with non-denatured soybean extracts and analyzed by histological staining and immune histochemistry showed an increase in elastin, fibrillin-1 and collagen production (73). These data suggest that non-denatured soybean extracts not only protect extracellular matrix from degradation, they also induce collagen and elastin synthesis, and increase the total amount of stable, cross-linked elastin fibers.

Protection against UV radiation

Chronic exposure of human skin to UV radiation is known to damage the structure and function of the skin. These changes are referred to collectively as photo-aging, which is characterized by wrinkles, laxity, roughness and irregular pigmentation (74). Photo-aged skin displays prominent alterations in the cellular component and extracellular matrix of the connective tissues such as an accumulation of disorganized elastin fibers (elastosis), a marked increase in glycosaminoglycans (GAGs), and a loss of interstitial collagens (75). The unifying pathogenic agents responsible for these changes are UV-induced reactive oxygen species (ROS) that deplete and damage the non-enzymatic and enzymatic antioxidant defense systems of the skin, leading to oxidative damage of the cellular and non-cellular components and ultimately skin cancer, immune-suppression and premature skin aging (76). ROS are believed to activate the cytoplasmic signal transduction pathways in the resident fibroblasts, which are related to growth, differentiation, senescence and connective tissue degradation, as well as causing permanent genetic changes (77). Considering that UV induces oxidative stress-mediated adverse effects in the skin, the regular intake of antioxidants and antioxidant nutrients as well as an antioxidant topical treatment is suggested to be a useful way to reduce the harmful effects of UV radiation (78).

In recent years, isoflavones have attracted increased attention owing to their health-related beneficial aspects. In addition to its diphenolic structure-based estrogen-like effect, isoflavones are associated with a broad range of biological activities that include antioxidant properties and inhibitory

effects on the several enzymes of the estrogen receptor-independent signal pathways (79). Genistein, the primary isoflavone from soy products, is known to enhance the antioxidant enzyme activities such as superoxide dismutase, catalase and glutathione reductase in various mouse organs (80), and it has also been shown to inhibit tyrosine kinase and topoisomerase (81, 82). Therefore, an investigation into the protective effects of dietary soy isoflavones on UV-damaged skin in the nutritional aspect is warranted. Also several experimental studies have suggested that the topical treatment of soybean isoflavone genistein inhibits UVB-induced skin tumorigenesis in a hairless mice model (83).

Potent anti-oxidant scavenging peroxy radicals

Intracellular and extracellular oxidative stress initiated by ROS promotes skin-aging, which is characterized by wrinkles and atypical pigmentation. Because UV enhances ROS generation in cells, skin aging is usually discussed in relation to UV exposure. The use of antioxidants is an effective approach to prevent symptoms related to photo-induced aging of the skin (84). Several bioactive compounds, including phenolics such as phenolic acids, flavonoids and isoflavonoids have been identified in soybeans. Recent interest in these substances has been stimulated by the potential health benefits arising from the antioxidant activity of these phenolic compounds (85). Genistein, the major component of soybean isoflavones, has been demonstrated to inhibit ultraviolet-B (UVB)-induced skin tumorigenesis in hairless mice. The antioxidant properties of genistein may explain the mechanisms of its anti-photocarcinogenic action because through either direct quenching of reactive oxygen species or indirect anti-inflammatory effects, genistein was found to substantially inhibit a series of oxidative events elicited by UVB irradiation, including hydrogen peroxide production, lipid peroxidation, and 8-hydroxy-2-deoxyguanosine formation (83).

Undesired hair growth inhibitory effect

Unlike other mammals, humans no longer use their hair for environmental protection, but keep or remove their hair for social and cosmetic purposes. Many procedures are used to remove unwanted hair, from simple home treatments like shaving, to laser and light therapies. These methods differ in the duration of hair elimination after removal, their price range, their pain and discomfort levels and their possible undesired effects (86). Shaving, the most popular hair-removal method, requires daily treatments, may result

in nicks and cuts, may increase the risk of infection, may leave a perception of an increased rate of hair growth, and may leave undesirable stubble. An alternative to at-home hair removal is hair dyeing or bleaching, used to reduce hair visibility in particular body areas. However, such methods are less preferred as the emerging portions of the hair shafts are always darker than the already treated parts. An alternative to these methods is desired; particularly a method that would reduce undesired hair growth, with a safe and simple at home procedure. As the biological activities of the non denatured soybean extracts were further explored, they were found to delay hair growth, resulting in smaller and thinner hair shafts (87). The use of a skin care product containing these extracts, therefore, would reduce the visibility of undesired hair growth. Topical daily treatments with STI or BBI visually delayed hair growth and reduced the length of the hair shafts of treated mice, with reduced hair follicles size observed histologically. Non-denatured soybean extracts (containing STI, BBI and isoflavones) were superior to either STI or BBI alone in this inhibitory activity. Non-denatured soybean extracts led to delayed and reduced hair growth, and hairs were visibly thinner, more “directionally organized”, and smoother to touch, relative to untreated controls (87). A statistically significant effect on hair follicle dimensions was observed, with hair shaft diameter reduced by an average of 42%, and hair bulb diameter reduced by an average of 23.8% (73). Additionally, the depigmenting effect of STI and BBI led to lighter colored hair shafts, which could potentially contribute to the reduced visibility of undesired hair growth. Heat-denatured soybean extract, or commercially available pasteurized soymilk, had no effect on hair growth or hair appearance (88, 89) further supporting the involvement of intact STI and BBI in the hair growth inhibitory effect.

CONCLUSION

In summary, *Glycine max* and its bioactive components have several dermatological and cosmeceutical effects such as anti-inflammatory, anti-oxidative, collagen stimulating, skin lightening, protection against UV radiation and removal of undesired hair growth. It seems that soybean seed extract and its active components such as phenolic acids, flavonoids, isoflavonoids (quercetin, genistein, and daidzein) and proteins (Bowman-Birk inhibitor and soybean trypsin inhibitor) are safe and effective in improving numerous skin care parameters. Thus, the use of soybean extracts provides multiple dermatological and cosmeceutical benefits, ranging from protection and restoration, to esthetic benefits. It is

even more apparent that there is a great deal of work still left to be done.

REFERENCES

1. Muller L.: J. C. Instituto de Tecnologia de Alimentos, Campinas 65, 11 (1981).
2. Henkel J.: Soy: Question About Other Components. FDA Consumer (Food and Drug Administration) 34, 18 (2000).
3. Messina M.J.: Am. J. Clin. Nutr. 70, 439S (1999).
4. Wallo W., Nebus J., Leyden J.J.: J. Drugs Dermatol. 6, 917 (2007).
5. King A., Young G.: J. Am. Diet. Assoc. 99, 2 (1999).
6. Robbins R.J.: J. Agric. Food Chem. 5, 10 (2003).
7. Rechner A.R., Spencer J.P., Kuhnle G., Hahn U., Rice-Evans C.A.: Free Radic. Biol. Med. 30, 11 (2001).
8. Mujic I., Sertovic E., Jokic S., Saric Z., Alibabic V., Vidovic S., Zivkovic N.: J. Food Sci. Technol. 3, 16 (2011).
9. Seo A., Morr C.V.: J. Agric. Food Chem. 32, 530 (1984).
10. Nijveldt R.J., van Nood E., van Leeuwen O.: Am. J. Clin. Nutr. 74, 418 (2001).
11. Namiki M.: Crit. Rev. Food Sci. Nutr. 29, 273 (1990).
12. Heim K.E., Tagliaferro A.R., Bobilya D.J.: J. Nutr. Biochem. 13, 572 (2002).
13. Cederroth C.R., Nef S.: Mol. Cell Endocrinol. 304, 30 (2009).
14. Kao T.H., Wu W.M., Hung C.F., Wu W.B., Chen B.H.: J. Agric. Food Chem. 55, 11068 (2007).
15. Wang H.J., Murphy P.A.: J. Agric. Food Chem. 42, 1666 (1994).
16. Carvalho A.W., Silva C.O., Dantas M.I.S., Natal D.I.G., Ribeiro S.M.R. et al.: Arch. Latinoam. Nutr. (In press).
17. Liu K.: Soybeans: chemistry, technology, and utilization. Chapman & Hall, New York 1997.
18. Brandon D.L., Friedman M.: J. Agric. Food Chem. 50, 6635 (2002).
19. Esteves EA., Martino H.S.D., Oliveira F.C.E., Bressan J., Costa N.M.B.: Food Chem. 122, 238 (2010).
20. Penha L.A.O., Fonseca I.C.B., Mandarino J.M., Benassi V.T.: B. Cent. Pesqui. Proc. A. 25, 91 (2007).
21. Birk Y.: Int. J. Pept. Protein Res. 25, 113 (1985).

22. Kennedy A.R.: *Am. J. Clin. Nutr.* 68, 1406S (1998).
23. Song H.K., Suh S.W.: *J. Mol. Biol.* 275, 347 (1998).
24. Billings P.C., Habres J.M.: *Proc. Natl. Acad. Sci. USA* 89, 3120 (1992).
25. Chang K.L., Kung M.L., Chow N.H. Su S.J.: *Biochem. Pharmacol.* 67, 717 (2004).
26. Hall W.L., Vafeiadou K., Hallund J., Bugel S., Koebnick C., Reimann M., Ferrari M. et al.: *Am. J. Clin. Nutr.* 82, 1260 (2005).
27. Kao T.H., Chen B.H.: *J. Agric. Food Chem.* 54, 7544 (2006).
28. Conklin C.M., Bechberger J.F., MacFabe D., Guthrie N., Kurowska E.M., Naus C.C.: *Carcinogenesis* 28, 9 (2007).
29. Chacko B.K., Chandler R.T., D'Alessandro T.L., Mundhekar A., Khoo N.K., Botting N., Barnes S., Patel R.P.: *J. Nutr.* 137, 34 (2007).
30. Fanti P., Asmis R., Stephenson T.J., Sawaya B.P., Franke A.A.: *Nephrol. Dial. Transplant.* 21, 2239 (2006).
31. Park J.S., Woo M.S., Kim D.H., Hyun J.W., Kim W.K., Lee J.C., Kim H.S.: *J. Pharmacol. Exp. Ther.* 320, 1237 (2007).
32. Parham P.: *The Immune System.* Garland Publishing, New York 2000.
33. Guha M., Mackman N.: *Cell Signal.* 13, 85 (2001).
34. Thornfeldt C.R.: *J. Cosmet. Dermatol.* 7, 78 (2008).
35. Mueller M.M.: *Eur. J. Cancer.* 42, 735 (2006).
36. Rundhaug J.E., Mikulec C., Pavone A., Fischer S.M.: *Mol. Carcinog.* 46, 692 (2007).
37. Chiu T.M., Huang C.C., Lin T.J., Fang J.Y., Wu N.L., Hung C.F.: *J. Ethnopharmacol.* 29, 108 (2009).
38. Yankep E., Njamen D., Fotsing M.T., Fomum Z.T., Mbanya J.C., Giner R.M., Recio M.C. et al.: *J. Nat. Prod.* 66, 1288 (2003).
39. Chacko B.K., Chandler R.T., Mundhekar A., Khoo N.K., H Pruitt H.M., Kocik D.F., Parks D. et al.: *Am. J. Physiol. Heart Circ. Physiol.* 289, H908 (2005).
40. Paradkar P.N., Blum P.S., Berhow M.A., Baumann H., Kuo S.M.: *Cancer Lett.* 215, 21 (2004).
41. Hall W.L., Vafeiadou K., Hallund J., Bügel S., Koebnick C., Reimann M., Ferrari M. et al.: *Am. J. Clin. Nutr.* 82, 6 (2005).
42. Park J.-S., Woo M.-S., Kim D.-H., Hyun J.-W., Kim W.-K., Lee J.-C., Kim H.-S.: *J. Pharmacol. Exp. Ther.* 320, 3 (2007).
43. Kao T., Wu W., Hung C., Wu W., Chen B.: *J. Agric. Food Chem.* 55, 26 (2007).
44. Ebanks J.P., Wickett R.R., Boissy R.E.: *Int. J. Mol. Sci.* 10, 4066 (2009).
45. Turner W.A., Taylor J.D., Tchen T.T.: *J. Ultrastruct. Res.* 51, 16 (1975).
46. Boissy R.E.: *Exp. Dermatol.* 12, 5 (2003).
47. Virador V., Matsunaga N., Matsunaga J., Valencia J., Oldham R.J., Kameyama K., Peck G.L. et al.: *Pigment Cell Res.* 14, 289 (2001).
48. Nystedt S., Emilsson K., Wahlestedt C., Sundelin J.: *Proc. Natl. Acad. Sci. USA* 91, 9208 (1994).
49. Nystedt S., Emilsson K., Larsson A.K.: *Eur. J. Biochem.* 232, 84 (1995a).
50. Nystedt S., Larsson A.K., Aberg H., Sundelin J.: *J. Biol. Chem.* 270, 5950 (1995).
51. Dery O., Corvera C.U., Steinhoff M., Bunnett N.W.: *Proteinase-activated receptors: novel mechanisms of signaling by serine proteases.* *Am. J. Physiol.* 247, C1429 (1998).
52. Dery O., Bunnett N.W.: *Biochem. Soc. Trans.* 27, 246 (2010).
53. Marthinuss J., Andrade-Gordon P., Seiberg M.: *Cell Grow. Differ.* 6, 807 (1995).
54. Seiberg M., Paine C., Sharlow E., Costanzo M.: *Exp. Cell Res.* 254, 25 (2000).
55. Seiberg M., Paine C., Sharlow E., Andrade-Gordon P., Costanzo M., Eisinger M., Shapiro S.: *J. Invest. Dermatol.* 115, 162 (2000).
56. Sharlow E.R., Paine C., Babiarz L., Eisinger M., Shapiro S.S., Seiberg M.: *J. Cell Sci.* 113, 3093 (2000).
57. Paine C., Sharlow E., Liebel F., Eisinger M., Shapiro S., Seiberg M.: *J. Invest. Dermatol.* 116, 587 (2001).
58. Paine C., Sharlow E., Liebel F., Eisinger M., Shapiro S., Seiberg M.: *J. Invest. Dermatol.* 116, 4 (2001).
59. Sharlow E., Paine C., Babiarz L., Eisinger M., Shapiro S., Seiberg M.: *J. Cell. Sci.* 113, 17 (2000).
60. Zhu W., Gao J.: *J. Invest. Dermatol. Symp. Proc.* 13, 20 (2008).
61. Hermanns J., Petit L., Martalo O., Pierard-Franchimont C., Cauwenbergh G., Pierard G.: *Dermatology* 201, 118 (2000).
62. Hermanns J.-F., Petit L., Piérard-Franchimont C., Paquet P., Piérard G.: *Dermatology* 204, 281 (2002).
63. Baumann L., Rodriguez D., Taylor S.C., Wu J.: *Cutis* 78 (Suppl. 6), 2 (2006).
64. Draelos Z.D.: *Dermatol. Ther.* 20,5(2007)
65. Jimbow K., Jimbow M.: *Chemical, pharmacologic and physical agents causing hypomelanoses.* in *The Pigmentary System: Physiology and Pathophysiology.* Nordlund J.J., Boissy

- R.E., Hearing V.J., King R.A., Ortonne J.P. Eds., Oxford University Press 1998.
66. Uitto J.: *Dermatol. Clin.* 4, 433 (1986).
 67. Uitto J.: *J. Drugs Dermatol.* 7, 12 (2008).
 68. Pasquali-Ronchetti I., Baccarani-Contri M.: *Microsc. Res. Tech.* 38, 428 (1997).
 69. Paine C., Sharlow E., Liebel F., Eisinger M., Shapiro S., Seiberg M.: *J. Invest. Dermatol.* 116, 587 (2001).
 70. Bailly C., Dreze S., Asselineau D., Nusgens B., Lapiere CM., Darmon M.: *J. Invest. Dermatol.* 94, 47 (1990).
 71. Tsukahara K., Takema Y., Moriwaki S., Tsuji N., Suzuki Y., Fujimura T., Imokawa G.: *J. Invest. Dermatol.* 117, 671 (2001).
 72. Tsukahara K., Moriwaki S., Fujimura T., Takema Y.: *Biol. Pharm. Bull.* 24, 998 (2001).
 73. Zhao R., Bruning E., Rossetti D., Starcher B., Seiberg M., Iotsova-Stone V.: *Exp. Dermatol.* 18, 883 (2009).
 74. Seiberg M.: *Non-denatured Soybean Extracts. in Skin Care: Multiple Anti-Aging Effects, Soybean – Biochemistry, Chemistry and Physiology.* Tzi-Bun Ng Ed., InTech, 2011.
 75. Scharffetter-Kochanek K., Brenneisen P., Wenk J., Herrmann G., Ma W., Kuhr L. et al.: *Exp. Gerontol.* 35, 307 (2000).
 76. Kligman L.H., Akin F.J., Kligman A M.: *J. Invest. Dermatol.* 84, 272 (1985).
 77. Miyachi Y.: *J. Dermatol. Sci.* 9, 79 (1995).
 78. Rittie L., Fisher G.J.: *Ageing Res.* 1, 705 (2002).
 79. Tham D.M., Gardner C.D., Haskell W.L.: *J. Clin. Endocrinol. Metab.* 83, 2223 (1998).
 80. Kurzer M.S., Xu X.: *Annu. Rev. Nutr.* 17, 353 (1997).
 81. Cai Q., Wei H.: *Nutr. Cancer.* 25, 1 (1996).
 82. Akiyama T., Ishida J., Nakagawa S., Ogawara H., Watanabe S., Itoh N., Shibuya M., Fukami Y.: *J. Biol. Chem.* 262, 5592 (1987).
 83. Markovits J., Linassier C., Fosse P., Couprie J., Pierre J., Jacquemin-Sablon A., Saucier J.M., Le Pecq J.B.: *Cancer Res.* 49, 5111 (1989).
 84. Wei H., Bowen R., Zhang X., Lebwohl M.: *Carcinogenesis* 19, 1509 (1998).
 85. Masaki H.: *J. Dermatol. Sci.* 58, 85 (2010).
 86. McCue P., Shetty K.: *Crit. Rev. Food Sci. Nutr.* 44, 361 (2004).
 87. Olsen E.A.: *J. Am. Acad. Dermatol.* 40, 143 (1999).
 88. Seiberg M., Liu J.C., Babiarz L., Sharlow E., Shapiro S.: *Exp. Dermatol.* 10, 405 (2001).
 89. Georgetti S.R., Casagrande R., Vicentini F.T., Baracat M.M., Verri W.A. Jr., Fonseca M.J.: *Biomed. Res. Int.* 2013, 340626 (2013).

Received: 6. 09. 2013

THE ROLE OF PROSTANOIDS IN THE URINARY BLADDER FUNCTION AND A POTENTIAL USE OF PROSTANOID-TARGETING PHARMACOLOGICAL AGENTS IN BLADDER OVERACTIVITY TREATMENT

ŁUKASZ DOBREK and PIOTR J. THOR

Department of Pathophysiology, Jagiellonian University Medical College,
Czysta 18, PL 31-121 Kraków, Poland

Abstract: Overactive bladder (OAB) is a syndrome involving urinary urgency with accompanying increased daytime urinary frequency and nocturia, with or without urgency urinary incontinence, in the absence of an urinary tract infection or other obvious pathology. The detailed OAB pathophysiology remains unclear. There is evidence that OAB pathogenesis also includes abnormal bladder paracrine activity, associated with release of local prostanoids. Those agents contribute to disturbances of peripheral neuronal bladder control resulting in detrusor instability. Thus, pharmacological agents abolishing prostanoid-induced bladder overactivity seem to be a potential, future OAB therapeutical option. This paper shortly describes the rationale for nonsteroidal anti-inflammatory drugs (NSAIDs) and EP-1 receptor antagonists administration in future OAB pharmacotherapy.

Keywords: overactive bladder, prostanoids, cyclooxygenase inhibitors, nonsteroidal anti-inflammatory drugs (NSAIDs), prostaglandin receptor antagonists

Abbreviations: AA – 5,8,11,14-eicosatetraenoic acid, COX – cyclooxygenase, DGLA – 8,11,14-eicosatrienoic acid, DP – D-prostaglandin receptor, EP – E-prostaglandin receptor, EPA – 5,8,11,14,17-eicosapentaenoic acid, FP – F-prostaglandin receptor, GAG – glycosaminoglycan, IC – interstitial cells, IP – prostacyclin receptor, LT – leukotrienes, NSAID (s) – nonsteroidal anti-inflammatory drug(s), OAB – overactive bladder, PG – prostaglandins, TP – thromboxane receptor, TX – thromboxanes

General introduction

Overactive bladder (OAB) is a complex syndrome defined by the International Continence Society (ICS) as the urinary urgency with accompanying increased daytime urinary frequency and nocturia, with (“wet” OAB) or without (“dry” OAB) urgency urinary incontinence, in the absence of an urinary tract infection or other obvious pathology (1–3). According to that report, urinary urgency is “a complaint of a sudden, compelling desire to pass urine which is difficult to defer”, increased daytime urinary frequency means “complaint that micturition occurs more frequently during waking hours than previously deemed normal”, nocturia is “complaint of interruption of sleep one or more times because of the need to micturate (each void is preceded and followed by sleep), urgency (urinary) incontinence is defined as “complaint of involuntary loss of urine associated with urgency (3).

The key OAB symptom is a sudden and strong desire to void that cannot be postponed – “urgency” and the term replaced “urge” as the “accepted” terminology for the abnormal rather than the normal phenomenon (3). The urgency and increased daily urination observed in OAB patients result from a reduced functional bladder capacity and the frequency is, at least partly, caused by adaptation of the patients to avoid urine leakage by maintaining a relatively low urinary volume inside the bladder (4).

OAB symptoms may also occur in neurological lesions involving central nervous system (stroke, Alzheimer disease, Parkinson one or multiple sclerosis) and the condition is referred to as neurogenic OAB, with a different etiology comparing to idiopathic OAB mentioned in the ICS definition above (4).

In overall estimation, OAB is reported to affect about 16.6% of European population, with the incidence increasing with age – thus being an increasing

* Corresponding author: e-mail: lukaszd@mp.pl

problem in aging societies (5). Despite the clinical importance of OAB, the detailed pathogenesis of this syndrome still remains unclear. In general, an unifying OAB development theory has been proposed, involving two main pathophysiological concepts: the neurogenic and the myogenic one. They have been described in many reviews in this field (6–11), also of our authorship (12). To sum up, disturbances of both central mechanisms and peripheral afferent/efferent bladder innervation contribute to neurogenic background of OAB while bladder smooth muscle and interstitial cells abnormal electrical activity are key factors of myogenic OAB pathophysiological theory. Considering the problem discussed in this paper, paracrine modulation of the peripheral, autonomic bladder neural control through many locally synthesized and released mediators is regarded to be critical.

According to the anatomical description, the urinary bladder is divided into the bladder dome and the base, composed of the trigone, ureterovesical junction, lateral wall of the detrusor along with the anterior bladder wall (4, 13). Cross-sections of that organ reveal three essential separate layers: the urothelium, the suburothelial layer and the detrusor muscle. Moreover, the urothelium surface is covered by a glycosaminoglycan (GAG) external layer, which is most probably responsible for maintenance of an osmotic barrier and constitutes an antibacterial coating (4, 13).

At present, some greater attention is being drawn to the urothelium (uro-epithelium), which is perceived no longer as a mere barrier separating the bladder lumen from its underlying tissues, but also as the sensor with a particular endocrine/paracrine activity. The urothelium consists of three layers: basal cells attached to a basement membrane, intermediate cells and superficial, apical cells referred to as “umbrella cells”, covered by GAG. The suburothelium is richly supplied by blood vessels, nerves and interstitial cells (IC) that are suggested to modulate the activity of the suburothelial afferents. The bladder muscle layer also contains IC cells; however, they are similar to intestinal interstitial cells of Cajal, mediating contractions. Therefore, the bladder IC detrusor cells are thought to play a pacing role (4, 13, 14). The term “lamina propria” has been also implemented to distinguish the bladder wall from the detrusor and all remaining tissues. The bladder lamina propria (urothelium and suburothelium) has been shown to release several substances, acting *via* appropriated receptors in response to various stimuli: bradykinin, purines, adenosine triphosphate (ATP), nitric oxide (NO), neuropeptides (e.g.,

substance P), cytokines and some others. Among them, there are also the – so-called – eicosanoids (involving prostaglandins, prostacyclins, thromboxanes and leukotrienes) that are treated as lipids mediators, being derivatives of 20-carbon unsaturated fatty acids (mostly the arachidonic one) (4, 13).

Prostanoids – a brief general outline

Eicosanoids (also known as icosanoids) are oxygenated derivatives of three different 20-carbon fatty acids. The origin of that term is associated with the Greek name “eikosi” meaning “twenty” (15). They are synthesized from either ω -3 (eicosapentaenoic; EPA – with 5 double bonds) or ω -6 (arachidonic; AA – with 4 double bonds or dihomo- γ -linolenic; DGLA – with 3 double bonds), 20-carbon, unsaturated fatty acids (16).

Current usage limits the term “eicosanoids” to leukotrienes (LT) and three types of prostanoids – prostaglandins (PG), prostacyclins (PGI) and thromboxanes (TX) (15). The further part of this paper will be limited to the description of the role of prostanoids (especially prostaglandins) in bladder physiology and pathophysiology. Prostaglandins contain a 5-membered cyclopentane ring and two side α and ω chains linked to the ring. The thromboxanes have a 6-membered ring (an oxane one), instead of the cyclopentane structure (16). As it has already been mentioned above, prostanoids may be synthesized from DGLA acid (8,11,14-eicosatrienoic acid), AA acid (5,8,11,14-eicosatetraenoic acid) and EPA acid (5,8,11,14,17-eicosapentaenoic acid). However, the second one is the most abundant in mammalian cells, therefore it is the main substrate for eicosanoid synthesis. The arachidonic acid (AA) is released from cell membrane phospholipids in response to various physiological and pathological stimuli by the action of phospholipases and converted into eicosanoids by subsequent synthases. Phospholipase A2 is a membrane-bound enzyme that cleaves AA from membrane phospholipids. The other enzyme that is also able to liberate the AA is phospholipase C. The released arachidonic acid is a substrate for prostanoid synthesis – along the cyclooxygenation pathway; or for leukotriene production – along the lipoxygenation pathway. The lipoxygenase pathway and leukotrienes will be not discussed in this paper. PG production is associated with the activity of PGH₂ synthase and PG endoperoxide synthase. Those enzymes are usually denoted to be cyclooxygenases (COXs; COX-1 and COX-2) and they were shown to occur in two isoforms, initially termed PGH₁ and PGH₂ synthases. The first “cyclooxygenation” reaction is based on the addition of

an oxygen molecule to the AA structure to form an intermediate compound named PGG₂. In the second step, PGG₂ is converted into PGH₂. The process uses the peroxidase activity of COX. Finally, the transformation of PGH₂ occurs, depending on the several, cell-specific enzymes, including synthases, isomerases and reductases. With regard to a specific cell, prostaglandins (PGE₂, PGI₂, PGD₂, PGF_{2α}), thromboxanes (TXA₂) or prostacyclin (PGI₂) are synthesized. Cyclooxygenases are encoded by genes located on the chromosome 9 (COX-1) and 1 (COX-2). COX-1 is expressed in most cells (mostly in vascular endothelial cells, stomach, kidney, vascular smooth muscles, blood cells but except red blood cells) and it is a source of – so called – housekeeping prostanoids, involved in numerous physiological functions, preserving homeostasis of most systems. COX-2 level is low in normal tissues but it becomes induced by inflammatory stimuli as well as hormones or growth factors and is responsible for prostanoids formation in inflammatory or cancer conditions (15, 17, 18).

Prostanoids exert their effect *via* the receptor mechanism. They are ligands for prostanoid receptors that belong to the rhodopsin-like 7-transmembrane-spanning G protein-coupled receptors family. The family is divided into 8 classes: E-prostaglandin receptor (EP); with further subclassification into 1–4 subtypes (EP₁–EP₄), PGD receptor – for prostaglandin D (DP₁); PGF receptor – for prostaglandin F (FP), PGI receptor (IP) and thromboxane (TP). Moreover, there is also another receptor that responds to PGD₂, called the chemoattractant receptor – homologous molecule expressed on T-helper 2 cells (CRTH₂ or DP₂) that belongs to the chemokine receptor family (N-formyl-methionyl-leucyl-phenyl-alanine chemoattractant receptor superfamily). Two additional isoforms of the TP receptor (TPα, TPβ) as well as of the FP receptor (FPA, FPB) may be also distinguished (17, 19).

The intracellular signalling pathway of prostanoid receptors differs between subtypes. EP₂, EP₄, IP and DP₁ receptors act through adenylyl cyclase activation *via* Gs protein resulting in intracellular cAMP elevation. EP₁ and FP are linked to the Gq and phosphatidylinositol with its derivatives (IP₃, DAG), finally leading to intracellular calcium mobilization. Moreover, FP receptors also act through a small G-protein Rho *via* a Gq-independent mechanism. TP receptors are associated with both Gq and G13 proteins and phospholipase C but they can be also coupled *via* Gh to phospholipase C as well as *via* Gi/Gs to adenylyl cyclase (17).

Prostanoids exert variety of actions. Usually, they affect smooth muscles causing either their

relaxation or contraction, acting *via* appropriate receptors and opening or closing calcium channels. Prostanoids are also demonstrated to modulate neuronal activity by several ways: inhibiting or stimulating neurotransmitter release, sensitizing sensory fibres, inducing some general actions (such as fever). One of the most important regulatory role of prostanoids is their modulatory influence on both secretion and motility of the gastrointestinal tract as well as on renal blood flow and transport of ions and water in kidneys. Prostanoids also regulate the activity of both platelets and endothelial cells and are involved in vascular homeostasis and hemostasis (15, 16).

Moreover, prostanoids belong to crucial mediators involved in various inflammatory mechanisms, resulting in development of pain, fever, redness and local edema. Those acute inflammatory symptoms result from both vascular (redness, local swelling) and central / peripheral neuronal (pain, fever) actions of prostanoids. Moreover, prostanoids exert other pro-inflammatory actions by their amplification in secretion of many cytokines, inflammatory cells activation and the role in the neuroinflammatory process (17). There are also reports confirming the role of prostanoids in transition and maintenance of chronic inflammation by development of a positive feedback loop and by induction of chemokines and recruitment of inflammatory cells to alternate active cell populations at affected sites or contribution in tissue remodelling as seen in angiogenesis and fibrosis (20). As it has already been mentioned above and according to the commonly accepted consensus, COX-1 is constitutively expressed under basic conditions in most cells, contributing to maintenance of local homeostasis, whereas COX-2 level is high in inflammatory states (15). Both COX isoforms are targets of non-steroidal anti-inflammatory drugs (NSAID), and that observation have become a background for general NSAID classification into non-selective, classical NSAID (inhibiting both COX isoforms) and selective COX-2 blocking agents. However, further studies resulted in more precise division of the NSAID group and according to recent arrangements, it is possible to distinguish selective COX-1 inhibitors, nonselective COX-1/2 ones, relatively selective – preferential COX-2 inhibitors and highly selective COX-2 ones. There are a lot of reviews (e.g., 21–24) offering detailed information on that subject.

Moreover, besides COX-1 and COX-2 isoforms, there is also a central COX-3 isoform currently distinguished, responsible for fever and co-responsible for central pain nociception, that is a

target for paracetamol (25). Nevertheless, the existence of that COX-3 as well as the central paracetamol action associated with its influence on that isoform are controversial and require further studies. That issue is also a subject of many reviews (e.g., 26, 27) in this field. The detailed discussion of numerous pharmacological aspects of NSAID is beyond the framework of this paper and can be found in many available reviews.

Prostanoids and their role in bladder function

The early interest in the prostanoids role in the bladder function is dated back to early 1970s when it was demonstrated for the first time that those agents were released inside the bladder in response to distention and mechanical or inflammatory injury of the mucosa (28, 29).

The primary prostanoids: PGE₂, PGF_{2α}, PGI₂, PGD₂ and TXA₂ are synthesized by cyclooxygenases in the bladder under both physiological and pathological conditions (29). There are some species-specific differences regarding the bladder prostanoid synthesis: in rabbits the main prostanoid is PGE₂, whereas PGI₂ is the principle prostanoid in rats (30, 31). In humans, the major prostanoid is PGI₂, followed by PGE₂, PGF_{2α} and TXA₂ (31). Those compounds are produced by both COX-1 and COX-2 found in various tissues of the bladder. There is a general belief that, similarly to other organs, bladder COX-1 is a constitutive enzyme responsible for prostanoids required for maintenance of local bladder homeostasis, while bladder COX-2 expression is induced by various pathophysiological factors (29).

The expression of COX-1 is demonstrated in the urothelium, especially in its basal and intermediate layers. It suggests that prostanoids belong to a complex signaling system connecting urothelium, suburothelial cells of the lamina propria and the muscular layer. Bladder muscular layer shows expression of both COX-1 and COX-2 (29, 32).

All the prostanoid receptors, except those for PGD₂ and PGF_{2α}, are expressed in the bladder (29). Moreover, the detailed distribution of bladder receptors for PGI₂ remains unknown. However, PGI₂ is produced inside the bladder in response to a distention, injury and inflammation (33). Additionally, no data have been published regarding bladder receptors for TXA₂, although it has been shown that thromboxane A₂ induced contractions of isolated smooth muscle of the bladder, while thromboxane A₂ receptor antagonist inhibited rhythmic rabbit bladder contractions (34, 35). A majority of reports referring to bladder prostanoids are associated with

PGE₂, that mediates their effects by EP receptors found in the urothelium and suburothelial layer. In general, EP₁ and EP₃ receptors are believed to cause bladder contractions, whereas EP₂ and EP₄ induce bladder relaxation (36). Moreover, it was shown that the EP₁ receptor is involved in the initiation of the micturition in both humans and animals (37).

It is well documented that prostaglandins alter bladder motility and influence the micturition reflex in both humans and animals. Those agents decrease functional bladder capacity and micturition volume and increase voiding contraction amplitudes in urodynamic recordings (29). Thus, prostaglandins seem to be one of the agents involved in bladder overactivity. Among prostaglandins contributing to bladder overactivity, PGE₂ is thought to be the most likely compound (29). That finding is also consistent with reports confirming that overactivation of the EP₁ receptors is responsible for bladder overactivity in animal model of bladder outlet obstruction (37). It seems, that prostaglandins, locally produced mostly in the urothelium, are likely to influence bladder contractility *via* at least three mechanisms: a direct, receptor-manner effect on smooth muscle cells of the bladder, effects mediated by the interstitial cells activation, and a neuromodulatory influence on sensory fibers (29).

Apart from experimental studies, the arachidonate cascade products abnormalities have also been demonstrated in clinical trials, although results seem to be conflicting so far. Urinary levels of PGE₂ and PGF_{2α} were found to be higher in patients with OAB symptoms compared to the control (38). However, another study did not confirm those findings, showing no differences in urinary PGE₂ level in patients with interstitial cystitis and healthy controls (39). The discrepancy requires some further studies to explicitly investigate the role of prostanoids and disturbances in OAB patients as well as in healthy individuals.

Prostanoids as a possible target for therapeutic OAB agents

Currently used OAB pharmacological agents diminish the increased bladder contractility and that way alleviate symptoms of bladder overactivity. Because of the fact, that final activity of the detrusor is initiated by excitation of cholinergic, muscarinic receptors (mostly M₂, M₃), drugs targeting that mechanism are considered to be the principal pharmacotherapy. Thus, antimuscarinics – antagonists of M₂/M₃ receptors – are the first-line treatment (4). The detailed description designed for current pharmacological OAB guidelines may be found in many

reviews, also of our authorship (40). There are also some new agents, studied as a potential novel OAB pharmacological options. They include drugs targeting the glutamate, glycinergic, GABA, enkephaline or purinergic systems, dopaminergic D₁ or adrenergic β ₂ receptor agonists, vanilloids affecting TRPV₁ receptors, calcium L-channels antagonists and some other. The rationale of both use of antimuscarinics and studies of new agents mentioned above is associated with OAB pathophysiological implications that may also be found in many reviews (e.g. 6–10), also written by us (12, 40). Therefore, it will not be discussed in this paper. Among new potential OAB drugs, the agents based on the prostanoids system are also being considered. As it has already been mentioned above, prostaglandins were demonstrated to be involved in bladder overactivity, thus inhibition of their synthesis or the use of prostaglandin receptor antagonists seem to be a rational way to treat OAB patients. That hypothesis was confirmed repeatedly in some animal studies. One of the first research in this field was the work by Bultiude et al. (41), who in 1976 reported that COX inhibitors affected detrusor muscle activity in both *in vivo* and *in vitro* experiments. Further studies clarified the effects of selected NSAIDs in amelioration of OAB symptoms in various animal models. Lecci et al. (42) studied the influence of both non-selective COX inhibitor – dexketoprofen and NS-398, a non-commercially available selective COX-2 inhibitor, in experimental cystitis in rats. They revealed that selective COX-2 inhibitors improved recorded urodynamic features resulting from inflammation-triggered bladder overactivity. Then, Angelico et al. (43) revealed that both non-selective and selective COX inhibitors were effective in suppression of the micturition reflex and in increasing of the bladder volume capacity in rats with overactive bladder, early following the bladder irritation evoked by intravesical instillation of diluted (0.2%) acetic acid. In the subsequent study, Kibar et al. (44) observed the tendency for reduced bladder contractile response to cholinergic stimulation following the intravesical aspirin administration in rabbit model of partially obstructed bladders. An interesting research also performed Takagi-Matsumoto et al. (45), who examined the effect of selected NSAIDs (aspirin, indomethacin, or ketoprofen) on urodynamic parameters in normal and cystitis rats and compared their ulcerogenic activity in the gastrointestinal mucosa. They revealed that NSAIDs (in the following rank order of potency: ketoprofen > indomethacin > aspirin) increased bladder capacity without any effect on micturition pressure in normal

rats, while in cystitis rats, bladder capacity was increased and micturition frequency was decreased. Moreover, the bladder levels of prostaglandin were significantly decreased in cystitis rats pretreated with NSAIDs. Those researchers demonstrated also that both ketoprofen and indomethacin administered intraduodenally induced lesions in the gastrointestinal mucosa, but aspirin had no significant effect. They concluded that since aspirin, in contrast to ketoprofen or indomethacin, did not cause any gastrointestinal lesions, aspirin might be the NSAIDs treatment of choice for overactive bladder (45). In one of the latest study, Jang et al. (46) examined the effects of intravesical cyclooxygenase-2 (COX-2) inhibitors on the expression of inducible nitric oxide synthase (iNOS) and nerve growth factor (NGF) in cyclophosphamide (CYP)-induced overactive bladder (OAB). They showed that COX-2 inhibitor-treated rats displayed significant elongation of the contraction and intercontraction intervals compared to OAB non-treated rats and the contraction time was significantly shorter. On immunohistochemical staining, there was no iNOS activity and NGF activity was minimally localized in the mucosa and submucosa in healthy animals. In OAB rats, NGF activity in the mucosa and submucosa were increased, and there was greater expression of iNOS in all layers and of NGF in detrusor while in the COX-2 inhibitor-treated rats, their expression was less pronounced in all layers. They concluded that intravesical instillation with COX-2 inhibitors may reduce CYP-induced bladder hyperactivity and expression of iNOS and NGF (46).

Despite the increasing number of encouraging results originating from experimental studies, the clinical trials of NSAIDs as a potential therapeutical OAB option are rather scant. Cardozo et al. tested non-selective COX inhibitors: flurbiprofen (47) and indomethacin (48). They demonstrated that both examined NSAIDs were effective in alleviation of OAB symptoms. Flurbiprofen, administered in 30 female OAB patients in a dose of 50 mg three times a day caused a significant reduction in frequency, urgency and urge incontinence. However, significant side effects (mostly indigestion, nausea, vomiting, dizziness, headache) occurred in 13 patients receiving flurbiprofen compared to 5 healthy individuals (47). Indomethacin, administered for 1 month in a group of 32 OAB patients, also displayed the improvement in both nocturnal and diurnal voiding frequency (48). A reliable clinical estimation was performed by Sprem et al. (49), who evaluated the therapeutic efficacy of intravesically administered ketoprofen in 30 patients with urodynamically verified detrusor instability in double-

blind randomized placebo-controlled cross-over study. They found that ketoprofen was a feasible and effective treatment for detrusor instability as the maximum cystometric capacity and the urinary bladder volume at which the patients felt urgency to void were larger after ketoprofen administration than before it. Moreover, ketoprofen administered intravesically produced no significant adverse effects (49). There are also reports concerning beneficial effects of EP₁ receptor antagonists in OAB. Wilbraham et al. (50) published a paper focusing on the assessment of the safety, tolerability and pharmacokinetic properties of ONO-8539, an EP₁ receptor antagonist, administered in OAB patients and healthy subjects in phase I of the clinical study. This agent has been followed into the next stage of the clinical trial.

CONCLUSIONS

It should be expected that NSAIDs will be further evaluated, both in experimental and clinical studies, as a potential, novel OAB pharmacological option. Despite the common agreement that prostanoids play an important role in the bladder physiology as well as in OAB pathogenesis, and despite the rationale for potential application of agents targeting prostanoids synthesis or blocking prostanoids receptors, the clinical approaches have not yet brought satisfactory results. None of the NSAIDs or EP receptor antagonists studied in animal models of OAB have entered the standard therapeutic arsenal for OAB treatment so far. This failure is at least due to the relatively small number of studied subjects in the clinical trials, observed numerous adverse drug reactions or clinically unpractical and patients' unfriendly route of administration (e.g., intravesically). However, those setbacks will not cease the efforts to find effective and safe prostanoids-based strategies to treat bladder overactivity and, therefore, it seems that NSAIDs (as well as EP receptor antagonists) will be able to be indicated also in that clinical entity in the future.

REFERENCES

- Abrams P., Cardozo L., Fall M., Griffiths D., Rosier P., Ulmsten U., Van Kerrebroeck Ph.E.V. et al.: *Urology* 61, 37 (2003).
- Abrams P., Artibani W., Cardozo L., Dmochowski R., van Kerrebroeck P., Sand P.: *Neurourol. Urodyn.* 25, 293 (2006).
- Haylen B.T., de Ridder D., Freeman R.M., Swift S.E., Berghmans B., Lee J., Monga A. et al.: *Int. Urogynecol. J.* 21, 5 (2010).
- Rahnama'i M.S., Van Koevringe G.A., Van Kerrebroeck P.E.: *Nephrourol. Mon.* 5, 933 (2013).
- Milsom I., Abrams P., Cardozo L., Roberts R.G., Thuroff J., Wein A.J.: *BJU Int.* 87, 760 (2001).
- Andersson K.E., Pehrson R.: *Drugs* 63, 2595 (2003).
- Chu F.M., Dmochowski R.: *Am. J. Med.* 119, 3S (2006).
- Hashim H., Abrams P.: *Curr. Opin. Urol.* 17, 231 (2007).
- Chapple C.: *Can. Urol. Assoc. J.* 5 (Suppl. 2), S126 (2011).
- Banakhar M.A., Al-Shaiji T.F., Hassouna M.M.: *Int. Urogynecol. J.* 23, 975 (2012).
- Birder L.A., Ruggieri M., Takeda M., van Koevringe G., Veltkamp S., Korstanje C., Parsons B., Fry C.H.: *Neurourol. Urodyn.* 31: 293 (2012).
- Dobrek Ł., Juszczak K., Wyczółkowski M., Thor P.J.: *Adv. Clin. Exp. Med.* 20, 119 (2011).
- Clemens J.Q.: *Urol. Clin. N. Am.* 37, 487 (2010).
- Moore C.K., Goldman H.B.: *Curr. Urol. Rep.* 7, 447 (2006).
- Miller S.B.: *Semin. Arthritis Rheum.* 36, 37 (2006).
- Narumiya S., Sugimoto Y., Ushikubi F.: *Physiol. Rev.* 79, 1193 (1999).
- Ricciotti E., FitzGerald G.A.: *Arterioscler. Thromb. Vasc. Biol.* 31, 986 (2011).
- Helliwell R.J.A., Adams L.F., Mitchell M.D.: *Prostaglandins Leukot. Essent. Fatty Acids* 70, 101 (2004).
- Breyer R.M., Bagdassarian C.K., Myers S.A., Breyer M.D.: *Annu. Rev. Pharmacol. Toxicol.* 41, 661 (2001).
- Aoki T., Narumiya S.: *Trends Pharmacol. Sci.* 33, 304 (2012).
- Frolich J.C.: *Trends Pharmacol. Sci.* 18, 30 (1997).
- Suleyman H., Demircan B., Karagoz Y.: *Pharmacol. Rep.* 59, 247 (2007).
- Korzeniowska K., Jankowski J., Jabłeczka A.: *Farm. Współ.* 3, 192 (2010).
- Batlouni M.: *Arq. Bras. Cardiol.* 94, 522 (2010).
- Botting R., Ayoub S.S.: *Prostaglandins Leukot. Essent. Fatty Acids* 72, 85 (2005).
- Davies N.M., Good R.L., Roupe K.A., Yáñez Y.A.: *J. Pharm. Pharm. Sci.* 7, 217 (2004).
- Schwab J.M.: *Lancet* 361, 981 (2003).
- Gilmore N.J., Vane J.R.: *Clin. Sci.* 41, 69 (1971).

29. Rahnama'i M.S., Van Kerrebroeck Ph.E.V., de Wachter S.G.G., van Koeveringe G.A.: *Nat. Rev. Urol.* 9, 283 (2012).
30. Leslie C.A., Pavlakis A.J., Wheeler J.S., Siroky M.B., Krane R.J.: *J. Urol.* 132, 376 (1984).
31. Jeremy J.Y., Mikhailidis D.P., Dandona P.: *Prostaglandins Leukot. Med.* 16, 235 (1984).
32. de Jongh R., Grol S., van Koeveringe G.A., Van Kerrebroeck Ph.E.V., de Vente J., Gillespie J.I.: *J. Cell. Mol. Med.* 13, 3069 (2009).
33. Jeremy J.Y., Tsang V., Mikhailidis D.P., Rogers H., Morgan R.J., Dandona P.: *Br. J. Urol.* 59, 36 (1987).
34. Palea S., Toson G., Pietra C., Trist D.G., Artibani W., Romano O., Corsi M.: *Br. J. Pharmacol.* 124, 865 (1998).
35. Collins C., Klausner A.P., Herrick B., Koo H.P., Miner A.S., Henderson S.C., Ratz P.H.: *J. Cell. Mol. Med.* 13, 3236 (2009).
36. Coleman R.A., Smith W.L., Narumiya S.: *Pharmacol. Rev.* 46, 205 (1994).
37. Lee T., Hedlund P., Newgreen D., Andersson K.E.: *J. Urol.* 177, 1562 (2007).
38. Kim J.C., Park E.Y., Seo S.I., Park Y.H., Hwang T.K.: *J. Urol.* 175, 1773 (2006).
39. Liu H.T., Tyagi P., Chancellor M.B., Kuo H.C.: *BJU Int.* 106, 1681 (2010).
40. Dobrek Ł., Juszcak K., Wyczółkowski M., Thor P.J.: *Acta Pol. Pharm. Drug Res.* 68, 807 (2011).
41. Bultitude M.I., Hills N.H., Shuttleworth K.E.: *Br. J. Urol.* 48, 631 (1976).
42. Lecci A., Birder L.A., Meini S., Catalioto R.M., Tramontana M., Gliuliani S., Criscuoli M., Maggi C.A.: *Br. J. Pharmacol.* 130, 331 (2000).
43. Angelico P., Guarneri L., Velasco C., Cova R., Leonardi A., Clarke D.E., Testa R.: *BJU Int.* 97, 837 (2006).
44. Kibar Y., Irkilata H.C., Yaman H., Onguru O., Coguplugil A.E., Ergin G., Seyrek M. et al.: *Neurourol. Urodyn.* 30, 1646 (2011).
45. Takagi-Matsumoto H., Ng B., Tsukimi Y, Tajimi M.: *J. Pharmacol. Sci.* 95, 458 (2004).
46. Jang J., Park E.Y., Seo S.I., Hwang T.K., Kim J.C.: *BJU Int.* 98, 435 (2006).
47. Cardozo L.D., Stanton S.L., Robinson H., Hole D.: *BMJ* 280, 281 (1980).
48. Cardozo L.D., Stanton S.L.: *J. Urol.* 123, 399 (1980).
49. Sprem M., Milicić D., Oresković S., Ljubojević N., Kalafatić D.: *Croat. Med. J.* 41, 423 (2000).
50. Wilbraham D., Masuda T., Deacon S., Kuwayama T., Vincent S.: *J. Urol.* 13, 271 (2006).

Received: 18. 03. 2014

ANALYSIS

SOLID STATE CHARACTERIZATION OF α -TOCOPHEROL IN INCLUSION COMPLEXES WITH CYCLODEXTRINS

KINGA LANGE* and TERESA GIERLACH-HŁADOŃ

Department of Inorganic and Analytical Chemistry, Karol Marcinkowski University of Medical Sciences,
6 Grunwaldzka St., 60-780 Poznań, Poland

Abstract: The alternative for a pure soluble, sensible for physical and chemical conditions oil form of α -tocopherol (α -T) is its complexation with cyclodextrins. A different influence of cyclodextrins on the included substance demands a stability investigation of the substance enclosed in a host-guest complex. Hence, the thermal stability of α -T in inclusion complexes (InCs) with cyclodextrins (CDs) was studied. The inclusion complexes were obtained by two different methods: a lyophilization and a kneading method, and their formation was examined by IR spectroscopy, differential scanning calorimetry and $^1\text{H-NMR}$ spectroscopy. The inclusion complexes were subjected to the test of accelerated aging at 323 K, 333 K, 338 and 343 K, for comparison α -T as a substance and physical mixtures (PhM) of α -T with CDs were used. Changes in α -T concentration during the experiment were followed by HPLC method and next, the products of thermal decomposition were studied by LC-ESI-MS/MS method. The reaction of α -T decomposition in inclusion complexes with CDs was found to be of the first order. The same order of a decomposition reaction was observed in a sample of α -T as a substance. It seems that cyclodextrins protect α -T against thermal decomposition, moreover, the protective effect of natural β -cyclodextrin (β -CD) appears to be greater than that of 2-hydroxypropyl- β -cyclodextrin (2-HP- β -CD). However, the CDs do not influence the type of a formed product of decomposition. This product, i.e., the dimer of α -T (m/z 859 Da), was found in all tested samples. The protective effect of CDs and transformation from the liquid state to the solid state of α -T can be used to create a new pharmaceutical form – tablets with α -T.

Keywords: inclusive complexes, cyclodextrins, tocopherol, solid state, $^1\text{H-NMR}$, mass spectrometry

For over a decade inclusion complexes of therapeutic substances with CDs have been of great interest to pharmaceutical industry due to their ability to modify the solubility, stability, bioavailability and even to diminish the toxicity of many therapeutic drugs (1, 2). CDs are oligosaccharides consisting of glucopyranose molecules linked by α -1,4-glycoside bonds to form a conical structure, with a hydrophobic cavity and hydrophilic outside part (3). This specific conformation enables them to form host-guest complexes (4). The ability of forming inclusion complexes with various molecules depends on the size and polarity of the included substance and the type of CD (3, 5). Cyclodextrins can stabilize the guest molecules but in some cases they can accelerate their degradation as well, e.g., bis(4-hydroxyphenyl)ethane (6–9). Hence, a different influence of CDs on the included substance demands the stability investigation of the substance enclosed in the host-guest complex.

A widely known significance of tocopherol in living organisms is the ability to sweep out free radicals and protect the cell lipid membranes against autocatalytic peroxidation. The following issues of its function have been analyzed so far: antioxidant- (anti-radical) activity, structure-function regulation of cell membranes and regulation of enzyme activity (10). The protection of cell membranes against oxidation is vital and essential to fight sclerosis of blood vessels, cardiac muscle ischemia or cardiac infarcts (11). The novelty of a tocopherol family application are anti-cancer properties which do not relate to their anti-radical activity (12, 13). This new discovered action by pro-apoptotic mechanisms, e.g., in human breast cancer cells, results in further finding a new form of tocopherol more stable and better soluble in water (14). So far, chemically stable have been tocopherol esters (acetate or succinate), but in these forms their bioavailability and effectiveness were not better than the present mole-

* Corresponding author: e-mail: klange@ump.edu.pl; phone: +48-618546608; fax: +48-618546609

cule (15–17). For this reason a new form of α -T has still been searched and the inclusion complexes with different derivatives of CDs have been proposed. The replacement of the natural β -CD in complexes with tocopherol by branched derivatives (e.g., HP- β -CD or HP- γ -CD) has not influenced the antioxidative properties of vitamin E, but considerably enhanced its light-induced decomposition, hence the selection of the CD's derivative during preparation of inclusion complexes is significant (18). The aim of this study was to choose the best way of inclusion complex preparation and to evaluate the stability of α -tocopherol (α -T) in inclusion complexes with β -CD and 2-HP- β -CD in conditions of storage for diet supplements. Moreover, the purpose of the study was to discuss whether the protecting effect of natural cyclodextrin and its 2-hydroxypropyl derivative exists and if these structures can be used in a new pharmaceutical form.

MATERIALS AND METHODS

Chemicals

α -T was purchased from Sigma-Aldrich Chemie (Germany). β -CD and 2-HP- β -CD were supplied by Fluka Sigma-Aldrich Chemie. Methanol LiChrosolv was purchased at Merck (Germany). All reagents were analytically examined by HPLC.

Preparation of inclusion complexes and physical mixtures

Inclusion complexes

Kneading method

2-HP- β -CD (1.380 g) was dissolved in distilled water and α -T (0.431 g) was dissolved in ethanol (760 g/L). Both saturated solutions were mixed and transferred quantitatively to the agate mortar. The mixture was kneaded for about 2.5 h to obtain dry powder. The product was dried at room temperature to a constant mass.

Lyophilization method

For the solid inclusion complex preparation, a saturated solution of α -T was added to an aqueous solution containing the β -CD. The molar ratio of the guest molecule to CD was 1 : 1. The dispersion of α -T in aqueous β -CD solution was shielded from light and stirred for 24 h at room temperature to achieve equilibrium of the complexation reaction. Next, after filtration through a 0.2 μ m nylon membrane, the solvent was removed and the remaining coprecipitate was collected. These solid complexes were frozen at -20°C and then lyophilized in a laboratory freeze-dryer (Alpha 1-2 Christ, Germany).

Physical mixtures

Physical mixtures were simply obtained by thorough mixing of testing substances.

Samples identification

Infrared spectroscopy (IR)

IR absorption spectra were measured using FT-IR Bruker IFS 66v/S spectrometer. The samples of the solid substances were previously mixed thoroughly with potassium bromide (KBr) and next, the KBr disks were prepared by compressing the powders under force of 10 ton in a hydraulic press. The measurement of α -T was performed using KBr discs due to its oily form. Scans were obtained at a resolution of 2 cm^{-1} , from 4000 to 500 cm^{-1} .

Differential scanning calorimetry (DSC)

DSC measurements were performed on a Shimadzu DSC-50 differential scanning calorimeter with a thermal analyzer. All accurately weighed samples (2.0 mg) were placed in aluminium pans before heating under nitrogen flow (30 mL/min) at a scanning rate of $10^{\circ}\text{C}/\text{min}$ from 20 to 400°C . An aluminium pan with accurately weighed Al_2O_3 (2.0 mg) was used as a reference standard.

Nuclear magnetic resonance spectroscopy ($^1\text{H-NMR}$)

The solid-state cross-polarization magic angle spinning (CP/MAS) NMR experiments were performed on 400 MHz Bruker Avance III spectrometer, equipped with a MAS probe head using 4-mm ZrO_2 rotors at a frequency of 400.13 MHz for ^1H . The conventional ^1H MAS spectra were performed using the following parameters: measurements temperature of 296 K, spinning rate of 8 kHz, proton 90° pulse length of 5 μs , repetition delay of 3 s, spectral width of 40 kHz and time domain size of 16 k data points. In $^1\text{H-NMR}$ measurements α -T was excluded due to its oily form.

Stability studies

The study was performed during 29 weeks in the atmosphere of dry air at 323, 333, 338 and 343 K. Accurately weighed samples of α -T (2.5 mg), InC with β -CD and InC with 2-HP- β -CD (10.0 mg, respectively) were placed in glass vials, which afterwards were placed in sand baths and closed in thermostats set at appropriate temperature. Prior to initiating studies, the sand baths were heated to required temperature during one day. Next, at certain intervals samples were taken and analyzed by HPLC method. On the basis of a diminished concentration of α -T in time the kinetic decomposition equation was set.

HPLC method**Equipment and chromatographic conditions**

Chromatographic analyses were made on the HPLC apparatus equipped with a DAD detector, made by Agilent Technologies series 1200. Separation was performed in the reversed phase system using a LiChroCART 250-4 column filled with LiChrospher 100 RP-18 (5 μ m). Results were analyzed on a computer integrated with the chromatograph using ChemStation software for LC 3D System.

Analyses of α -T, its inclusion complexes and physical mixtures with β -CD and 2-HP- β -CD were performed in the following conditions: 100% methanol as the mobile phase, at the flow rate of 1.3 mL/min, column thermostated at 25°C, injection volume of 20 μ L, detection at 292 nm.

Sample preparation

α -T (2.5 mg), InCs (10.0 mg) were transferred quantitatively into a measuring flask (10.0 mL) and the volume was supplemented with methanol. Prior to injection on the column all the solutions were filtered.

Validation

The method was validated according to the ICH recommendations (19). The method's selectivity, linearity, precision, accuracy and recovery were determined. The optimization and validation conditions for the HPLC method have already been published (20).

LC-ESI-MS/MS method

The analysis was carried out by using a system consisting of a liquid chromatograph Agilent

Table 1. Kinetic parameters of α -tocopherol decomposition.

Temp. [K]	(k \pm Δ k) [s ⁻¹]	(a \pm Δ a) [h ⁻¹]	t _{0.5} [h]	t _{0.1} [h]	S _a	r	n
343	(4.976 \pm 0.298) \cdot 10 ⁻⁷	(-1.79 \pm 0.11) \cdot 10 ⁻³	386.9	58.8	4.65 \cdot 10 ⁻⁵	-0.997	10
338	(4.189 \pm 0.342) \cdot 10 ⁻⁷	(-1.51 \pm 0.12) \cdot 10 ⁻³	459.5	69.9	4.43 \cdot 10 ⁻⁵	-0.997	10
333	(3.352 \pm 0.219) \cdot 10 ⁻⁷	(-1.21 \pm 0.08) \cdot 10 ⁻³	574.5	87.4	3.22 \cdot 10 ⁻⁵	-0.998	9
323	(2.081 \pm 0.082) \cdot 10 ⁻⁷	(-7.49 \pm 0.29) \cdot 10 ⁻⁴	924.6	140.6	1.30 \cdot 10 ⁻⁵	-0.998	11

k – rate constant of reaction, a – slope, S_a – standard deviation for a, r – correlation coefficient.

Table 2. Kinetic parameters of decomposition of α -T in inclusion complex with β -CD.

Temp. [K]	(k \pm Δ k) [s ⁻¹]	(a \pm Δ a) [h ⁻¹]	t _{0.5} [h]	t _{0.1} [h]	S _a	r	n
343	(1.019 \pm 0.069) \cdot 10 ⁻⁷	(-3.67 \pm 0.25) \cdot 10 ⁻⁴	1891.0	287.6	1.13 \cdot 10 ⁻⁵	-0.995	11
338	(7.798 \pm 0.304) \cdot 10 ⁻⁸	(-2.80 \pm 0.11) \cdot 10 ⁻⁴	2468.9	375.5	4.97 \cdot 10 ⁻⁶	-0.998	13
333	(5.334 \pm 0.188) \cdot 10 ⁻⁸	(-1.92 \pm 0.06) \cdot 10 ⁻⁴	3608.9	548.9	3.04 \cdot 10 ⁻⁶	-0.998	12
323	(2.812 \pm 0.174) \cdot 10 ⁻⁸	(-1.01 \pm 0.06) \cdot 10 ⁻⁴	6845.7	1041.2	2.87 \cdot 10 ⁻⁶	-0.996	12

k – rate constant of reaction, a – slope, S_a – standard deviation for a, r – correlation coefficient.

Table 3. Kinetic parameters of decomposition of α -T in inclusion complex with 2-HP- β -CD.

Temp. [K]	(k \pm Δ k) [s ⁻¹]	(a \pm Δ a) [h ⁻¹]	t _{0.5} [h]	t _{0.1} [h]	S _a	r	n
343	(3.033 \pm 0.175) \cdot 10 ⁻⁸	(-1.09 \pm 0.06) \cdot 10 ⁻³	634.7	96.6	2.67 \cdot 10 ⁻⁵	-0.998	9
338	(2.095 \pm 0.089) \cdot 10 ⁻⁷	(-7.54 \pm 0.32) \cdot 10 ⁻⁴	918.9	139.8	1.39 \cdot 10 ⁻⁵	-0.998	11
333	(1.607 \pm 0.121) \cdot 10 ⁻⁷	(-5.78 \pm 0.43) \cdot 10 ⁻⁴	1197.9	182.2	1.94 \cdot 10 ⁻⁵	-0.995	11
323	(9.538 \pm 0.742) \cdot 10 ⁻⁸	(-3.43 \pm 0.27) \cdot 10 ⁻⁴	2018.5	307.0	1.16 \cdot 10 ⁻⁵	-0.995	11

k – rate constant of reaction, a – slope, S_a – standard deviation for a, r – correlation coefficient.

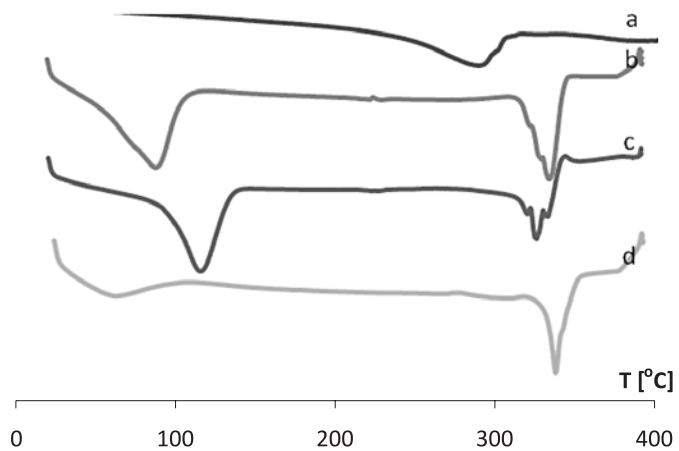


Figure 1. DSC thermograms of: a – α -tocopherol, b – β -CD, c – physical mixture of α -T- β -CD, d – inclusion complex of α -T- β -CD

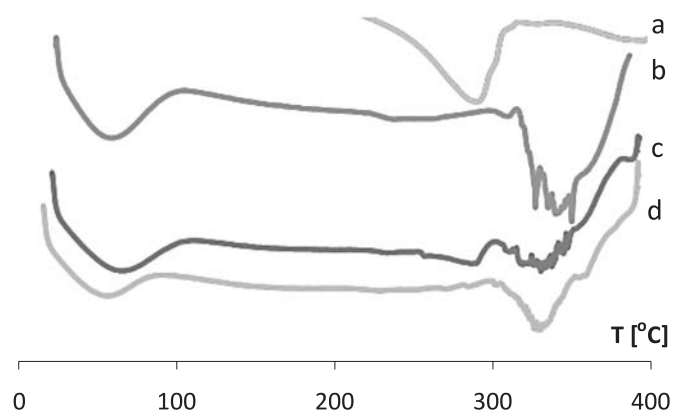


Figure 2. DSC thermograms of: a – α -tocopherol, b – 2-HP- β -CD, c – physical mixture of α -T-2-HP- β -CD, d – inclusion complex of α -T-2-HP- β -CD

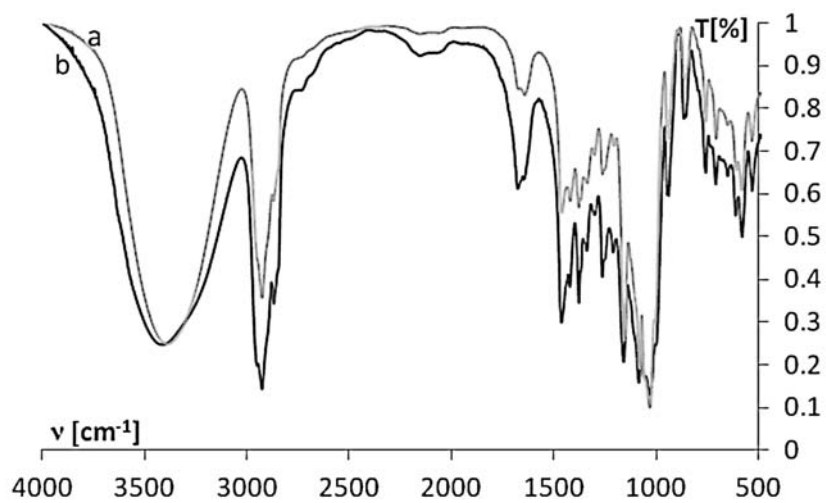


Figure 3. IR spectra of: a – inclusion complex of α -T- β -CD, b – physical mixture of α -T- β -CD

Infinity 1260 Series coupled with triple quadrupole QTRAP 4000 mass spectrometer equipped with electrospray ionization (ESI). LC separation was achieved using a LiChroCart (250 \times 4 mm) LiChrospher 100 RP-18 (5 μ m) analytical column and a solution of 5.0 mM ammonium acetate in methanol 100% as a mobile phase was used. The flow rate was set at 0.5 mL/min and the volume injected was 10 μ L. The column temperature was thermostated at 25°C. The analytes were ionized by a positive electrospray ionization mode. The standard solution of α -T (1 μ g/mL) was used for optimization of the mass spectrometer parameters, which was carried out using the commands and protocols incorporated in the instrument software. The final ionization conditions were set at 5.5 kV – capillary voltage, 350°C – desolvation temperature. Nitrogen was used as both the desolvation gas (70 psi) and as the cone gas (30 psi). The mass spectra were acquired between 100 and 900 at scan rate of 2 s per spectrum (full-scan mode).

RESULTS

Identification of samples

The products obtained by the kneading and lyophilization methods of α -T with β -CD and 2-HP- β -CD were analyzed by the thermal method (DSC), IR spectroscopy and 1 H-NMR spectroscopy. The three identification methods confirmed obtaining the inclusion complexes of α -T with β -CD and 2-HP- β -CD. The results of studies were illustrated graphically in Figures 1–6.

Kinetic parameters of decomposition of α -T and its inclusion complexes with CDs

Kinetic parameters of α -T decomposition in the uncomplexed form and in the inclusion complexes with CD were found from the semilogarithmic plots of $c = f(t)$, where c is the concentration of the substrate at time t . The regression coefficients a and b were calculated by the least squares method. The time after which 10% or 50% of the initial substrate concentration is decomposed was obtained from the formulae $t_{0.5} = 0.693/k$ and $t_{0.1} = 0.1054/k$.

The kinetic parameters of α -T decomposition in the uncomplexed form and in inclusion complexes with CDs are given in Tables 1–3.

Thermodynamic parameters of decomposition of α -T and in inclusion complexes with CDs

The effect of temperature on the stability of substances is described by the Arrhenius equation, illustrated graphically in Figure 7.

On the basis of the rate constants of α -T decomposition, the thermodynamic parameters were calculated and the results were subjected to the statistical analysis. Enthalpy and entropy were calculated from the equations: $\Delta H^\# = Ea - RT$ [J/mol]; $\Delta S^\# = R \cdot (\ln A - \ln(kT/h))$ [J/(K·mol)], where k is the Boltzmann constant ($1.3806 \cdot 10^{-23}$ [J/K]), h is the Planck constant ($6.6262 \cdot 10^{-34}$ [J·s]), R is the gas constant (8.314 [J/mol/K]), see Table 4.

Products decomposition of α -T in inclusion complexes with CDs

Products decomposition of α -T in inclusion complexes were checked by LC-ESI-MS/MS method in a full scan mode. As illustrated in Figure 8, in the full scan mode the spectrum showed an ion at m/z 431. Moreover, for samples treated with an elevated temperature the spectrum showed an ion at m/z 859. The result is given in Figure 9. The same situation takes place for the second inclusion complex of α -T with 2-HP- β -CD.

DISCUSSION

The inclusion complexes of α -tocopherol and cyclodextrins prepared by the kneading and lyophilization methods were identified by the thermal method (DSC), IR spectroscopy and NMR spectroscopy and obtaining of inclusion complexes was confirmed. The kneading method was ineffective in the case of preparation the inclusion complex with the hydroxypropyl derivative of cyclodextrin.

The thermogram of α -T shows a single endothermic peak at about 268.6°C, which corresponds to decomposition of this compound. The thermograms of β -CD and 2-HP- β -CD show two endothermic peaks at 91.6°C, 329.9°C and 56.6°C, 339.9°C, respectively. The peaks at lower temperatures were assigned to dehydration of cyclodextrins (21), whereas the peaks >300°C correspond to the melting point of the substance. The thermograms of the InCs (Fig 1, 2) do not exhibit a signal at about 268°C, which is assigned to α -T, but show peaks assigned to cyclodextrins shifted towards higher temperatures. This is the main opposite of the thermograms of physical mixtures where the endothermic peak assigned to α -T appears. The changes of the thermograms seem to testify the occurrence of physicochemical interactions of CDs and α -T, accompanied by the formation of inclusion complexes in a solid phase. Similar changes have been observed for substances such as sparfloxacin or tolbutamide (5, 21). The analogical situation takes places for both InCs with β -CD and 2-HP- β -CD.

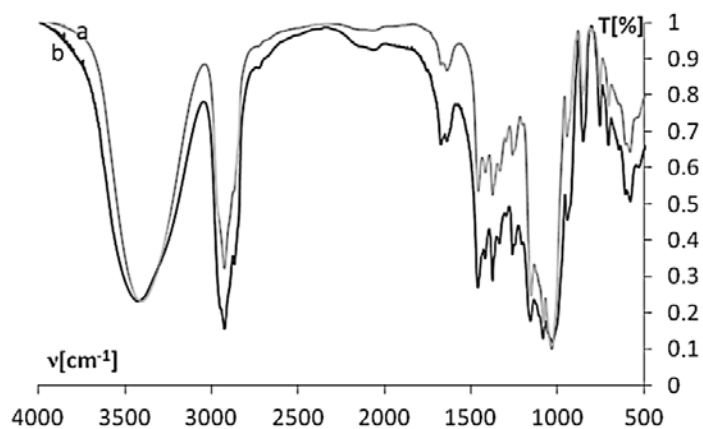


Figure 4. IR spectra of: a – inclusion complex of α -T-2-HP- β -CD, b – physical mixture of α -T-2-HP- β -CD

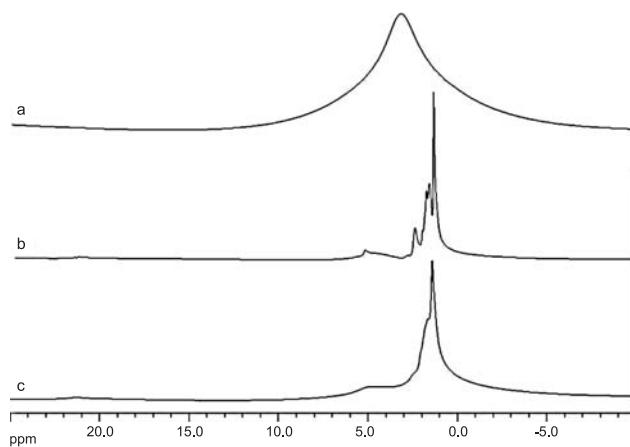


Figure 5. $^1\text{H-NMR}$ spectra of: a – β -CD, b – physical mixture of α -T- β -CD, c – inclusion complex of α -T- β -CD

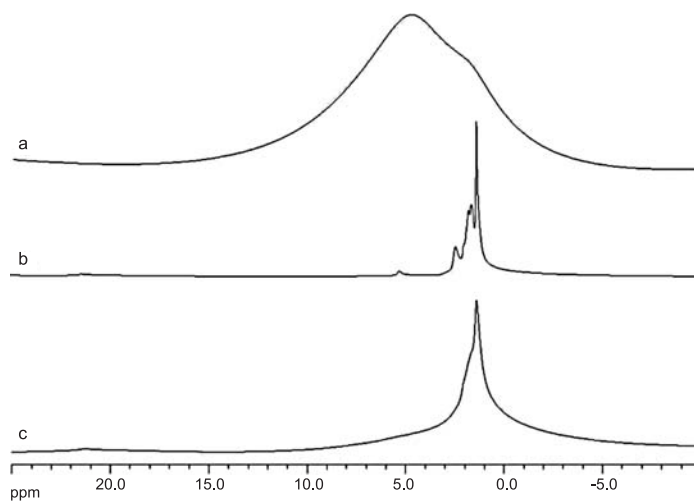


Figure 6. $^1\text{H-NMR}$ spectra of: a – 2-HP- β -CD, b – physical mixture of α -T-2-HP- β -CD, c – inclusion complex of α -T-2-HP- β -CD

The IR spectra of all tested substances were standardized to stretching vibrations of the secondary group OH (ν C-O 1038 cm^{-1}) band. The comparison of the inclusion complexes spectra and their physical mixtures (Fig. 3, 4) points to the formation of the hydrogen bond between the phenol OH group of α -T and the primary OH group of CDs. This is confirmed by shifts of the CDs (β -CD, 2-HP- β -CD) bands corresponding to their OH group stretching vibrations in the physical mixtures (3451, 3457 cm^{-1} , respectively) and in inclusion complexes (3442, 3438 cm^{-1} , respectively). The spectra of inclusion complexes exhibit lower intensities of the bands in the ranges corresponding to stretching vibrations of the aliphatic chain (2950-2720 cm^{-1}) and benzopyrene ring (1500-1000 cm^{-1}) of α -T. The disappearance of the bands in these ranges seems to be the result of the tocopherol incorporation into the cyclodextrin cavities, thus confirming these complexes formation for both situations.

More evidence of the complex formation was obtained from ^1H nuclear magnetic resonance study in the solid state. The spectra of InCs are very similar to the spectra of pure CDs. Spectra of PhMs of both CDs with α -T exhibit well-resolved five signals at δ 1.39; 1.63; 1.78; 2.45; 5.26 ppm, and at 1.39; 1.64; 1.78; 2.45; 5.31 ppm for mixture with β -CD and with 2-HP- β -CD, respectively. In turn, the spectra of InCs exhibit one singlet at δ 1.39 ppm and two broad defused signals at δ 1.69; 5.02 ppm for InC with β -CD, whereas one broad defused signal at δ 1.39 ppm for InC with 2-HP- β -CD. Interestingly, well resolved signals which appeared in PhMs spectra seem to come from α -T protons that are not involved in the formation of hydrogen bonds,

although should not be visible in NMR in solid state studies due to the liquid oil form of α -T. The proposed explanation of this phenomenon is the absorption of α -T on the surface of the CDs resulting in giving dimensions on the spectra of mixtures. Whereas the engagement of CDs and tocopherol protons in interaction results in significant changes in signal multiplicity, only one diffused broad signal is observed in InCs spectra. The disappearance of the signals and their significant overlapping suggest the formation of inclusive complexes between α -tocopherol and β -CD or 2-HP- β -CD. The ^1H -NMR spectra are presented in Figures 5 and 6.

The stability of α -T and α -T in inclusion complexes with β -CD and 2-HP- β -CD in the solid state was evaluated on the basis of kinetic and thermodynamic parameters of α -T decomposition at a certain temperature. The decomposition was accompanied by a change in the color from yellow to brown for α -T and from cream to yellow for α -T in InCs.

As follows from the semi-logarithmic character of the time dependence of concentration, the thermal decomposition of α -T, both uncomplexed and in inclusion complexes, can be described by a simple equation of a first order reaction $\ln[C] = [C_0] - kt$, where $[C]$ is the concentration of decomposition products upon heating, $[C_0]$ – the concentration of decomposition products at $t_0 = 0$, t – time of heating, k – the rate constant of a first order reaction. The character of the decomposition reaction was the same as that reported by Chung (22), who studied tocopherol decomposition in temperatures 100–200°C and claimed that it was the first order reaction. The reaction rate constants and activation energies may also indicate the same mechanism of

Table 4. Thermodynamic parameters of α -T and α -T in inclusion complexes with CDs decomposition.

	α -Tocopherol	α -T/ β -CD InC	α -T/2-HP- β -CD InC
Statistical evaluation of $\ln k = f(1/T)$			
$a \pm \Delta a$	-4874.10 ± 770.81	-7207.10 ± 1070.00	-6262.17 ± 1808.57
S_a	179.13	248.66	420.30
$b \pm \Delta b$	-0.28 ± 2.31	4.92 ± 3.20	3.20 ± 5.41
S_b	0.54	0.74	1.26
r	-0.999	-0.999	-0.996
Thermodynamic parameters			
E_a [kJ/mol]	40.53	59.92	52.07
ΔH^\ddagger [kJ/mol]	38.09	57.49	49.63
ΔS^\ddagger [J/(K·mol)]	-247.14	-203.85	-218.21

$\ln k$ – logarithm of rate constant of reaction; a – slope of Arrhenius plot; S_a – standard deviation for a , b – intercept of Arrhenius plot; S_b – standard deviation of b ; E_a – activation energy, ΔH^\ddagger – activation enthalpy; ΔS^\ddagger – activation entropy.

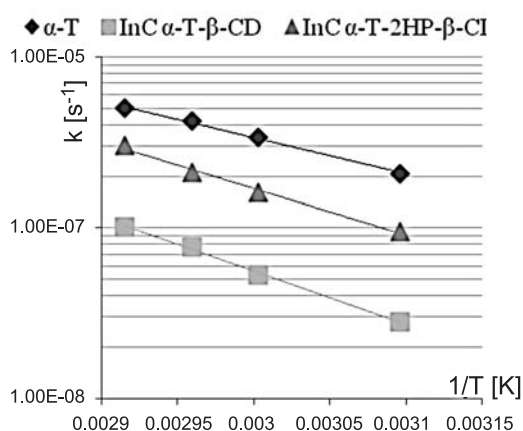


Figure 7. Arrhenius plots of the decomposition of: α -tocopherol, inclusion complex of α -T- β -CD (InC α -T- β -CD), inclusion complex of α -T-2-HP- β -CD (InC α -T-2-HP- β -CD)

α -T uncomplexed and complexed decomposition. The reaction rate constants were found to increase along with temperature, which means that temperature has an important effect on tocopherol decomposition (23). The lower rates constants of α -T decomposition in InCs with CDs than that for α -T indicate that in the solid phase α -T in inclusion complexes is more stable. The comparison of the $t_{0.1}$ and $t_{0.5}$ times for α -T and α -T in complexes with β -CD and 2-HP- β -CD showed that β -CD brings a stronger stabilizing effect, which confirms the values of $t_{0.1}$ time increased about 64% for 2-HP- β -CD and about 400% for β -CD at the highest temperature (Tables 1–3). The results obtained differ from those reported by Cho et al. (24), who studied the stability of tocopherol in the inclusion complex in several solvents e.g., distilled water. These authors reported

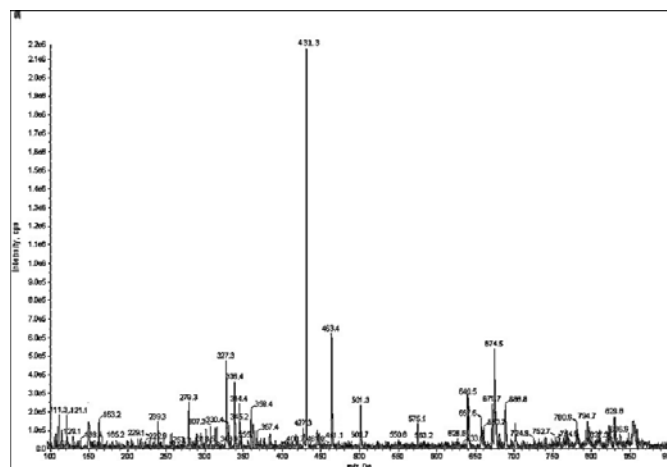


Figure 8. MS spectra of α -tocopherol (m/z 431 Da)

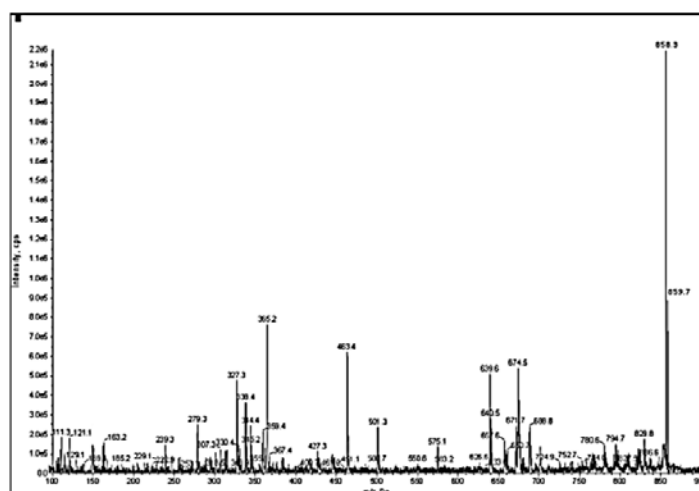


Figure 9. MS spectra of α -tocopherol in inclusion complex after decomposition (m/z 859 Da)

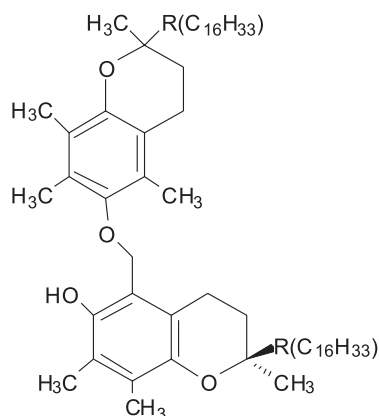


Figure 10. Proposed structure of α -tocopherol dimer

greater stability of tocopherol in the inclusion complex with 2-HP- β -CD than with β -CD. Most likely, the difference related to the greater hygroscopicity of HP- β -CD, which is an advantage from the viewpoint of water solubility but it is a disadvantage from the viewpoint of a given substance stabilization in the solid phase.

On the basis of the reaction rate constants and the Arrhenius relation it was possible to find a dependence between temperature and stability of α -T and α -T in inclusion complexes. This dependence was linear for α -T in InCs with both CDs. The energy of activation and changes in enthalpy and entropy were found from the parameters of the Arrhenius formula $\ln k = \ln A - (E_a/R) \cdot (1/T)$. The activation energy and enthalpy of α -T in inclusion complexes were higher than the corresponding values for the α -T (Table 4), which means that the uncomplexed α -T is more susceptible to temperature. Positive values of ΔH^\ddagger and negative values of ΔS^\ddagger confirm that the reaction of α -T decomposition both uncomplexed and in inclusion complexes is endothermic and the activation energy is greater for α -T in complexes.

Next, the samples of uncomplexed α -T and α -T in InCs with β -CD and 2-HP- β -CD treated with elevated temperature were studied by LC-ESI-MS/MS. The samples of α -T, and α -T in InCs with CDs not subjected to thermal heating were used as standards and the peak was found at m/z 431. However, on spectra of samples subjected to thermal decomposition the peak was detected at m/z 859 and was formed by the connection of two molecules of tocopherol. The same situation takes place for α -T as a substance and α -T in InCs with both CDs. The most probable structure of the dimer is presented in Figure 10 (25).

The results discussed above indicate that the α -T in inclusion complexes with CDs are more stable than the uncomplexed substance. The thermal decomposition of α -T in inclusion complexes with cyclodextrins proceeds according to the first order reaction. Cyclodextrins have a protective effect on α -T in the solid phase, which is higher for natural β -CD and lower for its 2-hydroxypropyl derivatives. The main decomposition product obtained in elevated temperature is α -tocopherol dimer. The improved stability of the tested substance in the obtained form results in new possibilities of a new pharmaceutical form of tablets with α -T.

CONCLUSIONS

1. In a stable phase inclusion complexes of α -T with β -CD and 2-HP- β -CD were produced by kneading and lyophilization. The identification of extracted products was carried out by a DSC, IR and $^1\text{H-NMR}$. The identity of both inclusion complexes has been confirmed.

2. A method of denoting the amount of α -T in inclusive complexes was HPLC, which had been subjected to validation previously. The method turned out to be the most useful.

3. The decomposition of α -T follows according to the simple first order reaction. The kinetic parameters like $t_{0.1}$ and $t_{0.5}$ indicate that cyclodextrins, both β -CD and 2-HP- β -CD, exhibit the protective influence on the α -T. $T_{0.1}$ for temperature 343 K increased by 400% for α -T in InC with β -CD and 64% for 2-HP- β -CD derivative.

4. Both β -CD and its 2-HP- β -CD derivative demonstrate the protective effect for α -T, after its inclusion to complexes, but β -CD effect was significantly greater.

5. The main product of α -T in inclusion complexes decomposition treated with an elevated temperature is α -tocopherol dimer.

REFERENCES

1. Van Hees T., Piel G., de Hassonville S.H., Evrard B., Delattre L.: *Eur. J. Pharm. Sci.* 15, 347 (2002).
2. Li J., Zhang M., Chao J., Shuang S.: *Spectrochim. Acta A Mol. Biomol. Spectrosc.* 73, 752 (2009).
3. Garnero C., Longhi M.: *J. Pharm. Biomed. Anal.* 45, 536 (2007).
4. Davis M.E., Brewster M.E.: *Nat. Rev. Drug Discov.* 3, 1023 (2004).
5. Chao J., Li J., Meng D., Huang S.: *Spectrochim. Acta A Mol. Biomol. Spectrosc.* 59, 705 (2003).

6. Loftsson T., Birna B.J., Olafsdottir J.: *Int. J. Pharm.* 67, R5 (1991).
7. Loftsson T., Jóhannesson H.R.: *Pharmazie* 49, 292 (1994).
8. Wanga G., Xuea X., Lib H., Wua F., Deng N.: *J. Mol. Catal. A: Chem.* 276, 143 (2007).
9. Schwartz A., Bar R.: *Appl. Environ. Microbiol.* 61, 2727 (1995).
10. Kobayashi N., DellaPenna D.: *Plant J.* 55, 607 (2008).
11. Kushi L.H., Folsom A.R., Prineas R.J., Mink P.J., Wu Y., Bostick R.M.: *N. Engl. J. Med.* 334, 1156 (1996).
12. Prasad K.N., Kumar B., Yan X.D., Hanson A.J., Cole W.C.: *J. Am. Coll. Nutr.* 22, 108 (2003).
13. Snyder R.M., Yu W., Jia L., Sanders B.G., Kline K.: *Nutr. Cancer* 60, 401 (2008).
14. Shun M.C., Yu W., Gapor A., Parsons R., Atkinson J., Sanders B.G., Kline K.: *Nutr. Cancer* 48, 95 (2004).
15. Almeida M.M., Alves J.M., Patto D.C., Lima C.R., Quenca-Guillen J.S., Santoro M.I., Kedor-Hackmann E.R.: *Int. J. Cosmet. Sci.* 31, 445 (2009).
16. Regiert M.: *SOFW Int. J. Appl. Sci.* 5, 10 (2005).
17. Uekama K., Horiuchi Y., Kikuchi M., Hirayama F.: *J. Incl. Phenom. Macrocycl. Chem.* 6, 167 (1988).
18. Iaconinoto A., Chicca M., Pinamonti S., Casolari A., Bianchi A., Scalia S.: *Pharmazie* 59, 30 (2004).
19. International Conference on Harmonization (ICH) Q2(R1) Validation of Analytical Procedures: Text and Methodology (2005).
20. Gierlach-Hładoń T., Lange K.: *Acta Pol. Pharm. Drug Res.* 69, 591 (2012).
21. Veiga I.F., Teixeira-Dias J.J.C., Kedzierewicz F., Sousa A., Maincent P.: *Int. J. Pharm.* 129, 63 (1996).
22. Chung H. Y.: *Prev. Nutr. Food Sci.* 12, 115 (2007).
23. Chung H.Y.: *Prev. Nutr. Food Sci.* 12, 131 (2007).
24. Hei S., Kim S.Y., Lee S.I., Lee Y. M.: *J. Ind. Eng. Chem.* 12, 50 (2006).
25. Krol S.E, Escalante J.D.D., Liebler C.D.: *Lipids* 36, 49 (2001).

Received: 12. 07. 2013

DETERMINATION OF NEOMYCIN IN THE FORM OF NEOMYCIN DERIVATIVE WITH DABSYL CHLORIDE BY THIN LAYER CHROMATOGRAPHY AND DENSITOMETRY

URSZULA HUBICKA, BARBARA ŻUROMSKA-WITEK, JOANNA PIOTROWSKA
and JAN KRZEK*

Department of Inorganic and Analytical Chemistry, Medical College of Jagiellonian University,
Medyczna 9, 30-688 Kraków, Poland

Abstract: A thin layer chromatographic–densitometric method has been developed for identification and quantitative determination of neomycin derivative with dabsyl chloride. The analysis of antibiotic was achieved on the silica gel TLC plates with fluorescent indicator with n-butanol – 2-butanone – 25% ammonia – water (10 : 6 : 2 : 2, v/v/v/v) as the mobile phase. The densitometric measurements were made at 460 nm. Under these conditions good separation of chosen aminoglycoside antibiotic from reagent used to make a complex was obtained. The method is characterized by high sensitivity, LOD from 0.1953 µg per band and LOQ from 0.5918 µg per band, wide linearity range from 0.5918 to 2.1960 µg per band for neomycin. The precision of the method was good; RSD varied from 1.17 to 2.05%. Satisfactory results of validation of the method were also confirmed by determination of selected antibiotic in pharmaceutical commercial preparation. The results obtained by TLC–densitometric method were compared with those obtained by spectrophotometric method.

Keywords: pharmaceutical research, neomycin, dabsyl chloride, TLC, densitometry

Neomycin is an aminoglycoside antibiotic that is produced naturally by the actinomycete bacterium *Streptomyces fradiae* via the fermentation process. It has bactericidal properties against Gram negative bacteria and partial also against Gram positive bacteria. Neomycin in a sulfate form is a common aminoglycoside indicated for treatment of gastrointestinal infections. Neomycin sulfate is mainly composed of the two isometric components neomycins B and C. The component B has higher antibiotic activity than component C (1). Neomycin is mostly administered in the form of powder, aerosols, creams and also drops and ointments often in complex preparations with bacitracin, dexamethasone, polymyxin, gramicidin, hydrocortisone, fluocinolone, etc. (2, 3, 4).

There are several methods described for the determination of neomycin in pharmaceutical preparations: colorimetric determination (5), fluorimetric determination (6), near-infrared spectroscopy (7) and spectrophotometric determination (8, 9). Some of the most popular methods are chromatographic methods: liquid chromatography with varied methods of detection like HPLC–PED (pulsed electro-

chemical detection) (10, 11), HPLC–ELSD (Evaporative Light Scattering Detection) (12), HPAE–IPAD (High-performance anion-exchange chromatography with integrated pulsed amperometric detection) (13) and thin layer chromatography (14, 15).

Pendela et al. described the analysis of ear drops containing neomycin sulfate, polymyxin B sulfate and dexamethasone sodium phosphate using liquid chromatography with pulsed electrochemical detection on a gold electrode (10). The similar study was performed to a formulation, which contained neomycin sulfate, polymyxin B sulfate and gramicidin (11). HPLC–ELSD method was applied successfully for the determination of neomycin and sulfate in raw materials, pharmaceutical formulations (powder, aerosols and creams) and medicated animal feeds (12). HPAE–IPAD was used to determine neomycin B and its impurities. The method was shown to be rugged for the intended application of neomycin identity, purity and assay (13). A thin layer chromatography with densitometric detection for simultaneous identification and quantitative determination of neomycin sulfate, polymyxin B sulfate, zinc

* Corresponding author: e-mail: jankrzek@cm-uj.krakow.pl

bacitracin and methyl and propyl hydroxybenzoate in ophthalmic ointment was described by Krzek et al. (14). Hubicka et al. described the analysis of amikacin, gentamicin, kanamycin, neomycin, netilmycin and tobramycin in pharmaceutical preparations (tobramycin ampoules, amikacin vials, tablets containing 250 mg of neomycin and eye drops containing 3 mg/mL of gentamicin) (15). The densitometric measurements were made after detection with a 0.2% ninhydrin solution in ethanol (14, 15).

Anionic capillary isotachopheresis (cITP) with conductometric detection was used for indirect determination of neomycin trisulfate as sulfate anion in pharmaceutical preparations (16, 17). Capillary electrophoresis with direct (18) and indirect (19, 20) UV detection for simultaneous determination of neomycin sulfate and such active substances as hydrocortisone, polymyxin in various pharmaceutical preparations have been reported (18–20).

Since 1975, dabsyl chloride (DBS) has been used for identification of N-terminal amino acid in polypeptide chain during analysis of compounds containing amine group (21). The first step in the process is condensation of DBS with polypeptide through N-terminal amino acid. The second step is hydrolysis in acidic environment that results in a product – sulfonamide derivative. The final third step is chromatographic identification of obtained product. This reaction is highly sensitive (10^9 – 10^{10} mol/L). For example, biogenic amines, bisoprolol, labetalol, and propafenone as dabsyl derivatives were determined (22–25).

The quantitative determination of bacitracin after condensation reaction with DBS was presented by Krzek and Piotrowska. Modification in the method of N-terminal amino acid determination with the use of DBS was done by exclusion of hydrolysis and establishing reaction conditions to enable direct spectrophotometric estimation of the product of DBS reaction with the antibiotic (26).

In this paper a new TLC–densitometric method was developed for the simultaneous identification and quantitative determination of neomycin derivative with dabsyl chloride (NDC), directly without the requirement of chromatogram visualization. The developed method was validated and used for the quantitative determination of neomycin in pharmaceutical preparation.

EXPERIMENTAL

Reagents

Acetone, sodium carbonate, sodium bicarbonate, 25% ammonia, butanol, 2-butanone were of

analytical grade and were purchased either from POCh (Gliwice, Poland) or Chempur (Piekary Śląskie, Poland).

Dabsyl chloride (DBS) – assay = 97.5% (AT) no. 39068 (Fluka, Chemie AG Buchs, Switzerland). Solutions of DBS in acetone were prepared at concentrations 0.3238 mg/mL and 0.1619 mg/mL.

Standard solutions and substance

The following pharmaceutical raw material of neomycin sulfate was used: 25 g PPH Galfarm – no. 011209. Neomycin met the requirements described in a monograph in Polish Pharmacopoeia (FP VIII) within the scope of identity, purity and biological activity. Standard solutions in water were prepared at concentrations from 1.8603 to 0.1970 mg/mL calculated on neomycin.

Pharmaceutical preparation and solution

Neomycinum – tablets (250 mg neomycin sulfate, macrogol 4000, sodium starch glycolate type A, talc, magnesium stearate, saccharose about 260 mg in one tablet). Polfa Tarchomin S.A., Poland, series No. 1010904.

A solutions of Neomycinum – to prepare sample solution from powdered mass of 20 tablets, 50.10 mg corresponding to 15.52 mg of neomycin was accurately weighed. Then, 15.0 mL of water was added into the sample and the solution was shaken for 15 min. Then, the solution was filled up with water to 25.0 mL. The suspension was filtered directly into a 25.0 mL volumetric flask through qualitative filter paper. For testing by spectrophotometric method, the solution of neomycin at a concentration of 1.8600 mg/mL was prepared similarly.

TLC method

Preparation of neomycin derivative with dabsyl chloride (NDC)

A product of reaction was formed when 0.5 mL of neomycin solution was mixed with 1.0 mL of DBS (0.1619 mg/mL) and 0.2 mL of carbonate buffer (pH = 9.0). The samples and blank solution were heated up in water bath at 70°C for 15 min, and then cooled down and adjusted with acetone to the final volume of 5.0 mL. A blank solution containing identical volume of carbonate buffer (pH = 9.00) and DBS concentration as in the study sample was prepared.

TLC analysis

TLC was performed on 10 × 12 cm TLC plates cut from 20 × 20 cm aluminium foil-backed plates precoated with silica gel 60 F₂₅₄ (Merck, Germany;

#1.05548). Solutions of the NDC obtained for standard solutions and for preparation solution (30 μL) were applied to the plates as 0.8 cm bands, 1.0 cm from the bottom edge, 1.0 cm from the sides and 0.8 cm apart, by use of a Linomat V sample applicator (Camag, Switzerland). Chromatograms were developed to a distance of 12 cm with n-butanol – 2-butanone – 25% ammonia – water (10 : 6 : 2 : 2, v/v/v/v) as a mobile phase in a chromatographic chamber (18 \times 9 \times 18 cm Sigma-Aldrich, USA, #Z20,415-3). The mobile phase was chosen experimentally by checking different solvent mixtures. Plates were dried at room temperature for one hour. Bands on the chromatograms retain durable yellow color within 24 h. Color of bands contrasts with a white background of chromatogram. Bands were visible and could be used for quantitative densitometric determination. Detection was carried out by Camag TLC Scanner 3 with winCats 1.3.4 software at $\lambda = 460$ nm; this wavelength was selected on the basis of the recorded absorption spectra. In addition to the R_f values, identification of analyzed substances were done. Peak areas of NDC obtained for standard solutions and for preparation solution were recorded directly from the chromatograms and were used for quantitative analysis.

Method validation

The method was validated by checking the specificity, linearity, precision, recovery, limits of detection and quantification and also robustness in accordance with ICH guidelines (27).

Specificity

Specificity of the method was assessed by comparing chromatograms of NDC obtained for standard solutions and for preparation solution, chromatogram of blank solution and blank chromatogram.

In obtained chromatograms, the retardation factor (R_f) values of analyzed substances, resolution factor, peak areas, peak purity and spot color were taken into account. Resolution factor (R_s) was calculated according to the formula:

$R_s = 2 \times (\text{distance between the centers of two adjacent spots}) / (\text{sum of the two spots in the direction of development})$.

Linearity

The calibration plot for the method was constructed by analysis of seven solutions containing different concentrations of neomycin in the range 0.1970 – 0.7320 mg/mL after reaction with dabsyl chloride. Preparation of samples working solutions were described before. Further analytical procedure

was described in “TLC analysis”. Linearity was assessed in triplicate on the basis of the relationship between mean peak area and amount of neomycin in micrograms per band. Linearity was reported as regression equations, correlation coefficients (r) and determination coefficient (r^2).

The limit of detection (LOD) and quantification (LOQ)

Solutions of neomycin in the form of derivative with DBS (0.1220 – 0.3660 mg/mL) were applied on the plates. LOD and LOQ were calculated on the basis of the slope (a) of the calibration line and the standard error of the estimate (S_e), using formulas:

$$\text{LOD} = 3.3 S_e / a \text{ and } \text{LOQ} = 10 S_e / a.$$

Precision

The repeatability of the method was determined by analysis of five replicates of NDC obtained for standard solutions from individual weighings. Study was done for three concentration levels, 50% (0.5918 μg per band of NDC), 100% (1.0980 μg per band of NDC) and 150% (1.6470 μg per band of NDC). Intermediate precision was obtained by analysis of solutions at the same concentration by a different analyst who performed the analysis over a period of one week.

Accuracy

Accuracy was assessed by determination of the recovery (%) of the drug. Precisely known weighed amounts of the neomycin standard (from 80 to 120% of the declared content) were added to preparation solutions and percentage recovery was calculated on the basis of the determined amounts of added neomycin standard under conditions of developed method in relation to the amount weighed. For each level three determinations were done.

Robustness

Under conditions of the developed method, comparison of results with change of stationary phase from TLC (Merck, Germany) to TLC (polyester sheets precoated with silica gel 60 F₂₅₄ Macherey-Nagel, Germany; #805023) plates was done.

The impact of small changes of 25% ammonia in the composition of the mobile phase ($\pm 5\%$) for chromatographic separation was checked.

Determination of neomycin in pharmaceutical preparation

Determination of neomycin in tested tablets was carried out according to earlier described proce-

dure. The amount of 0.9150 μg per band of NDC obtained for standard solution and preparation solution were applied onto TLC plates for the determination of neomycin content. For each determination three measurements were performed and the mean value was taken for calculations.

Spectrophotometric method

In order to compare the test results obtained by TLC method for the determination of neomycin, spectrophotometric method was performed (26). The method was validated in accordance with ICH guidelines (27). The obtained results were used for statistical evaluation.

Formation of neomycin derivative with dabsyl chloride

A product of reaction was formed when 0.2 mL of neomycin solution (0.6100 mg/mL) in water was mixed with 1.2 mL of DBS solution (0.3238 mg/mL) and 0.2 mL of carbonate buffer (pH = 9.0), heated up at 70°C for 15 min, then cooled down to 25°C, 0.5 mL of distilled water added and adjusted with acetone to the final volume of 5.0 mL. A reference material containing identical volume of carbonate buffer (pH = 9.00) and DBS concentration as in the studied sample was prepared for each individual sample. Absorbance at 492 nm was measured by use of a UV/Vis spectrophotometer (Varian Cary 100 Conc.) in relation to appropriate reference material.

Determination of neomycin in pharmaceutical preparation

Determination of neomycin in tested tablets after formation of neomycin derivative with dabsyl

chloride was carried out according to earlier described procedure. For this purpose, a series of six solutions containing DBS with neomycin preparation solution at a concentration of 1.8600 mg/mL were prepared. Then, the content of neomycin in pharmaceutical preparation was calculated by comparing appropriate values of absorbance recorded at $\lambda_{\text{max}} = 492$ nm for standard and sample solutions.

RESULTS AND DISCUSSION

Reaction of free amine groups with DBS was used for the development of a new TLC method for the determination of neomycin in pharmaceutical preparation. In the first stage of studies, conditions for the separation of NDC and DBS were established (Fig. 1).

The mobile phase n-butanol – 2-butanone – 25% ammonia – water (10 : 6 : 2 : 2, v/v/v/v) enables good resolution of analyzed substances. NDC on TLC chromatogram appeared as a compact yellow band, which contrasts with the white background of the plate and its R_F value was 0.22. The NDC bands were stable after application to the plate for 24 h. Next to the NDC, band of DBS ($R_F = 0.53$) appeared in chromatogram and didn't interfere with the band of tested complex (Fig. 2).

The application of densitometric detection demonstrated that peaks in the chromatograms were well resolved, symmetrical and easy to identify and determine. Registration of peak areas for NDC was carried out at $\lambda = 460$ nm. The analytical wavelength chosen for densitometric registration corresponded to absorption maximum for NDC.

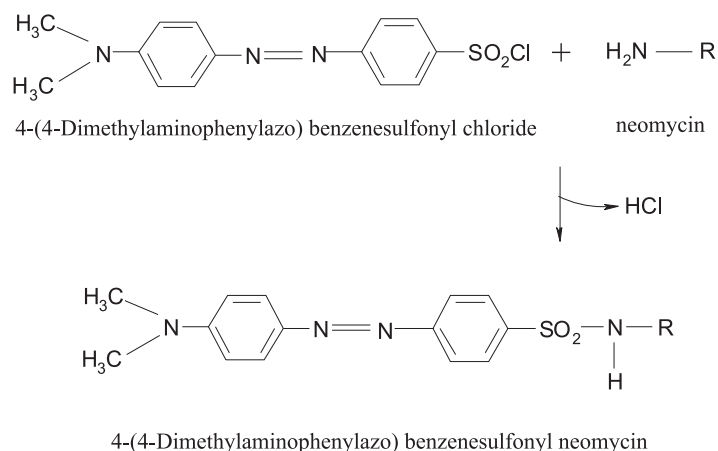


Figure 1. Scheme of synthesis of neomycin derivative

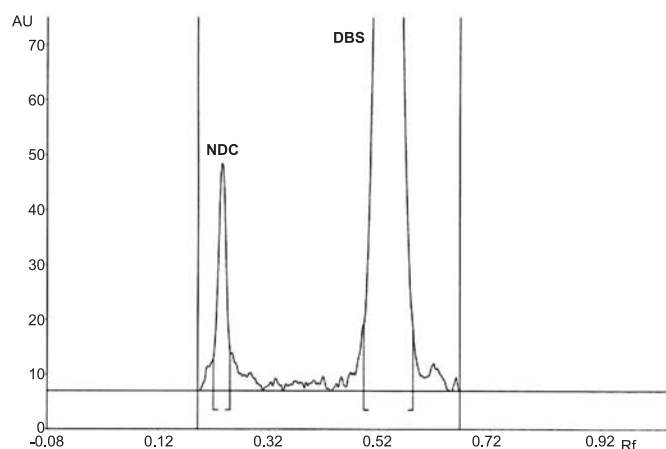


Figure 2. Densitogram of neomycin derivative with dabsyl chloride (NDC) and dabsyl chloride (DBS)

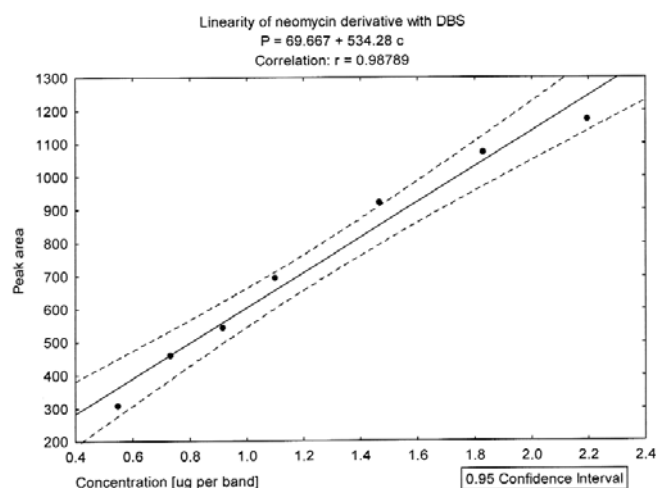


Figure 3. Linear relationship between peak area and concentration of NDC.

In the available literature there were some papers describing the determination of neomycin by thin-layer chromatography, where densitometric detection of neomycin was performed after previously spraying with a ninhydrin solution (14, 15). Application of ninhydrin required complete evaporation of ammonia (mobile phase component) from the stationary phase by heating plates at 100°C for about 1.5 h. The research presented in this paper revealed that the developed method for the determination of neomycin in the form of color derivative with DBS may be an alternative to time consuming method using ninhydrin solution for the visualization of chromatograms.

For estimation of reliability of the developed method according to ICH recommendations, the following parameters were determined: specificity, linearity, limits of detection and quantitation, recovery and robustness (27).

The developed method was specific against the studied components. There are no peaks in chromatogram recorded for blank solution, chromatograms of NDC obtained for standard solutions and for preparation solution and blank chromatogram where studied components occur. Good correlation between VIS spectra acquired from the standard and the pharmaceutical preparation indicated that NDC spot was free of any interference that

Table 1. The results of validation of TLC and spectrophotometric method.

Parameter	TLC – densitometry	VIS spectrophotometry
R_F	0.20 ± 0.03 –	
Limit of detection	0.1953 µg per band	1.48·10 ⁻³ mg/mL
Limit of quantitation	0.59 µg per band	4.48·10 ⁻³ mg/mL
Linearity range	0.59 – 2.20 µg per band	4.48·10 ⁻³ – 2.46·10 ⁻³ mg/mL
Regression coefficients $P = a c + b \pm S_c$	a = 534.28 b = 69.667 ± 55.29	a = 23.673 b = -0.0357 ± 0.01679
Standard deviation of the regression coefficients	$S_a = 37.52$ $S_b = 51.51$	$S_a = 0.709$ $S_b = 0.0106$
Correlation coefficient, r	r = 0.9879	r = 0.9969
Determination coefficient r ²	r ² = 0.9759	r ² = 0.9938
Precision n = 5 level 50%: level 100%: level 150%:	$x_m = 263.68$ RSD = 1.70% $x_m = 637.84$ RSD = 1.44% $x_m = 1026.26$ RSD = 1.17%	$x_m = 95.94\%$ RSD = 2.92% $x_m = 96.75\%$ RSD = 2.23% $x_m = 103.26\%$ RSD = 1.89%
Intermediate precision n = 5 level 50%: level 100%: level 150%:	$x_m = 228.10$ RSD = 2.05% $x_m = 743.42$ RSD = 2.01% $x_m = 1062.44$ RSD = 1.27%	$x_m = 100.22\%$ RSD = 3.38% $x_m = 99.98\%$ RSD = 3.30% $x_m = 99.60\%$ RSD = 2.04%
Recovery, (%) n = 3 level 80%: level 100%: level 120%:	101.48% RSD = 2.65% 101.26% RSD = 2.07% 100.97% RSD = 2.40%	105.31% RSD = 0.89% 97.29% RSD = 2.11% 97.75% RSD = 1.74%

P – peak area; c – concentration [µg per band]; a and b – regression coefficients, S_c – standard error of the estimate, S_a – standard deviation of the slope a, S_b – standard deviation of the intercept, x_m – arithmetic mean; RSD – relative standard deviation.

Table 2. The results of neomycin determination in pharmaceutical preparation with statistical evaluation.

Preparation	Declared concentration	Determined concentration	
		TLC method	Spectrophotometric method
Neomycinum (tablets)	250 mg	$x_m = 253.15$ SD = 5.2908 RSD = 2.09%	$x_m = 254.70$ SD = 2.5145 RSD = 2.47%
		Fisher-Snedecor test: $F_{obs} = 4.43$; $F_{1-\alpha} = 5.05$ for $f = 5$, $\alpha = 0.05$ $F_{obs} < F_{1-\alpha}$ statistically insignificant	

f – number of degrees of freedom, α – significance level, SD – standard deviation, RSD – relative standard deviation, F_{obs} – calculated experimental value; $F_{1-\alpha}$ – critical value from the Snedecor law table.

might be present in the analysis. Resolution of the peaks appearing in the chromatograms was 3.94.

A plot of concentration against mean peak area of NDC was linear over the range from 0.5918 µg per band to 2.1960 µg per band. The correlation coefficient (r) and determination coefficient (r²) obtained for significance level 0.05 and n = 7 were close to 0.99 that proved a highly significant linear correlation (Fig. 3). The y-intercept of the linear equation for NDC was statistically insignificant.

The regression equation of the calibration plot, values of standard deviation of the slope (S_a), standard deviation of the intercept (S_b) and standard error of the estimate (S_c) are presented in Table 1.

Based on parameters of the curve ($P = -25.48 + 650.27C$, $r = 0.9846$ and $S_c = 38.48$), in low range of concentrations, the LOD and LOQ (µg per band) values were 0.1953 and 0.5918, respectively. These low values indicated satisfactory sensitivity of the method.

Accuracy of the method expressed as % recovery at three concentration levels was from 100.97 to 101.48%. Good precision and intermediate precision with % RSD less than 2.10% was observed. Detailed results are presented in Table 1. In all the deliberately varied chromatographic conditions (composition of the mobile phase, change of stationary phase), the retention parameters of NDC remained unchanged.

The usefulness of the method was examined by determination of neomycin in the tablets. There was no influence of additional components present in tested preparation such as macrogol, sodium starch glycolate type A, talc, magnesium stearate, sucrose and the components of the substrate on the determination results. Satisfactory results of the quantitative determination were obtained, which were characterized by good repeatability of measurements (RSD = 2.09%). The concentration determined by the developed method was comparable to the results obtained by spectrophotometric method (Table 2).

The results of determination of neomycin obtained by TLC and spectrophotometric methods were analyzed statistically using Fisher-Snedecor test (Table 2). The calculated experimental value F_{obs} for TLC and spectrophotometric methods were compared with the critical value: $F_{1-\alpha}$ (for $f = 5$, $\alpha = 0.05$), extracted from the Snedecor law table. Based on the results of statistical analysis ($F_{obs} > F_{1-\alpha}$) it was found that the compared methods were not different considering precision in statistically significant way.

CONCLUSIONS

In reaction of neomycin with DBS a yellow complex of neomycin derivative was formed which can be used in direct TLC–densitometric analysis at $\lambda = 460$ nm.

The method meets the acceptance criteria for validation and may be useful for the determination of neomycin in the form of derivative with DBS in pharmaceutical products.

REFERENCES

1. Zejc A., Górczyca M. Chemistry of Drugs (Polish), PZWL, Warszawa 2002.
2. Bonomo R.A., Van Zile P.S., Li Q., Shermock K.M., McCormik W.G., Kohut B.: Expert Rev. Anti Infect. Ther. 5, 773 (2007).
3. Sheth V.M., Weitzul S.: Dermatitit 19, 181 (2008).
4. Gennaro A.R. Ed.: Remington's Pharmaceutical Sciences, 17th edn., p. 1181, Mack Publ., Easton, PA 1985.
5. Amin A.S., Issa Y.M.: Spectrochim. Acta A 59, 663 (2003).
6. El-Shabrawy V.: Spectrosc. Lett. 35, 99 (2002).
7. Cruz Sarraguça M., Oliveira Soares S., Almeida Lopes J.: Vib. Spectrosc. 56, 184 (2011).
8. Confinop M., Bontchev V, P.: Microchim. Acta 102, 305 (1990).
9. Marques M.R.C., Hackmann E.R.M., Saito T.: Anal. Lett. 23, 1005 (1990).
10. Pendela M., Adams E., Hoogmartens J.: J. Pharm. Biomed. Anal. 36, 751 (2004).
11. Adams E., Schepers R., Gathu L.W., Kibaya R., Roets E., Hoogmartens J.: J. Pharm. Biomed. Anal. 15, 505 (1997).
12. Megoulas N.C., Koupparis M.A.: J. Chromatogr. A 1057, 125 (2004).
13. Hanco V.P., Rohrer J.S.: J. Pharm. Biomed. Anal. 43, 131 (2007).
14. Krzek J., Starek M., Kwiecień A., Rzeszutko W.: J. Pharm. Biomed. Anal. 24, 629 (2001).
15. Hubicka U., Krzek J., Woltyńska H., Stachacz B.: J. AOAC Int. 92, 1068 (2009).
16. Kurzawa M., Jastrzębska A., Szłyk E.: Chem. Pap. 63, 255 (2009).
17. Kurzawa M., Jastrzębska A., Szłyk E.: Acta Pol. Pharm. Drug Res. 62, 163 (2005).
18. Huidobro A.L., García A., Barbas C.: J. Pharm. Biomed. Anal. 49, 1303 (2009).
19. Srisom P., Liawruangrath B., Liawruangrath S., Slater J.M., Wangkam S.: J. Pharm. Biomed. Anal. 43, 1013 (2007).
20. Ackermans M.T., Everaerts F.M., Beckers J.L.: J. Chromatogr. 606, 229 (1992).
21. Lin J.-K., Chang J.-Y.: Anal. Chem. 47, 1634 (1975).
22. Romero R., Bagur M.G.; Sánchez-Viñas M., Gázquez D.: Chromatographia 51, 404 (2000).
23. Romero R., Sánchez-Viñas M., Gázquez D., Bagur M.G., Cuadros-Rodríguez L.: Chromatographia 53, 481 (2001).
24. Castillo M.A., Castells R.C.: Chromatographia 54, 711 (2001).
25. Witek A., Hopkala H., Matysik G.: Chromatographia 50, 41 (1999).
26. Krzek J., Piotrowska J.: Acta Pol. Pharm. Drug Res. 68, 853 (2011).
27. ICH-Q2 (R1) Validation and Analytical Procedures: Text and Methodology, International Conference on Harmonization, Geneva, November 2005: <http://www.ich.org>.

Received: 5, II, 2013

EFFECT OF CHROMATOGRAPHIC CONDITIONS ON RETENTION BEHAVIOR AND SYSTEM EFFICIENCY FOR HPTLC OF SELECTED PSYCHOTROPIC DRUGS ON CHEMICALLY BONDED STATIONARY PHASES

ANNA PETRUCZYNIK, KAROL WRÓBLEWSKI and MONIKA WAKSMUNDZKA-HAJNOS*

Department of Inorganic Chemistry, Medical University of Lublin, Staszica 4a, 20-093 Lublin, Poland

Abstract: Selected psychotropic drug standards have been chromatographed on RP18, CN and diol layers with a variety of aqueous and nonaqueous mobile phases. The effect of buffers at acidic or basic pH, acetic acid, ammonia and diethylamine (DEA) in aqueous mobile phases on retention, efficiency and peak symmetry was examined. Improved peak symmetry and separation selectivity for investigated compounds were observed when ammonia or DEA were used as mobile phase additives. The effect of diethylamine concentration in aqueous eluents on retention, peak symmetry and theoretical plate number obtained on CN plates was also investigated. Because of the strong retention of these basic drugs on stationary phases bonded on silica matrix, nonaqueous eluents containing medium polar diluents, strongly polar modifiers and silanol blockers (ammonia or diethylamine) were applied. Aqueous and nonaqueous eluent systems with the best selectivity and efficiency were used for separate psychotropic drug standards' mixture on CN layer by 2D TLC.

Keywords: HPTLC, psychotropic drugs, system efficiency, 2D-TLC

Psychotropic drugs are prescribed to treat a variety of mental health problems when these problems cause significant impairment to healthy functioning. Psychotropic drugs typically act by changing the secretion of important chemicals in the brain called neurotransmitters. This group of drugs is one of the most toxic groups among different groups of substances used in medicine. In case of poisoning by them, there are serious health and life hazards. Diagnostics of poisoning by psychotropic drugs, determination of their content in pharmaceutical preparations and monitoring of their concentration in biological fluids have special significance.

Different chromatographic techniques play an important role in the analysis of these drugs e.g., gas chromatography (GC) (1, 2), high performance liquid chromatography (HPLC) (3–5), thin layer chromatography (TLC) (6, 7). TLC is particularly useful for rapid analysis of large number of samples.

Most often, psychotropic drugs have been analyzed by TLC on silica gel with mobile phase of high eluent strength containing e.g., mixture of toluene and methanol (6, 8), butanol, acetic acid and water (9), methanol, toluene and acetic acid (10),

methanol and chloroform (7), acetone, methanol and triethylamine (11), hexane, dioxane and propylamine (12), ethyl acetate, methanol and ammonia (13), methanol, toluene, ammonia (14), ethanol, hexane, ammonia (15).

Alkyl bonded plates were also used for analysis of these drugs e.g., on C18 layers with eluent system containing tetrahydrofuran and phosphate buffer at pH 9.0 (12), on C8 layers eluted with tetrahydrofuran and phosphate buffer at pH 3.5 (16).

Rarely, these compounds were chromatographed on other chemically bonded stationary phases e.g., on aminopropyl (NH₂) and cyanopropyl (CN) layers with eluents containing acetone, diethylamine, dioxane, ethanol, isopropanol, or tetrahydrofuran in *n*-hexane (15). Some antidepressants were analyzed on CN plates in systems containing as mobile phases mixture of acetonitrile, ether, hexane or petroleum ether; diethyl ether, acetonitrile and ethyl methyl ketone (17).

Psychotropic drugs, which are basic compounds, caused a number of analytical problems – the peaks on chromatograms are asymmetric, the efficiency of systems is low, the reproducibility and

* Corresponding author: e-mail: monika.hajnos@umlub.pl; phone +48 81535 7378

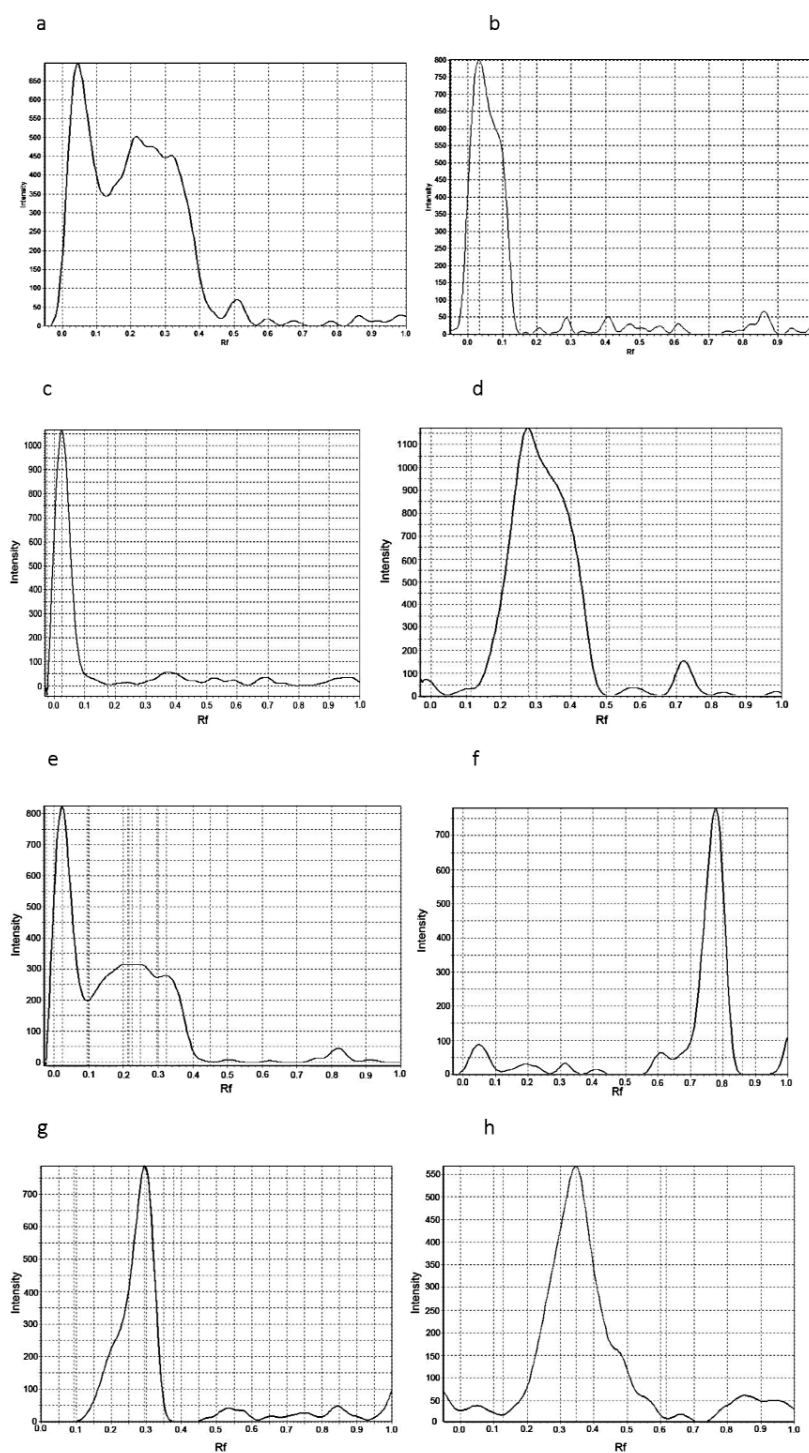


Figure 1. Densitograms of quetiapine chromatographed on HPTLC plates in different systems: a. C18/MeOH-H₂O (60 : 40, v/v); b. CN/MeOH-H₂O (60 : 40, v/v); c. C18/MeOH-H₂O (70 : 30, v/v) buffered with acetate buffer at pH 3.5; d. CN/MeOH-H₂O (70 : 30, v/v) buffered with acetate buffer at pH 3.5; e. C18/MeOH-H₂O (70 : 30, v/v) buffered with ammonium buffer at pH 8.3; f. CN/MeOH-H₂O (70 : 30, v/v) buffered with ammonium buffer at pH 8.3; g. C18/MeOH-H₂O (70 : 30v/v) containing 1% acetic acid; h. CN/MeOH-H₂O (70 : 30, v/v) containing 1% acetic acid.

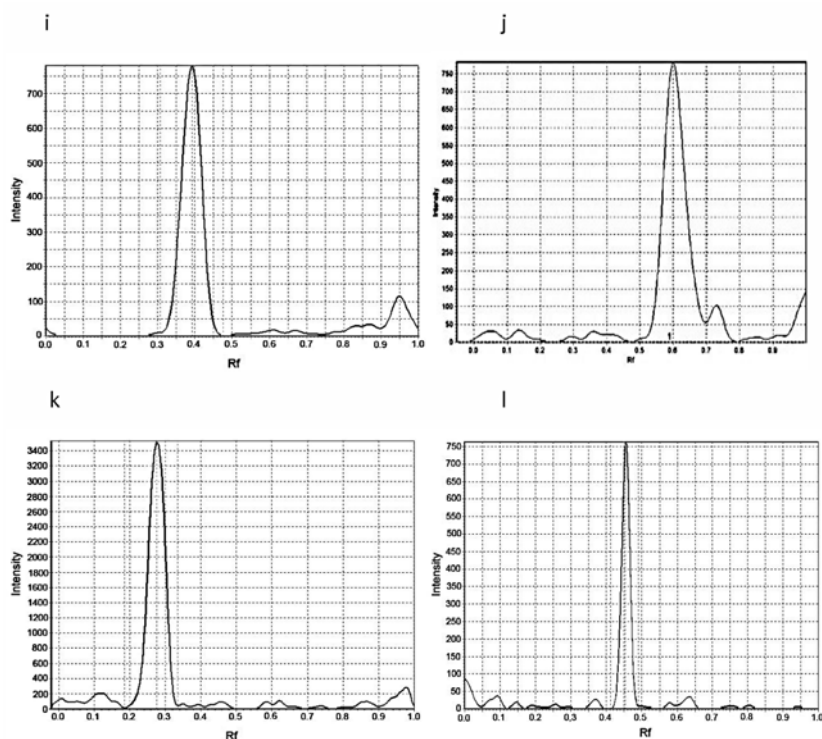


Figure 1. cont.: i. C18/MeOH-H₂O (80 : 20, v/v) containing 1% ammonia; j. CN/MeOH-H₂O (80 : 20, v/v) containing 1% ammonia; k. C18/MeOH-H₂O (80 : 20, v/v) buffered with acetate buffer at pH 3.5 containing 0.05M DEA; l. CN/MeOH-H₂O (80 : 20, v/v) buffered

selectivity of the separation can often be unsatisfactory. This is caused by the partial dissociation of these compounds in aqueous solutions and the different interactions of neutral and ionic form with the stationary phase residual silanols. For this reason, optimization of the chromatographic system for obtaining correct results is necessary.

The aim of this paper was an investigation of retention behavior of selected psychotropic drugs in normal-phase and reversed-phase systems on different chemically bonded stationary phases with various eluents. Influence of various composition of mobile phases on retention, peak shape, efficiency and separation selectivity of these drugs on C18, CN and diol stationary phases was investigated. Systems with the best parameters and highest selectivity were used for the analysis of psychotropic drug standards' mixtures. The application of the most selective systems in 2D-TLC separations of standards' mixture of investigated drugs has been also presented.

EXPERIMENTAL

HPTLC was performed on 10 × 10 cm glass plates precoated with 0.2 mm layer of RP-18F₂₅₄S,

CN F₂₅₄S, and diol F₂₅₄ produced by E. Merck (Darmstadt, Germany). Plates were developed face down to a distance of 9 cm from the origin at 20 ± 1°C in horizontal DS-chambers (Chromdes, Lublin, Poland).

Solvents: methanol (MeOH), acetonitrile (MeCN), tetrahydrofuran (THF), methyl ethyl ketone (MEK), diisopropyl ether (iPr₂O), diethylamine (DEA), and aqueous ammonia 25% were of HPLC grade produced by E. Merck. Acetic acid was of analytical grade produced by Polish Reagents (Gliwice, Poland). Bidistilled water was used as a component of aqueous solutions.

Photos of the plate were taken by the digital camera Kodak EasyShare C913. The treatment of the photographs was performed using the computer programme Sorbfil TLC.

Asymmetry factor (A_s) was calculated by the computer programme at 10% of peak height, theoretical plate number (N) was calculated from chromatograms using equation:

$$N = 16\left(\frac{z}{w}\right)^2$$

where: z – substance migration distance; w – peak width at base.

RESULTS AND DISCUSSION

The retention of 10 psychotropic drugs (Table 1) was investigated on RP18 plates with aqueous eluents, CN and diol plates by the use of aqueous and nonaqueous eluents.

The first experiments were performed on RP18 and CN plates with a mobile phase containing acetonitrile or methanol and water only. In mobile phases containing organic modifier and water, investigated psychotropic drugs – weak organic bases – are present in the ionized and neutral forms, which interact differently with active sites of the stationary phases. The ionized form interacts strongly with ionized free silanols, which causes tailing, and low efficiency of the chromatographic system. For this reason, poor spots shape, low system efficiency and separation selectivity were obtained. Figure 1a shows peaks obtained for quetiapine on RP18 and CN layers in eluent system containing mixture of methanol and water with a very bad shape.

In order to obtain better spot shapes, higher efficiency and improved separation selectivity, mobile phases containing different additives (such as: acetic acid, ammonia, buffers at different pH or diethylamine) were applied. The application of mobile phases containing organic modifier and acetate buffer at pH 3.5 on RP18 and CN adsorbents, where the silanol ionization was partially suppressed, caused an improvement of spot shapes, but they were still asymmetric for most of investigated compounds and some compounds were still strongly retained on RP18 plates e.g., quetiapine (Fig. 1b). The use of a mobile phase containing a buffer at pH 8.3 (Fig. 1c), when the dissociation of the analytes is partially suppressed, does not cause significant improvement of peak shapes and increase the system efficiency for most investigated drugs in comparison to a system containing the acidic buffer.

In the next series of experiments, the retention, peak symmetry, theoretical plate number on both tested adsorbents in systems containing aqueous mixtures of methanol or acetonitrile with addition of 1% acetic acid as mobile phase were examined (Fig. 1d). In this systems, a slightly better peak shapes and an increase of theoretical plate number, compared with a system with acidic buffer can be observed, however, the asymmetry factor for all investigated drugs was not in the optimal range of A_s values ($0.8 < A_s < 1.5$).

A significant improvement of the spot shapes and an increase of theoretical plate number was obtained on C18 and CN adsorbents in the eluent system with addition of 1% ammonia. The addition

of ammonia caused suppression of basic analytes' dissociation and blocking of free silanols. Good results were obtained by use both stationary phases and MeOH or MeCN as organic modifiers, but the most symmetric spots and highest system efficiency were obtained for mobile phases with ammonia on RP18 layers, when MeOH was used as organic modifier. Figure 1e depicts the peaks obtained for quetiapine on both adsorbents in this eluent system. Most symmetric spots were also obtained for olanzapine and lamotrigine.

Further improvement of efficiency, peak symmetry, and separation selectivity for psychotropic drugs on both adsorbents was obtained when DEA was added to the mobile phase. In Figure 1f, densitogram obtained for quetiapine on RP18 plate in eluent containing DEA additive is presented. DEA, as strong base, interacts with ionized silanols, blocking the interactions of these groups with the compounds analyzed. This explains why considerable improvement in peak symmetry, system efficiency, and often separation selectivity was observed in chromatographic systems containing amines.

The retention of psychotropic drugs on CN stationary phase as a function of DEA concentration (0.005–0.05 M) is presented in Figure 2. The increase of DEA concentration initially causes an increase of retention of most investigated drugs and then retention decreases, as an effect of silanols' blocking. Significant differences in retention for most investigated compounds were observed in range 0.005 – 0.02 M of DEA concentration. Further increasing of DEA concentration from 0.02 – 0.05 M does not cause distinct differences in retention. With the change of DEA concentration, the changes in separation selectivity can be also observed.

The increase of DEA concentration causes also the significant improvement of system efficiency and spot symmetry. In the system with 0.005 M of DEA $N/m > 5000$ were obtained only for venlafaxine and lamotrigine, while in the system with 0.04 or 0.05 M DEA, 6 or 7 drugs have $N/m > 5000$ and for other investigated compounds $N/m > 1000$. In most cases, increasing the concentration of diethylamine results in improvement of peak symmetry. In the concentration of 0.005 M DEA, only six investigated drugs have the acceptable asymmetry factors. In chromatographic system with mobile phases containing 0.03–0.05 M DEA, symmetry of spots was acceptable for all investigated compounds and for nine of compounds it was excellent ($0.9 > A_s > 1.2$). In the next series of experiments, the effects of composition of nonaqueous mobile phases on retention, spot shape and system efficiency on CN and diol

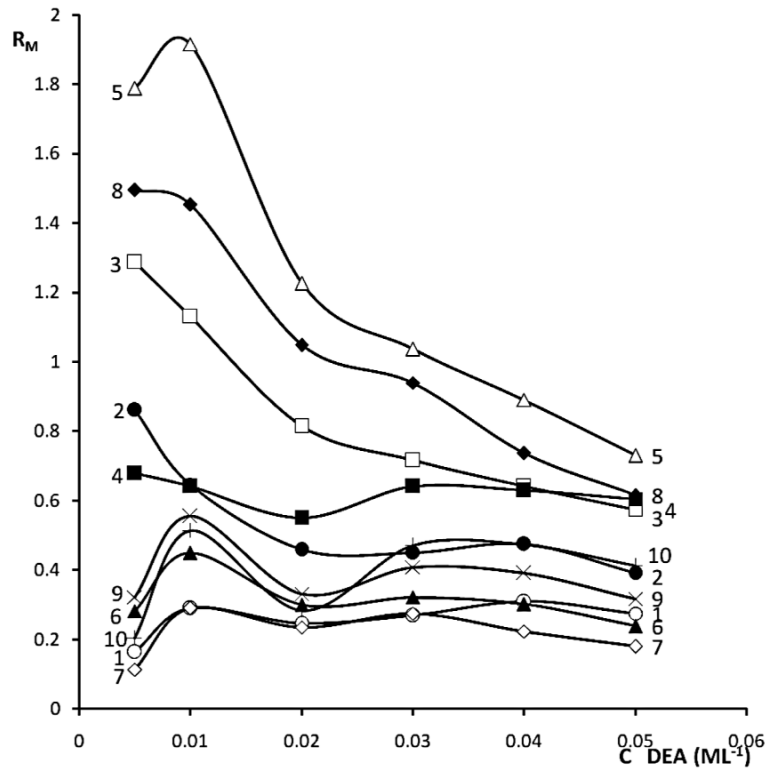


Figure 2. Relationships between R_M and DEA concentration in mobile phase for psychotropic drugs. System: CN, MeOH-H₂O (80 : 20, v/v) buffered with acetate buffer at pH 3.5 containing 0.005 – 0.05 M DEA

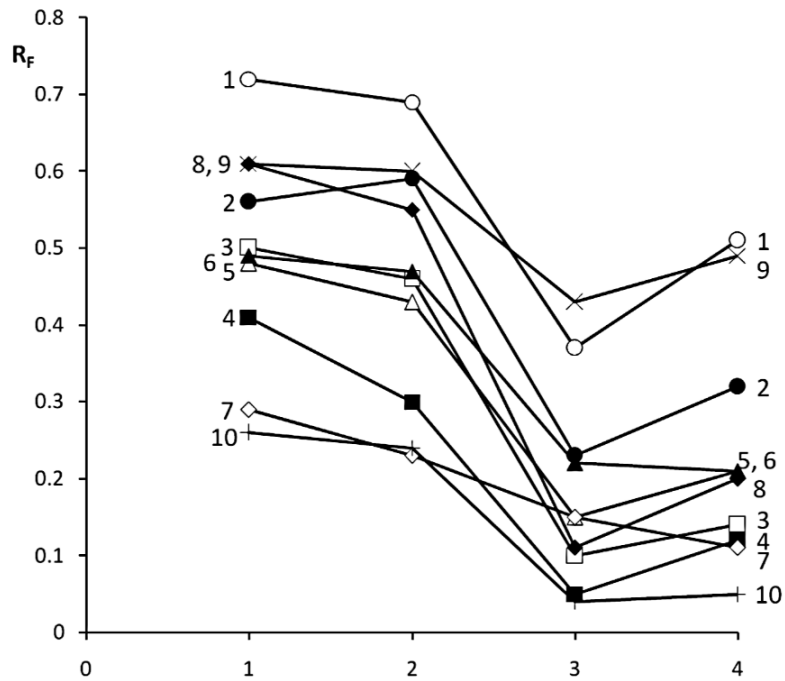


Figure 3. Graphical comparison of R_F values obtained for psychotropic drugs in chromatographic systems: 1. CN; 10% MeOH + 5% MEK + iPr₂O + 1% ammonia; 2. CN; 15% MeOH + iPr₂O + 1% ammonia; 3. Diol; 10% MeOH + 5% MEK + iPr₂O + 1% ammonia; 4. CN; 15% MeOH + iPr₂O + 1% ammonia

Table 1. Structure of the investigated compounds.

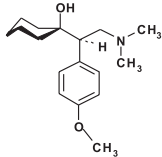
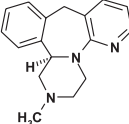
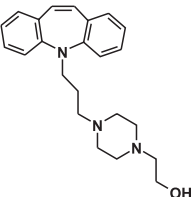
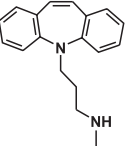
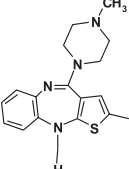
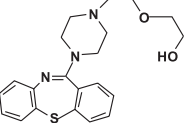
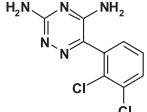
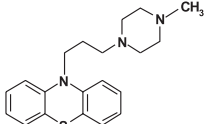
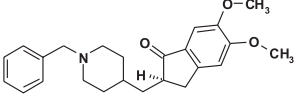
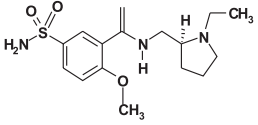
	Name of compound	Structure
1	Venlafaxine	
2	Mirtazapine	
3	Opi Pramole	
4	Desipramine	
5	Olanzapine	
6	Quetiapine	
7	Lamotrigine	
8	Perazine	
9	Donazepil	
10	Sulpiride	

Table 2. Asymmetry factor (A_s) and theoretical plate number (N/m) values for investigated psychotropic drugs obtained on CN or diol plates in different nonaqueous eluent systems.

No.	CN 10% MOH + 5% MEK + iPr ₂ O + 1% ammonia		CN 15% MOH + iPr ₂ O + 1% ammonia		Diol 10% MOH + 5% MEK + iPr ₂ O + 1% ammonia		Diol 15% MOH + iPr ₂ O + 1% ammonia	
	A_s	N/m	A_s	N/m	A_s	N/m	A_s	N/m
1	0.94	20530	1	52900	0.58	9360	0.55	10940
2	1.07	34840	1.08	50520	1.1	16330	0.71	15750
3	0.91	21950	0.92	30710	0.91	3670	0.83	3870
4	0.93	18680	0.85	10000	0.89	920	0.91	2840
5	0.86	25600	0.92	16980	0.9	9070	0.91	8710
6	0.92	41680	1	38350	0.91	13770	0.91	8160
7	0.92	13730	0.83	10450	0.91	5920	1	3440
8	0.92	26460	0.86	27780	0.82	3740	0.83	6940
9	1	54000	1.08	40000	0.92	36520	1	32940
10	1	7510	1	9400	0.71	1260	1	1110

stationary phases were examined. The investigated psychotropic drugs were strongly retained on cyanopropyl and diol phases, when nonaqueous eluents were used, and the use of strongly polar modifiers and diluents of medium polarity was necessary. With most binary solvent combinations such as MeOH, ethyl acetate (AcOEt), ethyl methyl ketone (EMK) as modifiers and dichloromethane or diisopropyl ether (iPr₂O) as diluents, the spots were wide and asymmetric.

For this reason, the use of DEA or ammonia, to reduce ion-exchange processes, was necessary. In the systems with addition of DEA to mobile phase containing mixture of MeOH and dichloromethane or iPr₂O, a slight improvement of peak shapes was observed, but they were still asymmetric. Similar results in chromatographic systems with DEA was obtained on diol layers. The addition of ammonia to mobile phase containing MeOH and dichloromethane on both stationary phases also does not improve symmetry of spots and system efficiency.

A significant improvement of peak symmetry, efficiency and separation selectivity for the compounds was achieved when ammonia was added to mobile phase containing MeOH or its mixture with MEK and iPr₂O on both CN and diol plates. The use of mixture of MeOH and MEK resulted in different separation selectivity compared to system containing only MeOH as a modifier. Large differences in separation selectivity of investigated drugs were obtained on both layers, e.g., in eluent containing

MeOH, MEK and ammonia. Venlafaxine and sulpiride or olanzapine and lamotrigine are eluted together on diol but are well separated on CN, while pipramol, olanzapine and quetiapine or perazine and donazepil are eluted together on CN but separated on diol stationary phase (Fig. 3).

A_s and N/m values for the psychotropic drugs chromatographed on CN and diol plates with nonaqueous mobile phases containing ammonia are presented in Table 2. The better spot shapes and especially greater system efficiency for most investigated compounds were obtained on CN plates. On CN stationary phase spots symmetry was acceptable for all investigated drugs, whereas when diol plates were used for eight drugs in two tested nonaqueous eluent systems with addition of ammonia the results are acceptable. On CN plate with eluent containing MEK for nine psychotropic drugs excellent A_s values were obtained. On CN plates in both eluents N/m > 10 000 were for nine, on diol plates only for three investigated compounds.

Good spot shape and system efficiency for investigated drugs were obtained in several chromatographic systems such as: C18 stationary phase with eluents containing mixture of MeOH, water and ammonia or MeOH, buffer pH at 3.5 and DEA; CN stationary phase with aqueous eluent containing MeOH, buffer pH at 3.5 and DEA or with nonaqueous eluents containing mixture of MeOH, iPr₂O and ammonia or MeOH, MEK, iPr₂O and ammonia; diol stationary phase with nonaqueous eluents contain-

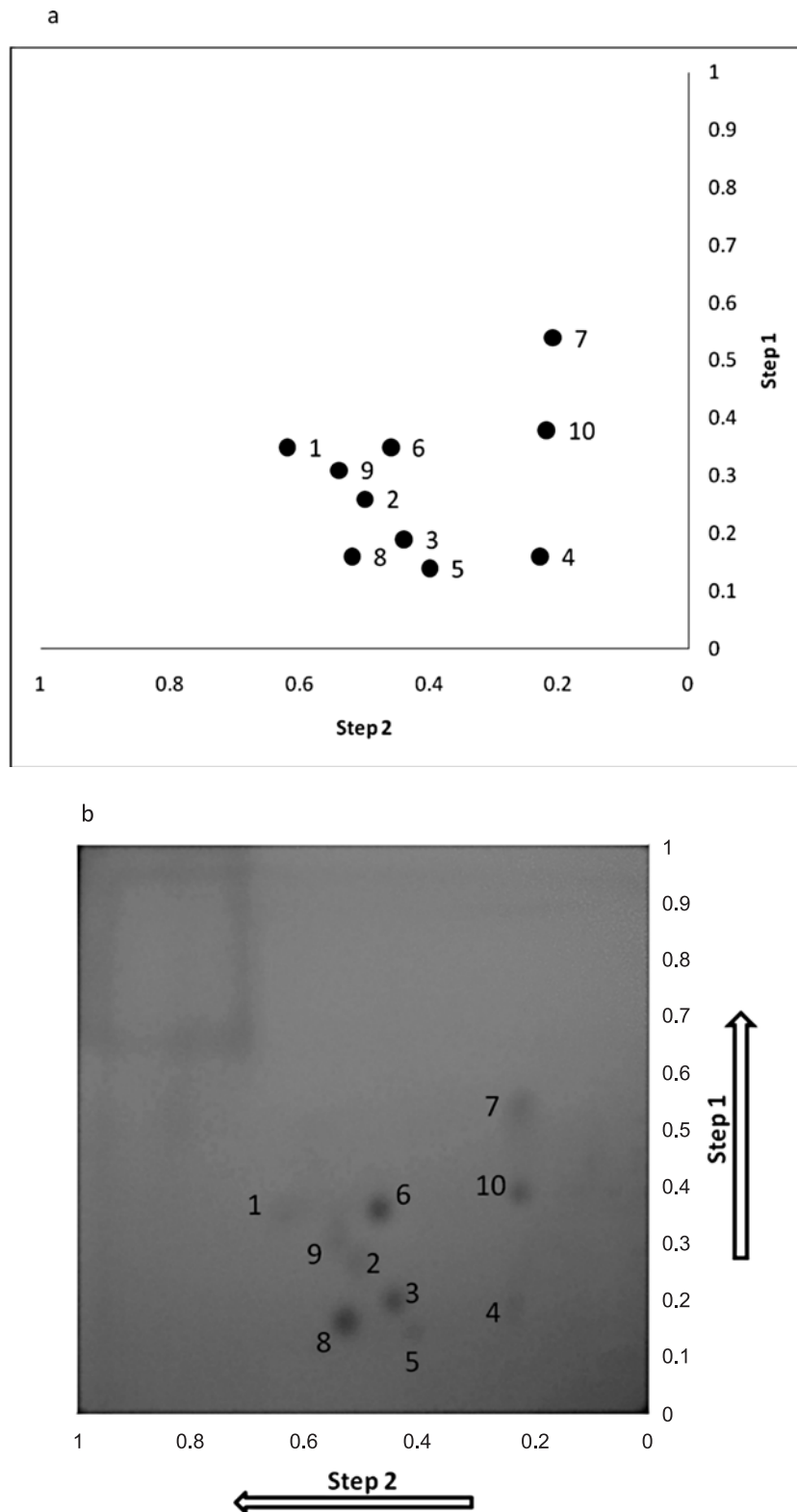


Figure 4. a. Correlation diagram of R_f values obtained in systems: I direction: CN; 80% methanol + acetate buffer at pH 3.5 + 0.05 M DEA; II direction: CN; 10% MeOH + 5% MEK + iPr_2O + 1% ammonia

b. Photo of the 2D-TLC chromatogram of psychotropic drug standards at $\lambda = 254$ nm obtained in systems: I direction: CN; 80% methanol + acetate buffer at pH 3.5 + 0.05 M DEA; II direction: CN; 10% MeOH + 5% MEK + iPr_2O + 1% ammonia

ing mixture of MeOH, iPr_2O and ammonia or MeOH, MEK, iPr_2O and ammonia, but in all systems the mixture of the investigated drugs was not completely separated. It means, that the identification of all investigated drugs in one run by 1D-HPTLC in examined systems is impossible. On the basis of the results, optimal eluent systems for the analysis of drugs on CN-layer by two-dimensional TLC (2D-TLC) were chosen.

The correlation of R_F values obtained on CN layer in aqueous mobile phase containing 80% MeOH + 20% acetic buffer pH 3.5 + 0.05 M DEA and nonaqueous mobile phase containing 10% MeOH + 5% MEK + iPr_2O + 1% ammonia is presented in Figure 4a. The dispersion of points indicates the differences of the retention parameters obtained in both eluent systems. These correlations are very useful for planning the two-dimensional separation of complex mixtures, and the selectivity differences can be employed in practical applications. The data obtained from the correlation were put into practice for the separation of a mixture containing all investigated psychotropic drugs by the 2D-TLC method. Figure 4b presents the chromatogram of psychotropic drugs separated on CN plate in the same eluent systems. By the use of these selected mobile phase systems with their differing selectivities, the identification of the psychotropic drug is possible by the R_F values obtained for each drug in two eluent systems.

CONCLUSIONS

On RP18 and CN stationary phases, for mobile phases containing organic modifier and water, the investigated psychotropic drugs, which occur as neutral and ionic forms, give highly asymmetric spots, and system efficiency is poor. An addition of buffer to the mobile phase, at acidic or basic pH, leads to slight improvement of spot shape and system efficiency. An addition of acetic acid to the aqueous mobile phases results in further improvement in spot shape, but they are still asymmetric. The best efficiency and most symmetrical spots were obtained for aqueous mobile phase systems by use of mobile phases with addition of DEA.

On CN and diol plates in NP systems, the best results for the separation of psychotropic drugs were obtained with the mobile phase composed of MeOH, MEK, iPr_2O and aqueous ammonia.

On the basis of the retention data of the investigated drugs, obtained on CN stationary phase, the systems of orthogonal selectivity were chosen for two-dimensional thin-layer chromatography of the psychotropic drugs mixture.

REFERENCES

1. Sasaki C., Shinozuka T., Murakami C., Irie W., Maeda K., Watanabe T., Nakamaru N. et al.: *Forensic Sci. Int.* 227, 90 (2013).
2. de la Torre C.S., Martinez M.A., Almarza E.: *Forensic Sci. Int.* 155, 193 (2005).
3. Choong E., Rudaz S., Kottelat A., Guillaume D., Veuthey J.-L., Eap C.B.: *J. Pharm. Biomed. Anal.* 50, 1000 (2009).
4. Xiong C., Ruan J., Cai Y., Tang Y.: *J. Pharm. Biomed. Anal.* 49, 572 (2009).
5. Sabbioni C., Bugamelli F., Varani G., Mercolini L., Musenga A., Saracino M.A., Fanali S., Raggi M.A.: *J. Pharm. Biomed. Anal.* 36, 351 (2004).
6. Shirvi V.D., Channabasavaraj K.P., Kumar G.V., Mani T.T.: *J. Planar Chromatogr.* 23, 369 (2010).
7. Potale L.V., Khodke A.S., Patole, M.C. Damle S.M.: *J. Planar Chromatogr.* 25, 72 (2012).
8. Dhaneshwar S.R., Patre N.G., Mahadik M.V.: *Acta Chromatogr.* 21, 83 (2009).
9. Ramesh B., Narayana P.S., Reddy A.S., Devi P.S.: *J. Planar Chromatogr.* 24, 160 (2011).
10. Shah D.A., Nakrani R.S., Baldania S.L., Chhalotiya U.K., Bhatt K.K.: *J. Planar Chromatogr.* 25, 174 (2012).
11. Patel S.K., Patel N.J., Patel P.U., Patel D.B., Prajapati A.M., Patel S.A.: *J. Planar Chromatogr.* 22, 121 (2009).
12. Skibiński R., Komsta Ł., Koszyła I.: *J. Planar Chromatogr.* 21, 289 (2008).
13. Ahrens B., Blankenhorn D., Spangenberg B.: *J. Chromatogr. B* 772, 11 (2002).
14. Tantawy M.A., Hassan N.Y., Elragehy N.A., Abdelkawy M.: *J. Adv. Res.* 4, 173 (2013).
15. Skibiński R., Misztal G., Komsta Ł., Korólczyk A.: *J. Planar Chromatogr.* 19, 73 (2006).
16. Skibiński R., Komsta Ł., Hopkała H., Suchodolska I.: *Anal. Chim. Acta* 590, 195 (2007).
17. Oztunc A., Onal A., Erturk S.: *J. Chromatogr. B* 774, 149 (2002).

Received: 18. 01. 2014

DRUG BIOCHEMISTRY

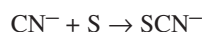
THE EFFECT OF LIPOIC ACID ADMINISTRATION ON THE URINARY
EXCRETION OF THIOCYANATE IN RATS EXPOSED
TO POTASSIUM CYANIDEANNA BILSKA-WILKOSZ¹, MAGDALENA DUDEK², JOANNA KNUTELSKA³
and LIDIA WŁODEK^{1*}¹Chair of Medical Biochemistry, Jagiellonian University, Medical College,
7 Kopernika St., 31-034 Kraków, Poland²Chair of Pharmacodynamics, ³Department of Pharmacological Screening, Chair of Pharmacodynamics,
Jagiellonian University, Medical College, 9 Medyczna St., PL 30-688 Kraków, Poland

Abstract: The oxidation of cyanide (CN⁻) to a much less toxic thiocyanate (SCN⁻) is the main *in vivo* biochemical pathway for CN⁻ detoxification. SCN⁻ is excreted mainly in urine. This study was performed to investigate the effect of lipoic acid (LA) on the urinary excretion of thiocyanate (SCN⁻; rhodanate) in rats. Groups of the animals were treated intraperitoneally (*i.p.*) as follows: group 1: potassium cyanide (KCN) (1 mg/kg); group 2: KCN (1 mg/kg) + LA (100 mg/kg). Urine was collected for 24 h and the pooled samples were examined for SCN⁻ levels. The obtained results indicated that the treatment of animals with potassium cyanide and LA in combination significantly increased the urinary excretion of SCN⁻ in comparison with the respective values in the KCN-alone-treated group. It indicates that LA increased the rate of CN⁻ detoxification in rats.

Keywords: lipoic acid, dihydrolipoic acid, cyanides, thiocyanates (rhodanates), sulfane sulfur

Cyanides (CN⁻), salts of hydrogen cyanide (HCN), and HCN itself have always been feared as poisons because of their toxic properties. Cyanides are synthesized, excreted and degraded in nature by many species of bacteria, plants and insects. Cyanides have also been used for various purposes in industry. Toxic level of cyanides in the body is generated after administration of certain drugs, like laetrile and sodium nitroprusside. Cyanide targets primarily mitochondrial cytochrome oxidase, thereby causing the inhibition of cellular respiration, acceleration of anaerobic glycolysis, and consequent tissue hypoxia and metabolic lactic acidosis.

The oxidation of CN⁻ to a much less toxic thiocyanate (the oral LD₅₀ values of cyanide and thiocyanate in rats are 3 and 854 mg/kg, respectively) (1) is the main *in vivo* biochemical pathway for CN⁻ detoxification according to the following reaction:



The conversion of CN⁻ to SCN⁻ is catalyzed by sulfurtransferases: rhodanase (EC. 2.8.1.1; TST), 3-mercaptopyruvate sulfurtransferase (EC 2.8.1.2; MST) and cystathionine γ -lyase (EC 4.4.1.1; CSE). The role of these enzymes consists in sulfane sulfur transfer to CN⁻.

Sulfane sulfur is a divalent sulfur atom (-S-) covalently bound to another sulfur atom (R-S-S-H). The elemental sulfur (S₈) and outer sulfur atom of thiosulfate (S=SO₃⁻) exhibit also sulfane sulfur properties. The sulfane sulfur-containing compounds are endogenous metabolites formed from cysteine. Cysteine is synthesized from the essential amino acid methionine to a limited extent and for this reason, it is called a semi-essential amino acid. Cysteine and methionine are only two of the twenty amino acids normally present in proteins and belong to the sulfur-containing amino acids (SAA). Thiocyanate is excreted mainly in urine.

* Corresponding author: e-mail: mbwlodek@cyf-kr.edu.pl

Lipoic acid (R)-5-(1,2-dithiolan-3-yl)pentanoic acid, LA, $C_8H_{14}O_2S_2$), a naturally occurring dithiol compound, is a cofactor for a number of multienzymatic complexes involved in energy metabolism. Dihydrolipoic acid (6,8-dimercaptooctanoic acid, DHLA, $C_8H_{16}O_2S_2$) is the reduced form of LA. Exogenous LA has been shown to exhibit pharmacological activities (2–6). Literature data indicate that the LA/DHLA system participates also in sulfane sulfur metabolism. Namely, it was shown that DHLA serves as a sulfane sulfur acceptor in the TST- and MST-catalyzed sulfane sulfur transfer. In these reactions DHLA hydropersulfide is formed, from which sulfane sulfur is released in the form of hydrogen sulfide (H_2S) and LA is produced concomitantly (7, 8).

Thus, it can be assumed that LA may be involved in cyanide detoxification reactions in the body. This study was undertaken to investigate for the first time the effect of LA administration on the urinary excretion of SCN^- in rats exposed to CN^- .

EXPERIMENTAL

Animals

The experiments were carried out on male Wistar rats (300–350 g). Animals were housed in metabolic cages for urine collection, in a room at a constant temperature of $20 \pm 2^\circ C$ with a natural light-dark cycle. They had free access to standard pellet diet and water. Groups consisted of 6 animals each. The pharmaceutical with the commercial name Thiogamma, which contains LA as an active substance was used in our experiments as a source of LA. All procedures were approved by the Ethics Committee for Animal Research in Kraków (license no. 44/2012).

Groups were treated as follows: Group 1: KCN (1 mg/kg b.w., *i.p.*). Group 2: KCN (1 mg/kg b.w.; *i.p.*) + LA (100 mg/kg b.w.; *i.p.*).

Urine was collected for 24 h after drug injection and the pooled samples were examined for SCN^- levels.

Methods

Determination of thiocyanate level in the urine of rats

The content of SCN^- was determined by the method of Goldstein (9). SCN^- present in the urine reacts with Fe^{3+} ions to form the colored compound $Fe(SCN)_3$, the concentration of which is measured spectrophotometrically at a wavelength of $\lambda = 450$ nm. SCN^- concentration is calculated based on a standard curve prepared for potassium thiocyanate (KSCN).

Statistical analysis

Data are presented as the means \pm SEM. The statistical significance of the differences between the means was analyzed using Student's *t*-test. A level of $p \leq 0.001$ was adopted to indicate statistical significance.

RESULTS

The results presented in Table 1 indicated that 24-h urinary excretion of SCN^- was significantly higher in rats which were administered KCN and LA in combination in comparison with the group treated with KCN alone ($4.86 \mu\text{mol}/24 \pm 0.23$ h vs. $2.5 \mu\text{mol}/24 \pm 0.37$ h, respectively).

DISCUSSION AND CONCLUSIONS

The obtained results showed that LA increased CN^- detoxification rate in rats, which indicates that this compound can act as a CN^- antidote. It was confirmed also by studies of other authors. Müller and Krieglstein reported that one hour of preincubation with $1 \mu\text{M}$ DHLA reduced damage of neurons from chick embryo telencephalon caused by 1 mM sodium cyanide (10). Abdel-Zaher et al. demonstrated that intraperitoneal injection of KCN into mice produced clonic and tonic seizures. The severity of convulsions was dose-dependent. The ED_{50} value of KCN was 4.8 mg/kg. In contrast, animals administered LA at a dose of 100 mg/kg before KCN injection showed the increase in CN^- ED_{50} values from 4.8 mg/kg to 9.4 mg/kg (10). The same authors also demonstrated that LA (25, 50 and 100 mg/kg) given to mice 15 min before KCN injection increased the CN^- LD_{50} values (based on 24 h mortality) from 6 mg/kg to 6.2, 7.2 and 11.2 mg/kg, respectively (11). It has also been reported that LA protects cholinergic cells against sodium nitroprusside neurotoxicity (12).

Therefore, it is a plausible proposal that LA plays a role in cyanide detoxification process. However, further studies are necessary to explain the mechanisms of these processes. Swenne et al. exposed normal and protein-malnourished rats to the cyanogenic compound acetonitrile (CH_3CN); that study indicated that urinary excretion of SCN^- was lower in rats fed a low-protein diet compared to rats fed a normal-protein diet (13). Analysis of the above data suggests that there may be some analogy with the present results. Namely, when rats are exposed to CN^- the urinary SCN^- excretion is higher in animals, which were fed a normal protein diet and in those which were administered LA. It indicates that

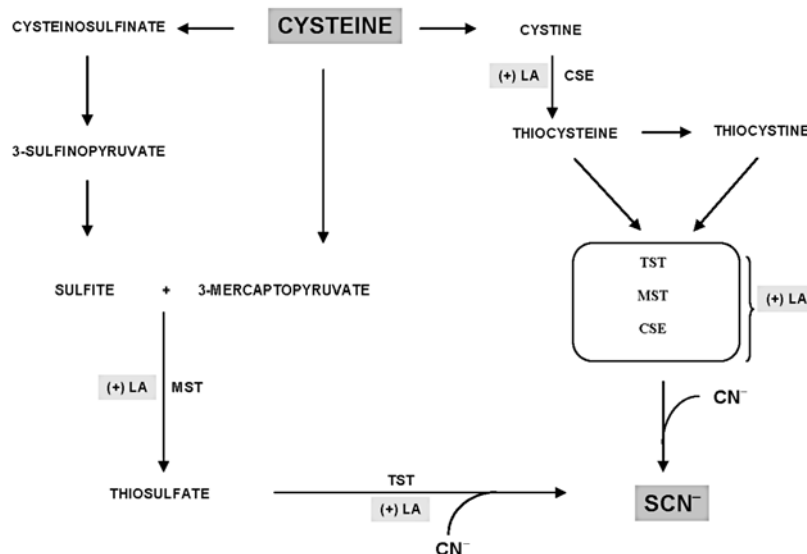


Figure 1. A proposal of the mechanism of LA action in processes leading to the formation of sulfane sulfur compounds: thiosulfate, thiocysteine and thiocystine, and in the CN^- to SCN^- transformation. TST – thiosulfate: cyanide sulfurtransferase (EC 2.8.1.1; rhodanese). MST – 3-mercaptopyruvate:cyanide sulfurtransferase (EC 2.8.1.2). CSE – cystathionine γ -lyase (EC 4.4.1.1; cystathionase)

Table 1. The urinary excretion of SCN^- in rats treated with KCN in the absence or presence of LA.

Treatment	SCN^- [$\mu\text{mol}/24 \text{ h}$]
KCN	2.50 ± 0.37
KCN + LA	$4.86^a \pm 0.23$

^aStudent's *t*-test, significance $p < 0.001$ in comparison with KCN group

LA acted in that case like a normal-protein diet. The literature data indicate that a low-protein diet increases CN^- toxicity, because the concentrations of sulfane sulfur compounds are dependent on the availability of SAA from dietary protein (14). Tor-Agbidye et al. proposed that SAA deficiency might be a risk factor for human neurological diseases among protein-poor populations subsisting on cassava (*Manihot esculenta*), a cyanophoric plant (15). In 1981, Westley found that purified bovine liver TST had a high turnover rate of almost 20,000/min *in vitro*, which meant that 1 mole of TST could convert 20,000 moles of CN^- to SCN^- per 1 minute. This high turnover rate means that the availability of sulfane sulfur compounds, rather than the TST activity, is the rate limiting factor for CN^- conversion to SCN^- (16).

Therefore, it appears that all the data warrant hypothesis that LA increases CN^- to SCN^- trans-

formation rate by elevation of the level of sulfane sulfur compounds in the body. It was confirmed also by data from Bilska et al. studies, which demonstrated for the first time *in vivo* that the level of sulfane sulfur compounds in the heart, liver and kidney of rats given LA at a dose of 100 mg/kg/24 h for 8 days was significantly higher than in the control LA-free group (17). The same experiments indicated that LA elevated also TST activity in several tissues of rats (17). However, in the light of the present knowledge, LA sulfur is not a sulfane sulfur, and TST does not participate in its formation. However, on the other hand, Frankenberg indicated that the administration of TST together with sulfane sulfur compounds had a good antidotic effect against CN^- poisoning in mice, yet, when sulfane sulfur compounds were given without TST, the antidotic effect was weaker (18).

So, based on literature data, it can be hypothesized that, apart from TST, LA also elevates activity of MST and/or CSE (Fig. 1). It is known that CSE and MST belong to enzymes which are directly involved in the generation of sulfane sulfur compounds. MST is also known to be implicated in the CN^- to SCN^- conversion reaction. As for CSE, *in vivo* studies indicated that the inhibition of this enzyme by L-propargylglycine increased the toxicity of CN^- (19). It can indicate that, like for MST, the CSE-catalyzed reactions lead both to the production of sulfane sulfur compounds, and to CN^- to SCN^-

conversion. Already in the 1960s, it was documented that the products of CSE-catalyzed cleavage of cystine (Cys-S-S-Cys) produced sulfane sulfur donors for TST (20, 21).

In summary, this paper clearly demonstrated that the treatment of rats with KCN and LA in combination significantly increased the urinary excretion of SCN^- in comparison with the respective values in the KCN-alone-treated group, which confirms the hypothesis suggesting that LA plays a role in the CN^- detoxification process. These results suggest that biological activity of LA may be connected with sulfane sulfur metabolism (Fig. 1). It points to potential new pharmacological properties of LA. However, confirmation of this hypothesis requires further studies.

Acknowledgments

This work was supported by statutory funds of the Faculty of Medicine and Faculty of Pharmacy, Jagiellonian University Medical College, Kraków, Poland.

The authors have declared no conflict of interest.

REFERENCES

1. Beasley D.M., Glass W.I.: *Occup. Med.* 48, 427 (1998).
2. Gorąca A., Huk-Kolega H., Piechota A., Kleniewska P., Ciejka E., Skibska B.: *Pharmacol. Rep.* 63, 84 (2011).
3. Lyzogub V.H., Altunina N.V., Bondarchuk O.M.: *Lik. Sprava* 7-8, 20 (2011).
4. Rochette L., Ghibu S., Richard C., Zeller M., Cottin Y., Vergely C.: *Mol. Nutr. Food Res.* 57, 114 (2013).
5. Sałat K., Moniczewski A., Librowski T.: *Mini Rev. Med. Chem.* 13, 335 (2013).
6. Zygmunt M., Dudek M., Bilaska-Wilkosz A., Bednarski M., Mogilski S., Knutelska J., Sapa J.: *Acta Pol. Pharm. Drug Res.* 70, 899 (2013).
7. Mikami Y., Shibuya N., Kimura Y., Nagahara N., Ogasawara Y., Kimura H.: *Biochem. J.* 439, 485 (2011).
8. Villarejo M., Westley J.: *J. Biol. Chem.* 238, 4016 (1963).
9. Goldstein F.: *J. Biol. Chem.* 187, 523 (1950).
10. Müller U., Kriegelstein J.: *J. Cereb. Blood Flow Metab.* 15, 624 (1995).
11. Abdel-Zaher A.O., Abdel-Hady R.H., Abdel Moneim W.M. Salim, S.Y.: *Exp. Toxicol. Pathol.* 63, 161 (2011).
12. Bielarczyk H., Gul S., Ronowska A., Bizon-Zygmańska D., Pawełczyk T., Szutowicz A.: *J. Neurochem.* 98, 1242 (2006).
13. Swenne I., Eriksson U.J., Christofferson R., Kagedal B., Lundquist P., Nilsson L., Tylleskär T., Rosling H.: *Fundam. Appl. Toxicol.* 32, 66 (1996).
14. Cliff J., Lundquist P., Martenson J., Rosling H., Sörbo B.: *Lancet* 2, 1211 (1985).
15. Tor-Agbidye J., Palmer V.S., Lasarev M.R., Craig A.M., Blythe L.L., Sabri M.I., Spencer P.S.: *Toxicol. Sci.* 50, 228 (1999).
16. Westley J.: *Methods Enzymol.* 77, 285 (1981).
17. Bilaska A., Dudek M., Iciek M., Kwiecień I., Sokołowska-Jeżewicz M., Filipek B., Włodek L.: *Pharmacol. Rep.* 60, 225 (2008).
18. Frankenberg L.: *Arch. Toxicol.* 45, 315 (1980).
19. Porter D.W., Nealley E.W., Baskin S.I.: *Biochem. Pharmacol.* 52, 941 (1996).
20. Cavallini D., De Marco C., Mondovi B., Mori B.G.: *Enzymologia* 22, 161 (1960).
21. Szczepkowski T.W., Wood J.L.: *Biochim. Biophys. Acta* 139, 469 (1967).

Received: 10. 12. 2013

DRUG SYNTHESIS

SYNTHESIS AND ANTIBACTERIAL PROPERTIES OF PYRIMIDINE DERIVATIVES

JERZY CIEPLIK ^{1*}, MARCIN STOLARCZYK ¹, JANUSZ PLUTA ², OLAF GUBRYNOWICZ ², IWONA BRYNDAL ³, TADEUSZ LIS ⁴ and MARCIN MIKULEWICZ ⁵¹ Department of Organic Chemistry, Wrocław Medical University,
9 Grodzka St., 50-137 Wrocław, Poland² Department of Applied Pharmacy, Wrocław Medical University,
38 Szewska St., 50-137 Wrocław, Poland³ Faculty of Chemistry, University of Economics, Wrocław,
118/120 Komandorska St., 54-435 Wrocław, Poland⁴ Faculty of Chemistry, University of Wrocław, 14 Joliot-Curie St., 50-383 Wrocław, Poland⁵ Department of Dentofacial Orthodontics, Wrocław Medical University,
26 Krakowska St., 50-425 Wrocław, Poland

Abstract: In this study, a series of syntheses was conducted on the pyrimidine system, obtaining bisulfite carboxyl derivatives **4** and hydroxy derivatives **5**. In addition, a series of syntheses were carried out as a result of which both alkyl and aromatic amines were obtained. Then, the attempt was made to cyclize these amines in the Mannich reaction to pyrimido[4,5-d]pyrimidines **11**, **12**. After determination of chemical structure using physicochemical tests, also by means of crystallographic tests, all the newly obtained derivatives underwent microbiological tests on bacterial strains and fungi. The most interesting results of the microbiological tests are included later in the study.

Keywords: pyrimidine derivatives, antibacterial effect, pyrimido[4,5-d]pyrimidines

Our earlier work on the synthesis and biological properties of the pyrimidine ring proved that this system is extremely active biologically. The derivatives obtained showed cytostatic (1, 2), immunomodulatory (3, 4), and most of all antibacterial (5–9) properties. Therefore, it was advisable to conduct a series of syntheses aimed at obtaining pyrimido-pyrimidine derivatives and subjecting them to microbiological tests. During synthesis of the new pyrimidine derivatives, it turned out completely unexpectedly that the pyrimido[4,5-d]pyrimidine system can be obtained using two methods fully independent of each other.

The substrate in our study was ethyl 4-methyl-2-phenyl-6-sulfanylpyrimidine-5-carboxylate (**1**), which, when heated in the presence of phenylhydrazine, condensed to bisulfite fusion of diethyl 4,4'-disulfanediyldis[6-(methyl-2-phenylpyrimidine-5-carboxylate) (**2**). Before that, similar fusions

on ethyl ester were obtained by Brazilian scientists, Cunta and coworkers (10). Bisulfite ester **2** was subjected to LiAlH₄, a THF and CS₂ reduction, as a result of which tetrasulfite fusion with reduced carboxyl group down to hydroxyl group [tetrasulfane-1,4-diylbis-(methyl-2-phenylpyrimidine-4,5-diyl)]dimethanol (**3**) was obtained. Initial ester **1** was exposed to SOCl₂, thus yielding diethyl 4,4'-disulfanediyldis[6-(methoxycarbothionyl)-2-phenylpyrimidine-5-carboxylate] (**4**). Structures of **3** and **4** were confirmed using crystallographic tests. Initial substrate **1** melted with aromatic amines gave aminoesters **5** which, when hydrolyzed, changed into 5-carboxyl amino acids **6**. Both esters **5** and amino acids **6** were reduced with LiAlH₄ to 5-hydroxy derivatives **7**. Hydroxy derivatives **7**, under the influence of SOCl₂, gave 5-chloro derivatives **8** which, when condensed with aromatic amines, changed into 5-amino-substituted pyrimidines **10**.

* Corresponding author: e-mail: jerczieplik@o2.pl

Fusions **10** were cyclized in the Mannich reaction to compounds **11** and **12** which showed strong antibacterial properties.

Ester **1** melted with aromatic amines yielded a series of derivatives ethyl-4-methyl-2-phenyl-6-aryloaminopyrimidine-5-carboxylate (**5**) which also hydrolyzed to 4-methyl-2-phenyl-6-arylaminopyrimidine-5-carboxylate acid (**6**). Ester **5** or acid **6** were reduced with LiAlH_4 to (4-methyl-2-phenyl)-6-aryloaminopyrimidin-5-yl-methanol (**7**). By exposing compound **7** to SOCl_2 , pyrimidine chloroderivatives **8** were obtained. Compound **8** was treated with ammonia and aromatic amines, thus yielding compounds **9** and **10**, confirmed with crystallographic tests. The attempt to obtain compound **13** by means of the Mannich reaction was not successful.

EXPERIMENTAL

Chemistry

Melting points were determined in Kofler apparatus. ^1H NMR spectra were recorded on a BS-487-C-80 MHz Tesla spectrometer. Infrared (IR) spectra were recorded in nujol with a Specord spectrophotometer, at the Elemental Laboratory of the Medical University in Wrocław. Elemental analyses indicated by the symbols were within $\pm 0.4\%$ of theoretical values.

[Tetrasulfane-1,4-diylbis-(6-methyl-2-phenylpyrimidine-4,5-diyl)]dimethanol (**3**)

Four grams (0.005 mol) of diethyl 4,4'-disulfanediybis-(6-methyl-2-phenylpyrimidine)-5-carboxylate (**2**) was dissolved in anhydrous tetrahydrofuran (THF) and CS_2 , and LiAlH_4 was added in small quantities until the solution stopped foaming. After this time, 100 mL of chloroform was added to the post-reaction mixture. This mixture was poured into 500 mL of cold water and extracted three times with 50 mL of chloroform. Chloroform extracts were combined and evaporated under vacuum; the oily reaction mixture was crystallized from methanol, yielding 4.5 g (47.5%) of crystals (**3**) with m.p. 145–147°C.

The structure of compound **3** was confirmed with crystallographic tests and IR and ^1H NMR spectra. IR (KBr, cm^{-1}): 2560 (C-S), 650 (C-S). ^1H NMR (CDCl_3 , δ , ppm): 1.85 (s, 3H, CH_3), 3.5 (s, 1H, OH), 7.20–8.35 (m, 10 H, arom.).

Diethyl 4,4'-disulfanediybis[6-(methoxycarbothioyl)-2-phenylpyrimidine-5-carboxylate] (**4**)

Four grams (0.014 mol) of ethyl 4-methyl-2-phenyl-6-sulfanylpurimidine-5-carboxylate (**1**) was

dissolved in 50.0 mL of benzene and 5.0 mL SOCl_2 (thionyl chloride) was added. The reaction mixture was refluxed for 3 h. Then, the excess of SOCl_2 was distilled off and the residue was recrystallized from methanol, yielding 6.1 g (56.5%) of crystals (**4**) with m.p. 165–166°C.

The structure of compound **4** was confirmed with crystallographic tests and IR and ^1H NMR spectra. IR (KBr, cm^{-1}): 2560 (C-S), 650 (C-S). ^1H NMR (CDCl_3 , δ , ppm): 1.20 (t, 3H, CH_2CH_3), 1.55 (s, 3H, OCH_3), 2.50 (q, 3H, CH_2CH_3), 1.85 (s, 3H, CH_3), 7.20–8.35 (m, 10 H, arom.).

Ethyl 4-methyl-2-phenyl-6-[3-(trifluoromethyl)phenylamino]pyrimidine-5-carboxylate (**5a**)

Four grams (0.014 mol) of ethyl 4-methyl-2-phenyl-6-sulfanylpurimidine-5-carboxylate (**1**) was melted with 2.0 g of 3-trifluoroaniline for 4 h in a round-bottom flask under the reflux condenser. After this time, the reaction mixture was poured into 50.0 mL of methanol and cooled down. The precipitate was filtered and recrystallized from methanol, yielding 3.9 g (68%) of crystals (**5a**). M.p. 137–137°C. IR (KBr, cm^{-1}): 3440 (NH), 940 (NH). ^1H NMR (CDCl_3 , δ , ppm): 1.20 (t, 3H, CH_2CH_3), 2.50 (q, 3H, CH_2CH_3), (s, 3H, CH_3), 3.85 (s, 1H, NH), 7.20–8.35 (m, 9 H, arom.).

In a similar way, compound **5b** was obtained. IR (KBr, cm^{-1}): 3450 (NH), 945 (NH). ^1H NMR (CDCl_3 , δ , ppm): 1.25 (t, 3H, CH_2CH_3), 2.45 (q, 3H, CH_2CH_3), 1.80 (s, 3H, CH_3); 7.20–8.35 (m, 9 H, arom.).

4-Methyl-2-phenyl-6-[3-(trifluoromethyl)phenylamino]pyrimidine-5-carboxylic acid (**6a**)

Four grams (0.009 mol) of ethyl 4-methyl-2-phenyl-6-[3-(trifluoromethyl)phenylamino]pyrimidine-5-carboxylate (**5a**) was dissolved in 10% methanol solution of NaOH. The mixture was refluxed in the round-bottom flask for 24 h. After this time, the solution was neutralized with HCl to pH = 7. The precipitate was filtered and recrystallized from methanol, yielding 3.4 g (92%) of crystals (**6a**). M.p. 205–206°C. IR (KBr, cm^{-1}): 3440 (NH), 940 (NH). ^1H NMR (CDCl_3 , δ , ppm): 1.85 (s, 3H, CH_3), 3.85 (s, 1H, NH), 7.20–8.35 (m, 9 H, arom.).

In the same way, compound **6b** was obtained. IR (KBr, cm^{-1}): 3445 (NH), 945 (NH). ^1H NMR (CDCl_3 , δ , ppm): 1.80 (s, 3H, CH_3), 3.80 (s, 1H, NH), 7.20–8.35 (m, 9 H, arom.).

4-Methyl-2-phenyl-6-[3-(trifluoromethyl)phenylamino](pyrimidin-5-yl)methanol (**7**)

Four grams (0.009 mol) of ethyl 4-methyl-2-phenyl-6-[3-(trifluoromethyl)phenylamino]pyr-

imidine-5-carboxylate (**5a**) was dissolved in 50.0 mL THF and LiAlH₄ was added in small portions until the solution stopped foaming. After this time, 100.0 mL of chloroform was added to the reaction mixture and it was poured into water with ice in order to destroy any unreacted LiAlH₄. The solution was filtered and extracted three times with chloroform. Chloroform extracts were combined and dried with MgSO₄. The dried solution was concentrated under vacuum and the precipitate was filtered and crystallized from methanol yielding 2.3 g (65.5%) of crystals (**7**). M.p. 150–152°C. IR (KBr, cm⁻¹): 3445 (NH), 3450 (OH), 945 (NH). ¹H NMR (CDCl₃, δ, ppm): 1.80 (s, 3H, CH₃), 2.50 (s, 1H, OH), 3.80 (s, 1H NH), 4.30 (s, 2H CH₂), 7.20–8.35 (m, 9 H, arom.).

5-(Chloromethyl)-6-methyl-2-phenyl-N-[3-(trifluoromethyl)phenyl]pyrimidine (**8**)

Four grams (0.011 mol) of, (4-methyl-2-phenyl)-6-[[3-(trifluoromethyl)phenyl]amino](pyrimidin-5-yl)methanol (**7**) was dissolved in 50.0 mL of benzene and 3.0 mL SOCl₂ was added. The reaction mixture was left for 24 h at room temperature. After this time, the excess of thionyl chlorine was distilled off and the oily residue was crystallized from chloroform, yielding 3.1 (74%) of crystals (**8**). M.p. 196–198°C. IR (KBr, cm⁻¹): 3445 (NH), 945 (NH), 725 (C-Cl). ¹H NMR (CDCl₃, δ, ppm): 1.80 (s, 3H, CH₃), 3.80 (s, 1H NH), 4.30 (s, 2H CH₂), 7.20–8.35 (m, 9 H, arom.).

5-(Aminomethyl)-6-methyl-2-phenyl-N-[3-(trifluoromethyl)phenyl]pyrimidine-4-amine (**9**)

Four grams (0.010 mol) of (**8**) was dissolved in 50.0 mL of THF and 10.0 mL of 25% of ammonia solution was added. The mixture was intensively mixed in the round-bottom flask under the reflux condenser at 80°C for 8 h. After this time, the reaction mixture was poured into 500.0 mL of water and extracted three times with 50.0 mL of chloroform. Chloroform extracts were combined and dried with MgSO₄. The solution was filtered and the filtrate was concentrated under vacuum. The oily residue was cleaned by passing it through the chromatographic column filled with silica gel (200–300 mesh). Chloroform was distilled off from the eluate and the residue was recrystallized from methanol, yielding 3.1 g (82.0 %) of crystals (**9**) with m.p. 158–160°C. IR (KBr, cm⁻¹): 3445 (NH), 945 (NH), 725 (C-Cl). ¹H NMR (CDCl₃, δ, ppm): 1.80 (s, 3H, CH₃), 2.12 (s, 2H, NH₂), 3.80 (s, 1H NH), 4.30 (s, 2H CH₂), 7.20–8.35 (m, 9 H, arom.).

5-[[4-(4-Ethoxyphenyl)amino]methyl]-N-(3-trifluoromethyl)phenyl-6-methyl-2-phenylpyrimidine-4-amine (**10a**)

Four grams (0.010 mol) of (**8**) was dissolved in 50.0 mL of THF and 2.0 g of p-phenetidine was added. The reaction mixture was refluxed at 80°C for 8 h. After this time, the solution was poured into 500.0 mL of cold water and extracted three times with 50.0 mL of chloroform. Chloroform extracts were combined and dried with MgSO₄. The solution was filtered and the filtrate was concentrated and cleaned by passing it through the chromatographic column filled with silica gel (200–300 mesh). The eluate was concentrated again and the precipitate was recrystallized from methanol, yielding 3.9 g (78.5%) of crystals (**10a**) with m.p. 120–121°C. IR (KBr, cm⁻¹): 3445 (NH), 945 (NH). ¹H NMR (CDCl₃, δ, ppm): 1.25 (t, 3H, CH₂CH₃), 1.80 (s, 3H, CH₃), 2.12 (s, 1H, NH), 2.45 (q, 3H, CH₂CH₃), 3.80 (s, 1H NH), 4.30 (s, 2H CH₂), 7.20–8.35 (m, 13 H, arom.).

Similarly, compounds: **10b–e** were obtained.

10b: IR (KBr, cm⁻¹): 3450 (NH), 940 (NH). ¹H NMR (CDCl₃, δ, ppm): 1.25 (t, 3H, CH₂CH₃), 1.80 (s, 3H, CH₃), 2.12 (s, 1H, NH), 2.45 (q, 3H, CH₂CH₃), 3.80 (s, 1H NH), 4.30 (s, 2H CH₂), 7.20–8.35 (m, 13 H, arom.).

10c: IR (KBr, cm⁻¹): 3445 (NH), 945 (NH). ¹H NMR (CDCl₃, δ, ppm): 1.25 (t, 3H, CH₃), 1.80 (s, 3H, CH₃), 2.12 (s, 1H, NH), 3.80 (s, 1H NH), 4.30 (s, 2H CH₂), 7.20–8.35 (m, 13 H, arom.).

10d: IR (KBr, cm⁻¹): 3445 (NH), 945 (NH). ¹H NMR (CDCl₃, δ, ppm): 1.25 (t, 3H, CH₂CH₃), 1.80 (s, 3H, CH₃), 2.12 (s, 1H, NH), 2.45 (q, 3H, CH₂CH₃), 3.80 (s, 1H NH), 4.30 (s, 2H CH₂), 7.20–8.35 (m, 13 H, arom.).

10e: IR (KBr, cm⁻¹): 3440 (NH), 940 (NH). ¹H NMR (CDCl₃, δ, ppm): 1.25 (t, 3H, CH₂CH₃), 1.80 (s, 3H, CH₃), 2.12 (s, 1H, NH), 2.45 (q, 3H, CH₂CH₃), 3.80 (s, 1H NH), 4.30 (s, 2H CH₂), 7.20–8.35 (m, 13 H, arom.).

3-(4-Ethoxyphenyl)-2-(4-nitrophenyl)-1-[3-(trifluoromethyl)phenyl]-5-methyl-7-phenyl-1,2,3,4-tetrahydropyrimido[4,5-d]pyrimidine (**11a**)

Four grams (0.010 mol) of (**10a**) was dissolved in 50.0 mL of THF and 2.0 g of p-nitrobenzaldehyde was added. The reaction mixture was refluxed with intensive mixing at 80°C for 8 h. Then, the reaction mixture was poured into 500 mL of cold water and extracted three times with chloroform. Chloroform extracts were combined and dried with MgSO₄. The solution was filtered, concentrated under vacuum and cleaned by passing it through the chromatographic column filled with silica gel (200–300

mesh). The chloroform eluate was concentrated again and the precipitate was filtered and crystallized from methanol, yielding 5.2 g (81.5%) of crystals (**11a**) with m.p. 162–164°C. IR (KBr, cm^{-1}), 1325 (N). ^1H NMR (CDCl_3 , δ , ppm): 1.25 (t, 3H, CH_2CH_3), 1.80 (s, 3H, CH_3), 2.45 (q, 3H, CH_2CH_3), 4.30 (s, 2H CH_2), 7.20–8.55 (m, 17 H, arom.).

In similar way, compounds **11b** and **11c** were obtained.

11b: IR (KBr, cm^{-1}): 1335 (N). ^1H NMR (CDCl_3 , δ , ppm): 1.30 (t, 3H, CH_2CH_3), 1.85 (s, 3H, CH_3), 2.55 (q, 3H, CH_2CH_3), 4.40 (s, 2H CH_2), 7.30–8.65 (m, 17 H, arom.).

Table 1. Physical properties of the tested compounds.

Compound	R ^{1*}	R ^{2*}	Formula (m.w.)	M.p. [°C]	Yield [%]	Analysis			
						C	H	N	Cl
3			$\text{C}_{24}\text{H}_{22}\text{N}_4\text{O}_2\text{S}_4$ (526.71)	145–147	47.5	54.73 54.55	4.21 4.33	10.64 10.72	
4			$\text{C}_{36}\text{H}_{32}\text{N}_4\text{O}_6\text{S}_4$ (744.92)	165–166	56.5	58.04 58.22	4.33 4.38	7.52 7.62	
5a	3- CF_3		$\text{C}_{21}\text{H}_{18}\text{F}_3\text{N}_3\text{O}_2$ (401.38)	137–139	68.0	62.84 62.66	4.52 4.68	10.47 10.73	
5b	2- CF_3		$\text{C}_{21}\text{H}_{18}\text{F}_3\text{N}_3\text{O}_2$ (401.38)	145–147	69.5	62.84 63.02	4.52 4.33	11.26 11.51	
6a	3- CF_3		$\text{C}_{19}\text{H}_{14}\text{F}_3\text{N}_3\text{O}_2$ (373.32)	205–207	86.0	61.13 61.44	3.78 3.84	11.26 11.37	
6b	2- CF_3		$\text{C}_{19}\text{H}_{14}\text{F}_3\text{N}_3\text{O}_2$ (373.32)	200–202	82.5	61.13 61.24	3.78 3.41	11.26 11.35	
7	3- CF_3		$\text{C}_{19}\text{H}_{16}\text{F}_3\text{N}_3\text{O}$ (359.34)	150–152	65.5	63.51 63.67	4.49 4.55	11.69 11.72	
8	3- CF_3		$\text{C}_{19}\text{H}_{15}\text{ClF}_3\text{N}_4$ (377.79)	196–198	74.0	60.40 60.42	4.00 4.12	11.12 11.31	
9	3- CF_3		$\text{C}_{19}\text{H}_{17}\text{F}_3\text{N}_4$ (358.36)	158–160	82.0	63.68 63.72	4.78 4.82	15.63 15.73	9.38 9.43
10a	3- CF_3	4- OC_2H_5	$\text{C}_{27}\text{H}_{25}\text{F}_3\text{N}_4\text{O}$ (478.50)	120–121	78.5	67.77 67.88	5.27 5.33	11.71 11.82	
10b	4- OC_2H_5	3- CF_3	$\text{C}_{27}\text{H}_{25}\text{F}_3\text{N}_4\text{O}$ (478.51)	116–117	72.0	67.77 67.42	5.27 5.12	11.71 12.02	
10c	4- OCH_3	4- CF_3	$\text{C}_{26}\text{H}_{23}\text{F}_3\text{N}_4\text{O}$ (464.48)	196–198	77.5	67.23 67.42	4.99 5.12	12.06 11.88	
10d	4- OC_2H_5	2- CF_3	$\text{C}_{27}\text{H}_{25}\text{F}_3\text{N}_4\text{O}$ (411.49)	128–130	79.0	67.77 67.62	5.27 5.22	11.71 11.62	
10e	4- OC_2H_5	$\text{C}_6\text{H}_5\text{N}$	$\text{C}_{25}\text{H}_{25}\text{N}_3\text{O}$ (411.49)	182–184	79.0	72.97 72.84	6.12 6.22	17.02 17.25	
11a	3- CF_3	4- OC_2H_5	$\text{C}_{34}\text{H}_{28}\text{F}_3\text{N}_5\text{O}_3$ (611.61)	162–165	81.5	66.77 66.45	4.61 4.72	11.45 11.55	
11b	4- OCH_3	4- CF_3	$\text{C}_{33}\text{H}_{26}\text{F}_3\text{N}_5\text{O}_3$ (597.58)	115–117	82.5	66.33 66.14	4.39 4.42	11.72 11.83	
11c	4- OC_2H_5	3- CF_3	$\text{C}_{34}\text{H}_{28}\text{F}_3\text{N}_5\text{O}_3$ (611.61)	127–128	77.5	66.77 66.53	4.61 4.58	11.45 11.32	
12a	3- CF_3	4- OC_2H_5	$\text{C}_{28}\text{H}_{25}\text{F}_3\text{N}_4\text{O}$ (490.52)	172–174	79.0	68.56 68.43	5.14 5.21	11.42 11.53	
12b	4- OCH_3	4- CF_3	$\text{C}_{27}\text{H}_{23}\text{F}_3\text{N}_4\text{O}$ (476.49)	156–157	83.5	68.06 67.93	4.87 4.92	11.76 11.83	
12c	4- OC_2H_5	3- CF_3	$\text{C}_{28}\text{H}_{25}\text{F}_3\text{N}_4\text{O}$ (490.52)	177–178	78.5	68.56 68.22	5.14 5.43	11.42 11.53	

* R¹ and R² see Scheme 1.

Table 2. Minimal inhibitory concentrations (MIC) (mg/mL), Testing M-7, A-5.

Microorganism	Compound			
	3	4	10a	Erythromycin
<i>Bacillus subtilis</i> PCM 2021 (ATCC 6633)	4	8	16	0.25
<i>Escherichia coli</i> PCM 2057 (ATCC 25922)	16	16	8	32
<i>Klebsiella pneumoniae</i> PCM 1 (ATCC 13886)	32	32	8	0.5
<i>Proteus vulgaris</i> PCM 542 (ATCC 13315)	32	32	4	128
<i>Serratia marcescens</i> PCM 549 (ATCC 274)	16	16	32	64
<i>Pseudomonas aeruginosa</i> PCM 2058 (ATCC 27853)	16	16	32	128
<i>Enterococcus faecalis</i> PMC 2673 (ATCC 29212)	8	8	16	4
<i>Staphylococcus epidermidis</i> PCM 2118 (ATC 14990)	4	4	8	8
<i>Staphylococcus aureus</i> PCM 1932 (ATCC 6538 P)	8	8	4	0.5
<i>Candida albicans</i> PCM 2566 (ATCC 10231)	4	16	16	256

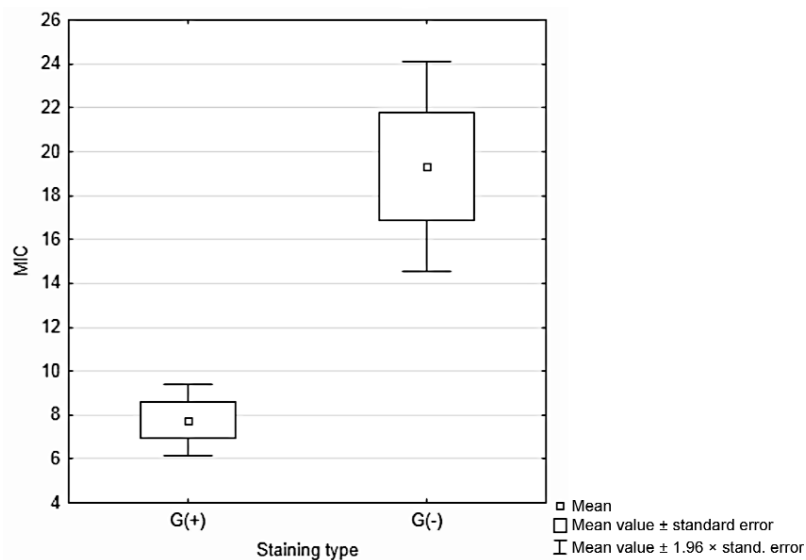


Figure 1. Effect of bacteria type depending on the color stain using the Gram method on MIC values

Table 3. Minimal inhibitory concentrations (MIC) (mg/mL), Testing M-7, A-5.

Microorganism	Compound			
	10d	11a	12b	Erythromycin
<i>Bacillus subtilis</i> PCM 2021 (ATCC 6633)	8	4	8	0.25
<i>Escherichia coli</i> PCM 2057 (ATCC 25922)	16	8	8	32
<i>Klebsiella pneumoniae</i> PCM 1 (ATCC 13886)	4	4	16	0.5
<i>Proteus vulgaris</i> PCM 542 (ATCC 13315)	8	8	32	128
<i>Serratia marcescens</i> PCM 549 (ATCC 274)	16	16	64	64
<i>Pseudomonas aeruginosa</i> PCM 2058 (ATCC 27853)	32	8	32	128
<i>Enterococcus faecalis</i> PMC 2673 (ATCC 29212)	16	2	8	4
<i>Staphylococcus epidermidis</i> PCM 2118 (ATC 14990)	8	4	8	8
<i>Staphylococcus aureus</i> PCM 1932 (ATCC 6538 P)	4	4	16	0.5
<i>Candida albicans</i> PCM 2566 (ATCC 10231)	8	2	4	256

Table 4. *t*-Tests; Grouping: Dyeing Group 1: G(+) Group 2 G(-).

	Mean – G(+)	Mean – G(-)	t	df	p	N valid – G(+)	N valid – G(-)	Std. var. – G(+)	Std. var. – G(-)	quotient F variance	p variances
MIC	7.76000	19.33333	4.167	53	0.000114	25	30	4.176123	13.33	10.191	1.74E-07

Table 5. Mann-Whitney U test; *Versus* variable: Dyeing Marked results are valid with p < 0.05.

	Sum. rang. – G(+)	Sum. rang. – G(-)	U	Z	p	Z – correct.	p	N valid – G(+)	N valid – G(-)	2 × 1 side – cur. p
MIC	475.00	1065.	150.00	3.79	0.00014	-3.93455	0.000083	25	30	0.000082

Table 6. Wald-Wolfowitz (runs) test; *Versus* variable: Dyeing Marked results are valid with p < 0.05.

	N valid – G(+)	N valid – G(-)	Mean – G(+)	Mean – G(-)	Z	p	Z correct.	p	Number – runs	Number – connected
MIC	25	30	7.760000	19.33333	-2.820	0.0048	2.68284	0.0073	18	15

Table 7. Analysis of variances. Marked effects are valid with p < .05 Inclusion requirement: grouping variable = G(+).

	SS – Effect	df – Effect	MS – Effect	SS – Error	df – Error	MS – Error	F	p
MIC	226.8705	6	37.81176	302.6719	21	14.41295	2.623458	0.046649

11c: IR (KBr, cm^{-1}): 1325 (N). ^1H NMR (CDCl_3 , δ , ppm): 1.30 (t, 3H, CH_3), 1.85 (s, 3H, CH_3), 4.40 (s, 2H CH_2), 7.30–8.65 (m, 17 H, arom.).

1-(4-Methoxyphenyl)-3-(4-trifluoromethylphenyl)-5-methyl-7-phenyl-1,2,3,4-tetrahydropyrimido[4,5-d]pyrimidine(1,4-d)pyrimidine (12c).

Four grams (0.008 mol) of (**10c**) was dissolved in 50.0 mL THF and 20.0 mL of formaldehyde was added. The reaction mixture was refluxed with intensive mixing for 8 h. After this time, the reaction mixture was poured into 500.0 mL of cold water and extracted three times with 50.0 mL of chloroform. The chloroform extracts were combined and dried with MgSO_4 . The solution was filtered, concentrated under vacuum and cleaned preliminarily in the chromatographic column filled with silica gel (200–300 mesh). The obtained chloroform eluate was concentrated and crystalized from methanol, yielding 3.4 g (83.5%) of crystals (**12c**) with m.p. 156–157°C.

IR (KBr, cm^{-1}): 3445 (NH), 945 (NH). ^1H NMR (CDCl_3 , δ , ppm): 1.25 (t, 3H, CH_3), 1.80 (s, 3H, CH_3), 2.12 (s, 1H, NH), 3.80 (s, 1H NH), 4.30 (s, 2H CH_2), 4.45 (s, 2H CH_2), 7.20–8.40 (m, 13 H, arom.).

In similar way, compounds **12a** and **12b** were obtained.

12a: IR (KBr, cm^{-1}): 3445 (NH), 945 (NH). ^1H NMR (CDCl_3 , δ , ppm): 1.25 (t, 3H, CH_2CH_3), 1.80 (s, 3H, CH_3), 2.12 (s, 1H, NH), 2.45 (q, 3H, CH_2CH_3), 3.80 (s, 1H NH), 4.35 (s, 2H CH_2), 4.50 (s, 2H CH_2), 7.20–8.45 (m, 13 H, arom.).

12b: IR (KBr, cm^{-1}): 3450 (NH), 940 (NH). ^1H NMR (CDCl_3 , δ , ppm): 1.25 (t, 3H, CH_2CH_3), 1.80 (s, 3H, CH_3), 2.12 (s, 1H, NH);, 2.45 (q, 3H, CH_2CH_3), 3.80 (s, 1H NH), 4.30 (s, 2H CH_2), 4.45 (s, 2H CH_2), 7.20–8.50 (m, 13 H, arom.).

Microbiological methods

The obtained chemical compounds were investigated microbiologically on selected strains, in order to evaluate their bioactivity. The investigation was based on M-7, A-5 standards (MIC testing) (11). The fungal strains also were cultivated on this standard recommended broth – Mueller Hinton Broth II.

Sample bacterial cultures were suspended in 3 mL of a sterile solution of PBS according to 0.5 McFarland's standard (corresponding to 1 to 2×10^8 cfu/mL), and next were diluted with a sterile 1 : 10 PBS solution (giving 1×10^7 CFU / mL).

The obtained inoculum (0.01 mL) was added to 0.2 mL of sterile final dilutions of the investigated

substances according to Table 1, obtaining 5×10^4 concentration of bacteria in the investigated samples. Six trials were carried out for every dilution of the investigated substance – one control without the inoculum.

Statistical methods used in microbiological tests

Based on the determined experimental data, the effect of two parameters was evaluated: the type of substituent of the tested chemical compound and type of bacteria depending on dyeing color using the Gram method

The obtained mean MIC values for seven tested compounds (6 compounds + erythromycin as a reference) were compared with each other using parametric analysis of ANOVA variances and non-parametric Kruskal-Wallis ANOVA analysis. Normality of distributions for analyzed random variables was checked using the Shapiro-Wilk and Kolmogorov-Smirnov tests with Lilliefors correction at the assumed confidence level of $p = 0.05$. Uniformity of variances was determined using the Levene and Brown-Forsythe tests at the confidence level of $p = 0.05$. In order to establish differences between two mean values, parametric Student t-test was used for independent samples and its non-parametric equivalents: the Mann-Whitney U test and the Wald-Wolfowitz (runs) test. For all completed statistical tests, confidence level of $p = 0.05$ was assumed.

Effect of the bacteria type depending on the dyeing color using the Gram method on mean MIC values

Microbiological tests were conducted on 4 bacteria species G(+) and 5 bacteria species G(-). Using parametric t test for independent samples and non-parametric tests: the Mann-Whitney U and Wald-Wolfowitz tests, the statistical validity of differences between mean MIC values obtained in both groups was evaluated, and results were summarized in Tables 1–3 and in Figure 1.

Effect of the substituent type on mean MIC values

Mean MIC values determined for six tested compounds were compared using parametric analysis of variances together with *post-hoc* NIR tests. Normality of distributions for analyzed random variables was confirmed with the Shapiro-Wilk and Kolmogorov-Smirnov tests with Lilliefors correction at the assumed confidence level of $p = 0.05$, and uniformity of variances using the Brown-Forsythe test at the confidence level of $p = 0.05$.

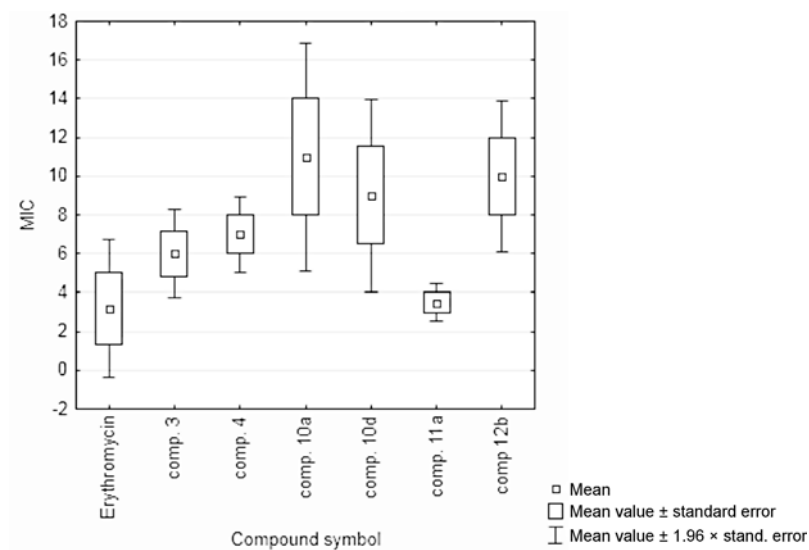


Figure 2. Effect of substituent type on mean MIC values of bacteria G(+)

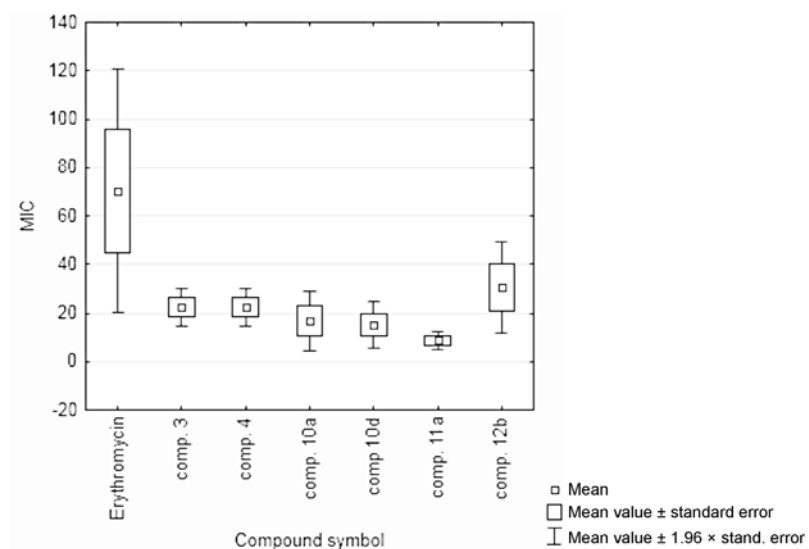


Figure 3. Effect of substituent type on mean MIC values for bacteria G(-)

The analysis was carried out separately for bacteria G(+) and G(-), and results were summarized in tables and figures

The completed statistical analysis showed that with the assumed confidence level of $p = 0.05$ both the type of substituent and type of bacteria depending on the dyeing color using the Gram method had

a statistically valid effect on the experimentally determined mean MIC values.

1. The tested chemical compounds showed higher, statistically valid antibacterial effectiveness for bacteria G(+) compared to bacteria G(-) (Fig. 1 and Tables 1–3).

2. All tested compounds showed higher, statistically valid antibacterial effectiveness for bacterial G(-) compared to the standard substance which was erythromycin, and not statistically valid differences were observed in antibacterial effectiveness for bacteria G(-) between them (Fig. 3, Tables 6, 7).

3. The highest antibacterial effectiveness for bacteria G(-) was shown by compound **11a**.

4. No statistically valid difference was found between antibacterial effectiveness for bacteria G(-) for erythromycin and compound: **3**, **4** and **11a** (Table 7).

5. Out of all tested compounds, the strongest antibacterial properties for the analyzed bacteria were shown by compound **11a**.

CONCLUSIONS

Seventeen newly obtained pyrimidine derivatives were tested microbiologically on 9 bacterial strains and one fungal strain: *Bacillus subtilis*, *Escherichia coli*, *Klebsiella pneumoniae*, *Proteus vulgaris*, *Serratia marcescens*, *Pseudomonas aeruginosa*, *Enterococcus faecalis*, *Staphylococcus epider-*

Table 8. NIR test. Marked differences are valid with $p < 0.05$ Inclusion requirement: grouping variable = G(+).

Compound	{1} – M = 3.1875	{2} – M = 6.0000	{3} – M = 7.0000	{4} – M = 11.000	{5} – M = 9.0000	{6} – M = 3.5000	{7} – M = 10.000
Erythr. {1}		-	-	+	+	-	+
Compd. 3 {2}	-		-	-	-	-	-
Compd. 4 {3}	-	-		-	-	-	-
Compd. 10a {4}	+	-	-		-	+	-
Compd. 10d {5}	+	-	-	-		-	-
Compd. 11a {6}	-	-	-	+	-		+
Compd. 12b {7}	+	-	-	-	-	+	

Erythr. – erythromycin

Table 9. Analysis of variances; Marked effects are valid with $p < .05$; Inclusion requirement: grouping variable = G(-).

	SS – Effect	df – Effect	MS – Effect	SS – Error	df – Error	MS – Error	F	p
MIC	12598.79	6	2099.798	16813.00	28	600.4643	3.496957	0.010449

Table 10. NIR test; Marked differences are valid with $p < 0.05$; Inclusion requirement: grouping variables = G(-).

Compound	{1} – M = 70.500	{2} – M = 22.400	{3} – M = 22.400	{4} – M = 16.800	{5} – M = 15.200	{6} – M = 8.8000	{7} – M = 30.400
Erythromycin {1}		+	+	+	+	+	+
3 {2}	+		-	-	-	-	-
4 {3}	+	-		-	-	-	-
10a {4}	+	-	-		-	-	-
10d {5}	+	-	-	-		-	-
11a {6}	+	-	-	-	-		-
12b {7}	+	-	-	-	-	-	

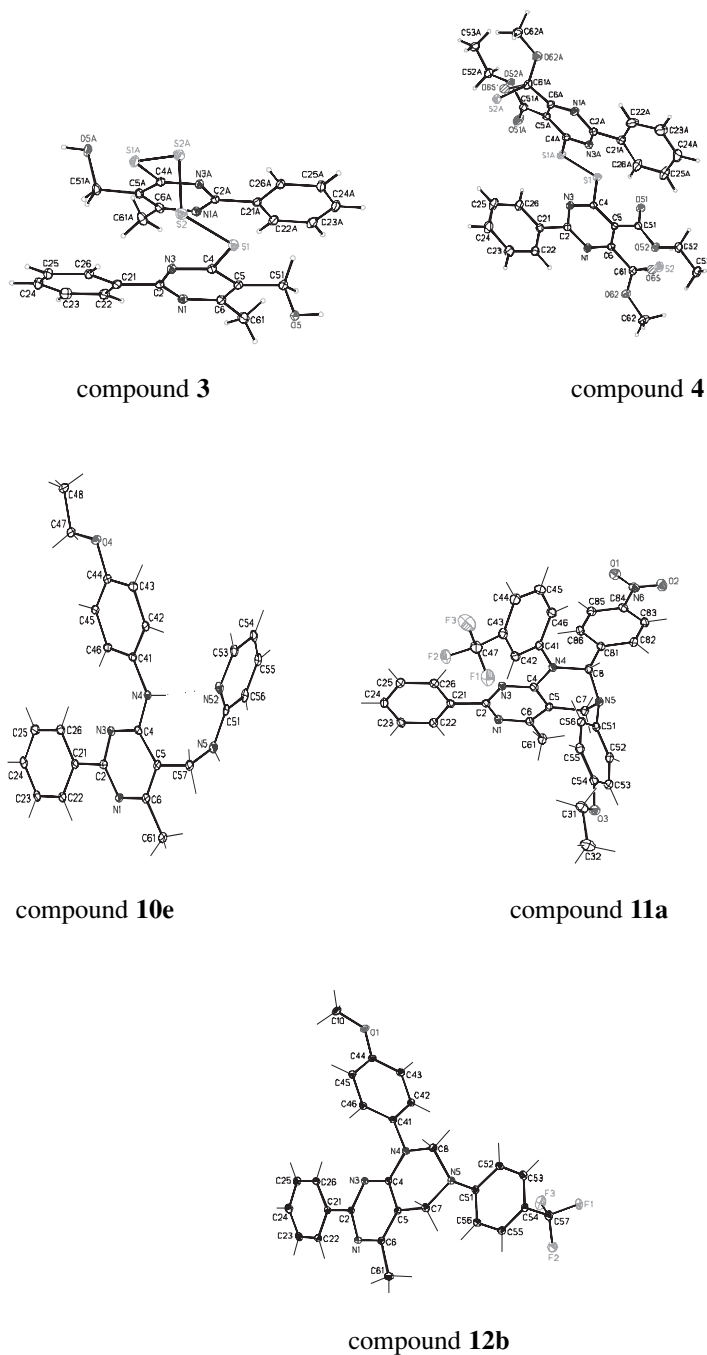
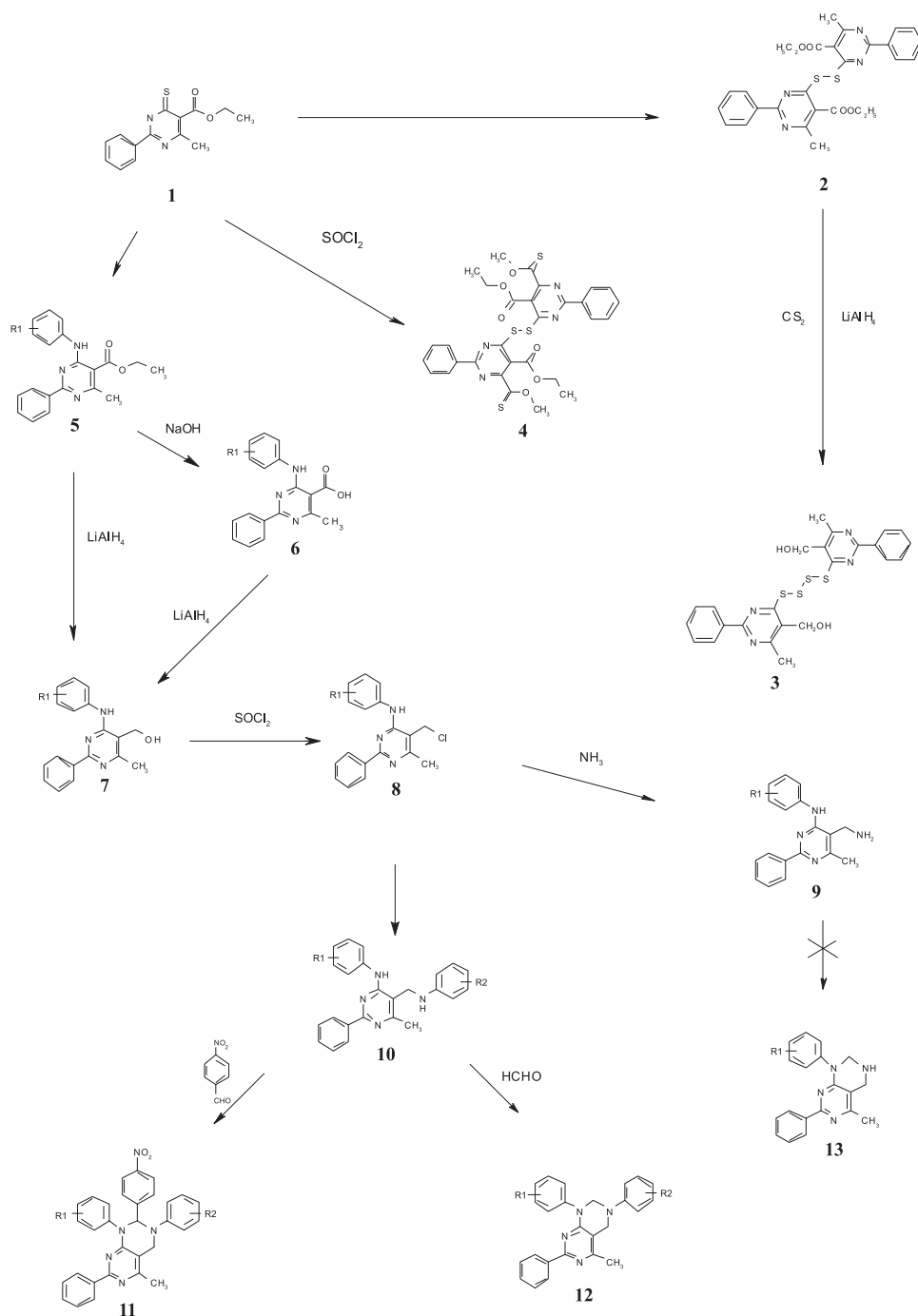


Figure 4. Crystallographic structures of selected synthesized compounds

midis, *Staphylococcus aureus* and *Candida albicans*. Some of the obtained compounds showed extremely interesting antibacterial activity.

Pyrimidine bibonding with multiple sulfide bridge showed interesting microbiological activity which was affected also by the functional group in

position 5. Higher microbiological activity was shown by sulfide compounds (**3**, **4**). Antibacterial activity was shown also by 5-amine pyrimidine derivatives (compounds **10a** and **10d**), and their activity to a considerable extent depends on substituted amine in position 5, which undoubtedly causes better solubili-



Scheme 1. Synthesis of pyrimidine derivatives

ty of the given compound. Cyclization of amines **10** in the Mannich reaction to pyrimido[4,5-d]pyrimidine moieties (**11**) increases their microbiological activity which becomes slightly weaker, if nitrophenyl substituent (**12**) is missing in the pyrimido[4,5-d]pyrimidine system in position 2.

Acknowledgment

Study sponsored by funds from "Farmacja Dolnośląska".

REFERENCES

1. Machoń Z., Cieplik J.: *Synthesis* 2, 142 (1986).
2. Machoń Z., Cieplik J.: *Pol. J. Pharmacol. Pharm.* 40, 201 (1988).
3. Cieplik J., Machoń Z., Zimecki M., Wieczorek Z.: *Arch. Immunol. Ther. Exp.* 41, 11 (1993).
4. Cieplik J., Machoń Z., Zimecki M., Wieczorek Z.: *Farmaco* 50, 131 (1995).
5. Machoń Z., Cieplik J.: *Eur. J. Med. Chem-Chim. Ther.* 19, 359 (1984).
6. Pluta J., Flendrich M., Cieplik J.: *Boll. Chim. Farm.* 135, 459 (1996).
7. Cieplik J., Pluta J., Meler G.: *Arch. Pharm. (Weinheim)* 330, 237 (1997).
8. Cieplik J., Pluta J., Gubrynowicz O.: *Sci. Pharm.* 68, 333 (2000).
9. Cieplik J., Pluta J., Gubrynowicz O.: *Sci. Pharm.* 70, 245 (2002).
10. Cunha S., Bastos R., Silva P., Costa G., Vencato I., Luriucci C., Napolitano H. et al.: *Monatsh. Chem.* 138, 111 (2007).
11. CLSI: *Methods for Dilution Antimicrobial Susceptibility Tests for Bacteria That Grow Aerobically; Approved Standard 9th edn.* CLSI document M07-A9. Clinical and Laboratory Standards Institute, Wayne, PA 2012.

Received: 28. 05. 2013

NOVEL PYRROLOPYRIMIDINES AND TRIAZOLOPYRROLOPYRIMIDINES CARRYING A BIOLOGICALLY ACTIVE SULFONAMIDE MOIETIES AS ANTICANCER AGENTS

MOSTAFA M. GHORAB^{1*}, MANSOUR S. ALSAID¹ and YASSIN M. NISSAN²

¹Department of Pharmacognosy, College of Pharmacy, King Saud University,
P.O. Box 2457, Riyadh 11451, Saudi Arabia

²Pharmaceutical Chemistry Department, Faculty of Pharmacy, Cairo University, Egypt

Abstract: A new series of pyrroles **5**, **6**, pyrrolopyrimidines **8**, **11–14**, **16–29**, triazolo-pyrrolopyrimidines **9**, **10** and **15** carrying a biologically active sulfonamide moieties were synthesized using 2-amino-3-cyano-4-(4-bromophenyl)pyrrole **5** as a strategic starting material. The structures of the prepared compounds were confirmed by elemental analyses, IR, ¹H-NMR and ¹³C-NMR data. All of the synthesized compounds showed promising anticancer activity against breast cancer cell line (MCF7) compared to doxorubicin as reference drug, especially compounds **5–17**, **21–24** and **28** with better IC₅₀ than that of doxorubicin. In order to suggest the mechanism of action of their cytotoxic activities, molecular docking on the active site of c-Src was done and good results were obtained.

Keywords: anticancer, pyrrolopyrimidines, triazolopyrrolopyrimidines, sulfonamides

The design as well as identification of some new molecules for the treatment of diseases such as cancer is an important undertaking in medicinal chemistry research. The pyrrole, pyrrolopyrimidine and triazolopyrrolopyrimidine derivatives have been known to possess wide spectrum of biological properties specially anticancer activity (1–10). Pyrrolo[2,3-d]pyrimidines have aroused recent attention from chemical and biological points of view, since they have useful properties as antimetabolites in purine biochemical reactions (11). Several mechanisms of action explaining their anticancer activity include protein kinases inhibition such as c-Src, Akt and EGFR (12–14). On the other hand, sulfonamides have recently been reported to show potent anticancer activity (15–17). To explore the synergistic effect resulting from combining pyrrole, pyrrolopyrimidine and triazolopyrrolopyrimidines with sulfonamide moiety, the present work describes the synthesis and molecular docking of these novel derivatives on the active site of c-Src enzyme hoping to discover novel anticancer agents and suggest a mechanism of action for their cytotoxic activities.

EXPERIMENTAL

Chemistry

Melting points (°C) were determined in open capillaries on a Gallenkamp melting point apparatus (Sanyo Gallenkamp, Southborough, UK) and were uncorrected. Precoated silica gel plates (silica gel 0.25 mm, 60 GF254, Merck, Germany) were used for thin layer chromatography, dichloromethane/methanol (9.5 : 0.5, v/v) mixture was used as a developing solvent system and the spots were visualized by ultraviolet light and/or iodine. Infrared spectra were recorded in KBr discs using IR-470 Shimadzu spectrometer (Shimadzu, Tokyo, Japan). NMR spectra in DMSO-d₆ were recorded on Bruker Ac-500 UltraShield NMR spectrometer (Bruker, Flawil, Switzerland; δ, ppm) at 500 MHz, using TMS as internal standard and peak multiplicities are designed as follows: s, singlet; d, doublet; t, triplet; m, multiplet. Elemental analyses were performed on Carlo Erba 1108 Elemental Analyzer (Heraeus, Hanau, Germany). All compounds gave results within ± 0.4% of the theoretical values.

* Corresponding author: e-mail: mmsghorab@gmail.com; phone: +966 534292860; fax: +966 01 4670560

4-(2-(4-Bromophenyl)-2-oxoethylamino)benzenesulfonamide (**3**)

A mixture of sulfanilamide **1** (1.72 g, 0.01 mol) and 4-bromophenacylbromide **2** (2.77 g, 0.01 mol) was refluxed in *N,N'*-dimethylformamide (20 mL) in the presence of catalytic amount of triethylamine for 6 h. The solid obtained was filtered off and recrystallized from ethanol to give **3**. Yield 89%, m.p. 232.6°C. IR (KBr, cm^{-1}): 3358, 3255 (NH, NH₂), 3100 (CH arom.), 2970, 2863 (CH aliph.), 1685 (C=O), 1381, 1157 (SO₂). ¹H-NMR (DMSO-*d*₆, δ , ppm): 4.7 (s, 2H, CH₂), 6.6 (s, 1H, NH, D₂O exchangeable), 6.7, 7.5 (2d, 4H, Ar-H, AB system, *J* = 7.1 Hz), 7.8, 8.0 (2d, 4H, Ar-H, AB system, *J* = 6.9 Hz). ¹³C-NMR (DMSO-*d*₆, δ , ppm): 49.4, 111.4 (2), 127.1, 127.7, 129.9 (2), 130.7 (2), 131.8 (2), 133.9, 150.8, 195.3. Analysis: calcd. for C₁₄H₁₃BrN₂O₃S (369.23): C, 45.54; H, 3.55; N, 7.59%; found: C, 45.54; H, 3.31; N, 7.24%.

4-(2-Amino-4-(4-bromophenyl)-3-cyano-1H-pyrrol-1-yl)benzenesulfonamide (**5**)

A mixture of compound **3** (3.69 g, 0.01 mol) and malononitrile (0.66 g, 0.01 mol) in ethanol (20 mL) containing sodium ethoxide (0.5 g) was refluxed for 8 h. The reaction mixture was cooled and acidified with dil. HCl. The solid obtained was filtered off and recrystallized from dioxane to give **5**. Yield 78%, m.p. 221.2°C. IR (KBr, cm^{-1}): 3419, 3344, 3238 (NH₂), 3095 (CH arom.), 2187 (C=N), 1635 (C=N), 1342, 1176 (SO₂). ¹H-NMR (DMSO-*d*₆, δ , ppm): 6.1 (s, 2H, NH₂, D₂O exchangeable), 7.0 (s, 1H, CH pyrrole), 7.5–7.9 (m, 10H, Ar-H + SO₂NH₂). ¹³C-NMR (DMSO-*d*₆, δ , ppm): 70.5, 113.5, 117.5, 119.5, 121.3 (2), 125.2, 127.3, 131.2 (2), 131.6 (2), 132.3 (2), 139.5, 142.9, 148.5. Analysis: calcd. for C₁₇H₁₃BrN₄O₂S (417.28): C, 48.93; H, 3.14; N, 13.43%; found: C, 48.71; H, 3.50; N, 13.16%.

Ethyl N-4-(4-bromophenyl)-3-cyano-1-(4-sulfamoylphenyl)-1H-pyrrol-2-ylformimidate (**6**)

A mixture of compound **5** (4.17 g, 0.01 mol) and triethylorthoformate (20 mL) was refluxed for 6 h. The reaction mixture was cooled and then poured onto ice/water. The formed residue was recrystallized from ethanol to give **6**. Yield 78%, m.p. 160.2°C. IR (KBr, cm^{-1}): 3151, 3136 (NH₂), 2987, 2865 (CH aliph.), 2206 (C≡N), 1629 (C=N), 1354, 1155 (SO₂). ¹H-NMR (DMSO-*d*₆, δ , ppm): 1.0 (t, 3H, CH₃), 4.3 (q, 2H, CH₂), 7.6–7.9 (m, 8H, Ar-H), 8.1 (s, 1H, CH pyrrole), 8.5 (s, 2H, SO₂NH₂, D₂O exchangeable), 8.7 (s, 1H, N=CH). ¹³C-NMR (DMSO-*d*₆, δ , ppm): 13.6, 63.6, 79.1, 116.8, 117.4,

120.3, 122.8 (2), 125.4, 127.7, 127.8 (2), 131.5 (2), 131.8 (2), 138.5, 140.6, 145.3, 161.9. Analysis: calcd. for C₂₀H₁₇BrN₄O₃S (473.34): C, 50.75; H, 3.62; N, 11.84%; found: C, 50.48; H, 3.91; N, 11.54%.

4-(3-Amino-5-(4-bromophenyl)-4-imino-3,4-dihydropyrrolo[2,3-d]pyrimidin-7-yl)benzenesulfonamide (**8**)

A mixture of **6** (4.73 g, 0.01 mol) and hydrazine hydrate (1.0 g, 0.02 mol) was stirred in ethanol (20 mL) at room temperature for 1 h, the solid formed was filtered and recrystallized from ethanol to give **8**. Yield 91%, m.p. 184.5°C. IR (KBr, cm^{-1}): 3294, 3230, 3150 (NH, NH₂), 1639 (C=N), 1375, 1163 (SO₂). ¹H-NMR (DMSO-*d*₆, δ , ppm): 5.6 (s, 2H, NH₂, D₂O exchangeable), 6.9 (s, 1H, CH pyrrole), 7.4–7.9 (m, 10H, Ar-H + SO₂NH₂), 8.0 (s, 1H, CH pyrimidine), 8.1 (s, 1H, NH, D₂O exchangeable). ¹³C-NMR (DMSO-*d*₆, δ , ppm): 103.7, 119.8, 120.1, 121.1 (2), 124.0, 126.7, 130.8 (2), 131.1 (2), 132.9 (2), 139.5, 141.9, 142.8, 147.6, 152.9. Analysis: calcd. for C₁₈H₁₅BrN₆O₂S (459.32): C, 47.07; H, 3.29; N, 18.30%; found: C, 47.39; H, 3.51; N, 18.64%.

4-(9-(4-Bromophenyl)-7H-pyrrolo[3,2-e][1,2,4]triazolo[1,5-c]pyrimidin-7-yl)benzenesulfonamide (**9**)

A solution of **8** (4.59 g, 0.01 mol) in formic acid (20 mL) was refluxed for 6 h, and the reaction mixture was then concentrated. The separated crystals were recrystallized from ethanol to give **9**. Yield 82%, m.p. 347.2°C. IR (KBr, cm^{-1}): 3402, 3267 (NH₂), 3082 (CH arom.), 1620 (C=N), 1370, 1165 (SO₂). ¹H-NMR (DMSO-*d*₆, δ , ppm): 7.5 (s, 1H, CH pyrrole), 7.6–8.2 (m, 10H, Ar-H + SO₂NH₂), 8.6 (s, 1H, CH triazole), 9.6 (s, 1H, CH pyrimidine). ¹³C-NMR (DMSO-*d*₆, δ , ppm): 104.1, 117.1, 120.0 (2), 124.7, 124.9 (2), 126.8, 129.2 (2), 131.3 (2), 131.7, 136.5, 139.2, 141.3, 142.7, 148.4, 154.3. Analysis: calcd. for C₁₉H₁₃BrN₆O₂S (469.31): C, 48.62; H, 2.79; N, 17.91%; found: C, 48.96; H, 2.49; N, 17.59%.

4-(9-(4-Bromophenyl)-2-(cyanomethyl)-7H-pyrrolo[3,2-e][1,2,4]triazolo[1,5-c]pyrimidin-7-yl)benzenesulfonamide (**10**)

A mixture of **8** (4.59 g, 0.01 mol) and ethylcyanoacetate (1.13 g, 0.01 mol) was refluxed for 10 h, in ethanol (20 mL) containing sodium ethoxide (0.23 g, 0.01 mol), the reaction mixture was then acidified with dil. HCl. The obtained solid was recrystallized from dioxane to give **10**. Yield 79%,

m.p. 301.2°C. IR (KBr, cm^{-1}): 3344, 3251 (NH_2), 3062 (CH arom.), 2922, 2861 (CH aliph.), 2270 ($\text{C}\equiv\text{N}$), 1625 ($\text{C}=\text{N}$), 1365, 1161 (SO_2). $^1\text{H-NMR}$ (DMSO-d_6 , δ , ppm): 4.5 (s, 2H, CH_2), 7.5 (s, 1H, CH pyrrole), 7.6–8.3 (m, 10H, Ar-H + SO_2NH_2), 9.6 (s, 1H, CH pyrimidine). $^{13}\text{C-NMR}$ (DMSO-d_6 , δ , ppm): 18.0, 109.1, 117.1, 120.1, 124.6 (2), 125.0, 126.8 (2), 129.3, 131.3 (2), 131.6 (2), 136.3, 139.1, 141.5, 142.7, 149.4, 158.4, 164.2. Analysis: calcd. for $\text{C}_{21}\text{H}_{14}\text{BrN}_7\text{O}_2\text{S}$ (508.35): C, 49.62; H, 2.78; N, 19.29%; found: C, 49.38; H, 2.46; N, 19.58%.

N-(5-(4-bromophenyl)-4-imino-7-(4-sulfamoylphenyl)-4H-pyrrolo[2,3-d]pyrimidin-3-(7H)-yl)acetamide (11)

A solution of **8** (4.59 g, 0.01 mol) in acetic anhydride (20 mL) was refluxed for 2 h. The solid obtained was recrystallized from acetic acid to give **11**. Yield 68%, m.p. 337.5°C. IR (KBr, cm^{-1}): 3420, 3280 (NH , NH_2), 3082 (CH arom.), 2940, 2860 (CH aliph.), 1710 ($\text{C}=\text{O}$), 1625 ($\text{C}=\text{N}$), 1348, 1161 (SO_2). $^1\text{H-NMR}$ (DMSO-d_6 , δ , ppm): 2.1 (s, 3H, COCH_3), 7.4 (s, 1H, CH pyrrole), 7.6–8.4 (m, 10H, Ar-H + SO_2NH_2), 8.5 (s, 1H, CH pyrimidine), 9.6 (s, 1H, NH imino, D_2O exchangeable), 12.2 (s, 1H, NHCO , D_2O exchangeable). $^{13}\text{C-NMR}$ (DMSO-d_6 , δ , ppm): 23.2, 103.6, 117.2, 120.0, 124.2 (2), 124.3, 128.8, 129.2 (2), 131.5 (2), 137.3 (2), 140.7, 141.2, 148.8, 163.6, 168.9, 172.0. Analysis: calcd. for $\text{C}_{20}\text{H}_{17}\text{BrN}_6\text{O}_3\text{S}$ (501.36): C, 47.91; H, 3.42; N, 16.76%; found: C, 47.66; H, 3.68; N, 16.50%.

General procedure for the synthesis of compounds (12–14)

A mixture of compound **8** (4.59 g, 0.01 mol) and benzoyl chloride derivatives (0.01 mol) in pyridine (20 mL) was refluxed for 6 h. The reaction mixture was poured onto ice water. The formed residue was recrystallized from dioxane to give **12–14**, respectively.

N-(5-(4-bromophenyl)-4-imino-7-(4-sulfamoylphenyl)-4H-pyrrolo[2,3-d]pyrimidin-3-(7H)-yl)benzamide (12)

Yield 68%, m.p. 247.8°C. IR (KBr, cm^{-1}): 3217, 3186, 3130 (NH , NH_2), 3093 (CH arom.), 1683 ($\text{C}=\text{O}$), 1591 ($\text{C}=\text{N}$), 1393, 1174 (SO_2). $^1\text{H-NMR}$ (DMSO-d_6 , δ , ppm): 7.4 (s, 1H, CH pyrrole), 7.5–8.4 (m, 15H, Ar-H + SO_2NH_2), 9.5 (s, 1H, CH pyrimidine), 9.6 (s, 1H, NH imino, D_2O exchangeable), 12.8 (s, 1H, NHCO , D_2O exchangeable). $^{13}\text{C-NMR}$ (DMSO-d_6 , δ , ppm): 104.8, 117.6, 120.6, 123.7 (2), 124.5, 126.5, 127.1 (2), 128.6 (2), 129.7 (2), 131.4 (2), 132.8 (2), 133.2, 133.4, 136.1, 136.4,

143.7, 162.9, 165.5, 167.2. Analysis: calcd. for $\text{C}_{25}\text{H}_{19}\text{BrN}_6\text{O}_3\text{S}$ (563.43): C, 53.29; H, 3.40; N, 14.92% found: C, 53.50; H, 3.68; N, 14.66%.

N-(5-(4-bromophenyl)-4-imino-7-(4-sulfamoylphenyl)-4H-pyrrolo[2,3-d]pyrimidin-3-(7H)-yl)-4-chlorobenzamide (13)

Yield 71%, m.p. 258.6°C. IR (KBr, cm^{-1}): 3220, 3165 (NH , NH_2), 3056 (CH arom.), 1683 ($\text{C}=\text{O}$), 1591 ($\text{C}=\text{N}$), 1391, 1176 (SO_2), 761 (C-Cl). $^1\text{H-NMR}$ (DMSO-d_6 , δ , ppm): 7.5 (s, 1H, CH pyrrole), 7.6–7.9 (m, 14H, Ar-H + SO_2NH_2), 8.0 (s, 1H, CH pyrimidine), 9.7 (s, 1H, NH imino, D_2O exchangeable), 12.9 (s, 1H, NHCO , D_2O exchangeable). $^{13}\text{C-NMR}$ (DMSO-d_6 , δ , ppm): 109.8, 119.3, 121.4, 123.3 (2), 125.2, 128.8, 129.5 (2), 130.3 (2), 130.8 (2), 131.0 (2), 134.0 (2), 134.9, 136.1, 136.9, 137.7, 146.1, 161.7, 165.1, 166.4. Analysis: calcd. for $\text{C}_{25}\text{H}_{18}\text{BrClN}_6\text{O}_3\text{S}$ (596.00): C, 50.22; H, 3.03; N, 14.06%; found: C, 50.01; H, 3.28; N, 14.36%.

N-(5-(4-bromophenyl)-4-imino-7-(4-sulfamoylphenyl)-4H-pyrrolo[2,3-d]pyrimidin-3-(7H)-yl)-3,4,5-trimethoxybenzamide (14)

Yield 73%, m.p. 260.8°C. IR (KBr, cm^{-1}): 3323, 3300, 3277 (NH , NH_2), 3081 (CH arom.), 2946, 2871 (CH aliph.), 1656 ($\text{C}=\text{O}$), 1593 ($\text{C}=\text{N}$), 1391, 1163 (SO_2). $^1\text{H-NMR}$ (DMSO-d_6 , δ , ppm): 3.7, 3.9 (2s, 9H, 3OCH_3), 7.0 (s, 1H, CH pyrrole), 7.5–8.4 (m, 12H, Ar-H + SO_2NH_2), 8.5 (s, 1H, CH pyrimidine), 9.5 (s, 1H, NH imino, D_2O exchangeable), 12.9 (s, 1H, NHCO , D_2O exchangeable). $^{13}\text{C-NMR}$ (DMSO-d_6 , δ , ppm): 55.9 (2), 60.5, 103.7 (2), 108.3, 117.2, 119.3, 120.0 (2), 124.5, 125.6, 126.8 (2), 129.3, 131.8 (2), 136.2 (2), 139.3, 141.3, 142.5, 142.6, 148.6 (2), 152.5, 155.1, 162.0. Analysis: calcd. for $\text{C}_{28}\text{H}_{25}\text{BrN}_6\text{O}_6\text{S}$ (652.07): C, 51.46; H, 3.86; N, 12.86%; found: C, 51.81; H, 3.57; N, 12.61%.

4-(9-(4-Bromophenyl)-2-thioxo-2H-pyrrolo[3,2-e][1,2,4]triazolo[1,5-c]pyrimidin-7(3H)-yl)benzenesulfonamide (15)

A mixture of **8** (4.59 g, 0.01 mol), carbon disulfide (2 mL) in pyridine (20 mL) was refluxed for 12 h, the reaction mixture was cooled and poured onto ice water. The separated solid was filtered off and recrystallized from acetic acid to give **15**. Yield 82%, m.p. 315.1°C. IR (KBr, cm^{-1}): 3346, 3311, 3248 (NH , NH_2), 3095 (CH arom.), 1581 ($\text{C}=\text{N}$), 1359, 1159 (SO_2), 1242 ($\text{C}=\text{S}$). $^1\text{H-NMR}$ (DMSO-d_6 , δ , ppm): 7.4 (s, 1H, CH pyrrole), 7.5–8.0 (m, 10H, Ar-H + SO_2NH_2), 9.6 (s, 1H, NH, D_2O exchangeable). $^{13}\text{C-NMR}$ (DMSO-d_6 , δ , ppm): 110.2, 117.0, 119.2, 121.9

(2), 124.6, 127.0, 129.9 (2), 130.3 (2), 132.2 (2), 138.0, 138.1, 142.8, 143.4, 153.3, 178.9. Analysis: calcd. for $C_{19}H_{13}BrN_6O_2S_2$ (501.38): C, 45.52; H, 2.61; N, 16.76%; found: C, 45.19; H, 2.38; N, 16.98%.

4-(5-(4-Bromophenyl)-4-imino-3-(propan-2-ylideneamino)-3H-pyrrolo[2,3-d]pyrimidin-7(4H)-yl)benzenesulfonamide (16)

A mixture of **8** (4.59 g, 0.01 mol) and dry acetone (30 mL) was refluxed for 18 h; on cooling the reaction mixture was concentrated and the product obtained was filtered and recrystallized from a mixture of acetic acid and ethanol (1 : 2, v/v) to give **16**. Yield 78%, m.p. 228.2°C. IR (KBr, cm^{-1}): 3365, 3246, 3176 (NH, NH_2), 3100 (CH arom.), 2972, 2927 (CH aliph.), 1595 (C=N), 1381, 1161 (SO_2). 1H -NMR (DMSO- d_6 , δ , ppm): 1.1 (s, 6H, 2 CH_3), 6.8 (s, 1H, CH pyrrole), 7.1–8.0 (m, 10H, Ar-H + SO_2NH_2), 8.1 (s, 1H, CH pyrimidine), 8.2 (s, 1H, NH, D_2O exchangeable). ^{13}C -NMR (DMSO- d_6 , δ , ppm): 19.8, 27.1, 100.0, 118.8, 119.6, 124.0 (2), 124.4, 126.6, 129.7 (2), 131.2 (2), 132.2 (2), 140.2, 142.2, 147.3, 154.6, 166.2, 208.3. Analysis: calcd. for $C_{21}H_{19}BrN_6O_2S$ (499.38): C, 50.51; H, 3.83; N, 16.83%; found: C, 50.27; H, 3.59; N, 16.55%.

General procedure for the synthesis of compounds (17–19)

A mixture of **8** (4.59 g, 0.01 mol) and sulfonyl chloride derivatives (0.01 mol) in dry benzene (30 mL) containing pyridine (1 mL) was refluxed for 8 h. The solid obtained was recrystallized from ethanol to give **17–19**, respectively.

4-(5-(4-Bromophenyl)-4-imino-3-(sulfamoylphenyl)-3,4-dihydropyrrolo[2,3-d]pyrimidin-7-yl)benzenesulfonamide (17)

Yield 74%, m.p. 188.8°C. IR (KBr, cm^{-1}): 3340, 3219, 3219 (NH, NH_2), 3066 (CH arom.), 1618 (C=N), 1326, 1161 (SO_2). 1H -NMR (DMSO- d_6 , δ , ppm): 7.3 (s, 1H, CH pyrrole), 7.4–8.3 (m, 15H, Ar-H + SO_2NH_2), 8.5 (s, 1H, CH pyrimidine), 8.9 (s, 1H, NH imino, D_2O exchangeable), 12.7 (s, 1H, $NHSO_2$, D_2O exchangeable). ^{13}C -NMR (DMSO- d_6 , δ , ppm): 111.4, 119.2, 124.8, 125.4 (2), 125.6, 126.9, 127.6 (2), 128.3 (2), 128.9 (2), 130.3 (2), 130.6 (2), 131.6, 132.0, 142.6, 145.4, 148.2, 151.9, 152.4. Analysis: calcd. for $C_{24}H_{19}BrN_6O_4S_2$ (598.00): C, 48.08; H, 3.19; N, 14.02%; found: C, 47.79; H, 3.52; N, 14.32%.

4-(5-(4-Bromophenyl)-4-imino-3-(sulfamoylphenyl)-3,4-dihydropyrrolo[2,3-d]pyrimidin-7-yl)-4-methylbenzenesulfonamide (18)

Yield 69%, m.p. 324.6°C. IR (KBr, cm^{-1}): 3331, 3263, 3171 (NH, NH_2), 3084 (CH arom.), 2932, 2867 (CH aliph.), 1595 (C=N), 1332, 1172 (SO_2). 1H -NMR (DMSO- d_6 , δ , ppm): 2.2 (s, 3H, CH_3), 6.7 (s, 1H, CH pyrrole), 7.0–7.9 (m, 14H, Ar-H + SO_2NH_2), 8.0 (s, 1H, CH pyrimidine), 8.1 (s, 1H, NH imino, D_2O exchangeable), 8.6 (s, 1H, $NHSO_2$, D_2O exchangeable). ^{13}C -NMR (DMSO- d_6 , δ , ppm): 20.7, 100.0, 118.6, 121.4, 124.8 (2), 125.4, 126.8, 126.9 (2), 128.0 (2), 130.7 (2), 130.8 (2), 132.0 (2), 138.2, 142.9, 143.2, 145.1, 145.3, 147.5, 152.3. Analysis: calcd. for $C_{25}H_{21}BrN_6O_4S_2$ (613.51): C, 48.94; H, 3.45; N, 13.70%; found: C, 48.60; H, 3.71; N, 13.47%.

4-Bromo-N-(5-(4-bromophenyl)-4-imino-7-(4-sulfamoylphenyl)-4H-pyrrolo[2,3-d]pyrimidin-3-(7H)-yl)benzenesulfonamide (19)

Yield 62%, m.p. 296.6°C. IR (KBr, cm^{-1}): 3405, 3332, 3261 (NH, NH_2), 3084 (CH arom.), 1595 (C=N), 1384, 1174 (SO_2). 1H -NMR (DMSO- d_6 , δ , ppm): 6.6 (s, 1H, CH pyrrole), 7.4–8.0 (m, 14H, Ar-H + SO_2NH_2), 8.1 (s, 1H, CH pyrimidine), 8.6 (s, 1H, NH imino, D_2O exchangeable), 8.8 (s, 1H, $NHSO_2$, D_2O exchangeable). ^{13}C -NMR (DMSO- d_6 , δ , ppm): 100.0, 118.6, 121.4, 121.6 (2), 124.8, 126.2, 126.9, 127.0 (2), 127.6 (2), 130.7 (2), 130.8 (2), 132.0 (2), 138.1, 143.3, 144.2, 145.1, 147.5, 152.4. Analysis: calcd. for $C_{24}H_{18}Br_2N_6O_4S_2$ (678.38): C, 42.49; H, 2.67; N, 12.39%; found: C, 42.76; H, 2.48; N, 12.08%.

General procedure for the synthesis of compounds (20 and 21)

A mixture of **8** (4.59 g, 0.01 mol) and isothiocyanate derivatives (0.01 mol) in absolute ethanol (20 mL) was refluxed for 6 h, the reaction mixture was concentrated and the separated crystals were recrystallized from dioxane to give **20** and **21**, respectively.

4-(5-(4-Bromophenyl)-3-(3-butylthioureido)-4-imino-3,4-dihydropyrrolo[2,3-d]pyrimidin-7-yl)benzenesulfonamide (20)

Yield 59%, m.p. 245.6°C. IR (KBr, cm^{-1}): 3415, 3390 (NH, NH_2), 3084 (CH arom.), 2958, 2872 (CH aliph.), 1637 (C=N), 1340, 1182 (SO_2), 1265 (C=S). 1H -NMR (DMSO- d_6 , δ , ppm): 0.9 (s, 3H, CH_3), 1.3 (m, 2H, CH_2CH_3), 1.4–1.5 (m, 2H, CH_2CH_2NH), 3.2 (t, 2H, CH_2NH), 6.9 (s, 1H, CH pyrrole), 7.4–8.0 (m, 10H, Ar-H + SO_2NH_2), 8.1 (s, 1H, CH pyrimidine), 8.3 (s, 1H, NH imino, D_2O exchangeable), 9.1 (s, 2H, 2NH, D_2O exchangeable). ^{13}C -NMR (DMSO- d_6 , δ , ppm): 13.4, 19.6,

31.1, 44.1, 102.3, 119.7, 122.5, 123.7 (2), 124.5, 126.7, 129.4 (2), 131.7 (2), 132.9 (2), 134.8, 139.5, 148.6, 157.6, 166.2, 189.2. Analysis: calcd. for $C_{23}H_{24}BrN_7O_4S_2$ (574.52): C, 48.08; H, 4.21; N, 17.07%; found: C, 48.33; H, 4.49; N, 17.36%.

4-(5-(4-Bromophenyl)-4-imino-3-(3-phenylthio-ureido)-3,4-dihydropyrrolo[2,3-d]pyrimidin-7-yl)benzenesulfonamide (21)

Yield 74%, m.p. 83.6°C. IR (KBr, cm^{-1}): 3215, 3196, 3116 (NH, NH_2), 3049 (CH arom.), 1597 (C=N), 1375, 1157 (SO_2), 1292 (C=S). 1H -NMR (DMSO- d_6 , δ , ppm): 7.1 (s, 1H, CH pyrrole), 7.3–7.9 (m, 15H, Ar-H + SO_2NH_2), 8.1 (s, 1H, CH pyrimidine), 8.4 (s, 1H, NH imino, D_2O exchangeable), 11.0 (s, 2H, 2NH, D_2O exchangeable). ^{13}C -NMR (DMSO- d_6 , δ , ppm): 102.7, 118.1, 121.5, 122.5 (2), 123.5, 124.9, 126.8, 127.6 (2), 128.7 (2), 130.5 (2), 131.3 (2), 135.3 (2), 139.9, 140.8, 142.1, 147.9, 157.6, 162.2, 187.1. Analysis: calcd. for $C_{25}H_{20}BrN_7O_2S_2$ (594.51): C, 50.51; H, 3.39; N, 16.49%; found: C, 50.21; H, 3.10; N, 16.87%.

General procedure for the synthesis of compounds (22–29)

A mixture of **8** (4.59 g, 0.01 mol) and the corresponding aromatic aldehydes (0.01 mol) was refluxed in acetic acid (30 mL) for 5 h, the reaction mixture was then concentrated and the separated solid crystals were recrystallized from dioxane to give **22–29**, respectively.

4-(5-(4-Bromophenyl)-4-imino-3-(4-methylbenzylideneamino)-3,4-dihydropyrrolo[2,3-d]pyrimidin-7-yl)benzenesulfonamide (22)

Yield 88%, m.p. 314.1°C. IR (KBr, cm^{-1}): 3321, 3191, 3136 (NH, NH_2), 1624 (C=N), 1330, 1161 (SO_2). 1H -NMR (DMSO- d_6 , δ , ppm): 2.2 (s, 3H, CH_3), 7.2 (s, 1H, CH pyrrole), 7.3–8.2 (m, 14H, Ar-H + SO_2NH_2), 8.4 (s, 1H, CH pyrimidine), 9.5 (s, 1H, NH imino, D_2O exchangeable), 9.9 (s, 1H, N=CH). ^{13}C -NMR (DMSO- d_6 , δ , ppm): 21.0, 103.8, 117.2, 122.6, 123.2 (2), 124.4, 126.9, 128.8 (2), 129.3 (2), 129.5 (2), 130.5 (2), 131.3, 133.9 (2), 136.1, 139.2, 141.3, 142.5, 145.1, 163.2, 192.5. Analysis: calcd. for $C_{26}H_{21}BrN_6O_2S$ (561.45): C, 55.62; H, 3.77; N, 14.97%; found: C, 55.96; H, 3.44; N, 14.66%.

4-(5-(4-Bromophenyl)-3-(4-hydroxybenzylideneamino)-4-imino-3,4-dihydropyrrolo[2,3-d]pyrimidin-7-yl)benzenesulfonamide (23)

Yield 82%, m.p. >350°C. IR (KBr, cm^{-1}): 3470 (OH), 3385, 3321, 3196 (NH, NH_2), 1593 (C=N),

1381, 1159 (SO_2). 1H -NMR (DMSO- d_6 , δ , ppm): 6.9 (s, 1H, CH pyrrole), 7.5–8.1 (m, 14H, Ar-H + SO_2NH_2), 8.5 (s, 1H, NH imino, D_2O exchangeable), 8.6 (s, 1H, CH pyrimidine), 9.5 (s, 1H, N=CH), 10.0 (s, 1H, OH, D_2O exchangeable). ^{13}C -NMR (DMSO- d_6 , δ , ppm): 103.7, 115.7 (2), 117.6, 120.0, 120.6 (2), 123.2, 124.5, 126.8, 128.8 (2), 129.4 (2), 130.5 (2), 131.4 (2), 131.8, 139.3, 142.6, 149.3, 159.7, 161.0, 162.9. Analysis: calcd. for $C_{25}H_{19}BrN_6O_3S$ (563.43): C, 53.29; H, 3.40; N, 14.92%; found: C, 53.55; H, 3.71; N, 14.60%.

4-(5-(4-Bromophenyl)-4-imino-3-(4-methoxybenzylideneamino)-3,4-dihydropyrrolo[2,3-d]pyrimidin-7-yl)benzenesulfonamide (24)

Yield 79%, m.p. 253.0°C. IR (KBr, cm^{-1}): 3292, 3230, 3101 (NH, NH_2), 2970, 2841 (CH aliph.), 1591 (C=N), 1340, 1157 (SO_2). 1H -NMR (DMSO- d_6 , δ , ppm): 3.7 (s, 3H, OCH_3), 6.8 (s, 1H, CH pyrrole), 6.9–8.1 (m, 14H, Ar-H + SO_2NH_2), 8.2 (s, 1H, CH pyrimidine), 9.6 (s, 1H, NH, D_2O exchangeable), 9.9 (s, 1H, N=CH). ^{13}C -NMR (DMSO- d_6 , δ , ppm): 55.0, 113.6, 114.4 (2), 118.9, 119.6, 121.0 (2), 124.4, 126.6, 127.9, 129.6 (2), 131.7 (2), 132.3 (2), 133.7 (2), 139.6, 140.0, 142.1, 145.3, 148.7, 158.9, 160.1. Analysis: calcd. for $C_{26}H_{21}BrN_6O_3S$ (577.45): C, 54.08; H, 3.67; N, 14.55%; found: C, 54.39; H, 3.29; N, 14.26%.

4-(3-Benzo[d][1,3]dioxol-5-ylmethyleneamino)-5-(4-bromophenyl)-4-imino-3,4-dihydropyrrolo[2,3-d]pyrimidin-7-yl)benzenesulfonamide (25)

Yield 66%, m.p. 310.4°C. IR (KBr, cm^{-1}): 3385, 3261, 3141 (NH, NH_2), 2976, 2895 (CH aliph.), 1595 (C=N), 1363, 1161 (SO_2). 1H -NMR (DMSO- d_6 , δ , ppm): 6.1 (s, 2H, CH_2), 6.9 (s, 1H, CH pyrrole), 7.0–8.1 (m, 13H, Ar-H + SO_2NH_2), 8.4 (s, 1H, CH pyrimidine), 9.5 (s, 1H, NH imino, D_2O exchangeable), 9.8 (s, 1H, N=CH). ^{13}C -NMR (DMSO- d_6 , δ , ppm): 101.6, 108.5, 117.3, 118.9, 119.6, 121.8, 123.7 (2), 124.4, 124.5, 126.8, 128.5, 129.4 (2), 131.7 (2), 132.3 (2), 136.1, 139.9, 145.3, 147.7, 148.7, 149.3, 163.0, 190.9. Analysis: calcd. for $C_{26}H_{19}BrN_6O_4S$ (591.44): C, 52.80; H, 3.24; N, 14.21%; found: C, 52.48; H, 3.56; N, 14.50%.

4-(5-(4-Bromophenyl)-3-(4-chlorobenzylideneamino)-4-imino-3,4-dihydropyrrolo[2,3-d]pyrimidin-7-yl)benzenesulfonamide (26)

Yield 83%, m.p. 375.0°C. IR (KBr, cm^{-1}): 3421, 3271 (NH, NH_2), 3051 (CH arom.), 1595 (C=N), 1334, 1161 (SO_2), 727 (C-Cl). 1H -NMR (DMSO- d_6 , δ , ppm): 7.4 (s, 1H, CH pyrrole), 7.5–8.3 (m, 14H, Ar-H + SO_2NH_2), 8.4 (s, 1H, CH

pyrimidine), 8.5 (s, 1H, NH imino, D₂O exchangeable), 9.6 (s, 1H, N=CH). ¹³C-NMR (DMSO-d₆, δ, ppm): 104.6, 118.6, 121.2, 122.0 (2), 123.9, 124.6, 126.8 (2), 128.8 (2), 129.4 (2), 131.4 (2), 133.5, 134.6 (2), 136.0, 136.4, 139.3, 143.1, 162.2, 167.2. Analysis: calcd. for C₂₅H₁₈BrClN₆O₂S (581.87): C, 51.60; H, 3.12; N, 14.44%; found: C, 51.35; H, 3.49; N, 14.12%.

4-(5-(4-Bromophenyl)-4-imino-3-(4-nitrobenzylideneamino)-3,4-dihydropyrrolo[2,3-d]pyrimidin-7-yl)benzenesulfonamide (27)

Yield 75%, m.p. 375.5°C. IR (KBr, cm⁻¹): 3350, 3271 (NH, NH₂), 3072 (CH arom.), 1625 (C=N), 1346, 1163 (SO₂). ¹H-NMR (DMSO-d₆, δ, ppm): 7.4 (s, 1H, CH pyrrole), 7.5–8.2 (m, 14H, Ar-H + SO₂NH₂), 8.4 (s, 1H, CH pyrimidine), 9.6 (s, 1H, NH imino, D₂O exchangeable), 10.1 (s, 1H, N=CH). ¹³C-NMR (DMSO-d₆, δ, ppm): 103.9, 117.7, 122.6, 123.4 (2), 124.2, 124.6 (2), 126.8, 129.3 (2), 130.2 (2), 130.6 (2), 131.7 (2), 136.7, 137.0, 138.1, 143.0, 144.3, 151.2, 162.8, 192.3. Analysis: calcd. for C₂₅H₁₈BrN₇O₂S (592.42): C, 50.68; H, 3.06; N, 16.55%; found: C, 50.37; H, 3.30; N, 16.82%.

4-(5-(4-Bromophenyl)-4-imino-3-(2,3,4-trimethoxybenzylideneamino)-3,4-dihydropyrrolo[2,3-d]pyrimidin-7-yl)benzenesulfonamide (28)

Yield 71%, m.p. 275.5°C. IR (KB, cm⁻¹): 3371, 3298, 3221 (NH, NH₂), 2939, 2839 (CH aliph.), 1624 (C=N), 1338, 1165 (SO₂). ¹H-NMR (DMSO-d₆, D₂O, δ, ppm): 3.7, 3.8 (2s, 9H, 3OCH₃), 6.7 (s, 1H, CH pyrrole), 7.3–8.1 (m, 12H, Ar-H + SO₂NH₂), 8.4 (s, 1H, CH pyrimidine), 8.6 (s, 1H, NH imino, D₂O exchangeable), 9.5 (s, 1H, N=CH). ¹³C-NMR (DMSO-d₆, δ, ppm): 55.6 (2), 59.2, 104.6, 106.8, 107.8, 119.6, 122.1, 124.3 (2), 124.4, 124.8, 126.7, 130.2 (2), 130.8 (2), 133.1 (2), 136.1, 137.2, 139.8, 142.6, 147.3, 154.0, 157.3, 163.4, 163.8. Analysis: calcd. for C₂₈H₂₅BrN₆O₅S (637.50): C, 52.75; H, 3.95; N, 13.18%; found: C, 52.40; H, 3.64; N, 13.55%.

4-(5-(4-Bromophenyl)-4-imino-3-(thiophen-2-ylmethyleneamino)-3,4-dihydropyrrolo[2,3-d]pyrimidin-7-yl)benzenesulfonamide (29)

Yield 56%, m.p. 334.2°C. IR (KBr, cm⁻¹): 3321, 3195 (NH, NH₂), 3055 (CH arom.), 1627 (C=N), 1327, 1159 (SO₂). ¹H-NMR (DMSO-d₆, δ, ppm): 7.0 (s, 1H, CH pyrrole), 7.1–8.1 (m, 13H, Ar-H + SO₂NH₂), 8.4 (s, 1H, CH pyrimidine), 9.5 (s, 1H, NH imino, D₂O exchangeable), 11.6 (s, 1H, N=CH). ¹³C-NMR (DMSO-d₆, δ, ppm): 103.6, 119.6, 120.0,

123.6 (2), 124.4, 124.6, 126.6, 126.8, 128.3, 128.9, 129.3 (2), 130.7 (2), 136.1 (2), 139.2, 141.5, 142.6, 149.2, 159.4, 184.2. Analysis: calcd. for C₂₃H₁₇BrN₆O₂S₂ (553.45): C, 49.91; H, 3.10; N, 15.18%; found: C, 49.66; H, 3.43; N, 15.55%.

Molecular docking

All the molecular modeling studies were carried out on an Intel Pentium 1.6 GHz processor, 512 MB memory with Windows XP operating system using Molecular Operating Environment (MOE, 10.2008) software. All the minimizations were performed with MOE until a RMSD gradient of 0.05 kcal mol⁻¹Å⁻¹ with MMFF94X force field and the partial charges were automatically calculated. The X-ray crystallographic structure of c-Src complex with its ligand (PDB ID: 1YOL) was obtained from the protein data bank. The enzyme was prepared for docking studies where: (i) Ligand molecule was removed from the enzyme active site. (ii) Hydrogen atoms were added to the structure with their standard geometry. (iii) MOE Alpha Site Finder was used for the active sites search in the enzyme structure and dummy atoms were created from the obtained alpha spheres. (iv) The obtained model was then used in predicting the ligand enzymes interactions at the active site (Table 1).

In vitro antitumor activity

Human tumor breast cell line (MCF7) was used in this study. The cytotoxic activity was measured *in vitro* for the newly synthesized compounds using the sulforhodamine-B stain (SRB) assay using the method of Skehan et al. (18). The *in vitro* anticancer screening was done by the pharmacology unit at the National Cancer Institute, Cairo University. Cells were plated in 96-multiwell plate (104 cells/well) for 24 h before treatment with the compound(s) to allow attachment of cell to the wall of the plate. The tested compounds were dissolved in dimethyl sulfoxide. Different concentrations of the compound under test (10, 25, 50, and 100 μM) were added to the cell monolayer. Triplicate wells were prepared for each individual concentration. Monolayer cells were incubated with the compound(s) for 48 h at 37°C and in atmosphere of 5% CO₂. After 48 h, cells were fixed, washed and stained for 30 min with 0.4% (w/v) SRB dissolved in 1% acetic acid. Excess unbound dye was removed by four washes with 1% acetic acid and attached stain was recovered with Tris EDTA buffer. Color intensity was measured in an ELISA reader. The relation between surviving fraction and drug con-

Table 1. Binding scores and amino acid interactions of the docked compounds on the active site of c-Src.

Compd. No.	S Kcal/mol	Amino acid interactions	Interacting groups	H bond length [Å]
5	-13.6201	Asp 350, Met 343 Ser 347	NH ₂ , N pyrimidine	3.22, 2.22 3.09
6	-12.7631	Asp 350	SO ₂ NH ₂	1.62
8	-10.6603	Met 343, Gln 277	NH ₂ , SO ₂ NH ₂	2.9, 2.51
9	-12.3317	Gln 277	N imidazole	2.78
10	-13.1892	Thr 340	SO ₂ NH ₂	2.27
11	-16.1225	Gln 277, Lys 274	C=NH, C=O	3.03, 2.94
12	-17.7816	Leu 275	NH, NH	1.59, 1.69
13	-17.7263	Met 343, Gln 277	SO ₂ NH ₂ , NH, C=O	1.94, 3.18, 2.50, 2.53
14	-14.4151	Thr 340, Gln 277	SO ₂ NH ₂ , C=O	1.94, 2.79
15	-8.0453	Leu 275	SO ₂ NH ₂	2.83
16	-16.6572	Asp 350, Asp 406	SO ₂ NH ₂ , C=NH	1.63, 1.53
17	-8.8088	Asp 350	SO ₂ NH	2.73
18	-13.2570	Gln 277	C=NH	2.55, 2.57
19	-14.0169	Gln 277	C=NH	2.58, 2.57
20	-15.3704	Leu 275	C=NH	1.81
21	-14.2411	Met 343, Gln 277	SO ₂ NH ₂ , C=NH	2.1, 1.4
22	-12.7915	Gln 277, Asp 350	C=NH, C=NH	2.91, 2.71
23	-13.9751	Thr 340	OH	2.47
24	-14.5953	Leu 275	C=NH	1.87
25	-19.0510	Gln 277	C=NH	2.93, 3.21
26	-18.3491	Met 343	SO ₂ NH ₂ , SO ₂ NH ₂	1.73, 2.75
27	-14.1116	Leu 275	C=NH	2.02
28	-18.5521	Thr 340	SO ₂ NH ₂	2.19
29	-18.3311	Asp 406, Asp 350	C=NH, SO ₂ NH ₂	1.78, 2.07

centration is plotted to get the survival curve for breast tumor cell line after the specified time. The molar concentration required for 50% inhibition of cell viability (IC₅₀) was calculated and compared to the reference drug doxorubicin (CAS, 25316-40-9). The surviving fractions were expressed as the means ± standard error and the results are given in Table 2.

RESULTS AND DISCUSSION

Chemistry

The synthetic procedures adopted to obtain the target compounds are depicted in Schemes 1 and 2. In this work, the reactivity of sulfanilamide **1** towards phenacyl bromide was studied. Thus, interaction of sulfanilamide **1** with 2-bromo-1-(4-bromophenyl)ethanone **2** furnished the corresponding

4-(2-(4-bromophenyl)-2-oxoethylamino)benzenesulfonamide **3**, which upon reaction with malononitrile in refluxing ethanol containing sodium ethoxide yielded the strategic starting material, pyrrole-2-amino-3-carbonitrile **5** (Scheme 1). The formation of compound **5** was assumed to proceed *via* condensation of compound **3** with malononitrile to give the intermediate **4** followed by intramolecular cyclization to give the pyrrole derivative **5**. The structure of compound **3** was proved *via* elemental analysis and spectral data. The IR spectrum of compound **3** revealed the presence of characteristic bands for NH, NH₂, C=O and SO₂. Also ¹H-NMR spectrum indicated the presence of a singlet at 4.7 ppm, which could be assigned to CH₂ group. The IR spectrum of compound **5** exhibited bands for NH₂, CN and SO₂ groups. The ¹H-NMR spectrum of **5** showed signals

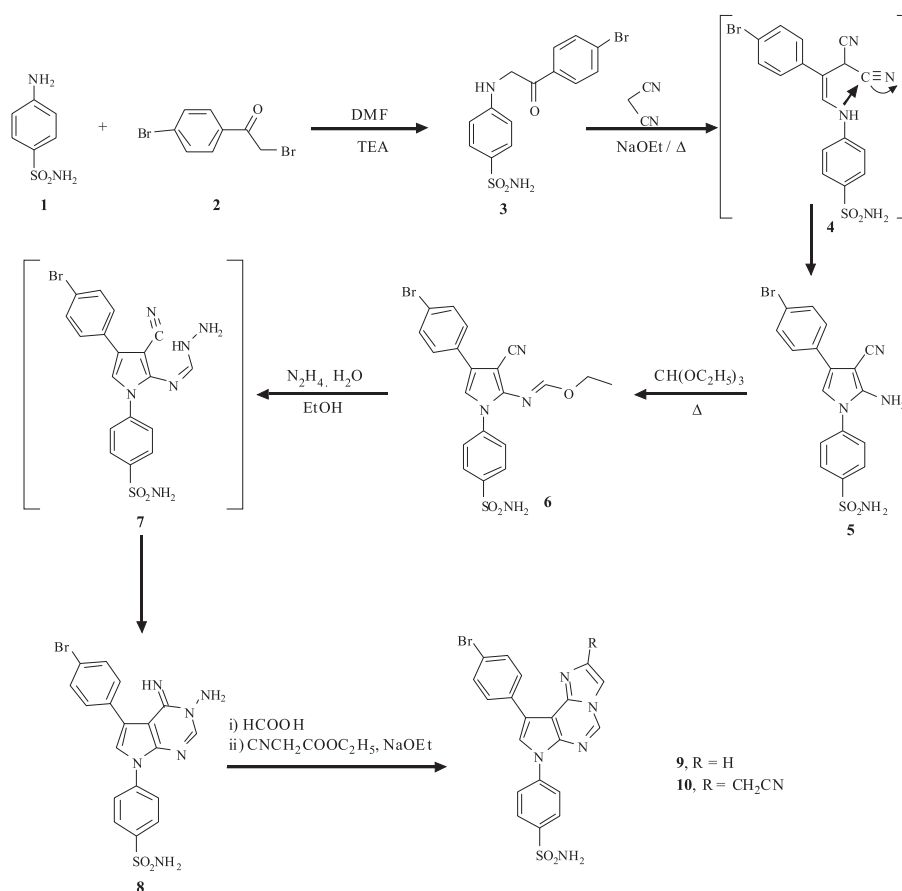
at 6.1 ppm due to NH₂ group and 7.9 ppm for SO₂NH₂ group. Compound **5** was reacted with triethylorthoformate to give the corresponding ethoxymethylene amino derivative **6**. The IR spectrum of compound **6** revealed the presence of characteristic bands for NH₂, CN and SO₂ groups. The ¹H-NMR spectrum of **6** showed a triplet for CH₃ group and a quartet for CH₂ group. When compound **6** was reacted with hydrazine hydrate in ethanol at room temperature, the *N*-amino-imino derivative **8** was obtained in good yield. The structure of compound **8** was supported on the basis of elemental analyses and spectral data. The IR spectrum exhibited the disappearance of the C=N band and the presence of bands at 3294, 3230, 3150 cm⁻¹ for NH, NH₂,

1639 cm⁻¹ for C=N and 1375, 1163 cm⁻¹ for SO₂. Moreover, the ¹H-NMR spectrum of compound **8** exhibited singlet at 5.6 ppm due to NH₂ group. Compound **8** was reacted with different one carbon cyclizing agents to prepare some new pyrrolopyrimidine derivatives carrying 1,2,4-triazole moiety. Thus, the corresponding 1,2,4-triazolopyrrolopyrimidine derivatives **9** and **10** were obtained *via* reaction of compound **8** with formic acid or ethyl cyanoacetate in the presence of sodium ethoxide. The IR spectrum of compound **9** revealed a band at 1620 cm⁻¹ for C=N. The ¹H-NMR spectrum of **9** showed singlet at 8.6 ppm attributed to CH of triazole. Also the IR spectrum of **10** revealed band at 2270 cm⁻¹ C=N. The ¹H-NMR spectrum of **10** in DMSO-d₆

Table 2. *In vitro* anticancer screening of the synthesized compounds against human breast cancer cell line (MCF7).

Compound	Compound concentration (μM)				IC ₅₀ (μM)
	10 μM	25 μM	50 μM	100 μM	
	Surviving fraction (Mean ± S.E.)*				
Doxorubicin	0.314 ± 0.032	0.309 ± 0.016	0.251 ± 0.023	0.266 ± 0.032	8.02
5	0.327 ± 0.121	0.273 ± 0.043	0.233 ± 0.011	0.255 ± 0.020	7.56
6	0.340 ± 0.090	0.294 ± 0.021	0.246 ± 0.110	0.256 ± 0.002	7.56
8	0.330 ± 0.211	0.309 ± 0.016	0.227 ± 0.110	0.268 ± 0.132	7.29
9	0.310 ± 0.101	0.318 ± 0.104	0.298 ± 0.100	0.322 ± 0.018	7.29
10	0.344 ± 0.004	0.312 ± 0.111	0.276 ± 0.040	0.343 ± 0.011	7.56
11	0.340 ± 0.149	0.284 ± 0.101	0.212 ± 0.146	0.266 ± 0.155	7.56
12	0.377 ± 0.021	0.356 ± 0.100	0.260 ± 0.001	0.294 ± 0.088	7.84
13	0.361 ± 0.021	0.324 ± 0.048	0.260 ± 0.099	0.245 ± 0.011	7.84
14	0.256 ± 0.044	0.211 ± 0.001	0.187 ± 0.032	0.270 ± 0.001	6.46
15	0.316 ± 0.010	0.323 ± 0.001	0.370 ± 0.124	0.311 ± 0.100	7.29
16	0.305 ± 0.007	0.263 ± 0.071	0.218 ± 0.100	0.244 ± 0.029	7.01
17	0.316 ± 0.011	0.264 ± 0.001	0.195 ± 0.021	0.177 ± 0.049	7.56
18	0.321 ± 0.001	0.311 ± 0.111	0.299 ± 0.029	0.299 ± 0.056	8.19
19	0.344 ± 0.092	0.310 ± 0.044	0.299 ± 0.008	0.280 ± 0.019	8.20
20	0.401 ± 0.001	0.367 ± 0.066	0.281 ± 0.047	0.300 ± 0.100	8.21
21	0.266 ± 0.011	0.269 ± 0.009	0.187 ± 0.006	0.266 ± 0.018	6.74
22	0.307 ± 0.001	0.256 ± 0.011	0.249 ± 0.096	0.259 ± 0.077	7.29
23	0.285 ± 0.001	0.246 ± 0.042	0.212 ± 0.033	0.218 ± 0.011	7.29
24	0.358 ± 0.010	0.300 ± 0.085	0.289 ± 0.011	0.355 ± 0.021	7.84
25	0.367 ± 0.093	0.345 ± 0.088	0.299 ± 0.024	0.299 ± 0.001	8.10
26	0.399 ± 0.001	0.387 ± 0.001	0.299 ± 0.077	0.310 ± 0.019	8.16
27	0.393 ± 0.012	0.289 ± 0.001	0.290 ± 0.044	0.300 ± 0.078	8.16
28	0.303 ± 0.011	0.280 ± 0.067	0.249 ± 0.067	0.352 ± 0.011	7.01
29	0.389 ± 0.001	0.389 ± 0.001	0.284 ± 0.022	0.300 ± 0.019	8.16

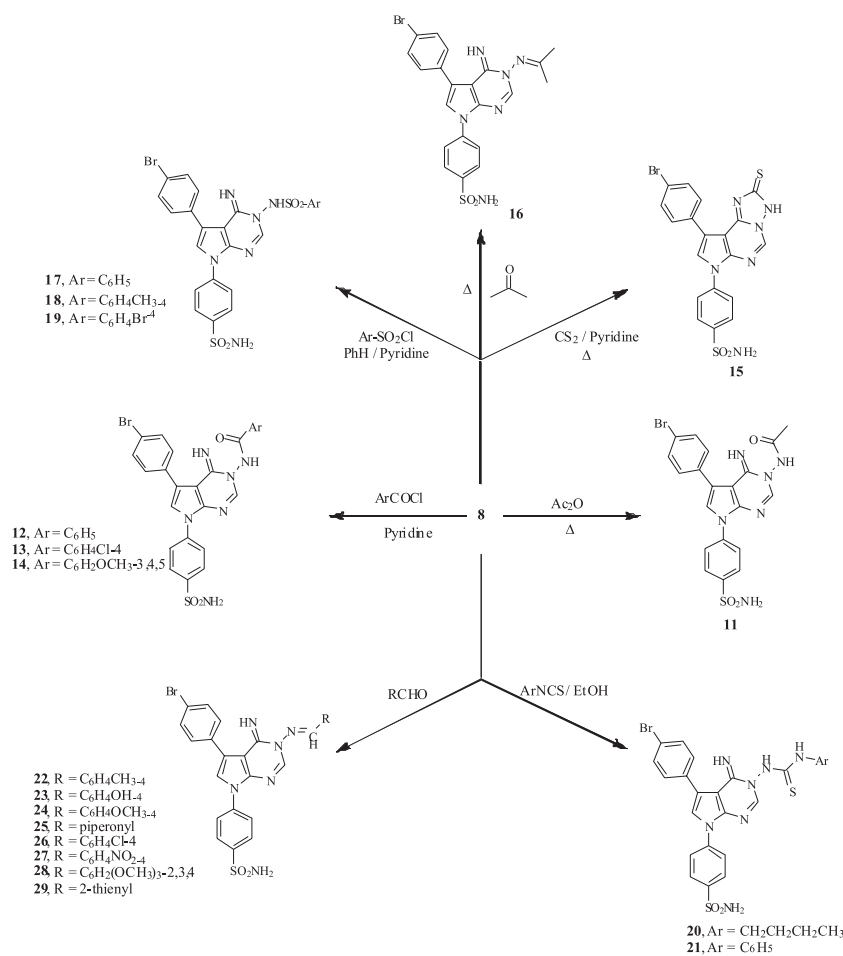
* Each value is the mean of three values ± standard error.



Scheme 1. Synthetic pathways for compounds 3–10

exhibited singlet at 4.5 ppm due to CH₂CN group. The monoacetyl derivative **11** was obtained *via* reaction of **8** with acetic anhydride (Scheme 2). The IR spectrum of **11** revealed the presence of a characteristic band at 1710 cm⁻¹ for C=O group, while its ¹H-NMR showed singlet at 2.1 ppm attributed to the presence of acetyl group. Interaction of compound **8** with benzoyl chloride derivatives in pyridine afforded the corresponding benzamide derivatives **12–14**, respectively. The IR spectrum of **12** showed band at 1683 cm⁻¹ (C=O). The ¹H-NMR spectrum of **12** revealed the presence of singlet at 9.6 ppm for imino group. The IR spectrum of **13** showed band at 761 cm⁻¹ (C-Cl). The ¹H-NMR spectrum of **14** exhibited signals at 3.7, 3.9 ppm attributed to three methoxy groups. When compound **8** was allowed to react with CS₂, the triazolopyrimidine-2-thione **15** was obtained. The IR spectrum of **15** revealed bands at 1242 cm⁻¹ (C=S), 1359, 1159 cm⁻¹ (SO₂). In addition, condensation of the key compound **8** with dry acetone gave the condensed product **16**, its ¹H-NMR

revealed singlet at 1.1 ppm attributed to two methyl groups. On the other hand, interaction of compound **8** with sulfonyl derivatives in dry benzene containing few drops of pyridine yielded the corresponding sulfonamide derivatives **17–19**, respectively. The ¹H-NMR spectrum of **18** revealed the presence of singlet at 2.2 ppm attributed to tolyl group. Nucleophilic reaction of compound **8** on the highly positive carbon of the isothiocyanate yielded the corresponding thiourea derivatives **20, 21** (Scheme 2). Their structures were confirmed based on their spectral data, where the IR spectra of compounds **20** and **21** showed bands at 1292, 1265 cm⁻¹ (C=S). The ¹H-NMR spectrum of compound **20** showed a triplet at 0.9 ppm due to the methyl group. The benzylidene derivatives **22–29** were obtained in a good yield *via* the reaction of compound **8** with aromatic aldehydes. The IR spectra showed the presence of bands of imino groups. Also ¹H-NMR spectra of compounds **22–29** showed singlets at 9.5–11.6 ppm for N=CH groups.



Molecular docking

Several classes of inhibitors are currently used to inhibit the activity of c-Src in a number of cell types. However, they often show poor selectivity within the c-Src family, which in mammals comprises at least eight members involved in many key functions of the cell (19). Recently, we have shown that c-Src inhibitors of the pyrrolopyrimidine class exhibit a powerful inhibitory activity and a several-fold greater selectivity for c-Src against most tyrosine kinases (20–22). This suggests that c-Src can be activated downstream of receptor activator of NF- κ B (RANK) (23), a member of the tumor necrosis factor (TNF) receptor superfamily that is involved in cell differentiation, function, and survival (24–26). In order to perform the aim of the present investigations, the authors have performed molecular docking of the synthesized compounds on the active sites of c-Src, which may lead to an understanding of

their effect as antitumor agents. The protein data bank file (PDB ID:1YOL) was selected for this purpose. The file contains c-Src enzyme co-crystallized with a pyrrolopyrimidine ligand. All docking procedures were achieved by MOE (Molecular Operating Environment) software 10.2008 provided by chemical computing group, Canada. Docking on the active site of c-Src enzyme was performed for all synthesized compounds. Docking protocol was verified by redocking of the co-crystallized ligand in the vicinity of the active site of the enzyme with energy score (S) = -22.6799 Kcal/mol and root mean standard deviation (RMSD) = 0.8205 (Fig. 1). The ligand interacts with the active site amino acids by three interactions: with Met 343 with hydrogen bond of 3.09 Å, with Glu 341 with hydrogen bond of 2.22 Å and with Thr 340 with hydrogen bond of 3.22 Å. All the synthesized compounds were docked on the active site of the enzyme showing good fitting. The

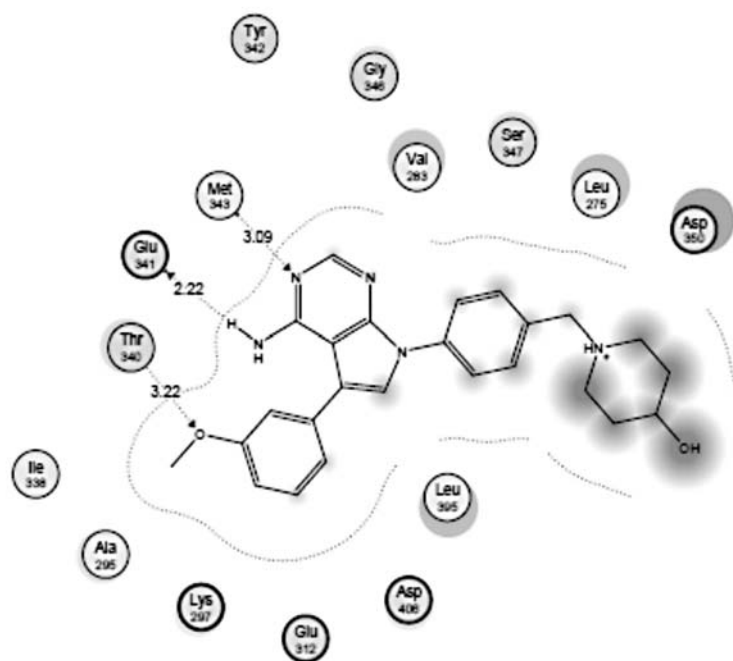


Figure 1. Pyrrolopyrimidine ligand on the active site c-Src enzyme

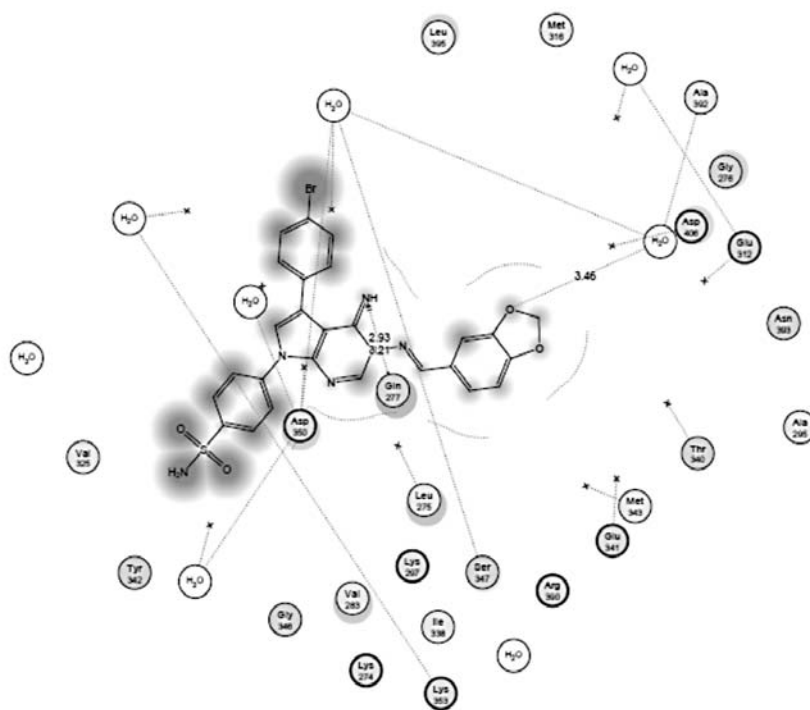


Figure 2. Compound 25 on the active site c-Src enzyme

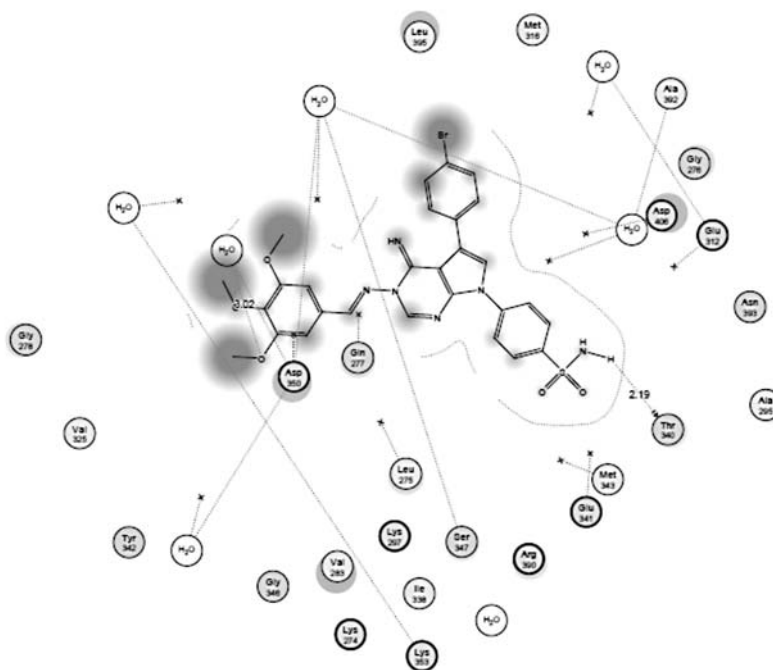


Figure 3. Compound **28** on the active site c-Src enzyme

energy score (S) as well as amino acid interactions of the synthesized compounds were listed in (Table 1). The best energy scores were exhibited by compounds **25** and **28** with $S = -19.0510$ and -18.5521 , respectively. Figures 2 and 3 show the amino acid interactions with compounds **25** and **28**, respectively. On the other hand, one or more of the amino acids that were interacting with the co-crystallized ligand has/have interacted with compounds **5**, **8**, **13**, **14**, **21**, **23**, **26** and **28**. This was not the case in the rest of compounds as they interacted with different amino acids of the active site other than the ones interacted with the co-crystallized ligand.

In vitro antitumor activity

The newly synthesized compounds were evaluated for their *in vitro* cytotoxic activity against human breast cancer cell line (MCF7). Doxorubicin, which is one of the most effective anticancer agents, was used as the reference drug in this study. The relationship between surviving fraction and drug concentration was plotted to obtain the survival curve of breast cancer cell line (MCF7). The response parameter calculated was the IC_{50} value, which corresponds to the concentration required for 50% inhibition of cell viability. Table 2 shows the *in vitro* cytotoxic activity of the synthesized com-

pounds where all compounds exhibited significant activity compared to the reference drug. All the synthesized compounds showed promising cytotoxic activities especially compounds **5–17**, **21–24** and **28** with IC_{50} values in the range of 6.46–7.84 μM , which is better than that of doxorubicin with IC_{50} value of 8.02 μM . On the other hand, compounds **18–20**, **25–27** and **29** showed IC_{50} values in the range of 8.16–8.21 μM , which indicated lower activity but comparable to that of doxorubicin.

The strategic synthone – compound **5**, showed IC_{50} value of 7.56 μM and upon reaction with ethyl orthoformate to give compound **6** did not lead to a more active derivative, as its IC_{50} value remains the same, while cyclization to the iminoamino pyrrolopyrimidine derivative **8** improved the activity, as its IC_{50} yielded 7.29 μM . Annulation to imidazo derivatives **9** did not improve the activity with the same IC_{50} value but substitution with CH_2CN as in compound **10** again returned the IC_{50} to that of the starting compound **5**. This was also the case in the acetyl derivative **11** with the same IC_{50} value of 7.56 μM . The activity decreased upon treatment of compound **8** with benzoyl chloride and/or 4-chlorobenzoyl chloride to reach 7.84 μM for compounds **12** and **13**. A marked increase in activity was observed with the trimethoxy derivative **14**

having $IC_{50} = 6.46 \mu\text{M}$. The triazolo derivative **15** showed IC_{50} value of $7.29 \mu\text{M}$ which was improved in case of the iminopyrrolopyrimidine derivative **16** to reach $7.01 \mu\text{M}$. Treatment of compound **8** with several sulfonylchloride derivatives lead to the formation of compounds **17–19** in which the unsubstituted aromatic derivative **17** was the best one among them with IC_{50} value of $7.56 \mu\text{M}$, while compounds **18** and **19** showed IC_{50} values of 8.19 and $8.20 \mu\text{M}$, respectively. The aliphatic thiourea derivative **20** had the worst IC_{50} of $8.21 \mu\text{M}$, while its aromatic analogue **21** showed very good IC_{50} value of $6.74 \mu\text{M}$. Finally, the Schiff's base derivatives **22–29** showed IC_{50} values in the range of $7.01–8.16 \mu\text{M}$. Again the trimethoxy derivative **28** was the most active among this series with IC_{50} value of $7.01 \mu\text{M}$, while compounds **26**, **27** and **29** with a substitution with electron withdrawing groups chloro, nitro and 2-thienyl showed IC_{50} value of $8.16 \mu\text{M}$. On the other hand, compounds **22**, **23** and **24** with electron donating groups CH_3 , OH and OCH_3 showed IC_{50} value of 7.29 , 7.29 and $7.84 \mu\text{M}$, respectively.

Relationship between molecular docking and cytotoxic activity

All of the synthesized compounds were fit in the active site of c-Src enzyme. The docking scores range between -19.0510 and -8.0453 kcal/mol. However, only compounds **5**, **8**, **13**, **14**, **21**, **23**, **26** and **28** interacted with either Met 343 or Thr 340, which are two of the amino acids that interacted with the co-crystallized ligand. The above mentioned compounds have shown better IC_{50} values than that of doxorubicin except for compound **26** with IC_{50} value of $8.16 \mu\text{M}$. Compound **28** case was interesting as its docking score was one of the best docking score of -18.5521 kcal/mol and its interaction with one of the amino acids that interacted with the co-crystallized ligand (Thr 340) with a hydrogen bond of 2.19 \AA . In spite of these findings, no linear relationship could be postulated between docking results and biological activities and this could be a trial to suggest a mechanism of action for the cytotoxic activities of the synthesized compounds that still needs further investigations.

CONCLUSION

A novel series of pyrrolopyrimidines and triazolopyrimidines carrying a biologically active sulfonamide moieties were synthesized and evaluated for their anti-breast cancer activity. Most of the synthesized compounds showed promising anticancer

activity against breast cancer cell line (MCF7) compared to doxorubicin as positive control especially compounds **5–17**, **21–24** and **28** with better IC_{50} than that of doxorubicin.

Acknowledgment

The authors would like to extend their sincere appreciation to the Deanship of Scientific Research at King Saud University for its funding of this research through the Research Group Project no. RGP-VPP- 302.

REFERENCES

1. Azas, N., Rathelot P., Djekou S., Delmas F., Gellis A., Di-Giorgio C., Vanelle P., Timon-David P.: *Farmaco* 58, 1263 (2003).
2. Ismail M., Ghorab M., Noaman E., Ammar A., Heiba H., Sayed Y.: *Arzneimittelforschung*. 56, 301 (2006).
3. Ghorab M., Noaman E., Ismail M., Heiba H., Ammar A., Sayed Y.: *Arzneimittelforschung*. 56, 405 (2006).
4. Ghorab M., Heiba H., Khalil A., Abou El Ella D., Noaman E.: *Phosphorus Sulfur Silicon Relat. Elem.* 183, 1 (2007).
5. Abou El Ella D., Ghorab M., Noaman E., Heiba H., Khalil A.: *Bioorg. Med. Chem.* 16, 2391 (2008).
6. Atul R.G., Kiran S.T., Fazal S., Mukund V.D., Kumar V.S: *Tetrahedron* 64, 10214 (2008).
7. Deshmukh M.B., Salunkhe S.M., Patil D.R., Anbhule P.V.: *Eur. J. Med. Chem.* 44, 2651 (2009).
8. Mohamed M.S., El-Domany R.A., Abd El-Hameed R.H.: *Acta Pharm.* 59, 145 (2009).
9. Said A., Abd El-Galil A., Sabry N., Abdalla M.: *Eur. J. Med. Chem.* 44, 4787 (2009).
10. Ghorab M., Ragab F., Heiba H., Youssef H., El-Gazzar M.: *Bioorg. Med. Chem. Lett.* 20, 6316 (2010).
11. Shih C., Habeck L.L., Mendelsohn L.G., Chen V.J., Schultz R.M.: *Adv. Enzyme Regul.* 38, 135 (1998).
12. Recchia I., Rucci N., Festuccia C., Bologna M., MacKay A.R., Migliaccio S., Longo M. et al.: *Eur. J. Cancer* 39, 1927 (2003).
13. Blake J.F., Kallan N.C., Xiao D., Xu R., Bencsik J.R., Skelton N.J., Spencer K.L. et al.: *Bioorg. Med. Chem. Lett.* 20, 5607 (2010).
14. Kawakita Y., Miwa K., Seto M., Banno H., Ohta Y., Tamura T., Yusa T. et al.: *Bioorg. Med. Chem.* 20, 6171 (2012).

15. Owa T., Yoshino H., Okauchi T., Yoshimatsu K., Ozawa Y., Sugi N.H., Nagasu T. et al.: *J. Med. Chem.* 42, 3798 (1999).
16. Casini A., Scozzafava A., Mastrolorenzo A., Supuran L.T.: *Curr. Cancer Drug Targets* 2, 55 (2002).
17. Rostom S.A.: *Bioorg. Med. Chem.* 14, 6475 (2006).
18. Skehan P., Storeng R., Scudiero D., Monks A., McMahon J., Vistica D., Warren J.T. et al.: *J. Natl. Cancer Inst.* 82, 1107 (1990).
19. Thomas S.M., Brugge J.S.: *Annu. Rev. Cell. Dev. Biol.* 13, 513 (1997).
20. Missbach M., Jeschke M., Feyen J., Muller K., Glatt M., Green J., Susa M.: *Bone* 24, 437 (1999).
21. Missbach M., Altmann E., Widler L., Susa M., Buchdunger E., Mett H., Meyer T., Green J.: *Bioorg. Med. Chem. Lett.* 10, 945 (2000).
22. Susa M., Luong-Nguyen N.H., Crespo J., Maier R., Missbach M., McMaster G.: *Protein Expr. Purif.* 19, 99 (2000).
23. Wong B.R., Josien R., Choi Y.: *J. Leukoc. Biol.* 65, 715 (1999).
24. Fuller K., Wong B., Fox S., Choi Y., Chambers T.J.: *J. Exp. Med.* 188, 997 (1998).
25. Dougall W. C., Glaccum M., Charrier K., Rohrbach K., Brasel K., De Smedt T., Daro E. et al.: *Genes Dev.* 13, 2412 (1999).
26. Hofbauer L.C., Khosla S., Dunstan C.R., Lacey D.L., Boyle W.J., Riggs B.L.: *J. Bone Miner. Res.* 15, 2 (2000).

Received: 12. 11. 2013

CYTOTOXIC ACTIVITY OF SOME NOVEL SULFONAMIDE DERIVATIVES

MOSTAFA M. GHORAB^{1,2*}, MANSOUR S. ALSAID¹, ABDULLAH-AL-DHFYAN³
and REEM K. ARAFA⁴¹Department of Pharmacognosy, College of Pharmacy, King Saud University,
P.O. Box 2457, Riyadh 11451, Saudi Arabia²Department of Drug Radiation Research, National Center for Radiation Research And Technology,
Atomic Energy Authority, P.O. Box 29, Nasr City, Cairo, Egypt³Stem Cell & Tissue Re-engineering Program, Research Centre, King Faisal Specialized Hospital,
P.O. Box 3354, Riyadh 11211, Saudi Arabia⁴ Department of Pharmaceutical Chemistry, Faculty of Pharmacy, Cairo University,
P.O. Box 11562, Cairo, Egypt

Abstract: The versatile synthons 2-chloro-*N*-(4-sulfamoylphenyl)acetamides **1a,b** were used as a key intermediates for the synthesis of sulfonamide derivatives with adamantyl **2**, indene **3**, morpholinophenyl **4**, piperonyl **5**, benzothiazole **6–8**, pyrazole **9**, thiaziazole **10, 11**, quinoline **12**, isoquinoline **13**, thiazoles **14–19**, acrylamides **20–24** and benzochromene **25** moieties *via* reaction with several nitrogen nucleophiles. The newly synthesized compounds were screened *in vitro* for their anticancer activity against breast cancer (MDA-MB-231) and colon cancer (HT-29) cell lines. Compound **17** was found to be the most potent against breast cancer cell lines with IC₅₀ value 66.6 μM compared with the reference drug 5-fluorouracil with IC₅₀ value 77.28 μM.

Keywords: synthesis, sulfonamides, anticancer activity

Although there has been great progress in the development of treatment and prevention for cancer, it still remains an enormous threat to people's health in the 21st century, representing the second primary cause of death in the world (1). In the past years, considerable efforts have been made to develop innovative strategies for finding safe and effective methods of treating this disease. With the increasing understanding of the biological process involved in cancer cell survival and the discovering of new targets, more and more novel chemical therapeutic drugs have been designed for treatment of cancer. Sulfonamides have attracted great interest over many years due to their broad bioactivities (2–4). The heterocyclic compounds are very important part of medicinal chemistry, among them it is worth to pay attention on derivatives of adamantyl, morpholine, piperonyl, benzothiazole, pyrazole, thiaziazole, quinoline and isoquinoline. They have a broad spectrum of pharmacological activities like anticancer (5–9), antibacterial (10–12) and antifungal activity (13–15). Moreover, it was also reported that acrylamides and chromenes have an interesting anticancer activity against differ-

ent cell lines (16–19). Generally, it seems that a sulfonamide group combined with acetamide having different type of aryl, heteroaryl as well as alkyl substituents exhibited a wide range of pharmacological applications. In our earlier work, we also showed that compounds containing short amine fragments exhibit anticancer activity (20–22). It has been known that aryl/heteroaryl sulfonamides may act as anticancer agents through a variety of mechanisms such as: cell cycle perturbation in the G1 phase, disruption of microtubule assembly, angiogenesis inhibition, and functional suppression of the transcriptional activator NF- κ B. Moreover, following an extensive evaluation, numerous sulfonamides were found to act as carbonic anhydrase (CA) inhibitors (23–26). The most prominent mechanism was the inhibition of carbonic anhydrase isozymes (CAs) (27). In light of this information and in continuation of our interest in the biologically active heterocyclic compounds, we have decided to continue the study on the antiproliferative activity of some newer sulfonamide moiety bearing aryl amines, acetamide, acrylamide and chromene derivatives.

* Corresponding author: e-mail: mmsghorab@yahoo.com, mmsghorab@gmail.com

EXPERIMENTAL

Chemistry

Melting points (°C, uncorrected) were determined in open capillaries on a Gallenkemp melting point apparatus (Sanyo Gallenkemp, Southborough, UK). Pre-coated silica gel plates (silica gel 0.25 mm, 60 GF-254; Merck, Germany) were used for thin layer chromatography, dichloromethane/methanol (9.5 : 0.5 v/v) mixture was used as a developing solvent system. IR spectra were recorded in KBr discs using IR-470 Shimadzu spectrometer (Shimadzu, Tokyo, Japan). NMR spectra in DMSO- d_6 were recorded on Bruker Ac-500 UltraShield NMR spectrometer (Bruker, Flawil, Switzerland, δ , ppm) at 500 MHz, using TMS as an internal standard. Elemental analyses were performed on Carlo Erba 1108 Elemental Analyzer (Heraeus, Hanau, Germany). For all compounds they were within \pm 0.4% of the theoretical values. All chemicals were commercially supplied from Sigma-Aldrich, USA.

General procedure for the synthesis of sulfonamides (2–13)

A mixture of compound **1a** (2.489 g, 0.01 mol) and required amines, namely: adamantylamine, 5-aminoindanone, 4-morpholinobenzamine, piperonylamine, 2-amino-6-fluorobenzothiazole, 2-amino-6-ethoxybenzothiazole, 2-amino-5,6-dimethylbenzothiazole, 2-amino-1-ethylpyrazole, 2-amino-5-ethylthiadiazole, 2-amino-5-thioethylthiadiazole, 3-aminoquinoline and 2-aminoisoquinoline (0.01 mol) in dimethylformamide (20 mL) containing 3 drops of triethylamine was refluxed for 17 h. The reaction mixture was collected and poured onto ice/water. The obtained solid was recrystallized from dioxane to give derivatives **2–13**, respectively.

2-(Adamant-2-ylamino)-*N*-(4-sulfamoylphenyl)acetamide(**2**)

Yield 89%, m.p. 244.5°C. IR (KBr, cm^{-1}): 3425, 3310, 3278 (NH, NH₂), 3068 (CH arom.), 2976, 2881 (CH aliph.), 1684 (C=O), 1383, 1160 (SO₂). ¹H-NMR (DMSO- d_6 , δ , ppm): 1.5–2.0 (m, 12H, 6CH₂, adamantyl), 1.59–1.67 (m, 4H, CH adamantyl), 3.5 (s, 2H, CH₂CO), 7.2 (s, 1H, NHCH₂, D₂O-exchangeable), 7.7–7.9 (m, 4H, Ar-H), 10.2 (s, 1H, NH-Ph, D₂O-exchangeable), 11.1 (s, 2H, SO₂NH, D₂O-exchangeable). ¹³C-NMR (DMSO- d_6 , δ , ppm): 28.6 (3), 36.1 (3), 40.1 (3), 44.4, 50.2, 118.5 (2), 126.8 (2), 138.4, 141.2, 171.7 (C=O). Analysis: calcd. for C₁₈H₂₅N₃O₃S (363.47): C, 59.48; H, 6.93; N, 11.56%; found: C, 59.12; H, 6.68; N, 11.23%.

2-(2,3-Dihydro-1*H*-inden-5-ylamino)-*N*-(4-sulfamoylphenyl)acetamide(**3**)

Yield 79%, m.p. 188.9°C. IR (KBr, cm^{-1}): 3391, 3362, 3212 (NH, NH₂), 3072 (CH arom.), 1681 (C=O), 1378, 1156 (SO₂). ¹H-NMR (DMSO- d_6 , δ , ppm): 1.9–2.0 (m, 2H, CH₂-CH₂-CH₂, cyclopentyl), 2.6–2.8 (m, 4H, 2CH₂ cyclopentyl), 3.9 (s, 2H, CH₂CO), 5.9 (s, 1H, NHCH₂, D₂O-exchangeable), 6.4–7.8 (m, 9H, Ar-H + SO₂NH₂), 10.2 (s, 1H, NHCO, D₂O-exchangeable). ¹³C-NMR (DMSO- d_6 , δ , ppm): 25.1, 32.5 (2), 47.9, 110.8, 115.3, 124.3 (2), 126.8 (2), 131.6, 136.4, 138.4, 141.6, 144.3, 146.9, 171.2 (C=O). Analysis: calcd. for C₁₇H₁₉N₃O₃S (345.41): C, 59.11; H, 5.54; N, 12.17%; found: C, 59.32; H, 5.22; N, 12.50%.

2-(4-Morpholinophenylamino)-*N*-(4-sulfamoylphenyl)acetamide (**4**)

Yield 77%, m.p. 222.8°C. IR (KBr, cm^{-1}): 3406, 3385, 3261 (NH, NH₂), 3099 (CH arom.), 2962, 2909 (CH aliph.), 1378, 1161 (SO₂). ¹H-NMR (DMSO- d_6 , δ , ppm): 3.0–3.7 (m, 8H, 4CH₂, morpholino), 4.3 (d, 2H, CH₂CO, J = 7.0 Hz), 6.8 (s, 1H, NHCH₂, D₂O-exchangeable), 7.0–7.9 (m, 10H, Ar-H + SO₂NH₂), 11.1 (s, 1H, NHCO, D₂O-exchangeable). ¹³C-NMR (DMSO- d_6 , δ , ppm): 48.5 (2), 57.0, 66.1 (2), 115.0 (2), 117.4 (2), 120.2 (2), 126.8 (2), 138.8, 140.4, 141.4, 143.3, 171.2 (C=O). Analysis: calcd. for C₁₈H₂₂N₄O₄S (390.46): C, 55.37; H, 5.68; N, 14.35%; found: C, 55.62; H, 5.33; N, 14.16%.

2-(Benzo[d][1,3]dioxol-5-ylmethylamino)-*N*-(4-sulfamoylphenyl)acetamide (**5**)

Yield 91%, m.p. 263.7°C. IR (KBr, cm^{-1}): 3386, 3318, 3256 (NH, NH₂), 3100 (CH arom.), 2991, 2868 (CH aliph.), 1386, 1156 (SO₂). ¹H-NMR (DMSO- d_6 , δ , ppm): 3.9 (s, 2H, CH₂CO), 4.1 (s, 2H, CH₂NH), 6.0 (s, 2H, OCH₂O), 6.9–7.9 (m, 9H, Ar-H + SO₂NH₂), 9.6 (s, 1H, NHCH₂, D₂O-exchangeable), 11.2 (s, 1H, NHCO, D₂O-exchangeable). ¹³C-NMR (DMSO- d_6 , δ , ppm): 47.2, 49.7, 100.8, 110.4, 118.9, 124.4, 124.8 (2), 126.6 (2), 126.7, 139.0, 141.0, 147.3, 147.8, 164.2. Analysis: calcd. for C₁₆H₁₇N₃O₅S (363.39): C, 52.88; H, 4.72; N, 11.56%; found: C, 52.56; H, 4.48; N, 11.21%.

2-(6-Fluorobenzo[d]thiazol-2-ylamino)-*N*-(4-sulfamoylphenyl)acetamide (**6**)

Yield 68%, m.p. 207.6°C; IR (KBr, cm^{-1}): 3410, 3368, 3271 (NH, NH₂), 3081 (CH arom.), 2936, 2836 (CH aliph.), 1688 (C=O), 1612 (C=N), 1383, 1160 (SO₂). ¹H-NMR (DMSO- d_6 , δ , ppm): 4.2 (s, 2H, CH₂CO), 7.0–8.0 (m, 9H, Ar-H + SO₂NH₂), 8.5 (s, 1H, NHCH₂, D₂O-exchangeable), 10.7 (s, 1H,

NHCO, D₂O-exchangeable). ¹³C-NMR (DMSO-d₆, δ, ppm): 64.6, 107.1, 114.6, 117.3 (2), 118.6, 120.1, 124.8 (2), 130.8, 131.7, 146.2, 154.6, 163.6, 168.4 (C=O). Analysis: calcd. for C₁₅H₁₃FN₄O₃S₂ (380.42): C, 47.36; H, 3.44; N, 14.73%; found: C, 47.16; H, 3.19; N, 14.46%.

2-(6-Ethoxybenzo[d]thiazol-2-ylamino)-N-(4-sulfamoylphenyl)acetamide (7)

Yield 59%, m.p. 144.2°C. IR (KBr, cm⁻¹): 3425, 3390, 3278 (NH, NH₂), 3077 (CH arom.), 2981, 2876 (CH aliph.), 1662 (C=O), 1628 (C=N), 1365, 1160 (SO₂). ¹H-NMR (DMSO-d₆, δ, ppm): 1.3 (t, 3H, CH₃), 4.0 (s, 2H, CH₂CO), 4.1 (q, 2H, CH₂), 6.8–8.1 (m, 9H, Ar-H + SO₂NH₂), 8.6 (s, 1H, NHCH₂, D₂O-exchangeable), 10.4 (s, 1H, NHCO, D₂O-exchangeable). ¹³C-NMR (DMSO-d₆, δ, ppm): 14.7, 60.9, 63.7, 105.5, 113.5, 118.1 (2), 119.1, 121.4, 126.7 (2), 132.0, 132.9, 146.8, 153.6, 164.8, 169.9. Analysis: calcd. for C₁₇H₁₈N₄O₄S₂ (406.48): C, 50.23; H, 4.46; N, 13.78%; found: C, 50.49; H, 4.18; N, 13.48%.

2-(5,6-Dimethylbenzo[d]thiazol-2-ylamino)-N-(4-sulfamoylphenyl)acetamide (8)

Yield 73%, m.p. 147.1°C. IR (KBr, cm⁻¹): 3410, 3376, 3312 (NH, NH₂), 3092 (CH arom.), 2936, 2872 (CH aliph.), 1689 (C=O), 1618 (C=N), 1382, 1155 (SO₂). ¹H-NMR (DMSO-d₆, δ, ppm): 2.3 (s, 6H, 2CH₃), 4.1 (s, 2H, CH₂), 7.1–8.1 (m, 8H, Ar-H + SO₂NH₂), 9.9 (s, 1H, NH, D₂O-exchangeable), 10.6 (s, 1H, NHCO, D₂O-exchangeable). ¹³C-NMR (DMSO-d₆, δ, ppm): 19.2, 19.6, 60.8, 118.7, 119.1, 121.1, 121.5 (2), 126.7 (2), 128.0, 129.2, 133.6, 138.6, 151.9, 165.9, 170.0. Analysis: calcd. for C₁₇H₁₈N₄O₃S₂ (390.48): C, 52.29; H, 4.65; N, 14.35%; found: C, 52.61; H, 4.39; N, 14.55%.

2-(1-Ethyl-1H-pyrazol-5-ylamino)-N-(4-sulfamoylphenyl)acetamide (9)

Yield 64%, m.p. 238.7°C. IR (KBr, cm⁻¹): 3368, 3290, 3186 (NH, NH₂), 3075 (CH arom.), 2978, 2912 (CH aliph.), 1694 (C=O), 1599 (C=N), 1378, 1156 (SO₂). ¹H-NMR (DMSO-d₆, δ, ppm): 1.3 (t, 3H, CH₃), 3.9 (q, 2H, CH₂), 4.0 (s, 2H, CH₂CO), 6.6–8.1 (m, 8H, Ar-H + 2 CH pyrazole + SO₂NH₂), 10.5 (s, 1H, NH, D₂O-exchangeable), 10.7 (s, 1H, NHCO, D₂O-exchangeable). ¹³C-NMR (DMSO-d₆, δ, ppm): 14.2, 49.1, 56.8, 94.6, 119.7 (2), 126.6 (2), 139.0, 141.4, 142.6, 150.8, 163.7. Analysis: calcd. for C₁₃H₁₇N₅O₃S (323.37): C, 48.28; H, 5.30; N, 21.66%; found: C, 48.09; H, 5.63; N, 21.42%.

2-(5-Ethyl-1,3,4-thiadiazol-2-ylamino)-N-(4-sulfamoylphenyl)acetamide (10)

Yield 68%, m.p. 128.4°C. IR (KBr, cm⁻¹): 3388, 3266, 3214 (NH, NH₂), 3100 (CH arom.), 2984, 2836 (CH aliph.), 1678 (C=O), 1619 (C=N), 1377, 1161 (SO₂). ¹H-NMR (DMSO-d₆, δ, ppm): 1.1 (t, 3H, CH₃), 2.9 (d, 2H, CH₂NH, *J* = 6.9 Hz), 5.4 (s, 1H, NH, D₂O-exchangeable), 7.0–7.9 (m, 6H, Ar-H + SO₂NH₂), 10.7 (s, 1H, NHCO, D₂O-exchangeable). ¹³C-NMR (DMSO-d₆, δ, ppm): 13.7, 24.4, 53.1, 120.6 (2), 126.7 (2), 138.8, 141.3, 162.2, 164.2, 165.5. Analysis: calcd. for C₁₂H₁₅N₅O₃S₂ (341.41): C, 42.22; H, 4.43; N, 20.51%; found: C, 42.46; H, 4.11; N, 20.19%.

2-(5-(Ethylthio)-1,3,4-thiadiazol-2-ylamino)-N-(4-sulfamoylphenyl)acetamide (11)

Yield 74%, m.p. 154.1°C. IR (KBr, cm⁻¹): 3441, 3377, 3189 (NH, NH₂), 3086 (CH arom.), 2976, 2880 (CH aliph.), 1666 (C=O), 1627 (C=N), 1388, 1160 (SO₂). ¹H-NMR (DMSO-d₆, δ, ppm): 1.2 (t, 3H, CH₃), 3.1 (q, 2H, CH₂), 4.1 (s, 2H, CH₂), 7.0–8.0 (m, 6H, Ar-H + SO₂NH₂), 8.9 (s, 1H, NH, D₂O-exchangeable), 10.6 (s, 1H, NHCO, D₂O-exchangeable). ¹³C-NMR (DMSO-d₆, δ, ppm): 14.3, 28.2, 55.6, 119.1 (2), 126.7 (2), 138.6, 140.9, 160.1, 166.6, 169.9. Analysis: calcd. for C₁₂H₁₅N₅O₃S₃ (373.47): C, 38.59; H, 4.05; N, 18.75%; found: C, 38.29; H, 4.27; N, 18.51%.

2-(Quinolin-3-ylamino)-N-(4-sulfamoylphenyl)acetamide (12)

Yield 59%, m.p. 144.1°C. IR (KBr, cm⁻¹): 3328, 3291, 3191 (NH, NH₂), 3056 (CH arom.), 2967, 2871 (CH aliph.), 1696 (C=O), 1619 (C=N), 1378, 1154 (SO₂). ¹H-NMR (DMSO-d₆, δ, ppm): 4.1 (d, 2H, CH₂, *J* = 6.8 Hz), 6.6 (s, 1H, NH, D₂O-exchangeable), 7.0–7.9 (m, 11H, Ar-H + SO₂NH₂), 8.2 (s, 1H, N=CH quinoline), 10.5 (s, 1H, NHCO, D₂O-exchangeable). ¹³C-NMR (DMSO-d₆, δ, ppm): 60.8, 123.8 (2), 124.2, 125.4, 126.9, 127.6, 128.4 (2), 129.2, 129.6, 136.3, 138.5, 141.6, 142.0, 143.4, 169.7. Analysis: calcd. for C₁₇H₁₆N₄O₃S (356.40): C, 57.29; H, 4.52; N, 15.72%; found: C, 57.48; H, 4.21; N, 15.50%.

2-(Isoquinolin-3-ylamino)-N-(4-sulfamoylphenyl)acetamide (13)

Yield 61%, m.p. 180.7°C. IR (KBr, cm⁻¹): 3406, 3366, 3218 (NH, NH₂), 3062 (CH arom.), 2968, 2866 (CH aliph.), 1677 (C=O), 1611 (C=N), 1376, 1161 (SO₂). ¹H-NMR (DMSO-d₆, δ, ppm): 4.0 (s, 3H, CH₃), 6.6–8.6 (m, 12H, Ar-H + SO₂NH₂), 9.1 (s, 1H, NH, D₂O-exchangeable), 11.8 (s, 1H, NHCO, D₂O-exchangeable). ¹³C-NMR (DMSO-d₆, δ, ppm): 58.1, 96.6, 124.3 (3), 126.0 (3), 126.6 (2),

130.8, 138.8 (2), 143.4, 155.2, 157.3, 169.0. Analysis: calcd. for $C_{17}H_{16}N_4O_3S$ (356.40): C, 57.29; H, 4.52; N, 15.72%; found: C, 56.91; H, 4.75; N, 15.40%.

General procedure for the synthesis of 4-amino-N-(4-sulfamoylphenyl)-2-thioxo-3-substituted phenyl-2,3-dihydrothiazole-5-carboxamides (14–19)

To a solution of **1b** (2.39 g; 0.01 mol) in absolute ethanol (30 mL) and dimethylformamide (10 mL) containing triethylamine (1 mL), the isothiocyanate derivatives (0.01 mol) together with elemental sulfur (0.32 g; 0.01 mol) were added. The reaction mixture was refluxed for 5 h, and poured onto ice/water. The obtained solid was crystallized from dioxane to give **14–19**, respectively.

4-Amino-N-(4-sulfamoylphenyl)-2-thioxo-3-p-tolyl-2,3-dihydrothiazole-5-carboxamide (14)

Yield 66%, m.p. 117.7°C. IR (KBr, cm^{-1}): 3368, 3305, 3226 (NH, NH_2), 2981, 2848 (CH aliph.), 1687 (C=O), 1378, 1160 (SO_2), 1276 (C=S). 1H -NMR (DMSO- d_6 , δ , ppm): 2.2 (s, 3H, CH_3), 6.5 (s, 2H, NH_2 , D_2O -exchangeable), 6.7–7.9 (m, 10H, Ar-H + SO_2NH_2), 10.6 (s, 1H, NH, D_2O -exchangeable). ^{13}C -NMR (DMSO- d_6 , δ , ppm): 23.2, 81.6, 122.6 (2), 127.6 (2), 128.6 (2), 130.8 (2), 133.6 (2), 139.7, 144.1, 160.6, 165.4, 178.4. Analysis: calcd. for $C_{17}H_{16}N_4O_3S_3$ (420.53): C, 48.55; H, 3.83; N, 13.32%; found: C, 48.29; H, 3.52; N, 13.62%.

4-Amino-3-(4-methoxyphenyl)-N-(4-sulfamoylphenyl)-2-thioxo-2,3-dihydrothiazole-5-carboxamide (15)

Yield 66%, m.p. 139.7°C. IR (KBr, cm^{-1}): 3385, 3315, 3271 (NH, NH_2), 3095 (CH arom.), 2961, 2861 (CH aliph.), 1681 (C=O), 1388, 1156 (SO_2), 1276 (C=S). 1H -NMR (DMSO- d_6 , δ , ppm): 3.8 (s, 3H, OCH_3), 6.6 (s, 2H, NH_2 , D_2O -exchangeable), 6.7–8.0 (m, 10H, Ar-H + SO_2NH_2), 10.9 (s, 1H, NH, D_2O -exchangeable). ^{13}C -NMR (DMSO- d_6 , δ , ppm): 54.2, 79.2, 113.6 (2), 123.7 (2), 124.3, 125.6 (2), 126.0 (2), 133.2, 140.6, 155.7, 158.6, 166.7, 189.6. Analysis: calcd. for $C_{17}H_{16}N_4O_4S_3$ (436.53): C, 46.77; H, 3.69; N, 12.83%; found: C, 46.48; H, 3.42; N, 12.49%.

4-Amino-3-(4-fluorophenyl)-N-(4-sulfamoylphenyl)-2-thioxo-2,3-dihydrothiazole-5-carboxamide (16)

Yield 81%, m.p. 196.8°C. IR (KBr, cm^{-1}): 3410, 3391, 3246 (NH, NH_2), 3100 (CH arom.),

1672 (C=O), 1376, 1152 (SO_2), 1269 (C=S). 1H -NMR (DMSO- d_6 , δ , ppm): 6.4 (s, 2H, NH_2 , D_2O -exchangeable), 7.0–8.1 (m, 10H, Ar-H + SO_2NH_2), 11.2 (s, 1H, NH, D_2O -exchangeable). ^{13}C -NMR (DMSO- d_6 , δ , ppm): 76.1, 114.6 (2), 122.7 (2), 128.4 (2), 129.6 (2), 131.1, 137.8, 141.2, 157.0, 160.2, 165.5, 187.4. Analysis: calcd. for $C_{16}H_{13}FN_4O_3S_3$ (424.49): C, 45.27; H, 3.09; N, 13.20%; found: C, 45.53; H, 3.28; N, 13.46%.

4-Amino-3-(4-nitrophenyl)-N-(4-sulfamoylphenyl)-2-thioxo-2,3-dihydrothiazole-5-carboxamide (17)

Yield 78%, m.p. 175.3°C. IR (KBr, cm^{-1}): 3284, 3220, 3186 (NH, NH_2), 3066 (CH arom.), 1654 (C=O), 1508, 1307 (NO_2), 1379, 1198 (SO_2), 1203 (C=S). 1H -NMR (DMSO- d_6 , δ , ppm): 6.7 (s, 2H, NH_2 , D_2O -exchangeable), 6.9–7.9 (m, 10H, Ar-H + SO_2NH_2), 10.9 (s, 1H, NH, D_2O -exchangeable). ^{13}C -NMR (DMSO- d_6 , δ , ppm): 77.4, 120.7 (2), 123.6 (2), 126.4 (2), 128.1 (2), 133.7, 141.4, 142.6, 145.0, 158.2, 162.7, 190.1. Analysis: calcd. for $C_{16}H_{13}N_5O_3S_3$ (451.50): C, 42.56; H, 2.90; N, 15.51%; found: C, 42.31; H, 2.60; N, 15.74%.

4-Amino-3-(4-bromophenyl)-N-(4-sulfamoylphenyl)-2-thioxo-2,3-dihydrothiazole-5-carboxamide (18)

Yield 71%, m.p. 290.9°C. IR (KBr, cm^{-1}): 3376, 3212, 3186 (NH, NH_2), 3056 (CH arom.), 1676 (C=O), 1376, 1165 (SO_2), 1218 (C=S). 1H -NMR (DMSO- d_6 , δ , ppm): 6.2 (s, 2H, NH_2 , D_2O -exchangeable), 7.2–8.0 (m, 10H, Ar-H + SO_2NH_2), 10.8 (s, 1H, NH, D_2O -exchangeable). ^{13}C -NMR (DMSO- d_6 , δ , ppm): 72.3, 120.6, 122.7 (2), 126.8 (2), 127.4 (2), 130.6 (2), 133.7, 136.1, 138.8, 156.7, 162.9, 186.8. Analysis: calcd. for $C_{16}H_{13}BrN_4O_3S_3$ (485.40): C, 39.59; H, 2.70; N, 11.54%; found: C, 39.81; H, 2.96; N, 11.36%.

4-Amino-3-(4-iodophenyl)-N-(4-sulfamoylphenyl)-2-thioxo-2,3-dihydrothiazole-5-carboxamide (19)

Yield 69%, m.p. 272.2°C. IR (KBr, cm^{-1}): 3385, 3318, 3190 (NH, NH_2), 3076 (CH arom.), 1684 (C=O), 1394, 1161 (SO_2), 1254 (C=S). 1H -NMR (DMSO- d_6 , δ , ppm): 6.5 (s, 2H, NH_2 , D_2O -exchangeable), 7.0–8.1 (m, 10H, Ar-H + SO_2NH_2), 10.6 (s, 1H, NH, D_2O -exchangeable). ^{13}C -NMR (DMSO- d_6 , δ , ppm): 74.3, 91.6, 120.4 (2), 128.7 (2), 129.6 (2), 131.3, 133.6, 139.1 (2), 141.4, 157.6, 164.2, 189.6. Analysis: calcd. for $C_{16}H_{13}IN_4O_3S_3$ (532.40): C, 36.10; H, 2.46; N, 10.52%; found: C, 36.41; H, 2.70; N, 10.19%.

General procedure for the synthesis of 2-cyano-3-(4-substituted phenyl)-*N*-(4-sulfamoylphenyl)acrylamides (20-24)

A mixture of **1b** (2.39 g; 0.01 mol) and aromatic aldehydes (0.01 mol) in ethanol (20 mL) containing 3 drops of piperidine was refluxed for 8 h. The obtained solid was crystallized from ethanol to give **20–24**, respectively.

2-Cyano-3-(4-fluorophenyl)-*N*-(4-sulfamoylphenyl)acrylamide (20)

Yield 83%; m.p. 265.9°C. IR (KBr, cm⁻¹): 3337, 3310, 3290 (NH, NH₂), 3065 (CH arom.), 2966, 2876 (CH aliph.), 2205 (C≡N), 1685 (C=O), 1396, 1184 (SO₂). ¹H-NMR in (DMSO-d₆, δ, ppm): 7.0–8.1 (m, 10H, Ar-H + SO₂NH₂), 8.3 (s, 1H, CH), 10.9 (s, 1H, NH, D₂O-exchangeable). ¹³C-NMR in (DMSO-d₆, δ, ppm): 105.6, 114.3 (2), 114.9, 122.6 (2), 126.7 (2), 127.8 (2), 129.9, 130.8, 133.7, 152.6, 163.1, 164.9. Analysis: calcd. for C₁₆H₁₂FN₃O₃S (345.35): C, 55.65; H, 3.50; N, 12.17%; found: C, 55.38; H, 3.22; N, 12.51%.

3-(3-Bromophenyl)-2-cyano-*N*-(4-sulfamoylphenyl)acrylamide (21)

Yield 86%, m.p. 167.2°C. IR (KBr, cm⁻¹): 3412, 3391, 3212 (NH, NH₂), 3095 (CH arom.), 2971, 2836 (CH aliph.), 2218 (C≡N), 1685 (C=O), 1328, 1155 (SO₂). ¹H-NMR (DMSO-d₆, δ, ppm): 7.0–7.9 (m, 10H, Ar-H + SO₂NH₂), 8.9 (s, 1H, CH), 10.6 (s, 1H, NH, D₂O-exchangeable). ¹³C-NMR (DMSO-d₆, δ, ppm): 109.0, 115.8, 121.1 (2), 126.2, 126.5, 127.3 (2), 130.3, 130.8, 131.8, 137.5, 138.3, 141.3, 152.6, 170.3. Analysis: calcd. for C₁₆H₁₂BrN₃O₃S (406.25): C, 47.30; H, 2.98; N, 10.34%; found: C, 47.62; H, 2.66; N, 10.12%.

3-(4-Bromophenyl)-2-cyano-*N*-(4-sulfamoylphenyl)acrylamide (22)

Yield 80%, m.p. 233.3°C. IR (KBr, cm⁻¹): 3390, 3309, 3287 (NH, NH₂), 3100 (CH arom.), 2992, 2920 (CH aliph.), 2219 (C≡N), 1689 (C=O), 1336, 1156 (SO₂). ¹H-NMR (DMSO-d₆, δ, ppm): 7.0–7.9 (m, 10H, Ar-H + SO₂NH₂), 8.4 (s, 1H, CH), 11.2 (s, 1H, NH, D₂O-exchangeable). ¹³C-NMR (DMSO-d₆, δ, ppm): 108.2, 115.1, 119.8 (2), 121.7, 128.4 (2), 129.6 (2), 130.7 (2), 133.8, 136.7, 140.8, 155.1, 164.6. Analysis: calcd. for C₁₆H₁₂BrN₃O₃S (406.25): C, 47.30; H, 2.98; N, 10.34%; found: C, 47.07; H, 2.66; N, 10.59%.

2-Cyano-3-(3-methoxynaphthalen-2-yl)-*N*-(4-sulfamoylphenyl)acrylamide (23)

Yield 69%, m.p. 104.5°C. IR (KBr, cm⁻¹): 3364, 3310, 3206 (NH, NH₂), 3066 (CH arom.),

2980, 2942 (CH aliph.), 2212 (C≡N), 1652 (C=O), 1376, 1156 (SO₂). ¹H-NMR (DMSO-d₆, δ, ppm): 4.0 (s, 3H, OCH₃), 7.0–8.0 (m, 12H, Ar-H + SO₂NH₂), 9.1 (s, 1H, CH), 10.7 (s, 1H, NH, D₂O-exchangeable). ¹³C-NMR (DMSO-d₆, δ, ppm): 56.2, 109.7, 110.2, 115.4, 121.2 (2), 123.3, 126.5 (3), 127.3 (2), 127.9, 128.5, 129.7, 133.8, 137.9, 139.3, 155.8, 160.5, 164.0. Analysis: calcd. for C₂₁H₁₇N₃O₄S (407.44): C, 61.90; H, 4.21; N, 10.31%; found: C, 61.59; H, 4.44; N, 10.02%.

2-Cyano-5-(4-dimethylamino)phenyl)-*N*-(4-sulfamoylphenyl)penta-2,4-dienamide (24)

Yield 59%, m.p. 240.2°C. IR (KBr, cm⁻¹): 3360, 3315, 3272 (NH, NH₂), 3091 (CH arom.), 2946, 2860 (CH aliph.), 2212 (C≡N), 1676 (C=O), 1377, 1156 (SO₂). ¹H-NMR (DMSO-d₆, δ, ppm): 3.0 (s, 6H, N(CH₃)₂), 6.6, 6.9 (2d, 2H, CH=CH, *J* = 7.0, 7.1 Hz), 7.5 (s, 1H, CH, *J* = 7.2 Hz), 7.7–8.0 (m, 10H, Ar-H + SO₂NH₂), 10.3 (s, 1H, NH, D₂O-exchangeable). ¹³C-NMR (DMSO-d₆, δ, ppm): 40.1 (2), 96.7, 112.4 (2), 115.8, 122.1 (2), 122.8, 126.4, 126.8 (2), 129.3 (2), 130.6, 131.0, 138.9, 141.5, 149.7, 164.2. Analysis: calcd. for C₂₀H₂₀N₄O₃S (396.46): C, 60.59; H, 5.08; N, 14.13%; found: C, 60.92; H, 5.30; N, 14.41%.

3-Oxo-*N*-(4-sulfamoylphenyl)-3*H*-benzo[*f*]chromone-2-carboxamide (25)

Yield 79%, m.p. 287.1°C. IR (KBr, cm⁻¹): 3343, 3309, 3275 (NH, NH₂), 3076 (CH arom.), 1700, 1673 (2C=O), 1374, 1184 (SO₂). ¹H-NMR (DMSO-d₆, δ, ppm): 7.4–8.1 (m, 12H, Ar-H + SO₂NH₂), 8.5 (s, 1H, CH), 10.3 (s, 1H, NH, D₂O-exchangeable). ¹³C-NMR (DMSO-d₆, δ, ppm): 116.3, 116.9, 118.2, 120.7 (2), 121.4, 122.6, 125.2, 127.3 (2), 128.2 (2), 131.7 (2), 135.7 (2), 142.6, 154.8, 168.9, 172.0. Analysis: calcd. for C₂₀H₁₄N₂O₅S (394.40): C, 60.91; H, 3.58; N, 7.10%; found: C, 60.64; H, 3.29; N, 7.33%.

In vitro antiproliferative activity

Antiproliferative activity *in vitro* was measured by the cell growth inhibition assay. The general *in vitro* anticancer evaluation of the synthesized compounds was conducted by using WST-1 reagent for determination of IC₅₀ for each compound. Results are given in Table 1.

WST-1 cell proliferation assay

MDA-MB-231 breast cancer and HT-29 colon cancer cell lines were purchased from the American Type Culture Collection. Cells were maintained in RPMI 1640 (Sigma), supplemented with 10% FBS

Table 1. *In vitro* antiproliferative activity of the novel synthesized compounds against breast (MDA-MB-231) and colon (HT-29) cancer cell lines.

Compd. No.	MDA-MB-231 IC ₅₀ (μM) ^a	HT-29 IC ₅₀ (μM) ^a
1b	NA ^b	49.22 ± 0.02
2	NA	109.94 ± 0.01
3	147 ± 0.3	NA
4	NA	NA
5	NA	NA
6	NA	96.61 ± 0.085
7	NA	NA
8	171.76 ± 0.7	45.62 ± 0.04
9	NA	NA
10	NA	NA
11	221.53 ± 0.08	NA
12	271.67 ± 0.03	NA
13	184.82 ± 0.08	NA
14	NA	NA
15	NA	NA
16	NA	NA
17	66.6 ± 0.04	NA
18	NA	77.96 ± 0.01
19	139.4 ± 0.2	74.46 ± 0.09
20	NA	60.84
21	NA	NA
22	NA	NA
23	236.78 ± 0.11	NA
24	85.31 ± 0.02	131.86 ± 0.018
5-Fluorouracil	77.28 ± 0.2	10.23 ± 0.09

^a IC₅₀: Concentration of the synthesized compounds (μM) producing 50% cell growth inhibition after 48 h of compound exposure, as determined by the WST-1 assay. Each experiment was run at least three times, and the results are presented as average values ± standard deviation. ^b Activity is above 150 μM.

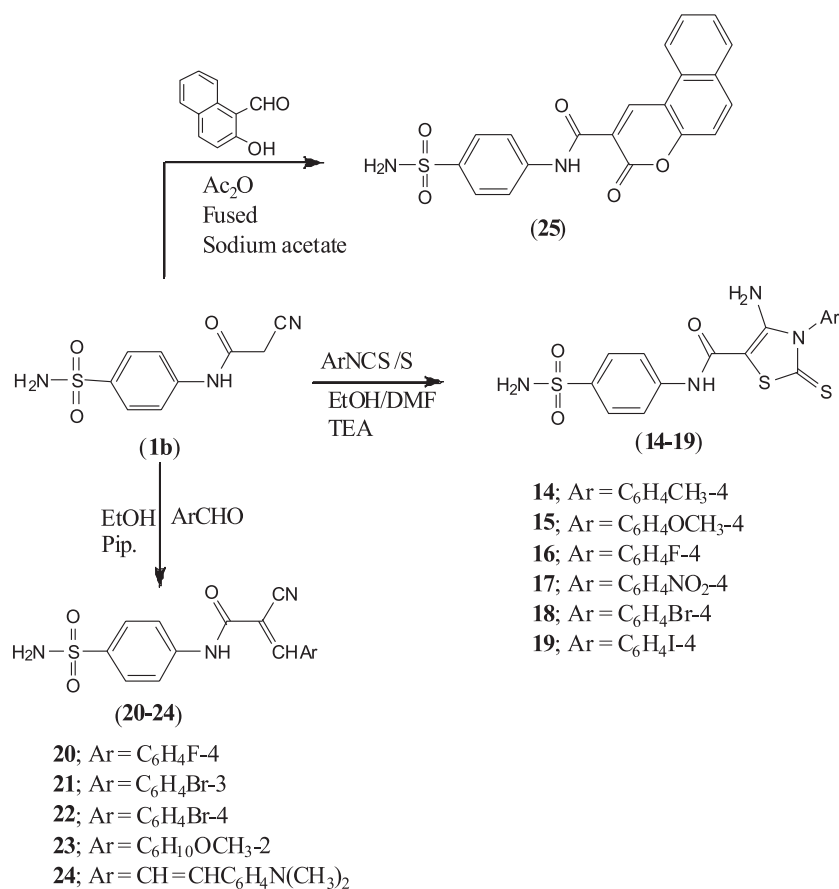
(Lonza), 100 IU/mL penicillin, 100 μg/mL streptomycin and 2 mmol/L L-glutamine (Sigma). Cells were seeded into 96-well plates at 0.4×10^4 /well and incubated overnight. The medium was replaced with fresh one containing the desired concentrations of the synthesized compounds. After 48 h, 10 μL of the WST-1 reagent was added to each well and the plates were re-incubated for 4 h at 37°C. The amount of formazan was quantified using ELISA reader at 450 nm (28, 29).

RESULTS AND DISCUSSION

Chemistry

The starting material – 2-chloro-*N*-(4-sulfamoylphenyl)acetamide **1a** was prepared accord-

ing to the reported method (29) and converted to the corresponding acetamide derivatives **2–13** by reaction with different amines such as adamantylamine, 5-aminoindanone, 4-morpholino-benzeneamine, piperonylamine, 2-aminobenzothiophenes, 2-amino-1-ethylpyrazole, 2-amino-5-ethyl-1,3,4-thiadiazole, 3-aminoquinoline and 2-aminoisoquinoline (Scheme 1). The structures of compounds **2–13** were established on the basis of microanalysis and spectral data. The IR spectra showed the presence of characteristic bands for (NH, NH₂), (CH aromatic), (CH aliphatic), (C=O), (SO₂). ¹H-NMR spectra of **2–13** revealed signals around 3.5–4.9 ppm assigned to CH₂CO group. In addition, interaction of 2-cyano-*N*-(4-sulfamoylphenyl)acetamide **1b** (23) with elemental sulfur and arylisothiocyanate yielded

Scheme 2. Synthesis of novel sulfonamide derivatives (**14–25**)

disappearance of CH₂ group and the presence of a new peak at 10.3–11.2 ppm assigned to NH group. Furthermore, Perkin reaction was carried out by reaction of **1b** with 2-hydroxy-1-naphthaldehyde in acetic anhydride in the presence of fused sodium acetate and yielded the corresponding benzochromene-2-one derivative **25**. The reaction went in analogy with the reported method (10). The IR spectrum of **25** exhibited the absence of C≡N band and the presence of 2 C=O bands. ¹H-NMR spectrum of **25** showed a singlet at 8.5 ppm assigned to CH chromene group and 10.3 ppm due to NH group consistent with the proposed structure.

In-vitro antiproliferative activity

Antiproliferative activity of all the synthesized compounds was assessed against breast cancer (MDA-MB-231) and colon cancer (HT-29) cell lines. The results of antiproliferative activity indicated that

sulfonamide **17** carrying 2,3-dihydrothiazole with free amino group at 4-position, 4-nitrophenyl at 3-position and thioxo at 2-position was found to exert the most powerful effect on MDA-MB-231 with IC₅₀ of 66.6 μM compared with that of the positive control – 5-fluorouracil (IC₅₀ = 77.28 μM). Also, the sulfonamide **24** containing 2-cyano-5-(4-*N,N*-dimethylphenylamino)penta-2,4-dienamide was slightly less active than 5-fluorouracil as reference drug against MDA-MB-231 (IC₅₀ = 85.31 μM). On the other hand, sulfonamides having cyano and acetamide groups **1b** and 5,6-dimethylbenzothiazole with acetamide moiety **8** were found to be the most active compounds against HT-29 with IC₅₀ values of 49.22 and 45.62 μM, respectively, but less active than 5-fluorouracil. In addition, compounds **18–20** exhibited a moderate activity with IC₅₀ values 77.96, 74.46 and 60.84 μM against HT-29, while, compounds **3–7**, **9–16** and **21–23** showed no activity (Table 1).

CONCLUSION

The objective of the present study was to synthesize and investigate the antiproliferative activity of some novel sulfonamide derivatives carrying the biologically active acetamide, dihydrothiazole, acrylamide and benzochromene moieties. Compound **17** was found to be the most potent against breast cancer cell lines compared with the reference drug – 5-fluorouracil. Also, compound **24** is nearly as active as 5-fluorouracil. In addition, compounds **1b** and **8** exhibited a moderate activity against colon cancer cell line but less active than the positive control.

Acknowledgments

The authors would like to extend their sincere appreciation to the Deanship of Scientific Research at King Saud University for its funding of this research through the Research Group Project no. GP-VPP-302.

REFERENCES

- Gibbs J.B.: *Science* 287, 1969 (2000).
- Genc Y., Ozkanca R., Bekdemir Y.: *Clin. Microbiol. Antimicrob.* 7, 17 (2008).
- Cassini A., Scozzafava A., Mastrolorenzo A., Supuran C.T.: *Curr. Cancer Drug Targets* 2, 55 (2000).
- Denko N.C.: *Nat. Rev. Cancer* 8, 705 (2008).
- Dawson M.I., Fontana J.A.: *Mini Rev. Med. Chem.* 10, 455 (2010).
- Yurttas L., Demirayak S., Cifteci G.A., Yildirim S.U., Kaplancikli Z.A.: *Arch. Pharm.* 346, 403 (2013).
- Brandoni E.F., Meijerman I., Klijn J.S., Arend D.D., Sparidons R.W., Lazaro L.L., Beijnen J.H., Schellens J.H.: *Anticancer Drugs* 16, 935 (2005).
- Bhuva H.A., Kini S.G.: *J. Mol. Graph. Model.* 29, 32 (2010).
- El-Sayed W.A., Flefel M.M., Morsy E.M.H.: *Der Pharma Chem.* 4, 23 (2012).
- Kumar D., Maruthi Kumar N., Chang K.H., Shah K.: *Eur. J. Med. Chem.* 45, 4664 (2010).
- Solomon V.R., Lee H.: *Curr. Med. Chem.* 18, 1488 (2011).
- Vasquez D., Taine A., Theoduloz R.C., Verrax J., Calderon P.B., Valderrama J.A.: *Bioorg. Med. Chem. Lett.* 19, 5060 (2009).
- Zhang W., Hu J. F., Lv W., Zhao Q.C., Shi G.B.: *Molecules* 17, 12950 (2012).
- Eswaran S., Adhikari A.V., Chowdhury I.H., Pal N.K., Thomas K.D.: *Eur. J. Med. Chem.* 45, 3374 (2010).
- Eswaran S., Adhikari A.V., Kumar R.A.: *Eur. J. Med. Chem.* 45, 957 (2010).
- Patil S.A., Wang J., Li X.S., Chen J., Jones S.T., Ahmed H.A., Patil R. et al.: *Bioorg. Med. Chem. Lett.* 22, 4458 (2012).
- Abuhaie M., Bicu E., Rigo B., Gautred P., Belei., Farce A., Dubois J., Ghiet A.: *Bioorg. Med. Chem. Lett.* 23, 147 (2013).
- Chen J., Hsu M.H., Kuo S.C., Lai Y.Y., Chung J.G., Huang L.J.: *Anticancer Res.* 27, 343 (2007).
- Lee S.M., Kwon J.I., Choi Y.H., Eom H.S., Chi G.Y.: *Phytother. Res.* 22, 752 (2008).
- Alsaid M.S., Bashandy M.S., Alqasomi S.I., Ghorab M.M.: *Eur. J. Med. Chem.* 46, 137 (2011).
- Alsaid M.S., Ghorab M.M., Al-Dosari M.S., Hamed M.M.: *Eur. J. Med. Chem.* 46, 201 (2011).
- Ghorab M.M., Ragab F.A., Hamed M.M.: *Eur. J. Med. Chem.* 44, 4211 (2009).
- Kivela A.J., Kivela J., Saarnio J., Parkkila S.: *World J. Gastroenterol.* 11, 155 (2005).
- Scozzafava A., Owa T., Mastrolorenzo A., Supuran C.T.: *Curr. Med. Chem.* 10, 925 (2003).
- Supuran C.T.: *Nat. Rev. Drug Discov.* 7, 168 (2008).
- Trivedi J.M., Mehta C.M.: *J. Indian Chem. Soc.* LII, 708 (1975).
- Thomas G.L., Johannes C.W.: *Curr. Opin. Chem. Biol.* 15, 516 (2011).
- Supuran C.T., Scozzafava A.: *Bioorg. Med. Chem.* 15, 4336 (2007).
- Casini A., Scozzafava A., Mastrolorenzo A., Supuran C.T.: *Curr. Cancer Drug Targets* 2, 55 (2002).

Received: 13. 11 2013

SYNTHESIS AND EVALUATION OF ANTICONVULSANT ACTIVITY OF *N*-(2,5-DIMETHYLPHENOXY)- AND *N*-[(2,3,5-TRIMETHYLPHENOXY)ALKYL]AMINOALKANOLS

ANNA MARIA WASZKIELEWICZ^{1*}, AGNIESZKA GUNIA-KRZYŻAK¹, MAREK CEGŁA²
and HENRYK MARONA¹

¹Department of Bioorganic Chemistry, ²Chair of Organic Chemistry, Faculty of Pharmacy,
Jagiellonian University Medical College, Medyczna 9, 30-688 Kraków, Poland

Abstract: A series of new *N*-(2,5-dimethylphenoxy)- and *N*-(2,3,5-trimethylphenoxy)alkylaminoalkanols [I–XVII] was synthesized and evaluated for anticonvulsant activity. Pharmacological tests included maximal electroshock (MES) and subcutaneous pentetrazole seizure threshold (scMet) assays as well as neurotoxicity (TOX) evaluation in mice after intraperitoneal (*i.p.*) administration and/or in rats after oral (*p.o.*) administration. The most active compound was *R*-2*N*-[(2,3,5-trimethylphenoxy)ethyl]aminobutan-1-ol, which exhibited 100% activity in MES at the dose of 30 mg/kg body weight (mice, *i.p.*) and 75% activity in MES at 30 mg/kg b.w. (rats, *p.o.*) without neurotoxicity at the active doses.

Keywords: anticonvulsant, epilepsy, MES, neurotoxicity, aminoalkanols, synthesis

Epilepsy is a set of neurological disorders affecting about 1% of world human population. The disorders have various etiology and progress, resulting in clinically different seizures, which start in the cerebral cortex. Despite great development of pharmacotherapy of epilepsy, about 30% of all seizures are resistant to drugs. Moreover, many patients who manage to control the symptoms using two or three medicines face numerous side effects enlarged by drug interactions. Therefore, there are strong premises for further research in this field (1, 2).

Currently available antiepileptic drugs (AEDs) have been mostly discovered by means of the maximum electroshock (MES), subcutaneous pentetrazole (scMet), and rotarod neurotoxicity (TOX) screens. However, pathophysiology of drug-resistant seizures does not resemble mechanism of the above stimuli, therefore 6 Hz test was introduced. It has been proved that it mimics epileptogenesis – the process where damaged neuronal tissue exhibits pathological processes leading to epilepsy. Examples of drugs active in 6 Hz test and inactive in MES are levetiracetam and its analog – seletracetam (3, 4).

Research concerning anticonvulsant activity of well-known antiarrhythmic drugs, such as propa-

nolol and mexiletine (Fig. 1), has revealed that both these medicines prevent seizures in the maximum electroshock seizure test (MES, mice, *i.p.*). Among the likely mechanisms in both cases there is inhibition of sodium channels, apart from their main molecular mechanisms (blocking β -adrenergic receptors and opening potassium channels, respectively) (5, 6). The effect of potential stabilization within neurons by those two drugs was a starting point for searching new anticonvulsant compounds among aroxyalkylaminoalkanols (7).

In our previous studies (8–14), we reported anticonvulsant activity of some amido- and aminoalkanols which were examined within the Anticonvulsant Screening Program (ASP) carried out at National Institute of Neurological Disorders and Stroke, National Institutes of Health, Rockville, USA (15). One of them, (*S*)-(+)-2-*N*-[(2,6-dimethylphenoxy)ethyl]aminobutan-1-ol hydrochloride displayed sufficient protection against MES-induced seizures and low toxicity (mice, *i.p.*) with ED_{50} = 7.57 mg/kg and PI = 4.55 (8). Another compound, (*R,S*)-*trans*-2-*N*-[(2,6-dimethylphenoxy)ethyl]aminocyclohexan-1-ol exhibited ED_{50} = 7.73 mg/kg and PI = 3.90 (MES, mice, *i.p.*) (Fig. 2) (9). We consistently report lipophilicity parameters as important

* Corresponding author: e-mail: awaszkie@cm-uj.krakow.pl; phone: +48126205576, fax: +48126205405

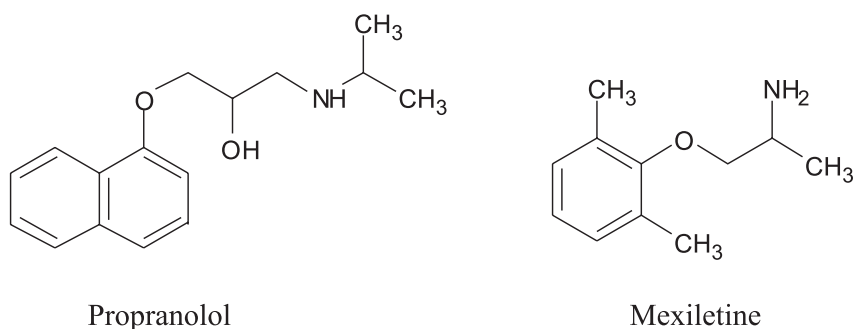


Figure 1. Structures of cardiovascular drugs with anticonvulsant activity

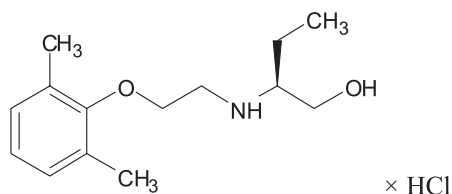
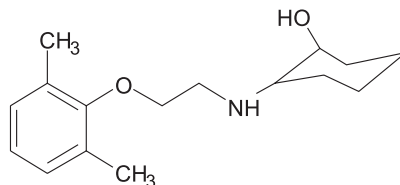
*(S)*-(+)-2-*N*-[(2,6-dimethylphenoxy)ethyl]amino butan-1-ol hydrochloride (8).*(R,S)*-*trans*-2-*N*-[(2,6-dimethylphenoxy)ethyl]aminocyclohexan-1-ol (9).

Figure 2. Structures of (2,6-dimethylphenoxy)ethyl aminoalkanol derivatives with anticonvulsant activity

physicochemical feature in CNS drug discovery (10). From the preliminary assay data, it was proposed that anticonvulsant activity was associated mainly with aminoalkanol type and configuration. Such anticonvulsant activity of the appropriate aminoalkanols drew our attention onto influence of position and type of substituents in the phenyl ring. So far, appropriate derivatives of 4-methylphenol, 2,6-dimethylphenol (8, 9), 4-chlor-3-methylphenol and 2-chlor-5-methylphenol (10), as well as 4-chlor-2-methylphenol (11) have been evaluated. Herein we report results of synthesis and anticonvulsant screening of novel *N*-(2,3-dimethylphenoxy) and *N*-(2,3,5-trimethylphenoxy)alkyl]aminoalkanols [I–XVII].

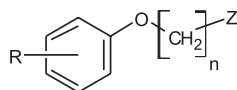
EXPERIMENTAL

Chemistry

Apparatus and reagents

Melting points (m.p.) were determined by means of a Büchi SMP-20 apparatus (Büchi Labortechnik, Switzerland) and are uncorrected. Elemental analyses were performed on Vario El III (Elementar Analysensysteme GmbH, Germany). Thin-layer chromatography was performed on pre-coated aluminum sheets (silica gel 60 F₂₅₄, Merck) using mobile phase indicated below. The theoretical values of the partition coefficient (LogP) of the tested compounds were calculated by means of ACD-

Table 1. Chemical structures of the tested compounds [I–XVII].



R	n	Compound	Z	Configuration
2,5-(CH ₃) ₂	2	I		R,S
		II		R,S
		III		R,S
		IV		R,S
		V		trans, R,S
		VI		R,S
	3	VII		R,S
		VIII		R,S
		IX		trans, R,S
2,3,5-(CH ₃) ₃	2	X		R,S
		XI		R,S
		XII		R,S
		XIII		R
		XIV		S
		XV		trans, R,S
		XVI		trans
XVII		R,S		

LABS 12.0 program. Specific rotation (for compounds **XIII** and **XIV**) was measured on Jasco P-2000 polarimeter (1% w/v solutions in CH₃OH, sodium light 589 nm). The proton magnetic resonance spectra were recorded by means of Varian VX 300 spectrometer (USA) or Bruker 500 spectrometer (Germany) using DMSO-d₆ or CDCl₃ as solvents and DMSO or TMS as internal standards, respectively. The results are presented in the following format: chemical shift δ (ppm), multiplicity, coupling constants (J) values in Hertz (Hz), number of protons, proton's position. Multiplicities are shown as the abbreviations: s (singlet), bs (broad singlet), d (doublet), dd (doublet of doublets), t (triplet), quin (quintet), m (multiplet). *D,L-trans*-2-aminocyclohexan-1-ol for synthesis of compounds **V**, **IX** and **XV** was synthesized according to published procedures (9). Other reagents were purchased from Alfa Aesar (Germany) or Merck (Germany). Solvents were commercially available materials of reagent grade.

General procedure of synthesis of tested compounds

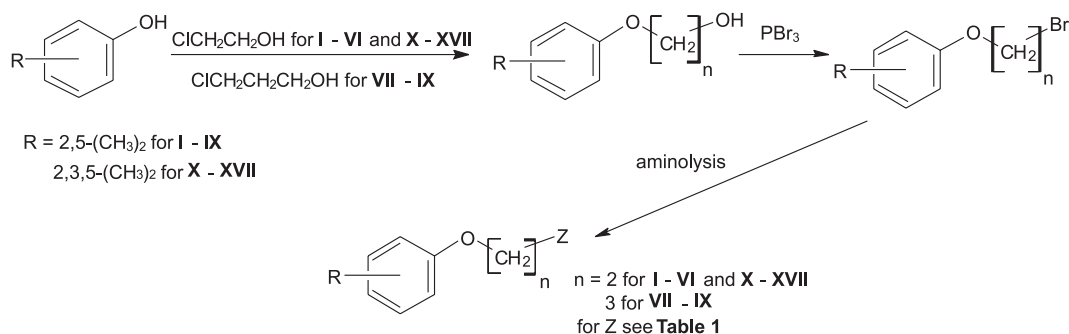
The tested compounds were synthesized according to formerly published procedures (7–10, 16). The general route of synthesis is shown in Scheme 1 and the chemical structures of the tested compounds in Table 1.

First step of the synthesis included *O*-alkylation of 0.1 mole of appropriate substituted phenol: 2,5-dimethyl for compounds **I–IX** or 2,3,5-trimethyl for compounds **X–XVII** with use of 10% excess of 2-chloroethanol (for **I–VI** and **X–XVII**) or 3-chloropropan-1-ol (for **VII–IX**). The reaction was carried out in 50% mixture of acetone with sodium ethanolate or sodium propanolate, respectively, at the presence of anhydrous K₂CO₃. The reaction mixture was refluxed for 48 h. Then, it was filtered and

50 mL of 2% aqueous solution of NaOH was added to the filtrate. The mixture was extracted with toluene (2 × 50 mL). Then, organic solvent was separated, dried over Na₂SO₄, and evaporated under reduced pressure. Raw residue was used for bromination reaction by means of 10% excess of PBr₃. The reaction mixture was refluxed for 2 h in water bath, then it was poured on ice. Raw product was extracted by toluene, and the extract was dried over anhydrous Na₂SO₄ and evaporated under reduced pressure yielding bromide derivative. In the final step, a mixture of 0.01 mole of an appropriate aminoalkanol or amine and 0.01 mole of appropriate bromide was refluxed for 6 h in 30 mL of toluene at the presence of 0.015 mole of anhydrous K₂CO₃ as a proton acceptor. Then, inorganic salts were filtered off and organic solvent was evaporated under reduced pressure. Oily residues were recrystallized from toluene/*n*-heptane 1 : 5 v/v mixture. In order to obtain compound **XVII**, the base was converted into hydrochloride salt upon treatment with excess of ethanolic solution of gaseous HCl. The hydrochloride was recrystallized from acetone.

R,S-1*N*-[(2,5-dimethylphenoxy)ethyl]amino-propan-2-ol [**I**]

Yield 60%; C₁₃H₂₁NO₂, M.w. = 223.31, m.p.: 64–66°C. R_f = 0.39 (CH₃OH : ethyl acetate 1 : 1, v/v). Log P = 2.22 ± 0.28. ¹H-NMR (500 MHz, DMSO, δ , ppm): 6.98 (d, J = 7.4, 1H, Ar-H3); 6.73 (s, 1H, Ar-H6); 6.63 (d, J = 7.4 Hz, 1H, Ar-H4); 4.44 (d, J = 4.3 Hz, 1H, OH); 4.03–3.94 (m, 2H, CH₂-O); 3.71–3.64 (m, 1H, HO-CH); 2.88 (t, J = 5.5 Hz, 2H, O-CH₂-CH₂-N); 2.54–2.45 (m, 2H, N-CH₂); 2.25 (s, 3H, Ar-CH₃); 2.09 (s, 3H, Ar-CH₃); 1.85 (bs, 1H, NH); 1.04 (d, J = 6.3 Hz, 2H, CH₃-R). Analysis: calcd.: C, 69.92; H, 9.48; N, 6.27%; found: C, 69.90; H, 9.38; N, 6.21%.



Scheme 1. Synthesis of the tested compounds [**I–XVII**]

R,S-2N-[(2,5-dimethylphenoxy)ethyl]amino-propan-1-ol [II]

Yield 72%; $C_{13}H_{21}NO_2$, M. w. = 223.31, m.p.: 74–76°C. R_f = 0.36 (CH₃OH : ethyl acetate 1 : 1, v/v). Log P = 2.22 ± 0.28. ¹H-NMR (500 MHz, DMSO, δ , ppm): 6.98 (d, J = 7.4 Hz, 1H, Ar-H3); 6.73 (s, 1H, Ar-H6); 6.63 (d, J = 7.4 Hz, 1H, Ar-H4); 4.53 (t, J = 5.0 Hz, 1H, OH); 4.04–3.98 (m, 1H, O-CHH); 3.98–3.93 (m, 1H, O-CHH); 3.33–3.28 (m, 1H, N-CHH); 3.24–3.18 (m, 1H, N-CHH); 2.96–2.90 (m, 1H, CHHOH); 2.89–2.84 (m, 1H, CHHOH); 2.71–2.64 (m, 1H, CH); 2.25 (s, 3H, Ar-CH₃); 2.10 (s, 3H, Ar-CH₃); 1.88 (bs, 1H, NH); 0.92 (d, J = 6.3 Hz, 3H, CH₃-R). Analysis: calcd.: C, 69.92; H, 9.48; N, 6.27%; found: C, 69.90; H, 9.32; N, 6.19%.

R,S-2N-[(2,5-dimethylphenoxy)ethyl]aminobutan-1-ol [III]

Yield 59%; $C_{14}H_{23}NO_2$, M.w. = 237.34, m.p.: 66–68°C. R_f = 0.44 (CH₃OH : ethyl acetate 1 : 1, v/v). Log P = 2.75 ± 0.28. ¹H-NMR (500 MHz, DMSO, δ , ppm): 6.98 (d, J = 7.4 Hz, 1H, Ar-H3); 6.73 (s, 1H, Ar-H6); 6.63 (d, J = 7.4 Hz, 1H, Ar-H4); 4.40 (t, J = 5.4 Hz, 1H, OH); 4.03–3.93 (m, 2H, CH₂-O); 3.42–3.22 (m, 2H, CH₂-O); 2.90 (t, J = 5.5 Hz, 2H, N-CH₂); 2.49–2.42 (m, 1H, CH); 2.25 (s, 3H, Ar-CH₃); 2.09 (s, 3H, Ar-CH₃); 1.76 (bs, 1H, NH); 1.41–1.30 (m, 2H, R-CH₂-R); 0.85 (t, J = 7.5 Hz, 3H, CH₃-R). Analysis: calcd.: C, 70.85; H, 9.77; N, 5.90%; found: C, 70.76; H, 9.69; N, 5.74%.

R,S-1N-[(2,5-dimethylphenoxy)ethyl]aminobutan-2-ol [IV]

Yield 65%; $C_{14}H_{23}NO_2$, M.w. = 237.34, m.p.: 63–65°C. R_f = 0.39 (CH₃OH : ethyl acetate 1 : 1, v/v). Log P = 2.75 ± 0.28. ¹H-NMR (500 MHz, DMSO, δ , ppm): 6.97 (d, J = 7.4 Hz, 1H, Ar-H3); 6.73 (s, 1H, Ar-H6); 6.63 (d, J = 7.4 Hz, 1H, Ar-H4); 4.41 (bs, 1H, OH); 4.03–3.95 (m, 2H, O-CH₂); 3.42 (bs, 1H, CH); 2.88 (t, J = 5.5 Hz, 2H, O-CH₂-CH₂-N); 2.57 (dd, J = 11.6, J = 4.0 Hz, 1H, N-CHH); 2.48 (dd, J = 11.6 Hz, J = 4.0 Hz, 1H, N-CHH); 2.26 (s, 3H, Ar-CH₃); 2.10 (s, 3H, Ar-CH₃); 1.84 (bs, 1H, NH); 1.45–1.26 (m, 2H, CH₂); 0.86 (t, J = 7.5 Hz, 3H, CH₃-R). Analysis: calcd.: C, 70.85; H, 9.77; N, 5.90%; found: C, 70.80; H, 9.77; N, 5.78%.

R,S-trans-2N-[(2,5-dimethylphenoxy)ethyl]aminocyclohexan-1-ol [V]

Yield 65%; $C_{16}H_{25}NO_2$, M.w. = 263.38, m.p.: 99–101°C. R_f = 0.57 (CH₃OH : ethyl acetate 1 : 1, v/v). Log P = 2.90 ± 0.27. ¹H-NMR (300 MHz, CDCl₃, δ , ppm): 7.01 (d, J = 7.4 Hz, 1H, Ar-H4);

6.67 (d, J = 7.4 Hz, 1H, Ar-H3); 6.64 (s, 1H, Ar-H6); 4.05 (t, J = 5.4 Hz, 2H, O-CH₂); 3.26–3.14 (m, 2H, -CHH-NH + CH-OH); 2.92–2.85 (m, 1H, CHH-NH); 2.31 (s, 3H, Ar-CH₃), 2.17 (s, 3H, Ar-CH₃); 2.29–0.95 (m, 9H, cyclohexyl). Analysis: calcd.: C, 72.97; H, 9.57; N, 5.32%; found: C, 73.10; H, 9.83; N, 5.49%.

R,S-2N-[(2,5-dimethylphenoxy)ethyl]amino-1-phenylethan-1-ol [VI]

Yield 60%; $C_{18}H_{23}NO_2$, M.w. = 285.38, m.p.: 124–126°C. R_f = 0.62 (CH₃OH); Log P = 3.54 ± 0.30. ¹H-NMR (500 MHz, DMSO, δ , ppm): 7.39–7.26 (m, 4H, Ar-H); 7.25–7.20 (m, 1H, Ar-H); 6.98 (d, J = 7.4 Hz, 1H, Ar-H3); 6.73 (s, 1H, Ar-H6); 6.63 (d, J = 7.4 Hz, 1H, Ar-H4); 5.26 (d, J = 3.5 Hz, 1H, OH); 4.68–4.61 (m, 1H, CH); 3.98 (t, J = 5.5 Hz, 2H, O-CH₂); 2.92 (t, J = 5.5 Hz, 2H, O-CH₂-CH₂-N); 2.72 (d, J = 6.2 Hz, 2H, N-CH₂-CH); 2.25 (s, 3H, Ar-CH₃); 2.05 (s, 3H, Ar-CH₃); 1.89 (bs, 1H, NH). Analysis: calcd.: C, 75.76; H, 8.12; N, 4.91%; found: C, 75.49; H, 8.05; N, 4.90%.

R,S-2N-[(2,5-dimethylphenoxy)propyl]amino-propan-1-ol [VII]

Yield 76%; $C_{14}H_{23}NO_2$, M. w. = 237.34, m.p.: 80–81°C. R_f = 0.16 (CH₃OH : ethyl acetate 1 : 1, v/v). Log P = 2.47 ± 0.27. ¹H NMR (500 MHz, DMSO, δ , ppm): 7.00 (d, J = 7.44 Hz, 1 H, Ar-H3), 6.61–6.71 (m, 2 H, Ar-H4,6), 4.04 (t, J = 5.96 Hz, 2 H, O-CH₂-CH₂-CH₂-N), 3.61 (dd, J = 10.64, 3.98 Hz, 1 H, CH₂-OH), 3.29 (dd, J = 10.77, 7.05 Hz, 1 H, CH₂-OH), 2.98 (dt, J = 11.70, 6.91 Hz, 1 H, O-CH₂-CH₂-CH₂-N), 2.73–2.91 (m, 2 H, O-CH₂-CH₂-CH₂-N, CH-NH), 2.34 (bs, 2 H, OH, NH), 2.31 (s, 3 H, Ar-CH₃), 2.17 (s, 3 H, Ar-CH₃), 2.02 (quin, J = 6.41 Hz, 2 H, O-CH₂-CH₂-CH₂-N), 1.10 (d, J = 6.54 Hz, 3 H, CH₃-CH). Analysis: calcd.: C, 70.85; H, 9.77; N, 5.90%; found: C, 70.80; H, 9.61; N, 5.91%.

R,S-2N-[(2,5-dimethylphenoxy)propyl]aminobutan-1-ol [VIII]

Yield 66%; $C_{15}H_{23}NO_2$, M.w. = 251.36, m.p.: 53–54°C. R_f = 0.22 (CH₃OH : ethyl acetate 1 : 1, v/v). Log P = 3.00 ± 0.27. ¹H NMR (300 MHz, CDCl₃, δ , ppm): 7.00 (d, J = 7.4 Hz, 1H, Ar-H3), 6.71–6.61 (m, 2H, Ar-H4,6), 4.04 (t, J = 6.0 Hz, 2H, Ar-O-CH₂), 3.62 (dd, J = 10.5, J = 4.1 Hz, 1H, CH-CH₂-OH), 3.27 (dd, J = 10.6, J = 6.6 Hz, 1H, CH-CH₂-OH), 2.97–2.86 (m, 1H, CH₂-NH), 2.82–2.72 (m, 1H, CH₂-NH), 2.61–2.51 (m, 1H, NH-CH-CH₂-OH), 2.31 (s, 3H, Ar-CH₃), 2.17 (s, 3H, Ar-CH₃), 1.97 (quin, J = 6.4 Hz, 2 H, CH-CH₂-CH₃), 1.62–1.31 (m, 2H, O-CH₂-CH₂-CH₂-NH), 0.91 (t, J

= 7.5 Hz, 1 H, CH-CH₂-CH₃). Analysis: calcd.: C, 71.67; H, 10.02; N, 5.57%; found: C, 71.39; H, 9.95; N, 5.51%.

R,S-trans-2N-[(2,5-dimethylphenoxy)propyl]aminocyclohexan-1-ol [IX]

Yield 67%; C₁₇H₂₇NO₂, M. w. = 277.41, m.p.: 92–93°C. R_f = 0.30 (CH₃OH : ethyl acetate 1 : 1, v/v). Log P = 3.15 ± 0.25. ¹H NMR (500 MHz, DMSO, δ, ppm): 7.00 (d, *J* = 7.6 Hz, 1H, Ar-H3), 6.71–6.60 (m, 2H, Ar-H4,6), 4.03 (t, *J* = 6.0 Hz, 2H, Ar-O-CH₂), 3.20–3.10 (m, 1H, cyclohexyl-H1/CH-OH), 3.03 (dt, *J* = 11.6, *J* = 6.9 Hz; 1 H, CH₂-NH), 2.68 (dt, *J* = 11.6, *J* = 6.7 Hz, 1H, CH₂-NH), 2.31 (s, 3H, Ar-CH₃), 2.26–2.18 (m, 1H, cyclohexyl-H2/CH-NH), 2.17 (s, 3H, Ar-CH₃), 2.15–2.03 (m, 2H, cyclohexyl-H6), 2.02–1.91 (m, 2H, cyclohexyl-H3), 1.78–1.66 (m, 2H, cyclohexyl-H5), 1.34–1.15 (m, 2H, cyclohexyl-H4). Analysis: calcd.: C, 73.61; H, 9.81; N, 5.05%; found: C, 74.01; H, 9.84; N, 5.03%.

R,S-1N-[(2,3,5-trimethylphenoxy)ethyl]amino-propan-2-ol [X]

Yield 69%; C₁₄H₂₃NO₂, M.w. = 237.3, m.p.: 74–76°C. R_f = 0.52 (CH₃OH : ethyl acetate 1 : 1, v/v). Log P = 2.68 ± 0.28. ¹H NMR (300 MHz, CDCl₃, δ, ppm): 6.62 (s, 1H, Ar-H4), 6.54 (s, 1H, Ar-H6), 4.05 (t, *J* = 5.1 Hz, 2H, O-CH₂-CH₂-N), 3.81 (quin, *J* = 9.4, *J* = 6.3, *J* = 3.1 Hz, 1H, CH₂-CH(OH)-CH₃), 3.16–2.96 (m, 2H, O-CH₂-CH₂-N), 2.83 (dd, *J* = 12.1, *J* = 3.1 Hz, 1 H, CH₂-CH(OH)-CH₃), 2.56 (bs., 2H, OH, NH), 2.49 (dd, *J* = 12.1, *J* = 9.5 Hz, 1 H, CH₂-CH(OH)-CH₃), 2.28 (s, 3H, Ar-CH₃), 2.23 (s, 3H, Ar-CH₃), 2.10 (s, 3H, Ar-CH₃), 1.17 (d, *J* = 6.2 Hz, 3H, CH₂-CH(OH)-CH₃). Analysis: calcd.: C, 70.79; H, 9.77; N, 5.90%; found: C, 70.85; H, 9.46; N, 5.59%.

R,S-2N-[(2,3,5-trimethylphenoxy)ethyl]amino-propan-1-ol [XI]

Yield 62%; C₁₄H₂₃NO₂, M.w. = 237.3, m.p.: 73–75°C. R_f = 0.25 (CH₃OH : benzene (1 : 5, v/v)). Log P = 2.68 ± 0.28. ¹H-NMR (300 MHz, CDCl₃, δ, ppm): 6.62 (s, 1H, Ar-H4); 6.54 (s, 1H, Ar-H6); 4.05–4.02 (m, 2H, Ar-O-CH₂); 3.61 (dd, *J* = 4.1, *J* = 10.5 Hz, 1H, CHHOH); 3.27 (dd, *J* = 5.0, *J* = 10.5 Hz, 1H, CHHOH); 3.15–3.11 (m, 1H, CHH-N); 2.96–2.91 (m, 1H, CHH-N); 2.88–2.84 (m, 1H, N-CH); 2.28 (s, 3H, Ar-CH₃); 2.23 (s, 3H, Ar-CH₃); 2.10 (s, 3H, Ar-CH₃); 1.10 (d, *J* = 6.5 Hz 3H, CH-CH₃); 2.50–1.50 (bs, 2H, NH, OH). Analysis: calcd.: C, 70.79; H, 9.77; N, 5.90%; found: C, 71.13; H, 9.36; N, 5.78%.

R,S-2N-[(2,3,5-trimethylphenoxy)ethyl]aminobutan-1-ol [XII]

Yield 60%; C₁₅H₂₅NO₂, M.w. = 251.35, m.p.: 61–62°C (toluene : heptane 1 : 1, v/v); R_f = 0.63 (CH₃OH : ethyl acetate 5 : 1, v/v). Log P = 3.21 ± 0.28. ¹H-NMR (500 MHz, DMSO, δ, ppm): 6.59 (s, 1H, Ar-H4); 6.56 (s, 1H, Ar-H6); 4.45 (bs, 1H, OH); 3.95 (t, *J* = 5.3 Hz, 2H, Ar-O-CH₂); 3.50–3.20 (m, 2H, CH₂-OH); 2.90 (t, 2H, CH₂-N); 2.55–2.40 (m, 1H, CH); 2.21 (s, 3H, Ar-CH₃); 2.16 (s, 3H, Ar-CH₃); 2.02 (s, 3H, Ar-CH₃); 1.45–1.3 (m, CH₂-CH₃); 0.85 (t, *J* = 7.2 Hz, 3H, CH₂-CH₃). Analysis: calcd.: C, 71.68; H, 10.03; N, 5.57%; found: C, 71.30; H, 9.90; N, 5.54%.

R-(-)-2N-[(2,3,5-trimethylphenoxy)ethyl]aminobutan-1-ol [XIII]

Yield 58%; C₁₅H₂₅NO₂, M.w. = 251.35, m.p.: 47–49°C. R_f = 0.37 (CH₃OH : benzene 1 : 5, v/v). [α]_D²⁰ = –19.4. ¹H NMR (300 MHz, CDCl₃, δ, ppm): 6.62 (s, 1H, Ar-H4), 6.53 (s, 1H, Ar-H6), 4.12–3.95 (m, 2 H, Ar-O-CH₂), 3.64 (dd, *J* = 10.6, *J* = 4.1 Hz, 1H, CH-CHH-OH), 3.32 (dd, *J* = 10.6, *J* = 6.4 Hz, 1H, CH-CHH-OH), 3.17–3.04 (m, 1H, CHH-NH), 3.01–2.89 (m, 1H, CHH-NH), 2.70–2.58 (m, 1H, NH-CH-CH₂-OH), 2.28 (s, 3H, Ar-CH₃), 2.23 (s, 3H, Ar-CH₃), 2.10 (s, 3H, Ar-CH₃), 1.61–1.38 (m, 2H, CH-CH₂-CH₃), 0.95 (t, *J* = 7.4 Hz, 3H, CH-CH₂-CH₃). Analysis: calcd.: C, 71.66; H, 10.02; N, 5.57%; found: C, 71.01; H, 9.80; N, 5.37%.

S-(+)-2N-[(2,3,5-trimethylphenoxy)ethyl]aminobutan-1-ol [XIV]

Yield 56%; C₁₅H₂₅NO₂, M.w. = 251.35, m.p.: 47–49°C. R_f = 0.37 (CH₃OH : benzene 1 : 5, v/v). [α]_D²⁰ = 22.2. ¹H NMR (300 MHz, CDCl₃, δ, ppm): 6.62 (s, 1H, Ar-H4), 6.53 (s, 1H, Ar-H6), 4.13–3.99 (m, 2H, Ar-O-CH₂), 3.67 (dd, *J* = 10.8, *J* = 4.0 Hz, 1H, CH-CH₂-OH), 3.36 (dd, *J* = 10.8, *J* = 6.4 Hz, 1H, CH-CH₂-OH), 3.20–3.08 (m, 1H, CH₂-NH), 3.04–2.94 (m, 1H, CH₂-NH), 2.75–2.64 (m, 1H, NH-CH-CH₂-OH), 2.27 (s, 3H, Ar-CH₃), 2.23 (s, 3H, Ar-CH₃), 2.10 (s, 3H, Ar-CH₃), 1.67–1.42 (m, 2H, CH-CH₂-CH₃), 0.96 (t, *J* = 7.4 Hz, 3H, CH-CH₂-CH₃). Analysis: calcd.: C, 71.66; H, 10.02; N, 5.57%; found: C, 71.31; H, 9.95; N, 5.48%.

R,S-trans-2N-[(2,3,5-trimethylphenoxy)ethyl]aminocyclohexan-1-ol [XV]

Yield 70%; C₁₇H₂₇NO₂, M.w. = 277.47, m.p.: 117–119°C. R_f = 0.54 (CH₃OH : benzene 1 : 5, v/v). Log P = 3.36 ± 0.27. ¹H-NMR (300 MHz, CDCl₃, δ, ppm): 6.59 (d, *J* = 8.8, 1H, Ar-H4); 6.56 (d, *J* = 3.0,

1H, Ar-H6); 4.62 (d, $J = 5.1$ Hz, 1H, OH); 4.04–3.98 (m, 1H, Ar-O-CHH); 3.94–3.86 (m, 1H, Ar-O-CHH); 3.13–3.04 (m, 1H, HO-CH); 2.97–2.89 (m, 1H, CHH-N); 2.86–2.78 (m, 1H, CHH-N); 2.23–2.15 (m, 1H, NH); 2.21 (s, 3H, Ar-CH₃); 2.15 (s, 3H, Ar-CH₃); 2.02 (s, 3H, Ar-CH₃); 1.96–1.88 (m, 1H, cyclohex.); 1.83–1.75 (m, 1H, cyclohex.); 1.66–1.54 (m, 2H, cyclohex.); 1.24–1.09 (m, 3H, cyclohex.); 0.96–0.86 (m, 1H, cyclohex.). Analysis: calcd.: C, 73.58; H, 9.81; N, 5.07%; found: C, 72.83; H, 9.48; N, 5.24%.

R,S-trans-4N-[(2,3,5-trimethylphenoxy)ethyl]aminocyclohexan-1-ol [XVI]

Yield 68%; C₁₇H₂₇NO₂, M.w. = 277.41 m.p.: 109–111°C. R_f = 0.45 (CHCl₃ : CH₃OH 1 : 1, v/v). Log P = 3.22 ± 0.26. ¹H NMR (500 MHz, DMSO, δ, ppm): 6.62 (s, 1H, Ar-H4), 6.53 (s, 1H, Ar-H6), 4.06 (t, $J = 5.3$ Hz, 2H, O-CH₂-CH₂-N), 3.71–3.56 (m, 1H, CH-OH), 3.06 (t, $J = 5.2$ Hz, 2H, O-CH₂-CH₂-N), 2.68–2.51 (m, 1H, CH-NH), 2.27 (s, 3H, Ar-CH₃), 2.22 (s, 3H, Ar-CH₃), 2.10 (s, 3H, Ar-CH₃), 2.00 (m, 4H, cyclohex-H2,6), 1.88 (bs, 2H, OH, NH), 1.43–1.12 (m, 4H, cyclohex-H3,5). Analysis: calcd.: C, 73.61; H, 9.81; N, 5.05%; found: C, 73.59; H, 9.89; N, 5.06%.

R,S-2N-[(2,3,5-trimethylphenoxy)ethyl]amino-1-phenylethan-1-ol hydrochloride [XVII]

Yield 58%; C₁₉H₂₆NO₂Cl, M.w. = 335.86; m.p.: 146–148°C. R_f = 0.36 (CH₃OH : benzene 1 : 5, v/v). Log P = 4.00 ± 0.30. ¹H-NMR (300 MHz, DMSO, δ, ppm): 9.37 (bs, 2H, NH₂⁺); 7.48–7.23 (m, 5H, Ar-H); 6.62 (d, $J = 4.7$ Hz, 2H, Ar-H); 6.26 (d, $J = 4.7$ Hz, 1H, OH); 5.13–5.00 (m, 1H, CH); 4.34–4.19 (m, 2H, O-CH₂); 3.40–3.03 (m, 4H, CH₂-N); 2.22 (s, 3H, Ar-CH₃); 2.15 (s, 3H, Ar-CH₃); 2.02 (s, 3H, Ar-CH₃). Analysis: calcd.: C, 67.94; H, 7.80; N, 4.17%; found: C, 67.91; H, 7.8042; N, 4.02%.

Pharmacology

Evaluation of anticonvulsant activity and neurotoxicity was carried out according to the Anticonvulsant Screening Program (ASP) at National Institute of Neurological Disorders and Stroke (NINDS), National Institutes of Health (NIH), Rockville, USA. Tests were performed in mice (adult male Carworth Farms No. 1) after intraperitoneal (*i.p.*) administration and/or in rats (Sprague-Dawley) after oral (*p.o.*) administration. The tested compounds were administered as solutions or suspensions in 0.5% methylcellulose. The total volume of used suspension was 0.01 mL/1 g b.w. for mice and 0.04 mL/10 g b.w. for rats. Initial

dosage for evaluation in mice was 30, 100, and 300 mg/kg, and in rats 30 mg/kg. Tests were performed at certain time points after administration of the compound i.e., at 0.5 and 4.0 h after *i.p.* administration or at 0.25, 0.5, 1.0, 2.0 and 4.0 h after *p.o.* administration. All procedures were published elsewhere (15, 17), below we provide short description of the experiments.

Maximal electroshock (MES)

At certain time after administration of the tested compound, 60 Hz alternating current at 50 mA for mice or 150 mA for rats was delivered for 0.2 s *via* corneal electrodes. Protection in MES test was defined as the abolition of the hindlimb tonic extension component of the seizure (15, 17).

Subcutaneous pentetrazole induced seizures (scMet)

The scMet was conducted in mice at certain time after administration of the tested compound by subcutaneous administration of pentetrazole dissolved in 0.9% NaCl solution at the dose of 85 mg/kg. The animal was placed in isolation cage and observed for next 30 min. Failure of observing even a threshold seizure (a single episode of clonic spasm which remains at least 5 s) was classified as protection (15, 17).

Neurotoxicity assays (TOX)

Neurotoxicity in mice was measured by the rotarod test. A mouse was placed on a 1 inch diameter knurled plastic rod rotating at 6 rpm. Neurotoxicity was indicated by the inability of the animal to maintain equilibrium on the rod for at least 1 min in each of the three trials. In rats, neurological deficit was indicated by ataxia, loss of placing response and muscle tone (15, 17).

6 Hz psychomotor seizure test

The 6 Hz model test was carried out according to the protocol originally described by Brown et al. (18) and more recently by Barton et al. (19) and Kaminski et al. (20). 6 Hz test was performed in mice. Seizures were induced by delivering 0.2 ms pulses of electric current at 6 Hz and 32 mA for 3 s *via* corneal electrodes. Untreated animals display seizures after such stimulation described as minimal clonic phase, whereas mice not displaying this behavioral are considered protected.

RESULTS

The synthesis of the tested compounds consisted of *O*-alkylation of the appropriate substituted

Table 2. Anticonvulsant activity of the tested compounds (I–XVII) (mice, *i.p.*).

Compound	Dose [mg/kg b.w.]	MES ^{a)}		scMet ^{a)}		TOX ^{b)}		ASP class ^{c)}
		0.5 h	4.0 h	0.5 h	4.0 h	0.5 h	4.0 h	
I	30	0/1	0/1	0/1	0/1	0/4	0/2	1
	100	3/3	0/3	0/1	0/1	8/8	1/4	
	300					4/4		
II	30	0/1	0/1	0/1	0/1	2/4	1/2	4
	100	3/3	3/3	0/1	0/1	8/8	1/4	
	300	1/1		0/1		4/4		
III	30	0/1	0/1	0/1	0/1	0/4	0/4	1
	100	3/3	0/3	0/1	0/1	8/8	0/4	
	300					4/4		
IV	30	0/1	0/1	0/1	0/1	0/4	0/2	1
	100	3/3	0/3	0/1	0/1	8/8	0/4	
	100	1/1				4/4		
VI	30	0/1	0/1	0/1	0/1	0/4	0/2	3
	100	0/3	0/3	0/1	0/1	7/8	0/4	
	300	0/1	0/1	0/1	0/1	3/4	1/2	
VII	30	0/1	0/1	0/1	0/1	0/4	0/2	1
	100	2/2	0/3	0/1	0/1	8/8	0/4	
	300					4/4		
VIII	30	0/1	0/1	0/1	0/1	0/4	0/2	1
	100	2/2	0/3	0/1	0/1	8/8	0/4	
	300					4/4		
IX	30	0/1	0/1	0/1	0/1	0/4	0/2	1
	100	1/3	0/3		0/1	4/8	0/4	
	300		0/1			4/4	0/2	
X	30	0/1	0/1	0/1	0/1	3/4	1/2	4
	100	3/3	0/3	0/1	0/1	8/8	1/4	
	300					4/4		
XI	3	0/4				0/4		4
	10	0/4				0/4		
	30	1/1		0/1	0/1	1/4	1/2	
	100	3/3		2/2	0/1	8/8	1/3	
	300					4/4		
XII	3	0/4				0/4		1
	10	0/4				0/4		
	30	1/1	0/1	0/1	0/1	0/4	0/2	
	100	3/3	1/3	0/1	0/1	7/8	0/4	
	300		0/1			4/4	0/2	
XIII	3							1
	10	0/4				0/4		
	30	1/1	0/1	0/1	0/1	0/4	0/2	
	100	2/3	1/3	0/1	0/1	4/8	0/4	
	300					4/4		
XIV	3	0/4				0/4		4
	10	0/4				0/4		
	30	1/1	0/1	0/1	0/1	3/4	0/2	
	100	3/3	0/3		0/1	7/8	0/4	
	300					4/4		
XV	3	0/4				0/4		4
	10	0/4				0/4		
	30	1/1	0/1	0/1	0/1	1/4	0/2	
	100	3/3	0/3	0/1	0/1	7/8	1/4	
	300					4/4		
XVI	30	0/1	0/1	0/1	0/1	0/4	0/2	1
	100	3/3	0/3	0/1	0/1	8/8	0/4	
	300					4/4		
XVII	30	0/1	0/1	0/1	0/1	3/4	1/2	4
	100	3/3	1/3	0/1	0/1	8/8	4/4	
	300	1/1			0/1	4/4	1/1	

^{a)}Number of animals protected / number of animals tested; ^{b)} number of animals exhibiting toxicity / number of animals tested in the rotarod test; ^{c)} ASP classification: 1 – anticonvulsant activity at dose 100 mg/kg or less; 2 – anticonvulsant activity at doses greater than 100 mg/kg; 3 – compound inactive at 300 mg/kg; 4 – compound either active or inactive but toxic at dose of 30 mg/kg; | – the compound was not tested in the particular conditions.

Table 3. Anticonvulsant activity of compounds **XIII** and **XV** tested in rats, *p.o.*

Compound	Test	Dose [mg/kg b.w.]	Time [h]				
			0.25	0.5	1.0	2.0	4.0
XIII ED ₅₀ (1 h) > 120	MES ^{a)}	30	1/4	3/4	2/4	0/4	0/4
	TOX ^{a)}	30	0/4	0/4	0/4	0/4	0/4
XV	MES ^{a)}	30	0/4	0/4	0/4	1/4	2/4
	TOX ^{a)}	30	0/4	0/4	0/4	0/4	0/4

^{a)} Number of animals protected / number of animals tested in anticonvulsant or neurotoxicity assays.

Table 4. Anticonvulsant activity in 6-Hz test of compounds **I** and **V** (mice, *i.p.*).

Compound	Test	Dose [mg/kg b.w.]	Time [h]				
			0.25	0.5	1.0	2.0	4.0
I	6-Hz ^{a)}	30	1/4	3/4	2/4	0/4	0/4
	TOX ^{b)}	30	0/4	0/4	0/4	0/4	0/4
V	6-Hz ^{a)}	30	0/4	0/4	0/4	1/4	2/4
	TOX ^{b)}	30	0/4	0/4	0/4	0/4	0/4

^{a)} Number of animals protected / number of animals tested; ^{b)} number of animals exhibiting toxicity / number of animals tested in the rotorod test.

phenol by means of 2-chloroethanol or 3-chloropropan-1-ol in the first step. Then, the obtained 2-phenoxyalkanols were converted to bromides by means of phosphorus tribromide. Finally, the obtained bromide derivatives were used in *N*-alkylation of chosen aminoalkanols.

After confirmation of structure and chemical purity, the synthesized compounds were subjected to anticonvulsant and neurotoxicity evaluation according to the protocols within Anticonvulsant Screening Program (ASP). Pharmacological tests were performed at National Institute of Neurological Disorders and Stroke, National Institutes of Health, Rockville, USA. Most of the compounds were qualified to standard procedures and tested in mice after *i.p.* administration. The results are shown in Table 2. The protective activity in MES was found for majority of the compounds. Most of substances showed full protection at the dose 100 mg/kg. Compounds **XI–XV** were also active at 30 mg/kg. Considering scMet evaluation, compound **XI** was the only one in the series which showed protection. Anticonvulsant properties of the tested substances were in all cases

accompanied by neurotoxicity, especially at the doses of 100 and 300 mg/kg. Most promising compounds, **XII**, **XIII**, and **XIV** proved anticonvulsant activity at 30 mg/kg and no neurotoxicity at the same dose. They are derivatives of 2-aminobutan-1-ol – the racemate and the two enantiomers.

Additional tests in rats after oral administration (*p.o.*) were performed for compounds **XIII** and **XV**, results are presented in Table 3. Both substances caused no neurological impairment at all tested time points. Interestingly, compound **XIII** showed protection until 1.0 h after administration while **XV** only at 2.0 and 4.0 h, whereas in mice *i.p.* evaluation both compounds were active at 0.5 h. Compound **XIII** was also used in a more advanced test in order to find ED₅₀ value. ED₅₀ indicates dose in which the compound is effective in 50% of tested animals (17). The dose was found to be more than 120 mg/kg b. w. (rats, *p.o.*) while tested after 1 h of administration of the compound.

Compound **V** was qualified to modified protocols and was tested initially in 6 Hz model. The obtained results were not good enough to have the

compound tested in MES. On the other hand, compound **I** was qualified for 6 Hz evaluation after successful MES screen. Results of 6 Hz model are shown in Table 4. Both compounds showed some protection.

DISCUSSION AND CONCLUSION

The anticonvulsant activity and neurotoxicity of all synthesized compounds **I–XVII** were evaluated according to the protocols of ASP, NIH, USA (15, 17). The reported series of compounds was characterized by good anticonvulsant activity in MES (mice, *i.p.*). It is visible that among aminoalkanols used as moieties – aminopropanol and aminobutanol with various configuration are more promising compared to more bulky moieties such as 2-amino-1-phenylethanol – compounds **I–IV** and **X–XIV** are the most active. Within this group, the use of ethyl or propyl linker does not make any significant difference in terms of activity – comparing compounds **II** and **VII** as well as **III** and **VIII** in pairs in Table 2.

In terms of substitution of the phenyl ring it is clearly visible that 2,3,5-trimethyl derivatives are more active than 2,5-dimethyl ones – the most active compound is **XIII** – *R-2N*-(2,3,5-trimethylphenoxy)ethyl]aminobutan-1-ol which was advanced to testing in rats, *p.o.*

The activity of **I–XVII** was mostly accompanied by neurotoxicity which excluded the compounds from further testing. The important factors in the group are the values of calculated partition coefficient (log P) ranging from 2.22 ± 0.28 to 4.00 ± 0.30 . Literature references indicate that in order to reach optimum activity within the central nervous system log P as a measure of lipophilicity should be around 2 (21, 22). In case of some more lipophilic compounds one of the reason of neurotoxicity might be high values of log P.

In terms of structure-anticonvulsant activity relationship, the obtained results in the reported series of compounds combined together with former results indicated that parameters such as type of substituents and their location in the phenyl ring, the aminoalkanol moiety, configuration may have impact on anticonvulsant activity. In conclusion, in the light of formerly published results, the conducted research confirmed that aroxyalkyl derivatives of aminoalkanols are an interesting group in terms of anticonvulsant activity, although 2,5-dimethyl and 2,3,5-trimethyl derivatives exhibit concomitant neurotoxicity.

Acknowledgments

The authors would like to thank prof. James P. Stables, prof. Jeff Jiang and Tracy Chen, Ph.D. for providing the results of pharmacological assays through ASP at National Institute of Neurological Disorders and Stroke, National Institutes of Health (Rockville, USA), as well as prof. Katarzyna Kieć-Kononowicz coordination of the cooperation between the NIH and Faculty of Pharmacy, Jagiellonian University Medical College.

This work was supported by the European Regional Development Fund through the Innovative Economy Program and Jagiellonian University Medical College in Kraków (grant no K/ZDS/003328).

REFERENCES

- Banerjee P.N., Filippi, D., Allen Hauser W.: *Epilepsy Res.* 85, 31 (2009).
- Bialer M., White, H.S.: *Nat. Rev. Drug Discov.* 9, 68 (2010).
- Löscher W.: *Seizure* 20, 359 (2011).
- Löscher W., Schmidt D.: *Epilepsia* 53, 1841 (2012).
- Fischer W.: *Seizure* 11, 285 (2002).
- Chew C., Collett J., Singh B.: *Drugs* 17, 161 (1979).
- Marona H., Waszkielewicz A., Kieć-Kononowicz K.: Patent App. WO 2009/093916A3, Jagiellonian University.
- Marona H., Antkiewicz-Michaluk L.: *Acta Pol. Pharm. Drug Res.* 55, 487 (1998).
- Pękała E., Waszkielewicz A.M., Szneler E., Walczak M., Marona H.: *Bioorg. Med. Chem.* 19, 6927 (2011).
- Waszkielewicz A.M., Szkaradek N., Pękała E., Galzarano F., Marona H.: *Biomed. Chromatogr.* 24, 1365 (2010).
- Waszkielewicz A.M., Szneler E., Cegła M., Marona H.: *Lett. Drug Des. Discov.* 10, 35 (2013).
- Marona H., Waszkielewicz A.M., Szneler E.: *Acta Pol. Pharm. Drug Res.* 62, 345 (2005).
- Marona H., Szneler E.: *Acta Pol. Pharm. Drug Res.* 60, 477 (2003).
- Gunia A., Waszkielewicz A.M., Cegła M., Marona H.: *Lett. Drug Des. Discov.* 9, 37 (2012).
- Stables J.P., Kupferberg H.J.: In *Molecular and Cellular Targets for Antiepileptic Drugs*, Avanzini G., Regesta P., Tanganelli A., Avoli

- M. Eds., pp. 191–198, John Libbey & Company Ltd., London 1997.
16. Augstein J., Austin W.C., Boscott R.J., Green S.M., Worthing C.R.: *J. Med. Chem.* 8, 356 (1964).
 17. White H.S., Woodhead J.H., Wilcox K.S., Stables J.P., Kupferberg H.J., Wolf H.H.D.: In *Antiepileptic Drugs*, 5th edn., Levy R.H., Mattson R.H., Meldrum B.S., Perucca E. Eds., pp. 36–48, Lippincott Williams & Wilkins, Philadelphia 2002.
 18. Brown W.C., Schiffman D.O., Swinyard E.A., Goodman L.S.: *J. Pharmacol. Exp. Ther.* 107, 273 (1953).
 19. Barton M.E., Klein B.D., Wolf H.H., White H.S.: *Epilepsy Res.* 47, 217 (2001).
 20. Kaminski R.F., Livingood M.R., Rogawski M.A.: *Epilepsia* 45, 864 (2004).
 21. Hansch C., Björkroth J.P., Leo A.: *J. Pharm. Sci.* 76, 663 (1987).
 22. Pajouhesh H., Lenz G.R.: *NeuroRx* 2, 541 (2005).

Received: 13. 01. 2014

SYNTHESIS AND ANTIPROLIFERATIVE ACTIVITY *IN VITRO*
OF NEW 2-THIOXOIMIDAZO[4,5-*B*]PYRIDINE DERIVATIVESANNA NOWICKA^{1*}, HANNA LISZKIEWICZ¹, WANDA P. NAWROCKA¹,
JOANNA WIETRZYK², AGNIESZKA ZUBIAK³ and WOJCIECH KOŁODZIEJCZYK³¹Wrocław Medical University, Department of Drug Technology,
Borowska 211A, 50-556 Wrocław, Poland²Ludwik Hirszfeld Institute of Immunology and Experimental Therapy, Polish Academy of Science,
“NeoLek” Laboratory of Experimental Anticancer Therapy, Wrocław, Poland³Wrocław Medical University, Department of Physical Chemistry, Wrocław, Poland

Abstract: Two series of 2-thioxoimidazo[4,5-*b*]pyridine derivatives have been synthesized from 2,3-diaminopyridine (**1**) and 5-halogenosubstituted-2,3-diaminopyridines **2**, **3**. Mannich bases **7** – **12** and **24** – **29**, derivatives of 1-arylamino-6-halogeno-2-thioxoimidazo[4,5-*b*]pyridine were obtained with selected secondary amines: morpholine, piperidine, 2-methoxyphenylpiperazine, pyrimidin-2-yl-piperazine and formaldehyde in ethanol. The structures **7** – **12** and **24** – **29** were confirmed by the results of elementary analysis and their IR, ¹H-NMR and MS spectra. All given structures **7** – **12** have been optimized to get the most stable low energy conformers. Synthesized compounds were of interest for biological studies or can be substrates for further synthesis. The selected compounds **7** – **10**, **12** – **17**, **22**, **25**, **27** – **29** were screened for their antiproliferative activity *in vitro* against human cancer and normal mouse fibroblast cell lines.

Keywords: 2-amino-3-arylideneamino-5-halogenopyridine, 2-thioxoimidazo[4,5-*b*]pyridine derivatives, Mannich bases, Schiff bases, IR, ¹H-NMR spectra, antiproliferative activity *in vitro*

There are some drugs, imidazo[4,5-*b*]pyridine derivatives, registered in the world, which exhibit diverse pharmacological activities. Antihistaminic H₂ generation drug with selective activity to H₁ receptors is represented by naberastine (**1**). Sulmazole (**2**), a new cardiotonic agent, is an A₁ adenosine receptor antagonist. Tenatoprazole (**3**) possesses antiulcer activity and is a novel proton pump inhibitor with a prolonged plasma half-life.

Based on the review of the chemical literature, derivatives of imidazole[4,5-*b*]pyridine showed a multiparmacological effects. A number of the imidazo[4,5-*b*]pyridine possess antidepressant (**4**), anticancer (**5**, **6**), antimicrobial (**7**, **8**) activities. There were also described derivatives of imidazo[4,5-*b*]pyridine with the potential uses in the treatment of diabetes and hyperlipidemia (**9**). Some chemical compounds which contain in their structure the imidazo[4,5-*b*]pyridine system inhibit neurodegeneration (**10**) and can be used in the treatment of neurodegenerative disorders e.g., multiple sclerosis, Alzheimer's disease or Parkinson's disease. Among

compounds of this class, antagonists of angiotensin II receptors that exhibit hypotensive activity are also known (**11**). Some of them can be used in the treatment of heart diseases.

Recently published works, showed that chemical modification of various heterocyclic compounds containing azomethine bond – Schiff base (**12**, **13**) and aminomethyl group – Mannich base provides biological activity (**14**, **15**). Many studies have shown that Mannich bases possess potent biological activities: antibacterial (**16**, **17**), antiviral (**18**), anti-tumor (**19**, **20**) properties. They may be potential drugs in epilepsy treatment (**21**).

In our recently published papers, we have described synthesis and antiproliferative activity *in vitro* of imidazo[4,5-*b*]pyridine derivatives (**22** – **24**).

The aim of this work was to synthesize the new Mannich bases, 2-thioxo-imidazo[4,5-*b*]pyridine derivatives using selected pharmacophore – secondary amines: morpholine, piperidine, 2-methoxyphenylpiperazine, pyrimidin-2-yl-piperazine together with formaldehyde.

* Corresponding author: e-mail: anna.nowicka@umed.wroc.pl

Selected compounds of different chemical structures, were examined for their antiproliferative activity *in vitro* against the cells of human cancer cell lines and normal mouse fibroblasts.

EXPERIMENTAL

Chemistry

Melting points were measured with a Boethius melting point apparatus. The new products were analyzed using a Perkin Elmer 2400 analyzer. IR spectra (in KBr) were recorded with an IR 75 spectrophotometer, ¹H NMR spectra – on a Bruker AVANCE DRX 300 MHz using DMSO-d₆ as an internal standard. The course of reaction and the purity of products were checked by TLC (Kieselgel G, Merck) in diethyl ether : ethanol 5 : 1, v/v as eluent. The syntheses of 6-bromo- (5) and 2-thioxoimidazo[4,5-*b*]pyridine (4) have been presented in our previous paper (23).

General procedure for the synthesis of Mannich bases 7 – 12

A mixture of 0.01 mol of thioxo-1*H*,3*H*-imidazo[4,5-*b*]pyridine (4) or 6-halogen-2-thioxo-1*H*,3*H*-imidazo[4,5-*b*]pyridine (5, 6), 0.03 mol of formaldehyde and 0.03 mol of selected secondary amine: morpholine, piperidine, 2-methoxyphenylpiperazine, pyrimidin-2-yl-piperazine in absolute ethanol was stirred at room temperature for 5 h. The precipitate formed was filtrated off and crystallized from ethanol.

1,3-Di-(morpholinemethyl)-2-thioxoimidazo[4,5-*b*]pyridine (7)

Yield: 1.64 g (47%); white solid from ethanol; m.p. 213–214°C. IR (KBr, cm⁻¹): 2910, 2850 (-CH₂-), 1450 (N-CS-N), 1125 (CS); ¹H NMR (DMSO, δ, ppm): 8.24 (dd, 1H, *J* = 4.8 Hz, *J* = 1.0 Hz, H-5), 8.10 (dd, 1H, *J* = 1.0 Hz, *J* = 8.1 Hz, H-7), 7.30 (dd, 1H, *J* = 4.8 Hz, *J* = 8.1 Hz, H-6), 5.20 (s, 2H, -CH₂-) 5.10 (s, 2H, -CH₂-), 3.50 (m, 8H, -CH₂-O-CH₂-), 2.70 (m, 8H, -CH₂-N-CH₂-). MS (70 eV): *m/z* (%): 351 (M⁺ + 2, 28), 350 (M⁺ + 1, 100), 348 (M⁺ - 1, 15); Analysis: calcd. for C₁₆H₂₃N₅O₂S₂ (349.46) C, 54.99; H, 6.63; N, 20.04%; found: C, 54.56, H, 6.63; N, 19.92%.

6-Chloro-1,3-di(morpholinemethyl)-2-thioxoimidazo[4,5-*b*]pyridine (8)

Yield: 3.22 g (85%); white solid from ethanol; m.p. 220–222°C. IR (KBr, cm⁻¹): 2950, 2850 (-CH₂-), 1000 (arom.); ¹H NMR (DMSO, δ, ppm): 7.92 (d, 1H, H-5), 7.63 (d, 1H, H-7), 5.15 (d, 2H, -CH₂-),

5.06 (d, 2H, -CH₂-), 3.53 (m, 4H, -CH₂-O-CH₂-), 2.60 (m, 4H, -CH₂-N-CH₂-). MS (70 eV): *m/z* (%): 386 (M⁺ - 3, 48), 385 (M⁺ - 2, 36), 384 (M⁺ 100), 285 (8), 186 (10). Analysis: calcd. for C₁₆H₂₂N₅ClO₂S (383.90) C, 50.06; H, 5.78; N, 18.24%; found: C, 49.89; H, 5.97; N, 18.06%.

1,3-Di-(piperidinemethyl)-2-thioxoimidazo[4,5-*b*]pyridine (9)

Yield: 1.82 g (53%); white solid from ethanol; m.p. 170–172°C. IR (KBr, cm⁻¹): 2950 (CH₂), 1450 (N-CS-N), 1125 (CS); ¹H NMR (DMSO, δ, ppm): 8.16 (d, 1H, H-5), 7.75 (dd, 1H, *J* = 7.8 Hz, *J* = 1.2 Hz, H-7), 5.15 (s, 2H, -CH₂-), 5.02 (s, 2H, -CH₂-), 2.65 (m, 8H, -CH₂-NH-CH₂-), 1.32 (m, 12H, -CH₂-CH₂-CH₂-); Analysis: calcd. for C₁₈H₂₇N₅S (345.51) C, 62.57; H, 7.88; N, 20.27%; found: C, 62.94; H, 9.29; N, 20.32%.

1,3-Di-[4-(2-methoxyphenyl)piperazinemethyl]-2-thioxoimidazo[4,5-*b*]pyridine (10)

Yield 3.18 g (57%); white solid from ethanol; m.p. 185–187°C. IR (KBr, cm⁻¹): 2950 (-CH₂-), 2825 (-OCH₃), 1500, 1450 (-CH₂-), 1175, 1060 (arom.); ¹H NMR (CDCl₃, δ, ppm): 8.20 (d, 1H, H-5), 7.60 (d, 1H, H-7), 7.10 (dd, 1H, H-6), 6.90 (m, 8H, arom.) 5.50 (s, 2H, -CH₂-), 5.20 (s, 2H, -CH₂-), 3.80 (s, 3H, -OCH₃), 3.70 (s, 3H, -OCH₃), 3.00 (m, 16H, 8× -CH₂-). Analysis: calcd. for C₃₀H₃₇N₇O₂S (559.73) C, 64.38; H, 6.66; N, 17.52%; found: C, 63.91; H, 6.64; N, 17.64%.

6-Chloro-1,3-di-[4-(2-methoxyphenyl)piperazinemethyl]-2-thioxoimidazo[4,5-*b*]pyridine (11)

Yield 4.93 g (83%); white solid from ethanol; m.p. 220–222°C. IR (KBr, cm⁻¹): 2940, 2880 (-CH₂-), 2840 (-OCH₃), 1450, 1160 (N-CS-N), 1010, 880 (-CH₂-), 750 (arom.); ¹H NMR (DMSO, δ, ppm): 8.19 (d, 1H, H-5), 7.58 (d, 1H, H-7), 7.01 (m, 8H, Ar-H), 5.45 (s, 2H, -CH₂-), 5.14 (s, 2H, -CH₂-), 3.85 (s, 3H, -OCH₃), 3.80 (s, 3H, -OCH₃), 3.06 (m, 8H, 2× -CH₂-N-CH₂-) 2.53 (m, 8H, 2× -CH₂-N-CH₂-). Analysis: calcd. for C₃₀H₃₆N₇ClO₂S (594.17) C, 60.64; H, 6.11; N, 16.50%; found: C, 60.86; H, 6.03; N, 16.41%.

1,3-Di-[4-(pyrimidin-2-yl)piperazinemethyl]-2-thioxoimidazo[4,5-*b*]pyridine (12)

1-(2-Pyrimidyl)piperazine hydrochloride (2.4 g, 0.01 mol) and 4.2 mL (0.03 mol) triethylamine in 30 mL ethanol were stirred at room temperature for 0.5 h. Next, 1.5 g (0.01 mol) of compound 2 and 2.5 mL (0.03 mol) of formaldehyde were added. A mixture was stirred at room temperature. After the com-

pletion of reaction, the solvent was evaporated and water (50 mL) was added to the dry residue. The precipitate formed was filtered off, dried decolorized with charcoal and crystallized from ethanol.

Yield 1.95 g (56%); white solid from ethanol; m.p. 165–167°C. IR (KBr, cm^{-1}): 2975 ($-\text{CH}_2-$), 1550 ($-\text{CH}_2-$), 1230, 1175 (arom.). ^1H NMR (DMSO, δ , ppm): 8.30 (m, 5H, H-5 + arom.), 7.90 (dd, 1H, $J = 1.80$ Hz, $J = 8.10$ Hz, H-7) 7.3 (dd, 1H, $J = 5.10$ Hz, $J = 8.10$ Hz, H-6) 6.50 (m, 2H, arom.) 5.30 (s, 2H, $-\text{CH}_2-$) 5.20 (s, 2H, $-\text{CH}_2-$) 3.70 (m, 8H, $4 \times -\text{CH}_2-$) 2.7 (m, 8H, $4 \times -\text{CH}_2-$). Analysis: calcd. for $\text{C}_{24}\text{H}_{29}\text{N}_{11}\text{S}$ (503.64) C, 57.24; H, 5.80; N, 30.59%; found: C, 57.59; H, 5.79; N, 30.82%.

General procedure for the synthesis of Schiff bases 13 – 15

A mixture of 0.01 mol of 2,3-diaminopyridine (**1**) or 5-bromo-2,3-diaminopyridine (**2**), 0.01 mol appropriate aldehyde: p-methoxy- or benzaldehyde and catalytic amount of triflate (trifluoromethanesulfonate indium) in 30 mL of ethanol was stirred and refluxed for 5 h. The precipitate formed was filtered off and crystallized from ethanol.

2-Amino-3-(p-methoxybenzylideneamino)pyridine (**13**)

Yield: 2.06 g (91%); yellow solid from ethanol; m.p. 128–130°C. IR (KBr, cm^{-1}): 3460, 3400 (NH_2), 2920 ($-\text{CH}-$), 2850 ($-\text{OCH}_3$), 1640 ($\text{CH}=\text{N}$, chain), 1605 ($\text{CH}=\text{N}$, ring), 1020, 850 (arom.); ^1H NMR (DMSO, δ , ppm): 8.56 (s, 1H, $-\text{CH}=\text{N}-$), 7.95 (d, 2H, Ar-H), 7.82 (d, 1H, $J = 1.5$ Hz, $J = 4.8$ Hz, H-6), 7.34 (d, 1H, $J = 1.5$ Hz, $J = 7.5$ Hz, H-4), 7.05 (d, 2H, Ar-H), 6.56 (dd, 1H, $J = 4.8$ Hz, $J = 7.5$ Hz, H-5), 5.88 (s, 2H, $-\text{NH}_2$), 3.83 (s, 3H, $-\text{OCH}_3$). Analysis: calcd. for $\text{C}_{13}\text{H}_{13}\text{N}_3\text{O}$ (227.27) C, 68.71; H, 5.77; N, 18.49%; found: C, 69.26; H, 5.84; N, 18.17%.

2-Amino-5-bromo-3-benzylideneaminopyridine (**14**)

Yield: 1.60 g (58%); yellow solid from ethanol; m.p. 126–128°C. IR (KBr, cm^{-1}): 4360, 3280 (NH_2), 1630 ($\text{CH}=\text{N}$, chain), 910, 780 (arom.). ^1H NMR (CDCl_3 , δ , ppm): 8.44 (s, 1H, $\text{CH}=\text{N}$), 7.93 (d, 1H, H-6), 7.81 (m, 2H, Ar-H), 7.41 (m, 3H, Ar-H), 7.29 (d, 1H, H-4), 5.10 (br, 2H, $-\text{NH}_2$). Analysis: calcd. for $\text{C}_{12}\text{H}_{10}\text{N}_3\text{Br}$ (276.14) C, 52.20; H, 3.65; N, 15.22%; found: C, 52.02; H, 3.52; N, 14.93%.

2-Amino-5-bromo-3-(p-methoxybenzylideneamino)pyridine (**15**)

Yield: 1.98 g (65%); yellow solid from ethanol; m.p. 110–113°C. IR (KBr, cm^{-1}): 3460,

3440 (NH_2), 1650 ($\text{N}=\text{CH}$, chain), 1175, 1125, 830 (arom.). ^1H NMR (CDCl_3 , δ , ppm): 8.41 (s, 1H, $\text{N}=\text{CH}$), 7.97 (d, H-6), 7.83 (m, 2H, Ar-H), 7.32 (d, 1H, H-4), 6.9 (m, Ar-H) (br, 2H, NH_2), 3.88 (s, 3H, $-\text{OCH}_3$). Analysis: calcd. for $\text{C}_{13}\text{H}_{12}\text{N}_3\text{BrO}$ (306.15) C, 51.00; H, 3.95; N, 13.72%; found: C, 51.36; H, 3.81; N, 13.52%.

Synthesis of 2-amino-5-chloro-3-(4-fluorobenzylidene)aminopyridine (**16**) and 6-chloro-2-(4-fluorophenyl)-3H-imidazo[4,5-*b*]pyridine (**17**)

A mixture of 5-chloro-2,3-diaminopyridine (**3**) 7.2 g (0.05 mol), 4-fluorobenzaldehyde 5.3 mL (0.05 mol) and catalytic amount of triflate in 30 mL absolute ethanol was refluxed for 5 h. After cooling, the solid of compound **16** was filtered off, the filtrate was evaporated and resulting residue was crystallized to obtain compound **17**.

2-Amino-5-chloro-3-(4-fluorobenzylidene) aminopyridine (**16**)

Yield: 1.99 g (80%); yellow solid from ethanol; m.p. 150–153°C. IR (KBr, cm^{-1}): 3300, 3150 (NH_2), 1660 ($\text{N}=\text{CH}$, chain), 1605 ($\text{N}=\text{CH}$, ring), 1175, 1150 (arom.). ^1H NMR (DMSO, δ , ppm): 8.74 (s, 1H, $-\text{N}=\text{CH}-$), 8.11 (m, 2H, H-6, Ar-H), 7.84 (d, 1H, Ar-H), 7.54 (d, 1H, Ar-H), 7.39 (m, 2H, H-4 + Ar-H), 6.22 (s, 2H, $-\text{NH}_2$). Analysis: calcd. for $\text{C}_{12}\text{H}_9\text{N}_3\text{ClF}$ (249.67) C, 56.73; H, 3.63; N, 16.83%; found: C, 57.71; H, 3.53; N, 16.42%.

6-Chloro-2-(4-fluorophenyl)-3H-imidazo[4,5-*b*]pyridine (**17**)

Yield: 0.37 g (15%); beige solid from ethanol; m.p. 347–348°C. IR (KBr, cm^{-1}): 3450, 1625 (NH), 1110, 950 (arom.). ^1H NMR (DMSO, δ , ppm): 13.65 (br, 1H, $-\text{NH}$), 8.32 (m, 4H, H-5 + Ar-H), 7.43 (m, 2H, H-6 + Ar-H). Analysis: calcd. for $\text{C}_{12}\text{H}_7\text{N}_3\text{ClF}$ (247.66) C, 58.20; H, 3.85; N, 16.97%; found: C, 58.09; H, 3.79; N, 16.82%.

General procedure for the synthesis of compounds 18 – 20

Sodium borohydride (0.01 mol) was added to the solution of Schiff base **4**, **5** or **6** (0.01 mol) in ethanol (50 mL). The reaction mixture was stirred and refluxed for ca. 8–10 h. The solvent was evaporated and water (150 mL) was added. The aqueous solution was left for 24 h. The precipitate formed was filtered off, dried, decolorized with charcoal and crystallized from ethanol.

2-Amino-3-(p-methoxybenzylamino)pyridine (**18**)

Yield: 1.12 g (49%); beige solid from ethanol; m.p. 105–106°C. IR (KBr, cm^{-1}): 3450, 3360 (NH_2), 3110 (NH), 2840 ($-\text{OCH}_3$), 1650, 1590 (NH), 1460 ($-\text{CH}_2-$), 1050, 805, 780 (arom.); ^1H NMR (DMSO, δ , ppm): 7.27 (m, 3H, Ar-H), 6.88 (m, 2H, Ar-H), 6.49 (d, 1H, Ar-H), 6.37 (dd, 1H, $J = 4.8$ Hz, $J = 7.5$ Hz, H-5), 5.49 (br, 2H, NH_2), 5.31 (t, 1H, NH), 4.20 (d, 2H, $-\text{CH}_2-$), 3.72 (s, 3H, $-\text{OCH}_3$). Analysis: calcd. for $\text{C}_{13}\text{H}_{15}\text{N}_3\text{O}$ (229.28) C, 68.10; H, 6.59; N, 18.33%; found: C, 67.81; H, 6.89; N, 18.80%.

2-Amino-3-benzylamino-5-bromopyridine (19)

Yield: 2.61 g (94%); beige solid from ethanol; m.p. 112–114°C. IR (KBr, cm^{-1}): 3380, 3310 (NH_2), 2920, 2850 (CH), 1650, 1580 (NH), 1480 (CH_2), 910, 850, 750 (arom.); ^1H NMR (DMSO, δ , ppm): 7.31 (m, 6H, Ar-H), 6.55 (s, 1H, Ar-H), 5.77 (m, 3H, $\text{NH}_2 + \text{NH}$), 4.30 (d, 2H, $-\text{CH}_2-$). Analysis: calcd. for $\text{C}_{12}\text{H}_{12}\text{N}_3\text{Br}$ (278.15) C, 51.82; H, 4.35; N, 15.11%; found: C, 52.20; H, 4.12; N, 14.98%.

2-Amino-5-chloro-3-(4-fluorobenzyl)aminopyridine (20)

Yield: 2.81 g (87%); beige solid from ethanol; m.p. 155–158°C. IR (KBr, cm^{-1}): 1400 (NH_2), 1170 (NH), 2270 ($-\text{CH}_2-$), 1650 (NH), 1490 ($-\text{CH}_2-$), 1150, 1100 (arom.). ^1H NMR (DMSO, δ , ppm): 7.42 (d, 1H, H-6), 7.38 (d, 1H, H-4), 7.20 (m, 3H, Ar-H), 6.46 (d, 1H, Ar-H), 5.77 (m, 3H, $-\text{NH} + -\text{NH}_2$), 4.29 (d, 2H, $-\text{CH}_2-$). Analysis: calcd. for $\text{C}_{12}\text{H}_{11}\text{N}_3\text{ClF}$ (251.65) C, 57.27; H, 4.41; N, 16.70%; found: C, 57.04; H, 4.22; N, 16.48%.

General procedure for the synthesis of compounds 5 and 21–23

The mixture of compound 3, 18, 19 or 20 (0.01 mol), CS_2 (0.01 mol) and NaOH 0.4 g (0.01 mol) in 30 mL of ethanol was stirred and refluxed for 8 h. After the completion of reaction, the solvent was evaporated and water (100 mL) was added to the dry residue. Aqueous solution of sodium 2-thioxoderivative was decolorized with charcoal. The filtrate was acidified to pH 4–5 with dilute hydrochloric acid. The precipitate formed was filtered off, dried, and crystallized from ethanol.

6-Chloro-2-thioxo-1H,3H-imidazo[4,5-*b*]pyridine (5)

Yield: 1.20 g (65%); beige solid; m.p. 345–348°C. IR (KBr, cm^{-1}): 3440, 1620 (NH), 1380 (HN-CS-NH), 1200 (C=S), 1080, 940 (arom.); ^1H NMR (DMSO, δ , ppm): 13.30 (br, 1H, NH), 12.91 (br, 1H, NH), 8.08 (d, 1H, H-5), 7.55 (dd, 1H, H-7). Analysis: calcd. for $\text{C}_6\text{H}_4\text{N}_3\text{ClS}$ (185.63) C, 38.82;

H, 2.17; N, 22.64%; found: C, 38.53; H, 2.36; N, 22.85%.

1-(*p*-Methoxybenzyl)-2-thioxo-3H-imidazo[4,5-*b*]pyridine (21)

Yield: 2.54 g (94%); beige solid from ethanol; m.p. 145–147°C. IR (KBr, cm^{-1}): 3350 (NH), 2925 ($-\text{CH}_2-$), 2850 ($-\text{OCH}_3$), 1650, 1560 (NH), 1425, 1350 (N-CS-N), 1025, 780 (arom.); ^1H NMR (DMSO, δ , ppm): 13.46 (br, 1H, NH), 8.13 (dd, 1H, $J = 1.2$ Hz, $J = 5.1$ Hz, H-5), 7.63 (dd, 1H, $J = 1.2$ Hz, $J = 8.1$ Hz, H-7), 7.36 (m, 2H, Ar-H), 7.28 (m, 2H, Ar-H), 7.14 (dd, 1H, $J = 5.1$ Hz, $J = 8.1$ Hz, H-6), 5.44 (s, 2H, $-\text{CH}_2-$), 3.71 (s, 3H, $-\text{OCH}_3$). Analysis: calcd. for $\text{C}_{14}\text{H}_{13}\text{N}_3\text{OS}$ (271.33) C, 61.87; H, 4.83; N, 15.49%; found: C, 62.15; H, 5.09; N, 15.17%.

1-Benzyl-6-bromo-2-thioxo-3H-imidazo[4,5-*b*]pyridine (22)

Yield: 2.52 g (79%); solid from ethanol; m.p. 191–194°C. IR (KBr, cm^{-1}): 3280 (NH), 2880 ($-\text{CH}_2-$), 1675, 1560 (NH), 1050 (C=S), 810, 720, 700 (arom.); ^1H NMR (DMSO, δ , ppm): 7.48 (d, 1H, Ar-H), 7.33 (m, 5H, Ar-H), 6.82 (d, 1H, Ar-H), 4.41 (s, 2H, $-\text{CH}_2-$). Analysis: calcd. for $\text{C}_{13}\text{H}_{10}\text{N}_3\text{BrS}$ (320.21) C, 48.76; H, 3.15; N, 13.12%; found: C, 48.51; H, 3.31; N, 13.50%.

6-Chloro-1-(4-fluorobenzyl)-3H-2-thioxoimidazo[4,5-*b*]pyridine (23)

Yield: 2.05 g (83%); solid from ethanol; m.p. 260–263°C. IR (KBr, cm^{-1}): 2850 ($-\text{CH}_2-$), 1605 (NH), 1480 (N-CS-N), 1325 (NH), 1240, 910, 880 (arom.); ^1H NMR (DMSO, δ , ppm): 13.72 (br, 1H, NH), 7.66 (m, 6H, H-5 + H-7 + Ar-H), 5.47 (s, 2H, $-\text{CH}_2-$). Analysis: calcd. for $\text{C}_{13}\text{H}_9\text{N}_3\text{ClFS}$ (247.66) C, 53.16; H, 3.09; N, 14.30%; found: C, 53.37; H, 2.87; N, 13.95%.

General procedure for the synthesis of Mannich bases 24–30

A mixture of (0.01 mol) of 6-halogeno-2-thioxo-1H,3H-imidazo[4,5-*b*]pyridine (21–23), 0.03 mol) of formaldehyde and (0.03 mol) of selected secondary amine: morpholine, piperidine, 2-methoxyphenylpiperazine or pyrimidin-2-yl-piperazine in absolute ethanol was stirred at room temperature for 5 h. The precipitate formed was filtered off and crystallized from ethanol.

6-Chloro-1-(4-fluorobenzyl)-3-[4-(2-methoxyphenylene)piperazinemethyl]-2-thioxoimidazo[4,5-*b*]pyridine (24)

Yield: 1.82 g (75%); white solid from ethanol; m.p. 177–180°C. IR (KBr, cm^{-1}): 2950 (CH_2), 2880

(OCH₃), 2850 (CH₂), 1450, 1160 (N-CS-N), 1010, 870 (-CH₂-); ¹H NMR (DMSO, δ, ppm): 8.17 (d, 1H, H-5), 7.16 (m, 9H, H-7 + Ar-H), 5.52 (s, 2H, CH₂), 5.50 (s, 2H, -CH₂-), 3.82 (s, 3H, -OCH₃), 3.09 (t, 4× -CH₂-). Analysis: calcd. for C₂₅H₂₅N₅ClFOS (498.01) C, 60.29; H, 5.06; N, 14.06%; found: C, 60.47; H, 5.23; N, 13.97%.

1-(p-Methoxybenzyl)-3-[4-(2-methoxyphenyl)piperazinemethyl]-2-thioxoimidazo[4,5-*b*]pyridine (25)

Yield: 3.13 g (66%); white solid from ethanol; m.p. 184–186°C; IR (KBr, cm⁻¹): 3080, 2930, 1500 (-CH₂-), 2825 (-OCH₃), 1300 (N=), 1150 (C=S), 1000, 800, 750 (arom.); ¹H NMR (DMSO, δ, ppm): 8.25 (d, 1H, H-5), 7.75 (d, 1H, H-7), 7.39 (d, 1H, Ar-H), 7.25 (dd, 1H, H-6), 6.88 (m, 7H, Ar-H), 5.55 (s, 2H, -CH₂-), 5.33 (s, 2H, -CH₂-), 3.70 (s, 6H, 2× -OCH₃), 2.90 (m, 8H, 4× -CH₂-). Analysis: calcd. for C₂₆H₂₉N₅O₂S (475.67): C, 65.65; H, 6.16; N, 14.73%; found: C, 65.66; H, 6.08; N, 14.37%.

1-(p-Methoxybenzyl)-3-[4-(pyrimidin-2-yl)piperazinemethyl]-2-thioxoimidazo[4,5-*b*]pyridine (26)

Yield: 1.40 g (63%); white solid from ethanol; m.p. 167–169°C; IR (KBr, cm⁻¹): 2925 (-CH₂-), 2850 (-OCH₃), 1590 (CH₂), 1440, 1300 (N-CS-N), 1250 (C=S), 990, 805, 780 (arom.); ¹H NMR (DMSO, δ, ppm): 8.29 (d, 2H, Ar-H), 8.23 (d, 1H, H-5), 7.72 (d, 1H, H-7), 7.34 (d, 2H, Ar-H), 7.22 (dd, 1H, H-6), 6.85 (m, 2H, Ar-H), 6.57 (m, 1H, Ar-H), 5.51 (s, 2H, -CH₂), 5.30 (s, 2H, -CH₂), 3.69 (m, 8H, 4× -CH₂), 2.80 (s, 3H, -OCH₃). Analysis: calcd. for C₂₃H₂₅N₇O₂S (447.55) C, 61.72; H, 5.63; N, 21.91%; found: C, 61.58; H, 5.75; N, 21.72%.

1-Benzyl-6-bromo-3-morpholinemethyl-2-thioxoimidazo[4,5-*b*]pyridine (27)

Yield: 1.59 g (38%); white solid from ethanol; m.p. 154–156°C; IR (KBr, cm⁻¹): 2940, 1480 (-CH₂-), 1430 (N-CS-N), 1205 (C=S). ¹H NMR (DMSO, δ, ppm): 7.79 (d, 1H, Ar-H), 7.46 (d, 1H, H-5), 7.33 (m, 4H, Ar-H), 6.96 (d, 1H, H-7), 5.72 (s, 2H, CH₂), 4.99 (s, 2H, CH₂), 4.41 (m, 4H, CH₂-O-CH₂), 3.97 (m, 4H, CH₂-N-CH₂); Analysis: calcd. for C₁₈H₁₉N₄BrOS (419.34) C, 51.56; H, 4.57; N, 13.36%; found: C, 51.19; H, 4.99; N, 13.35%.

1-(p-Methoxybenzyl)-3-morpholinemethyl-2-thioxoimidazo[4,5-*b*]pyridine (28)

Yield: 1.40 g (38%); white solid from ethanol; m.p. 134–137°C; IR (KBr, cm⁻¹): 2930 (-CH₂-), 2850 (-OCH₃), 1430, 1330 (N-CS-N), 1250 (C=S), 1000,

810, 750 (arom.). ¹H NMR (DMSO, δ, ppm): 8.22 (d, 1H, H-5), 7.73 (d, 1H, H-7), 7.36 (d, 2H, Ar-H), 7.24 (dd, 1H, *J* = 5.1 Hz, *J* = 7.8 Hz, H-6), 6.88 (d, 2H, Ar-H), 5.48 (s, 2H, -CH₂), 5.24 (s, 2H, -CH₂), 3.70 (m, 4H, CH₂-O-CH₂), 3.53 (m, 4H, -CH₂-N-CH₂-), 2.74 (s, 3H, -OCH₃). Analysis: calcd. for C₁₉H₂₂N₄O₂S (370.47) C, 61.60; H, 5.99; N, 15.12%; found: C, 62.01, H, 6.02; N, 14.72%.

6-Chloro-1-(4-fluorobenzyl)-3-morpholinemethyl-2-thioxoimidazo[4,5-*b*]pyridine (29)

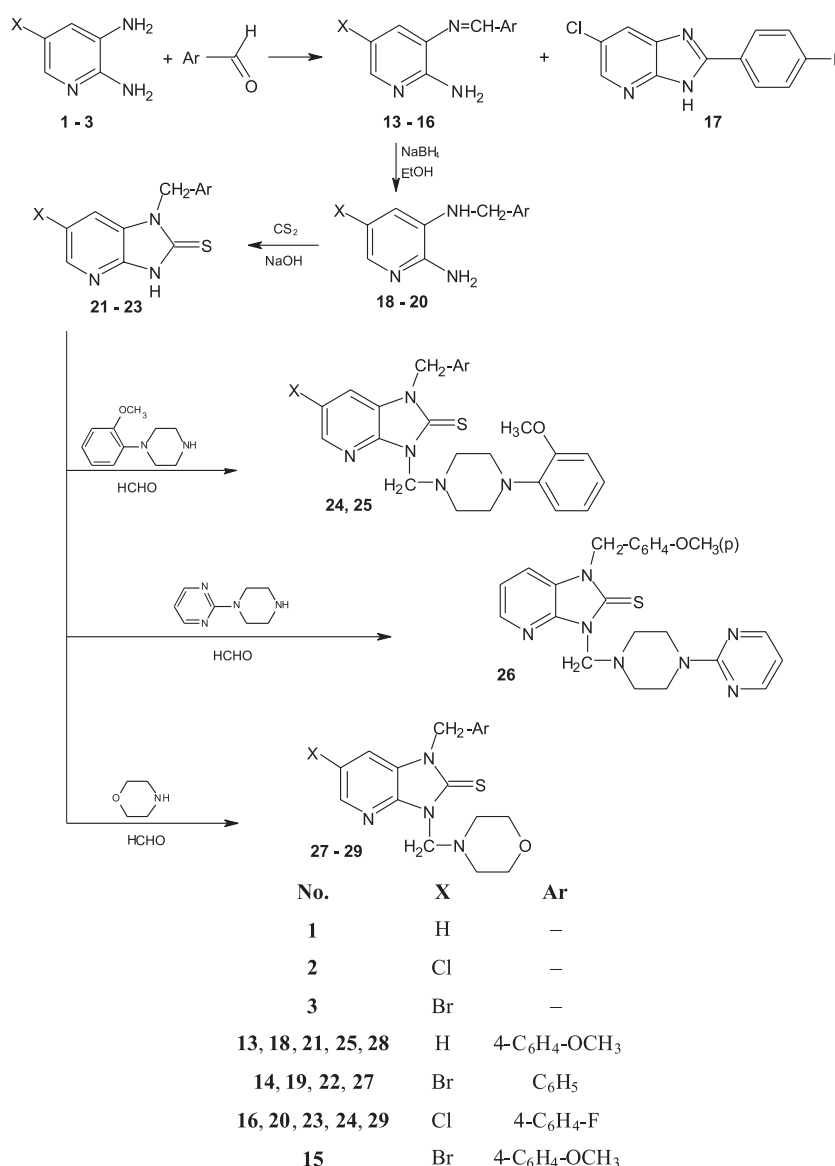
Yield: 2.66 g (70%); beige solid from ethanol; m.p. 169–172°C. IR (KBr, cm⁻¹): 2950, 2850 (-CH₂-), 1460, 1160 (N-CS-N), 1000, 750 (-CH₂-); ¹H NMR (DMSO, δ, ppm): 8.16 (d, 1H, H-5), 7.21 (m, 5H, H-7 + Ar-H), 5.52 (s, 2H, -CH₂), 5.36 (s, 2H, -CH₂), 3.69 (t, 4H, -CH₂-O-CH₂-), 2.88 (t, 4H, -CH₂-N-CH₂-). Analysis: calc. for C₁₇H₁₈N₄ClFOS (380.87). C, 53.61; H, 4.78; N, 14.71%; found: C, 54.03; H, 4.53; N, 14.50%.

Computational methods

Potential energy surfaces have been scanned, and all minima have been optimized to find all possible conformers of the molecules. All structures have been obtained using a relaxed dihedral angle scan to generate a potential energy surface. Points were then optimized using density functional theory's (25) B3LYP (26, 27) hybrid functional with 6-31G and 6-31G(d,p) basis sets. Second order Møller Plesset (MP2) (28) calculations have been performed to calibrate all structures. The thermodynamic parameters of all compounds have been calculated using statistical mechanics expressions. All calculations have been conducted using Gaussian 09 (29).

***In vitro* antiproliferative assay**

Antiproliferative tests were performed on human cancer cell lines: A549 (lung), MCF-7 (breast), leukemia MV4-11 and mouse embryonic fibroblast BALB/3T3 according to standard procedure (30). All cell lines were obtained from American Type Culture Collection (Rockville, Maryland, USA) and have been maintained in culture or frozen in thaw Cell Culture Collection of the Institute of Immunology and Experimental Therapy, Polish Academy of Sciences (IET, PAS, Wrocław, Poland). The A549 cells were cultured in a mixture of Opti-MEM and RPMI 1640 medium (1 : 1, both from Gibco, Scotland, UK) supplemented with 2 mM L-glutamine and 5% fetal bovine serum. MCF-7 cells were cultured in Eagle medium (IET, Wrocław, Poland), supplemented

Scheme 2. Synthesis of Mannich bases – 1-benzyl-2-thioxoimidazo[4,5-*b*]pyridine derivatives

compound was tested at every concentration in triplicate in a single experiment, which was repeated 3 times. The activity of tested compounds was compared to the activity of cisplatin used as a reference agent.

RESULTS AND DISCUSSION

Chemistry

In this paper, Mannich bases – imidazo[4,5-*b*]pyridine derivatives were prepared according to synthesis presented in Schemes 1 and 2.

In the first step of synthesis, 2-thioxo- (4) (23), 6-chloro- (5) or 6-bromo-2-thioxoimidazo[4,5-*b*]pyridine (6) (23) were obtained from 2,3-diaminopyridine derivatives with CS₂/NaOH in ethanol. Imidazo[4,5-*b*]pyridine derivatives 4 – 6 were substrates in Mannich condensation with triple excess of selected, secondary amines: morpholine, piperidine, 1-(2-methoxyphenyl)piperazine, 1-(2-pyridyl)piperazine and formaldehyde. The reaction was carried out in ethanol at room temperature (Scheme 1).

In all reactions single products were obtained. In this reaction products of various chemical struc-

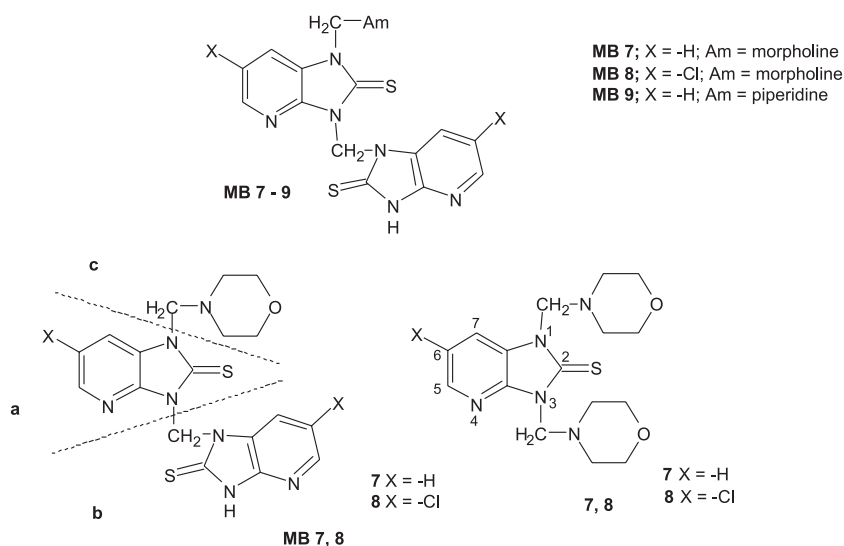


Figure 1. Exemplary structures of Mannich bases **MB 7–9** for calculated binding energies

Table 1. The antiproliferative activity of screened compounds against MV4-11 human biphenotypic B myelomonocytic leukemia cells.

Compound	IC ₅₀ [µg/mL]
7	19.90 ± 4.27
8	16.79 ± 12.37
9	19.66 ± 12.69
10	22.06 ± 5.59
12	12.87 ± 5.22
13	22.80 ± 6.38
14	3.98 ± 1.73
15	1.82 ± 0.84
16	7.41 ± 2.01
17	5.89 ± 0.17
22	3.61 ± 0.61
25	14.69 ± 6.68
27	2.82 ± 0.61
28	22.86 ± 7.65
29	8.60 ± 2.45
cisplatin	0.22 ± 0.07

tures could be obtained e.g., compound **MB**, 3-aminomethyl- **MB I** or 1,3-disubstituted aminomethyl compounds **7 – 12**.

Elementary analyses and MS, IR and ¹H NMR spectra showed that 1,3-disubstituted aminomethyl

products **7 – 12** were obtained. Also quantum-chemical calculations at Density Functional Theory level have confirmed such reaction path (Fig. 1).

IR spectra of Mannich base **7** contain at 2910 and 2850 cm⁻¹ bands characteristic for -CH₂- group, instead of secondary NH groups. In ¹H NMR spectra of compound **7** are two two protons singlets at δ = 5.10 and δ = 5.20 ppm, ascribed for methylene groups in 1 and 3 position. Protons characteristic for morpholine: -CH₂-N-CH₂- and -CH₂-O-CH₂- were observed as 8 protons two multiplets at δ = 2.70 and δ = 3.50 ppm, respectively. Additionally, number of signals for the pyridine protons in the ¹H NMR spectra of all Mannich bases is in good agreement with their structures.

The another route of synthesis was reaction of 5-substituted 2,3-diaminopyridines **1 – 3** with selected aromatic aldehydes: 4-methoxy-, 4-fluoro- and benzaldehyde (Scheme 2). The reactions were carried out in boiling ethanol with the presence of catalytic amounts of triflate. IR spectra of Schiff bases contain, among other absorption bands, those in the range of ~ 1650 cm⁻¹ characteristic for the chain groups C=N. The presence of azamethine bond CH=N protons was confirmed by ¹H NMR spectra of all imines, in which one-proton singlets in the range δ = 8.41–8.74 ppm were observed. In the reaction of 5-chloro-2,3-diaminopyridine (**2**) with 4-fluorobenzaldehyde, together with Schiff base **16** cyclic product 6-chloro-2-(4-fluorophenyl)-3*H*-imidazo[4,5-*b*]pyridine (**17**) was obtained.

Table 2. The antiproliferative activity of selected compounds against human breast (MCF-7) and lung (A549) cancer and normal mouse fibroblasts (BALB/3T3) cell lines.

Compound	IC ₅₀ [µg/mL]/cell line		
	A549	MCF-7	BALB/3T3
14	30.67 ± 1.94	30.86 ± 0.96	73.94 ± 3.83
15	7.96 ± 1.39	10.44 ± 1.65	91.66 ± 4.22
22	11.57 ± 1.20	12.56 ± 4.78	30.41 ± 3.88
27	11.24 ± 4.03	15.80 ± 7.38	22.88 ± 7.16
cisplatin	2.47 ± 0.97	1.71 ± 1.21	1.97 ± 1.20

In the next step of synthesis, the azamethine bond in obtained Schiff bases **13**, **14** and **16** have been subjected to selective reduction using NaBH₄ in boiling ethanol. The extent of the hydrogenation has been monitored by TLC and decoloration of yellow solution. In ¹H NMR spectra of 2-amino-3-benzylaminopyridine derivatives **18** – **20** the absence of one-proton singlets at $\delta = 8.41$ – 8.74 ppm was observed, whereas, two-proton doublets at $\delta = 4.20$ – 4.30 ppm ascribed to NH-CH₂ protons were present. Triplet or multiplet signal at $\delta \sim 5.50$ ppm was ascribed to NH-CH₂ protons.

1-Benzyl-2-thioxoimidazo[4,5-*b*]pyridine derivatives **21** – **23** were obtained in cyclization of compounds **18** – **20**, using CS₂ and NaOH in ethanol.

The synthesized derivatives **21** – **23** were used as a substrates for the Mannich condensation with selected pharmacophore, secondary amines: 1-(2-methoxyphenyl)piperazine, 1-(2-pyridyl)piperazine and morpholine and formaldehyde. The reactions were carried in ethanol at room temperature. Mannich bases, 1-benzyl-3-aminomethyl-2-thioxoimidazo[4,5-*b*]pyridine derivatives, were obtained. The product structures have been confirmed by elemental analysis and IR, ¹H-NMR and MS spectra. The signals corresponding to aromatic protons were observed in the range of $\delta \sim 6.80$ – 8.20 ppm, respectively.

Twenty four new compounds **5**, **7** – **29** of various chemical structures assigned for antiproliferative *in vitro* studies were obtained from the syntheses described here. These derivatives may also be used as starting materials for further syntheses.

Quantum-chemical calculations

All given structures **7** – **12** have been optimized to get the most stable low energy conformers. We have studied Molecular Electrostatic Potential

Surfaces (MEPS) of molecules to find the reactive area of moieties. The most active area of structure **7** and **8** is located on N-3 atom and H-6 or Cl-6, respectively (Fig. 1). Adding amine moiety moves the most active region to the N-1 atom. In order to examine the affinity of the individual reactions, binding energies of the various parts of moieties were calculated. Binding energy for moieties **MB 7**, **8** consisting of part **a–b** is positive. Binding energy for compounds **MB 7**, **8**, consisting of part **a–c** is negative. The analogical results have been obtained for all synthesized structures **7** – **12**. The given results have shown that the structure of 1,3-disubstituted aminomethyl compounds **7–12** is more preferable than that of compounds **MB 7** – **9**.

In vitro antiproliferative assay

The compounds were screened for their antiproliferative activity using cells of MV4-11 human leukemia (Table 1). Comparing to cisplatin, the activity of tested compounds was lower, however, we selected four of them **14**, **15**, **22**, **27**, with IC₅₀ value ranged between 1.82–3.98 µg/mL for further studies on the cells of breast and lung cancer, as well as on normal mouse fibroblasts to assess its selectivity towards cancer cells. The antiproliferative activity of selected compounds was remarkably lower against lung and breast cancer cells, comparing results obtained against MV4-11 cells. Interestingly, their activity towards mouse fibroblasts was much more lower, suggesting low toxicity (Table 2). Particularly, the most active on all cancer cells compound **15** was 9–50 times less cytotoxic towards normal fibroblasts than cancer cells.

CONCLUSIONS

Twenty four new compounds of different chemical structures: Schiff bases **13** – **16** and reduction of azamethine bond products **18** – **20**, 2-thioxo-

imidazo[4,5-*b*]pyridine derivatives and Mannich bases **7** – **12** and **24** – **29** were obtained from the syntheses described here. Their structures were confirmed by elemental analysis, IR, ¹H NMR and MS spectra. Selected new compounds **7** – **10**, **12** – **17**, **22**, **25**, **27** – **29** were screened for their antiproliferative activity *in vitro*. Four of them: 2-amino-5-bromo-3-benzylideneaminopyridine (**14**), 2-amino-5-bromo-3-(*p*-methoxybenzylideneamino)pyridine (**15**), 1-benzyl-6-bromo-2-thioxo-3H-imidazo[4,5-*b*]pyridine (**22**), 1-benzyl-6-bromo-3-morpholinemethyl-2-thioxoimidazo[4,5-*b*]pyridine (**27**) with high antiproliferative activity were screened on human breast (MCF-7) and lung (A549) cancer and normal mouse fibroblasts (BALB/3T3) cell lines. The most active and in parallel selective towards cancer cells was 2-amino-5-bromo-3-(*p*-methoxybenzylideneamino)pyridine (**15**).

Acknowledgment

The authors thank the Foundation of Lower Silesian Pharmacy (Fundacja Farmacji Dolnośląskiej) for financial support for publication charges.

REFERENCES

- Janssens M.M.L., Howarth P.H.: *Clin. Rev. Allergy* 11, 111 (1993).
- Barracough P., Black J.W., Cambridge D., Collard D., Firmin D., Gerskowitch V.P., Glen R.C. et al.: *J. Med. Chem.* 33, 2231 (1990).
- Matsuishi N., Takeda H., Iizumi K., Murakami K., Hisamitsu A.: patent US 4808596 (1989).
- Zhang L., Brodney M.A., Candler J., Doran A.C., Duplantier A.J., Efremov I.V., Evrard E. et al.: *J. Med. Chem.* 54, 1724 (2011).
- Bavetsias V., Sun C., Bouloc N., Reynisson J., Workman P., Linardopoulos S., MacDonald E.: *Bioorg. Med. Chem. Lett.* 17, 6567 (2007).
- Gillerman I., Fischer B.: *J. Med. Chem.* 54, 107 (2011).
- Kim D., Wang L., Hale J.J., Lynch C.L., Budhu R.J., Maccoss M., Mills S.G. et al.: *Bioorg. Med. Chem. Lett.* 15, 2129 (2005).
- Cundy D.J., Holan G., Otaegui M., Simpson G.W.: *Bioorg. Med. Chem. Lett.* 7, 669 (1997).
- Oguchi M., Wada K., Honma H., Tanaka A., Kaneko T., Sakakibara S., Ohsumi J. et al.: *J. Med. Chem.* 43, 3052 (2000).
- McGiunness B.F., Cole A.G., Dong G., Brescia M.R., Shao Y., Henderson I., Wines P.G., Quadros E.: *Bioorg. Med. Chem. Lett.* 20, 6845 (2010).
- Chakravarty P.K., Naylor E.M., Chen A., Chen A., Chang R.S., Chen T.B., Faust K.A. et al.: *J. Med. Chem.* 37, 4068 (1994).
- Przybylski P., Huczyński A., Pyta K., Brzeziński B., Bartl F.: *Curr. Org. Chem.* 13, 124 (2009).
- Makawana J.A., Sangani C.B., Teraiya S.B., Zhu H.L.: *Med. Chem. Res.* 23, 471 (2014).
- Murthy Y.L.N., Govindh B., Diwakar B.S., Nagalakshmi K., Rao K.V.R.: *Med. Chem. Res.* 21, 3104 (2012).
- Hu G., Wang G., Duan N., Wen X., Cao T., Xie S., Huang W.: *Acta Pharm. Sinica B* 2, 312 (2012).
- Sriram D., Bal T.R., Yogeewari P.: *Med. Chem. Res.* 14, 211 (2005).
- Malhotra M., Sharma S., Deep A.: *Med. Chem. Res.* 21, 1237 (2012).
- Asundaria S.T., Pannecouque C., De Clercq E., Supuran C.T., Patel K.C.: *Med. Chem. Res.* 22, 5752 (2013).
- Sunil D., Isloor A.M., Shetty P., Chandrakantha B., Satyamoorthy K.: *Med. Chem. Res.* 20, 1024 (2011).
- Tian J., Li D., Zhai F., Wang X., Li R.: *Med. Chem. Res.* 19, 1162 (2010).
- Obniska J., Rzepka S., Kamiński K.: *Bioorg. Med. Chem.* 20, 4872 (2012).
- Liszkiewicz H., Kowalska M.W., Nawrocka W., Wójcicka A., Wietrzyk J., Nasulewicz A., Pełczyńska M., Opolski A.: *Phosphorus Sulfur Silicon Relat. Elem.* 178, 2725 (2003).
- Liszkiewicz H., Kowalska M.W., Wietrzyk J.: *Phosphorus Sulfur Silicon Relat. Elem.* 182, 199 (2007).
- Liszkiewicz H., Nawrocka W.P., Sztuba B., Wietrzyk J., Jaroszewicz J., Nasulewicz, A., Pełczyńska M.: *Acta Pol. Pharm. Drug Res.* 68, 349 (2011).
- Parr R.G., Yang W.: *Density Functional Theory of Atoms and Molecules*. Oxford University Press, New York 1989.
- Becke A.D.: *J. Chem. Phys.* 98, 5648 (1993).
- Lee C., Wang W.P., Parr R.G.: *Phys. Rev. B* 37, 785 (1988).
- Møller C., Plesset M.S.: *Phys. Rev.* 46, 618 (1943).
- Frisch M.J., Trucks G.W., Schlegel H.B., Scuseria G.E., Robb M.A., Cheeseman J.R., Scalmani G., Barone V., Mennucci B., Petersson G.A., Nakatsuji H., Caricato M., Li X., Hratchian H.P., Izmaylov A.F., Bloino J., Zheng G., Sonnenberg J.L., Hada M., Ehara M., Toyota K., Fukuda R., Hasegawa J., Ishida M.,

- Nakajima T., Honda Y., Kitao O., Nakai H., Vreven T., Montgomery J.A. Jr., Peralta J.E., Ogliaro F., Bearpark M., Heyd J.J., Brothers E., Kudin K.N., Staroverov V.N., Kobayashi R., Normand J., Raghavachari K., Rendell A., Burant J.C., Iyengar S. S., Tomasi J., Cossi M., Rega N., Millam M.J., Klene M., Knox J.E., Cross J.B., Bakken V., Adamo C., Jaramillo J., Gomperts R., Stratmann R.E., Yazyev O., Austin A.J., Cammi R., Pomelli C., Ochterski J.W., Martin R.L., Morokuma K., Zakrzewski V.G., Voth G.A., Salvador P., Dannenberg J.J., Dapprich S., Daniels A.D., Farkas Ö., Foresman J.B., Ortiz J.V., Cioslowski J., Fox D.J.: "Gaussian 2009." Gaussian, Inc., Wallingford CT 2009.
30. Wietrzyk J., Chodynski M., Fitak H., Wojdat E., Kutner A., Opolski A.: *Anticancer Drugs* 18, 447 (2007).

Received: 2. 09. 2014

NATURAL DRUGS

EVALUATION OF ANTI-INFLAMMATORY, ANALGESIC AND ANTIPYRETIC ACTIVITIES OF *THYMUS SERPHYLLUM* LINN. IN MICE

ALAMGEER^{1*}, UZMA MAZHAR¹, MUHAMMAD NAVEED MUSHTAQ¹, HAFEEZ ULLAH KHAN¹, SAFIRAH MAHEEN¹, MUHAMMAD NASIR HAYAT MALIK¹, TASEER AHMAD¹, FOUZIA LATIF², NAZIA TABASSUM², ABDUL QAYYUM KHAN¹, HASEEB AHSAN¹, WASIM KHAN¹, IBRAHIM JAVED¹ and HAIDER ALI³

¹Faculty of Pharmacy, University of Sargodha, Sargodha, Pakistan

²Faculty of Pharmacy, the University of Lahore, Pakistan

³Faculty of Agriculture, University of Sargodha, Pakistan

Abstract: The present study was conducted to evaluate the analgesic, anti-inflammatory and antipyretic activities of *Thymus serphyllum* Linn. in mice. Anti-inflammatory activity was evaluated by carrageenan and egg albumin induced paw edema in mice, while analgesic activity was assessed using formalin induced paw licking and acetic acid induced abdominal writhing in mice. For determination of antipyretic activity, pyrexia was induced by subcutaneous injection of 20% yeast. All the extracts produced significant anti-inflammatory effect however, ether extract produced maximum effect 34% inhibition ($p < 0.001$) against carrageenan and 22% ($p < 0.01$) inhibition against egg albumin induced paw edema in mice at the end of 3 h. Ether extract produced prominent analgesic effect 77% ($p < 0.001$) inhibition in acetic acid induced abdominal writhing and 59% inhibition in formalin induced paw licking model in mice, respectively. Ether extract also demonstrated significant ($p < 0.001$) antipyretic activity against yeast induced pyrexia. The plant showed no sign of toxicity up to the dose of 2000 mg/kg in mice. This study supports the use of *Thymus serphyllum* in traditional medicine for inflammation accompanied by pain and fever.

Keywords: analgesic, anti-inflammatory, antipyretic, *Thymus serphyllum* Linn.

Inflammation is considered as a primary physiological defense mechanism and is associated with the protection of the body against burns, infections, toxic chemicals, allergens and other harmful stimuli. If the inflammation is left uncontrolled, it would act as an etiologic factor for a number of other chronic diseases (1). It involves a complex array of enzyme activation, mediator release, extravasation of fluid, cell migration, tissue breakdown and repair (2). Earlier, inflammation was considered as a single disease caused by disturbances of body fluids, however, in the modern medical science, inflammation is considered as a healthy process resulting from some disturbances or diseases (3). Currently, inflammatory conditions and accompanied pain and fever are managed by either narcotics e.g., opioids or non-narcotics e.g., salicylates and corticosteroids e.g., hydrocortisone. These synthetic drugs are associated with serious side effects (4). Moreover, these

conventional drugs are either too expensive or toxic and not commonly available to the rural folks that constitute the major populace of the globe. Therefore, the development of newer and more potent anti-inflammatory drugs with lesser side effects is necessary. Drugs of plant origin have been used since long time and have comparatively less adverse effects. It is therefore essential that efforts should be made to introduce new medicinal plants to develop cheaper drugs. Many plants had been used to ameliorate the inflammatory conditions and associated pain and fever on the basis of folklore claim. Purified natural compounds from plants can serve as a template for the synthesis of new generation anti-inflammatory drugs with low toxicity and higher therapeutic value (3). Many medicinal plants have been used in developing countries for the management of pain and inflammatory conditions. *Thymus serphyllum* Linn. is a widely growing herbal plant in

* Corresponding author: e-mail: alam_yuchi@yahoo.com

the northern hilly area, Gilgit-Baltistan. *Thymus serpyllum* is commonly used by local people for various purposes such as antiseptic, anthelmintic, carminative and expectorant (5). Its analgesic effect has been reported in Chinese literature. It has also been reported to have antipyretic properties (6). The present study was conducted to ascertain the traditional use of *Thymus serpyllum* for inflammation and associated pain and fever.

MATERIAL AND METHODS

Drugs and reagents

Carrageenan, fresh egg-albumin, formalin, acetic acid, Brewer's yeast, Tween-80 and aspirin.

Plant material

Aerial parts of *Thymus serpyllum* were used in this study. The plant was collected from the village Shikyote, District Gilgit, Gilgit-Baltistan, Pakistan during the month of July 2010. The plant was identified and authenticated by Dr. Sher Wali, Assistant Professor of Botany, Karakoram International University, Gilgit-Baltistan. A voucher specimen has been kept for future reference in the Herbarium of Faculty of Pharmacy, Department of Pharmacognosy with the number of TS-1150. It was shade dried and then, powdered using grinder.

Preparation of extracts

The powdered plant was extracted successively by method of cold maceration to prepare ether, ethanolic and aqueous extracts. For extraction with each solvent, the powder was soaked for 48 h with occasional shaking. It was passed through muslin cloth and then filtered through the filter paper. The extracts were dried with the help of rotary evaporator and lyophilized.

Animals used

Adult healthy mice of either sex weighing 25–30 g were used in the study. Animals were housed in the animal house of Faculty of Pharmacy, University of Sargodha under natural light and dark cycles at a temperature of $28 \pm 4^\circ\text{C}$, given a standard pellet diet and water *ad libitum*. Animals received human care. The study protocol was approved by the local Ethical Committee, Faculty of Pharmacy, University of Sargodha. All animals were treated according to the standard procedures guided by NIH (7).

Analgesic activity

Analgesic activity of ether, ethanolic and water extracts of *Thymus serpyllum* against acetic acid

induced writhing (abdominal constrictions and stretching of hind limbs) and formalin induced paw licking in mice was conducted according to methods described earlier with some modifications (8, 9). Briefly; after an overnight fasting, mice were divided into 5 groups of 5 mice each. Group I served as control and was treated with 2 mL/kg body weight of normal saline *i.p.* Group 2, 3 and 4 were given ether, aqueous and ethanolic extracts in a dose of 100 mg/kg *p.o.*, respectively. Group 5 was treated with standard drug, aspirin 100 mg/kg body weight (*i.p.*). After 30 min of treatment, the mice were injected *i.p.* with 0.2 mL of 3% acetic acid solution to induce writhing. The number of abdominal constrictions (writhing) and stretching with a jerk of the hind limb was counted between 5 and 15 min after acetic acid injection. The same procedure of grouping of mice was adopted in paw licking test, however, this time after 1 h of treatment with drugs, 20 μL of 2.5% formalin solution was injected subcutaneously under the surface of the left hind paw of each mice and responses were observed for 30 min, immediately after injecting formalin. The time spent by mice in licking the injected paw was noted and was indicative of pain.

Anti-inflammatory activity

Anti-inflammatory activity of ether, ethanolic and water extracts against carrageenan and egg-albumin induced paw edema in mice was evaluated according to the methods described earlier with some modifications (10).

Briefly; after an overnight fasting, mice were divided into 5 groups of 5 mice each. Group I served as control and was treated with normal saline 2 mL/kg *p.o.* Group 2, 3 and 4 were given ether, aqueous and ethanolic extracts of *Thymus serpyllum* 100 mg/kg *p.o.* respectively and Group 5 was treated with standard drug, aspirin 100 mg/kg *p.o.* The same group pattern was adopted for egg albumin induced inflammation. After 1 h of treatment, the inflammation in the hind paw was produced by injecting 0.1 mL of freshly prepared carrageenan suspension (1%) in normal saline and fresh egg-albumin into the sub planer-surface of the right hind paw. The linear circumference of the injected paw was measured at 0, 1, 2 and 3 h of the administration of carrageenan and egg-albumin, with the help of a vernier caliper. The increase in paw circumference at 1, 2 and 3 h after administration of carrageenan injection was adopted as the parameter for measurement of inflammation. The ability of the extracts to suppress the paw inflammation was expressed as a percent inhibition of

paw edema (11) and was calculated according to the following equation:

$$\text{Percentage of inhibition (\%)} = 100 \times (1 - x/y)$$

where x = mean increase in paw thickness of treated mice; y = mean increase in paw thickness of control mice.

Antipyretic activity

Antipyretic activity of various ether, water and ethanolic extracts of *Thymus serpyllum* against yeast induced pyrexia in mice was performed according to the methods described earlier with some modifications (12, 13).

Briefly; after an overnight fasting, mice were divided into 5 groups of 5 mice each. Pyrexia was induced by subcutaneous administration of 2

mL/100 g of 20% aqueous suspension of brewer's yeast. Group I served as a control group and was treated with normal saline 2 mL/kg *p.o.* Group 2, 3 and 4 were treated with ether, aqueous and ethanolic extracts of *Thymus serpyllum* 100 mg/kg *p.o.*, respectively, while group 5 was treated with standard drug, aspirin 100 mg/kg *p.o.* After 24 h of induction of pyrexia, rectal temperatures were noted. Then, the animals were treated as described earlier with control, standard and plant extracts. Rectal temperature of animals was taken at 30, 90 and 150 min after drug administration.

Acute toxicity

Acute toxicity was tested in mice of either sex; the animals received plant extract (ether, aqueous

Table 1. Effect of various extracts of *Thymus serpyllum* on writhing induced by acetic acid in mice.

Treatment	No. of writhings	Inhibition [%]
	Mean \pm SEM	
Control (2 mL/kg)	39.2 \pm 1.35	–
Ether extract (100 mg/kg)	16 \pm 0.7 ^d	59
Aqueous extract (100 mg/kg)	30.4 \pm 0.81 ^b	22
Ethanolic extract (100 mg/kg)	21.6 \pm 1 ^c	45
Aspirin (100 mg/kg)	17.2 \pm 0.8 ^d	57

Data are expressed as the mean \pm SEM. (p < 0.05) was considered as significant ^b = (p < 0.01), ^c = (p < 0.001) and ^d = (p < 0.0001), compared to control group. The means sharing the same letters are not significant to each other.

Table 2. Effect of various extracts of *Thymus serpyllum* on formalin induced paw licking in mice.

Treatment	No. of paw lickings	Inhibition [%]
	Mean \pm SEM	
Control (2 mL/kg)	324.6 \pm 10.4	–
Ether extract (100 mg/kg)	74.4 \pm 5.4 ^d	77
Aqueous extract (100 mg/kg)	121 \pm 6.66 ^c	63
Ethanolic extract (100 mg/kg)	182.8 \pm 7.34 ^b	44
Aspirin (100 mg/kg)	109.8 \pm 2.85 ^c	66

Data are expressed as the mean \pm SEM. (p < 0.05) was considered as significant ^b = (p < 0.01), ^c = (p < 0.001) and ^d = (p < 0.0001), compared to control group. The means sharing the same letters are not significant to each other.

and ethanolic) in doses of 500, 1000, 1500, 2000 mg/kg and vehicle – normal saline by the intragastric route. The mortality rate was observed for 24 h (14).

Statistical analysis

Values are presented as the mean \pm SEM and data were analyzed by ANOVA followed by Tukey's test using Mini Tab software. A value of $p < 0.05$ was considered significant.

RESULTS

Analgesic activity

All the three extracts significantly reduced the acetic acid induced writhing and formalin induced paw licking in mice. The analgesic effect of ether extract was highly significant ($p < 0.0001$) in both experimental models (Tables 1, 2).

Anti-inflammatory activity

All the extracts produced a significant anti-inflammatory effect between 2–3 h after induction of inflammation. However, ether extract produced maximum effect 34% inhibition ($p < 0.001$) against carrageenan and 28% ($p < 0.01$) inhibition against egg albumin induced paw edema in mice at the end of 3 h (Tables 3, 4).

Antipyretic activity

All the extracts were found to produce significant effects against yeast induced pyrexia but the ether extract exhibited a highly significant ($p < 0.0001$) antipyretic effect as compared to control group (Table 5).

Acute toxicity

Animals treated up to 2000 mg/kg of ether, aqueous and ethanolic extracts of *Thymus serpyllum*-

Table 3. Effect of various extracts of *Thymus serpyllum* on carrageenan induced paw edema in mice.

Treatment	Paw circumference in mm at indicated time*			
	0 h	1 h	2 h	3 h
Control (2 mL/kg)	3.60 \pm 0.10	4.09 \pm 0.06	4.30 \pm 0.10	4.51 \pm 0.09
Ether extract (100 mg/kg)	3.57 \pm 0.25	3.79 \pm 0.22 ^b	3.85 \pm 0.28 ^d	3.85 \pm 0.27 ^c
Aqueous extract (100 mg/kg)	3.64 \pm 0.04	3.54 \pm 0.07 ^b	3.36 \pm 0.07 ^{bc}	3.35 \pm 0.08 ^b
Ethanolic extract (100 mg/kg)	3.88 \pm 0.21	3.15 \pm 0.26 ^b	3.02 \pm 0.28 ^{bc}	2.65 \pm 0.27 ^b
Aspirin (100 mg/kg)	4.03 \pm 0.13	4.35 \pm 0.05 ^b	4.47 \pm 0.07 ^b	4.55 \pm 0.07 ^b

* Data are expressed as the mean \pm SEM; $p < 0.05$ was considered as significant ^b = $p < 0.01$, ^c = $p < 0.001$ and ^d = $p < 0.0001$ compared to control group.

Table 4. Effect of various extracts of *Thymus serpyllum* on paw edema induced by egg albumin in mice.

Treatment	Paw circumference in mm at indicated time*			
	0 h	1 h	2 h	3 h
Control (2 mL/kg)	3.56 \pm 0.14	3.57 \pm 0.15 ^a	3.71 \pm 0.15 ^a	3.92 \pm 0.14 ^a
Ether extract (100 mg/kg)	4.48 \pm 0.13	4.29 \pm 0.10 ^b	4.12 \pm 0.06 ^{ab}	3.80 \pm 0.06 ^b
Aqueous extract (100 mg/kg)	4.02 \pm 0.15	4.00 \pm 0.13 ^{ab}	4.04 \pm 0.14 ^{ab}	3.80 \pm 0.12 ^{ab b}
Ethanolic extract (100 mg/kg)	3.95 \pm 0.13	4.01 \pm 0.22 ^{ab}	4.02 \pm 0.34 ^{ab}	3.70 \pm 0.31 ^b
Aspirin (100 mg/kg)	3.87 \pm 0.10	3.64 \pm 0.08 ^b	3.54 \pm 0.09 ^b	3.40 \pm 0.11 ^b

* Data are expressed as the mean \pm SEM; $p < 0.05$ was considered as significant ^a = $p < 0.05$, ^b = $p < 0.01$, ^c = $p < 0.001$ and ^d = $p < 0.0001$ compared to control group.

Table 5. Effect of various extracts of *Thymus serpyllum* on Brewer's yeast-induced pyrexia in mice.

Treatments	Temperature at 0 min [°]	Temperature at 30 min [°]	Temperature at 90 min [°]	Temperature at 150 min [°]
	Mean ± SEM	Mean ± SEM	Mean ± SEM	Mean ± SEM
Control (2 mL/kg)	36.82 ± 0.23	37.10 ± 0.24 ^a	37.26 ± 0.14 ^a	37.42 ± 0.19 ^a
Ether extract (100 mg/kg)	36.68 ± 0.31	36.24 ± 0.39 ^a	36.00 ± 0.23 ^b	35.90 ± 0.4 ^c
Aqueous extract (100 mg/kg)	36.40 ± 0.46	36.22 ± 0.22 ^a	36.40 ± 0.35 ^b	36.42 ± 0.23 ^b
Ethanol extract (100 mg/kg)	36.90 ± 0.19	36.16 ± 0.15 ^b	36.90 ± 0.29 ^a	37.22 ± 0.25 ^b
Aspirin (100 mg/kg)	36.70 ± 0.39	37.54 ± 0.41 ^b	36.66 ± 0.47 ^b	36.74 ± 0.38 ^a

Data are expressed as the mean ± SEM. ($p < 0.05$) was considered as significant ^a = $p < 0.05$, ^b = $p < 0.01$, ^c = $p < 0.001$ and ^d = $p < 0.0001$ compared to control group. The means sharing the same letters are not significant to each other.

lum produced no death and changes in behavior, a fact indicating low toxicity of the extract.

DISCUSSION

The folkloric use of *Thymus serpyllum* Linn. in fever, inflammation and pain has been reported in literature along with several other traditional claims. Hence, it was thought that investigations of these medicinal properties should be scientifically authenticated to validate the traditional claims. Moreover, this plant has not been subjected to the above mentioned pharmacological screening so far. The results obtained after experimental work indicated that all of the three extracts exhibited analgesic activity by reducing both the acetic acid induced writhing and formalin induced paw licking in mice. Acetic acid causes inflammatory pain by inducing capillary permeability, while formalin exhibits neurogenic and inflammatory pain (15). In acetic acid induced models of pain, analgesic activities were supposed to be present, due to some sterols. Plants possessing some organic acid, and flavonoid also showed significant analgesic activities (16). These results of ether extract exhibited a mode of action similar to those drugs which act through inhibiting Cox-3, enzyme like paracetamol, which has been reported to lack or possess a weak anti-inflammatory activity but possesses a strong analgesic and antipyretic activities and was reported to inhibit centrally the synthesis of prostaglandin in the brain (17).

However, these drugs do not inhibit peripheral biosynthesis of prostaglandin and therefore lacks peripheral anti-inflammatory effect. Ether extract

has also been reported to inhibit acetic acid induced writhing. The central action of the extracts is further supported by its ability to inhibit both phases of formalin induced paw licking, which is the characteristic of drugs (as narcotic) that act centrally (18). Although all the three extracts exhibited analgesic activity, the ether extract showed more pronounced ($p < 0.0001$) analgesic activity even compared to standard drug, aspirin.

In the study of anti-inflammatory activity, we evaluated the extracts against egg-albumin and carrageenan induced paw edema. Synthesis or release of mediators of the injured site has been reported to occur. Prostaglandins, especially the E series, histamine, bradykinins, leukotrienes and serotonin are included in these mediators, all of which also cause pain and fever (19). Inflammation, and other symptoms are normally ameliorated by inhibition of these mediators from reaching the injured site or from bringing out their pharmacological effects.

Development of carrageenan induced paw edema is commonly correlated with early inflammatory oxidative stage. Carrageenan edema is a multi-mediated phenomenon. It is believed to be biphasic; in the first phase (1 h) serotonin and histamine are released while in the second phase (over 1 h) prostaglandins, cyclooxygenase products are mediated and kinins provide the continuity between the two phases (20). Thus, the carrageenan induced inflammation model is a significant predictive test for inflammation. The anti-inflammatory activity of various extracts of *Thymus serpyllum* against carrageenan induced inflammation in mice was observed but the ethanolic extract at the dose of 100

mg/kg significantly ($p < 0.05 - p < 0.0001$) inhibited the carrageenan induced mice paw edema. The anti-inflammatory activity of ether, aqueous and ethanolic extracts of *Thymus serpyllum* was observed in mice against egg-albumin induced paw edema. Histamine is an important mediator of inflammation, a potent vasodilator and is also involved in increasing the vascular permeability (21). As the plant extracts effectively suppressed the edema produced by egg-albumin, it showed that the extract might exhibited anti-inflammatory actions by inhibiting the synthesis, release or action of inflammatory mediators such as histamine, serotonin and prostaglandins.

In this study, antipyretic effect was evaluated and the ether extract produced a prominent effect ($p < 0.001$) against yeast induced pyrexia. As discussed above, the extracts might exhibit analgesic effects by acting centrally. The extract was likely to reduce pyrexia by reducing the brain concentration of prostaglandin E₂ especially in the hypothalamus through its action on Cox-3 or by enhancement of the production of the body's own antipyretic substances like vasopressin and arginine (22).

In acute toxicity testing, animals treated with up to 2000 mg/kg of ether, aqueous and ethanolic extracts of *Thymus serpyllum* produced no death and no changes in behavior of mice that indicates low toxicity of the extracts.

From these investigations, it might be concluded that various (ether, aqueous and ethanolic) extracts of *Thymus serpyllum* exhibited analgesic, anti-inflammatory and antipyretic effects. It justifies the traditional use of this plant in the treatment of various types of pain, fever and inflammation. However, further studies are required to isolate active compounds from the potent extracts and to elucidate their exact mechanism of action.

Acknowledgment

The authors are thankful to Dr. Sher Wali, Assistant Professor of Botany, Karakoram International University, Gilgit-Baltistan for the identification of the plant used in the present study.

REFERENCES

1. Kumar V., Abbas A.K., Fausto N., Eds.: Robbins and Cotran Pathologic Basis of Disease, 7th edn., pp. 47–86, Elsevier Saunders, Philadelphia, PA 2004.
2. Vane J.R., Botting R.M.: *Inflamm. Res.* 44, 1 (1995).
3. Anilkumar M.: *Ethnomedicine* 34, 267 (2010).
4. Gaddi A., Cícero A.F.G., Pedro E.J.: *Arch. Gerontol. Geriatr.* 38, 201 (2004).
5. Qureshi R.A., Ghufuran M.A., Gilani S.A., Sultana K., Ashraf M.: *Pak. J. Bot.* 39, 2275 (2007).
6. Zachar O.: *Int. J. Pharmacol.*: 7, 435 (2008).
7. Zaman R., Ahmad M.: *J. Biol. Sci.* 4, 463 (2004).
8. Koster R., Anderson., De Boer E.J.: *Fed. Proc.* 18, 412 (1959).
9. Hunskaar S., Fasmer O.B., Hole K.: *J. Neurosci.* 4, 69 (1987).
10. Akah P.A., Nwambie A.L.: *J. Ethnopharmacol.* 42, 179 (1994).
11. Jain B.B., Rathi B.S., Thakurdesai P.A., Bodhankar S.L.: *Indian J. Nat. Prod.* 23, 26 (2007).
12. Metowogo K., Agbonon A., Eklun-Gadegbeku K., Aklikokou A.K., Gbeassor M.: *Trop. J. Pharm. Res.* 7, 907 (2008).
13. Brito A.S.: UNICAMP Press, Campinas 1994.
14. Vaz Z.R., Cechinel V., Yunes R.A., Calixto J.B.: *J. Pharmacol. Exp. Ther.* 278, 304 (1996).
15. Bittar M., De Sousa M., Yunes R., Lento R.A., Delle-Monache F., Cechinel Filho V.: *Planta Med.* 66, 84 (2000).
16. Botting R.M.: *Clin. Infect. Dis.* 31 (5), 202 (2001).
17. Santos A.R., Cechinel Filho V., Niero R., Viana A.M., Moreno F.N., Campos M.M., Yunes R.A. et al.: *J. Pharm. Pharmacol.* 46, 755 (1994).
18. Asongalem E., Foyet H.S., Ekoo S., Dimo T., Kamtchouing P.: *J. Ethnopharmacol.* 95, 63 (2004).
19. Silva G.N., Martins F.R., Matheus M.E., Leitão S.G., Fernandes P.D.: *J. Ethnopharmacol.* 100, 254 (2005).
20. Cumin R.K.N., Bersani Amadio C.A., Fortes Z.B.: *Inflamm. Res.* 50, 460 (2001).
21. Chandrasekharan., Dai N.V., Roos H., Evanson K.L., Tomsik N.K., Elton J., Simmons T.S.: *Proc. Natl. Acad. Sci. USA* 99, 13926 (2002).

Received: 19. 10. 2013

**IN VITRO ANTIOXIDANT ACTIVITY AND GC-MS ANALYSIS
OF THE ETHANOL AND AQUEOUS EXTRACTS OF *CISSUS CORNIFOLIA*
(BAKER) SPLANCH (VITACEAE) PARTS**

TALENT CHIPITI¹, MOHAMMED AUWAL IBRAHIM¹, NEIL ANTHONY KOORBANALLY²
and MD. SHAHIDUL ISLAM^{1*}

¹School of Life Sciences and ²School of Chemistry and Physics,
University of KwaZulu-Natal (Westville Campus), Durban, 4000, South Africa

Abstract: The study was intended to explore the antioxidant potential and phytochemical content of the ethanol and aqueous extracts of the leaf and root samples of *Cissus comifolia* (Baker) Splanck (Vitaceae) across a series of four *in vitro* models. The results showed that all the extracts had reducing power (Fe³⁺- Fe²⁺), and DPPH, hydroxyl and nitric oxide radical scavenging abilities to varying extents. However, the ethanol root extract had more potent antioxidant power in all the experimental models than other extracts and possessed a higher total phenol content of 136.1 ± 6.7 mg/g. The GC-MS analysis of the aqueous and ethanol extracts of the roots indicated the presence of the common aromatic phenolic compounds, pyrogallol, resorcinol and catechol, a fatty acid, n-hexadecanoic acid and an aldehyde, vanillin. Data from this study suggest that both the leaves and roots of *C. comifolia* possessed anti-oxidative activities with the best anti-oxidant activity being exhibited by the ethanolic extract of the root. The antioxidant properties of the root extracts can be attributed to the phenolic compounds present in the extracts.

Keywords: antioxidant, *Cissus comifolia*, *in vitro*, polyphenols

The biochemical state of the body, when there is an imbalance between the production of reactive oxygen and a biological system's ability to readily detoxify the reactive intermediates or easily repair the resulting damage, is termed oxidative stress (OST). Oxidative stress has been implicated in the pathogenesis of a number of diseases such as atherosclerosis, Parkinson's, heart failure, myocardial infarction, Alzheimer's disease, fragile X syndrome, chronic fatigue syndrome and diabetes (1).

The deleterious effects of oxidative stress in a number of metabolic chronic disorders has prompted scientists to search for antioxidative compounds that can impede the oxidation of biomolecules in a chain reaction, which could be vital in the therapy and prevention of many metabolic disorders (2). The synthetic antioxidative agents, such as butylated hydroxyanisole (BHA), butylated hydroxytoluene (BHT), propylgallate (PG), and tert. butylhydroxytoluene exhibit potent free radical scavenging effects but they induce liver and kidney dysfunction and have also been reported to be carcinogenic in laboratory animals (3-5). Thus, there is a need to identify and utilize more antioxidants of natural ori-

gin, which can relieve the deleterious effects of free radicals and other biological oxidants (5).

Plants have a long history of use in medicinal applications, especially in Sub-saharan Africa where access to medical supplies, pharmaceuticals and medical doctors are limited. The uses of these medicinal plants have been well documented over the years and their use, especially in the rural areas of African countries is quite popular (6). Based on this, research activities on medicinal plants, especially on the phytochemistry and bioactivity of medicinal plants have been stimulated in order to develop alternative therapies for a number of diseases (7). Thus, in recent years the screening of medicinal plants with potential antioxidant properties has received significant attention due to an increasing concern for safe and non-toxic alternative antioxidants (8).

Cissus cornifolia (Baker) Splanck (Vitaceae), commonly called the "Ivy grape" is indigenous to Zimbabwe. It is locally called "Mudzambiringa" and "Idebelebe" by the Shona and Ndebele-speaking Zimbabweans, respectively. *Cissus* is a genus of approximately 350 species. Most of the members of

* Corresponding author: e-mail: islamd@ukzn.ac.za or sislam1974@yahoo.com; phone: +27 31 260 8717; fax: +27 31 260 7942

this genus have a wide array of uses in African traditional medicine (9). *C. cornifolia*, commonly found in Zimbabwe, is traditionally used by the Shona speaking people as a remedy for gonorrhoea while the leaf-sap is used among the Tanganyika as a sedative in cases of mental derangement; the root-decoction is also used for malaria, septic tonsil, diabetes, cardiac problems and pharyngitis (10). Currently, there have been no phytochemical or biological activity studies on *C. cornifolia*. Phytochemical studies on other species of *Cissus* have revealed the presence of glycosides, flavonoids, saponins, steroids, terpenoids and tannins (11-14).

Bioactivity and isolation of various compounds have been carried out in a number of species from the genus *Cissus* and had shown impressive results. *Cissus quadrangularis* Linn. Wall. Ex which is commonly used as a food supplement in India, was evaluated for its protective effects against tissue injury (13). Jainu and Devi (15) reported that *Cissus quadrangularis* has antimicrobial, antiulcer, antioxidative and cholinergic activity as well as potent fracture healing properties and a beneficial effect on cardiovascular diseases. In addition, the same group reported cytoprotective properties of the methanolic extract of the same plant (16). Attawish et al. (17) isolated vitamin C, β -carotene, two asymmetric tetracyclic triterpenoids, β -sitosterol, α -amyrin, α -amyrone from *Cissus quadrangularis* which they accredited to the observed activities and Potu et al. (18) also reported several phytochemical constituents, such as ascorbic acid, flavonoids, and triterpenoids in *Cissus quadrangularis*.

Cissus sicyoides L. has been widely used in folk medicine against stomach ache and indigestion (19) and has been reported to treat diabetes, pain, inflammation, rheumatism, abscesses, muscle inflammation, convulsions, epilepsy, stroke and hypertension (20). Ferreira et al. (20) also reported a coumarin glycoside, coumarin sabandin, flavonoids, steroids, sitosterol and hydrolyzable tannins from the plant. *Cissus populnea* has been reported as a food supplement in Nigeria (21), however there are no reports on the phytochemistry of the plant in the literature. Ojekale et al. (22) reported *Cissus populnea* to have a myriad of uses as a medicinal agent globally.

This study was undertaken to investigate the ethnomedicinal efficacy of the leaf and root ethanol and aqueous extracts of the plant as potential sources of therapeutic agents which can be of use in ameliorating oxidative stress related parameters using various models *in vitro*. We also subjected the

extracts to GC-MS analysis in order to partially explore the phytochemistry of the plant.

MATERIALS AND METHODS

Chemicals and reagent

All chemicals used were of analytical grade. Gallic acid, ascorbic acid, 2,2-diphenyl-1-picrylhydrazyl radical (DPPH), 2-deoxy-D-ribose, iron chloride, sodium carbonate, trichloroacetic acid, ethylenediaminetetraacetic acid (EDTA), H_2O_2 , 2-deoxy-D-ribose and potassium ferricyanide were procured from Sigma-Aldrich through Capital Lab Supplies, New Germany, South Africa. Griess reagent, sodium nitroprusside, thiobarbituric acid (TBA) and Folin Ciocalteu's phenol reagent were purchased from Merck Chemical Company, Durban, South Africa.

Plant material

The fresh leaf and root samples of *C. cornifolia* were collected in the month of March, 2012 from Mrewa, Mashonaland East province, Zimbabwe. The plant samples were identified and authenticated at the herbarium unit of the Harare botanical garden and herbarium, Zimbabwe and a voucher specimen number CC082 was deposited. The leaves and roots were immediately washed with distilled water, cut into small pieces and shade-dried until constant weights were attained. The dried samples were ground to a fine powder using a blender, and stored individually in air-tight polyethylene bags for transport to the University of KwaZulu-Natal, Westville campus, Durban, South Africa for further analysis.

Preparation of the plant extracts

Forty grams of the fine powdered plant parts were separately defatted with hexane. The defatted materials were sequentially extracted with ethanol and water by soaking for 48 h in 200 mL of the relevant solvent. For ethanol extracts, after filtration through Whatmann filter paper (No. 1), the ethanol was evaporated under reduced pressure using a rotary evaporator (Buchi Rotavapor II) at 40°C. Aqueous extracts were dried using a freeze dryer. The solvent extracts in each case was weighed, transferred to micro tubes and stored in a refrigerator at 4°C until required.

Estimation of total phenolic content

The total phenolic content of each extract was determined (as gallic acid equivalents) according to the method described by McDonald et al. (23), with slight modifications. Briefly, 200 μ L of the extract

(240 µg/mL) was incubated with 1 ml of ten-fold diluted Folin Ciocalteu's phenol reagent and 800 µL of 0.7 M Na₂CO₃ for 30 min at room temperature. Absorbance values were determined at 765 nm on a Shimadzu UV mini 1240 spectrophotometer (Shimadzu Corporation, Kyoto, Japan) using a special glass cuvette with a 10 mm optical path length. All measurements were done in triplicate.

Ferric (Fe³⁺) reducing antioxidant power assay (FRAP)

The FRAP method of Oyaizu (24) with slight modifications was used to measure the total reducing capacity of the extracts. To perform this assay, 1 mL of different extract concentrations (15–240 µg/mL) were incubated with 1 mL of 0.2 M sodium phosphate buffer (pH 6.6) and 1% potassium ferricyanide at 50°C for 30 min. After 30 min incubation, the reaction mixture was acidified with 1 mL of 10 % trichloroacetic acid (pH 0.211). Thereafter, 1 mL of the acidified sample of this solution was mixed with 1 mL of distilled water and 200 µL of FeCl₃ (0.1%) in another test tube and the absorbance was measured at 700 nm using above-mentioned cuvette and spectrophotometer. Increased absorbance of the reaction mixture indicates higher reduction capacity of the extracts. Results were expressed as a percentage of absorbance of the sample to the absorbance of gallic acid:

$$\text{Ferric reducing antioxidant power (\%)} = \frac{\text{Absorbance of sample}}{\text{Absorbance of gallic acid}} \times 100$$

Free radical scavenging activity (DPPH assay)

The free radical scavenging activity of the extracts was determined and compared to that of ascorbic and gallic acids using a method described by Tuba and Gulcin (25) with slight modifications. In order to perform this assay, a 0.3 mM solution of DPPH was prepared in methanol and 500 µL of this solution was added to 1 mL of the extract at different concentrations (15–240 µg/mL). These solutions were mixed and incubated in the dark for 30 min at room temperature. The absorbance was measured at 517 nm against a blank lacking the scavenger.

Deoxyribose assay/hydroxyl radical scavenging (HRS) assay

The hydroxyl radical scavenging activity was measured by studying the competition between deoxyribose and the solvent extracts for hydroxyl radicals generated by the ascorbate – EDTA – H₂O₂ system (Fenton reaction) as described by Hinneburg et al. (26). The assay was performed by adding 200 µL of premixed 100 µM FeCl₃ and 100 µM EDTA (1

: 1, v/v) solution, 100 µL of 10 mM H₂O₂, 360 µL of 10 mM 2-deoxy-D-ribose, 1 mL of different extract concentrations (15–240 µg/mL), 400 µL of 50 mM sodium phosphate buffer (pH 7.4) and 100 µL of 1 mM ascorbic acid in sequence. The mixture was incubated at 50°C for 2 h. Thereafter, 1 mL of 2.8% TCA and 1 mL of 1.0% TBA (in 0.025 M NaOH) were added to each test tube. The samples were further incubated in a water bath at 50°C for 30 min to develop the pink chromogen color. The extent of oxidation was estimated from the absorbance of the solution at 532 nm and the hydroxyl radical scavenging activity of the extract is reported as a percentage inhibition of deoxyribose degradation.

Nitric oxide (NO) radical scavenging assay

Sodium nitroprusside in aqueous solution at physiological pH spontaneously generates nitric oxide (NO), which interacts with oxygen to produce nitrite ions that can be estimated by use of Griess reagent. Scavengers of NO compete with oxygen, leading to reduce the production of NO. The assay was carried out by incubating 500 µL of 10 mM sodium nitroprusside in phosphate buffer (pH 7.4) and 500 µL of different extract concentrations (15–240 µg/mL) at 37°C for 2 h. The reaction mixture was then mixed with 500 µL of Griess reagent. The absorbance of the chromophore formed during the diazotization of nitrite with sulfanilamide and subsequent coupling with naphthylethylenediamine was read at 546 nm. The percentage inhibition of nitric oxide generated was measured in comparison with the absorbance value of a control (sodium nitroprusside in phosphate buffer).

The scavenging effects of the solvent extracts in the DPPH, hydroxyl and nitric oxide radical scavenging assays were calculated as:

$$\text{Scavenging activity (\%)} = \left(\frac{\text{Ac} - \text{As}}{\text{Ac}} \right) \times 100$$

where: Ac is absorbance of control and As absorbance of the sample or standard.

Gas chromatography-mass spectrometric (GC-MS) analysis

The aqueous and ethanol extracts of the leaf and root samples of the plant were subjected to GC-MS analysis. The analysis was conducted with an Agilent Technologies 6890 Series gas chromatograph coupled with (an Agilent) 5973 Mass Selective detector and driven by Agilent chemstation software. A eHP-5MS capillary column was used (30 m × 0.25 mm internal diameter, 0.25 µm film thickness). The carrier gas was ultra-pure helium at a flow rate of 1.0 mL/min and a linear veloc-

ity of 37 cm/s. The injector temperature was set at 250°C. The initial oven temperature was at 60°C which was programmed to increase to 280°C at the rate of 10°C/min with a hold time of 4 min at each increment. Injections of 2 µL were made in the splitless mode with a split ratio of 20 : 1. The mass spectrometer was operated in the electron ionization mode at 70 eV and electron multiplier voltage at 1859 V. Other MS operating parameters were as follows: ion source temperature 230°C, quadrupole temperature 150°C, solvent delay 4 min and scan range 50–700 amu. The compounds were identified by direct comparison of the retention times and mass spectral data and fragmentation pattern with those in the National Institute of Standards and Technology (NIST) library.

Statistical analysis

Data are presented as the mean ± SD of triplicate determinations. Data were analyzed by SPSS statistical software (version 19) using Tukey's multiple range *post-hoc* test. Values were considered significantly different at $p < 0.05$.

RESULTS

A higher yield of aqueous extract was recorded in the two parts of the plant. The highest total phenolic content was recorded in the ethanol extract of the roots (136.1 ± 10.6 mg/g GAE) (Table 1). All the extracts of *C. cornifolia* showed an ability to donate electrons to convert $Fe^{3+} \rightarrow Fe^{2+}$ as indicated by the concentration dependent increase in the percentage

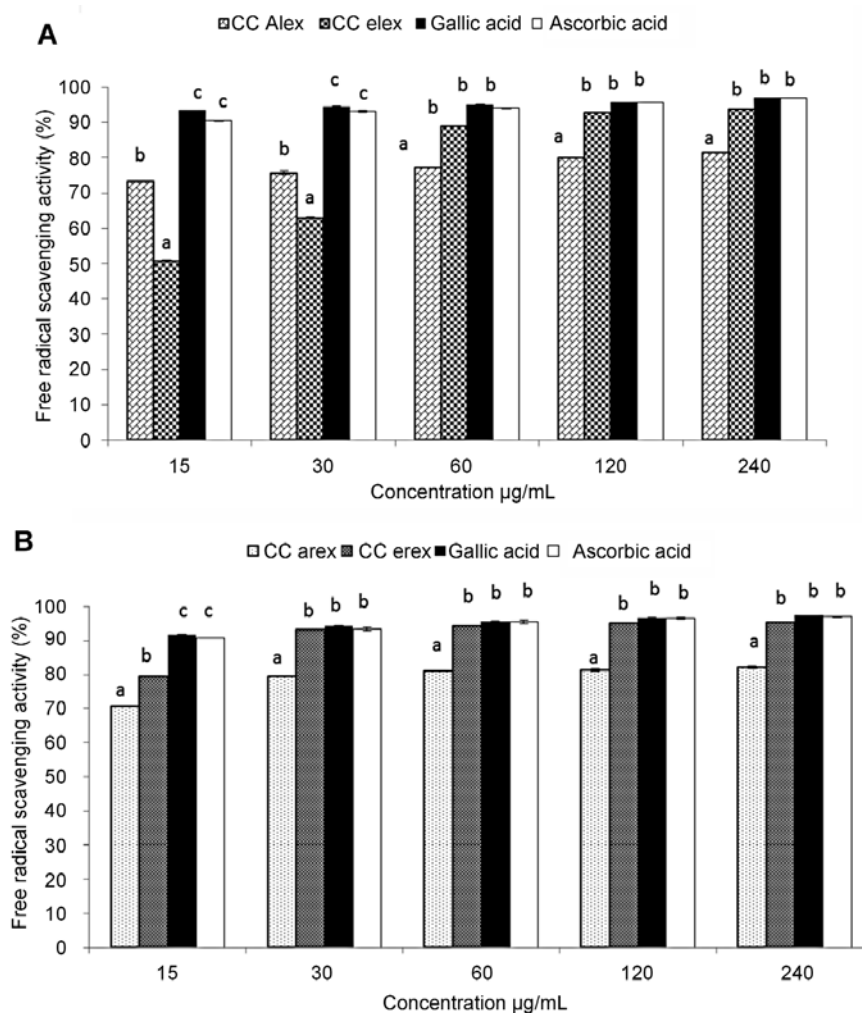


Figure 1. DPPH radical scavenging activity of ethanol and aqueous extracts of the leaves (A) and roots (B) of *C. cornifolia*. Data are presented as mean ± SD of triplicate determinations.

^{a-c}Values with different letters over the bars for a given concentration of each extract are significantly different from each other (Tukey's-HSD multiple range *post hoc* test, $p < 0.05$). Arex = aqueous root extract and Erex = ethanol root extract; Alex = aqueous leaf extract and Elex = ethanol leaf extract

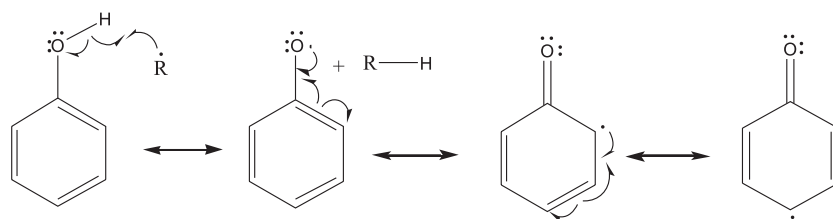


Figure 2. Hydrogen radical donation to a reactive radical species and stabilization of the resultant radical

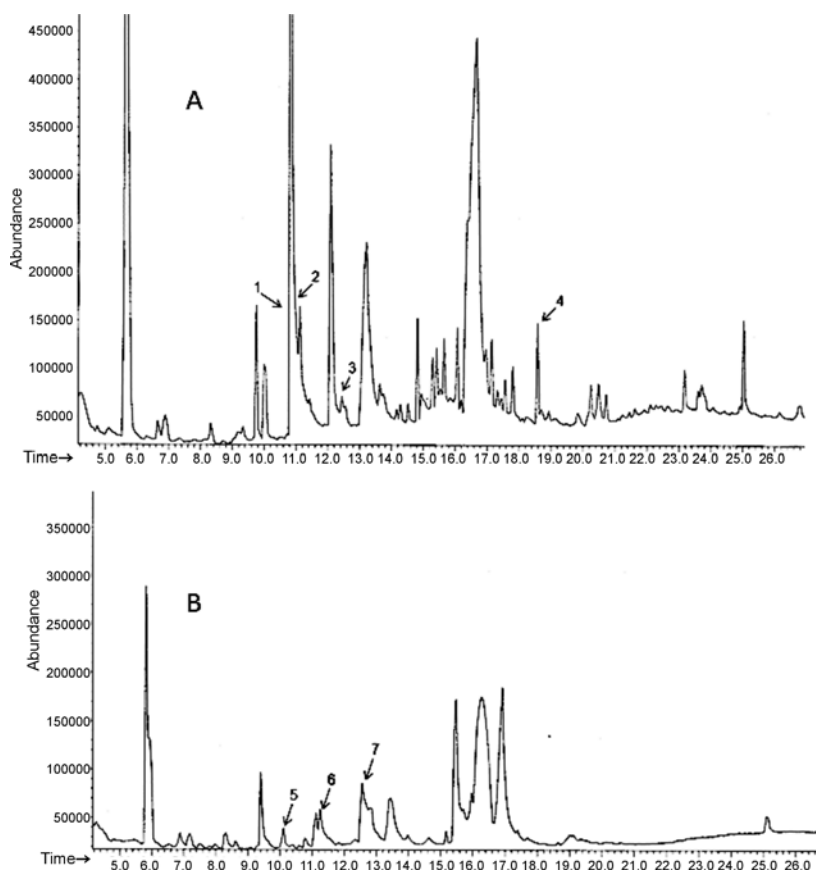


Figure 3. GC-MS chromatogram of the ethanol (A) and aqueous (B) extracts of the root of *C. comifolia*

reducing power (Table 2). However, the ethanol extract of the root had a consistent and significantly ($p < 0.05$) higher total reducing power than other extracts.

Figure 1A and 1B, shows the DPPH radical scavenging activities of the leaf and root extracts of *C. comifolia*. The ability to quench DPPH free radicals was evident in all extracts as indicated by the concentration dependent increase in the percentage inhibitions. Further to this, the ethanol root extract

indicated a consistently higher free radical scavenging activity than all other extracts tested.

All the extracts possess the ability to scavenge hydroxyl radicals generated by Fenton's reaction with the ethanol extracts displaying a significantly ($p < 0.05$) higher HRS ability compared to the aqueous extracts and the standards used (Table 3). The ethanol extract of the leaves demonstrated a higher ($p < 0.05$) HRS activity than the same extract in the roots at lower concentrations (15–60 $\mu\text{g}/\text{mL}$) but at

Table 1. Percentage recovery (w/w) and total phenolic content of various solvent extracts of *C. cornifolia* parts.

Samples	% Recovery (w/w)	Total polyphenol (mg/g GAE)
Leaves		
EtOH	2.70	52.9 ± 12.5 ^a
Aqueous	5.91	89.9 ± 7.40 ^b
Root		
EtOH	1.69	136.1 ± 10.6 ^d
Aqueous	7.60	106.0 ± 23.6 ^c

Data are presented as the mean ± SD values of triplicate determinations. ^{a-d}Different superscript letters for a given value within a column are significantly different from each other (Tukey's-HSD multiple range *post hoc* test, $p < 0.05$).

Table 2. Percentage total reducing power (GAE) of solvent extracts from various parts of *C. cornifolia*.

Extracts	Concentration (µg/mL)				
	15	30	60	120	240
Leaves					
EtOH	9.81 ± 1.30 ^a	14.12 ± 2.45 ^a	21.37 ± 1.33 ^b	28.59 ± 1.14 ^a	34.00 ± 9.07 ^a
Aqueous	4.65 ± 3.39 ^a	10.79 ± 4.54 ^a	14.51 ± 0.88 ^a	29.15 ± 5.69 ^a	30.71 ± 1.00 ^a
Root					
EtOH	29.75 ± 1.12 ^c	45.75 ± 2.66 ^c	52.80 ± 0.45 ^d	75.22 ± 2.39 ^c	93.09 ± 1.05 ^c
Aqueous	15.95 ± 2.02 ^b	30.18 ± 0.20 ^b	40.69 ± 0.63 ^c	45.71 ± 1.80 ^b	75.51 ± 1.10 ^b
Standard					
Ascorbic acid	76.83 ± 4.92 ^d	80.24 ± 3.00 ^d	90.26 ± 5.51 ^c	91.08 ± 5.43 ^d	93.60 ± 6.21 ^c

Data are presented as the mean ± SD values of triplicate determinations. ^{a-e}Different superscript letters for a given value within a column are significantly different from each other (Tukey's-HSD multiple range *post hoc* test, $p < 0.05$).

Table 3. Percentage hydroxyl radical scavenging activity of extracts from the root and leaves of *C. cornifolia*.

Extracts	Concentration (µg/mL)				
	15	30	60	120	240
Leaves					
Ethanol	38.96 ± 1.2 ^c	55.41 ± 1.3 ^c	70.34 ± 0.3 ^d	78.57 ± 0.1 ^d	83.54 ± 0.7 ^d
Aqueous	24.98 ± 1.0 ^b	27.89 ± 1.2 ^b	43.51 ± 4.8 ^c	48.63 ± 3.3 ^c	54.12 ± 2.2 ^b
Root					
Ethanol	27.51 ± 1.7 ^b	47.40 ± 1.3 ^d	64.71 ± 0.2 ^d	88.46 ± 2.0 ^e	92.96 ± 2.1 ^e
Aqueous	26.82 ± 1.3 ^b	20.42 ± 1.6 ^a	32.13 ± 2.0 ^b	51.50 ± 0.3 ^c	69.90 ± 5.6 ^c
Standard					
Ascorbic acid	14.50 ± 2.20 ^a	17.35 ± 3.10 ^a	21.85 ± 0.10 ^a	26.80 ± 0.70 ^a	30.30 ± 1.20 ^a
Gallic acid	32.00 ± 0.60 ^c	35.57 ± 2.30 ^c	36.75 ± 1.80 ^b	38.90 ± 1.10 ^b	40.20 ± 0.20 ^a

Data are presented as the mean ± SD values of triplicate determinations. ^{a-e}Different superscript letters for a given value within a column are significantly different from each other (Tukey's-HSD multiple range *post hoc* test, $p < 0.05$).

Table 4. Percentage nitric oxide (NO) scavenging activities of extracts from various parts *C. cornifolia*.

Extracts	Concentration ($\mu\text{g/mL}$)				
	15	30	60	120	240
Leaves					
Ethanol	18.75 \pm 2.5 ^a	27.48 \pm 1.9 ^b	28.24 \pm 0.7 ^b	43.51 \pm 1.4 ^b	48.85 \pm 0.5 ^b
Aqueous	ND	11.19 \pm 0.6 ^a	12.91 \pm 1.0 ^a	16.28 \pm 0.7 ^a	22.95 \pm 0.7 ^a
Root					
Ethanol	42.23 \pm 1.4 ^b	44.52 \pm 0.9 ^c	57.58 \pm 1.0 ^c	83.11 \pm 2.2 ^d	91.18 \pm 1.5 ^d
Aqueous	46.56 \pm 2.4 ^b	50.63 \pm 1.0 ^c	54.7 \pm 0.7 ^c	63.15 \pm 0.1 ^c	70.48 \pm 0.8 ^c
Standard					
Ascorbic acid	51.44 \pm 0.05 ^c	56.94 \pm 0.90 ^c	58.37 \pm 1.40 ^c	62.44 \pm 0.70 ^c	77.22 \pm 1.20 ^c
Gallic acid	43.06 \pm 9.20 ^b	47.36 \pm 0.70 ^c	49.76 \pm 0.70 ^c	59.33 \pm 3.20 ^c	64.59 \pm 6.20 ^c

Data are presented as the mean \pm SD values of triplicate determinations. ^{a-d}Different superscript letters for a given value within a column are significantly different from each other (Tukey's-HSD multiple range *post hoc* test, $p < 0.05$); ND = not determined.

Table 5. Compounds identified from the root of *Cissus cornifolia* by GCMS

Name of compound	Retention time (min)	Percentage match (%)	Molecular mass (g/mol)
Ethanol extract			
Hydroquinone	10.71	86	110
Resorcinol	10.83	99	110
Vanillin	12.56	92	152
n-Hexanoic acid	18.58	91	256
Aqueous extract			
Catechol	10.12	95	110
Resorcinol	11.25	97	110
Pyrogallol	12.55	72	126

higher concentrations (120–240 $\mu\text{g/mL}$), the HRS activity in the ethanol extract of the roots were higher than in the leaves.

Table 4 presents the NO inhibition activities of the ethanol and aqueous extracts of *C. cornifolia* leaves and roots. All the extracts were found to exhibit NO inhibition activity to an extent, however the root extracts demonstrated a higher NO inhibition potential than the leaf extracts. Notably, the ethanol extract of the root had significantly higher NO inhibition potential compared to the other extracts and the standards used.

The crude aqueous and ethanol leaf and root extracts were analyzed by GCMS to identify compounds in the extracts by comparison with standard mass spectra in the NIST library. Three polyhydroxylated phenols, pyrogallol, catechol and resorcinol

were identified in the aqueous extract of the roots, with resorcinol also being present in the ethanol extract along with hydroquinone, vanillin and a long chain fatty acid, n-hexadecanoic acid (Table 5, Figs. 2 and 3).

DISCUSSION

Cissus cornifolia has been reported to have a variety of uses among which, the root decoction is used by traditional healers and herbalists to treat and manage a vast array of non-metabolic chronic disorders and ailments such as diarrhea and other stomach ailments, back pain, sore throat, wounds, diabetes and cardiac problems in the Mrewa district in Zimbabwe (personal communication with traditional healers).

Preliminary investigations on the *in vivo* neuropharmacological activity of the methanolic leaf extract as well as its hypoglycemic activity on normoglycemic rats have been reported (7, 11). Nevertheless, according to our current knowledge, there is no report on detailed anti-oxidative activities from any part of the plant or its phytochemistry. A set of *in vitro* assays were employed to cover most possible known mechanisms by which different antioxidants operate to inhibit oxidative chain reactions.

The results from all the experimental models (total reducing power ($\text{Fe}^{3+} \rightarrow \text{Fe}^{2+}$), DPPH, hydroxyl radical and nitric oxide reducing ability) indicated that all the different parts of *C. cornifolia* extracted in ethanol and water possess antioxidant potential in a concentration dependent manner to varying extents. The ethanolic root extract has consistently shown to have exceptionally high antioxidant ability and the recorded high phenolics content (136.1 ± 10.6 mg/g GAE), which supported the observed high activity and effectiveness of the extract in the *in vitro* assays.

To identify the responsible phytochemicals, we carried out GC/MS analysis of the aqueous and ethanol extracts of the leaves and roots. Only long chain aliphatic compounds were identified in the ethanol and aqueous extract of the leaves. Palmitic acid, arachidic acid and nonacosane were identified by comparing their MS spectra to those of standard spectra from the NIST library. While no phytochemicals could be identified in the leaf extracts of the plant, the root extracts contained polyphenol compounds, known to be potent antioxidant compounds and is most likely responsible for the antioxidant activity in the root extract of the plant. Two isomers of benzenediol (hydroquinone and resorcinol) were found in the ethanol extract of the roots.

It is highly probable that the polyphenols in the roots are the reason why the roots are more active as antioxidants than the leaves. The mechanism by which these compounds act as radical scavengers is *via* the transfer of a hydrogen atom to a radical species, thereby creating a radical charge on the polyphenol, which is delocalized on the aromatic ring stabilizing the radical charge (Fig. 2). The radical benzene molecule can be quenched by reacting with other radical species.

In conclusion, the results of this study suggest that the ethanolic extracts of leaf and root have strong anti-oxidative effects which might be contributed by some major bioactive active compounds such as hydroquinone, resorcinol, vanillin and n-hexanoic acid. The anti-oxidative effects of the root

ethanolic extract were better than the leaf ethanolic extract which can be used to investigate the *in vivo* anti-oxidative and anti-diabetic effects in the animal model of type 2 diabetes. Additionally, findings of this study further support the use of the root and leaf extracts by traditional healers as an anti-diabetic medicine.

Acknowledgments

This study was supported by the competitive research grant from the Research Office, University of KwaZulu-Natal (UKZN), Durban; an incentive grant for rated researchers and a grant support for women and young researchers from the National Research Foundation (NRF), Pretoria, South Africa. The first author received a scholarship from the College of Agriculture, Engineering and Science, University of KwaZulu-Natal, South Africa.

REFERENCES

1. Calabrese V., Cornelius C., Leso V., Trovato-Salinaro A., Ventimiglia B. et al.: *Biochim. Biophys. Acta* 1822, 729 (2012).
2. Wright E.J., Scism-Bacon J.L., Glass L.C.: *Int. J. Clin. Pract.* 60, 308 (2006).
3. Saito M., Sakagami H., Fujisawa S.: *Anti-Cancer Res.* 23, 4693 (2003).
4. Subhasree B., Baskar R., Laxmi Keerthana R., Lijina Susan R., Rajasekaran P.: *Food Chem.* 115, 1213 (2009).
5. Djeridane A., Yousfi M., Brunel J.M., Stocker P.: *Food Chem. Toxicol.* 48, 2599 (2010).
6. van Wyk B.E.: *J. Ethnopharmacol.* 119, 342 (2008).
7. Musa A.M., Yaro A.H., Usman H., Magaji M.G., Habu M.: *Int. J. Pharmacol.* 4, 145 (2008).
8. Aliyu A.B., Ibrahim M.A., Musa A.M., Bulus T., Oyewale A. O.: *Int. J. Biol. Chem.* 5, 352 (2012).
9. Wild H., Drummond R.B., Gonçalves M.L.: *Centro de Botanica* 50, 24 (1969).
10. Burkill H.M.: *The Useful Plants of West Tropical Africa*. 2nd edn., pp: 293–294, Royal Botanical Garden, Kew 2000.
11. Jimoh A., Tanko Y., Mohammed A.: *Eur. J. Exp. Biol.* 3, 22 (2013).
12. Musa S.M., Fathelrhman E.A., Elsheikh A.E., Lubna A.M.N.A., Abdel Latif E. M., Sakina M.Y.: *J. Med. Plants Res.* 5, 4287 (2011).
13. Jainu M., Mohan K.V., Devi C.S.: *J. Ethnopharmacol.* 104, 302 (2006).

14. Varadarajan P., Rathinaswamy G., Asirvatham D.: *Ethnobot. Leaflet* 12, 841 (2008).
15. Jainu M., Devi C.S.: *J. Clin. Biochem. Nutr.* 34, 43 (2003).
16. Jainu M., Devi C.S.: *J. Med. Food* 7, 372 (2004).
17. Attawish D., Chavalitumrong S., Chivapat S., Chuthaputti S., Rattarajarasroj S.: *J. Sci. Technol.* 24, 39 (2002).
18. Potu B.K., Rao M.S., Nampurath G.K., Rao M.C., Nayak S.R., Thomas H.: *Chang Gung Med. J.* 33, 252 (2010).
19. Asprey G.F., Thornton P.: *West Indian Med. J.* 3, 17 (1954).
20. Ferreira M.P., Nishijima C.M., Seito L.N., Dokkedal A.L., Lopes-Ferreira M. et al.: *J. Ethnopharmacol.* 117, 170 (2008).
21. Ibrahim M.A., Dawes V.N.: *Pharm. Ind.* 62, 243 (2000).
22. Ojekale A.B., Ojiako O.A., Saibu G.M., Olodude O.A.: *Afr. J. Biotechnol.* 6, 247 (2007).
23. McDonald S., Prenzler P.D., Autolovich M., Robards K.: *Food Chem.* 73, 73 (2001).
24. Oyaizu M.: *Japan J. Nutr.* 44, 307 (1986).
25. Tuba A.K., Gulcin I.: *Chem. Biol. Interact.* 174, 27 (2008).
26. Hinneburg I., Dorman H.J.D., Hiltunen R.: *Food Chem.* 97, 122 (2006).

Received: 24. 10. 2013

DIURETIC ACTIVITY OF AQUEOUS EXTRACT OF *NIGELLA SATIVA* IN ALBINO RATS

MUHAMMAD ASIF*¹, QAISER JABEEN², AMIN MALIK SHAH ABDUL MAJID¹
and MUHAMMAD ATIF²

¹School of Pharmaceutical Sciences, Universiti Sains Malaysia,
11800, Minden, Penang, Malaysia

²Department of Pharmacy, The Islamia University of Bahawalpur, Punjab, Pakistan

Abstract: The study aims to evaluate the diuretic effect and acute toxicity of a crude aqueous extract of *Nigella sativa* using animal models. To evaluate the diuretic activity of the plant, Albino rats were divided into five groups. The control group received normal saline (10 mL/kg), the reference group received furosemide (10 mg/kg) and the test groups were administered different doses (i.e., 10, 30 and 50 mg/kg) of the crude extract by intra-peritoneal route, respectively. Graph Pad Prism was used for the statistical analysis and p-values less than 0.05 were considered statistically significant. We observed significant diuretic, kaliuretic and natriuretic effects in the treated groups in a dose dependent manner. However, urinary pH remained unchanged during the course of the study. The diuretic index values showed good diuretic activity of the crude extract. The Lipschitz values demonstrated that the crude extract, at the dose of 50 mg/kg, showed 46% diuretic activity compared with furosemide. With regard to the acute toxicity study, no lethal effects were observed among Albino mice even at the higher dose of 5000 mg/kg. The extract of *Nigella sativa*, at the dose of 50 mg/kg, significantly increased the urinary volume and modified the concentration of urinary electrolytes, and there was observed no signs of acute toxicity associated with the crude extract. Further studies are encouraged to isolate the pure phytochemical responsible for diuresis.

Keywords: *Nigella sativa*, saluretic, natriuretic, Lipschitz value, diuretic index, Na⁺/K⁺ ratio

Herbal plants as medicines are still the mainstay of health care in several developing as well as underdeveloping countries where people mostly rely on local herbs for food and cure of different ailments. The practice of traditional medicine is widespread in China, Japan, Pakistan, Sri Lanka and Thailand. In Pakistan, the local communities of different regions have centuries old knowledge and traditional practices of most of the plants occurring in their regions (1). This indigenous knowledge of plants has been transferred from generation to generation through oral communication and personal experiences (2). In early 1950's, up to 84% of Pakistani population relied on indigenous medicines for traditional health practices (3), but now this practice is only limited to the remote areas due to assorted reasons which are beyond the scope of this paper. *Nigella sativa* (family Ranunculaceae) (Ns) commonly known as Black Cumin is an annual herb that grows in the Mediterranean region and Western Asian countries including Pakistan. Black Cumin has been used as a natural healing aid in various cul-

tures and civilizations around the world, as well as a supplement to help maintaining good health (4).

Seeds of Ns are traditionally used as aromatic, diuretic, diaphoretic, stomachic, carminative, condiment, liver tonic and digestive aid (5, 6). Many studies have been conducted to scientifically prove the effects of Ns on cardiovascular and renal system. The oil of Ns has profound cardiovascular depressant effects, potent centrally acting antihypertensive and cardioprotective properties (7). The seed extract of Ns has also been proved to have renoprotective effects in a number of animal models (8, 9). Additionally, it has been demonstrated to have antioxidant, free radical scavenger and antibacterial activities against Gram-positive and Gram-negative bacteria (10, 11).

The aim of our study was to evaluate the diuretic properties of the aqueous extract of Ns seed in normal Albino rats. We also aimed to study the effect of the crude drug extract on the excretion of urinary electrolytes. Finally, the acute toxicity of the aqueous crude extract was studied in Albino mice.

* Corresponding author: e-mail: asif_pharmacist45@yahoo.com; phone: +60125303242

EXPERIMENTAL

Collection of plant material

About 600 g of dried seeds of *Ns* were purchased from the local market of Bahawalpur, Pakistan, and the well identified sample was deposited in the herbarium of Pharmacology laboratory at the Pharmacy Department, the Islamia University of Bahawalpur (IUB), Pakistan, and a voucher no. NS-SD-06-10-002 was allotted to the seeds for future reference.

Aqueous extraction

After removing the foreign material, the seeds were ground with an electric grinder (National, MJ-176NR, China) into a coarse powder. Approximately, 0.5 kg of ground material was soaked in hot boiling water (1 L) at room temperature (23–25°C) for 3 days with occasional shaking followed by filtration (muslin cloth and filter paper [Whatman, Grade 1]). This procedure was repeated three times. Finally, the resultant filtrate was evaporated in a rotary evaporator (Heidolph Laborota 4000 efficient, Germany) under reduced pressure (-760 mm Hg) to a thick, semi-solid pasty mass of dark greenish color (the crude extract). The yield of the crude extract of *Nigella sativa* (Ns.Cr.) was about 8%. Ns.Cr. was completely solubilized in distilled water and normal saline for use in *in vitro* and *in vivo* experiments (12).

Experimental controls

A loop diuretic (Furosemide; Lasix, Aventis Pharma, Pakistan), was used as positive control (reference drug) and 0.9% sodium chloride (Merck, Germany) was used as control drug, respectively.

Animal housing and treatment

Animals (Albino rats and mice) were kept in polycarbonate cages (Techniplast, Italy), and were housed under the standard conditions of temperature, humidity and dark/light cycles (12 h/12 h). The animals were given pelleted food and drinking water *ad libitum*. The bedding of the animal cages was changed after every 48 h. Ns.Cr. was given by intraperitoneal (*i.p.*) route for the diuretic activity, and by the oral route for the acute toxicity study (13). Three days prior to the experimentation, the animals were caged daily for 6 h in the metabolic cages for acclimatization to the experimental conditions. The animals were also kept in an isolated area away from the normal flow of the students to avoid the stress and other psychological effects which may influence diuresis.

Phytochemical screening

The standard procedures were used to test the presence of a variety of secondary metabolites (alkaloids, flavonoids, saponins, anthraquinones, coumarins, and tannins) in the crude aqueous extract (12–14).

Diuretic activity

Adult Albino rats of either sex, weighing 200–220 g, were divided into five groups of six animals each. Prior to experimentation, the animals were screened for any visible signs of disease, and only the healthy animals were selected for the study. The study was performed at a normal room temperature (25 ± 2°C). Before the administration of the extract/controls, the bladder of the rat was emptied by gentle compression of pelvic area and pulling of tails. Group I (the control group) was given 10 mL/kg of normal saline, Group II (the reference group) was given 10 mg/kg of furosemide and the test groups (III, IV and V) were administered different doses of Ns.Cr., respectively. All the doses were prepared in the same volume of normal saline in order to ensure that each animal received the same volume of liquids. Owing to ease of administration and freedom to administer large volume of fluids, the *i.p.* route was used for the administration of extract/controls. Immediately after administration, the animals were placed in metabolic cages (one animal per cage), specially designed to separate urine and feces. The urine, collected in graduated vials, was measured at the end of 6 h and expressed as mL/100 g of body weight per 6 h (12, 15). The animal handling protocol was approved by board of advanced studies under the registration number of IU/125 M.Phil/2009.

Urinary parameters

The concentration of Na⁺ and K⁺ ions in the fresh urine samples was estimated using calibrated flame photometer (Corning 410, UK) and was expressed in parts per million (ppm). Before estimating the electrolyte levels, the samples were filtered to remove debris and shedding (16, 17).

A calibrated pH meter (WTW-Series pH-720) was used to measure the pH of the fresh urine samples (12).

Calculation of diuretic index, Lipschitz value, saluretic index and Na⁺/K⁺ ratio

The following formulas were used for the calculation of different urinary parameters (16, 17):
diuretic index = Mean urine volume of the test group/Mean urine volume of the control group;

Lipschitz value = Mean urine volume of the test group/Mean urine volume of the reference group;

saliuretic index = Concentration of electrolyte in urine of the test group/Concentration of electrolyte in urine of the control group;

Na^+/K^+ ratio = Concentration of Na^+ in urine of a group/Concentration of K^+ in urine of the same group.

Acute toxicity

Albino mice of 18–25 g body weight were used to study acute toxicity of Ns.Cr. The animals were divided into five groups of five mice each. The control group of mice was administered normal saline (10 mL/kg), while other groups received increasing doses of extracts, up to 5000 mg/kg. All the treatments were administered by oral gavage.

After administration, the animals were observed closely for 2 h, and then at 30 min intervals for 6 h for any visible sign of toxicity (i.e., salivation, lachrymation, ptosis, squinted eyes, writhing, convulsions, tremors, yellowing of fur, loss of hair),

stress (i.e., erection of fur and exophthalmia), behavioral abnormalities (i.e., impairment of spontaneous movement, climbing, cleaning of face and ataxia, and other postural changes), aggressive behavior (i.e., biting and scratching behavior, licking of tail, paw and penis, intense grooming behavior and vocalization) and diarrhea. Mortality of the animals was noted at the end of 24 h (12, 13).

Data analysis

The data were expressed as the mean \pm standard error of the mean (S.E.M.). Student *t*-test was applied to test difference among the groups, and *p*-values less than 0.05 were considered significant. We used Graph Pad Prism (Graph PAD, San Diego, USA) for statistical analysis.

RESULTS

Phytochemical screening

The preliminary qualitative phytochemical analysis of Ns.Cr. revealed that it was positive for

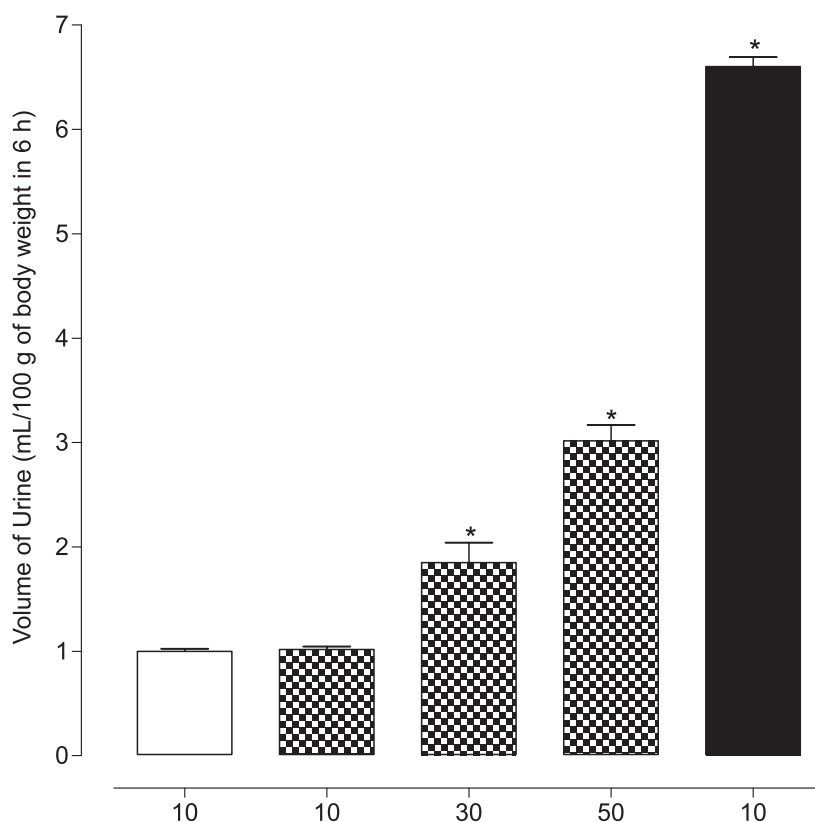


Figure 1. The effect of the Ns.Cr. on urination in Albino rats. Values shown are the mean \pm SEM of six observations and the values are compared with control group and considered significant as $*p < 0.05$. \square = Normal saline [mL/kg]; \checkmark = Ns.Cr [mg/kg]; \blacksquare = Furosemide [mg/kg]

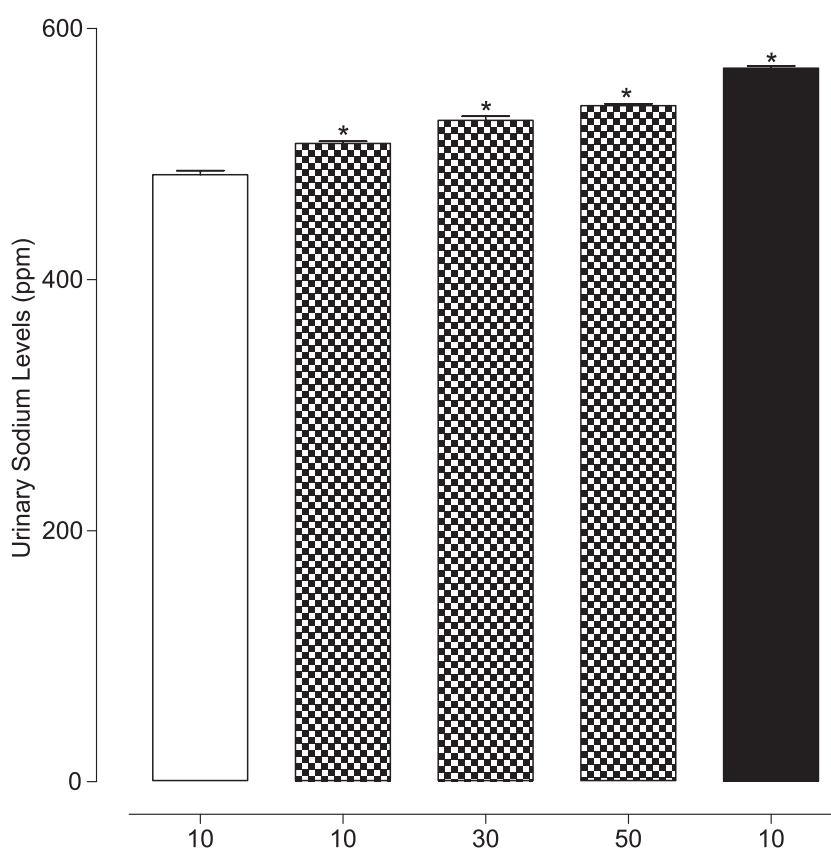


Figure 2. The effect of the Ns.Cr. on urinary sodium levels in urine. The values shown are the mean \pm SEM of six observations and the values are compared with the control group and considered significant at $*p < 0.001$. \square = Normal saline [mL/kg]; \checkmark = Ns.Cr. [mg/kg]; \blacksquare = furosemide [mg/kg]

Table 1. Effect of *Nigella sativa* aqueous extract on urinary volume and electrolyte concentration.

Group	Extract & dose [mg/kg]	Volume of urine [mL/6 h]	Urine sodium [ppm]	Urine potassium [ppm]	pH	Diuretic index	Lipschitz value	Saliuretic index		Na ⁺ /K ⁺
								Na	K	
1	Normal saline 10 [mL/kg]	1.0 \pm 0.3	483.3 \pm 3.3	26.3 \pm 0.2	7.0	—	—	—	—	18.38
2	Furosemide 10	*6.5 \pm 0.1	*568.3 \pm 1.7	*48.8 \pm 0.5	7.8	6.5	—	1.18	1.86	11.64
3	Ns.Cr. 10	1.0 \pm 0.1	*508.3 \pm 1.6	*42.1 \pm 0.1	6.9	1.0	0.15	1.05	1.60	12.07
4	Ns.Cr. 30	*1.9 \pm 0.2	*526.7 \pm 3.3	*47.1 \pm 0.1	6.9	1.9	0.29	1.09	1.79	11.18
5	Ns.Cr. 50	*3.0 \pm 0.1	*538.3 \pm 1.7	*47.8 \pm 0.1	7.0	3.0	0.46	1.11	1.81	11.26

Values given are the mean \pm SEM of six observations. All values are compared with control group and considered significant at $*p < 0.001$.

alkaloids, anthraquinones, flavonoids, saponins and tannins, while negative for coumarins.

Diuretic effects

The *i.p.* administration of Ns.Cr. increased the urinary flow in a dose-dependent manner (Fig. 1). When compared with the control group, 1.9 and 3.0

fold increase in urine output was observed in the group IV and V, respectively.

The diuretic index values of the test groups (group III, IV and V) were 1.0, 1.9 and 3.0, respectively, which indicated a good diuretic activity at the dose of 50 mg/kg (Table 1). The Lipschitz values demonstrated that, at the doses of 10, 30 and 50

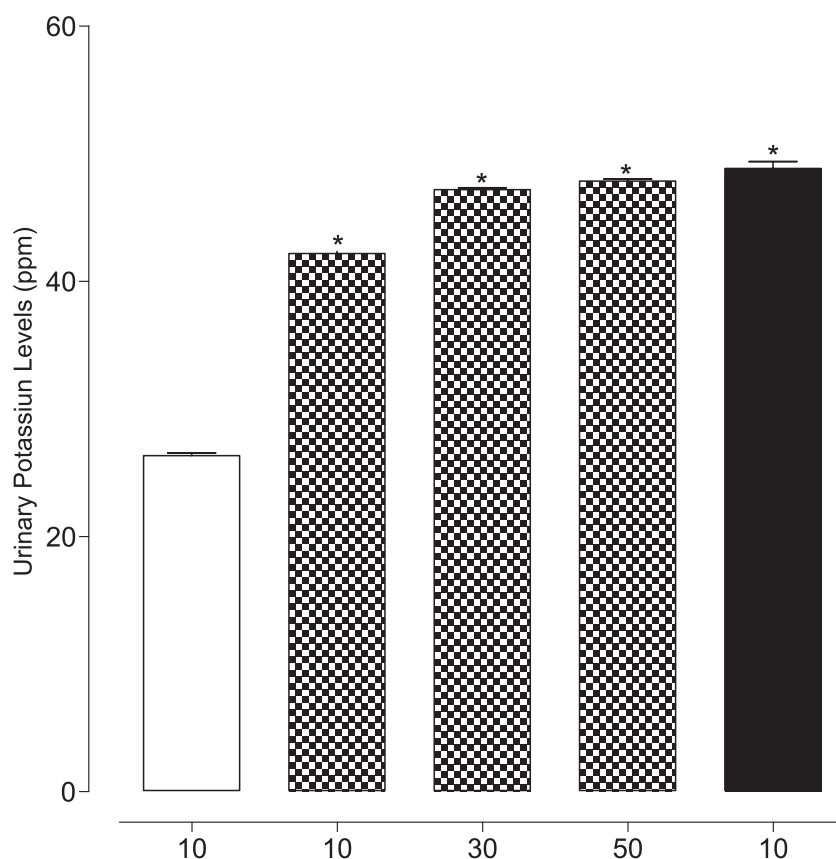


Figure 3. The effect of the Ns.Cr. on urinary potassium levels in urine. The values shown are the mean \pm SEM of six observations and the values are compared with the control group and considered significant at *** $p < 0.001$. \square = Normal saline [mL/kg]; \square (checkered) = Ns.Cr. [mg/kg]; \blacksquare = furosemide [mg/kg]

mg/kg, Ns.Cr. showed 15%, 29% and 46% of diuretic activity, respectively, compared with furosemide (Table 1).

Urinary electrolyte and pH

Ns.Cr. produced significant natriuretic effects in a dose dependent manner, especially at the dose of 50 mg/kg (Fig. 2).

A dose-dependent increase in the excretion of urinary potassium was observed after the *i.p.* administration of Ns.Cr. (Fig. 3). Especially, at the dose of 50 mg/kg, the concentration of potassium excretion was almost the same compared to the furosemide treated group. The saluretic index values also showed a stepwise increase in the excretion of Na^+ and K^+ in the urine samples of the treated groups. The Na^+/K^+ ratio was also calculated to estimate the degree of excretion of the electrolytes with respect to each other. The values of Na^+/K^+ ratio showed that, with the increase in dose, K^+ excretion was relatively higher than Na^+ .

The pH of fresh urine samples in control and treated groups was not significantly different (Table 1).

Acute toxicity

In the acute toxicity study, no visible signs of toxicity or any other abnormal behavior were observed in the test animals even, at the dose of 5000 mg/kg of body weight.

DISCUSSION

Due to a broad range of medicinal uses and extremely safe nature of Ns, it is studied extensively for a variety of secondary metabolites, and is scientifically proved to have proteins, carbohydrates, fats, mucilage, alkaloids, flavonoids, glycosidal saponins, tannins, resins, bitter principles and minerals (18). Our preliminary phytochemical investigation also confirmed the presence of alkaloids, anthraquinones, flavonoids, saponins and tannins in

the Ns.Cr, which was in accordance with the above mentioned studies. Alkaloids, flavonoids, saponins and organic acids have been shown to produce diuresis (13, 19), which indicates that, in our study, the diuretic activity of Ns.Cr. might be due to these secondary metabolites.

Herbal medicine, which is also called as botanical medicine, is the use of herbs as a medicine. Herbal plants produce and contain different classes of chemical substances eliciting a variety of pharmacological actions. Herbalists use the fruits, flowers, leaves, roots, stems and seeds of the plants for the prevention and treatment of various disorders. It is a fact that many well known treatments of the twentieth century were developed from the plants. Today, science has explored the medicinal properties of a large number of botanicals, and their healing components have been extracted and analyzed. Many plant components are now synthesized in large laboratories for use in the pharmaceutical preparations. For example, vincristine (an antitumor drug), digitalis (a heart regulator), and ephedrine (a bronchodilator) were all originally discovered through research on plants (20).

In the developed as well as in developing countries, still the use of medicinal plants for the cure of different ailments is a common practice. In some cases, extracts of medicinal plants are used by the traditional healers for renal disorders (21). A number of different botanical medicines have shown the promise in the treatment of a variety of urologic disorders and around 85 species of plants belonging to diverse families have been demonstrated to have diuretic activity. In addition, the Commission E approves at least 12 plant extracts as diuretics, indicating the need of further detailed studies of natural herbs for the treatment of different ailments (22).

It is now evident through research that the renal dysfunction is a common comorbidity accompanying the uncontrolled hypertension. By controlling high blood pressure, progression of renal disease may be halted. Likewise, the antioxidants are scientifically proven to have renoprotective effects in numerous animal models and may be administered as an adjuvant therapy in hypertensive patients with compromised renal function.

Within this context, plants like *Nigella sativa*, which contains secondary metabolites with diuretic and antioxidant activities (23), are expected to be the ideal candidates for the treatment of hypertension associated with renal disorders. The results of our study showed that Ns.Cr. have dose dependent diuretic effects. Studies have shown that the crude herbal extracts have dual activity at different doses

due to the presence of a variety of phytochemical constituents acting on different components of the biological system (24).

The diuretic activity of an extract is considered to be good if the diuretic index values of treated groups are greater than 1.50 (13, 19). In our study, the diuretic index values of the treated groups (III, IV and V) were 1.0, 1.9 and 3.0, respectively. This indicates 3-fold increase in the urine volume in the Group V. Lipschitz values also showed that, at the maximal dose (50 mg/kg), the plant showed 46% of diuretic activity compared with furosemide. The mild diuretic activity of crude extract, as compared to the standard drug, necessitates further fractionation and isolation of pure secondary metabolite(s) responsible for the diuretic activity of this plant extract.

An excess of Na^+ in body fluids is considered to be one of the important external factors in idiopathic hypertension and one of the main reasons for the deformities of arterial blood pressure (25). Our study showed that, compared with the saline treated group, the *i.p.* administration of Ns.Cr. produced significant natriuretic effects in a dose dependent manner. This finding highlights the medicinal use of Ns.Cr in the control of hypertension. However, at the dose of 50 mg/kg, the amount of Na^+ excretion was significantly lower than that of the reference standard indicating a lower probability of inducing hyponatremia. Likewise, the excretion of K^+ in the urine was also significantly increased in a dose-dependent manner but it is noteworthy that concentration of K^+ in the urine of the treated groups, especially at the dose of 50 mg/kg, was the same as that of the reference treated animals, reflecting the loop diuretic like activity of our extract.

CONCLUSION

Combined with published antioxidant and renoprotective effects of Ns (10, 11, 23), the present study indicates that Ns.Cr. has strong potential to be used as a diuretic agent. However, activity guided fractionation is required to separate the potent diuretic phytochemical constituents.

Acknowledgment

We would like to thank Professor Dr. Karamat Mehmood at Department of Chemistry, IUB for his valuable contribution in phytochemical analysis. We are extremely thankful to the laboratory staff at the Department of Pharmacy, IUB, for the supply of chemicals, reagents and animals. The bench work

was performed at the Department of Pharmacy, the Islamia University of Bahawalpur, Punjab, Pakistan.

Conflict of interest: Not declared.

REFERENCES

1. Alam N., Shinwari Z.K., Ilyas M., Zahid U.: Pak. J. Bot. 43, 773 (2011).
2. Shinwari Z.K.: J. Med. Plants Res. 4, 161 (2010).
3. Hocking G.M.: Pakistan Medicinal Plants. T. Qual. Plant. Mater. Veg. 5, 145 (1958).
4. Abu-Zinadah O.A.: J. King Abdulaziz Univ. Sci. 21, 335 (2009).
5. Usmanghani K., Saeed A., Alam, M.T.: Indusynic Medicine: Traditional Medicine of Herbal, Animal and Mineral Origin in Pakistan. p. 310–311. B.C.C. and T. Press, University of Karachi, Pakistan 1997.
6. Gilani A.H., Jabeen Q., Khan A.U.: Pak. J. Biol. Sci. 7, 441 (2004).
7. Ebru U., Burak U., Yusuf S., Reyhan B., Arif K., Faruk T.H., Emin M. et al.: Basic Clin. Pharmacol. Toxicol. 103, 574 (2008).
8. Ragheb A., Attia A., Eldin W. S., Elbarbry F., Gazarin S., Shoker, A.: Saudi J. Kidney Dis. Transpl. 20, 741 (2009).
9. Yaman I., Balikci E.: Exp. Toxicol. Pathol. 62, 183 (2010).
10. Khan M. A., Ashfaq M. K., Zuberi H. S., Mahmood M. S., Gilani A.H.: Phytother. Res. 17, 183 (2003).
11. Sen N., Kar Y., Tekeli Y.: J. Food Biochem. 34, 105 (2010).
12. Asif M., Jabeen Q., Abdul Majid A.M.S., Atif M.: Pak. J. Pharm. Sci. 27, 1811 (2014).
13. Asif M., Atif M., Malik A.S.A., Dan Z.C., Ahmad I., Ahmad A.: Trop. J. Pharm. Res. 12, 967 (2013).
14. Tona L., Kambu K., Ngimbi N., Cimanga K., Vliellnck A.J.: J. Ethnopharmacol. 61, 57 (1998).
15. Asif M., Atif M., Sulaiman S.A.S., Hassali M.A., Shafie A.A., Haq N., Saleem F.: Value Health 15, A644 (2012).
16. Sathianarayanan S., Jose A., Rajasekaran A., George R.M., Chittethu A.B.: Phytomedicine 2, 7 (2011).
17. Danamma K.A.K., Jayasimha B.G., Basha S.N.: Int. J. Pharm. Biol. Sci. 1, 160 (2011).
18. Shabina I., Muhammad A., Muhammad Q.H., Mudassir A. Int. J. Agri. Bio. 15, 1151 (2013).
19. Patel U., Kulkarni M., Undale V., Bhosale A.: Trop. J. Pharm. Res. 8, 215 (2009).
20. Srichaikul B., Supachai S., Gordon B., Sunthorn D., Saksum J.: Advan. Natur. Sci. 5, 11 (2012).
21. Yarnell E.: World J. Urol. 20, 285 (2002).
22. Clare B.A., Conroy R.S., Spelman K.: J. Altern. Complement. Med. 15, 929 (2009).
23. Rastogi L., Feroz S., Pandey B.N., Jagtap A., Mishra K.P.: Int. J. Radiat. Biol. 86, 719 (2010).
24. Mehmood M.H., Aziz N., Ghayur M.N., Gilani A.H.: Dig. Dis. Sci. 56, 1460 (2011).
25. Hoareau L., DaSilva E.J.: Electron. J. Biotechnol. 2, 56 (2009).

Received: 27. 11. 2013

ANTIOXIDANT AND ANTI-INFLAMMATORY ACTIVITY
OF *POTENTILLA REPTANS* L.MARINA T. TOMOVIC^{1*}, SNEZANA M. CUPARA¹, MARIJA T. POPOVIC-MILENKOVIC²,
BILJANA T. LJUJIC³, MARINA J. KOSTIC⁴ and SLOBODAN M. JANKOVIC⁴¹Department of Pharmacy, Faculty of Medical Sciences, University of Kragujevac,
Svetozara Markovica 69, 34000 Kragujevac, Serbia²Community Pharmacy Kragujevac, Kralja Aleksandra I Karadjordjevic 36, 34000 Kragujevac, Serbia³Center for Molecular Medicine and Stem Cell Research, Faculty of Medical Sciences,
University of Kragujevac, Svetozara Markovica 69, 34000 Kragujevac, Serbia⁴Department of Pharmacology, Faculty of Medical Sciences, University of Kragujevac,
Svetozara Markovica 69, 34000 Kragujevac, Serbia

Abstract: *Potentilla* species have been used in traditional medicine in the treatment of different ailment, disease or malady. *Potentilla reptans* (*P. reptans*) has been scarcely studied. The aim of this study was to test antioxidant and anti-inflammatory activity of *P. reptans* aerial part and rhizome. DPPH assay was used to measure antioxidant activity of aqueous plant extracts. Anti-inflammatory effect was evaluated by experimental animal model of phenol-in-acetone induced mice ear edema. DPPH radical-scavenging activity of both tested extracts was concentration dependent with IC₅₀ values 12.11 µg/mL (aerial part) and 2.57 µg/mL (rhizome). Maximum anti-inflammatory effect (61.37%) was observed after administration of 10 mg/ear of the rhizome extract and it was 89.24% of effect induced by dexamethasone as a standard. In conclusion, *P. reptans* rhizome aqueous extract possesses anti-inflammatory effect and higher antioxidant activity than aerial part.

Keywords: *Potentilla reptans*, DPPH, anti-inflammatory effect, total phenols, flavonoids, procyanidins

Potentilla species have been used for a long time in traditional medicine of cultures in Europe, Asia and Northern America, such as *Potentilla erecta* which is official in pharmacopoeias of different European countries and was used for the treatment of purulent facial eczema and buccal ulcerations. Plants were mainly prepared in the form of water or alcoholic extract and applied either topically for the treatment of mouth ulcers, throat inflammation, wound-healing or internally in jaundice and dysentery. Traditional medicine sporadically employed *Potentilla* species in the treatment of hepatitis, rheumatism, scabies, diarrhea, viral infections and as a remedy for detoxification (1).

P. erecta, *P. anserina*, *P. aurea* and *P. reptans* were included in homeopathic pharmacopoeias for preparation of homeopathic remedies. In spite of a big variety of traditional uses for *Potentilla* species, studying phytochemistry and pharmacology of this genus has not been completed. Clinical studies of *P. erecta* rhizome extracts showed positive results in

the treatments of colitis ulcerosa and viral children diarrhea (2, 3).

Potentilla reptans (*P. reptans*) has been the least studied among the members of genus. Nine compounds have been found in aerial parts of *P. reptans*. They are flavonoids (kaempferol, quercetin, quercetin-3'-glucoside, quercetin-3,7-diglucuronide, 2',4',6',4-tetrahydroxychalkon-2'-O-β-D-glucoside), ellagic acid, p-coumaric acid, caffeic acid and ferulic acid (1). Animal models were used to test antiulcerogenic and antioxidant activities of *P. reptans* (4, 5). There are no data about chemical content or pharmacology available for the underground part of *P. reptans*.

P. reptans is a perennial plant with thick vertical rhizome, prostrate and elongated stem with a rosette of leaves. Petals are golden yellow, usually twice as long as sepals. The flowers have five petals, rarely four (6).

The aim of this study was to determine principle active compounds in aqueous extracts of *P. rep-*

* Corresponding author: e-mail: marinapop@gmail.com; phone: +381 34 306 800 ext. 225; fax:+381 34 306 800 ext. 112

tans rhizome and aerial part and to evaluate and compare antioxidative potential and anti-inflammatory effects of studied extracts.

EXPERIMENTAL

Extract preparation

P. reptans was collected from autochthonous sources in Serbia. The voucher specimens were deposited in Department of Biology, Faculty of Natural Sciences, University of Kragujevac and botanical garden of Department of Biology, Faculty of Natural Sciences, University of Belgrade, with number BEOU 16405.

Aerial part and rhizome were collected in May to August 2010 and separated. Sources of plant material were three different locations in Serbia: Sumarice nearby city of Kragujevac, Oplanić and Dobroselica on the mountain Zlatibor. The collected material was dried under the shade. Aqueous extracts were prepared separately extracting aerial part and rhizome of *P. reptans*. Forty grams of dried, milled parts of the plant were extracted by 600 mL of hot distilled water (7). Dry extracts were obtained by evaporation under reduced pressure (RV05 basic IKA, Germany).

Determination of the total phenols

Determination of the total phenols was performed according to the standard method of Singleton et al. (8), customized for 96-well microplates (9). We used Folin-Ciocalteu's reagent (FC) (Fisher Scientific, UK), anhydrous Na_2CO_3 (Analytika, Czech Republic) and gallic acid (Sigma Aldrich, Germany) as standard. The following concentrations of extracts were prepared: 0.5, 0.25, 0.125 and 0.063 mg/mL. Gallic acid (100–0.063 $\mu\text{g/mL}$), was used as a standard for plotting a calibration curve. Thirty microliters of each extract or standard solution was added to 150 μL of 0.1 mol/L FC reagent and mixed with 120 μL of sodium carbonate (7.5%) after 6 min. Absorbance at 760 nm was measured after 120 min. The content of total phenol compounds in examined extracts was expressed as mg of gallic acid equivalents (GA) per gram of dry extract weight.

Analysis of individual phenol compounds (HPLC)

Prepared extracts were diluted in mobile phase (0.05% HCOOH : MeOH , 1 : 1, v/v) to final concentrations of 20 mg/mL and 2 mg/mL and analyzed by HPLC with LC-MS/MS detection. A series of dilutions of 45 reference standards mixture was pre-

pared in 1.5 ng/mL to 25 $\mu\text{g/mL}$ range, to perform quantification. Separation was achieved using Series liquid chromatograph (Agilent Technologies 1200) coupled with Triple Quad mass selective detector with electrospray ion source (Agilent Technologies 6410A). Five microliters of extract/standard was injected and compounds were resolved on a Zorbax Eclipse XDB-C18 (50 \times 4.6 mm, 1.8 μm) column, set at 50°C. Mobile phase consisting of 0.05 % HCOOH and MeOH , was delivered in gradient mode (0 min 30% B, 6 min 70%, 9–12 min 100%, post time 3 min), at 1 mL/min flow. Eluted compounds were detected in dynamic SRM mode. Obtained results were analyzed using MassHunter Workstation Software – Qualitative Analysis (B.03.01). A calibration curve (MRM peak area vs. concentration) was plotted for each compound.

Determination of procyanidins

The content of procyanidins was calculated using the method described in European Pharmacopoeia 6.0 (10) and expressed as equivalent of cyanidin chloride. We used butanol (BuOH) (POCH, Poland) and cyanidin-chloride (Carl Roth, Germany). The investigated extract was hydrolyzed under reflux by an EtOH/HCl mixture. Procyanidins were separated with BuOH from the aqueous layer. The absorbance was measured at 550 nm by spectrophotometer (Cecil CE 2021) (11).

Determination of flavonoids

The content of flavonoids was calculated by aluminum chloride colorimetric method (12) adapted for 96-well microplates (9). We used $\text{AlCl}_3 \times 6\text{H}_2\text{O}$, $\text{CH}_3\text{COONa} \times 3\text{H}_2\text{O}$ (Centrohem, Serbia), quercetin (Sigma-Aldrich, Germany), methanol (MeOH) (J.T. Baker, USA). Test samples were prepared in concentrations of 10.0, 5.0, 2.5, 1.25 and 0.625 mg/mL. As standard we used quercetin. Thirty microliters of extract or standard was diluted by 90 μL of methanol and 6 μL of 10% aluminum chloride, 6 μL of 1 mol/L sodium acetate and 170 μL of distilled water were added. Absorbance at 415 nm was measured after 30 min. All samples were made in triplicate and mean values for flavonoid content were expressed as milligrams of quercetin equivalents per gram of dry extract weight calculated according to the standard calibration curve.

Evaluation of antioxidative activity

Investigated plant extracts were tested by DPPH assay according to the method of Soler-Rivas et al. (13). It was adapted for 96-well microplates (9, 14). We used the following materials: DPPH (α,α -

diphenyl- β -picrylhydrazyl) (Fluka, Switzerland), butylated hydroxytoluene (BHT) (Alfa Aesar, USA), butylated hydroxyanisole (BHA) (Merck, Germany), quercetin (Sigma-Aldrich, Germany), rutin (Fluka, Switzerland), propyl gallate (PG) (Alfa Aesar, USA), dimethyl sulfoxide (DMSO) (Sigma-Aldrich, Germany). Ten microliters of examined extract solutions, in series of seven concentrations of double dilution in DMSO (5.0–0.078 mg/mL for *P. reptans* aerial part and 0.345–0.005 mg/mL for *P. reptans* rhizome as initial concentration), were added to 100 μ L of 90 μ mol/L DPPH solution in methanol and the mixture was diluted with 190 μ L of methanol. After that, we have obtained final concentration for *P. reptans* aerial part 166.7–2.6 μ g/mL and for *P. reptans* rhizome 11.49–0.180 μ g/mL. As a control, the exact amount of extract was substituted with DMSO. Absorption at 515 nm was measured by the microplate reader after 60 min (Multiskan Spectrum, Thermo Corporation). Synthetic antioxidants (BHT, BHA, PG, quercetin and rutin) served as a positive control. The radical-scavenging capacity (RSC) was calculated by the equation:

$$\text{RSC} = 100 - (A_a - A_{\text{corr}}) / A_{\text{control}} \times 100$$

where A_a = average absorbance of the probes for a given concentration sample level; A_{corr} = correction of extract absorbance (with no reagents); A_{control} = absorbance of the DPPH radical (with no extract).

The extract concentration which causes 50% of DPPH inhibition (IC_{50}), was calculated from the RSC concentration curve.

Experimental animal edema model

Anti-inflammatory effect of investigated extracts was evaluated by experimental mouse ear edema model. Inflammation was induced by application of an irritant agent on the mouse ear. Treated animals received investigated extracts, while control animals received distilled water or dexamethasone as positive control, 15 min prior to the application of irritant agent. The ear edema was measured and compared among different animal groups. It was expressed as the difference of ear weight, with and without inflammation (15).

We used dexamethasone (Dexason[®], Galenika, Serbia), acetone in phenol (irritant agent) (Zorkapharma, Serbia).

Female and male BALB/c 5–6 weeks old mice, were used in this study (purchased from the Military Medical Academy, Belgrade, Serbia). They were kept in environmentally controlled conditions (22°C, 12 h light/dark cycle), in cages, with free access to standard pellet diet and water. Prior to the experiment, they fasted for 15 h. Adaptation to the

test environment lasted 2 h before the experiment. The experiment was approved by the Ethics Committee of Medical Faculty, Kragujevac, number 016427/2. All of the animal procedures complied with the National Institutes of Health guidelines for humane treatment of laboratory animals.

Animals were divided into eight groups, 8 animals in each. Six groups were treated by different concentrations of investigated aqueous extracts of *P. reptans* aerial part and rhizome (2.5, 5.0, 10.0 mg/ear). Two groups served as control, receiving distilled water or dexamethasone (0.08 mg/ear). Treated groups received extracts on the right ear, 15 min before the application of the irritant agent (20 μ L of 10% phenol in acetone). Both irritant agent and investigated extracts were applied on the inner and outer surface of the right ear.

The ear edema measurements were performed 1 h after irritant agent application. Edema was expressed as the difference between left and right ear weight, which appeared due to inflammatory challenge. One hour after induction of inflammation, mice were sacrificed by the overdose of ether anesthesia and both ears were removed. Edema was quantified as the weight difference between the two ears (16).

The anti-inflammatory effect was calculated as a percent of edema inhibition in the treated group of animals relative to the control of animals, using the relation:

$$\text{Edema /inhibition (\%)} = 100 [(Rt - Lt)/(Rc - Lc)]$$

where Rt = mean weight of right ear of treated animals; Lt = mean weight of left ear of treated animals; Rc = mean weight of right ear of control animals; Lc = mean weight of left ear of control animals.

Statistical analysis

The results are expressed as the mean \pm standard error of measurement (SEM). For statistical analysis one-way analysis of variance (one-way ANOVA) was used, followed by Dunnett T3 *post hoc* test, where applicable. The probability of null hypothesis lower than 0.05 ($p < 0.05$) was considered to be an indicator of statistically significant difference among experimental groups. All calculations were made by statistical software SPSS version 18.

RESULTS

Quantitative phytochemical analysis of major compounds found in the rhizome and aerial part of *P. reptans* is presented in Table 1.

Table 1. Quantitative phytochemical analysis of aqueous extracts of *P. reptans* rhizome (Pr-R) and areal part (Pr-A) (the mean value \pm SD of three measurements).

Active constituents	Pr-A	Pr-R
Total phenols (mg of GA ^a /g)	116.0 \pm 16	468.6 \pm 60
Flavonoid content (mg of Q ^b /g)	10.1 \pm 1	3.9 \pm 2
Procyanidin content (mg of C ^c /g)	1.11 \pm 0.30	98.4 \pm 4.3

^aGA = gallic acid, ^bQ = quercetin, ^cC = cyanidin chloride

Table 2. Quantitative and qualitative analysis of individual compounds found in rhizome (Pr-R) and aerial part (Pr-A) of *P. reptans*.

Compound name ^a	t _r ^b (min)	t _r ^c (min)	t _r ^d (min)	Quantification (mg/kg)	
				Pr-R	Pr-A
Chinic acid	0.48	0.48	0.48	87.2	78.7
Gallic acid	0.57	0.55		65.9	
Catechin	0.74	0.67		20103	
Protocatechuic acid	0.76	0.73	0.72	34.3	16.2
Epicatechin	0.97	0.93		39.7	
Esculetin	1.08		1.03		9.05
Caffeic acid	1.13		1.08		164
p-Coumaric acid	1.64		1.59		3.14
Luteolin-7-O-glucoside	2.12	2.06	2.06	6.50	13.50
Quercetin-3-O-glucoside	2.22		2.16		38.3
Rutin	2.17		2.12		49.1
Quercetin	2.75	2.70	2.70	150	47.5
Kaempferol-3-O-glucoside	2.80		2.74		27.5
Apigenin-7-O-glucoside	2.67		2.60		21.6
Kaempferol	4.49		4.42		3.72

^a The numbers refer to compounds signed on the HPLC spectrum ^b Retention times of the standards ^c Retention times of the compounds identified in the extract *P. reptans* rhizome. ^d Retention times of the compounds identified in the extract *P. reptans* aerial part.

Table 3. DPPH free radical scavenging activity of the *P. reptans* extracts aerial part (Pr-A) and rhizome (Pr-R).

Sample	IC ₅₀ ^a (μg/mL)
Pr-A	12.11 \pm 0.216
Pr-R	2.57 \pm 0.340
BHT	11.65 \pm 1.144
BHA	1.57 \pm 0.093
Quercetin	0.41 \pm 0.169
Rutin	1.42 \pm 0.173
PG	0.62 \pm 0.030

^a The mean value \pm SD of three measurements.

Quantitative and qualitative analyses of individual compounds found in rhizome and aerial part of *P. reptans* are presented in Table 2, Figures 1 and 2

Both investigated extracts of *P. reptans* possessed DPPH free-radical-scavenging activity. Rhizome showed slightly better antioxidant effect. When the extract of *P. reptans* aerial part was applied in the concentration range of 166.7-2.6 μg/mL, its DPPH free-radical-scavenging activity varied from 98.9 to 12.3% (IC₅₀ value 12.11 \pm 0.216 μg/mL). Application of *P. reptans* rhizome extract in the concentration range of 11.49-0.180 μg/mL possessed DPPH free-radical-scavenging activity 91.2-

1.1% (IC_{50} value $2.57 \pm 0.340 \mu\text{g/mL}$). Results of DPPH assay performed on *P. reptans* extracts are presented in Table 3.

P. reptans aqueous extract of rhizome reduced edema in experimental mouse ear model in a dose-dependent manner. Maximum edema reduction of 61.37% was observed for the concentration 10 mg/ear of rhizome extract. In the same conditions of experiment, dexamethasone (used in concentration of 0.08 mg/ear) achieved 68.77% of edema inhibition. It should be noted that other investigated concentrations of *P. reptans* aerial part and rhizome have shown some edema reduction effect, only 10 mg/ear of rhizome extract and 0.08 mg/ear dexamethasone as positive control have produced statistically significant reduction (Table 4).

DISCUSSION AND CONCLUSION

Natural compounds with antioxidant properties play an important role as mediators in reactions where reactive oxygen species are being formed. Diminishing harmful potential of these reactive structures, natural antioxidants such as different types of phenol compounds, may prevent development of chronic and/or debilitating diseases such as cancer, cardiovascular diseases, etc. (17, 18).

Our results suggested that rhizome extract of *P. reptans* is four times richer in total phenol compounds than *P. reptans* aerial part. Interestingly, flavonoid content of aerial part is higher than flavonoid content of rhizome. We observed that procyanidins are main contributors to the high value

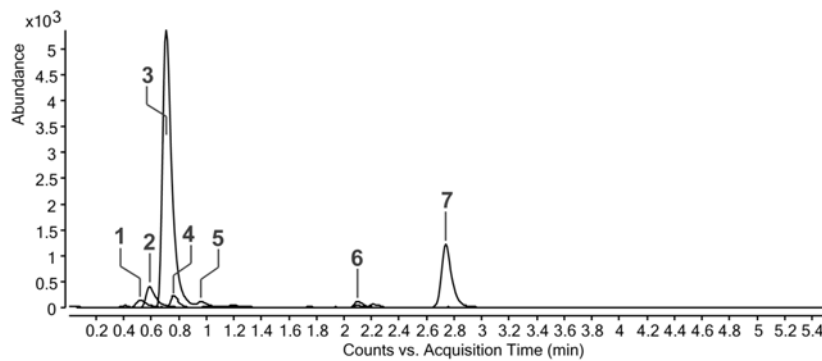


Figure 1. HPLC chromatogram of *Potentilla reptans* rhizome aqueous extract: 1 – chonic acid, 2 – gallic acid, 3 – catechin, 4 – protocatechuic acid, 5 – epicatechin, 6 – luteolin-7-O-glucoside, 7 – quercetin

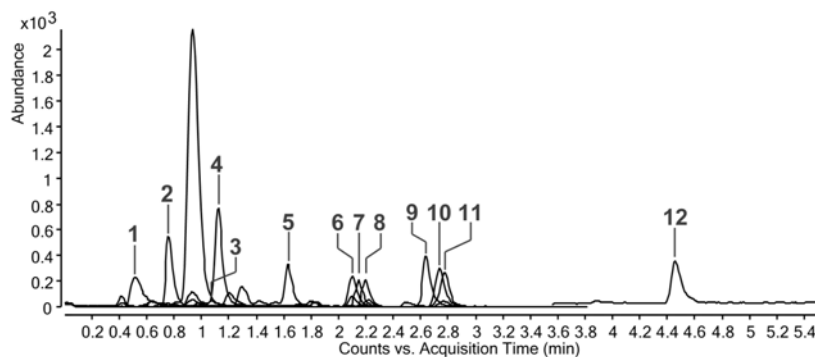


Figure 2. HPLC chromatogram of the aqueous extract of *Potentilla reptans* aerial parts: 1 – chonic acid, 2 – protocatechuic acid, 3 – esculetin, 4 – caffeic acid, 5 – p-coumaric acid, 6 – luteolin-7-O-glucoside, 7 – rutin, 8 – quercetin-3-O-glucoside, 9 – apigenin-7-O-glucoside, 10 – quercetin, 11 – kaempferol-3-O-glucoside, 12 – kaempferol

Table 4. Inhibition of edema by *P. reptans* aerial part (Pr-A) and *P. reptans* rhizome (Pr-R).

Sample	Concentration (mg/ear)	Edema (mg)	Inhibition (%)
Pr-R	2.5	21.61 ± 9.91	14.18
Pr-R	5	17.54 ± 11.78	30.34
Pr-R	10	9.73 ± 4.22 ^a	61.37
Pr-A	2.5	19.89 ± 9.46	21.00
Pr-A	5	26.36 ± 7.74	-4.71
Pr-A	10	18.47 ± 17.75	26.62
Dexamethasone (control)	0.08	7.86 ± 4.74 ^a	68.77
Water (control)	0	25.18 ± 9.24	0

^ap < 0.05 comparison with control groups.

of total phenols in *P. reptans* rhizome (Table 1). Comparing individual phenol compounds in *P. reptans* aerial part and rhizome we observed that most phenol compounds are present in aerial part in higher content than in rhizome, with exception of gallic acid, catechin, epicatechin, protocatechuic acid and quercetin, which are dominantly present in rhizome. Flavonoids are considered as powerful antioxidants among plant-derived phenols and particularly kaempferol, quercetin and rutin were studied (19, 20). Caffeic acid and p-coumaric acid also exhibit noticeable antioxidant effect (21, 22). Although literature data suggest that apigenin, luteolin and kaempferol have been found in rhizome of *P. species* (23-26), we have not identified these compounds in *P. reptans* rhizome. The amount of procyanidins we found in *P. reptans* rhizome (98.4 g/kg) is higher than the one found in *P. alba* root (80 g/kg dry weight) (27). We also compared our results with the content of total phenols, flavonoids and procyanidins found in the comparative study of aerial part of ten different species of *Potentilla*. *P. reptans* aerial part contains 116.0 mg/g of total phenols, which is the second highest value of phenols in comparative analysis, after *P. fruticosa* (116.3 mg/g). *P. reptans* aerial part is richer in total flavonoids (10.1 mg/g) than *P. fruticosa* (7.0 mg/g). Aerial part of *P. reptans* have the smallest quantity of procyanidins 1.1 mg/g among other compared species (28).

Catechin, condensed tannin which is thoroughly researched plant-derived phenol, shows anti-inflammatory effect and protects against oxidative stress (29). Studies on quantification of catechin in different plants, have various results. They differ and imply that some parts/organs of plants like fruits are scarce sources of catechin, while others are con-

sidered as dominant source of catechin (30, 31). We found unusually high quantity of catechin (20.1 g/kg) in rhizome, which is in accordance with data for some *Potentilla* species (1). On the contrary, catechin has not been found in *P. reptans* aerial part. The similar discrepancy between contents of aerial part and rhizome was observed for epicatechin, kaempferol, caffeic acid and p-coumaric acid. Kaempferol, caffeic acid and p-coumaric acid are present dominantly in aerial part, while epicatechin was found only in rhizome. We therefore, suggest that *P. reptans* rhizome represents a considerable source of epicatechin and catechin.

In our study we used DPPH method in order to determine antioxidant effect of *P. reptans* extracts. DPPH method is a useful and reliable tool for estimating free-radical scavenging activity of phenolic compounds (32). Antioxidant activity of *P. reptans* rhizome was observed to be more than five times higher than antioxidant activity of *P. reptans* aerial part (Table 3), though both extracts gave concentration dependent response. In relation to standards, antioxidant activity of rhizome was higher than BHT, lower than quercetin, BHA, PG and rutin.

Previous research of plant material noted a positive correlation between content of total phenols and antioxidant activity (33, 34). In our study, rhizome of *P. reptans* showed free-radical scavenging activity, as have done also other *P. species* extracts made by different solvents and tested by DPPH assay (27, 35, 36). As literature data suggest, catechin act as powerful antioxidant (29). We found catechin to be a major component of *P. reptans* rhizome and it guides to think that free-radical scavenging activity exerted by *P. reptans* rhizome depends in major on abundant presence of catechin. Our

assumption that catechin in rhizome may be a strong contributor to the observed antioxidant activity, is based on the fact that our results for IC_{50} finely correlate with results obtained in a similar experiment of aqueous extract of *Bergenia crassifolia* rhizome, (positive relation between catechin content and IC_{50}) (34). Therefore, we propose that high content of total phenols, particularly content of catechin in rhizome of *P. reptans*, significantly contributes to strong antioxidant effect performed by aqueous rhizome extract. Considering that substances possessing IC_{50} values = 50 $\mu\text{g/mL}$ in the DPPH assay have been categorized as active antioxidants (37, 38), we think that based on our results for IC_{50} (2.57 $\mu\text{g/mL}$ rhizome and 12.11 $\mu\text{g/mL}$ aerial part), both extracts may be categorized as active antioxidants. We are aware of synergic action of individual compounds found in plant material as a valid fact, but high amount of catechin present in rhizome seems to be mainly responsible for antioxidant effect exerted by rhizome extract. Analyzing content of individual phenol compounds in aerial part we found that the presence of caffeic acid is the highest. Since caffeic acid is categorized as an active antioxidant (21), we may attribute the effects of antioxidant activity of aerial part of *P. reptans* to its content of caffeic acid.

It is noticeable that the presence of procyanidins, which lately attracted attention of nutrition and medicine, as potent protective antioxidants for human health (39) may also contribute to antioxidant action of rhizome, since considerably higher content of procyanidins was found in rhizome of *P. reptans* than in aerial part.

Studies of *Potentilla* genus reveal that antioxidant effect of some *P. species* (*P. alba* root) is correlated to the content of phenol derivatives (catechin, epicatechin etc.) (28). Our opinion is that this study complements current research of *P. species* (1). *P. reptans* rhizome is richer in total phenols than aerial part and we think that it is why rhizome possessed stronger antioxidant activity than aerial part.

Natural plant-derived antioxidants prevent reactive oxygen species (ROS) to initiate or speed many conditions where inflammatory mediators are implicated (40, 41). Antioxidants lower presence of ROS, which induce release and production of various pro-inflammatory mediators responsible for the inflammation, such as IL-1, IL-6, IL-8, TNF- α , leukotrienes and prostaglandins (42). Experimental model for studying inflammation employees phenol as irritant agent (43). When phenol comes into direct contact with the skin, it damages membranes of keratinocytes. As a result, cytokines are released (IL-1 α , TNF- α and IL-8), which is followed by further

release of other inflammatory mediators (arachidonic acid metabolites) (44, 45). This way an acute local inflammatory response is produced and thus, phenol is a good irritant agent for simulating inflammation (44).

Numerous investigations have shown that phenol compounds found in plants, in particular flavonoids and phenolcarboxylic acids, may act as anti-inflammatory agents (45). In our experiment, *P. reptans* rhizome aqueous extract showed anti-inflammatory effect. *P. reptans* aerial part achieved no significant anti-inflammatory effect. Edema inhibition produced by 10 mg/ear of rhizome extract was 61.27% and is comparable with other results for aqueous plant extracts (57.0% by 5 mg/ear (16), 36.3% by 200 mg/ear (38)). In comparison with effect induced by dexamethasone as standard (15), concentration of 10 mg/ear of *P. reptans* rhizome extract produced maximum edema reduction of 89.24%.

Catechin inhibits release of proinflammatory cytokines (IL-1, TNF- α and prostaglandin E_2) (46). Quercetin, also found in our investigated extracts, is effective inflammation suppressor (45). The results of this investigation provided evidence that *P. reptans* rhizome extract is topically active in the attenuation of acute dermatitis induced by phenol, in a manner similar to dexamethasone, as the reference anti-inflammatory drug (47). On the basis of our results of DPPH assay and content of phenol compounds in rhizome of *P. reptans*, particularly of catechin present as a major component, we suggest hypothesis that phenol compounds in rhizome may be responsible for anti-inflammatory effect achieved by *P. reptans* rhizome extract.

Our study brings more information about little data available on *P. reptans*. We found that both rhizome and aerial part are good source of total phenols, which are more present in rhizome than in leaves. Rhizome also contains more procyanidins than aerial part. Content of catechin, as a major component is unusually high, catechin being present exclusively in rhizome of *P. reptans*. Aqueous extracts of rhizome and aerial part showed antioxidant activity on DPPH assay, rhizome being more potent antioxidant than aerial part. Both investigated extracts belong to group of active antioxidants. Aqueous extract of *P. reptans* rhizome possesses anti-inflammatory activity.

Since this plant has been scarcely studied up to now, this work may represent a modest contribution to completion of findings on *Potentilla species*. We consider that characterization of aqueous extracts of different parts of *P. species* con-

firms that traditional medicinal uses of this plant should not be disregarded. On the bases of different applications of this plant in ethno-medicine and the fact that it may be considered as an active antioxidant for health preservation, we find appropriate to suggest further pharmacological research of this plant.

Acknowledgment

The authors would like to express gratitude to the Medical Faculty, University of Kragujevac for Grant No. JP 28/10 and Ministry of Education and Science of the Republic of Serbia for Grant No. 175014.

Conflict of interest

The authors have declared that there is no conflict of interest.

REFERENCES

- Tomczyk M., Latté K.P.: *J. Ethnopharmacol.* 122, 184 (2009).
- Huber R., Dittfurth A.V., Amann F., Guthlin C., Rostock M., Trittler R., Kummerer K., Merfort I.: *J. Clin. Gastroenterol.* 41, 834 (2007).
- Subbotina M.D., Timchenko V.N., Vorobyov M.M., Konunova Y.S., Aleksandrovih Y.S., Shushunov S.: *Pediatr. Infect. Dis. J.* 22, 706 (2003).
- Gurbuz I., Ozkan A.M., Yesilada E., Kutsal O.: *J. Ethnopharmacol.* 101, 313 (2005).
- Avci G., Kupeli E., Eryavuz A., Yesilada E., Kucukkurt I.: *J. Ethnopharmacol.* 107, 418 (2006).
- Chaoluan L., Ikeda H., Ohba H.: *Flora of China* 9, 291 (2003).
- Tomczyk M., Leszczyńska K., Jakoniuk P.: *Fitoterapia* 79, 592 (2008).
- Singleton V.L., Orthofer R., Lamuela-Raventos R.M.: *Methods Enzymol.* 299, 152 (1999).
- Beara N.I., Lesjak M.M., Jovin Đ.E., Balog J.K., Anačkov T.G., Orčić Z.T., Mimica-Dukić M.N.: *J. Agric. Food Chem.* 57, 9268 (2009).
- European Pharmacopoeia 6.0, 5th edn., p. 1712, Council of Europe: Strasbourg, France 2008.
- Porter L.J., Hristich L.N., Chan B.G.: *Phytochemistry* 25, 223 (1986).
- Chang C.C., Yang M.H., Wen H.M., Chern J.C.: *J. Food Drug Anal.* 10, 178 (2002).
- Soler-Rivas C., Espin J.C., Wichers H.J.: *Phytochem. Anal.* 11, 330 (2000).
- Orčić Z.D., Mimica-Dukić M.N., Francišković M.M., Petrović S.S., Jovin D.E.: *Chem. Cent. J.* 5, 34 (2011).
- Leite G.O., Leite L., Sampaio R.S., Araruna M.K., Menezes I.R., Costa Ł.G., Campos A.R.: *Fitoterapia* 82, 208 (2011).
- Okoli C.O., Akah P.A., Onuoha N.J., Okoye T.C., Nwoye A.C., Nworu C.S.: *BMC Complement. Altern. Med.* 8, 27 (2008).
- Halliwell B.: *Free Radic. Res.* 25, 57 (1996).
- Halliwell B.: *Nutr. Rev.* 57, 104 (1999).
- Havsteen B.H.: *Pharmacol. Ther.* 96, 67 (2002).
- Sun C., Fu J., Chen J., Jiang L., Pan Y.: *J. Sep. Sci.* 33, 1018 (2010).
- Gülçin I.: *Toxicology* 16, 213 (2006).
- Gülçin I., Topal F., Çakmakçı R., Bilsel M., Gören A.C., Erdogan U.: *J. Food Sci.* 76, C585 (2011).
- Xue P., Zhao Y., Wang B., Liang H.: *J. Chromatogr. Sci.* 45, 216 (2007).
- Wollenweber E., Dorr M.: *Biochem. Syst. Ecol.* 36, 481 (2008).
- Xue P.F., Luo G., Zeng W.Z., Zhao Y.Y., Liang H.: *Biochem. Syst. Ecol.* 33, 725 (2005).
- Yang J., Wen X., Jia B., Mao Q., Wanga Q., Laib M.: *Phytochem. Anal.* 22, 6, 547 (2011).
- Oszmianski J., Wojdyło A., Lamer-Zarawska E., Świader K.: *Food Chem.* 100, 579 (2007).
- Tomczyk M., Pleszczyńska M., Wiater A.: *Molecules* 15, 4639 (2010).
- Katalinic V., Milos M., Modun D., Music I., Boban M.: *Food Chem.* 86, 593 (2004).
- Suzuki T., Someya S., Hu F., Tanokura M.: *Food Chem.* 93, 149 (2005).
- Tsanova-Savova S., Ribarova F., Gerova M.: *J. Food Compos. Anal.* 18, 691 (2005).
- Lebeau J., Furman C., Bernier J.L., Duriez P., Teissier E., Cotellet N.: *Free Radic. Biol. Med.* 29, 900 (2000).
- Ghasemzadeh A., Jaafar H., Rahmat A.: *Molecules* 15, 6231 (2010).
- Ivanov S., Nomura K., Malfanov I.L., Sklyar I.V., Ptitsyn L.R.: *Fitoterapia* 82, 212 (2011).
- Miliauskas G., Venskutonis P.R., Van Beek T.A.: *Food Chem.* 85, 231 (2004).
- Kalia K., Sharma K., Singh H.P., Singh B.: *J. Agric. Food Chem.* 56, 10129 (2008).
- Cheel J., Theoduloz C., RodriÄguez J., Schmeda-Hirschmann G.: *J. Agric. Food Chem.* 53, 2511 (2005).
- Tadic V.M., Dobric S., Markovic G.M., Đordjevic S.M., Arsic I.A., Menkovic N.R., Stevic T.: *J. Agric. Food Chem.* 56, 7700 (2008).
- Santos-Buelga C., Scalbert A.: *J. Sci. Food Agric.* 80, 1094 (2000).

40. Alder V., Yin, Z., Tew K.D., Ronai Z.: *Oncogene* 18, 6104 (1999).
41. Keane M.P., Strieter R.M.: *Respir. Res.* 3, 5 (2002).
42. Luger T.A., Schwarz T.: *J. Invest. Dermatol.* 95, 100S (1990).
43. Wilmer J.L., Burleson F.G., Kayama F., Kauno J., Luster M.I.: *J. Invest. Dermatol.* 102, 915 (1994).
44. Murray A.R., Kisin E., Castranova V., Kommineni C., Gunther M.R., Shvedova A.A.: *Chem. Res. Toxicol* 20, 1769 (2007).
45. Rogerio A.P., Kanashiro A., Fontanari C., Da Silva E.V.G., Lucisano-Valim Y.M., Soares E.G., Faccioli L.H.: *Inflammation Res.* 56, 402 (2007).
46. Tang L.Q., Wei W., Wang X.Y.: *Adv. Ther.* 24, 679 (2007).
47. Utsunomiya I., Nagai S., Oh-ishi S.: *Eur. J. Pharmacol.* 252, 213 (1994).

Received: 25. 11. 2013

IN VITRO AND IN VIVO ANTIMICROBIAL EVALUATION OF ALKALOIDAL EXTRACTS OF *ENANTIA CHLORANTHA* STEM BARK AND THEIR FORMULATED OINTMENTS

EMMANUEL E. NYONG¹, MICHAEL A. ODENIYI^{2*} and JONES O. MOODY¹

¹Department of Pharmacognosy, University of Ibadan, Ibadan, Nigeria

²Department of Pharmaceutics, University of Ibadan, Ibadan, Nigeria

Abstract: The *in vitro* and *in vivo* antimicrobial evaluation of the formulated ointment of alkaloidal extract of *Enantia chlorantha* Oliv. (Annonaceae) was the concern of this study. The alkaloidal fraction of the stem bark extract was formulated into simple ointment using British Pharmacopoeia formula for preparation of simple ointment. Agar diffusion and agar dilution methods were used for the *in vitro* antimicrobial studies. Ketoconazole 4000 µg/mL and tioconazole cream 1% were used as reference standards while normal saline was used as control. The fungicidal activity kinetics of the plant extract was carried out using selected concentrations of the plant extract against the most sensitive organism (*Candida albicans*). For the *in vivo* studies, 25 albino rats weighing between 180–200 g were divided into 5 groups, anesthetized (thiopental sodium 50 mg/kg), infected with overnight culture of *Candida albicans* and incubated at 37°C for three days to allow for growth of the microorganisms. Each of the five groups was treated on the third day of incubation with different concentrations of the formulated simple ointment (200 mg/mL, 100 mg/kg, 50 mg/mL), tioconazole cream 1% (reference standard) and normal saline control, respectively. The alkaloidal extract exhibited greater zones of inhibition with *Candida glabrata* and *Trichophyton tonsurans* while *Candida albicans* and *Trichophyton interdigitali* also showed some sensitivity. There was no surviving organism at the end of 240 min at 100 mg/mL concentration with 10⁴ dilution factor. Treatment of the infected rats with the formulated simple ointments (200, 100 and 50 mg/mL) showed that 50 mg/mL ointment had a better percentage reduction in the fungal loads at the end of the experiment when compared with the 200 mg/mL simple ointment as well as the standard tioconazole 1% cream and normal saline treated rats, respectively. The alkaloidal fraction of *Enantia chlorantha* stem bark as well as the formulated ointment exhibited significant *in vitro* and *in vivo* antifungal activities against different species of *Candida*, dermatophytes and plant fungi.

Keywords: anticandidal, *Candida albican*, *Enantia chlorantha*, ointment formulation

Current treatment of candidiasis and other infections caused by *Candida* species is becoming very expensive and unaffordable by a large section of the population in developing economies. Many plant extracts have folkloric use in the treatment of infections. *Enantia chlorantha* plant extract has previously been investigated for antifungal activities (1). The plant belongs to the family Annonaceae and is known locally in Yoruba as Awopa, Osopupa or Dokita Igbo. It is an under storey tree of high rain-forest. It is also an ornamental tree which may grow up to 30 m high, with dense foliage and spreading crown. The outer bark, which is thin and dark brown, is fissured geometrically while the inner bark is brown above and place cream beneath. The stem is fluted and aromatic while the elliptic leaves are about 0.14–0.15 m long and 0.05–0.14 m broad

(2). The leaves display up to 20 pairs of prominent lateral vein and parallel secondary nerves. It is a dense forest tree found in the Western and Southern forest of Cameroon, Southern part of Nigeria, Gabon, Angola and Zaire. It is widely distributed along the coasts of West and Central Africa (2). *Enantia chlorantha* is a medicinal tree used for the treatment of malaria and other ailments of the human body. Gill and Akinwunmi (3) reported the use of infusion of the plant bark for the treatment of cough and wounds. Wafo et al. (4) noted the antiviral activity of extracts from the dried stem bark. *Enantia chlorantha* is also used for the management of stomach problems in the southern forest zone of Cameroon as well as for the treatment of jaundice, tuberculosis, urinary tract infection, malaria, hepatitis and some forms of ulcer. The decoction of the

* Corresponding author: e-mail: deleodeniya@gmail.com; phone: +234-7088194371

root in addition to the root of *Carica papaya* is used for the management of malaria. The decoction of the stem bark of *Enantia chlorantha* is also used for the treatment of leprosy spots and liver damage. The stem bark has also been reported to be used as antipyretic and uterus stimulant (5). Palmatine chloride and jatrorrhizine chloride have been identified as the major antimicrobial constituents of the plant extracts (6).

Hence, this study is concerned with the formulation and antimicrobial evaluation of purified alkaloidal extracts obtained from the stem bark of *Enantia chlorantha* Oliv. (Annonaceae) found to be effective against *Candida albicans* and other fungal strains.

MATERIALS AND METHODS

Plant material

Enantia chlorantha (Annonaceae) stem bark was obtained from herb sellers in Bode Market in Ibadan, Nigeria and identified at the Department of Pharmacognosy, Faculty of Pharmacy, University of Ibadan, Nigeria. A voucher sample was deposited at the Department and compared with previously collected sample (IB 197/241).

Preparation of extract

One kilogram (1 kg) of the sun dried chopped *Enantia chlorantha* stem bark was pulverized with a hammer-mill to obtain a coarse powder and macerated in 70% ethanol for 72 h. After decantation, maceration was for 48 h to ensure thorough extraction. The combined filtered ethanolic extract was concentrated to dryness and the resulting residue weighed and refrigerated until use.

Preparation of alkaloidal fraction (AF)

Forty grams (40 g) of the crude ethanolic extract was acidified with 5% HCl (500 mL) and filtered through kieselghur under vacuum. The filtrate was lyophilized and the dried AF mixture was obtained.

Formulation of ointment

The dried alkaloid fraction was incorporated into Simple Ointment BP (7) to produce formulations yielding 50, 100, and 200 mg/mL *Enantia chlorantha* ointments by levigation.

Antimicrobial evaluation

The agar-well diffusion bioassay method (7, 8) was used. One hundred mL molten sterile nutrient broth was cooled to 50°C and inoculated with 1 mL

of overnight culture of test organism. Twenty mL quantities of the inoculated medium was each poured into a 9 cm agar plates and allowed to set. Equidistant wells of 6 mm were bored into the agar using a sterile cork borer and the wells were filled with appropriate concentrations of the extracts under test.

All extracts were reconstituted in 50% v/v aqueous methanol, which was used as a control while Bertrosil Cream (tioconazole), Trosyd Cream (tioconazole) and ketoconazole (4000 µg/mL) were used as reference standards. The plates were left at room temperature for 45 min and then incubated at 37°C for bacterial strains and 25°C for fungal strains. After an incubation period of 24 and 48 h for bacterial and fungal strains, respectively, the diameters of the zones of inhibition were measured. The minimal inhibitory concentration (MIC) and minimal bactericidal concentration (MBC) measures were determined by the broth dilution method (9).

Animal studies

Male and female albino rats weighing between 180 and 200 g, respectively, were purchased from the animal house of the University of Ibadan. Twenty five albino rats weighing between 180–200 g were divided into five groups for the *in vivo* anti-candidal studies and were fed with standard feeds and water. Thiopental sodium injection was used as an anesthetic agent and administered based on their body weight at a dose 50 mg/kg. The dorsal flank of the albino rats were carefully shaved and the exposed skin part were bruised. An overnight *Candida albicans* culture was applied on the bruised skin parts of the dorsal flank of the albino rats using sterile swab sticks and observed for a period of 3 days. The growth of the *Candida albicans* was established on the third day. Each of the five groups were then treated on daily basis with different concentrations of the *Enantia chlorantha* ointment (200, 100 and 50 mg/mL), tioconazole cream 1% (reference standard) and normal saline control, respectively. The swabs taken on days 0, 3, 7, 10 and 13 were placed on a tryptone soya broth and incubated for 3 days at 37°C. Serial dilutions were carried out and the fungal loads were counted using colony counter.

Statistical analysis

Statistical analysis was carried out using Students' *t*-test and ANOVA. At 95% confidence interval, *p* value lower or equal to 0.05 was considered the limit of significance (GraphPad Software Incorporation, San Diego, USA).

RESULTS AND DISCUSSION

The investigation of the antifungal activity of the alkaloidal fraction of the stem bark of *Enantia chlorantha* used ethno-medicinally for the management of various infectious diseases was carried out. The plant extract was tested against different species of *Candida*, dermatophytes and plant fungi, respectively. The fungal species used in these studies were *Candida valida*, *Candida pseudotropicalis*, *Candida tropicalis*, *Candida glabrata*, *Candida krusei*, *Candida albicans*, *Trichophyton rubrum*, *Trichophyton interdigitalis*, *Trichophyton tonsurans*, *Epidermo-*

phyton floccosum, *Coletotrichum gloesporoides*, *Trichoderma asperelum*, and *Fusarium* spp. The bacteria species used in these studies were *Staphylococcus aureus* and *Escherichia coli*.

The minimum inhibitory concentration of the alkaloidal fraction of the crude ethanolic extract of stem bark of *Enantia chlorantha* are shown in Tables 1 and 2, respectively. The results show that the alkaloidal fraction of the stem bark of *Enantia chlorantha* was active at various concentrations (200, 100, 50, 25, 12.5, 6.25, 3.125, 1.563 and 0.781 mg/mL) on test organisms. It was at the following order of decreasing sensitivity; *Candida albicans* >

Table 1. Minimum inhibitory concentration of the alkaloidal fraction of the stem bark of *Enantia chlorantha* using agar diffusion method.

	Conc. mg/mL	C1	C2	C3	C4	C5	C6	D1	D2	D3	D4	1	3	9	SA	EC
1	200	16	18	17	15	16	20	18	23	19	19	18	20	24	32	20
2	100	12	15	14	13	13	18	16	20	16	16	15	16	19	26	17
3	50	10	13	11	10	11	15	12	17	12	14	13	13	17	23	16
4	25	-	-	-	-	-	14	-	-	10	12	11	-	13	21	13
5	12.5	-	-	-	-	-	13	-	-	-	10	10	-	10	19	10
6	6.25	-	-	-	-	-	10	-	-	-	-	-	-	-	17	-
7	-ve	-	-	-	-	-	-	-	-	-	-	-	-	-	-	-
8	BC	-	-	-	-	-	-	-	-	-	-	-	-	-	27	-
9	TC	-	-	-	-	-	-	-	-	-	-	13	-	15	-	-
10	KE	-	-	-	25	-	12	-	12	20	-	-	-	-	-	-

Keys: -ve: Negative control (methanol), BC: Bertrosil Cream (Tioconazole cream by Drugfield Pharmaceuticals), TC: Trosyd Cream (Tioconazole cream by Pfizer), KE (4000 µg/mL) Ketoconazole, C1: *Candida valida*, C2: *Candida pseudotropicalis*, C3: *Candida tropicalis*, C4: *Candida glabrata*, C5: *Candida krusei*, C6: *Candida albicans*, D1: *Trichophyton rubrum*, D2: *Trichophyton interdigitalis*, D3: *Trichophyton tonsurans*, D4: *Epidermophyton floccosum*, 1: *Colletotrichum gloesporoides* from yam blight, 3: *Trichoderma asperelum* from banana fruit, 9: *Fusarium* spp from yam, SA: *Staphylococcus aureus*, EC: *E. coli*

Table 2. Agar dilution method used to determine the minimum inhibitory concentration of the alkaloidal fraction of the stem bark of *Enantia chlorantha*.

Conc. mg/mL	C1	C2	C3	C4	C5	C6	D1	D2	D3	D4	1	3	9	SA	EC
50	-	-	-	-	-	-	-	-	-	-	-	-	-	-	-
25	+	+	+	+	+	+	+	+	+	+	+	+	+	-	-
12.5	+	+	+	+	+	+	+	+	+	+	+	+	+	+	+
6.25	+	+	+	+	+	+	+	+	+	+	+	+	+	+	+
3.125	+	+	+	+	+	+	+	+	+	+	+	+	+	+	+
1.563	+	+	+	+	+	+	+	+	+	+	+	+	+	+	+
0.781	+	+	+	+	+	+	+	+	+	+	+	+	+	+	+

Keys: - Absence of growth, + Presence of growth, C1: *Candida valida*, C2: *Candida pseudotropicalis*, C3: *Candida tropicalis*, C4: *Candida glabrata*, C5: *Candida krusei*, C6: *Candida albicans*, D1: *Trichophyton rubrum*, D2: *Trichophyton interdigitalis*, D3: *Trichophyton tonsurans*, D4: *Epidermophyton floccosum*, 1: *Colletotrichum gloesporoides* from yam blight, 3: *Trichoderma asperelum* from banana fruit, 9: *Fusarium* spp from yam, SA: *Staphylococcus aureus*, EC: *E. coli*

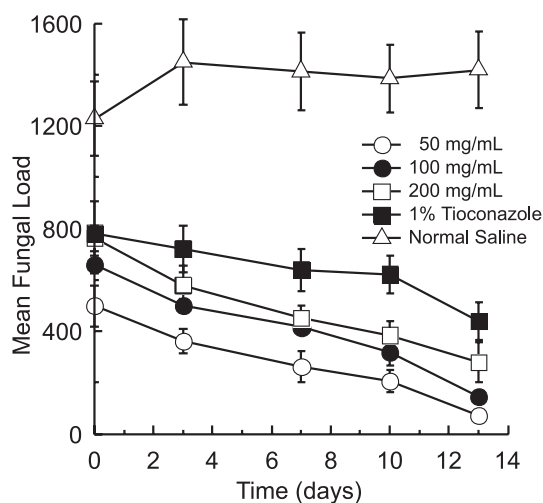


Figure 1. Effect of *Enantia chlorantha* ointment on the fungal load in rats

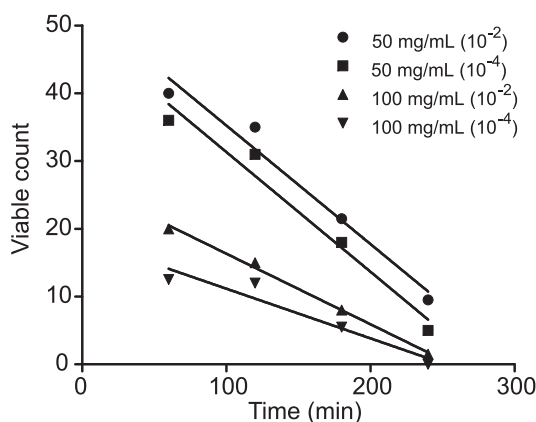


Figure 2. Kinetics of fungicidal activity of alkaloidal fractions of *Enantia chlorantha* against *Candida albicans* at different dilution factors

Candida krusei > *Candida glabrata* > *Candida pseudotropicalis* > *Candida tropicalis* > *Candida valida*. For the dermatophytes, the sensitivity was at the following order of decreasing sensitivity: *Trichophyton interdigitalis* > *Trichophyton rubrum* > *Epidermophyton floccosum* > *Trichophyton tonsurans*. For the plant fungi, the zone of inhibition was in the following order of decreasing sensitivity: *Fusarium* spp > *Trichoderma asperelum*, > *Colletotrichum gloeosporoide*, respectively. *Staphylococcus aureus* had a larger zone of inhibition compared to *Escherichia coli*, which were the bacterial species used for the studies.

Results of sensitivity testing for the antifungals used as reference standard (Table 1) revealed that ketoconazole showed larger zones of inhibition against *Candida glabrata* and *Trichophyton tonsurans*. *Candida albicans* and *Trichophyton interdigitalis* showed the same zone of inhibition with the 4000 mg/mL concentration of ketoconazole. Tioconazole cream 1% exhibited better zone of inhibition for the *Fusarium* spp., followed by *Trichophyton rubrum* (Table 1). Methanol, which was used as a negative control, showed no zone of inhibition.

The kill kinetics or the fungicidal activities (Table 3) of the extracts were also investigated using

Table 3. Kinetics of fungicidal concentration of alkaloidal fraction of the stem bark of *Enantia chlorantha* for 50 and 100 mg/mL concentration using 10^{-2} and 10^{-4} dilution factors.

Time (min)	VC (50 mg/mL) 10^{-2}	VC (50mg/mL) 10^{-4}	VC (100 mg/mL) 10^{-2}	VC (100 mg/mL) 10^{-4}
0	Numerous	Numerous	Numerous	Numerous
60	40.0	36.0	20.0	12.0
120	35.0	31.0	15.0	12.5
180	21.5	18.0	8.0	5.5
240	9.5	5.0	1.5	0.0

Key: VC – No. of viable colonies. Numerous – Values of viable colonies or growth above 1000.

Table 4. The percentage reduction of fungal load after 13 days of treatment with formulated ointment, Tioconazole cream 0.10 mg/mL and normal saline.

Sample	Concentration (mg/mL)	Fungal load after 13 days
Formulated ointment of alkaloidal extract	200	63.50
	100	77.97
	50	83.38
Tioconazole cream	0.10	43.93
Normal saline	–	–15.44

the most potent concentration of the plant extracts against the most sensitive organism (*Candida albicans*). The result obtained showed that the number of the viable organisms was reduced with contact time. At the end of 240 min at 100 mg/mL concentration with 10^{-4} dilution factor, there was no surviving organism. The kinetics were found to be linear ($r^2 > 0.9$) for all treatments except for the normal saline control (Fig. 2).

The fungal load for each of the formulated ointment concentrations (200, 100, 50 mg/mL) showed a reduction in the fungal load with respect to the days interval in which the swab were taken as shown in Table 4. Tioconazole cream 1% was used as a reference standard in the treatment of *Candida albicans* infected rats. It demonstrated a good reduction of the fungal load as could be seen in Table 4. Normal saline was used as a negative control to treat the *Candida* infected skin of the albino rats used. In this group, there was no significant reduction of the fungal load (Table 4).

The 50 mg/mL ointment formulation produced a higher percentage reduction of fungal load when compared to 200 and 100 mg/mL ointments, tioconazole cream 1% (reference standard) and normal saline control, respectively (Table 4). This significant reduction in fungal loads demonstrated by 50

mg/mL *Enantia chlorantha* ointment would appear to suggest that there is an optimal concentration of the alkaloidal fraction required to elicit maximal action against *C. albicans*. This observation therefore calls for further probe into the response pattern of *C. albicans* to various concentrations of the individual protoberberine alkaloids in the alkaloidal fraction used in preparing the ointment.

The alkaloidal fraction of the stem bark of *Enantia chlorantha* exhibited antifungal activity against the different strains of *Candida albicans*, dermatophytes and the plant fungi. The result obtained shows that the plant extracts possess antifungal property and can be effective in the treatment of fungal infections since they inhibit the growth of fungal causative agents of infections. This finding buttresses earlier reports of many researchers, that medicinal plants or traditional medicine have a critical role in the provision of health care coverage for over 80% of the world population especially in the developing world (10–13). Tables 1 and 2 show that the alkaloidal fraction of the stem bark of *Enantia chlorantha* have very large zones of inhibition with *Staphylococcus aureus* and *E. coli*, respectively (15). Of particular interest in this study, is the resistance of the test organisms to the conventional antifungal drugs but their sensitivity to the alkaloidal fraction

of *Enantia chlorantha* plant extracts. This is an indication that this plant if well harnessed, formulated under standard and good manufacturing practice can compete favorably with some of the existing antifungal drugs. This plant product can therefore be used in the management of *Candida*, dermatophyte and plant fungi infections. Following the result of these findings on different species of *Candida*, dermatophytes, and plant fungi, respectively, it is highly recommended that these plant extracts and constituents be incorporated into antifungal skin creams, causative organism responsible for skin fungal infections and vaginal candidiasis. Other forms of fungal infections like *Candida balanitis*, *Tinea barbae* and oropharyngeal candidiasis can as well be researched into using these same plant extracts.

Further investigations of the activities of these plant extract and constituents against a wider range of fungi, and bacteria should be carried out with a view to develop phytotherapeutic agents for enhanced and cost-effective healthcare delivery in developing economies considering the fact that the plant is safe owing to the toxicological investigation earlier carried out (16, 17), in addition to the relevant chemical constituents of the plant which has already been identified by Moody et al. (1).

REFERENCES

1. Moody J.O., Hylands P.J., Bray, D.H.: Pharm. Pharmacol. Lett. 2, 80 (1995).
2. Iwu M.M.: Handbook of African Medicinal Plants. p. 1, CRC Press, Boca Raton 1993.
3. Gill L.S., Akinwunmi C.: J. Ethnopharmacol. 18, 23 (1986).
4. Wafo P., Nyasse B., Fontaine C.: Phytochemistry 50, 279 (1999).
5. Oliver B.: Medicinal plants in Nigeria. p. 139, University of Ibadan, Nigeria 1960.
6. Moody J.O., Bloomfield S.F., Hylands P.J.: Afr. J. Med. Med. Sci. 24, 269 (1995).
7. Hugo W.B., Russell A.D.: Pharmaceutical Microbiology, 3rd edn., p. 167, Blackwell, Oxford 1983.
8. Ogundipe O.O., Moody J.O., Houghton, P.J., Odelola, H.A. J. Ethnopharmacol. 74, 275 (2001).
9. Onawunmi G.O.: Lett. Appl. Microbiol. 9, 105 (1986).
10. British Pharmacopoeia. Vol. 2, p. 713, Her Majesty's Stationery Office, London 1988.
11. WHO: Traditional Medicines Growing Needs and potentials. WHO policy perspectives on medicine. p. 1, World Health Organization, Geneva 2002.
12. Iwu M.M., Duncan A.R., Okunji C.O. :New antimicrobials of plant origin. p. 457, ASHS Press, Alexandria, VA 1999
13. Scheinman D.: The ancient and modern world unites to fight HIV/AIDS in Tanga, Tanzania, Merck: Science in Africa online magazine 2002
14. Kala C.P., Farooque N.A., Dhar U.: India J. Biodiver. Conserv. 13, 453 (2004).
15. Adesokan A.A., Akanji M.A., Yakubu, M.T.: Afr. J. Biotechnol. 6, 2502 (2007).
16. Moody J.O., Ogundipe O.O., Akang E.U.U., Agbedana, E.O.: Afr. J. Med. Sci. 36, 317 (2007).
17. Tan P.V., Boda, M., Enoworock G.E., Etoa F., Bitolog P.: Pharmacology Online 1, 304 (2007).

Received: 21. 12. 2013

EFFECTS OF WHITE MULBERRY (*MORUS ALBA*) LEAF TEA INVESTIGATED IN A TYPE 2 DIABETES MODEL OF RATS

RACHEL DOROTHY WILSON and MD. SHAHIDUL ISLAM*

Department of Biochemistry, School of Life Sciences, University of KwaZulu-Natal (Westville Campus), Durban 4000, South Africa

Abstract: The present study was aimed to investigate the anti-diabetic effects of a low (0.25%) and a high (0.5%) dose of white mulberry leaf tea in a rat model of type 2 diabetes (T2D). Six week old male Sprague-Dawley rats were divided into four groups: Normal control (NC), Diabetic control (DBC), Diabetic mulberry tea low (DMTL, 0.25%) and Diabetic mulberry tea high (DMTH, 0.50%). T2D was induced by feeding a 10% fructose solution in drinking water for 2 weeks to induce insulin resistance, followed by a single injection (*i.p.*) of streptozotocin (40 mg/kg body weight (b.w.)) to induce partial pancreatic β -cell dysfunction in all groups except the NC group, which only received a normal drinking water and citrate buffer (pH 4.4) instead of fructose solution and STZ injection, respectively. After 4 weeks feeding of brewed mulberry leaf tea, there were no significant improvements in polyphagia, polydipsia, body weight gain, blood glucose, glucose intolerance, serum insulin, fructosamine, AST, ALT, creatinine, albumin and uric acid levels and liver parameters when serum total cholesterol was significantly and LDL-cholesterol and triglyceride concentrations were markedly decreased in the DMTH group compared to the DBC and DMTL groups. Serum total proteins were significantly reduced in DMTL and DMTH groups compared to the DBC group. These results suggest that brewed white mulberry leaf tea has hypolipidemic rather than antidiabetic effects at least in this experimental condition. However, the effects of the different brands of white mulberry leaf tea may be varied due to various factors.

Keywords: mulberry leaf tea, *Morus alba*, type 2 diabetes, rats

Diabetes is an ongoing public health concern that has an increasing prevalence globally. According to International Diabetes Federation (IDF), at least 371 million people have diabetes worldwide in 2012, which is predicted to be 552 million by 2030 (1). Of all the diabetic cases, 90–95% of them suffer from type 2 diabetes (T2D) (2). Unlike type 1 diabetes (T1D), which is denoted as diminished insulin production, T2D is a heterogeneous disorder characterized by impaired cellular responses to insulin known as insulin resistance and followed by progressive partial pancreatic β -cell dysfunction (3). Due to insulin resistance, pancreatic β -cells secrete abnormally high levels of insulin in order to control blood glucose levels, however overtime, hyperglycemia, hyperinsulinemia, pancreatic β -cell dysfunction and subsequent progressive pancreatic β -cell destruction occur (4–6). Nowadays, diet and lifestyle choices tend toward high caloric intake and low physical activity, pro-

moting the development of obesity. An increased risk of developing T2D has been linked to obesity through its association with diets of high caloric content (7). Since T2D is characterized by 2 main pathogenesis; insulin resistance and partial pancreatic β -cell dysfunction (4), these are also the two predominant targets for disease control.

Despite the wide availability and range of existing anti-diabetic drug therapies, there is still an ever-growing need for better and/or alternative therapies to combat the rising numbers of global diabetic patients. Furthermore, the demand for new alternative therapies is increasing as patients search for cheaper options, wider availability as well as to avoid the dissatisfactory symptoms and consequences of traditional drug therapies, including weight gain, hypoglycemia or certain contraindications that may limit their use (8, 9).

White mulberry (*Morus alba*) has been used over the centuries in traditional Chinese medicine as

* Corresponding author: e-mail: islamd@ukzn.ac.za or sislam1974@yahoo.com; phone: +27 31 260 8717, fax: +27 31 260 7042

a common agent to treat a variety of conditions including diabetes, atherosclerosis, cancer as well as for boosting the immune system through potent antioxidant activity (10). Different parts of the mulberry plant (fruit, bark, leaf and root) have drawn interest in their role to treat diabetes, when the root and bark often was used to reduce hyperglycemia (11). Several studies have already investigated various alkaloids, flavonoids and phytochemicals in white mulberry, having found especially in leaves to exhibit anti-diabetic effects. These effects include inhibition of α -glycosidase, sucrase and maltase enzymes activity (12, 13), reducing carbohydrates metabolism and thus lowering blood glucose levels (12), prevention of lipid peroxidation (14), improvement of dyslipidemia, especially hypercholesterolemia (15) and inhibiting oxidation of LDL cholesterol (16). Kimura et al. (17) found 1-deoxynojirimycin (DNJ), an alkaloid in white mulberry leaf and reported to have non-fasting blood glucose (NFBG) lowering activity in humans. Nowadays, white mulberry leaf extracts are found in various food products especially sold as a tea and is readily available in many countries (15). Whilst all current research investigates white mulberry leaf extracts, none investigate the effect of white mulberry leaf tea, as consumed by humans, either in humans or experimental animals.

Hence, the present study was conducted to investigate the anti-diabetic effects of a low (0.25%) and a high (0.5%) dose of brewed white mulberry leaf tea in a T2D model of rats.

MATERIALS AND METHODS

Reagents and materials

Streptozotocin (STZ) (> 98%) (Sigma-Aldrich) was purchased from Capital Lab Supplies cc. Durban, South Africa. Fructose (Nature's Choice™ Wholefood specialists, Meyerton, South Africa 1960) was purchased from a local pharmacy. White mulberry leaf tea was purchased from Beautique Thai (Thailand). A glucometer (GlucoPlus Inc., Quebec, Canada) with a maximum measuring capacity of 600 mg/dL) was used for measuring blood glucose levels.

Animals

Twenty eight (6 weeks old) male Sprague-Dawley rats (mean body weight 191.88 ± 16.40 g) were procured from the Biomedical Resource Unit (BRU) at Westville Campus of the University of KwaZulu-Natal, Durban, South Africa. Animals were randomly subdivided into 4 groups of 6–7 rats in each group as follows: Normal control (NC),

Diabetic control (DBC), Diabetic culberry tea low (DMTL, 0.25%) and Diabetic mulberry tea high (DMTH, 0.50%). Two rats per polycarbonated cage were housed in a temperature and humidity controlled room with a set of 12 h light-dark cycle. The rats were fed a commercially available rat chow diet *ad libitum* throughout the 7 week experimental period. The animals were maintained according to the rules and regulations of the University of KwaZulu-Natal (UKZN) Animal Ethics Committee (Ethical approval number: 029/11/Animal).

Induction of diabetes

T2D was induced in the animals in DBC, DMTL and DMTH groups by feeding 10% fructose solution for the first 2 weeks followed by an injection (*i.p.*) of STZ (40 mg/kg b.w.) dissolved in citrate buffer (pH 4.4) when the animals in NC group were fed with normal drinking water and injected with citrate buffer, respectively (18). Non-fasting blood glucose (NFBG) levels of all animals were measured 1 week after STZ injection by using a portable glucometer in the blood collected from tail veins. Animals with a NFBG level > 300 mg/dL were considered as diabetic.

Tea preparation and intervention

White mulberry leaf tea was prepared in the following concentrations: 0.25 and 0.5%. According to the concentration, tea bags were brewed exactly for 10 min in boiling water, cooled to room temperature and supplied to the respective group of animals *ad libitum* during 4 weeks intervention period, starting from one week after the STZ injection. At the same time, the animals in the NC and DBC groups were supplied with normal drinking water instead of mulberry tea. Daily food and fluid intake and weekly body weight changes and NFBG were measured during the entire intervention period.

Oral glucose tolerance test (OGTT)

Oral glucose tolerance test (OGTT) was performed in all animals in the last week of the 4 week intervention period. In order to perform this test, after an overnight fast (12 h), rats were orally dosed with a D-glucose solution (2.0 g/kg b.w.) and glucose concentrations were subsequently measured in the blood collected from the tail veins at 0 (just prior to oral glucose dosing), 30, 60, 90 and 120 min after oral dosing of glucose.

Collection of blood and liver

At the end of the experimental period, animals were fasted for 14 h and sacrificed using halothane

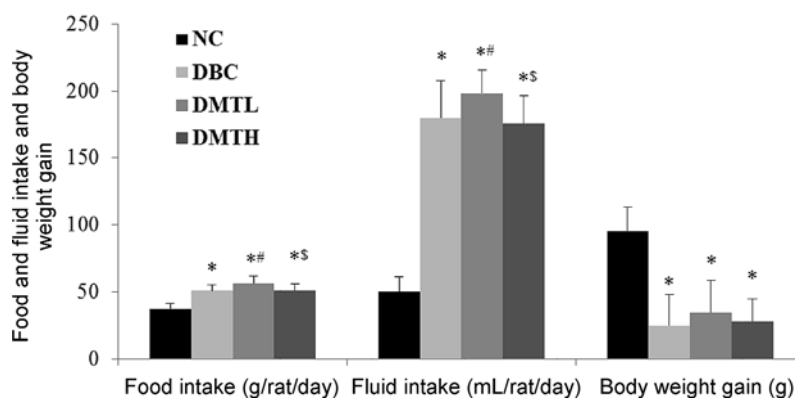


Figure 1. Food and fluid intake and body weight gain in different animal groups at the end of the experimental period. * $p < 0.05$ vs. NC, # $p < 0.05$ vs. DBC, \$ $p < 0.05$ vs. MTL (Tukey-Kramer's multiple range *post-hoc* test)

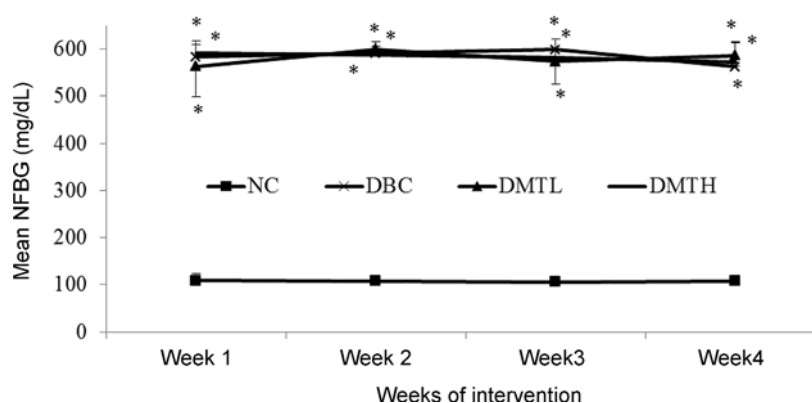


Figure 2. Non-fasting blood glucose (mg/dL) of different rat groups during the intervention trial period. * $p < 0.05$ vs. NC (Tukey-Kramer's multiple range *post-hoc* test).

ethanasia after which blood and liver were collected. Blood was collected through cardiac puncture and immediately placed into heparinized tubes and preserved on ice. The blood samples were centrifuged at 3000 rpm for 15 min and separated serum was stored at -30°C for further analysis. Liver samples were washed in cold saline, wiped dry with filter paper, weighed on an analytical balance and preserved at -30°C for subsequent analysis.

Analytical methods

Liver glycogen concentration was measured photometrically by using phenol-sulfuric acid method as described by Lo et al. (19). Serum insulin concentration was measured using an ultra-sensitive

rat insulin ELISA kit (Merckodia AB, Uppsala, Sweden) in a multi-plate ELISA reader (Biorad-680, BIORAD Ltd., Japan). Serum lipid profiles, serum creatinine, total proteins, serum albumin, fructosamine and liver function enzymes (AST and ALT) were measured using an Automated Chemistry Analyzer (LabmaxPlenno, Labtest, Costa Brava, Lagoa Santa, Brazil).

Statistical analysis

All data are presented as the mean \pm SD. The data were analyzed by a statistical software package (SPSS version 18) using the Tukey's HSD multiple range *post-hoc* test. The values were considered significantly different at $p < 0.05$.

RESULTS

During the experimental period, food intake and fluid intake in DMTL, but not DMTH group was significantly higher than the DBC group. Mean body weight gain amongst the groups was not significantly different from each other, except from that of the NC group (Fig. 1).

The DMTL and DMTH groups showed no significant improvement either for NFBG over 4 weeks (Fig. 2) when glucose tolerance ability was worsened by the feeding mulberry leaf tea (Fig. 3).

There was no significant difference in liver weight amongst the groups (Table 1); however, relative liver weights and liver glycogen concentrations were significantly higher in the diabetic groups

compared to the NC group. The liver function enzyme ALT was significantly higher in both DBC and DMTH compared to the NC group, whereas not in the DMTL group (Table 2). No significant difference was observed for serum AST and creatinine concentrations among the groups, however, serum total proteins were significantly lower in DMTL and DMTH compared to DBC, as well as serum albumin was significantly reduced in DMTL and DMTH compared to NC, but not DBC group. Serum uric acid was significantly lower in the DMTL group compared to the NC group when no difference observed among the other groups (Table 2). Serum insulin and fructosamine concentrations were also not affected by the consumption of the either dosages of mulberry leaf tea (Table 2).

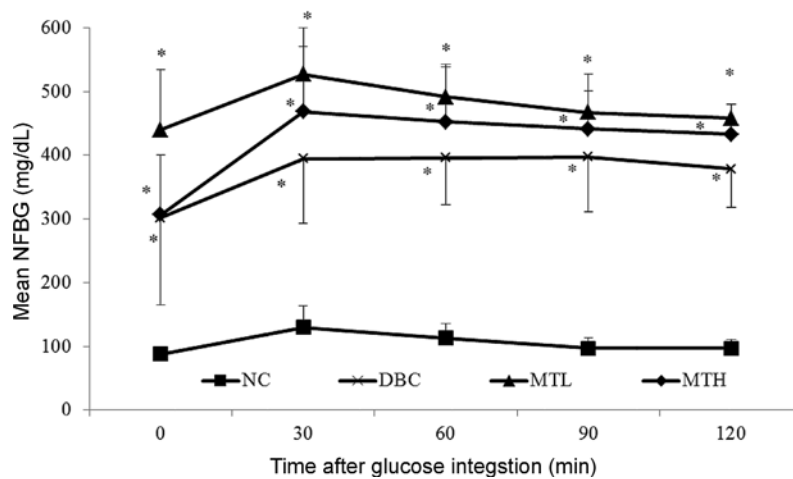


Figure 3. Oral glucose tolerance test over a 2 h period.*p < 0.05 vs. NC (Tukey-Kramer multiple range *post-hoc* test)

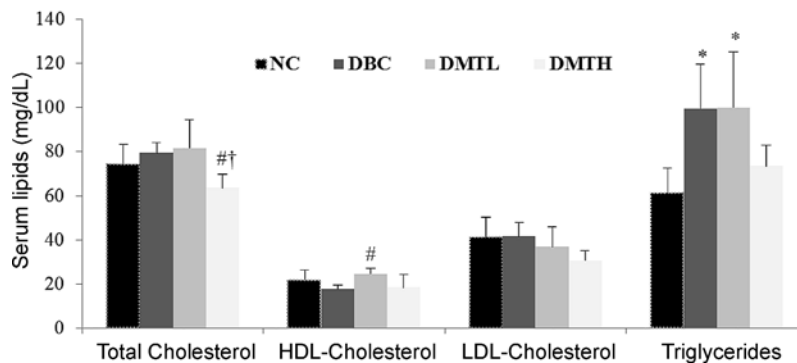


Figure 4. Serum lipid profile of the different animal groups at the end of the experimental period *p < 0.05 vs. NC, #p < 0.05 vs. DBC, †p < 0.05 vs. DMTL (Tukey-Kramer’s multiple range *post-hoc* test)

Total cholesterol was significantly lower in the DMTH group compared to DBC and DMTL groups, whereas HDL was significantly higher in DMTL compared to DBC group. Serum triglycerides were significantly higher in DBC and DMTL compared to the NC group, however, comparatively lower serum triglyceride and LDL-cholesterol concentrations were observed in the DMTH group compared to the DBC and DMTL groups (Fig. 4).

DISCUSSION

Due to the rapidly rising numbers of T2D patients, intensive research on diabetes therapy and prevention has similarly increased. Currently, oral drug therapies for T2D focus on improving insulin secretion and improving insulin sensitivity (20). Ideal alternative therapies must exhibit a similar degree of efficacy compared to conventional drug therapy, however without the negative side effects often associated with the conventional therapies (21). In late 1980's, with over 400 reported traditional medicines for the treatment of T2D, the World Health Organization Expert Committee on Diabetes has recognized the great potential of natural plants and functional foods as alternative treatments for

T2D and recommended to carry our further investigations on them (22). Today, the plant based individual alternative or isolated therapy of T2D is very common and popular in most developing and even in some developed countries.

Tea in traditional Asian medicine is believed to promote both good health and longevity (23). In recent years, leaves from the mulberry plant have gained much popularity as a tea drink for diabetics in many Asian countries (10). The major anti-diabetic compound in white mulberry leaves is a glucose analogue called 1-deoxynojirimycin (DNJ), which inhibits the intestinal enzyme α -glucosidase by binding to the active site in the enzyme (24). α -Glucosidase is considered to be one of the most important enzymes in starch digestion in the small intestine (25) and thus DNJ is believed to be responsible for the reduction in NFBG and hyperglycemia by reducing the rate of both carbohydrate and lipid absorption (24). It has been reported that a minimal dose of mulberry DNJ (6 mg/60 kg b.w.) is required to reduce NFBG and decrease insulin secretions in human subjects (17, 26).

Recently, Vichasilp et al. (26) investigated 35 mulberry tea varieties in Thailand to determine and develop a mulberry tea blend with the optimal DNJ

Table 1. Liver weight, relative liver weight, liver glycogen and liver function enzymes of the different animal groups at the end of the experimental period.

Rat groups/ liver parameters	NC	DBC	DMTL	DMTH
Liver weight (g)	11.81 ± 0.8	10.66 ± 1.3	10.51 ± 1.1	10.33 ± 1.8
Relative liver weight (%)	3.05 ± 0.1	3.90 ± 0.3*	3.72 ± 0.1*	3.80 ± 0.3*
Liver glycogen (mg/g tissue)	37.30 ± 28.9	95.76 ± 1.3*	91.69 ± 10.0*	87.02 ± 21.4*

Values are shown as the mean ± SD of 7 animals. *p < 0.05 vs. NC (Tukey-Kramer's multiple range *post-hoc* test).

Table 2. Serum data of the different animal groups at the end of the experimental period

Rat groups/ serum parameters	NC	DBC	DMTL	DMTH
Insulin (pmol/L)	65.8 ± 6.49	8.77 ± 2.24*	9.31 ± 2.45*	11.11 ± 2.98*
Fructosamine (µmol/L)	223.7 ± 26.7	242.0 ± 20.4	246.0 ± 17.10	233.0 ± 21.9
AST (U/L)	57.86 ± 3.9	59.20 ± 6.3	65.67 ± 14.7	53.20 ± 6.1
ALT (U/L)	34.86 ± 6.4	65.20 ± 21.7*	53.83 ± 13.7	62.20 ± 17.8*
Creatinine (mmol/L)	0.43 ± 0.1	0.38 ± 0.1	0.39 ± 0.1	0.41 ± 0.1
Total proteins (g/dL)	6.43 ± 0.4	5.58 ± 0.2*	4.88 ± 0.3*#	4.78 ± 0.2*#
Albumin (g/dL)	2.66 ± 0.3	2.47 ± 0.2	2.28 ± 0.1*	2.25 ± 0.1*
Uric acid (mg/dL)	2.71 ± 1.1	1.90 ± 0.9	1.55 ± 0.4*	1.76 ± 0.2

Values are shown as the mean ± SD of 7 animals. *p < 0.05 vs. NC, #p < 0.05 vs. DBC (Tukey-Kramer's multiple range *post-hoc* test).

concentration. Several critical findings were established, including determining that the selection of leaf area is essential to the level of medicinal potential. Shoots of mulberry leaves contained significantly higher DNJ content than young leaves, which in turn, had significantly higher DNJ content than older mulberry leaves (shoots > young leaves > mature leaves). These findings distinguished better commercial varieties from those with insufficient DNJ concentrations to elicit any beneficial effect on hyperglycemia. Moreover, they tested the quality of the tea-making protocol provided by the manufacturers for DNJ extraction at 90°C for 300 s. Upon modification of the protocol, the optimal tea making condition was in fact found to be at 98°C for 400 s and this increased DNJ extraction from 85 to 95%. This indicates any inferior mulberry leaf selections in tea harvesting and/or coupled with incorrect preparation would most likely provide tea brews containing less the required DNJ concentration to elicit any anti-diabetic effect. A major limitation of many mulberry tea brands is the non-specification of an effective dose to reduce NFBG, despite the packaging claims of anti-hyperglycemic effects of the tea (27). Furthermore, Vichasilp et al. (26) acknowledged the fact that for daily home use it is largely impractical to measure precise tea brewing temperatures for a specified time period in order to ensure sufficient active ingredients are obtained. Although the concentration of DNJ in our brewed mulberry tea has not been measured, no significant anti-diabetic effect might be due to insufficient DNJ concentration.

For this reason, despite much literature indicating the hypoglycemic effects (14, 28–30) of white mulberry leaf tea and extracts, it is most likely that the brand of tea used in this experiment might not provide sufficient DNJ to reduce NFBG as seen in Figures 1 and 2 and might have some other phytochemicals, which did not improve but relatively worsened the glucose tolerance ability as seen in Figure 3. There is, however in fact no record of brewed mulberry leaf tea tested in an animal model for T2D, with most of the studies having dosed the extract itself, or isolating and dosing DNJ into experimental animals to examine the anti-diabetic effects (16, 28, 30, 31). Since mulberry leaf teas are usually consumed after brewing but not as an extract so the aim of our study was to examine anti-diabetic effects of a low (0.25%) and a high (0.5%) concentration of brewed white mulberry leaf tea.

The fructosamine test is another test that is the result of a non-enzymatic reaction between glucose and amino acids in the serum and is an early glyca-

tion end product (32). Fructosamine can thus be used to predict the concentration of advanced glycation end products (AGES) and is an indicator of glycemic control over a 3 weeks or longer period (33). Studies indicate that in diabetic animals, fructosamine concentrations increase compared to normal controls (32). Low serum fructosamine thus indicates a good glycemic control and in the case of intervention trials, the effectiveness of the treatment regime. No significant difference in serum fructosamine and insulin in the mulberry tea consuming groups compared to the DBC group (Table 2) suggests that brewed white mulberry leaf tea have no hypoglycemic or insulinotropic effect but may have some hypolipidemic effects at least in this experimental condition.

Kojima et al. (24) tested the hypolipidemic effects of mulberry leaf extract in healthy non-diabetic human subjects and found no significant differences in serum total cholesterol, HDL- and LDL-cholesterols and triglyceride levels after 6 and 12 weeks, however the hypolipidemic effects of mulberry leaf tea may not be similar between normal and diabetic conditions. In our study, significantly lower total cholesterol and comparatively lower LDL-cholesterol and triglycerides in DMTH group compared to the DBC and DMTL groups suggest the possible hypolipidemic effects of mulberry leaf tea where DNJ might be involved since it has been shown to be effective in decreasing lipid accumulation not only *via* increasing β -oxidation but also by increasing adiponectin levels and activating AMP-activated protein-kinase (AMPK) in isolated rat liver (34).

Although hyperglycemia and hypercholesterolemia are the two major contributing factors to the severity of the diabetic condition, it is necessary to analyze other vital biochemical parameters in order to fully assess the anti-diabetic effects. Mild but chronic increases of these transaminases are also commonly seen in T2D due to hepatic insulin resistance from elevated levels of circulating free fatty acids, which in fact, are toxic to hepatocytes, presumably due to oxidative stress from lipid peroxidation and the recruitment of inflammatory cells (35). However, in our study, the either concentration of mulberry leaf tea could not significantly reduce these liver function enzymes (Table 2). The liver glycogen level was not also affected by the either dose of mulberry leaf tea (Table 1).

In summary, white mulberry leaf tea did not exhibit any hypoglycemic effects, contrary to many literature reports possibly due to the inferior blend of tea selection and hence was unable to correct

minor symptoms of T2D including polyphagia, polydipsia, weight gain and liver glycogen as well as major symptoms including glucose intolerance and insulin deficiency. Additionally, it was significantly increased serum ALT, as well as significantly decreased serum total protein and albumin and serum uric acid – the combined effect thus indicating poorly controlled diabetes and signifying insulin resistance. However, significantly lower serum total cholesterol and markedly and dose dependently lower serum LDL-cholesterol and triglycerides indicate the possible hypolipidemic effects of mulberry leaf tea. In conclusion, white mulberry leaf tea did not display any significantly beneficial anti-diabetic effects but may have some promising hypolipidemic effects at least in this experimental condition and further studies are needed to confirm this effect in humans. Additionally, the effects of the different brands of white mulberry leaf tea may be different due to various factors such as geographical location of tea, age of tea leaves, and processing as well as brewing condition of tea. Hence, the results of this study do not exclude the beneficial effects of the other brands of white mulberry leaf tea which has been proven in other studies.

Acknowledgments

This study was supported by the Competitive Research Grant from the Research Office, University of KwaZulu-Natal (UKZN), Durban; an Incentive Grant for Rated Researchers and a Grant Support for Women and Young Researchers from the National Research Foundation (NRF), Pretoria, South Africa. The authors would like to thank Linda Bester, David Mompe and Mitesh Indrajit for their assistance during the study.

Conflict of interest

There is no conflict of interest within this manuscript.

REFERENCES

1. International Diabetes Federation (IDF): IDF Diabetes Atlas, 5th edn., Brussels, Belgium 2012.
2. Chen D., Wang M.-W.: Diabetes Obes. Metabol. 7, 307 (2005).
3. DeFronzo R.A.: Med. Clin. North Am. 88, 787 (2004).
4. Stumvoll M., Goldstein B.J., Van Haeften T.W.: Lancet 365, 1333 (2004).
5. Liu Y., Wang Z., Yin W., Li Q., Cai M. et al.: Exp. Anim. 56, 11 (2007).
6. Srinivasan K., Viswanad B., Asrat L., Kaul C.L., Ramarao P.: Pharmacol. Res. 52, 313 (2005).
7. Marshall J.A., Hoag S., Shetterly S., Hamman R.F.: Diabetes Care 17, 50 (1994).
8. Amin K.A., Nagy M.A.: Diabetol. Metab. Syndr. 1, 17 (2009).
9. Tahrani A.A., Piya M.K., Kennedy A., Barnett A.H.: Pharmacol. Ther. 125, 328 (2010).
10. Butt M.S., Nazir A., Sultan M.T., Schroën K.: Trends Food Sci. Technol. 19, 505 (2008).
11. Bantle J.P., Slama G.: Is fructose the optimal low glycemic index sweetener, in Nutritional Management of Diabetes Mellitus and Dysmetabolic Syndrome, pp. 83–89, Karger, Basel 2006.
12. Oku T., Yamada M., Nakamura M., Sadamori N., Nakamura S.: Br. J. Nutr. 95, 933 (2006).
13. Hansawasdi C., Kawabata J.: Fitoterapia 77, 568 (2006).
14. Andallu B., Varadacharyulu N.: Clin. Chim. Acta 338, 3 (2003).
15. Kobayashi Y., Miyazawa M., Kamel A., Abe K., Kojima T.: Biosci. Biotechnol. Biochem. 74, 2385 (2010).
16. Enkhmaa B., Shiwaku K., Katsube T., Kitajima K., Anuurad E. et al.: J. Nutr. 135, 729 (2005).
17. Kimura T., Nakagawa K., Kubota H., Kojima Y., Goto Y. et al.: J. Agric. Food Chem. 55, 5869 (2007).
18. Wilson R.D., Islam M.S.: Pharmacol. Rep. 64, 129 (2012).
19. Lo S., Russel J.C., Taylor A.W.: J. Appl. Physiol. 28, 234 (1970).
20. Islam M.S., Choi H.: J. Food Sci. 73, H213 (2008).
21. Dey L., Attele A.S., Yuan C.-S.: Altern. Med. Rev. 7, 45 (2002).
22. Bailey C.J., Day C.: Diabetes Care 12, 553 (1989).
23. Yang C.S., Landau J.M.: J. Nutr. 130, 2409 (2000).
24. Kojima Y., Kimura T., Nakagawa K., Asai A., Hasumi K. et al.: J. Clin. Biochem. Nutr. 47, 155 (2010).
25. Herscovics A.: Biochim. Biophys. Acta 1473, 96 (1999).
26. Vichasilp C., Nakagawa K., Sookwong P., Higuchi O., Luemunkong S. et al.: LWT – Food Sci. Technol. 45, 226 (2012).
27. Kimura T., Nakagawa K., Saito Y., Yamagishi K., Suzuki M. et al.: J. Agric. Food Chem. 52, 1415 (2004).

28. Kong W.H., Oh S.H., Ahn Y.R., Kim K.W., Kim J.H. et al.: J. Agric. Food Chem. 56, 2613 (2008).
29. Miyahara C., Miyazawa M., Satoh S., Sakai A., Mizusaki S.: J. Nutr. Sci. Vitaminol. (Tokyo). 50, 161 (2004).
30. Naowaboot J., Pannangpetch P., Kukongviriyapan V., Kukongviriyapan U., Nakmareong S. et al.: Nutr. Res. 29, 602 (2009).
31. Kim S.Y., Gao J.J., Lee W.C., Ryu K.S., Lee R.R. et al.: Arch. Pharm. 22, 81 (1999).
32. Cheng-Tzu L., Chen K-M., Lee S-H., Tsai L-J.: Nutrition 21, 615 (2005).
33. Li K., Yang H.X.: Chin. Med. J. 119, 1861 (2006).
34. Tsuduki T., Nakamura Y., Honma T., Nakagawa K., Kimura T. et al.: J. Agric. Food Chem. 57, 11024 (2009).
35. Harris E.H.: Clin. Diabetes 23, 115 (2005).

Received: 3. 01. 2014

PHARMACEUTICAL TECHNOLOGY

**THE INFLUENCE OF LOW PROCESS TEMPERATURE
ON THE HYDRODYNAMIC RADIUS OF POLYNIPAM-CO-PEG
THERMOSENSITIVE NANOPARTICLES PRESUMED AS DRUG CARRIERS
FOR BIOACTIVE PROTEINS**WITOLD MUSIAŁ^{1*} and JIŘÍ MICHÁLEK²¹Department of Physical Chemistry, Wrocław Medical University, Borowska 211, 50-556 Wrocław, Poland²Department of Polymer Gels, Institute of Macromolecular Chemistry of the Academy of Sciences of Czech Republic, Heyrovského nám. 2, 162 06 Praha 6 – Břevnov, Czech Republic

Abstract: The aim of the work was to evaluate the influence of low process temperature on the hydrodynamic radius of the synthesized nanoparticles presumed for incorporation of bioactive proteins. The reaction prompted in temperatures of 22, 38 and 70°C. The first one reflected the ambient environmental temperature, at which the bioactive proteins may be implemented into the reactant mixture. The intermediate temperature should enable safe use of proteins during the reaction, and represents the upper limit of applied heat, due to the consequent denaturation of proteins at elevated temperatures. The reactant mixture heated up to 70°C provides excellent formation of nanoparticles, however the albuminous components will tend to degrade. Within the study we applied N,N,N',N'-tetramethylethane-1,2-diamine as an accelerator in the presence of the strong oxidizing agent – ammonium persulfate as radical initiator. Six batches of N-isopropylacrylamide derivatives with polyoxyethylene glycol diacrylamide co-monomer of molecular weight in the range of 2000 Da were synthesized within the course of surfactant free precipitation polymerization. The nanodispersions were assessed in the terms of hydrodynamic radius, by the dynamic light scattering method (DLS). The polydispersity index, as well as average hydrodynamic radius, and hydrodynamic radius of main population of particles, identified in the DLS device, were evaluated and discussed in the perspective of application of the nanogels as drug carriers for bioactive proteins.

Keywords: nanogel, N-isopropylacrylamide, thermosensitivity, protein stability, PEG

Controlled and targeted drug delivery in the case of proteins is developed intensively, due to the instable properties of the polypeptides in elevated temperatures. The model polypeptides e.g., insulin, BSA, β -galactosidase, calcitonin, lysozyme, and interleukin are loaded to the thermoresponsive nanogels, however the loading process is often ineffective (1, 2). Another approach includes the polymerization *in situ* with biologically active component implemented into reacting mixture (3). One of the attractive monomers applied in the studies on new polymeric drug carriers is N-isopropylacrylamide (NIPA) (4). Nanogels synthesized using NIPA enjoy a growing interest among specialists in drug form technology, bioengineering and biocompatible polymers. This is due to the fact of removal large amounts of water from particles of poly-N-iso-

propylacrylamide (polyNIPA), around volume phase transition temperature (VPTT). Consequently, one can expect the release of drug substance from the nanogels of polyNIPA under the influence of the thermal factor. Importantly, the VPTT is in the range of known physiological temperatures, e.g., in the range of the temperature of human skin surface. By modifying the composition and structure of derivatives of NIPA it is possible to obtain a number of macromolecules with programmed VPTT in the water system (5–7). The homogenous nucleation NIPA with co-monomers is usually performed at increased temperature (8), due to the fact that the key requirement for formation of the polymer in the microgel structure, is the insolubility of the obtained entity in the solvent, otherwise the macrogel will be obtained (9). The process uses an initiator, e.g.,

* Corresponding author: e-mail: witold.musial@gmail.com

ammonium persulfate (APS), yielding initiator radicals imparting surface-active properties to the particles of the growing polymer chain. Macromolecules prepared by this technique are stabilized by covalently bound sulfate groups of the radical species derived from the persulfate ion (10). The obtained nanostructures collapse *in situ* in the process conditions, so the definite nanogel structures are obtained. However, in this procedure, the temperature increases beyond the VPTT of the obtained material, so the incorporation of thermally instable protein entities is hardly possible in the course of the polymer synthesis. Rarely, the proteins of interesting prospective applications are thermally stable at temperatures beyond the physiological human body temperature. Moreover, few of them are stable in the temperature range of 60–80°C, which is suitable for the process of synthesis of nano- and microgels in aqueous conditions. For example, glyceraldehyde-3-phosphate dehydrogenase produced by *Bacillus stearothermophilus* is stable in the range of 40–65°C, however the human one is degraded by 37°C (11). Due to that fact, some studies were developed to enhance the stability of bioactive proteins at elevated temperatures, however the practical application of modified thermally stable proteins in drug delivery, seems to be a very future task – some of the approaches include modification of the internal composition of the protein, or attachment of the proteins to the protective components (12–16). Another way of overcoming the problem of implementation of bioactive proteins into the polymer bead, in the polymerization course, is use of low process temperatures.

During the growth of the polyNIPA, several structures may be formed due to various bibliographic reports and process conditions. Saunders proposed some possible structures: homogenous,

core-shell with uniform mesh size in the core and the shell, agglomerated, and agglomerated with core-shell microgels (17). The additional important factor, which influences the formation of nano- and microstructures is micellization (18). When the room temperature is applied in the polymerization course, the growing polyNIPA chains do not shrink, and additionally, the number of active polymerization loci may be decreased, comparing to the increased process temperature. The low temperature and low initiator content result in structures of high radius and low density. This may lead to the growth of macrogels, instead of microgel or nanogel. Anyway, the problem of synthesis of nanogels and microgels, in the conditions providing the thermal stability of proteins, is very attracting to the researchers. An attempt was made to resolve the problem applying the initiator system consisting of APS with N,N,N',N'-tetramethylethane-1,2-diamine (TEMED) for immobilization of avidin by one-pot copolymerization at temperature near VPTT (19). In several works authors evaluated the polyoxyethylene glycol diacrylates (PEGDA) and methacrylates as co-monomers with interesting properties (20).

The aim of the work was to evaluate the influence of thermal conditions on the hydrodynamic radius of polyNIPA-co-PEGDA nanogels synthesized at various temperatures in the presence of APS-TEMED initiator system.

EXPERIMENTAL

Materials

N-isopropylacrylamide (NIPA), polyethylene glycol diacrylate of molecular mass ca. 2000 (PEGDA), N,N,N',N'-tetramethylethane-1,2-diamine were purchased from Aldrich (Prague, Czech

Table 1. The feed composition of the substrates in surfactant free precipitation polymerization; NIPA – N-isopropylacrylamide, PEGDA – polyoxyethylene glycol diacrylate of molecular weight ca. 2000 Da, TEMED – N,N,N',N'-tetramethylethane-1,2-diamine, APS – ammonium persulfate.

Nanogel type	Acronym	Substrates [g]			
		NIPA	PEGDA	TEMED	APS
polyNIPA-co-PEGDA (1 : 22)	PA	0.720	0.250	0.010	0.020
polyNIPA-co-PEGDA (1 : 38)	PB	0.720	0.250	0.010	0.020
polyNIPA-co-PEGDA (1 : 70)	PC	0.720	0.250	0.010	0.020
polyNIPA-co-PEGDA (2 : 22)	PD	0.720	0.250	0.020	0.040
polyNIPA-co-PEGDA (2 : 38)	PE	0.720	0.250	0.020	0.040
polyNIPA-co-PEGDA (2 : 70)	PF	0.720	0.250	0.020	0.040

Republic). APS was supplied by Lachema (Prague, Czech Republic). The substrates obtained from commercial suppliers were used without further purification. A dialysis bag with a molecular weight cut-off of 12000–14000 Da was received from Sigma Aldrich (Prague, Czech Republic). Deionized water was produced in TKA DI 6000 system (Niederelbert, Germany) and we used it in all following procedures.

Synthesis of the thermosensitive nanoparticles

The surfactant-free precipitation polymerization (SFPP) was performed to obtain polyNIPA nanogel particles crosslinked by PEGDA. The polymerization was performed in deionized water under an inert nitrogen atmosphere according to the procedure evaluated by Pelton and Chibante (21, 22), and developed in groups of Snowden and Vincent (23–25). The radical initiator, APS, was placed in a 500 mL, three-necked round-bottomed flask and stirred continuously at 120 rpm. Pre-dissolved NIPA and cross-linking agent PEGDA were dissolved in 20 mL of deionized water with stirring and were then added to the reaction vessel. After 4 h, the dispersion was cooled to room temperature and filtered. Dry weight analysis of the nanogels showed the dispersion to have a concentration on the order of 0.1–0.5 wt.%. The starting composition of the substrates is given in Table 1, with respective acronyms of the nanodispersions.

Equilibrium dialysis – purification of nanogels

Dialysis – purification by diffusion through semipermeable membrane was performed in the set of glass vessels. The sample of 50 mL of nanogel dispersion was closed in dialysis bag, and transferred into 300 mL glass vessel. The system was stirred in IKA-VIBRAX-VXR device (Germany), at 100 rpm. The particles were dialyzed against deionized water until the conductivity was less than 1.0 $\mu\text{S}/\text{cm}$ (26). Within the first 30 h the conductivity in the acceptor compartment was measured and the water remained unchanged in the acceptor compartment. After 30 h, the water was replaced in acceptor compartment by fresh deionized water, and the conductivity measurement was taken after 24 h. The procedure was repeated every 24 h, through 18 days, till the conductivity did not exceed 1.0 $\mu\text{S}/\text{cm}$.

FTIR evaluations

Fourier transformed infrared spectra – FTIR of the obtained polymers were measured at ambient temperature with a Nicolet Nexus 870 FTIR spectrometer purged with dry air, and equipped with a

Golden Gate device ATR, with reproducible approximate sample loads of 3 kbar. Samples were measured in the dry state; the spectra were corrected for absorption of the solvent and H_2O vapors.

Assessment of the hydrodynamic radius

The hydrodynamic radius was assessed in aqueous dispersions by dynamic light scattering (DLS). From the ca. 50 mL sample, 50 μL was taken, and centrifugated within the Eppendorf tube filled with 1.0 mL of prefiltered water, in Roth MicroCentrifuge, at 6000 rpm for 45 min. From the tube 50 μL of supernatant were taken, and placed into polystyrene-single use fluorimeter cuvettes. Then, 1 mL of de-ionized water, filtered through 0.2 μm PVDF Whatmann nanofilter, was added to the cuvette and the sample was inserted into Zeta Sizer Nano with 173° backscatter measurement arrangement and settings of Mark-Houwkin parameters. The duration of measurements was extended for the case of large particles, with relaxation time multiplier of 100000. The measurements settings were automated to seek optimum position; the attenuator selection was also automated. Every measurement was multiplied five times. Three sets of data were excavated from every measurement: (1) average radius of the nanogels counted on the total measured nanogels (R_{ha}), (2) radius of the main fraction of nanogels present in the evaluated spectrum of sizes in the assessed dispersion (R_{hm}), and (3) polydispersity index of the assessed dispersions of thermosensitive nanogels (PI) in the Zetasizer Nano Software Version 5.03.

RESULTS

Due to the FTIR assessments within all the products, the polyNIPA polymer was synthesized in all the cases with implemented PEGDA crosslinker, as confirmed in previous work (12). The yield of the reaction was different, and depended on the applied conditions and feed compositions. The yields of nanogels PA-PF, estimated due to the gravimetric assessments, were in the range of 8–93%. The proposed structure of the obtained nanogel is visualized in Figure 1.

The measurements of synthesized nanogels performed *via* DLS give characteristic set of data, which is valuable in the terms of evaluation of the structure of thermosensitive macromolecules obtained on the basis of NIPA. We assessed in details three parameters in pure aqueous environment, as it is mentioned above: (1) average radius of the nanogels counted on the total measured nanogels

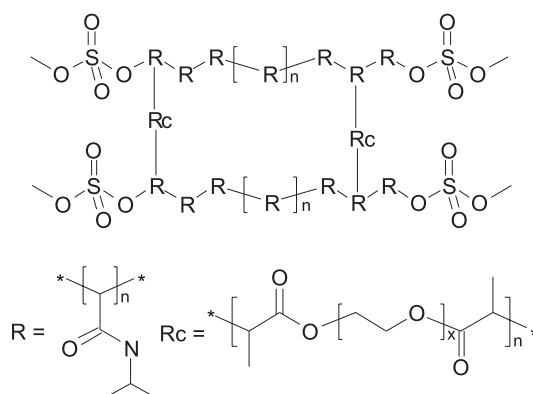


Figure 1. Visualization of proposed structure of the synthesized nanogels PA-PF

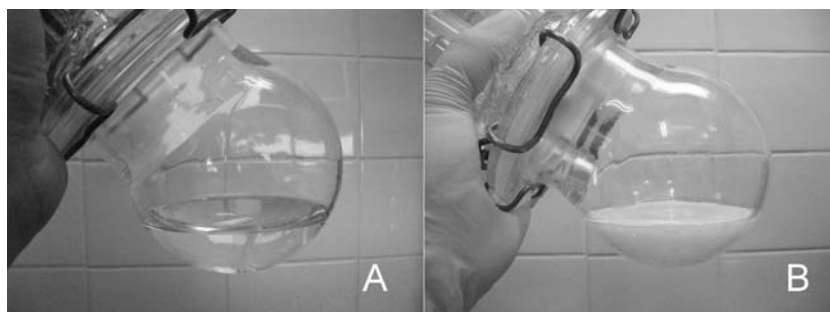


Figure 2. The synthesized system PD below (A) and over (B) VPTT

(R_{ha}), (2) radius of the main fraction of nanogels present in the evaluated spectrum of sizes in the assessed dispersion (R_{hm}), (3) polydispersity index of the assessed dispersions of thermosensitive nanogels (PI). In the macroscopic view, the dispersions may be defined as transparent below the VPTT, whereas at increased temperatures they are non-transparent, due to the aggregation of small particles as it is presented in Figure 2 for the system pilot PD synthesized in our laboratory.

The general observation of the data leads to the conclusion, that the radii at fixed temperature are higher in the case of lower concentration of the initiator/accelerator system, with the exception of the systems PA and PD. In the case of the both latter nanogels (PA, PD) the effective size, measured in DLS conditions, is better presented when the extreme values are rejected from the considerations.

Hydrodynamic radius of microspheres prepared at 22°C

The R_{ha} of nanogels synthesized in the temperature of 22°C, was in the range between 98 and 245

nm, and it was not possible to distinguish between the batch PA and PD in the entire range of evaluated temperatures of measurements i.e., 10–52°C. Notwithstanding, we noted the characteristic shape of the polynomial trend line, which took the form of obverse letter U. The average radii are presented in Figure 3A. When the extreme values were rejected from the considerations, we observed a decrease of radius, which is typical for the thermosensitive N-isopropylacrylamide derivatives as it is visualized in Figure 3B (R_{hm}). Notwithstanding, the diversity of radii was high.

Hydrodynamic radius of microspheres prepared at 38°C

The concentration of initiator influenced the direction of the R_{ha} changes, in the batches prepared in intermediate temperature of the synthesis (PB, PE). In PB batch, the R_{ha} increased slightly with increased temperature from ca. 183 nm at 10°C to 228 nm at 52°C, while the PE presented opposite tendency – the R_{ha} decreased with the increase of the temperature in the course of the size assessments

from 432 nm to 40 nm – Figure 4A. Similarly, the values of hydrodynamic radius after rejection of extreme values – R_{hm} , also decreased in the range between 1360 nm and 50 nm for PE. The batch PB did not change significantly the radius with the alteration of the temperature – the initial and final value corresponded, respectively, to 176 nm and 128 nm, as it is presented in Figure 4B.

Hydrodynamic radius of microspheres prepared at 70°C

The values from R_{ha} measurements performed on nanogels prepared at temperature of 70°C are gathered in Figures 5A and 5B. The PC batch has higher radii both in the case of initial and final temperature, i.e., 98 nm and 50 nm, comparing to the batch PF, with initial and final values of R_{ha} 89 and 47 nm, respectively (Fig. 5A). The initial values of R_{hm} were in the range of 110 nm for PC and 105 nm for PF, while the final values were 55 nm and 52 nm, respectively (Fig. 5B).

Polydispersity index

The PDI factor is illustrated on the Fig. 6A–6C. For the nanogels synthesized in temperature of 22°C the PDI is below the VPTT in the range of 0.01–0.37. The highest values were observed in the case of nanogels obtained in SFPP prompted in temperature of 38°C. Interestingly, the highest values of 1.0 were observed below VPTT for the the batch PE with high content of TEMED and APS, while over VPTT the highest values were observed in the case of PB with lower content of TEMED and APS. The nanogels obtained in the temperature of 70°C were characterized by highest homogeneity and the PDI did not exceed the range of 0.09–0.167 in the case of PF, and 0.04–0.164 in the case of PC, with exception of one point for PC equal to 0.249.

DISCUSSION

The often misleading notion “size” usually is referred in nanoscience to the hydrodynamic diame-

Table 2. Evaluation of the average hydrodynamic radii obtained in the DLS measurements.

Shift of average hydrodynamic radius (R_{ha}) with increase of temperature			
Concentration of initiator [mg/L]	Temperature of synthesis	Acronym	Change of radius of the nanogels, when the VPTT is crossed
TEMED: 10 APS: 20 (○)	22	PA	Similar radii, high diversity of radius, \cap shape
	38	PB	Slight increase
	70	PC	Typical decrease
TEMED: 20 APS: 40 (●)	22	PD	Similar radii, high diversity of radius, \cap shape
	38	PE	Decrease, L shape
	70	PF	Typical decrease

TEMED: N,N,N,N-tetramethylethane-1,2-diamine, APS: ammonium persulfate, PA-PF: synthesized nanoparticles, the descriptors (○), and (●) represent respective values on the Figures throughout the entire text.

Table 3. Evaluation of the hydrodynamic radii of main fraction of nanogels obtained in the DLS measurements.

Shift of hydrodynamic radius of main fraction of nanogels (R_{hm}) with an increase of temperature			
Concentration of initiator [mg/L]	Temperature of synthesis	Acronym	Change of radius of the nanogels, when the VPTT is crossed
TEMED: 10 APS: 20 (○)	22	PA	Decrease of radius, high diversity of radius
	38	PB	Similar radii, not shifted
	70	PC	Typical decrease
TEMED: 20 APS: 40 (●)	22	PD	Decrease of radius, high diversity of radius
	38	PE	High decrease
	70	PF	Typical decrease

TEMED: N,N,N,N-tetramethylethane-1,2-diamine, APS: ammonium persulfate, PA-PF: synthesized nanoparticles, the descriptors (○), and (●) represent respective values on the Figures throughout the entire text.

ter, or hydrodynamic radius. Due to the works of Dušek, the number of macromolecules obtained *via* SFPP, may increase with the parallel increase of initiator concentration (27–29). If the reacting systems consist of the same amount of monomer, but the concentration of the initiator increases, parallel the hydrodynamic radius of obtained macromolecule should decrease. The DLS system gives an opportunity to measure the hydrodynamic radius. Respectively, the DLS measurements should enable evaluation of the influence of the initiator concentration on the “size” of obtained nanogels. In Tables 2 and 3 we present the evaluated data in compact form.

The evaluation of R_{ha} gives an assumption, that the nanogels prepared at the 22°C are very varied in the terms of hydrodynamic radius. However, when the extreme data are excluded, the main fraction of the nanogels may be assigned to the range 138–235 nm at the temperature below VPTT, and respectively, to the range 53–153 nm at temperature overcoming VPTT. This result confirms the possibility of synthesis of thermosensitive co-polymer of NIPA and PEG in temperature below the values critical for the denaturation of the proteins. The PDI measured throughout the entire assessment process increased

(Fig. 6A), due to the fact of aggregation of the particles in the region of VPTT (Fig. 3A), according to the decrease of the size of the main fraction of the nanogels in the course of the heating (Fig. 3B).

The complications arise when the SFPP process is performed at the temperature of 38°C. This temperature would be acceptable for implementation of some proteins into the SFPP process, however the resulting nanogels are highly differentiated, due to the high PDI. In the polymeric system PB with low content of accelerator and initiator the nanogels aggregated when the temperature increase (Fig. 4A), and we did not observe any precise VPTT, however due to the measurements of R_{hm} , the main fraction of the macromolecules was practically thermally insensitive (Fig. 4B). At the temperature below VPTT in the polymeric system PE dominate the huge structures with radius in the range of 746–1360 nm, but in higher temperature they disaggregate to more homogenous macromolecules in the range of 50–100 nm, with PDI decreased to values not exceeding 0.437 – Fig. 5B. The uncertain results of the synthesis at the temperature of 38°C confirm the multilateral form of the NIPA in the region of VPTT – the nascent polymer may be formed in various shapes according to Wu and Wang (27), and var-

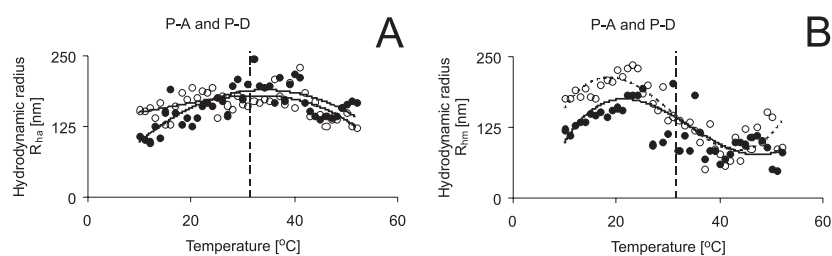


Figure 3. The influence of temperature on the average hydrodynamic radius (R_{ha} , **A**), and on the hydrodynamic radius of main fraction (R_{hm} , **B**) of nanogels obtained in the SFPP process, performed in the temperature of 22°C, respectively, at low (○) and high (●) concentrations of the accelerator/initiator system, the vertical discontinuous straight line represents VPTT, the dotted lines are the guides for the eye

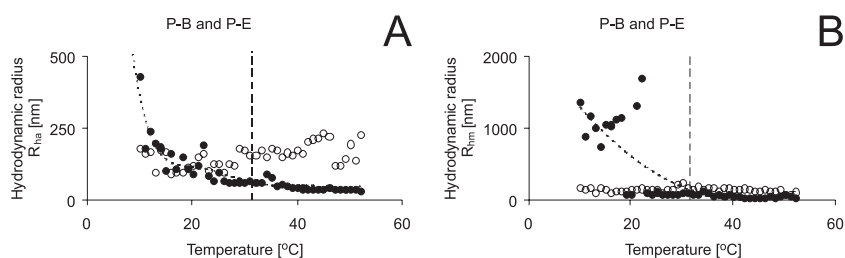


Figure 4. The influence of temperature on the average hydrodynamic radius (R_{ha} , **A**), and on the hydrodynamic radius of main fraction (R_{hm} , **B**) of nanogels obtained in the SFPP process, performed in the temperature of 38°C, respectively, at low (○) and high (●) concentrations of the accelerator/initiator system, the vertical discontinuous straight line represents VPTT, the dotted lines are the guides for the eye

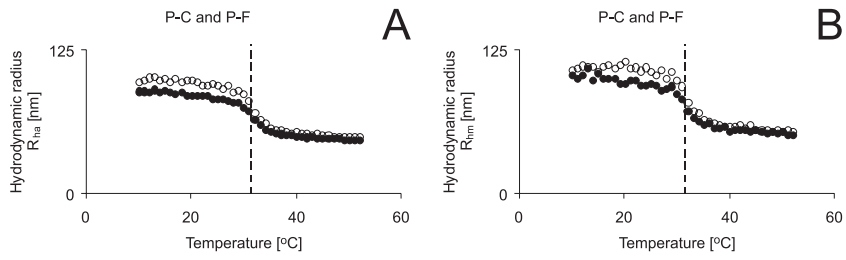


Figure 5. The influence of temperature on the average hydrodynamic radius (R_{h} , **A**), and on the hydrodynamic radius of main fraction (R_{fm} , **B**) of nanogels obtained in the SFPP process, performed in the temperature of 70°C, respectively, at low (○) and high (●) concentrations of the accelerator/initiator system, the vertical dotted line represents VPTT

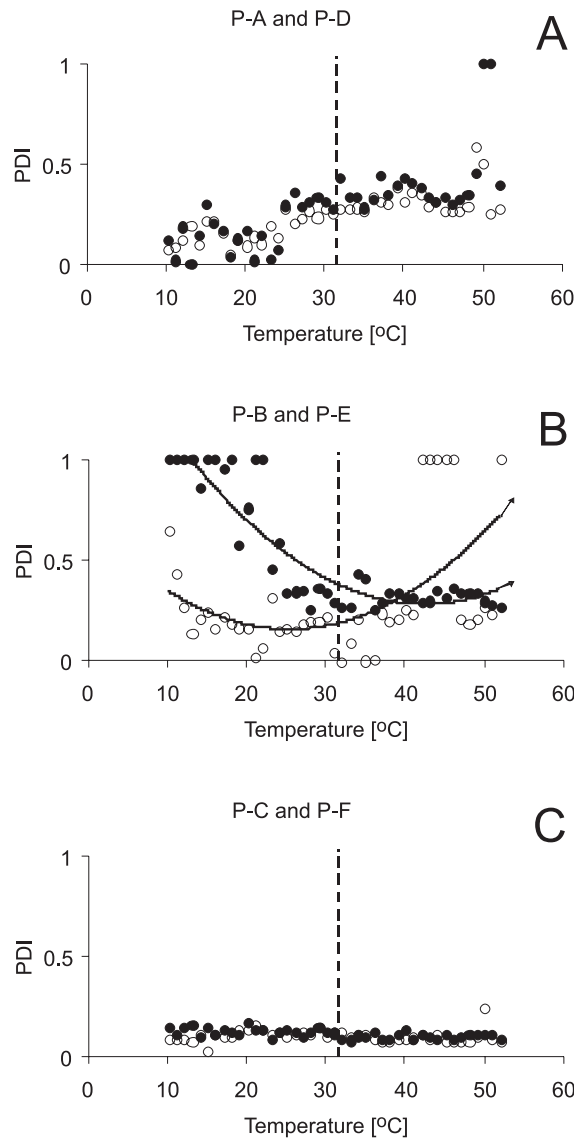


Figure 6. Polydispersity index of nanogels PA-P6, the vertical discontinuous straight line represents VPTT, the dotted lines are the guides for the eye

ious fractions of polymer may exist in this intermediate temperature, leading to high polydispersion.

Due to Wu and Wang (30), there are at least four thermodynamically stable states of a homopolymer chain in the coil-to-globule and the globule-to-coil transitions. At the low temperatures the particle is in the, so called, coiled state, and the chains movement is not hindered by molecular hindrances, what was confirmed in the work of Zhou et al. (31). On the opposite side, there is the, so called, globule state, when the chains of the macromolecule are definitively collapsed. However, between the two alternate states, two additional states are possible: crumpled coil, and molten globule. That phenomenon may explain the increase in R_{ha} value for the system PB and unsuspected high R_{hm} value for the PE system. The PB system was synthesized at intermediated temperature, when the growing polymer chain could be formed into crumpled coil or molten globule form. Moreover, the initiator system was in rather low concentration. Therefore, large particles were formed and the implemented crosslinker influenced growth of large and rigid structures, with tendency of aggregation. Also synthesis of PE system was prompted at interjacent temperature, however the increased initiator concentration should enhance the growth of large number of minor particles. From the graphs and the tables it is clear that at reduced temperatures the particles tend to aggregate, whereas after heating the particles are homogeneously dispersed in the medium. Their dimensions correlate with the assumption, that at increased initiator concentrations, the obtained nanoparticles should be smaller. The different behavior of PB and PE systems was confirmed also in terms of PDI – Fig. 6B. The system PB synthesized with low concentration of initiator tends to aggregate with the increase of temperature, so the PDI is increasing. In this case the long PEG chains may influence the increased interpenetration of the particles. The PE system tends to deaggregate at increased temperatures, due to the data from DLS.

The classical approach to the synthesis of the polyNIPAM-co-PEGDA system results in small particles – Fig. 5. They are in the radius range of ca. 100 nm – decreasing to ca. 50 nm after crossing the VPTT value. When the higher initiator concentration is applied, the particles seem to be slightly smaller, which is in agreement with the predictions of Dušek (24, 25) and Cio (32). From the R_{ha} values, it may be deduced that in the batches of polyNIPAM-co-PEGDA : PC and PF rather small particles are present, as the respective values are slightly lower. The standard temperature applied for

the synthesis of polyNIPAM in the SFPP process is in the range of 70°C. The comparative graphs of size vs. environmental temperature confirm that the optimal conditions for synthesis of polyNIPAM-co-PEG are at elevated temperatures, however similar results were obtained in the case of PD, when the synthesis of the nanoparticles is performed at 22°C, however we recommend development of the TEMED/APS system for the further research in the SFPP at reduced temperatures, even much more below 38°C, and close to 22°C.

CONCLUSIONS

The use of TEMED in the temperatures below the VPTT, and below the applied temperature of activation of the initiator, gives promising results at the temperature of 22°C. Due to our data, it is possible to synthesize thermosensitive nanogels, derivatives of NIPA and PEG in this low temperature conditions. When intermediate temperature 38°C is applied, with low concentration of TEMED and APS, the resulting nanogels tend to agglomerate, but they do not seem to be thermosensitive in the sense of typical polyNIPAM. The increased concentration of the accelerator and initiator favors synthesis of thermosensitive nanogels in the temperature of 38°C, but the produced nanogels are not homogeneous. The increased concentration of accelerator/initiator system promoted the decrease of the hydrodynamic radius in all the cases, irrespective of the temperature of measurement.

Acknowledgments

The study was supported by research fellowship within “Development program of Wrocław Medical University”, Poland, funded from European Social Fund, Human Capital, National Cohesion Strategy, contract no. UDA-POKL.04.01.01-00-010/08-00 in 2011. The authors would like to thank to the following colleagues for the scientific and technical help in the performance of the measurements in the Institute of Macromolecular Chemistry in Prague, Czech Republic: František Rypáček, Petr Štěpánek, Karel Dušek, and Miroslava Dušková-Smrčková.

REFERENCES

1. Bhuchar N., Sunasee R., Ishihara K., Thundat T., Narain R.: *Bioconjugate Chem.* 23, 75 (2012).
2. Bromberg L.E., Ron E.S.: *Adv. Drug Deliv. Rev.* 31, 197 (1998).

3. Ngwuluka N.: AAPS PharmSciTech 11, 1603 (2010).
4. Qiu Y., Park K.: Adv. Drug Deliv. Rev. 64, 49 (2012).
5. Quan C.Y., Wei H., Shi Y., Li Z.Y., Cheng S.X., Zhang X.Z., Zhuo R.X.: Colloid Polym. Sci. 289, 667 (2011).
6. Lee Y.J., Cheong I.W., Yeum J.H., Jeong Y.U.: Macromol. Res. 18, 208 (2010).
7. Dai W., Zhang Y., Du Z., Ru M., Lang M.: J. Mat. Sci. Mat. Med. 21, 1881 (2010).
8. Schild H.G.: Prog. Polym. Sci. 17, 163 (1992).
9. Pelton R., Hoare T.: in Microgel Suspensions, Fundamentals and Applications, 1st edn., Fernandez-Nieves A., Wyss H., Mattsson J. Eds., p. 11, Wiley-VCH, Weinheim 2011.
10. Odian G.: Surfactant Free Emulsion Polymerization: Principles of polymerization, p. 352, John Wiley and Sons, New Jersey 2004.
11. Vogt G., Woell S., Argos P.: J. Mol. Biol. 269, 631 (1997).
12. Menéndez-Arias L., Argos P.: J. Mol. Biol. 206, 397 (1989).
13. Kaushik J.K., Bhat R.: Protein Sci. 8, 222 (1999).
14. Wingreen N.S., Li H., Tang C.: Polymer 45, 699 (2004).
15. Noritomi H., Minamisawa K., Kamiya R., Kato S.: J. Biomed. Sci. Eng. 4, 94 (2011).
16. Prashar D., Cui D., Bandyopadhyay D., Luk Y.Y.: Langmuir 27, 13091 (2011).
17. Saunders B.R.: Langmuir 20, 3925 (2004).
18. Zheng S., Shi S., Xia Y., Wu Q., Su Z., Chen X.: J. Appl. Polym. Sci. 118, 671 (2010).
19. Hu X., Tong Z., Lyon A.: Langmuir 27, 4142 (2011).
20. Musial W., Kokol V., Fecko T., Voncina B.: Chem. Pap. 64, 791 (2010).
21. Pelton R.H., Chibante P.: Colloids Surf. 20, 247 (1986).
22. Pelton R.H.: Adv. Colloid Interface Sci. 85, 1, (2000).
23. Lowe J.S., Chowdhry B.Z., Parsonage J.R., Snowden M.J.: Polymer 39, 1207 (1998).
24. Nur H., Pinkrah V.T., Mitchell J.C.: Adv. Colloid Interface Sci. 158, 15 (2010).
25. Rasmusson M., Routh A., Vincent B.: Langmuir 20, 3536 (2004).
26. Senff H., Richtering W.: Colloid Polym. Sci. 278, 830 (2000).
27. Dušek K.: J. Polym. Sci. C, Polym. Symp. 16, 1289 (1967).
28. Dušek K.: J. Polym. Sci. C, 39, 83 (1972).
29. Dušek K.: Macromol. Chem. Macromol. Symp. 7, 37 (1987).
30. Wu C., Wang X.: Phys. Rev. Lett. 80, 4092 (1998).
31. Zhou S., Fan S., Auyeung S.C.F., Wu C.: Polymer 36, 1341 (1995).
32. Xiao X.C.: eXPRESS Polym. Lett. 1, 232 (2007).

Received: 30. 10. 2013

FAST ULTRA-FINE SELF-NANOEMULSIFYING DRUG DELIVERY SYSTEM FOR IMPROVING *IN VITRO* GASTRIC DISSOLUTION OF POOR WATER SOLUBLE DRUG

EHAB I. TAHA*, SALEH A. AL-SUWAYEH, MOUSTAFA M. TAYEL
and MOHAMED M. BADRAN

Department of Pharmaceutics, King Saud University, P.O. Box 2457, Riyadh 11451, Saudi Arabia

Abstract: Meloxicam (MLX) has poor water solubility which leads to slow absorption following oral administration; hence, immediate release tablet is unsuitable in the treatment of acute pain. The aim of this study was to prepare a novel fast ultra-fine self-nanoemulsifying drug delivery system (UF-SNEDDS) of MLX for oral administration to facilitate drug release process in the stomach as well as comparing its *in vitro* dissolution with commercial Mobic® and Mobitol® tablets. MLX solubility in oils, mixed glycerides and surfactants with different HLB values was investigated. Based on MLX solubility profiles, eight UF-SNEDDSs composed of MLX, Cremophor RH 40 as oily phase, Capmul MCM-C8 or Tween 80 as surfactant and PEG 400 as co-solvent were prepared and evaluated for their spontaneous formation of emulsion, droplet size, turbidity and *in vitro* dissolution. The prepared novel MLX formulations showed a significant very low droplets size (up to 25 nm), thermodynamically stable and spontaneously formed nanoemulsion. MLX UF-SNEDDS formulations showed significant high percentage of drug dissolution (up to 70%) in simulated gastric fluid, compared with Mobic® and Mobitol®. In conclusion, due to higher drug release from MLX UF-SNEDDS formulations they could enhance its absorption and hence its bioavailability.

Keywords: meloxicam, solubility, ultra-fine self-nanoemulsifying, lipid-based formulations, *in vitro* dissolution

Meloxicam (MLX) is a highly potent once daily non-steroidal anti-inflammatory drug (NSAID) of the enolic class. It is more selective in inhibiting cyclooxygenase COX-2 than COX-1 therefore; it possesses superior gastrointestinal safety profile and tolerability compared with regular NSAIDs (1). The drug is effective as analgesic for various pain conditions (2). After an oral dose, MLX is well absorbed from the gut, with an absolute bioavailability of 89%, with the plasma concentration peaking after 5–6 h, indicating the slow absorption of MLX after an oral administration (3). Consequently, intramuscular formulation of MLX is used to shorten the onset of action, since rapid pain relief is required in case of acute and painful exacerbations of rheumatoid arthritis (1). However, due to the potential local tissue irritation and necrosis, intramuscular administration of MLX is not recommended for the chronic use (4). It is therefore reasonable to investigate the approaches that may facilitate oral absorption of MLX for treating acute pain. MLX is practically insoluble in water (8 µg/mL) at

low pH value. Also it has a zwitterionic property with two pK_a values of 1.09 and 4.18 (3, 5). A zwitterionic drug possesses a large intramolecular multipole moment due to its multiplicity of oppositely charged groups. Consequently, most of these drugs show low solubility in polar and nonpolar media (3). MLX is classified as a Class II compound having a low solubility and high permeability according to the Biopharmaceutics Classification System (6). The pharmacokinetic profiles of these drugs can generally be changed by formulation techniques that increase their aqueous solubility (3), as the rate of dissolution remains one of the most challenging aspects in formulation development of poorly water-soluble drugs (7). To achieve adequate pharmacodynamic properties such as rapid onset of drug effect, improvement of dissolution is important factor (1, 7). Therefore, several attempts have been made to improve MLX solubility (8).

Self nanoemulsifying drug delivery system (SNEDDS) is a system which contains surfactants and usually, but not always, oils, co-solvents and a

* Corresponding author: e-mail: eelbadawi@ksu.edu.sa; ehab71328@yahoo.com; phone: +96614677366; mobile : +966567843885; fax : +96614676295

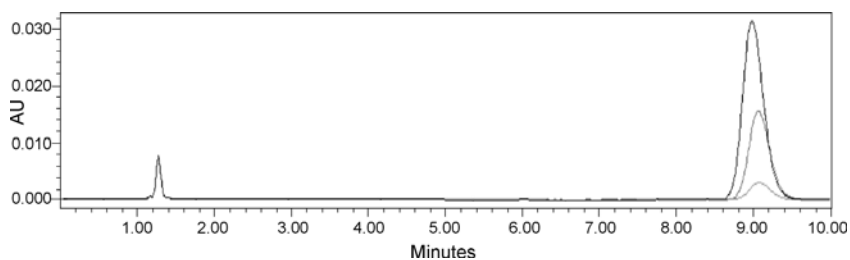


Figure 1. Overlaying chromatogram of 1, 10, 20 µg/mL MLX

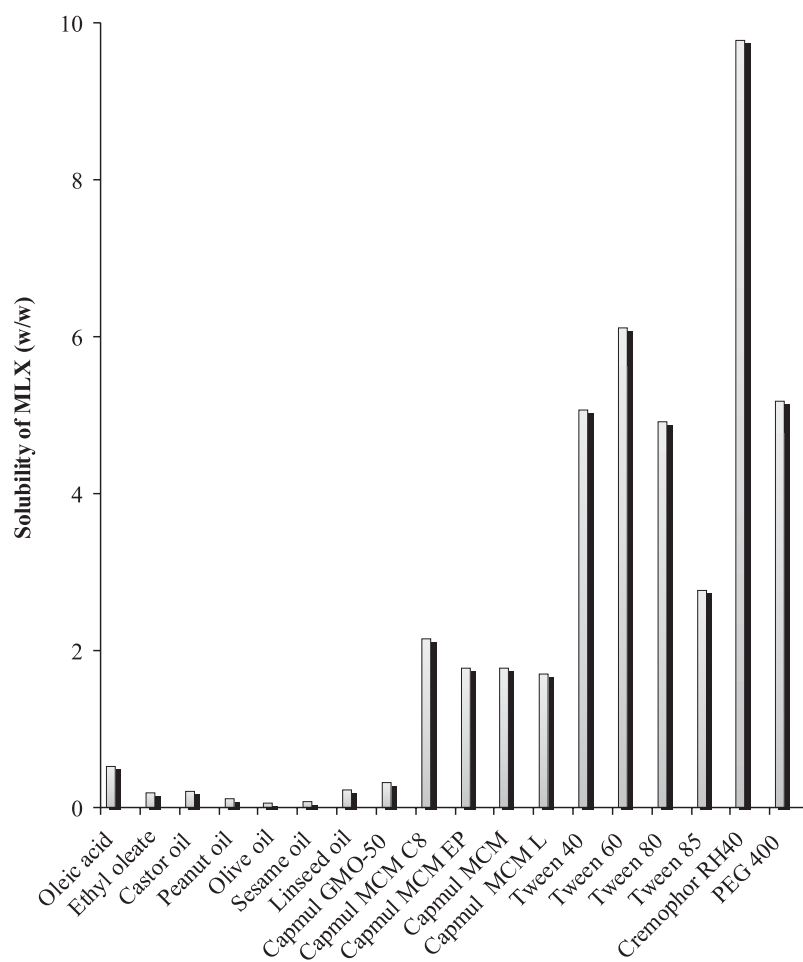


Figure 2. Solubility of MLX in different kinds of oils, polar oils and surfactants

drug (9). By optimizing various additives, a proper SNEDDS could be obtained. Upon dilution in aqueous media such as gastrointestinal fluids, these systems can form nanoemulsions (10). The ability of SNEDDS to enhance the oral bioavailability of poorly water-soluble drugs has been recognized. It

is commonly believed that increased luminal solubilization and improved drug dissolution in gastrointestinal tract are the main mechanisms responsible for enhanced class II drug bioavailability. Increased drug solubilization is achieved by the interaction of lipid formulations and their digestion products with

endogenous bile salts and phospholipids to form a range of vesicular and micellar species which enhance drug solubilization in gastrointestinal tract (11).

SNEDDSs were classified by Lipid Formulation Classification System (LFCS). LFCS was initially introduced by Pouton in 2000 (12), then six years later he updated it by including an extra type of formulation (13). Lipid-based delivery systems range from simple oil solutions to complex mixtures of oils, surfactants, co-surfactants and co-solvents. The latter mixtures are typically self-dispersing systems often referred to as self-emulsifying drug delivery systems (SEDDS or SNEDDS). Many poor water soluble drugs are much more soluble in co-solvents than oils, and such drugs may also dissolve in polyoxyethylene-rich environment present in water soluble non-ionic surfactant materials (14). This naturally encourages formulators to add water soluble surfactants and co-solvents at the expense of lipids, ultimately resulting in complete exclusion of lipid excipients to produce Type IV formulations (14). Ultra-fine SNEDDS (UF-SNEDDS) were recently developed. These systems form clear, transparent emulsion, upon dilution with an aqueous media and have droplet size of less than 50 nm (15, 16).

UF-SNEDDS formulation is, in theory, comparatively simple. The key step is to find a suitable oil/surfactant mixture that can dissolve the drug within the required therapeutic concentration. SNEDDS mixture can be filled in either soft or hard gelatin capsules (17).

Rapid entry of MLX into the blood stream is especially beneficial in the treatment of acute pain. So, the aim of this research work was to investigate the feasibility of preparation of MLX UF-SNEDDS in order to achieve fast dissolution, which would presumably yield quick onset of peak plasma concentration.

MATERIALS AND METHODS

Materials

MLX was a gift from Riyadh Pharma (Saudi Arabia). Peanut oil was purchased from Uni-Chem Chemical Reagents (England). Olive oil was obtained from Avonchem, Cheshire (England). Sesame oil was purchased from Fluka (Switzerland). Ethyl oleate, polyethylene glycol 400 (PEG 400), castor and linseed oil were purchased from Winlab (England). oleic acid was purchased from Riedel-de Haën (Germany). Cremophor RH40 was kindly supplied by BASF, Ludwigshafen

(Germany). Capmul grades were kindly supplied by ABITEC (USA). Tween grades were purchased from Sigma (USA). High-performance liquid chromatography (HPLC) grade methanol was purchased from BDH Chemicals (England). All other chemicals were of reagent grade and all solvents were HPLC grade.

Methods

HPLC method of analysis

MLX was analyzed using Autosampler, model no. 717 plus, binary HPLC pump, model no. 1525, Dual λ Absorbance, model no. 2487, Nova-Pak C₁₈ 3.9 × 150 mm Column (Waters, USA). The flow rate was adjusted at 1 mL/min and the mobile phase consisted of methanol and phosphate buffer (0.1 w/v potassium dihydrogen phosphate adjusted to pH 6 by potassium hydroxide) in ratio of 40 : 60. UV detector was adjusted at 356 nm. Figure 1 shows typical chromatograph of MLX at different concentrations.

Determination of MLX solubility

Solubility of drug in SNEDDS components is very important to obtain nanoemulsion. Therefore, appropriate oils, surfactants and cosurfactants were selected to determine MLX solubility. MLX solubility in different oils, mixed glycerides and surfactants was determined by addition of an excess amount of MLX to each compound. The mixtures were shaken at 37°C for 72 h, then were centrifuged in Eppendorf tubes for 30 min at 9000 rpm using centrifuge, model no. MIKRO 120 (Hettich-Zentrifugen, Germany). MLX concentrations in each supernatant were determined by the previously mentioned HPLC method. MLX solubility results are shown in Figure 2.

Preparation of MLX SNEDDS

According to the solubility study, Cremophor RH40 was chosen as the main hydrophilic surfactant. MLX SNEDDSs were prepared according to the design shown in Table 1 by mixing the exact compositions of each compound. The mixtures were slightly heated in water bath to liquefy the components. The melted components were shaken until the entire MLX amount was dissolved.

Evaluation of MLX nanoemulsions

Visual observations

To assess the self-emulsification properties, specific amount of MLX formulation was dispensed in 25 mL of water in a glass flask at ambient temperature, and the contents were gently stirred manu-

ally. The tendency to spontaneously form a transparent emulsion was judged as good and it was judged bad when there was poor or no emulsion formation. The measurements are shown in Table 2.

Turbidity measurements of MLX SNEDDSs

After diluting specific amount of MLX SMEDDS with 25 mL water in a stopped tube and gently mixed, the resultant nanoemulsions were evaluated for their turbidity. Turbidity given in nephelometric turbidity units (NTU) was measured using turbidity meter, model no. 415 (MARTINI Instruments, Romania). Turbidity measurements were performed with 10 mL of the nanoemulsion dispensed in clear screw-capped vials. The results are shown in Table 2.

Particle size measurements of MLX SNEDDSs

A specific amount of MLX SNEDDS was dispensed in adequate amount of water in a stopper flask and gently mixed. The resultant nanoemul-

sions were evaluated for its droplet size. The droplet size distribution of the resultant nanoemulsions was determined by laser diffraction analysis using Zetasizer (Nano ZS, England), which has a particle size measurement range of 0.3 nm – 10.0 μ m. The droplets size of MLX SNEDDS was determined in a small volume module. Samples were directly placed into the module and the data were collected for 10 min. Particle size was calculated from the volume size distribution. All studies were repeated in triplicates, with good agreement being found between measurements. The results are shown in Table 2.

In vitro dissolution of MLX SMEDDS

In vitro MLX release was conducted by using one gram of each MLX UF-SNEDDS filled in hard gelatin capsules size 00 and also two commercial MLX products namely Mobic® and Mobital® tablets (containing 7.5 mg MLX). The *in vitro* dissolution profiles were determined using USP2 rotating paddle apparatus (ERWEKA, DT-700, Germany) at

Table 1. Composition of 1 g MLX UF-SNEDDS each containing 7.5 mg of MLX dissolved in 80% (w/w) of Cremophor RH 40.

Formulation	Type	Capmul MCM C8	Tween 60	PEG 400
		% (w/w) of 20% of the formulation		
*F1	Type IV	–	–	–
F2	Type IV	0	100	0
F3	Type IV	0	0	100
F4	Type IIIB	100	0	0
F5	Type IV	0	90	10
F6	Type IIIB	90	0	10
F7	Type IV	0	85	15
F8	Type IIIB	85	0	15

*F1: containing 100% (w/w) of Cremophor RH 40

Table 2. Physical characterization of MLX UF-SNEDDS.

Formulation No.	Visual observation	Turbidity (NTU)	Particle size (nm)	% Release at 5 min	% Release at 20 min
F1	Good	4.8 \pm 0.5	25.6 \pm 1.3	10.6 \pm 5.5	59.1 \pm 7.1
F2	Good	3.7 \pm 0.3	12.8 \pm 1.4	22.2 \pm 8.4	66.1 \pm 8.6
F3	Good	4.2 \pm 0.3	16.5 \pm 1.6	30.1 \pm 6.8	64.8 \pm 2.3
F4	Good	3.6 \pm 0.3	13.9 \pm 1.3	40.8 \pm 7.2	75.7 \pm 1.8
F5	Good	3.3 \pm 0.2	16.2 \pm 1.3	12.5 \pm 0.8	64.6 \pm 4.9
F6	Good	2.3 \pm 0.2	14.3 \pm 1.3	48.3 \pm 9.0	73.7 \pm 2.4
F7	Good	2.5 \pm 0.2	16.8 \pm 1.5	20.7 \pm 5.8	69.1 \pm 6.1
F8	Good	1.9 \pm 0.2	14.7 \pm 1.3	55.2 \pm 7.6	82.7 \pm 0.5

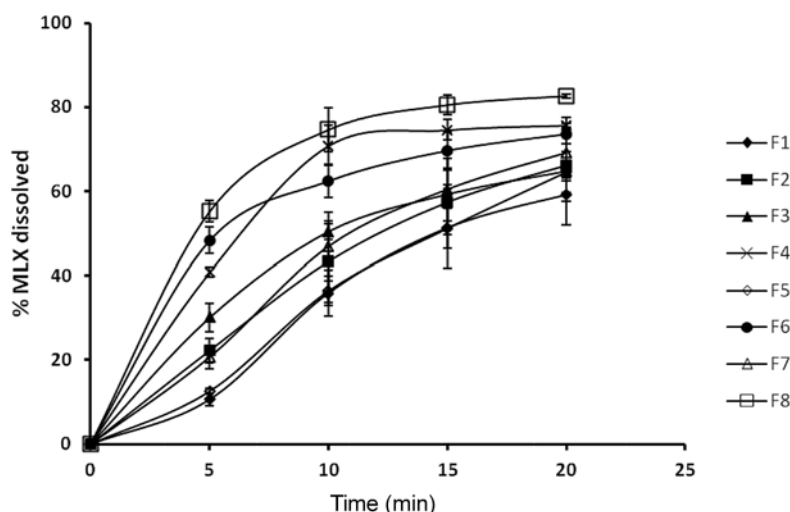


Figure 3. Dissolution profiles of MLX UF-SNEDDS

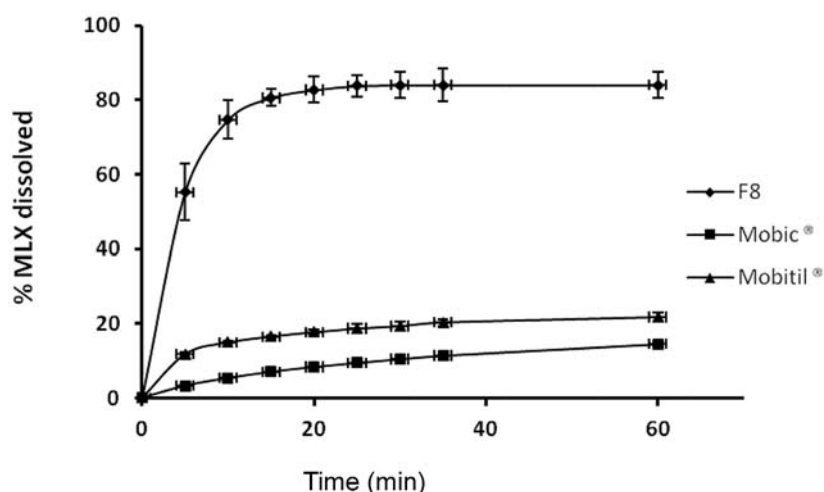


Figure 4. Dissolution profiles of MLX UF-SNEDDS (F8), Mobitic and Mobital tablets

rotating speed of 50 rpm in 900 mL of 0.1 M HCL maintained at $37 \pm 0.5^\circ\text{C}$. Samples were periodically withdrawn after 5, 10, 15, and 20 min using $1 \mu\text{m}$ cannula filters for MLX UF-SNEDDS and after 5, 10, 15, 20, 25, 30, 35 and 60 min for F8 capsules and Mobitic[®] and Mobital[®] tablets. MLX concentrations were assayed using HPLC method. The dissolution experiments were carried out in triplicates. The results are shown in Figures 3 and 4.

Statistical analysis

IBM[®] SPSS[®] statistics (version 19.0.0) software was used to analyze the data. One-way

ANOVA plus *post hoc* least significant difference (LSD) were applied to compare more than two groups or plus *post hoc* Dunnett test to compare groups with a control. A value of $p < 0.05$ was denoted significant throughout the analysis of data.

RESULTS AND DISCUSSION

Solubility of MLX

Drug solubility in the formulation and the ease of dispersion remain important design criteria especially in preparing SNEDDS (11). MLX was found to be very slightly soluble in oleic acid, ethyl oleate,

castor oil, peanut oil, and linseed oil and practically insoluble in olive oil and sesame oil (Fig. 2). MLX solubility in fatty acid, fatty acid ester and natural oils was ranged from 0.072 to 0.528 mg/g. The highest solubility was in oleic acid which is a fatty acid which belongs to the general group of polar oils (14).

Capmul products are mono-, di- and triglyceride emulsifiers prepared through the glycerolysis of selected fats and oils. They can be prepared by esterification of glycerin with specific fatty acids. They are lipophilic, insoluble in water (14). They are used to produce stable emulsions and to modify viscosity. MLX solubility in Capmul grades had shown a slight increase comparing to natural oils and fatty acids.

MLX solubility in non-ionic surfactants like Tween 40, 60, 80 and 85 were ranged between 5.06 to 2.77 mg/g. The lowest solubility was obviously with Tween 85. This decrease in solubility may be due to decreasing hydrophilic-lipophilic balance (HLB) value of this surfactant (5). In another words, increasing HLB increases MLX solubility.

The highest MLX solubility was found to be in Cremophor RH 40 (9.78 mg/g). Cremophor RH 40 is a polyoxy 40 hydrogenated castor oil. Polyoxyethylene castor oil derivatives are nonionic solubilizers and emulsifying agents used in oral, topical, and parenteral pharmaceutical formulations. MLX solubility in Cremophor RH 40 may be due to the changing happen in lipophilic moiety of the hydrogenated castor oil upon condensation with polyethylene. Also, Cremophor RH 40 has pH value of 6–7 which enhance MLX solubility. Many poor water soluble drugs are much more soluble in co-solvents than oils, and such compounds also dissolve in the polyoxyethylene-rich environment present in water-soluble non-ionic surfactants. This naturally encourages formulators to add water-soluble surfactants and co-solvents at the expense of lipids, which results in complete exclusion of lipid excipients to produce type IV lipid based formulations (14). It is worthy to mention that the regulatory status of Cremophor RH 40 is included in the FDA Inactive Ingredients Database (IV and ophthalmic solutions), parenteral medicines licensed in the UK and the Canadian List of Acceptable Non-medicinal Ingredients (18).

Also, Cremophor RH 40 has been used in about 35 FDA-approved drugs as seen from the FDA inactive ingredient database (19).

PEG 400 has the ability to form complexes with large number of poor water drugs. That is why it is widely used as solvent and solubilizing agent

mostly in liquid and semisolid formulations (20). Regarding MLX solubility in PEG 400, it was found to be 5.1 mg/g. However, for Type III and IV lipid based formulations which contain large quantities of water miscible surfactants and co-solvents, the likelihood of drug precipitation upon dispersion in water increases and care should be taken to minimize the quantity of formulation components such as PEG 400 that have limited 'on going' solubilization capacity after diluting the formulation with water or in gastrointestinal fluids (11).

Visual observations

For the development of self-emulsified formulations, a right blend of low and high HLB of the components is necessary for formation of a stable nanoemulsion (12). This is possible as surfactant strongly localized to the surface of the emulsion droplet reduces interfacial free energy and provide a mechanical barrier to coalescence resulting in a thermomechanically spontaneous dispersion. Furthermore, co-surfactant increases interfacial fluidity by penetrating into the surfactant film creating void space among surfactant molecules (21).

Droplet size and turbidity of dispersed MLX UF-SNEDDS

The droplet size of nanoemulsion is one of the most important parameters, because it governs the effective drug release (22). It has been confirmed that smaller droplet size resulted in large surface area providing high drug release for absorption (23). SNEDDS containing high proportions of water soluble surfactants provide small particle sizes on dispersion (11). MLX UF-SNEDDS Type IIIB and IV exhibit very small droplet size after dispersion in water (less than 25.6 nm). As a result, these systems are considered as UF-SNEDDS due the tiniest of the droplet size (15). Also these systems gave clear solutions with turbidity up to 4.8 NTU. The nanometer range particle size could enhance drug absorption and bioavailability.

MLX UF-SNEDDS dissolution profiles

It is clear from Figure 3 that MLX UF-SNEDDS prepared with Cremophor RH 40 (F1) showed the lowest MLX release rate among all formulations. It was also observed that incorporation of Tween 60 (F2) and PEG 400 (F3) separately, significantly improved MLX release rate in these formulations. Also the presence of Tween 60 and PEG in the same MLX UF-SNEDDS (F7) at a ratio of 85 : 15 has slight significant effect on MLX release rate while a ratio of 90 : 10 has no significant effect (F5),

suggesting that increasing PEG 400 percentage over that of Tween 60 could enhance MLX release rate. However, F3 slightly enhanced drug release, which could be due to a decrease in the solubilization capacity of this formulation in the dissolution medium. As was mentioned, incorporation of large quantities of water miscible surfactants and co-solvents like PEG 400 increases the chance of drug precipitation upon dispersion. Also from Figure 3 it could be observed that there is a delay in MLX release at 5 min. This may be due to fact that surfactants often take a considerable time to dissolve, due to the formation of viscous liquid crystalline (or gel crystalline) phases at the surfactant-water interface (14). There was no significant difference found between F2, F3 and F7.

MLX release was highly significant from F4, F6 and F8 comparing to that of F1. The enhancement in drug release from these formulations could be due to the presence of Capmul MCM C8. It was reported that Capmul MCM C8 (HLB < 6) is likely to increase the interfacial fluidity of Cremophor grades (HLB > 12) boundaries in micelles due to the entrapment of low HLB surfactant into high HLB one (22). This entrapment is due to lipophilic properties of Capmul MCM C8. As a result, the solubilization capacity of the formulation increases. There was no significant difference found between F4, F6 and F8.

Comparative dissolution study

Mobic® is a brand of MLX tablets which contain 7.5 mg of MLX with inactive ingredients including colloidal silicon dioxide, crospovidone, lactose monohydrate, magnesium stearate, microcrystalline cellulose, povidone and sodium citrate dehydrate. Mobital® is a novel formulation of MLX tablet also containing 7.5 mg of MLX with 37.5 mg β -cyclodextrin (β -CD) in an inclusion complex. Upon administration, an association-dissociation equilibrium is rapidly established with free MLX molecules readily available for absorption (in contrast to clumping which usually occurs with conventional tablet and capsule forms). Single MLX molecules are instantaneously absorbed and the equilibrium is rapidly shifted to the right hand side (MLX free side).

After 5 min, % dissolution of MLX from Mobic®, Mobital® and MLX UF-SNEDDS (F8) were 3.5, 11.8 and 74.7%, respectively.

Mobital® dissolution profile was increased by 7% dissolution over 60 min in acidic pH medium than that of Mobic® as shown in Figure 4. This could be attributed to the effect of β -CD which is included

with MLX in Mobital® tablet. MLX UF-SNEDDS dissolution profile was increased by 84% after 60 min in acidic pH medium compared to Mobic®, may be due to the effect of UF-SNEDDS formulation. The benefits of micellar solutions produced by MLX UF-SNEDDS as drug delivery system arise mainly from the solubilization power of surfactants and thus the elimination of dissolution as a rate-limiting step in the absorption process (24).

CONCLUSION

MLX was successfully formulated as a UF-SNEDDS that showed significant improved *in vitro* percentage of MLX released when compared to a commercially available MLX tablets (Mobic® and Mobital®). The results of this study revealed the better action of Capmul MCM C8 dispersion over Tween 60 for formulating MLX UF-SNEEDS.

The dissolution of MLX seems to depend on formulation and excipients. Using UF-SNEDDS could increase the dissolution rate in the stomach, and thereby, could potentially increase the absorption rate and bioavailability.

Acknowledgment

The authors would like to extend their sincere appreciation to the Deanship of Scientific Research at King Saud University for funding this work through the research group project No. RGP-VPP-287.

REFERENCES

1. Aboelwafa, A.A., Fahmy R.H.: Pharm. Dev. Technol. 17, 1 (2012).
2. Del Tacca M., Colucci R., Fornai M., Blandizzi C.: Clin. Drug Invest. 22, 799 (2002).
3. Han H.K., Choi H.K.: Eur. J. Pharm. Sci. 65, 99 (2007).
4. Euller-Ziegler L., Velicitat P., Bluhmki E., Turck D., Scheuerer S. Combe B.: Inflamm. Res. 50, S5 (2001).
5. Luger P., Daneck K. Engel W., Trummlitz G., Wagner K.: Eur. J. Pharm. Sci. 4, 175 (1996).
6. Lipka E. Amidon G.L.: J. Control. Release 62, 41 (1999).
7. Ambrus R., Kocbek P., Kristl J., Sibanc R., Rajko R., Szabo-Revesz P.: Int. J. Pharm. 381, 153 (2009).
8. El-Badry M.: Sci. Pharm. 79, 375 (2011).
9. Morozowich W., Gao P.: Chapter 19 – Improving the Oral Absorption of Poorly

- Soluble Drugs Using SEDDS and S-SEDDS Formulations, in *Developing Solid Oral Dosage Forms*, Qiu Y., Chen Y., Zhang G.G.Z., Liu L., Porter W.R. Eds., p. 443, Academic Press, San Diego 2009.
10. Garrigue J.-S., Lambert G., Benita S.: Self-Emulsifying Oral Lipid-Based Formulations for Improved Delivery of Lipophilic Drugs, in *Microencapsulation*, Benita S., Ed., p. 429, CRC Press, Boca Raton 2006.
 11. Porter C.J., Pouton C.W., Cuine J.F., Charman W.N.: *Adv. Drug Deliv. Rev.* 60, 673 (2008).
 12. Pouton C.W.: *Eur. J. Pharm. Sci.* 11, S93 (2000).
 13. Pouton C.W.: *Eur. J. Pharm. Sci.* 29, 278 (2006).
 14. Pouton C.W., Porter C.J.: *Adv. Drug Deliv. Rev.* 60, 625 (2008).
 15. Villar A.M., Naveros B.C., Campmany A.C., Trenchs M.A., Rocabert C.B., Bellowa L.H.: *Int. J. Pharm.* 431, 161 (2012).
 16. Faiyaz S., Nazrul H., Mahmoud E.B., Fars K.A., Ibrahim A.A.: *J. Mol. Liq.* 180, 89 (2013).
 17. Atef E., Belmonte A.A.: *Eur. J. Pharm. Sci.* 35, 257 (2008).
 18. Singh K.: Polyoxyethylene Castor Oil Derivatives, in *Handbook of Pharmaceutical Excipients*. 6th edn., Rowe R.C., Sheskey P.J., Quinn M.E. Eds., p. 542, Pharmaceutical Press and APhA, London, Washington 2009.
 19. Kanika S., Yogesh B.P., Arvind K.B.: *CRIPS* 11, 42 (2010).
 20. Beig A., Miller J.M., Dahan A.: *Eur. J. Pharm. Biopharm.* 81, 386 (2012).
 21. Taha M.O., Al-Ghazawi M., Abu-Amara H., Khalil E.: *Eur. J. Pharm. Sci.* 15, 461 (2002).
 22. Taha E.I., Samy A.M., Kassem A.A., Khan M.A.: *Pharm. Dev. Technol.* 10, 363 (2005).
 23. Shweta G., Sandip C., Krutika K.S.: *Colloids Surface A* 392, 145 (2011).
 24. Tarr B., Yalkowsky S.: *Pharm. Res.* 6, 40 (1989).

Received: 6. 11. 2013

AMORPHOUS SOLID DISPERSION STUDIES OF CAMPTOTHECIN–CYCLODEXTRIN INCLUSION COMPLEXES IN PEG 6000

SOFIANE FATMI^{1,2,3}, LAMINE BOURNINE⁴, MOKRANE IGUER-OUADA³, MALIKA LAHIANI-SKIBA¹, FATIHA BOUCHAL² and MOHAMED SKIBA^{1*}

¹ Technology Pharmaceutical and Biopharmaceutics Laboratory, UFR Medicine and Pharmacy, Rouen University, 22 Blvd. Gambetta, 76183, Rouen, France

² Technology Pharmaceutical Laboratory, Department of Engineering Processes,

³ Marine Ecosystems and Aquaculture Laboratory, ⁴ Plant Biotechnology and Ethnobotany Laboratory, Faculty of Natural Sciences and Life, Abderrahmane-Mira University, Targua Ouzemmour road, 06000 Bejaia, Algeria

Abstract: The present work focused on the solubility enhancement of the poorly water-soluble anti-cancer agent camptothecin which, in its natural state, presents poor solubility inducing lack of activity with a marked toxicity. A new approach is adopted by using a ternary system including camptothecin (CPT) and cyclodextrins (CDs) dispersed in polyethylene glycol (PEG) 6000. Camptothecin solubility variations in the presence of α -CD, β -CD, γ -CD, hydroxypropyl- α -CD (HP α -CD), hydroxypropyl- β -CD (HP β -CD), permethyl- β -CD (PM β -CD) and sulfobutyl ether- β -CD (SBE β -CD), were evaluated by Higuchi solubility experiments. In the second part, the most efficient camptothecin/ β -CDs binary systems, mainly HP β -CD and PM β -CD, were dispersed in PEG 6000. In addition to a drug release and modeling evaluation, the CPT interactions with CDs and PEG 6000 to prepared the amorphous solid dispersion in the binary and ternary systems were investigated by Fourier transformed infrared spectroscopy (FT-IR), differential scanning calorimetry (DSC), thermogravimetric analyses (TGA) and X-ray powder diffraction (XRPD). The results showed that HP β -CD and PM β -CD were the most efficient for camptothecin solubilization with highest apparent equilibrium constants. Dissolution studies showed that percentage of CPT alone after two hour in 0.1 M HCl medium, did not exceed 16%, whereas under the same conditions, CPT/PM β -CD complex reached 76%. When dispersing the binary systems CPT/ β -CDs in PEG 6000, the velocity and the percentage of CPT release were considerably improved whatever the CD used, reaching the same value of 85%. The binary and ternary systems characterization demonstrated that CPT included into the CDs cavity, replacing the water molecules. Furthermore, a drug transition from crystalline to amorphous form was obtained when solid dispersion is realized. The present work demonstrated that ternary complexes are promising systems for CPT encapsulation, and offer opportunities to use non toxic and commonly solubilizing carriers: β CD and PEG 6000 to improve bioavailability.

Keywords: camptothecin, cyclodextrins, kinetic model, PEG 6000, amorphous solid dispersion characterization, ternary complex

Camptothecin (CPT, Fig. 1) is an anti-cancer agent belonging to the family of the alkaloids, it is present in wood, bark and fruit of the Asian tree *Camptotheca acuminata* (1, 2). Camptothecin is known as DNA topoisomerase I inhibitor (3, 4) presenting a powerful anti-cancer activity against a wide spectrum of human malignancies, such as lung, prostate, breast, colon, stomach and ovarian carcinomas (5). However, the full therapeutic potential of CPT is limited in relation to its poor solubility (6) inducing lack of activity, with a marked toxicity (7). This limited activity is mainly in relation to the pH

dependent behavior of the lactone ring (Fig. 1) (7, 8).

Several approaches are proposed to improve CPT or analogs solubility; especially the use of various polymers such as: polyethylene glycol (PEG) (5, 9–11), poly(lactide-Co-glycolide), polycaprolactone (12), o-carboxymethylchitosan (13) and cyclodextrins (CDs) (14–16).

Cyclodextrins are cyclic oligosaccharides composed of glucose units linked to each other by α (1→4) glycosidic bond. Three natural types of cyclodextrins are reported: α -cyclodextrin (α -CD),

* Corresponding author: e-mail: mohamed.skiba@univ-rouen.fr

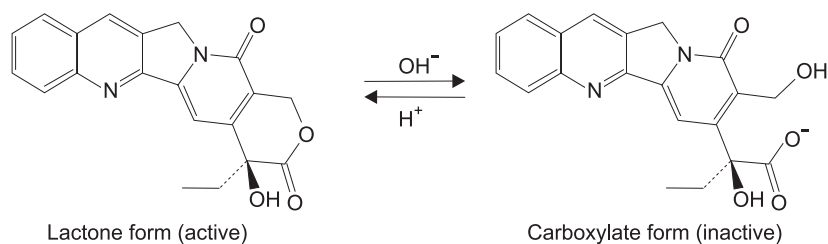


Figure 1. CPT structure (active and inactive form) (9)

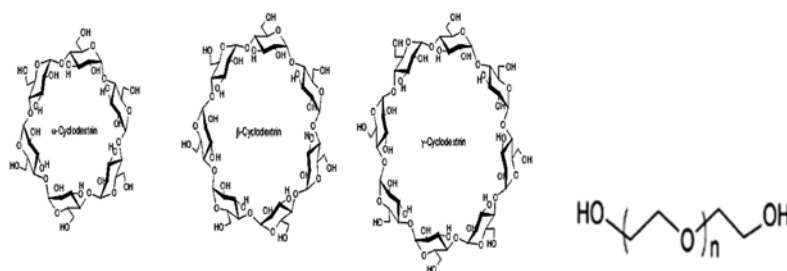


Figure 2. Molecular structure of natural cyclodextrins (24) and polyethylene glycol (25)

β -cyclodextrin (β -CD) and γ -cyclodextrin (γ -CD) composed of 6, 7 and 8 units of glucopyranoses (Fig. 2), respectively (17, 18). They result from the enzymatic degradation of the starch by cyclodextrins glucosyl transferases (CGTases) (18). The glucose units are bonded together to form a truncated cone shaped molecule with a broadest end containing secondary and tertiary hydroxyls, and a narrowest end containing primary hydroxyls (19). As a consequence, the inner cavity of cyclodextrins is hydrophobic and the exterior hydrophilic (20). This fact is used to increase molecules aqueous solubility by inclusion complexes (21).

In the present work, solubility of camptothecin in the presence of various CDs: α -CD, β -CD, γ -CD, hydroxypropyl- α -CD (HP α -CD), hydroxypropyl- γ -CD (HP γ -CD), hydroxypropyl- β -CD (HP β -CD), permethyl- β -CD (PM β -CD) and sulfobutyl ether- β -CD (SBE β -CD) was investigated and the equilibrium constants (K_c) were determined. Inclusion complexes were prepared and dissolution profiles were studied.

A new approach was also investigated to enhance CPT solubility by a ternary system: complexes CPT/CD dispersed in PEG (Fig. 2). The later, is a water-soluble, nontoxic, non-antigenic, biocompatible polymer that has been approved by the Food

and Drug Administration for human intravenous, oral, and dermal applications (22), its most common form is a linear or branched polyether ended with hydroxyl groups (23). In order to investigate the effect of PEG on both camptothecin and its corresponding inclusion complexes, dissolution profiles were realized. Finally, the nature of interaction in binary and ternary systems, were studied using different methods: Fourier transformed infrared spectroscopy (FT-IR), differential scanning calorimetry (DSC), thermogravimetric analyses (TGA) and X-ray powder diffraction (XRPD).

MATERIALS AND METHODS

Materials

Drug

Camptothecin (M.w. 348.11 g/mol) was purchased from Shenzhen Boda Natural Product laboratory (P. R. China).

Cyclodextrins

β -CD was obtained from Roquette Frères (France) (1135 g/mol), α -CD (972 g/mol), γ -CD (1297 g/mol), hydroxypropyl- β -CD (HP β -CD, 1488 g/mol), hydroxypropyl- α -CD (HP α -CD, 1285 g/mol) and hydroxypropyl- γ -CD (HP γ -CD, 1713

g/mol) were provided by Wacker (Germany). Permethyated β -CD (PM β -CD, 1330 g/mol) was received from Orsan (France). Sulfobutyl ether β -CD, SBE-CD (2163 g/mol) was purchased from Cydex, Inc. (USA).

Polyethylene glycol

PEG 4000 and 6000 were obtained from BASF (Germany).

All reagents were of analytical grade.

Methods

HPLC analyses

The analysis of lactone and carboxylate forms of CPT in solubility study, were performed using HPLC system which consisted of Jasco PU-980 pomp, Jasco AS-950 auto injector and Merck multi-channel photo Detector L 3000, equipped with C-18 analytical column. The mobile phase consisted of a mixture of a borate buffer and acetonitrile (65 : 35, v/v). Standard solution was prepared by dissolving CPT in a mixture of acetone / DMSO (95 : 5, v/v).

Solubility experiments and apparent equilibrium constant determination

The solubility measurement was carried out according to the method of Higuchi and Connors reported by Brewster and Loftsson (26). Excess of CPT was suspended in 5 mL pH 2.0 phosphate buffer solution (PBS pH 2) containing increasing concentrations of CDs : γ -CD (0–180 M), β -CD (0–16 mM), α -CD (0–150 mM), PM β -CD (0–300 mM), SBE β -CD (0–90 mM), HP γ -CD (0–350 M), HP β -CD (0–467 mM) and HP α -CD (0–300 mM), all solutions were shaken at 37°C under a constant agitation rate. Aliquots were withdrawn at the equilibrium after one week. The aliquots were filtered through 0.45 μ m membrane and quantified by HPLC. Each experiment was carried out in duplicate. The apparent binding constants were calculated from the straight line portion of the phase solubility diagram according to Higuchi-Connors, given in equation (1):

$$K_c = \text{slope} / S_0 (1 - \text{slope}) \quad (\text{Equation 1})$$

where S_0 = drug solubility without CDs.

Preparation of binary systems

Solid inclusion complexes prepared by solvent evaporation method

Cyclodextrins and CPT in a 1 : 1 molar ratio were dissolved in 50 mL of ethanol, the mixture was left under agitation for 1 h protected from light. After drying at 45°C during 1 h, the powder was preserved in a dessicator.

Solid dispersion (SD) CPT/ PEGs

Mixtures of CPT/ PEG 6000 or PEG 4000 at 5/95, 10/90, 15/85 and 30/70% (w/w) were dissolved in ethanol by agitation. After drying at 45°C during 1 h, the powder was preserved in a dessicator.

Preparation of ternary systems

Solid dispersion CPT complexes / PEG 6000

Nine parts of polyethylene glycol 6000 and one part of CPT in its complexes form were dissolved in ethanol by agitation. After drying at 45°C during 1 h, the powder was preserved in a dessicator.

Physical mixtures

Nine part of polyethylene glycol 6000 and one part of CPT in complexes form were mixed in a mortar until obtaining an apparent homogeneous powder. The latter was preserved in a dessicator.

Characterization of inclusion complexes and solid dispersions

Fourier transformed infrared spectroscopy (FT-IR)

The FT-IR spectra were taken from dried samples. An FT-IR machine from PerkinElmer equipped with an ATR was used in the frequency between 4000 cm^{-1} and 700 cm^{-1} .

Differential scanning calorimetry (DSC)

Thermal analysis was performed using a PerkinElmer differential scanning calorimeter (DSC-4), which was equipped with a compensated power system. All samples were weighed at around 5 mg and heated at a scanning rate of 10°C/min to a temperature level between 30 and 350°C under a nitrogen gas flow. Aluminum pans and lids were used for all samples.

Thermogravimetric analysis (TGA)

TGA was carried out using thermal analyzer (PerkinElmer, USA) with attached TG unit. The sample was heated under normal atmosphere at a rate of 10°C/min, and the loss of weight was recorded in temperature range 30 to 750°C for the pure drug and from 30 to 650°C for other samples.

X-ray powder diffraction (XRPD)

X-ray diffractograms of CPT, carriers, binary and ternary systems were recorded using an X-ray diffractometer (X'Pert Propan analytical, Netherlands) using RTMS detector, generated at 40 kV and 30 mA and scanning rate of 2°/min over a 2θ range of 0°–70°.

Dissolution studies

Dissolution profiles of free CPT, inclusion complexes or SDs were evaluated. Briefly, 10 mg of free CPT or its equivalent of complexes or SDs were added to 900 mL of hydrochloric acid (0.1 M) at $37 \pm 0.5^\circ\text{C}$, the rotation speed paddle was fixed at 75 rpm. The amount of dissolved CPT was evaluated on Beckman DU 640 B spectrophotometer at 286 nm. Each analysis was repeated in triplicate.

Drug release kinetics

In order to establish the mathematical model of CPT release from different preparations, the experimental data were fitted to commonly kinetic models (like zero order, first order, Higuchi, and Korsmeyer-Peppas) reported by Tapan et al. (27), where:

Zero-order model: $F = K_0 t$, where F represents the fraction of drug released in time t and K_0 is the apparent release rate constant or zero-order release constant.

First-order model: $\ln(1-F) = K_1 t$, where F represents the fraction of drug released in time t and K_1 is the first-order release constant.

Higuchi model: $F = K_H t^{1/2}$, where F represents the fraction of drug released in time t and K_H is the Higuchi dissolution constant.

Korsmeyer-Peppas model: $F = K_p t^n$, where F represents the fraction of drug released in time t , K_p is the rate constant and n is the diffusional exponent, it indicates the drug release mechanism (28–30).

RESULTS AND DISCUSSION

Solubility experiment

The solubility of CPT according to different CDs concentrations is shown in Figures 3–5. The CPT apparent solubility increased with CDs concen-

tration. When using natural or modified β -CDs, CPT solubility increased linearly, it exhibits typical *AL* curves corresponding to equivalent molar ratio between CD and CPT as reported by Kang et al. (15) and Foulon et al. (31). The apparent equilibrium constant (K_c), is calculated using an equation proposed by Higuchi and Connors:

$K_c = S_o / \text{intercept (1-slope)}$ (Equation 2) where S_o = drug solubility without CDs.

The modified and natural α - and γ -CDs showed *AP* curves. As described by Brewster (26), it is corresponding to CPT/CDs 1 : 2, 1 : 3 molar ratios. The K_c in this case is calculated using the linear portion of the curves. The maximal apparent CPT solubility and equilibrium constant are reported in Table 1.

Among the natural CDs, α CD induced the greatest increase in CPT solubility with approximately sixteen folds compared to CPT alone. β CD and γ CD, in contrast, increased two- and twelve folds CPT solubility, at their water solubility limit, respectively. These results suggest that α CD is the most effective solubilizing agent for CPT. This is in relation to its higher intrinsic solubility compared to β CD, with a more adequate size cavity compared to γ CD. However, when working at low CD concentrations, 1.5% (w/v) for β CD and 2.5% (w/v) for α CD and γ CD, respectively, Kang et al. (15) found that β CD is more effective in solubilizing CPT. According to Brewster (26), the solubility study should be realized at CDs water solubility limit.

Among the three modified HP-CDs (HP α , HP β and HP γ), HP- β -CD solubilized CPT to the greatest extent. Around water solubility limit of each HP-CDs (HP α , HP β and HP γ), camptothecin solubility was increased by factor of 47, 70 and 43, respectively, when compared to CPT alone. It has been shown previously that HP cyclodextrins

Table 1. Solubility and equilibrium constants (K_c) for camptothecin complexes calculated from the slope of the best-fit line of the phase solubility.

CDs	CPT max (10^{-3} mM)	S_o mM	slope	S_{max}/S_o	K_c (M^{-1})
β CD 16 mM	1.84E+01	8.15E-03	1.19E-03	2.26E+00	1.46E+02
α CD 150 mM	1.32E+02	8.15E-03	4.63E-04	1.62E+01	5.69E+01
γ CD 180 mM	1.03E+02	8.15E-03	5.07E-04	1.27E+01	6.22E+01
HP β CD 300 mM	5.71E+02	8.15E-03	1.97E-03	7.01E+01	2.43E+02
HP α CD 420.6 mM	3.80E+02	8.15E-03	1.04E-03	4.66E+01	1.28E+02
HP γ CD 350 mM	3.50E+02	8.15E-03	5.58E-04	4.29E+01	6.85E+01
SBE β CD 90 mM	2.32E+02	8.15E-03	2.30E-03	2.85E+01	2.83E+02
PM β -CD 300 mM	2.13E+03	8.15E-03	4.70E-03	2.61E+02	5.79E+02

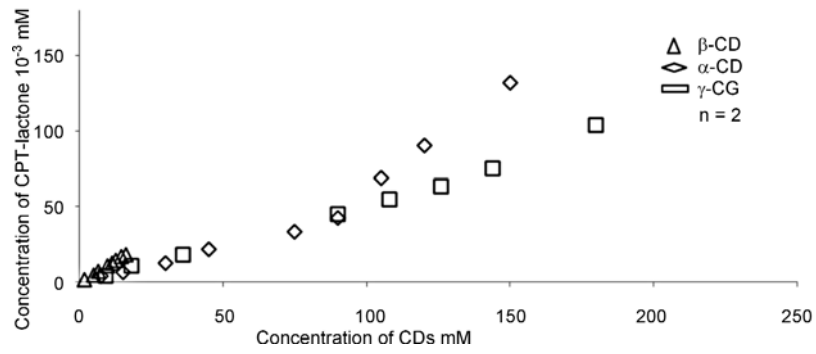


Figure 3. Solubility diagrams of camptothecin in the presence of natural CDs

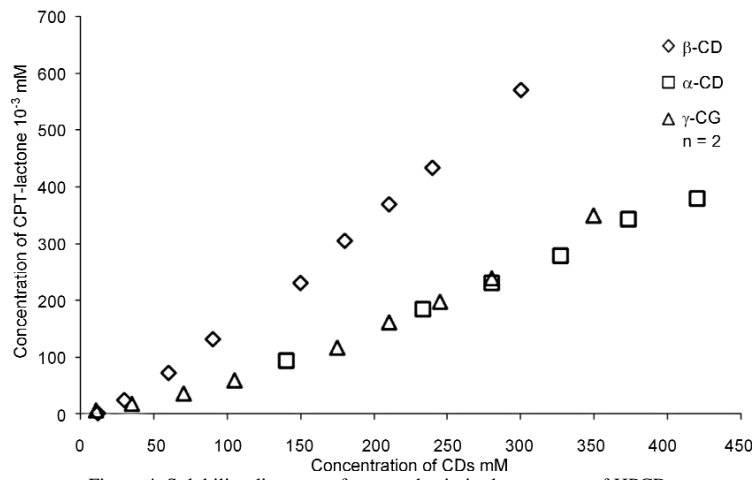
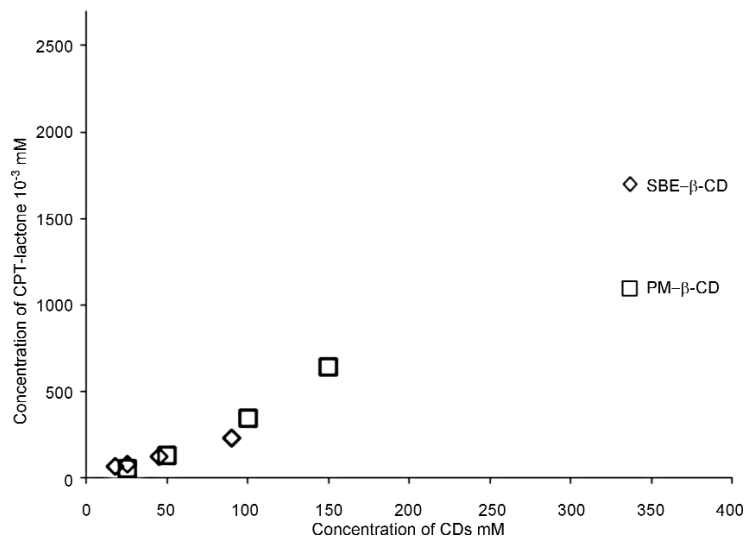


Figure 4. Solubility diagrams of camptothecin in the presence of HPCDs

Figure 5. Solubility diagrams of camptothecin in the presence of SBE- β -CD and PM- β -CD

improved solubility by the presence of hydroxypropyl groups (19). These results suggest also that β -CD cavity size is more adequate to CPT.

At 90 mM of SBE- β -CD, camptothecin solubility was increased by factor of 28 compared to the value obtained with CPT alone.

Among CDs tested in the present work, the most efficient is PM- β -CD in improving camptothecin solubility which was increased by 261 folds when compared to CPT alone. This could be attributed to the presence of methyl groups, which not only disrupt hydrogen bonding, but also enlarge the whole cavity (14).

The equilibrium constants (Table 1) were in agreement with the values described in the literature concerning drug-cyclodextrin complexation (32, 33). It can also be observed that the greatest value of K_c was obtained by complexation with β -CDs (natural and modified) compared to α -CDs and γ -CDs, indicating that the bonding strength between camptothecin and this type of CDs is more important, meaning that their size cavities are more adequate to load CPT. Similar equilibrium constants were obtained by Kang et al. (15) and Saetern et al. (8).

From these results, HP- β -CD and PM- β -CD, the two best CPT solubilizers, were selected for further experiments, considering β -CD as reference.

Selection of adequate polymer and concentration

The percentages of CPT released from each SD according to mass percentage and type of PEG are presented in Figure 6. Kinetic release of CPT from each SDs was realized in triplicate.

Improvement of the drug dissolution in all cases is probably attributed to the hydrophilic nature

of the polymers (26, 31), with wettability increasing (34) and amorphization of the drug by the carriers in solid dispersions (35). It clearly appeared that PEG 6000 was the best polymer improving CPT dissolution. Moreover, 90% of PEG (w/w) seems to be the most efficient with the less variation on the basis of relative standard deviation (36). For this reason, PEG 6000 at 90% (w/w) was selected for further experiments.

Characterization of inclusion complexes and solid dispersions

FT-IR analysis

Figures 7 and 8 represent the FT-IR spectra of CPT binary and ternary systems.

FT-IR spectroscopy analysis showed that there were weak interactions between the drug and the carrier used in complexation or solid dispersion. This is clearly observed with contracting and disappearance of the drug peaks around: 1750 cm^{-1} corresponding to C=O stretching vibration of lactone ring, 1655 cm^{-1} corresponding to C=O stretching vibration of ketone groups and 1490 cm^{-1} corresponding to vibrations of phenyl rings (37–40). The physical mixture FT-IR spectra showed simultaneously the presence of characteristic peaks of CPT, PEG 6000 and CDs, suggesting that there is no interaction. On the basis of these results, it can be retained that whole drug or at least some of drug groups are incorporated into cyclodextrin cavities and also suggest that there is intermolecular interaction between CPT and PEG molecules.

Differential scanning calorimetry (DSC)

Differential scanning calorimetry thermograms of pure drug and carriers, CPT binary systems and

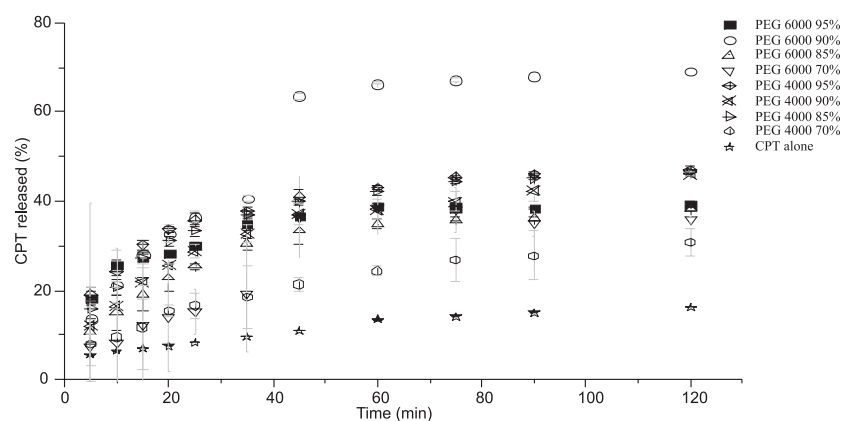


Figure 6. Camptothecin kinetic release from SDs at 5/95, 10/90, 15/85, 30/70 (w/w) percentages

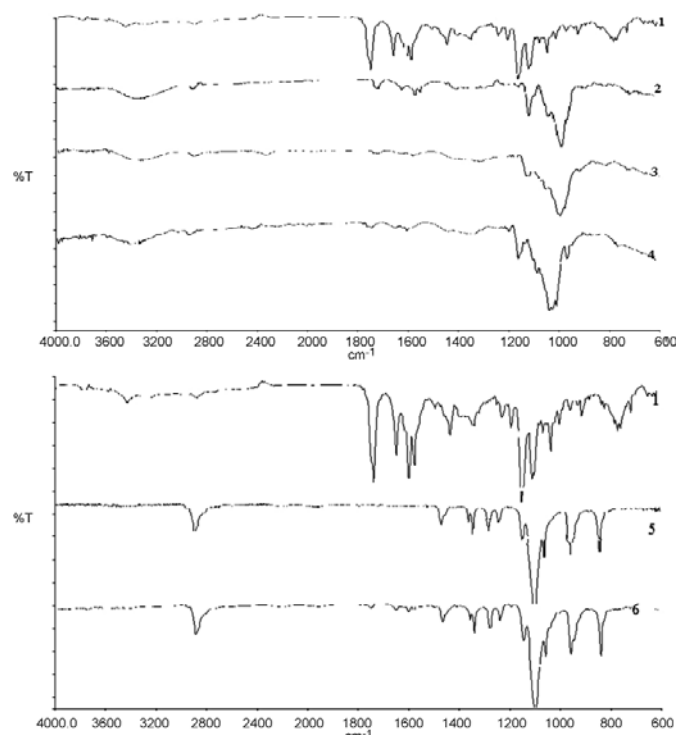


Figure 7. FT-IR spectra of: 1) CPT, 2) (CPT/ β -CD) complex, 3) (CPT/HP β -CD) complex, (CPT/PM β -CD) complex, 5) PEG 6000 and 6) (CPT/PEG 6000) SD

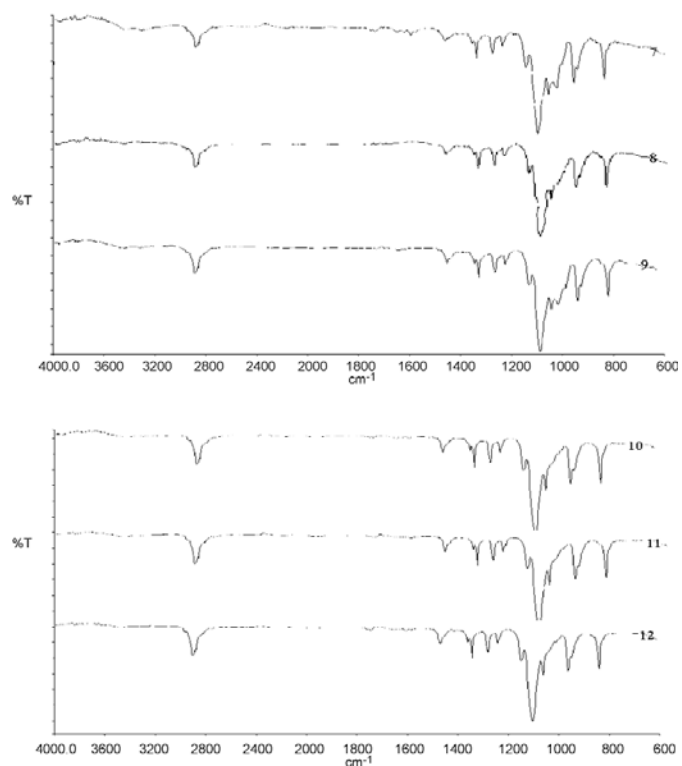


Figure 8. FT-IR spectra of: (7) SD1 ((CPT/ β -CD)/PEG 6000), (8) SD2 ((CPT/HP β -CD)/PEG 6000), (9) SD3 ((CPT/PM β -CD)/PEG 6000), (10) PM1 ((CPT/ β -CD)/PEG 6000), (11) PM2 ((CPT/HP β -CD)/PEG 6000) and (12) PM3 ((CPT/ β -CD)/PEG 6000)

CPT ternary systems are shown in Figures 9–11. Melting endotherms of CPT which are around 265 and 273°C (indicating crystalline nature of the drug (41)) disappeared totally in thermograms corresponding to CPT/CDs complexes, CPT/PEG 6000 SD (SDo) and CPT complexes/PEG 6000. In contrast,

they remained present in PM thermograms. This may indicate inclusion of CPT within the CD cavity replacing water. In case of SDs, only endothermic peak of PEG at 67°C is observed, the disappearance of CPT melting endotherms indicated the absence of crystalline drug replaced by its amorphous form (28,

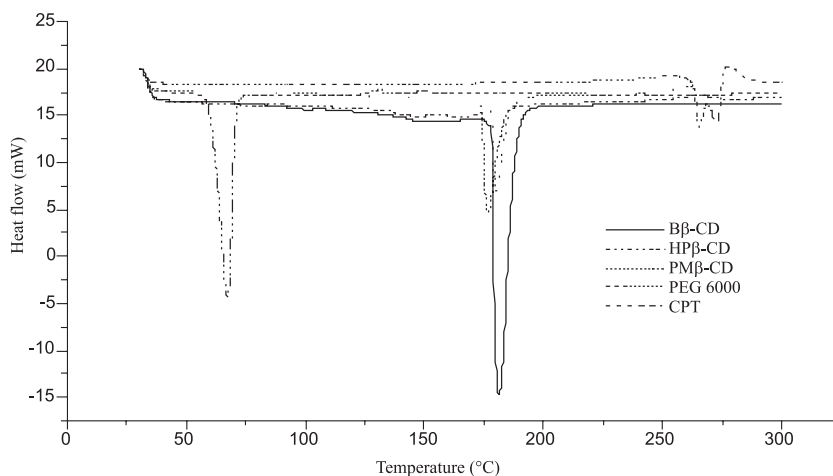


Figure 9. Differential scanning calorimetry thermograms of pure materials

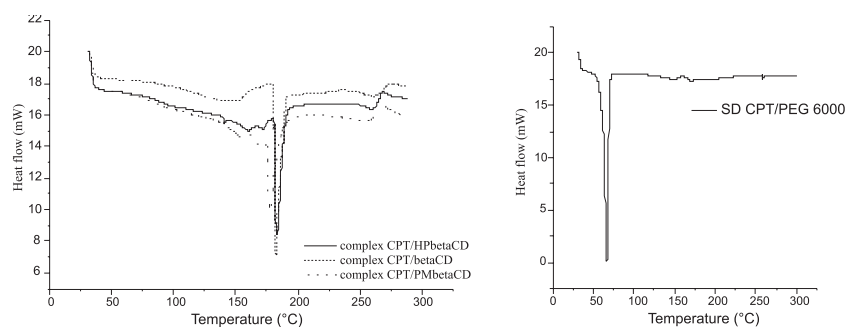


Figure 10. Differential scanning calorimetry thermograms of CPT binary systems, CPT complexes (left) and SD (right)

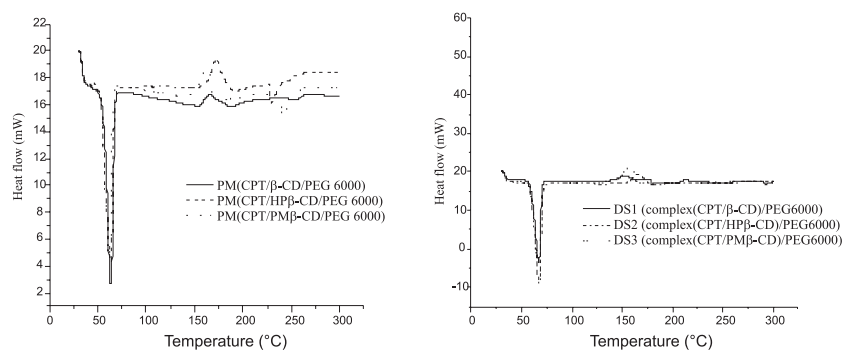


Figure 11. Differential scanning calorimetry thermograms of CPT ternary systems and corresponding physical mixtures

Table 2. Weight loss percentages of CDs, complexes and SDs calculated from dehydration step of TGA.

Analyzed products	Dehydration step		
	Temperature range (°C)		Weight loss (%)
β CD	30	119	12.60
HP- β CD	30	108	5.35
PM β CD	30	108	5.42
CPT/ β CD complex (IC 1)	30	102	4.98
CPT/ HP- β CD complex (IC 2)	30	102	4.50
CPT/ PM- β CD complex (IC 3)	30	102	4.80
SD (CPT/ β CD complex) / PEG (SD1)	30	107	1.57
SD (CPT/ HP- β CD complex)/PEG (SD2)	30	107	0.99
SD (CPT/ PM- β CD complex)/PEG (SD3)	30	107	1.40

Table 3. Drug release kinetic data obtained from fitting the drug release experimental data to different mathematical model of drug release.

	IC 1	IC 2	IC 3	SD 1	SD 2	SD 3	SDo
Zero order model							
K _o	0.0023	0.0028	0.0027	0.0022	0.0024	0.0027	0.0051
R ²	0.83	0.65	0.90	0.63	0.55	0.80	0.79
First order model							
K ₁	0.0035	0.0044	0.0070	0.0080	0.0090	0.0100	0.0100
R ²	0.87	0.69	0.96	0.75	0.67	0.90	0.83
Higuchi model							
K _H	0.031	0.041	0.037	0.033	0.037	0.039	0.072
R ²	0.94	0.80	0.98	0.79	0.71	0.91	0.90
Korsmeyer-Peppas model							
K _p	0.20	0.17	0.40	0.54	0.53	0.50	0.14
R ²	0.90	0.75	0.96	0.78	0.69	0.89	0.87
n	0.09	0.12	0.06	0.047	0.052	0.055	0.18

n = diffusional exponent; K = kinetic constant; R² = correlation coefficient.

40–42). The DSC thermograms indicated the formation of inclusion complex between CDs and CPT and also indicated a significant dispersion of CPT or its corresponding complexes in PEG 6000. Similar findings have been reported for CPT complexation with HP- β -CD and β -CD by Cirpanli et al. (32).

Thermogravimetric analysis (TGA)

It is reported that through the formation of host-guest inclusion complexes, the thermal stabilities of CDs and guests should be affected (43). The thermogravimetric graphs of pure drug, carriers, complexes and SDs are shown in Figures 12 and 13. Drug showed 84% weight loss, started around 145°C and stabilized around 639°C. This is probably

related to the decomposition of CPT structure induced by the transition from solid to liquid phase. PEG 6000 showed 98% weight loss, from 166 to 478°C indicating the decomposition of the polymer. Cyclodextrins presented three stages of weight loss (Fig. 12), where less than 120°C the lost weight indicates the loss of water molecules included in CDs cavities. The weight loss percentages of each CD are presented in Table 2.

Previous studies have reported the presence of water molecules, depending on the relative humidity in CDs (44, 45). Consequently, weight loss in the range 270–500°C was related to CD structure decomposition due to the transition from solid to liquid phase (44). Relatively slow weight decrease

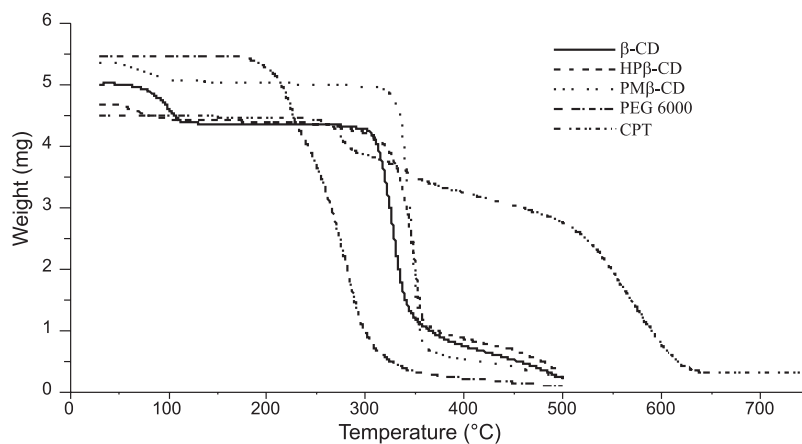


Figure 12. Thermogravimetric graphs of pure CPT and carriers.

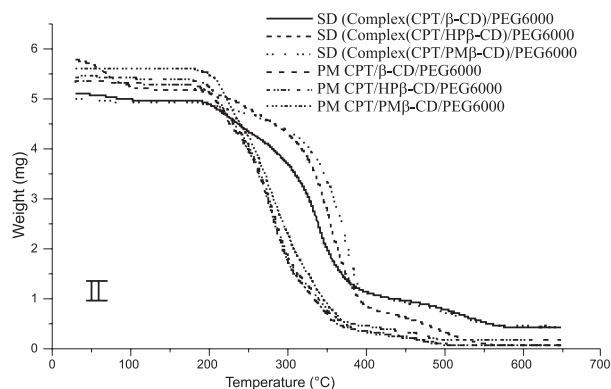
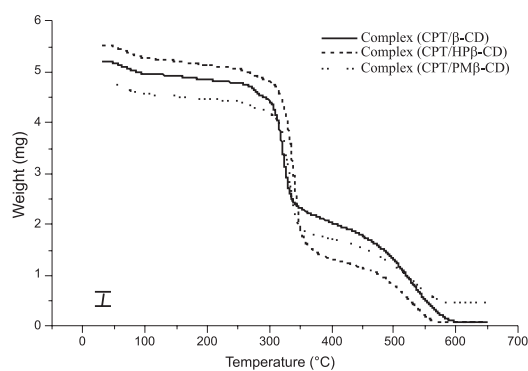


Figure 13. Thermogravimetric graphs of CPT/CDs complexes (I) and thermogravimetric graphs of (CPT/CDs complexes)/PEG 600 SDs (II)

around 500°C indicated the thermal degradation of “chars”, the residues formed during the second stage of CDs decomposition (44).

For the both binary and ternary systems, the thermogram patterns were different from the pure materials and since the ranges of degradation of both drug and carrier change, this difference indicates the

occurrence of interactions between the drug and carriers and in consequence, the formation of new systems. It is also found in the present study that the dehydration patterns of binary and ternary systems (Table 2) were different from the thermal behavior of pure CDs. The percentages of water evaporation decreased when complexes are formed indicating

substitution of water molecules by CPT, and this decrease was more important when complexes are dispersed in PEG 6000. This fact could be explained by the substitution of water molecules by CPT in one hand, and by the solid dispersion method itself that eliminates most water molecules, in other hand. Surprisingly, the thermogram patterns of PM (CPT/CDs/PEG 6000), did not show any evaporation of water molecules, probably in relation to mass dominance of PEG 6000 and to none homogenous systems. This can also be supported by the similarity of thermogram patterns of SDs and pure PEG 6000.

X-ray powder diffraction (XRPD)

XRPD of raw materials, binary and ternary systems are shown in Figures 14 and 15. The CPT diffractogram revealed a crystalline compound, showing a very strong diffraction peaks at 2θ of 6° , 9° , 11° , 12° , 17.6° and 25° . Nevertheless, the XRD pattern of CPT complexes and solid dispersions (binary and ternary systems) showed that some char-

acteristic peaks of pure CPT were absent and others appeared with a markedly reduced intensity. This suggests the formation of CD inclusion complexes by intermolecular interaction as reported earlier (46, 47). This also demonstrates that the CPT crystalline state dispersed in PEG 6000 had changed to an amorphous form, with improvement of drug dissolution as demonstrated below. This phenomenon had been reported for etoricoxib when it is dispersed in PEG (34).

Dissolution studies

The *in vitro* dissolution profiles of CPT, various ICs, SDo (binary systems) and various SDs of inclusion complexes in PEG 6000 (ternary systems) are shown in Figure 16.

Binary system

The fastest dissolution rate and the most important dissolved percentage of camptothecin were obtained with CPT/PM- β CD complex, 76% of the drug was dissolved within 120 min. It was also

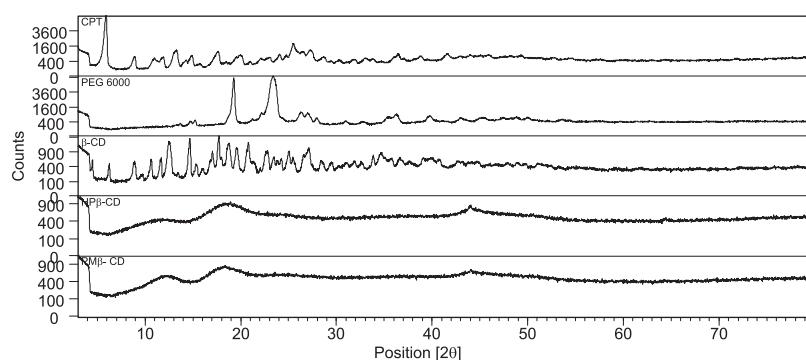


Figure 14. XRPD diffraction of raw materials

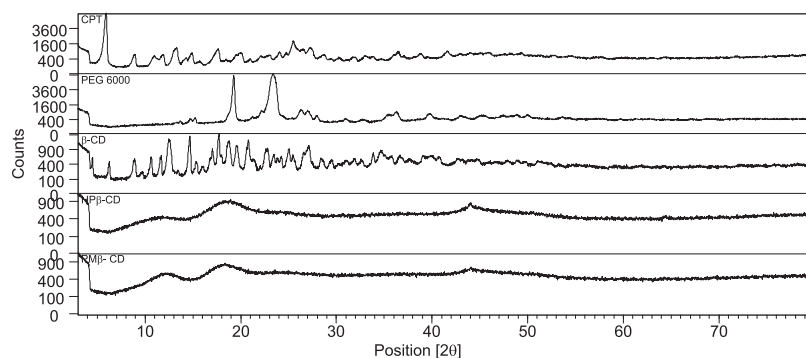


Figure 15. XRPD diffraction of CPT binary and ternary systems

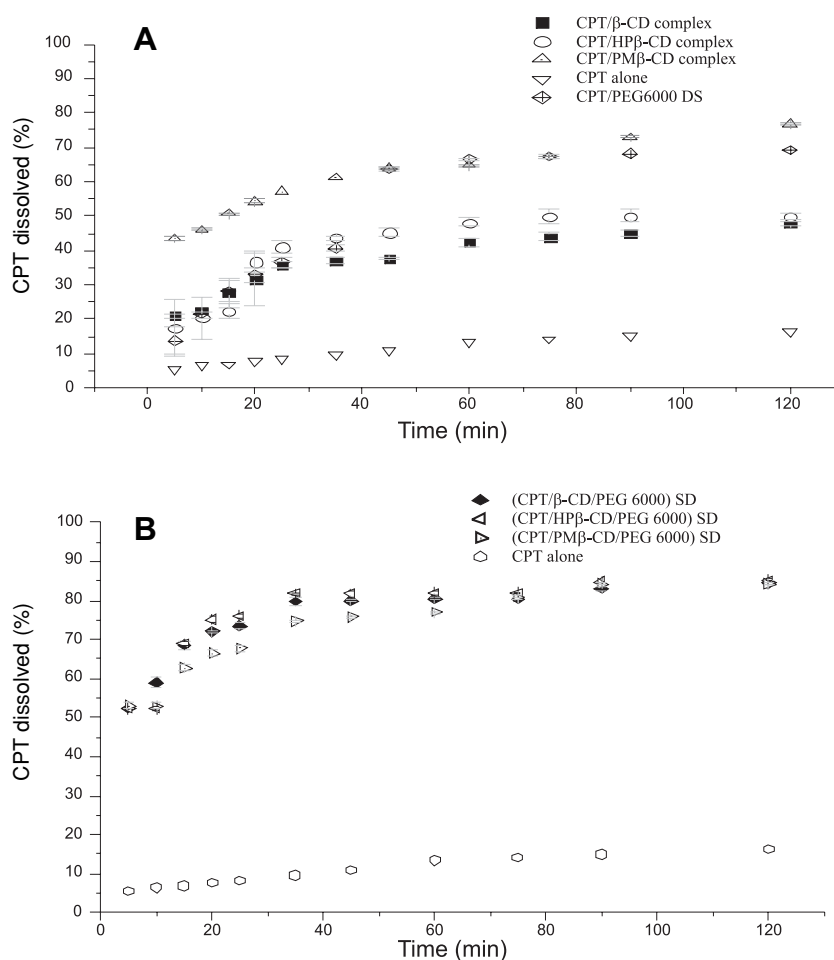


Figure 16. *In vitro* percentage of CPT released from binary (A) and ternary (B) systems in 0.1 M HCl. Triplicates for each sample except CPT ($n = 3$)

observed that solid dispersion was more effective in enhancing CPT dissolution (70%) than HP- β CD and β CD complexes. This is probably related to drug crystallinity decrease and the wettability improvement related to PEG 6000 as demonstrated for progesterone and indomethacin SDs (42, 48). The present results demonstrated that solid dispersion of CPT in PEG 6000 is a valuable concurrent to CPT / CD complexes.

Ternary system

All SDs samples showed dissolution improvement when compared to CPT alone. This is mainly attributed in one part to the formation of inclusion complex, in the second part to wettability increasing by PEG 6000 and to the amorphous state of CPT in SDs preparation. It is also observed that all solid dispersions revealed more CPT dissolution when com-

pared to their respective complexes. This is probably due to the effect of PEG 6000 and to the solid dispersion preparation. (35, 42, 48). Surprisingly, in all SDs preparations, whatever the IC used, 85% of dissolved CPT is reached, a recommendable value for tablet drug release (36), which indicates that there is a synergic effect between CDs and PEG 6000 without regards to the CD substitutions.

In order to establish the mathematical modeling of CPT release, the experimental data were fitted to kinetic models: zero order, first order, Higuchi, and Korsmeyer-Peppas models (49–51). The values for the diffusional exponent (n), correlation coefficient (R^2) and release rate coefficient (k) obtained are summarized in Table 3. The best correlation coefficients (R^2) were obtained with Higuchi model, as it was reported by Costa in his review (52). Higuchi describes drug release as a diffusion

process based in the Fick's law, square root time dependent. When modelization was done by Korsmeyer-Peppas model, the value of the exponent n for all formulations was below 0.43, which was further indicative of the drug releases following Fickian diffusion control mechanism (50, 53).

CONCLUSION

The purpose of the present paper was the improvement of camptothecin solubility and its dissolution rate. These aims were achieved either by forming CPT/CDs complexes, by solid dispersion of 10% of camptothecin in PEG 6000 (w/w) or by formation of ternary systems (CPT/CDs/PEG 6000). HP β -CD and PM β -CD appeared to be the most efficient in solubilizing CPT, these two CDs in addition to β -CD enhanced the velocity and the percentage of dissolved CPT, achieving 76% after 120 min, particularly when using PM β -CD. Moreover, CPT release from solid dispersion (CPT/PEG 6000, 10/90% (w/w)) reached a significant percentage (70%). However, the ternary systems, whatever the CPT complex used, appeared to be the most potent in enhancing the dissolution percentages and velocities. Physicochemical characterization (FT-IR, DSC, TGA and XRPD) demonstrated that camptothecin is incorporated into cyclodextrin cavity, replacing the water molecules. CPT 10% (w/w) or its complexes equivalent are well dispersed in PEG 6000, with appearance of amorphous state of the drug.

The synergic effect of complexation by cyclodextrins and solid dispersion in PEG 6000 conducted to a CPT release following Fickian diffusion reaching 85% in a gastric medium. This main result, offers promising perspectives of new CPT formulation tablets combining the use of non expensive, non toxic and commonly solubilizing carriers: β -CD and PEG 6000.

REFERENCES

1. Paranjpe P.V., Chen Y., Kholodovych V., Welsh W., Stein S., Sinko P.J.: *J. Control. Release* 100, 275 (2004).
2. Hsiang Y.H., Hertzberg R., Hecht S., Liu L.F.: *J. Biol. Chem.* 260, 14873 (1985).
3. Li Q.Y., Zu Y.G., Shi R.Z., Yao L.P.: *Curr. Med. Chem.* 13, 2021 (2006).
4. Thiele C., Auerbach D., Jung G., Wenz G.: *J. Incl. Phenom. Macrocycl. Chem.* 69,303 (2011).
5. Xie C., Li X., Luo X., Yang Y., Cui W., Zou J., Zhou S.: *Int. J. Pharm.* 391, 55 (2010).
6. Berrada M., Serreqi A., Dabbarh F., Owusu A., Gupta A., Lehnert S.: *Biomaterials* 26, 2115 (2005).
7. Lorence A., Nessler C.L.: *Phytochemistry* 65, 2735 (2004).
8. Saetern A.M., Nguyen N.B., Bauer-Brandl A., Brandl M.: *Int. J. Pharm.* 284,61 (2004).
9. Cheng J., Khin K.T., Jensen G.S., Liu A., Davis M.E.: *Bioconjugate Chem.* 14,1007 (2003).
10. Watanabe M., Kawano K., Yokoyama M., Opanasopit P., Okano T., Maitani Y.: *Int. J. Pharm.* 308,183 (2006).
11. Greenwald R.B., Pendri A., Conover C.D., Lee C., Choe Y.H., Gilbert C., Martinez A. et al.: *Bioorg. Med. Chem.* 6, 551 (1998).
12. Cýrpanli Y., Allard E., Passirani C., Bilensoy E., Lemaire L., Calph S., Benoit J.P.: *Int. J. Pharm.* 403, 201 (2011).
13. Aiping Z., Jianhong L., Wenhui Y.: *Carbohydr. Polym.* 63, 89 (2006).
14. Jiang Y., Sha X., Zhang W., Fang X.: *Int. J. Pharm.* 397, 116 (2010).
15. Kang J., Kumar V., Yang D., Chowdhury P.R., Hohl R.J.: *Eur. J. Pharm. Sci.* 15, 163 (2002).
16. Cirpanli Y., Bilensoy E., Dogan A.L., Calis S.: *J. Control. Release* 148, e21 (2010).
17. Bhaskara-Amrit U.R., Agrawal P.B., Warmoeskerken M.C.G.: *Autex Res. J.* 11, 94 (2011).
18. Katagery A., Sheikh M.: *Int. Res. J. Pharm.* 3, 52 (2012).
19. Lala R., Thorat A., Gargote C.: *IJRAP* 2, 1520 (2011).
20. Loftsson T., Duchene D.: *Int. J. Pharm.* 329, 1 (2007).
21. Chadha R., Kapoor V., Thankur D., Kaur R., Arora P., Jain D.V.S.: *J. Sci. Ind. Res. India* 67, 185 (2008).
22. Cheng T.L., Chuang K.H., Chen B.M., Roffler S.R.: *Bioconjugate Chem.* 23, 881 (2011).
23. Banerjee S.S., Aher N., Patil R., Khandare J.: *J. Drug Deliv.* 10, 1155 (2012).
24. Dodziuk H.: *Cyclodextrins and Their Complexes*, p. 2, Wiley-VCH, Weinheim 2006.
25. Li W., Zhan P., De Clercq E., Lou H., Liu X.: *Prog. Polym. Sci.* 38, 421 (2012).
26. Brewster M.E., Loftsson T.: *Adv. Drug Deliv. Rev.* 59, 645 (2007).
27. Giri T.K., Kumar K., Alexander A., Ajazuddin, Badwaik H., Tripathi D.K.: *Bulletin of Faculty of Pharmacy, Cairo University* 50, 147 (2012).
28. Hasnain M.S., Nayak A.K.: *Chemistry: Bulgarian Journal of Science Education* 21, 118 (2012).

29. Dash S., Murthy P.N., Nath L., Chowdhury P.: Acta Pol. Pharm. Drug Res. 67, 217 (2010).
30. Barzegar-Jalali M., Adibkia K., Valizadeh H., Shadbad M.R., Nokhodchi A., Omidi Y., Mohammadi G. et al.: J. Pharm. Pharm. Sci. 11, 167 (2008).
31. Foulon C., Tedou J., Lamerie T.Q., Vaccher C., Bonte J.P., Goossens J.F.: Tetrahedron Asymmetry 20, 2482 (2009).
32. Cirpanli Y., Bilensoy E., Lale Dođan A., Caliş S.: Eur. J. Pharm. Biopharm. 73, 82 (2009).
33. Bricout H., Hapiot F., Ponchel A., Tilloy S., Monflier E.: Sustainability 1, 924 (2009).
34. Suhagia B.N., Patel H.M., Shah S.A., Rathod I., Parmar V.K. Acta Pharm. 56, 285 (2006).
35. Almeida H.M., Cabral Marques H.M.: J. Incl. Phenom. Macrocycl. Chem. 70, 397(2011).
36. The United States Pharmacopeia 30, NF 25, p. 1010, Rockville, Maryland 2007.
37. Swaminathan S., Pastero L., Serpe L., Trotta F., Vavia P., Aquilano D., Trotta M. et al.: Eur. J. Pharm. Biopharm. 74, 193 (2010).
38. Dong L., Li Y., Hou W.G., Liu S.J.: J. Solid State Chem. 183, 1811 (2010).
39. Guijin L., Hongdi W., Yanbin J.: Ind. Eng. Chem. Res. 52, 15049 (2013).
40. Bai L., Song L.X., Wang M., Zhu L.H.: Chinese J. Chem. Phys. 23, 117 (2010).
41. Thakral N.K., Ray A.R., Bar-Shalom D., Eriksson A.H., Majumdar D.K.: AAPS PharmSciTech 13, 59 (2012).
42. Wulff M., Aldén M.: Eur. J. Pharm. Sci. 8, 269 (1999).
43. Dutet J., Lahiani-Skiba M., Didier L., Jezequel S., Bounoure F., Barbot C., Arnaud P., Skiba M.: J. Incl. Phenom. Macrocycl. Chem. 10, 203 (2007).
44. Zafid M.S., Afidah A.R., Abdullah J.M., Shariza A.R.: Biomed. Res. India 23, 513 (2012).
45. Moriwaki C., Costa G.L., Ferracini C.N., Moraes F.F., Zanin G.M., Pineda E.A.G., Matioli G.: Braz. J. Chem. Eng. 25, 225 (2008).
46. Shaikh J., Ankola D.D., Beniwal V., Singh D., Kumar M.N.: Eur. J. Pharm. Sci. 37, 223 (2009).
47. Yallapu M.M., Jaggi M., Chauhan S.C.: Colloids Surface B 79, 113 (2010).
48. Lahiani-Skiba M., Barbot C., Bounoure F., Joudieh S., Skiba M.: Drug Dev. Ind. Pharm. 32, 1043 (2006).
49. Takahashi A.I., Veiga F.J.B, Ferraz H.G.: Int. J. Pharm. Sci. Rev. Res. 12, 1 (2012).
50. Muthu M.S., Singh S.: Curr. Drug Deliv. 6, 62 (2009).
51. Dredan J., Antal I., Racz I.: Int. J. Pharm. 145, 61 (1996).
52. Costa P., Sousa Lobo J.M. : Eur. J. Pharm. Sci. 13, 123 (2001).
53. Zhang X., Zhang X., Wu Z., Gao X., Cheng C., Wang Z., Li C.: Acta Biomater. 7, 585 (2011).

Received: 10. 12. 2013

PREPARATION AND *IN VITRO* CHARACTERIZATION OF A NON-EFFERVESCENT FLOATING DRUG DELIVERY SYSTEM FOR POORLY SOLUBLE DRUG, GLIPIZIDE

VENKATA SRIKANTH MEKA^{*}, SHREENI PILLAI, SENTHIL RAJAN DHARMALINGHAM,
RAVI SHESHALA and ADINARAYANA GORAJANA

School of Pharmacy, International Medical University, Bukit Jalil, 57000, Kuala Lumpur, Malaysia

Abstract: The aim of the present study was to formulate a non-effervescent floating drug delivery system of glipizide, a poorly water soluble drug. The solubility of glipizide was initially enhanced using a solid dispersion (SD) strategy with the help of hydrophilic carriers such as poloxamer, cyclodextrin, and povidone. The optimized core material/SD was further formulated into non-effervescent floating tablets (NEFT) by using matrix ballooning inducers, such as crospovidone and release retarding agents including HPMC and PEO. Poloxamer-based solid dispersions prepared by a solvent evaporation technique showed the highest dissolution rate (1 : 10 drug to carrier ratio) compared with all other dispersions. NEFT were evaluated for all physico-chemical properties including *in vitro* buoyancy, dissolution, and release rate. All of the tablets were found to be within pharmacopoeial limits and all of the formulations exhibited good floating behavior. The formulations (F2 and F3) were optimized based on their 12 h drug retardation with continuous buoyancy. The optimized formulations were characterized using FTIR and DSC and no drug and excipient interaction was found. *In-vitro* buoyancy and dissolution studies showed that non-effervescent floating drug delivery systems provide a promising method of achieving prolonged gastric retention time and improved bioavailability of glipizide.

Keywords: non-effervescent, floating system, glipizide, solid dispersion

Oral controlled release drug delivery systems are widely used as they provide prolonged therapeutic effect by releasing the drug at a controlled rate after administration of a single dose. This improves patient compliance, reduces fluctuation of drug levels after multiple doses, reduces the total amount of drug administered, and reduces side effects. However, these systems are limited by the short gastrointestinal (GI) transit time, which prevents the drug from being completely released, leading to low bioavailability. To overcome this limitation, gastroretentive drug delivery systems were developed to retain the dosage form in the stomach (1, 2).

Although different types of gastroretentive systems are available, the floating drug delivery system (FDDS) has been described in detail. Floating drug delivery can be approached by either effervescent or non-effervescent techniques. Optimized effervescent FDDS of propranolol HCl prepared using polyethylene oxide (PEO) had good buoyancy and controlled drug release for up to 12 h (3). Ofloxacin effervescent floating tablets showed controlled drug

release for more than 12 h with excellent buoyancy properties (floating lag time < 1 min, floating duration > 16 h) (4).

FDDS have a bulk density < 1 g/mL, allowing them to float on the surface of the stomach contents (2). Effervescent FDDS incorporate gas generating agents, which provides buoyancy, whereas in non-effervescent systems, the swelling of polymers entraps air within the polymeric matrix, providing buoyancy to the dosage form (1, 2). While there has been much work on the development of effervescent drug delivery, non-effervescent technology is limited. The main drawback of the effervescent drug delivery is patient compliance, due to discomfort in the stomach after administration caused by the continuous liberation of gas.

Studies on non-effervescent systems include that of Garse et al. who formulated non-effervescent FDDS of labetalol hydrochloride using HPMC. Tablets had an insignificant floating lag time, a floating time > 12 h, and complete drug release (5). Patel et al. also designed a non-effervescent floating

^{*} Corresponding author: e-mail: venkatasrikanthmeaka@gmail.com

tablet for captopril. Combination of different viscosity grades HPMC showed > 96% drug release after 24 h (6). Sawicki and Łunio prepared floating pellets with verapamil hydrochloride and studied the influence of type of tablet press on the tableting of floating pellets and releasing rate of active substance (7). Development of gastroretentive drug delivery for poorly soluble drug presents a significant challenge. It is inadequate to formulate gastroretentive drug delivery of a poorly soluble drug without improving its solubility at the gastric pH. Hence, the present study targeted glipizide, a poorly soluble compound, as a model drug for the development of a gastroretentive drug delivery system. Solid dispersion is the best approach for the enhancement of solubility of the drugs.

Glipizide is a short acting antidiabetic sulfonylurea. It has a short half life (2–7.3 h) which requires it to be administered in 2–3 divided doses per day. Like all sulfonylureas, it may cause dose-dependent hypoglycemia (8). Therefore, a controlled release system is expected to provide more stable plasma glucose levels, reduce the dosing frequency and decrease the incidence of hypoglycemia. Moreover, the FDDS will be retained longer in the GI tract, providing sufficient time for the drug to be completely released.

Glipizide is a Class II drug according to the Biopharmaceutics Classification System; thus, its absorption is dissolution rate limited (9). Therefore, a solid dispersion approach was applied to improve the solubility and dissolution rate of the drug, followed by formulation into non-effervescent floating

tablets. Dehghan et al. concluded that the order of drug dissolution from different carriers is PEG > PVP > mannitol (10). Batra et al. showed that poloxamer 188 had a higher solubility enhancement effect than poloxamer 407 (11). In both studies, solid dispersions showed a higher dissolution compared with plain drug, or with a physical mixture of drug and carriers (10, 11). The objective of this study was to create a platform technology that enables the incorporation of poorly soluble drugs into FDDS.

EXPERIMENTAL

Materials

Glipizide was obtained from Dr. Reddy's Laboratories Ltd. (Hyderabad, India). Poloxamer 188, PVP K30, β -cyclodextrin, gelucire, PEO, HPMC, magnesium stearate, crospovidone, and lactose were obtained from Labchem Sdn. Bhd. Malaysia. All other reagents were of analytical grade.

Methods

UV analytical method development

Glipizide (100 mg) was dissolved in minimal quantity of methanol and volume was made up to 100 mL with 0.1 M HCl solution. From this, 10 mL of the solution was withdrawn and diluted to 100 mL using 0.1 M HCl solution, which yielded 100 μ g/mL of stock solution. Stock solution was scanned in a UV-Visible spectrometer at the wavelength range of 400–200 nm. Standard solutions of various concentrations of glipizide were prepared by subsequently

Table 1. Solid dispersions prepared by solvent evaporation and melt granulation.

Solid dispersion	Carrier	Drug-Polymer Ratio	Technique
G-PL-S 1:1	Poloxamer 188	1:1	Solvent evaporation
G-PL-S 1:2	Poloxamer 188	1:2	Solvent evaporation
G-PL-S 1:4	Poloxamer 188	1:4	Solvent evaporation
G-PL-S 1:6	Poloxamer 188	1:6	Solvent evaporation
G-PL-M 1:1	Poloxamer 188	1:1	Melt granulation
G-PL-M 1:2	Poloxamer 188	1:2	Melt granulation
G-PL-M 1:4	Poloxamer 188	1:4	Melt granulation
G-PL-M 1:6	Poloxamer 188	1:6	Melt granulation
G-PVP 1:6	PVP K30	1:6	Solvent evaporation
G-BCD 1:6	β -Cyclodextrin	1:6	Kneading
G-GEL 1:6	Gelucire	1:6	Melt granulation
G-PL-S 1:8	Poloxamer 188	1:8	Solvent evaporation
G-PL-S 1:10	Poloxamer 188	1:10	Solvent evaporation

*PL – poloxamer; PVP – polyvinylpyrrolidone; BCD – β -cyclodextrin; GEL – gelucire

Table 2. Formulae of glipizide non-effervescent floating tablets.

Ingredients	F1	F2	F3	F4	F5	F6
Solid dispersion (1 : 10 ratio)	55	55	55	55	55	55
HPMC K100M	15	30	40	–	–	–
PEO N12K	–	–	–	30	50	70
Crospovidone	50	50	50	50	50	50
Lactose	28.5	13.5	–	63	43	23
Mg Stearate	1.5	1.5	1.5	2	2	2
Tablet weight (mg)	150	150	150	200	200	200

Table 3. Mathematical models of drug release (12).

Model	Equation
Zero order	$Q_t = Q_0 + k_0 t$
First order	$\log Q_t = \log Q_0 - k_1 t$
Higuchi	$Q_t = k_H(t)^{1/2}$
Hixson-Crowell	$Q_0^{1/3} - Q_t^{1/3} = k_s t$
Korsmeyer-Peppas	$Q/Q_s = k_n t^n$

Q_t = amount of drug released in time t ; Q_0 = initial amount of drug in the tablet; t/Q_s = fraction of drug released at times t ; k_0 , k_1 , k_H , k_s , k_n = release rate constants; n = the release exponent indicative of the mechanism of drug release.

diluting suitable quantities of stock solution with respective media to obtain a series of standard solutions containing 10, 20, 30, 40, and 50 mg/mL of glipizide. The absorbances of these standard solutions of glipizide in respective media were measured individually at a wavelength of 275 nm against 0.1 M HCl as blank using UV-Visible spectrophotometer (UV-VIS Perkin-Elmer double beam spectrophotometer). A calibration curve was constructed by plotting the absorbance against the concentration of glipizide. The regression equation and the correlation coefficient value were derived from the plot and were used for the estimation of glipizide in 0.1 M HCl solution.

Preparation of solid dispersions

Solid dispersions were prepared using different carriers, techniques, and ratios, as summarized in Table 1.

Solvent evaporation

Glipizide and carrier were dissolved separately using the minimum quantity of methanol, and the two solutions combined. The resulting solution was evaporated at 50°C under reduced pressure in a rota evaporator and they were further dried in desiccator

over silica gel for 24 h to remove all the residual solvents. The dried mass was collected and packed in a closed container.

Kneading technique

Glipizide and β -cyclodextrin were mixed in a mortar. A drop of water was added, and the mixture was kneaded until a homogenous paste was obtained. The mixture was then placed in an oven at 50°C for 30 min, to remove water.

Melt granulation

The carrier was melted on a hot plate. Glipizide was added to the molten carrier with constant stirring to obtain a uniform melt, which was directly cooled in a refrigerator for 24 h to make it solidify. The final product was packed in a closed container for further use.

In vitro drug release of solid dispersions

Drug release studies were carried out using a USP type II (paddle) apparatus at 50 rpm. Solid dispersions equivalent to 5 mg of glipizide were tested in 900 mL of 0.1 M HCl (pH 1.2). Aliquots (5 mL) were withdrawn and filtered with cotton-filled canulae at predetermined intervals with replacement of equal volumes of fresh dissolution medium. Samples were tested spectrophotometrically at 275 nm, and compared against a calibration curve. Percent drug release *versus* time profiles were constructed.

Optimization of solid dispersion

The dissolution profiles of all the solid dispersions were compared. The technique, carrier and ratio were optimized based on the highest dissolution rate.

Preparation of floating tablets

The optimized solid dispersion was incorporated into floating tablets as the tablet core. Tablets were

prepared by direct compression. The ingredients used for each formulation are shown in Table 2. All excipients except magnesium stearate were passed through a 0.5 mm mesh sieve, while the dispersion was screened through a 1 mm mesh sieve. The pre-sifted ingredients were then manually blended in a polybag. The pre-lubricated blend was then mixed with magnesium stearate in the polybag for 3 min. Accurately weighed quantities of the final blend were manually fed into the die of an 8-station rotary tablet press, and then compressed with 8 mm punches.

Evaluation of tablet parameters

Tablets were evaluated for hardness (Monsanto hardness tester), weight variation, and friability (Roche friabilator, 100 revolutions in 4 min).

In vitro buoyancy

Tablets were placed in the dissolution vessel containing 900 mL of 0.1 M HCl. The time taken for the tablet to rise to the surface of the dissolution media (floating lag time) and total duration that the tablet remained on the surface (total floating time) were recorded.

In vitro drug release of floating tablets

Tablets were placed into dissolution vessels containing 900 mL of 0.1 M HCl (pH 1.2). Dissolution studies were carried out for 12 h, with samples withdrawn at predetermined intervals. The apparatus used and procedure is as described in step 4 (*in-vitro* drug release of solid dispersions).

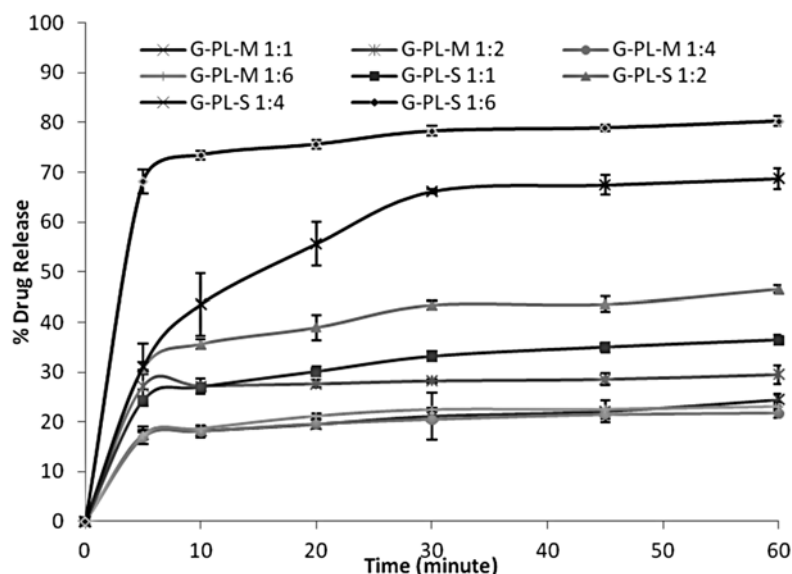


Figure 1. Dissolution profiles of poloxamer solid dispersions

Table 4. *In-vitro* drug release of pure drug and Poloxamer 188 solid dispersions.

Solid dispersion	% drug release					
	5 min	10 min	20 min	30 min	45 min	60 min
G-PL-S 1 : 1	24.29 ± 1.21	26.92 ± 2.89	30.05 ± 1.11	33.11 ± 0.96	34.96 ± 0.28	35.40 ± 1.55
G-PL-S 1 : 2	30.70 ± 1.22	35.60 ± 0.88	38.89 ± 2.56	43.39 ± 0.88	43.55 ± 1.53	46.53 ± 0.74
G-PL-S 1 : 4	31.10 ± 4.66	43.55 ± 6.19	55.61 ± 4.43	66.13 ± 0.46	67.42 ± 1.94	68.71 ± 2.16
G-PL-S 1 : 6	68.22 ± 2.44	73.45 ± 0.91	75.62 ± 0.91	78.27 ± 1.03	78.91 ± 0.74	80.06 ± 1.03
G-PL-M 1 : 1	17.44 ± 0.96	18.16 ± 0.88	19.53 ± 0.91	21.13 ± 4.66	22.10 ± 2.16	24.43 ± 1.14
G-PL-M 1 : 2	27.24 ± 3.11	27.24 ± 1.53	27.64 ± 0.74	28.21 ± 0.28	28.53 ± 1.20	29.49 ± 1.80
G-PL-M 1 : 4	16.79 ± 1.14	18.00 ± 1.20	19.53 ± 0.96	20.41 ± 0.34	21.38 ± 0.85	21.70 ± 0.97
G-PL-M 1 : 6	17.28 ± 1.82	18.64 ± 0.28	21.13 ± 0.51	22.42 ± 0.28	22.50 ± 0.00	23.06 ± 0.74

Table 5. *In vitro* drug release of solid dispersions prepared with different carriers.

Solid dispersion	% drug release					
	5 min	10 min	0 min	30 min	45 min	60 min
G-PL-S 1 : 6	68.22 ± 2.44	73.45 ± 0.91	75.62 ± 0.91	78.27 ± 1.03	78.91 ± 0.74	80.06 ± 1.03
Gel 1 : 6	13.42 ± 2.84	23.38 ± 1.08	33.35 ± 3.86	35.12 ± 0.34	39.70 ± 3.24	44.04 ± 1.48
BCD 1 : 6	14.06 ± 3.13	36.00 ± 2.39	44.60 ± 1.82	48.07 ± 1.25	50.30 ± 3.07	52.79 ± 3.30
PVP 1 : 6	46.93 ± 2.28	59.22 ± 3.24	62.28 ± 0.40	63.48 ± 0.74	64.37 ± 1.25	65.73 ± 1.31

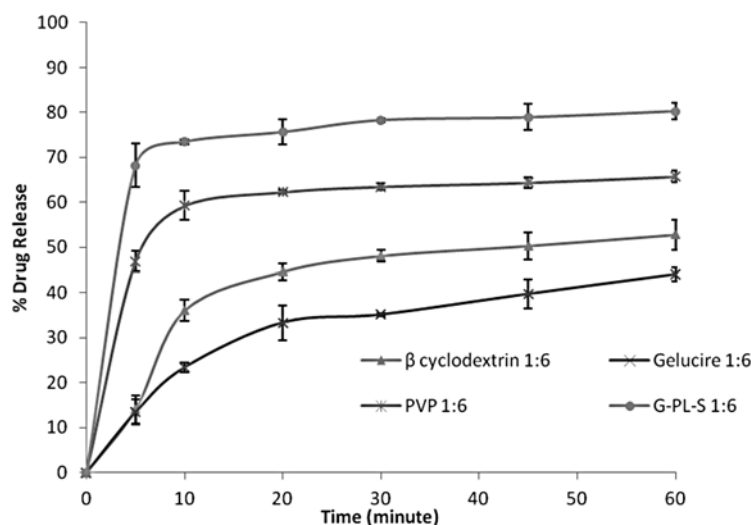


Figure 2. Dissolution profiles of dispersions prepared with different carriers

Determination of drug release kinetics

The dissolution data were fitted into various models of drug release as detailed in Table 3.

Optimization of floating tablets

Formulations with minimum floating lag time, maximum total floating time, and controlled drug release up to 12 h were selected as the optimized formulations.

Drug interaction studies

Fourier transformed infrared radiation (FTIR)

FTIR was performed on the drug, polymer, optimized solid dispersion, and optimized formulations. Samples were analyzed using the potassium bromide (KBr) pellet method (Shimadzu FTIR, scanning range 4000–400 cm^{-1}).

Differential scanning calorimetry (DSC)

DSC was performed with a Mettler Toledo DSC apparatus. Samples (3–10 mg) were heated in

nitrogen atmosphere from 10 to 250°C (heating rate 10°C per min).

RESULTS AND DISCUSSION

UV analytical method development

Glipizide λ_{max} was 275 nm. The calibration curve was linear (equation: $y = 0.0224x + 0.0072$) with regression (r^2) value of 0.9996.

In vitro drug release of solid dispersions

Poloxamer 188 solid dispersions prepared by solvent evaporation have a higher % drug release than melt granulation at all ratios (Table 4 and Fig. 1). In addition, higher drug: carrier ratios provided a higher % drug release. Therefore, solvent evaporation was selected as the optimized technique.

In melt granulation, maximum drug release was observed at 1 : 2 ratio (29.49%). Higher drug : carrier ratios did not increase the % drug release. This could be because the carrier formed a concentrated

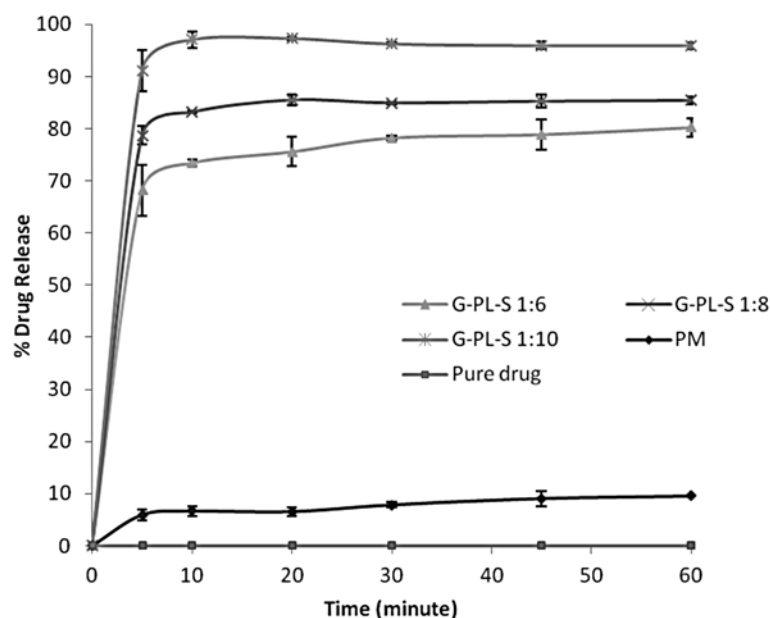


Figure 3. Dissolution profiles of pure drug, physical mixture and dispersions with different drug : poloxamer ratios

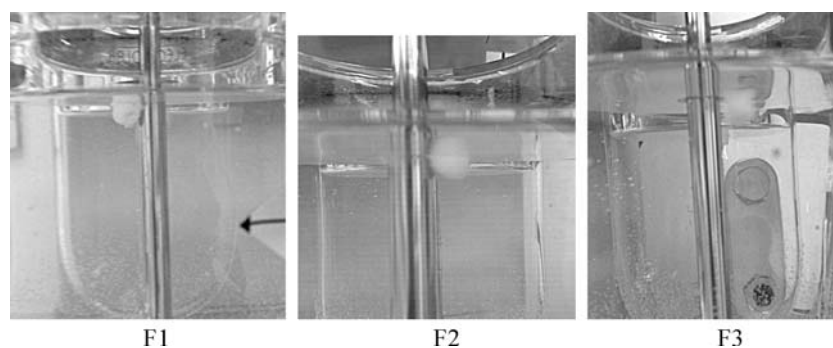


Figure 4. Floating tablets of glipizide at 2 h

layer surrounding the drug particles, acting as a diffusion barrier and slowing drug release (13). However, drug release of dispersions prepared by solvent evaporation at 1 : 6 ratio is only 80.6%. Therefore, different carriers were tried at 1 : 6 ratio to determine if they could further increase the drug release.

The order of drug release for different carriers was gelucire < β -cyclodextrin < PVP < poloxamer (Table 5 and Fig. 2). At 1 : 6 ratio, the other carriers could not provide higher drug release than poloxamer. Therefore, poloxamer 188 was selected as the optimized carrier. Higher drug : poloxamer ratios were investigated to obtain higher drug release.

As shown in Table 6 and Figure 3, 1 : 8 and 1 : 10 ratios released 85.42 and 95.95% of drug, respectively. The ratio 1 : 10 was selected as the optimized ratio as it had the highest % drug release. All dispersions had higher % drug release than pure drug and physical mixture.

The increased solubility of solid dispersions may be due to various mechanisms, including formation of eutectic mixtures or solid solutions, increased wetting by hydrophilic carriers, amorphization of drug, or particle size reduction (13). For example, gelucire decreases interfacial tension between drug particles and water by microemulsifi-

cation, while PVP systems may have formed interstitial solid solutions or an amorphous state; poloxamer systems increases dissolution by micellar solubilization (14), and cyclodextrin systems by formation of inclusion complexes (15). However, poloxamer systems seem to be the most efficient in increasing the solubility of glipizide.

Tableting parameters and *in vitro* buoyancy

The limits of weight variation for all formulations were less than 7.5% (Table 7). The hardness of

all formulations was between 3–4 kg/cm² and the % weight loss after friability was less than 1% (Table 7). Thus, all formulations fulfilled pharmacopoeial requirements.

All tablets floated (Fig. 4). The floating properties of HPMC formulations (F1, F2 and F3) were better than that of PEO (F3–F6), as shown by the shorter floating lag time and longer floating duration (Table 7). This could be due to the higher inherent swelling property of HPMC compared to that of PEO (8). Also, PEO based tablets floated for 8–10 h

Table 6. *In vitro* drug release of physical mixture and solid dispersions with different drug:carrier ratios.

Solid dispersion	% drug release					
	5 min	10 min	0 min	30 min	45 min	60 min
G-PL-S 1 : 6	68.22 ± 2.44	73.45 ± 0.91	75.62 ± 0.91	78.27 ± 1.03	78.91 ± 0.74	80.06 ± 1.03
G-PL-S 1 : 8	78.67 ± 1.76	83.17 ± 0.23	85.50 ± 1.08	84.94 ± 0.17	85.26 ± 1.20	85.42 ± 0.74
G-PL-S 1 : 10	91.13 ± 4.04	97.07 ± 1.59	97.31 ± 0.28	96.27 ± 0.17	95.95 ± 0.74	95.95 ± 0.63
Pure drug	< 1	< 1	< 1	< 1	< 1	< 1
Physical mixture (PM)	5.95 ± 1.08	6.67 ± 0.96	6.59 ± 0.79	7.88 ± 0.52	9.08 ± 1.41	9.56 ± 0.06

Table 7. Tableting and buoyancy characteristics of non-effervescent floating tablets.

Formulation	F1	F2	F3	F4	F5	F6
Hardness (kg/cm ²)	3–4	3–4	3–4	3–4	3–4	3–4
Weight variation (mg)	149.6 + 1.84	150.5 + 1.70	149.2 + 0.94	198.33 + 1.24	200.3 + 2.78	200.01 + 0.25
Friability (%)	0.3	0.6	0.4	0.5	0.02	0.1
Floating lag time (s)	< 1	< 1	< 1	25–30	10–11	5–9
Total floating time (h)	12	12	13	8	8	10

Table 8. Correlation coefficient values and drug release kinetics.

Formulation	Zero order		First order		Higuchi	Hixson-Crowell	Korsmeyer-Peppas	
	K ₀	r	K ₁	r	r	r	n	r
F1	3.8908	0.8882	0.1990	0.9573	0.9498	0.8556	0.2222	0.9710
F2	7.3383	0.9965	0.1338	0.9120	0.9925	0.9786	0.5798	0.9918
F3	7.815	0.9837	0.186	0.8516	0.9699	0.8416	0.4564	0.9826
F4	16.35	0.9001	0.1957	0.9252	0.9536	0.9854	1.0632	0.9912
F5	7.4484	0.9154	0.19	0.9041	0.9652	0.8773	0.9777	0.9991
F6	7.45	0.9254	0.197	0.8813	0.9531	0.8239	1.167	0.9887

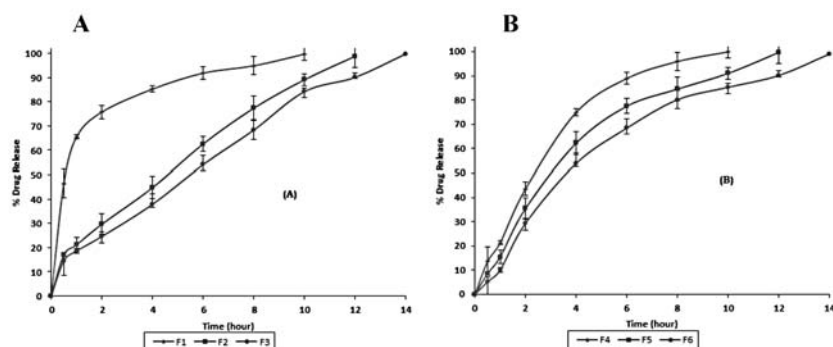


Figure 5. Dissolution profile of non-effervescent floating tablets prepared with A – HPMC; B – PEO

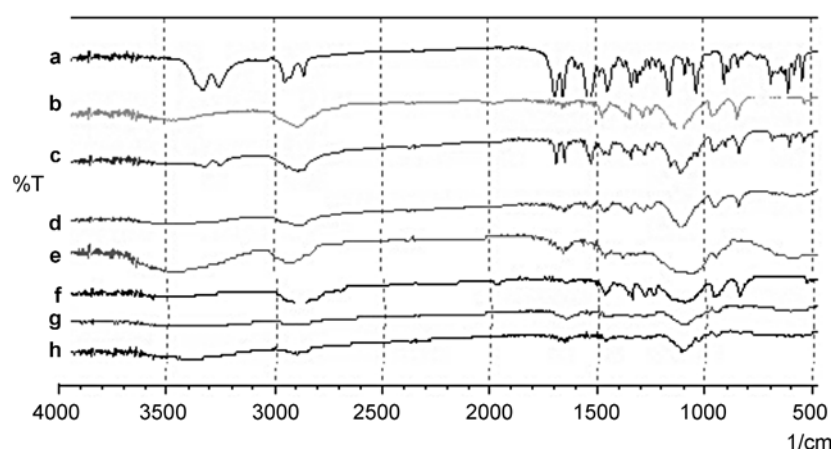


Figure 6. FTIR spectra of compounds. a) glipizide; b) poloxamers 188; c) physical mixture; d) solid dispersion (1 : 10); e) HPMC; f) formulation F2; g) PEO; h) formulation F5

as surface erosion of polymer took place (8), and the tablet was completely eroded by the end of 8 h, with insoluble residues visible at the bottom of the dissolution vessel.

Buoyancy of the tablets was provided by crospovidone. The quantity of crospovidone was constant in all the formulations based upon the preliminary studies. It is a super-disintegrant /matrix ballooning inducer, which swells and increases water uptake capacity of tablets. In the presence of hydrophilic polymers, it exhibits controlled swelling. Thus, the porosity of the matrix increased, and air bubbles were entrapped within the polymeric matrix, causing buoyancy of the dosage form (16, 17).

In vitro drug release

From Figure 5, drug release after 12 h reached > 90% for all formulations. F2 formulation showed

better controlled release than F1, which released > 90% of drug within 6 h. A higher HPMC content causes greater amount of gel to be formed, which increases the diffusion path length of the drug. This might lead to drug retardation. PEO based formulations also have good retardation properties. Lactose was the chosen diluent due to its water soluble and hydrophilic nature. It enables better matrix hydration, gel formation, and promotes free volume, which may have facilitated the drug release (8). When the dosage form is exposed to the dissolution medium, the medium can penetrate readily into the spaces between chains of the polymer. After polymer chain solvation, the dimensions of the polymer molecule increase due to the polymer relaxation by the stress of the penetrated solvent. This will form a gel-like network surrounding the tablet. This hydration property of the hydrophilic polymers such as HPMC and PEO can cause an immediate formation

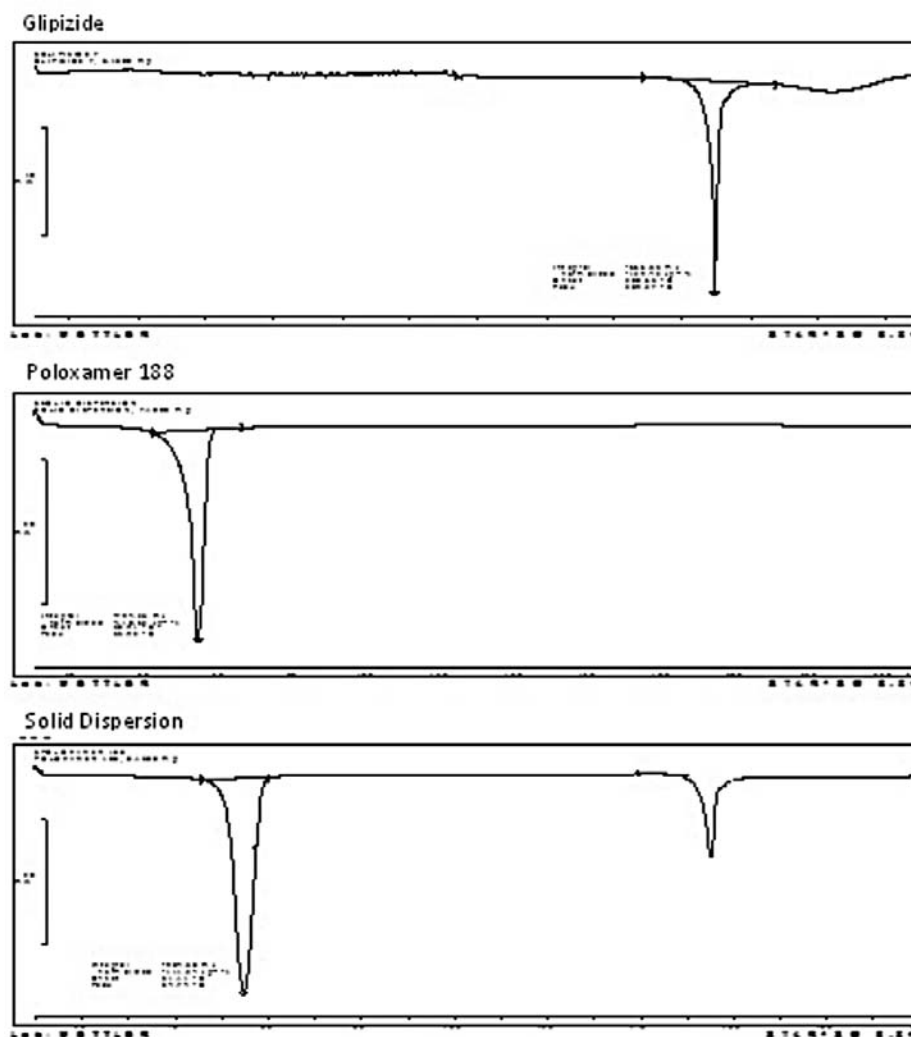


Figure 7. DSC spectra of glipizide, poloxamer 188 and solid dispersion

Table 9. FTIR assignment of bands of compounds (3, 18–21).

Compound	Major peaks (cm ⁻¹)	Assignment of bands
Glipizide	3325, 3250	N-H stretching
	1689, 1651	C = O stretching
	1159, 1132	S = O
	1527	Aromatic vibrations
	1444	Cyclohexane C-H bending
Poloxamer 188	2887	O-H stretch
	1109	C-O stretch
HPMC K100M	3437	O-H stretch
	1062	C-O (ether) stretch
PEO WSR N12K	3233	O-H stretch
	1097	C-O-C symmetric stretch
	1262	C-O-C asymmetric stretch

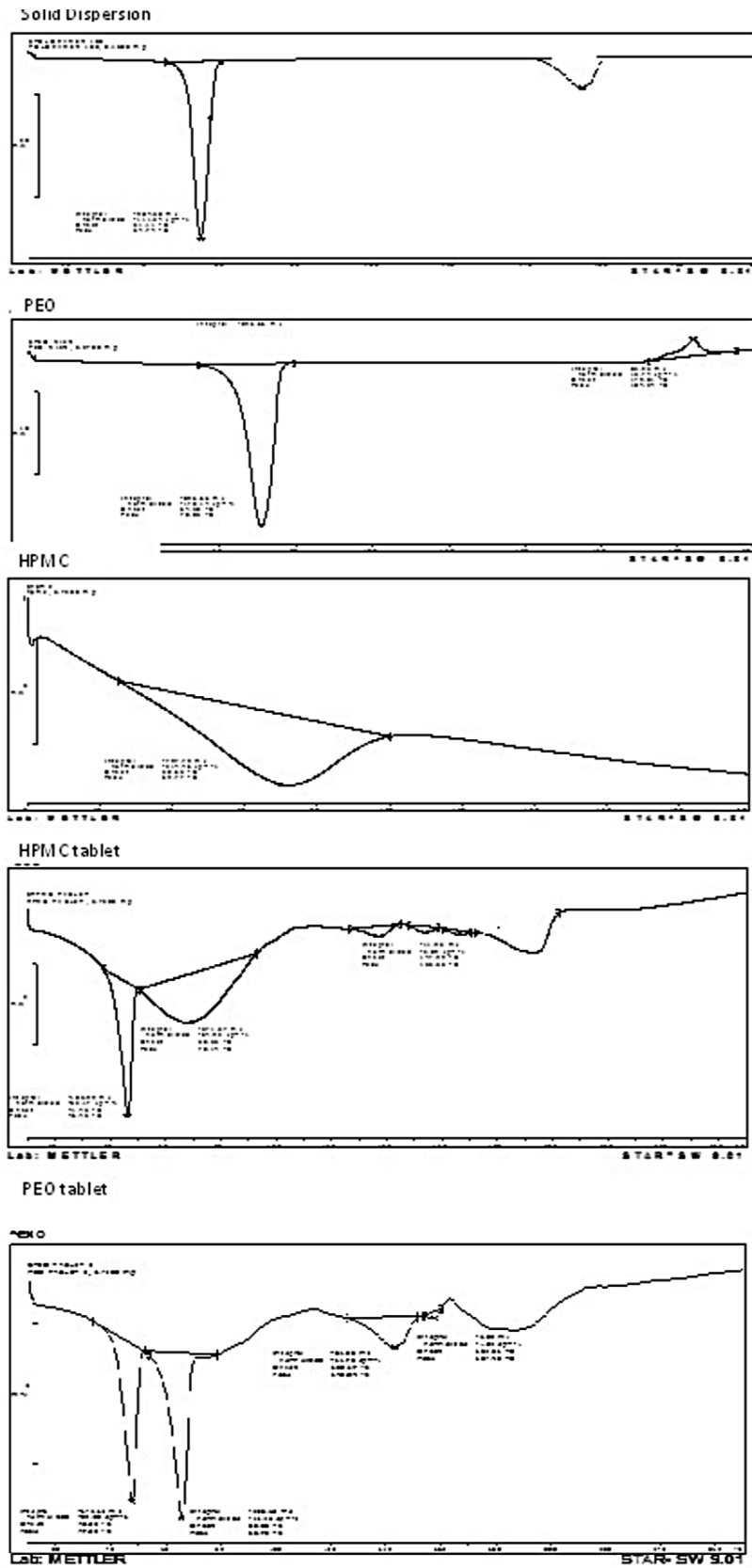


Figure 8. DSC thermograms of compounds

Table 10. DSC endothermic peaks.

Compound	DSC peak (°C)
Glipizide	209.27
Poloxamer	54.74
Solid dispersion	53.89
HPMC	69.77
PEO	70.83
Lactose	146.41
HPMC tablet	46.43, 70.14, 137.20
PEO tablet	47.60, 65.72, 143.04

of a surface barrier around the non-effervescent floating tablet that eliminates the burst release.

F2 and F5 were selected as optimized formulations based upon their drug retardation up to 12 h with continuous buoyancy properties.

Drug release kinetics

Among the HPMC based formulations, F1 followed first order rate kinetics and F2 and F3 followed zero order rate kinetics (Table 8). All HPMC based formulations follow the Higuchi model, indicating diffusion mechanisms. F1 follows Fickian diffusion, while F2 and F3 shows non-Fickian diffusion. This can be concluded from the higher correlation coefficient (*r* value) (12). The PEO based formulations F4 followed first order rate kinetics with erosion mechanism, which might be due to the lower concentration of the polymer. Other formulations F5 and F6 followed zero order kinetics with super case-II transport diffusion mechanism. The rate and mechanism of drug release depends on the type of polymer and the polymer concentration. For HPMC as well as PEO based formulations, higher polymer concentrations changed the rate from first order to zero order and the mechanism from Fickian to non-Fickian diffusion.

FTIR

Table 9 shows the major peaks of the compounds. From Figure 6 it can be seen that the physical mixture still retains the characteristic peaks of glipizide (3250, 3325, 1689, 1649, 1527, 1448 and 1159 cm^{-1}) and poloxamer (1112 and 2891 cm^{-1}). The solid dispersion spectrum also shows some peaks of glipizide (1527, 1637, and 1452 cm^{-1}) and poloxamer (1114 and 2877 cm^{-1}). However, the intensity of glipizide peaks are significantly reduced

(some to obscurity), and band broadening was observed at approximately 3600–3200 cm^{-1} (N-H stretching). The absence of any significant change in the IR spectral pattern in the physical mixture and solid dispersion indicate the absence of interaction between glipizide and carrier.

F2 tablets showed peaks at 1112 and 1097 cm^{-1} due to C-O of poloxamer and HPMC. A broad peak centered around 3375 cm^{-1} indicates the O-H group of HPMC. F3 tablets show a broad, high intensity peak from 3600 to 3000 cm^{-1} indicative of the O-H group of PEO. A peak at 1114 cm^{-1} indicates the C-O group of poloxamer and the 1097 cm^{-1} peak indicates C-O-C symmetric stretch of PEO. The absence of new, unidentified peaks indicates no drug- excipient interactions.

DSC

The endothermic peaks shown in Table 10 correspond to the melting points of glipizide, poloxamer, HPMC, PEO, and lactose. From Figure 7 and 8, the drug endothermic peak was suppressed in the solid dispersion, probably due to the small amount of drug compared to carrier, or due to the drug dissolving partially in the carrier to form a solid solution. This observation could also be due to the amorphous form of the drug in solid dispersion. The peaks of tablets F2 and F3 result from the superposition of their individual component DSC curves. The slight change in melting points could be due to a change in purity of the individual components in the tablets.

CONCLUSION

Incorporation of solid dispersion into floating tablets is a promising approach to enhance the solubility of poorly soluble drugs and achieve controlled release through gastric retention. Poloxamer 188 provided significant increase in solubility of glipizide. HPMC and PEO were able to provide *in vitro* buoyancy as well as controlled the drug release. Crospovidone was used successfully as a swelling agent.

Competing interests

The authors declare that they have no competing interests.

Acknowledgment

The authors would like to thank International Medical University for providing the necessary facilities for conducting the research.

REFERENCES

1. Arora S., Ali J., Ahuja A., Khar R.K., Baboota S.: AAPS PharmSciTech 6, 372 (2005).
2. Singh B.N., Kim K.H.: J. Control. Release 63, 235 (2000).
3. Srikanth M.V., Songa A.S., Nali S.R., Battu J.R., Kolapalli V.R.M.: Invest. Clin. 53, 60 (2012).
4. Shakya R., Thapa P., Saha R.N.: Asian J. Pharm. Sci. 8, 191 (2013).
5. Garse H., Vij M., Yamgar M., Kadam V., Hirlekar R.: Arch. Pharm. Res. 33, 405 (2010).
6. Patel P., Dand N., Somwanshi A., Kadam V.J., Hirlekar R.S.: AAPS PharmSciTech 9, 839 (2008).
7. Sawicki W., Łunio R.: Acta Pol. Pharm. Drug Res. 67, 103 (2010).
8. American Hospital Formulary Service. McEvoy G.K.: Antidiabetic agents. AHFS drug information. American Society of Health-System Pharmacists, Bethesda 2013.
9. Jamzad S., Fassihi R.: Int. J. Pharm. 312, 24 (2006).
10. Dehghan M.H.G., Saifee M., Hanwate R.M.: J. Pharm. Sci. Technol. 2, 293 (2010).
11. Batra V., Shirolkar V.S., Mahaparale P.R., Kasture P.V., Teshpande A.D.: Indian J. Pharm. Educ. Res. 42, 371 (2008).
12. Costa P., Lobo J.M.S.: Eur. J. Pharm. Sci. 13, 123 (2001).
13. Vo C.L.N., Park C., Lee B.J.: Eur. J. Pharm. Biopharm. 85, 799 (2013).
14. Ahuja N., Katare O.P, Singh B.: Eur. J. Pharm. Biopharm. 65, 26 (2007).
15. Martin Del Valle E.M.: Process Biochem. 39, 1033 (2004).
16. Ratnaparkhi M.P., Bhabad V.S., Chaudhari S.P.: Int. J. Pharm. Tech. Res. 4, 1041 (2012).
17. Mohamed M., Talari M.K., Tripathy M., Majeed A.B.A.: IJDFR 3, 13 (2012).
18. Tiwari G., Tiwari R., Srivastava B., Rai A.K.: Research J. Pharm. and Tech. 1, 14 (2008).
19. Kolašinac N., Kachrimanis K., Homšek I., Grujić B., Durić Z., Ibrić C.S.: Int. J. Pharm. 436, 161 (2012).
20. Patil S.A., Kuchekar B.S., Chabukswar A.R., Jagdale S.C.: J. Young Pharm. 2, 121 (2010).
21. Coates J.: Interpretation of Infrared Spectra, A Practical Approach, in Encyclopedia of Analytical Chemistry. Meyers R.A. Ed., p. 10815, John Wiley & Sons, Chichester 2000.

Received: 11. 12. 2013

PHARMACOLOGY

EFFECT OF ALLOFERON 1 ON CENTRAL NERVOUS SYSTEM IN RATS

MONIKA RYKACZEWSKA-CZERWIŃSKA^{1,2*}, PIOTR OLEŚ^{1,3}, MICHAŁ OLEŚ^{1,2},
MARIOLA KUCZER⁴, DANUTA KONOPIŃSKA⁴ and ANDRZEJ PLECH⁵¹Chair and Department of Pharmacology, Medical Faculty in Zabrze of the Medical University of Silesia
in Katowice, 28 Jordana St., 41-808 Zabrze, Poland²Department of Toxicology and Health Protection, Medical University of Silesia,
18 Medyków St., 40-752 Katowice, Poland³Department and Clinic of Internal Diseases, Angiology and Physical Medicine,
Medical University of Silesia, 15 Batorego St., 41-902 Bytom, Poland⁴Faculty of Chemistry, Wrocław University, 14 F. Joliot-Curie St., 50-383 Wrocław, Poland⁵Chair of Basic Medical Sciences, Higher Medical School, 6 Wojska Polskiego St. 41-200 Sosnowiec,
Poland

Abstract: Alloferon 1 is an insect-derived peptide with potent antimicrobial and antitumor activity. It was isolated from blood of an experimentally infected insect, the blow fly *Callifora vicina*. Synthetic alloferon 1 reveals a capacity to stimulate activity of NK cells and synthesis IFN in animal and human models. Moreover, it was demonstrated antiviral and antitumor activity of alloferon 1 in mice. There are no data on influence of alloferon 1 on central nervous system. The aim of present study was to determine an effect of alloferon 1 on rats' central nervous system by some behavioral tests: open field test, hole test, score of rats irritability, and determination of memory consolidation in the water maze test. Moreover, a probable antinociceptive effect of alloferon 1 in rats was determined by a tail immersion test and hot plate test. Experiments were performed on female Wistar rats. Seven days before experiments, rats were anesthetized with ketamine and xylazine and polyethylene cannulas were implanted into the right lateral brain ventricle (*i.c.v.*). On the day of experiment, alloferon 1 dissolved in a volume of 5 µL of saline was injected directly *i.c.v.* through implanted cannulas at doses of 5–100 nmol. It was found that alloferon 1 had slight effect on locomotor and exploratory activity, induced some decrease of rat irritability and a weak impairment of rats memory (only at the low dose of 5 nmol). On the other hand, the higher dose of this peptide exerts significant antinociceptive effect. Obtained results indicate that alloferon 1 do not exert any evidently toxic effect on central nervous system in rats. Therefore, alloferon 1 may be good new drug with antitumor and antinociceptive activity.

Tridecapeptide alloferon 1 (HGVS₁GHGQHG VGH) (Al 1) has been isolated from blood of experimentally infected larvae of the blow fly *Callifora vicina* (1). It does not possess any similarity of aminoacid sequence with other known immunomodulatory peptides. On the other hand, this peptide shows some functional similarity with interferon and therefore was named alloferon as a nonvertebrate-derived regulator of cytotoxic lymphocytes (1). Synthetic alloferon 1 reveals a capacity to stimulate activity of NK cells, and synthesis of interferon (IFN) in animal *in vivo* and in human models *in vitro* (1). Moreover, it was demonstrated antiviral and antitumor effect of alloferon 1 in mice

(1, 2). It was shown that several peptides of different length and aminoacid sequence of peptide chain act on central nervous system (CNS) (3–6). However, there are no data on influence of alloferon 1 on CNS. Present study was undertaken in order to define any effect of synthetic alloferon 1 on CNS in rats, determined by some behavioral tests.

METHODS

Animals

Experiments were performed on female Wistar rats weighing 230–280 g obtained from the animal farm of the Medical University of Silesia in

* Corresponding author: e-mail: monczer@gazeta.pl

Katowice. The animals were kept under 12 h light/12 h dark cycle (light from 6 a.m. to 6 p.m.) in a constant temperature with free access to the water and a standard food (Labofeed B, Kcynia, Poland).

Intracerebroventricular (*i.c.v.*) cannulation

One week before the beginning of the experiments, rats were implanted with polyethylene cannulas (length 35 mm, internal diameter 0.4 mm and external diameter 0.7 mm) into the right lateral brain ventricle (*i.c.v.*) using the same technique as in our previous investigations (3, 4). After intraperitoneal (*i.p.*) injection of xylazine hydrochloride (Xylavet 2% sol., ScanVet, Poland, 10 mg/kg *i.p.*) and of ketamine hydrochloride (Bioketan, Biovet, Poland, 100 mg/kg *i.p.*) heads of animals were fixed in the stereotaxic frame. Polyethylene cannulas (Tomel, Tomaszów Mazowiecki, Poland) were introduced into the right lateral brain ventricle (*i.c.v.*) according to the following coordinates: a depth 4 mm from the surface of the skull, 2 mm to the right from sagittal suture and 2 mm caudal from the coronal suture and fixed to the skull with dental cement (Duracryl, Spofa Dental, Prague, Czech Republic).

Drugs

Alloferon 1 was synthesized in the Faculty of Chemistry, University of Wrocław, Poland (7). It was injected directly *i.c.v.* through implanted cannulas in four doses of 5, 25, 50 and 100 nmol dissolved in 5 µL of 0.9% NaCl to unanesthetized rats using a Hamilton microsyringe. Control animals were treated *i.c.v.* with 5 µL of 0.9% NaCl.

Behavioral tests

Locomotor and exploratory activity was determined 10 min and 24 h after *i.c.v.* injection by means of an open field according to Janssen et al. (8), and 16 min and 24 h after injection in the hole test according to File et al. (9, 10). The open field test was performed in the dark room where was placed round black table with eight white lines. The punctual light was switching on the center of the table where all white lines cut through. Rats were placed on the table and for 3 min were count: ambulation, rearing, peeping, grooming and number of defecation. In the hole test during 3 min number of head dips were counted in rats placed on the wooden box with 16 circular holes of 7 cm diameter.

Irritability was measured 15 min and 24 h after *i.c.v.* injection of Al 1 using the score of Nakamura and Thoenen (11). In this test, rats reaction on blowing is measured, using 0–3 point score: blowing, touching with the glass rod of whiskers and back and holding by hand.

Antinociceptive effect was determined by two tests: the tail immersion (12) and a hot plate test (13) using apparatus HP – 41 (COTM, Białystok, Poland). The latencies for the tail immersion test were recorded before experiment and 10 min, 60 min and 24 h after injection, while the latencies for a hot plate test were recorded also before, and next 11 min, 61 min and 24 h after Al 1 injection.

Latencies determined in the tail immersion test were converted to percent of analgesia according to the formula:

$$\begin{array}{l} \% \text{ of analgesia} \\ (\% \text{ of maximal} \\ \text{antinociceptive effect}) \end{array} = \frac{T_x - T_o}{10 - T_o} \times 100$$

The determined latency time of each animal in the hot-plate test was converted to the coefficient: percent of analgesia according to the formula:

$$\begin{array}{l} \% \text{ of analgesia} \\ (\% \text{ of maximal} \\ \text{antinociceptive effect}) \end{array} = \frac{T_x - T_o}{20 - T_o} \times 100$$

where T_x – individual latency time determined at time intervals after Al 1 administration; T_o – individual latency time determined before Al 1 administration; 10 – maximal latency time in the tail immersion test (in s); 20 – maximal latency time in the hot-plate test (in s).

Space memory was determined by means of a water maze test according to Plech et al. (14). The time between placing the animal into a central part of the maze and entering onto platform was measured. A mean latency time for three probe trials of each animal was calculated. Latency time was measured one day before beginning of the experiment and 65 min and 24 h after *i.c.v.* injection of Al 1.

At the end of experiments, rats were sacrificed by xylazine and ketamine injection and *post mortem* the placements in the brain of cannulas' tips was checked by injecting *i.c.v.* 10 µL of 2% methylene blue dye solution and investigations of frontal brain slices cut with freezing microtome.

Data were subjected to ANOVA and *post-hoc* Dunnett test (15) (significance $p < 0.05$).

All these experiments were performed in accordance with guidelines for investigations of experimental pain in conscious animals (16).

The protocol of this study was approved by the local ethical committee of the Medical University of Silesia (KNW-0022/LKE-1-77/09).

RESULTS

Alloferon 1 decreases number of rearing (at doses: 5 and 25 nmol) and number of peeping (at

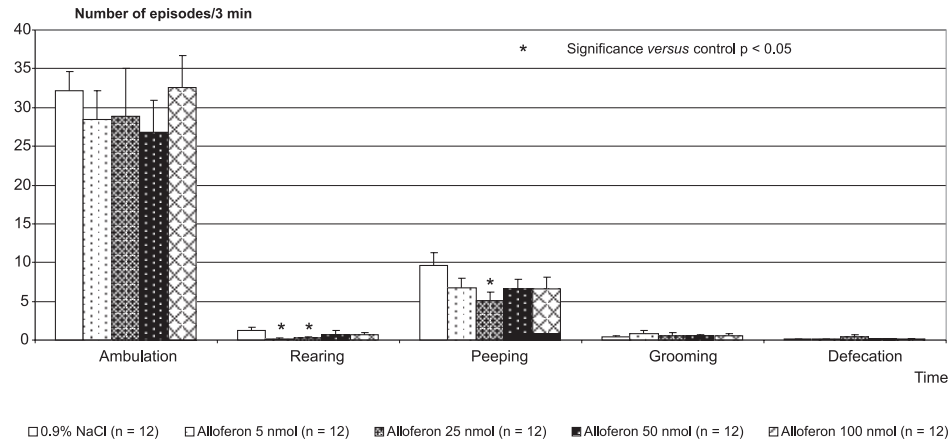


Figure 1. Affect of alloferon 1 on rat's behavior measured with an open field test 10 min after *i.c.v.* injection

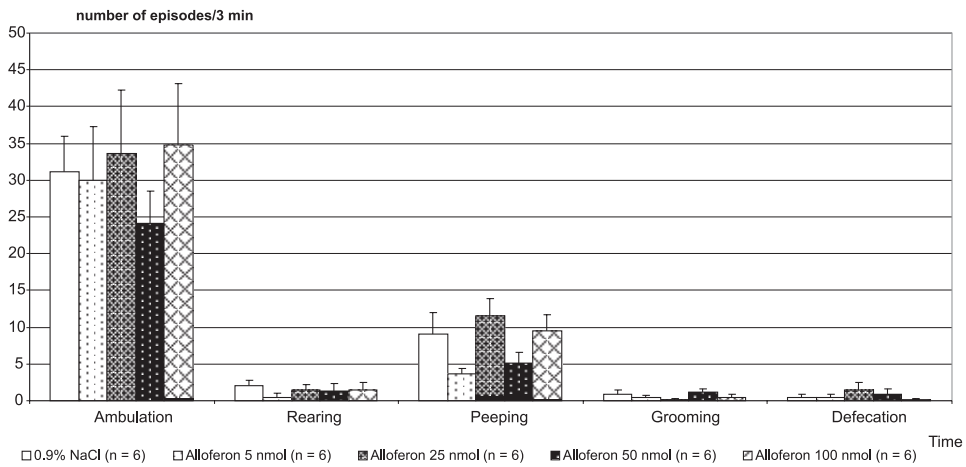


Figure 2. Effect of alloferon 1 on rat's behavior measured with an open field test 23 h after *i.c.v.* injection

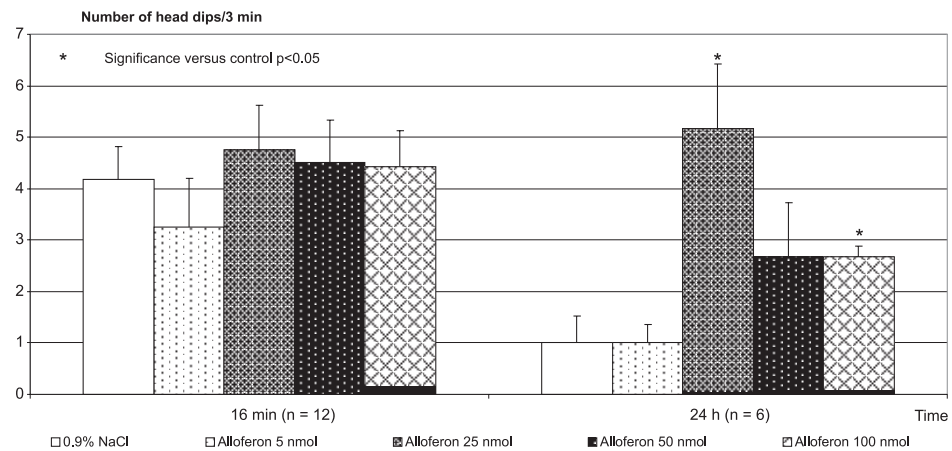


Figure 3. Effect of alloferon 1 on rat's exploratory activity measured by a hole test after *i.c.v.* injection

a dose 25 nmol) in rats 10 min after *i.c.v.* injection (Fig. 1). It does not change number of ambulation, grooming and defecation (Fig. 1) and it does not influence on rats behavior observed in the open field test after 24 h after *i.c.v.* injection (Fig. 2). Alloferon slightly increases rats' exploratory activity 24 h after *i.c.v.* administration, specially at a dose of 25 nmol (Fig. 3). The same dose 25 nmol of AI 1 exerts significant activity lowering rats' irritability (Fig. 4). Investigations of antinociceptive effect of AI 1 show slight antinociceptive effect at both used tests: tail immersion and hot plate test (Figs. 5 and 6). However, AI 1 at a dose 25 nmol *i.c.v.* 61 min after injection exerted some hyperalgesia determined by a hot plate test (Fig. 6). Alloferon exerts also a weak impairment on rats' memory measured by a water maze test (Fig. 7).

DISCUSSION

The method used in this study of direct, intracerebral administration – into the lateral brain ventricle (*i.c.v.*) of tridecapeptide AI 1 made it possible to overcome the blood-brain barrier and to determine the effect of this peptide on the function of rat brain. It is commonly known, since several years that different peptides poorly penetrated the blood-brain barrier (17). The method of *i.c.v.* administration of different peptides and of other drugs was used in several our earlier studies (18–20). *I.c.v.* administration of peptides or drugs resulted in their broad penetration to different brain areas of the rat (21, 22). Synthetic AI 1 was given *i.c.v.* in four increasing doses: 5, 25, 50 and 100 nmols. Such range of dosing was chosen in order to find their effect on rats behavior. Several of different synthetic peptides

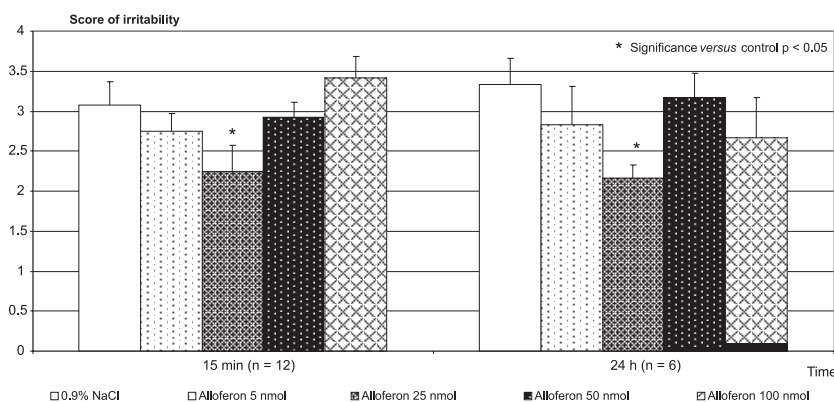


Figure 4. Effect of alloferon 1 on rat's irritability measured by Nakamura-Thoenen score after *i.c.v.* injection

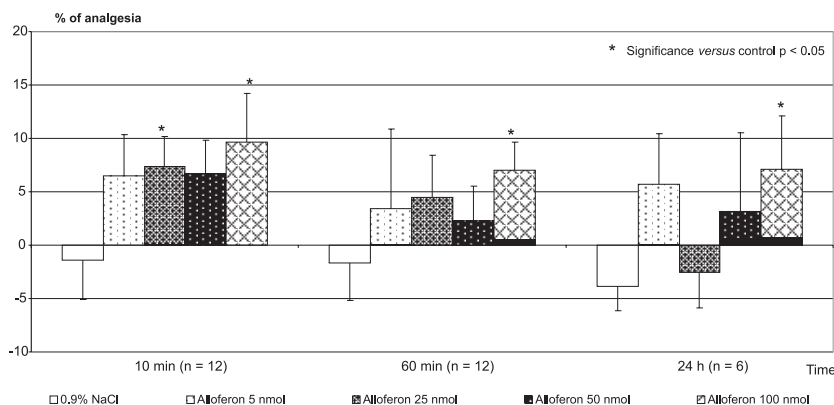


Figure 5. Antinociceptive effect of alloferon 1 determined by the tail immersion test after *i.c.v.* injection

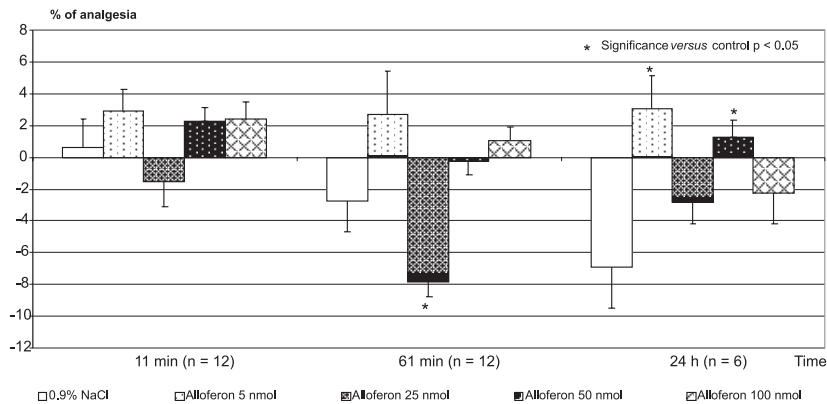


Figure 6. Antinociceptive effect of alloferon 1 determined by a hot plate test after *i.c.v.* injection

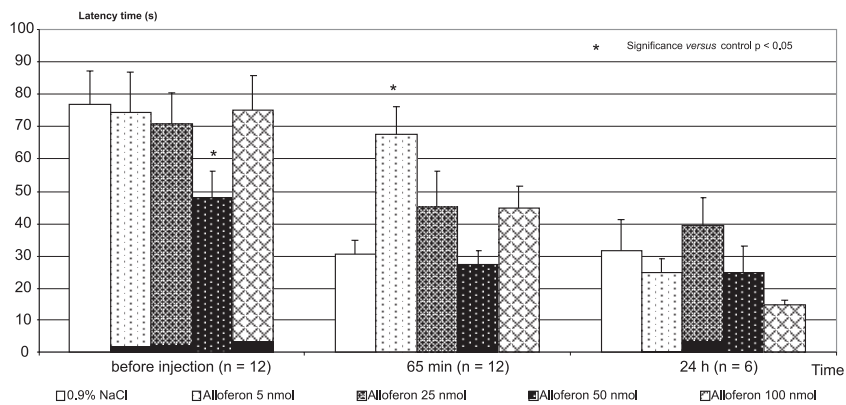


Figure 7. Memory effect of *i.c.v.* administration of alloferon 1 determined by water maze test

applied *i.c.v.* and in similar range of doses cause evident behavioral effects in rats (20, 23). Two used behavioral tests: of the hole and of an open field evaluated rats locomotor and exploratory activity. These both forms of rats behavior expressed an activity of the CNS. Obtained results proved that Al 1 slightly affected rats exploratory activity, as it was observed a prompt effect (in 10 min after it *i.c.v.* administration) of a decrease of the number of rats rearings in an open field test. However, this effect was not confirmed in the hole test. It was not found any prompt decrease on the number of head dips determined in a hole test. Moreover, *i.c.v.* administration of Al 1 elicited in rats a late (after 24 h after it *i.c.v.* administration) increase of rats exploratory activity, expressed as an increase of the number of rats head dips counted in a hole test. Thus, different, not distinct changes of rats locomotor and explorato-

ry activity indicated that Al 1 not disturbed the function of rats CNS. The results of the study of two other forms of rats behavior i.e., the determination of the intensity of rats irritability and the investigation of memory consolidation also did not show any neurotoxic effect of Al 1. All applied doses of Al 1 neither increase rats irritability nor elongated the latency time of entering rats onto platform in a water maze test in comparison to untreated control animals. All behavioral evaluations were performed on female rats. It is known that different behavioral effects in rats, including locomotor and exploratory activity, are modulated by gender, estrus cycle as well as by progesterone (24). Estradiol seems to be a main ovarian steroid modulating also an acquisition of conditioned avoidance response (25). On the other hand, it was found in earlier investigations that synthetic pentapeptide proctolin, the first discovered

insect neuropeptide, applied directly into the lateral brain ventricle to uncastrated female rats did not change rats exploratory activity in every of four phases of estrus cycle (26). The same, equimolar dose of proctolin, of 100 nmols applied *i.c.v.* in castrated female rats, also did not change their exploratory activity in comparison to control group (26). The results of our present investigations were obtained on intact, uncastrated female rats. These animals either of experimental or control groups were in different phases of estrus cycle, therefore, it was possible to avoid a distinct effect of estrus phase on rats behavior. Moreover, there were used different behavioral tests. Thus, we expect that probable effect of estrus cycle had not prominent influence on results of performed investigations of Al 1 activity.

Antinociceptive effect of the same, standard, equimolar doses of Al 1: 5–100 nmol was investigated in rats by two classic methods: the tail immersion and the hot plate. It was found a slight antinociceptive effect of Al 1. It was presented in several reports that opioid and non-opioid peptides displayed analgesic effect in rats and mice (19, 23, 27, 28). At present, the mechanism of analgesic effect of Al 1 is unknown. We hope that further study of this peptide may reveal the mechanism responsible for its analgesic effect. To our knowledge this report is a first on neurotoxic effect of Al 1.

In summary, all presented here behavioral studies allow to conclude that Al 1 is not a distinct neurotoxic agent for rats.

CONCLUSION

The results of present study did not prove any neurotoxic effect of Al 1 in rats, expressed as an impairment of rats behavior.

Acknowledgments

This work was supported by a grant from the Medical University of Silesia KNW-2-031/10 and by a grant from Ministry of Science and Higher Education NN 204085638.

REFERENCES

1. Chernysh S., Kim S.I., Bekker G., Pleskach V.A., Filatova N.A., Anikin V.B., Platonov V.G., Bulet P.: Proc. Natl. Acad. Sci. USA 99, 12628 (2002).
2. Lee N.E., Kang J.S., Kim J.E., Jung J.D., Lee S.K., Bae S., Kong J.M. et al.: FASEB J. 22 (Meeting Abstract Suppl.), 859, 19 (2008).
3. Rykaczewska-Czerwińska M., Oleś P., Konopińska D., Sipiński A., Plech A.: JAST 2, 702 (2012).
4. Rykaczewska-Czerwińska M., Radosz A., Szymanowska-Dziubasik K., Konopińska D., Plech A.: Pestycydy/Pesticides 3-4, 139 (2008).
5. Nusbaum M.P., Blitz D.M.: Curr. Opin. Neurobiol. 22, 592 (2012).
6. Holzer P., Reichmann F., Farzi A.: Neuropeptides 46, 261 (2012).
7. Kowalik-Jankowska T., Biega Ł., Kuczer M., Konopińska D.: J. Inorg. Biochem. 103, 135 (2009).
8. Janssen P.A.J., Jagenau A.H.M., Schellekens K.H.L.: Psychopharmacology 1, 389 (1960).
9. File S.E.: Br. J. Pharmacol. Chemother. 49, 303 (1973).
10. File S.E., Pope J.H.: Psychopharmacology 37, 249 (1974).
11. Nakamura K., Thoenen H.: Eur. J. Pharmacol. 16, 46 (1971).
12. Janssen P.A.J., Niemegeers C.J.E., Dony J.G.H.: Arzneimittel Forsch. 13, 502 (1964).
13. O'Callaghan J.P., Holtzman S.G.: J. Pharmacol. Exp. Ther. 192, 497 (1975).
14. Plech A., Klimkiewicz T., Jakrzewska H.: Pol. J. Environ. Stud. 9, 301 (2000).
15. Tallarida R.J., Murray R.B.: Manual of Pharmacologic Calculations with Computer Programs, 2nd ed., pp. 110–121, 146–148, Springer Verlag, New York 1987.
16. Zimmermann M.: Pain 16, 109 (1983).
17. Banks W.A., Kastin A.J.: Brain Res. Bull. 15, 287 (1985).
18. Plech A., Rykaczewska-Czerwińska M., Konopińska D.: Peptides 25, 1005 (2004).
19. Rykaczewska-Czerwińska M., Konopińska D., Plech A.: Comp. Biochem. Physiol. C 130, 271 (2001).
20. Plech A., Rykaczewska-Czerwińska M., Bartosz-Bechowski H., Lombarska-Śliwińska D., Małota M., Szewczyk M., Brus R., Konopińska D.: Pol. J. Pharmacol. 49, 119 (1997).
21. Plech A., Rykaczewska-Czerwińska M., Ryszka F., Suszka-Świtek A., Dolińska B., Konopińska D.: Int. J. Tissue React. 25, 65 (2003).
22. Plech A., Rykaczewska-Czerwińska M., Ryszka F., Suszka-Świtek A., Dolińska B., Konopińska D.: Acta Pol. Pharm. Drug Res. 62, 393 (2005).
23. Rykaczewska-Czerwińska M., Wróbel M., Kuczer M., Konopińska D., Plech A.: Pestycydy/Pesticides 1-2, 21 (2006).

24. Avitsur R., Donchin O., Barak O., Cohen E., Yirmiya R.: *Brain Behav. Immun.* 9, 234 (1995).
25. Diaz-Veliz G., Urresta F., Dussaubat N., Mora S.: *Psychoneuroendocrinology* 19, 387 (1994)
26. Plech A., Gabriel E.: (unpublished data).
27. Plech A., Rykaczewska-Czerwińska M., Sipiński A., Konopińska D.: *JAST* 2, 682 (2012).
28. Schorscher-Petcu A., Sotocinal S., Ciura S., Dupre A., Ritchie J., Sorge R.E., Crawley J.N. et al.: *J. Neurosci.* 30, 8274 (2010).

Received: 26. 11. 2013

SHORT COMMUNICATION

**VARIATION IN VITAMIN D PLASMA LEVELS ACCORDING TO STUDY
LOAD OF BIOMEDICAL STUDENTS**

OLIVERA Z. MILOVANOVIC¹, JASMINA R. MILOVANOVIC^{2*}, ALEKSANDAR DJUKIC³,
MILOVAN MATOVIC⁴, ALEKSANDRA TOMIC LUCIC⁵, NENAD GLUMBIC⁶,
ANA M. RADOVANOVIC¹ and SLOBODAN M. JANKOVIC²

¹Department of Pharmacy, ²Department of Pharmacology and Toxicology, ³Department of Internal Medicine – Endocrinology, ⁴Department of Nuclear Medicine, ⁵Department of Internal Medicine – Rheumatology, Faculty of Medical Sciences, University of Kragujevac, Kragujevac, Serbia

⁶Department of Special Education and Rehabilitation, Faculty for Special Education and Rehabilitation, University of Belgrade

Keywords: 25-hydroxyvitamin D, vitamin D deficiency, biomedical study, focus group

Students' life can be perceived by the different prisms. On one hand, that is the happiest time of life while on the other side, that is a period that changes lifestyle habits. Numerous studying commitments over a school year can decrease certain extracurricular activities such as spending time outdoors, playing a sport or just walking and consequently lead to reduced exposure to sunlight, which is the major risk factor for vitamin D deficiency. Vitamin D is substantial for achieving and up keeping calcium homeostasis and consequently accomplishing skeleton health. Besides the aforementioned, there is a great number of studies that showed a whole variety of vitamin D effects on human body such as prevention of cancer, cardiovascular, autoimmune, infectious and respiratory diseases, and preservation of mental health (cognitive impairment and depression) (1–3).

Our aim was to see how study load and some other factors correlate with vitamin D plasma levels of healthy students from the Faculty of Medical Sciences in Kragujevac. The study was approved by the Ethics Committee of the Faculty of Medical Sciences, University of Kragujevac, Serbia and the students signed informed consent for participation in the study. The study took place from April 2012 to August 2012. The students were from three different study courses (medicine, pharmacy and dentistry) and from various study years (from 1 to 5).

Average vitamin D level (25-hydroxyvitamin D) in the study population of 86 students was 13.263 ± 4.86 ng/mL that was significantly below cut off point for sufficient vitamin D level ($p < 0.001$) (2). Vitamin D deficiency was observed in 88.37% participants. Sex, study course, average study score, average vitamin D food intake (calculated for period of 30 days before blood samples were taken), body mass index, biochemical parameters (phosphate level, urea, creatine, total protein) and endocrine parameters (FT4, TSH and PTH level) did not correlate with vitamin D plasma levels ($p > 0.05$). There was weak but significant correlation between level of vitamin D (25-hydroxyvitamin D) and calcium level ($r = 0.228$; $p \geq 0.05$).

However, the year of study influenced vitamin D levels ($p \geq 0.05$): the students of the third year of study had the lowest average level while students of the fifth year had the highest average level of vitamin D, 11.825 ± 4.372 ng/mL and 15.397 ± 4.103 ng/mL, respectively (Fig. 1). We thought that reason for such results may be decreased exposure to sunlight of students in the third year in comparison with other years ($p \geq 0.05$).

In order to examine the influence of study load on variation of serum vitamin D level by biomedical students authors created a focus group that was composed of 15 graduated students by Faculty of

* Corresponding author: e-mail: Jasminamilo@yahoo.com; phone: +381 34 306800 111; fax: +381 34 306800

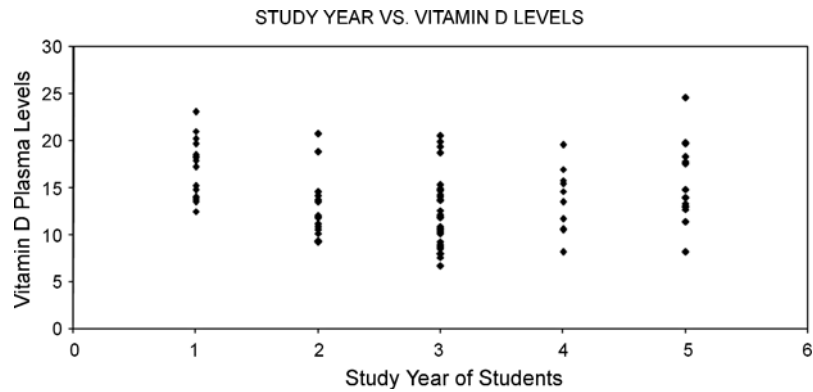


Figure 1. Vitamin D plasma level in relation to study year

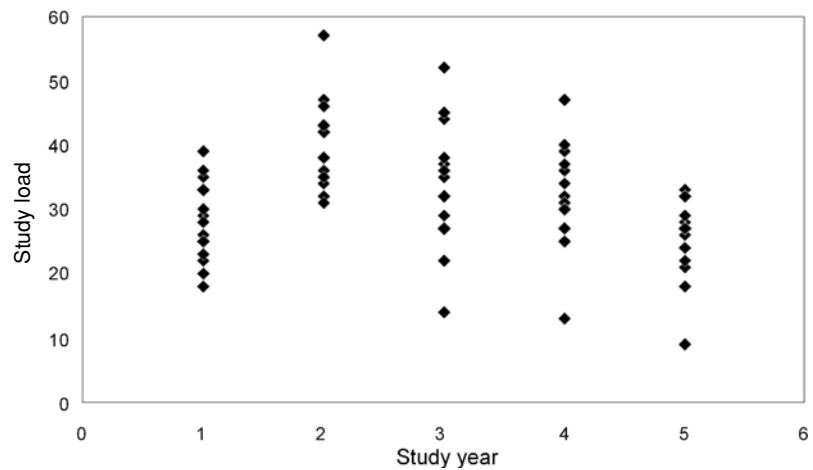


Figure 2. Perception of study load by focus group according to study year

Medical Sciences, in Kragujevac. After discussion about the topic, members of the focus group rated study load of each of the study subjects on a scale from 1 to 5 where mark 1 meant “the lowest load” while mark 5 presented “the highest load”. Estimate of the total study load for particular year of study was then calculated as the sum of estimated loads of each subject from that year. The results are shown in Figure 2, where it can be seen that the second year of study bears the highest student workload, then followed by the third, fourth and first study years, while the fifth study year bears the lowest load. We believe that this could explain the lowest vitamin D levels in the third study year. As the second study year had the highest study load, we may assume that decreased sun exposure during the second year of study created insufficient amounts of vitamin D, which then were spent during the winter, leading to low plasma levels in the next year, when the measurements took place (4).

Our results point out that vitamin D deficiency was presented in a majority of biomedical students, which is in accordance with epidemic nature of vitamin D deficiency all over the world (5). The study load has an effect on variation of vitamin D levels and it would be useful to supplement vitamin D and prevent its deficiency during the study years with the highest load in order to prevent myriad of adverse consequences of vitamin D deficiency on physical and psychical health (6, 7). Of course, our results remain to be confirmed by larger studies in the future.

Acknowledgments

This study was partially financially supported by Grant No. 175007 given by Serbian Ministry of Education, and by a Grant given by Ministry of Science, Montenegro.

Conflict of interest

All authors have no conflicts of interest.

REFERENCES

1. Wacker M., Holick M.F.: *Nutrients* 5, 111 (2013).
2. Gröber U., Spitz J., Reichrath J., Kisters K., Holick M.F.: *Dermatoendocrinology* 5, 331 (2013).
3. Hossein-nezhad A., Holick M.F.: *Mayo Clin. Proc.* 88, 720 (2013).
4. Holick M.F.: *Am. J. Clin. Nutr.* 80 (6 Suppl.), 1678S (2004).
5. Bosomworth N.J.: *Can. Fam. Physician* 57, 16 (2011).
6. van der Schaft J., Koek H.L., Dijkstra E., Verhaar H.J., van der Schouw Y.T., Emmelot-Vonk M.H.: *Ageing Res. Rev.* 12, 1013 (2013).
7. Maddock J., Geoffroy M.C., Power C., Hyppönen E.: *Br. J. Nutr.* 111, 904 (2014).

Received: 18.06.2014

Instruction for Authors

Submission of the manuscript

All papers (in duplicate and electronic version) should be submitted directly to Editor:

Editor
Acta Poloniae Pharmaceutica –
Drug Research
16 Długa St.
00-238 Warsaw
Poland

We understand that submitted papers are original and not published elsewhere.

Authors submitting a manuscript do so on the understanding that if it is accepted for publication, copyright of the article shall be assigned exclusively to the Publisher.

Scope of the Journal

Acta Poloniae Pharmaceutica - Drug Research publishes papers in all areas of research. Submitted original articles are published in the following sections: Reviews, Analysis, Biopharmacy, Drug Biochemistry, Drug Synthesis, Natural Drugs, Pharmaceutical Technology, Pharmacology, Immunopharmacology, General. Any paper that stimulates progress in drug research is welcomed. Both, Regular Articles as well as Short Communications and Letters to the Editor are accepted.

Preparation of the manuscript

Articles should be written in English, double-spaced. Full name (first, middle initial, last) and address of authors should follow the title written in CAPITAL LETTERS. The abstract should be followed by keywords. We suggest the following structure of paper: 1) introduction, 2) experimental, 3) results, 4) discussion and conclusion.

Instructions for citation of references in the e-journal:

1. In the text, sequential numbers of citations should be in order of appearance (not alphabetically) in parentheses (...) not in brackets [...].
2. In the list of references, for papers the correct order is: number of reference with dot, family name and initial(s) of author(s), colon, proper abbreviation(s) for journal (Pubmed, Web of Science, no dot neither comma after one word journal name), number of volume, number of issue (if necessary) in parentheses, first page or number of the paper, year of publication (in parentheses), dot. For books: number of reference with dot, family name and initial(s) of author(s), colon, title of chapter and/or book names and initials of editors (if any), edition number, page(s) of corresponding information (if necessary), publisher name, place and year of publication.

EXAMPLES:

1. Gadzikowska M., Gryniewicz G.: Acta Pol. Pharm. Drug Res. 59, 149 (2002).
2. Gilbert A.M., Stack G.P., Nilakantan R., Kodah J., Tran M. et al.: Bioorg. Med. Chem. Lett. 14, 515 (2004).
3. Roberts S.M.: Molecular Recognition: Chemical and Biochemical Problems, Royal Society of Chemistry, Cambridge 1989.
4. Salem I.I.: Clarithromycin, in Analytical Profiles of Drug Substances And Excipients. Brittain H.G. Ed., pp. 45-85, Academic Press, San Diego 1996.
5. Homan R.W., Rosenberg H.C.: The Treatment of Epilepsy, Principles and Practices. p. 932, Lea & Febiger, Philadelphia 1993.
6. Balderssarin R.J.: in The Pharmacological Basis of Therapeutics, 8th edn., Goodman L., Gilman A., Rall T.W., Nies A.S., Taylor P. Eds., Vol 1, p. 383, Pergamon Press, Maxwell Macmillan Publishing Corporation, New York 1985.
7. International Conference on Harmonization Guidelines, Validation of analytical procedures, Proceeding of the International Conference on Harmonisation (ICH), Commission of the European Communities, Geneva 1996.
8. <http://www.nhlbi.nih.gov/health/health-topics/topics/ms/> (accessed on 03. 10. 2012).

Chemical nomenclature should follow the rules established by the International Union of Pure and Applied Chemistry, the International Union of Biochemistry and Chemical Abstracts Service. Chemical names of drugs are preferred. If generic name is employed, its chemical name or structural formula should be given at point of first citation.

Articles should be written in the Past Tense and Impersonal style. I, we, me, us etc. are to be avoided, except in the Acknowledgment section.

Editor reserves the right to make any necessary corrections to a paper prior to publication.

Tables, illustrations

Each table, figure or scheme should be on a separate page together with the relevant legend and any explanatory notes. Tables ideally should not have more than 70, and certainly not more than 140, characters to the line (counting spaces between columns 4 characters) unless absolutely unavoidable.

Good quality line drawings using black ink on plain A4 paper or A4 tracing paper should be submitted with all lettering etc., included. Good black and white photographs are also acceptable. Captions for illustrations should be collected together and presented on a separate sheet.

All tables and illustrations should be specially referred to in the text.

Short Communications and Letters to the Editor

The same general rules apply like for regular articles, except that an abstract is not required, and the number of figures and/or tables should not be more than two in total.

The Editors reserve the right to publish (upon agreement of Author(s) as a Short Communication a paper originally submitted as a full-length research paper.

Preparation of the electronic manuscript

We encourage the use of Microsoft Word, however we will accept manuscripts prepared with other software. Compact Disc - Recordable are preferred. Write following information on the disk label: name the application software, and the version number used (e.g., Microsoft Word 2007) and specify what type of computer was used (either IBM compatible PC or Apple MacIntosh).

Fee for papers accepted for publication

Since January 2013 there is a publication fee for papers accepted for publication in Acta Poloniae Pharmaceutica Drug Research. The fee - 1000 PLN, should be paid before publication on the bank account:
Polish Pharmaceutical Society, Długa 16, 00-238 Warszawa
Millennium S.A. account no. 29 1160 2202 0000 0000 2770 0281
with a note „publication in Acta Pol. Pharm. Drug Res., paper no.

For foreign authors the payment (250 €) should be done according to the data:

1. SWIFT Address: BANK MILLENNIUM SA, 02-593 WARSZAWA, POLAND, STANISŁAWA ŻARYNA 2A St.
2. SWIFT CODE: BIGBPLPWXXX
3. Beneficiary account Number: PL 30 1160 2202 0000 0000 2777 0200
4. Bank Name: BANK MILLENNIUM SA
5. Favoring: POLSKIE TOWARZYSTWO FARMACEUTYCZNE (Polish Pharmaceutical Society), DŁUGA 16, 00-238 WARSZAWA, Poland, NIP 526-025-19-54
6. Purpose of sending money: Publication in Acta Pol. Pharm. Drug Res., paper no.

For payments by Western Union, the name of recipient is Katarzyna Trembulak at the address of Polish Pharmaceutical Society (see above).

